DEVELOPMENT OF A MODULAR STRATEGY TOWARDS THE TOTAL SYNTHESIS OF (+)-PLEUROMUTILIN AND PROGRESS TOWARDS THE SYNTHESIS OF (–)-MERRILACTONE A

Thesis by

Sean Feng

In Partial Fulfillment of the Requirements

for the Degree of

Doctor of Philosophy

CALIFORNIA INSTITUTE OF TECHNOLOGY

Pasadena, California

2020

(Defended April 13, 2020)

Sean Feng

ORCID: 0000-0002-8095-6402

To Mom, Dad, Eva, Woodson, and Julep.
For your unconditional love, support, and
bottomless pits of Patience.

ACKNOWLEDGEMENTS

First and foremost, I would like to thank my advisor, Sarah Reisman, not only for allowing me to spend my graduate career conducting research in her group, but also for being such a great source of support. One thing that I've come to appreciate about Sarah is that even though she makes it abundantly clear to us that she's the boss (she regularly says, "I'm the boss"), she cares deeply about each and every one of us like a big sister would. Coming to graduate school is a **huge** life transition for many of us. Beginning my first year at 22 and finishing at 26, I am a completely different person now from who I was when I first got here. With that came *a lot* of growing pains. I took comfort in knowing that any time I was struggling through a tough time, *work-related or personal*, Sarah's office was a safe space to unload. Talking *chemistry* at Magnolia House, admiring your front (and back) porch after the 2019 holiday party, and getting yelled at for not properly packing the bear lockers to your liking–these are all fond memories that I will never forget.

I would also like to thank my committee chair, Brian Stoltz, for being like a second advisor to all of us in the Reisman Group. I've appreciated all of the thoughtful discussions we've had regarding chemistry and also the not-so-thoughtful discussions we've had about "when's the wedding?" and the true novelty that is his beard.

Greg and Linda have been very supportive members of my committee. While I recognize our discussions have been limited to our annual meetings, I have always valued their input and insightful questions that have led me to think more deeply about the topics being discussed. Greg, I truly hope that in due time, there will be a doggy door between yours and Jonas' office so that not even a wall will be able to separate you from Bluejay.

I am deeply grateful to the Caltech staff who have helped make my time at Caltech proceed so seamlessly. I would like especially like to thank Alison Ross and Agnes Tong for their logistical help and for organizing the fun visiting weekends that we, graduate students, look forward to every year.

I have the utmost admiration for Scott Virgil, David Vander Velde, and Mona Shahgholi for their commitment to the Caltech students. They are indispensable resources that set Caltech apart from other universities, and none of this would have been possible without their hard work.

Of course, I would not be where I am today without the Reisman group posse! I would like to thank Maddi Kieffer for being a great first mentor (chemistry and dog parent) in the group when I got here in the summer of 2015. You and Kangway gave me the courage to get *two* puppies in graduate school and for that, Woodson, Julep, and I are eternally grateful. I would also like to thank Victor Mak, Karen Mak, Alice Wong, and Carson Matier for giving me a warm welcome into the group with Chinese food and *lots* of boba.

Throughout my five years at Caltech, I have had the privilege to work closely with a number of people either as project partners or as bay-mates. Despite our initial disagreements when I joined the group, I feel fortunate to call Julie Hofstra a friend and will miss our late night chats about exploring the outdoors. I will forever remember the time we hiked Mt. Wilson together when there was ice at the summit (my feet have never hurt so much). I'm so happy we were able to move past our differences; thank you for being a great bay-mate and friend.

I'd like to give a special shout out to Nick Fastuca who worked beside me for the past four years. I will never forget our ridiculous late night spot-to-spot dance parties in the lab and Spongebob sing-a-longs; there was never a dull day in the lab when working next to you. You will always be an enigma to me; please never change.

Prior to Nick Fastuca, I worked next to a visiting student from Germany, Kevin Sokol. Our friendship didn't blossom until he moved back to Germany. I'm happy that it eventually did, but also, dude! We could've hung out the entire time you were here! In 2018, I attended a conference in France and immediately after, I hopped on a plane to go visit him in Innsbruck, Austria. From biking around the streets of Innsbruck to climbing in Martinswand, it was the trip of a lifetime, and I'm glad I was able to spend it with Kevin. Thanks for being such a great friend, even from 6,000 miles away.

Luke Hanna and I are bonded by two things: 1) we are anteaters first and foremost (zot zot) and 2) merrilactone A. Firstly, thank you for laying down the foundation for the merrilactone project. It is undoubtedly your brain child and I am fortunate to have been part of it. Secondly, thank you for always being down to hang out. Grad school is exhausting, and having a friend who is happy to just sit with you on the couch and watch Rick and Morty really makes a huge difference.

The 2nd year cohort of graduate students are an exceptionally fun, talented, and driven crop of students that I have had the pleasure of overlapping with. Even before Yujia Tao got here, I knew she was a force to be reckoned with. She is a chemistry mastermind, twitter guru, snack connoisseur, and the most adorable person I have ever met despite her strangely dark sense of humor. I will miss startling her in the office and will never forget the shriek of Yujia.

I've always admired Jeff Kerkovius' enthusiasm for chemistry. This guy really just *loves chemistry*. But little do most people know, there's something he loves more than chemistry, and that's sushi. Jeff, I will miss our sushi adventures together and hope that you'll continue the weekly sushi tradition. I hope to receive regular updates on the status of our sushi chart; most importantly, I hope that you find a place that belongs in the ~palladium~ category. As much as I hate to say it, I will also miss your groan-worthy punslinging.

I don't think anyone has said "no" to me more times than Sara Dibrell has, and that's one of the reasons why I like her so much. Dibrell, even though you meant business most of the time, I always enjoyed our discussions in the office, even though you disagreed with me most of the time. I will cherish the handful of times you came over for game night and I will especially remember when you and Alex yelled at each other for an hour about whether mol was an acceptable word for Scrabble. I'm sorry Chris, Marco, and I were always such a nuisance in the office and thank you for putting up with us.

Whenever I had a question about a calculation, I knew I could count on Ray. Ray, thanks for always entertaining my calculation questions and for just being an all-around great person to work with. You are an incredible scientist and I enjoyed watching at your reactions change color and looking at your cool TLC plates.

As a graduate student, I had the pleasure of mentoring Ali Bodnar and Felix Schäfers. Ali, I had so much fun working with you in the lab; you were really the best undergraduate mentee I could've asked for despite all of your sass. I know you'll do great at Yale and I'm looking forward to seeing all that you can accomplish. Felix, it was a pleasure working with you on the pleuromutilin project. Those were some dark days we

had together, but we got through it! It was an honor to watch you grow as a scientist, from running your first (proper) TLC to setting up complicated reactions on 100 mmol scale. I know you'll do great in the Glorious group and whatever you decide to pursue next.

Arthur was single-handedly my greatest resource at Caltech. Arthur is like if *Cosmopolitan* magazine came out with a chemistry issue. He is an encyclopedia of chemistry knowledge, a Powerpoint and ChemDraw fashionista, and knows all the latest on who got a tenure-track position where. Arthur, I am so grateful to have you in my life not only as a source of inspiration, but also as a friend. I look forward to the day that you realize you are truly a Cali boy at heart so you can come back and we can hang out again.

I had the honor of working with my project partner and mentor, Elliot Farney. Anyone who knew Elliot would describe the man as a machine. His diligence, patience, and work-ethic were unparalleled and as a chemist, he is the embodiment of everything I strive to be. Elliot, thank you for being such a great mentor in lab and in life. I wouldn't be the scientist I am today if it weren't for you and for that I am eternally grateful. Peace. Love. Unity. And RESPECT.

Some of my fondest memories of Nat and Julia Kadunce were the front porch barbeques with marinated chicken hearts. They were SO good. But aside from that, thank you for being wonderful friends and overall just really lovely people! Nat, I will always admire your calm and collected nature. You are the most zen person I've ever met and hope that someday, I will also be zen like you.

There are several stressful aspects of joining a new group as a first year graduate student: 1) you don't know where anything is, 2) you don't know what equipment you need to get trained on, and perhaps the most challenging bit, 3) you have no friends and don't

know anyone. Matt Hesse made my transition into the Reisman group a seamless one. Not only did he help me with the stressful work aspects, but also he was my first friend at Caltech. Matt, thank you for being my friend when I had none and for all the fun adventures afterwards.

Graduate school is filled with so many unpredictable variables that are out of our control, but for me, Lauren Chapman has always been a constant. She has been an unwavering source of support through every stage of my graduate career, offering advice and wisdom in times of crisis. Lauren, thank you for being such a loyal, dependable, and an amazing friend. Your guidance and friendship are invaluable to me and I wouldn't have gotten through these past five years without you.

I will never forget all of the *treat-yo-self* nights with Denise Grünenfelder, be it getting dinner at Sugarfish or getting massages together. Denise, thank you for always being such a loyal friend. I knew I could always count on you for good time and to help me solve NMR structures! Yassss queeeeeeen.

Jordan Casey Beck is hands down the fiercest, sassiest, and wittiest person Schlinger has ever seen. Jordan has a thirst for life and I will look back fondly at the days we spent hanging out with CRUSH, getting our eyebrows threaded to perfection, and dying in Orangetheory. Jordan, I will always remember that day we went to Burbank for our TSA Precheck interview and I was like, "HE MADE ME LATE." I still can't believe you dragged me and Kelsey to Olive Garden afterwards. But seriously, thank you for making me get TSA Precheck, for always looking out for me and Kelsey, and for being a wonderful friend all these years. I am also thankful for Jon Nicolini for introducing me and Jordan to all the hottest sushi joints in town. I will never forget the night we spent $200 at Nozawa

Bar, only to have an A5 Wagyu steak at Maestro's for dessert. It's too bad Spasso was closed. We could've gotten tuna cones too.

And with Jordan, of course there is also Kelsey Poremba. I will always remember Kelsey as the sweetest girl you'll ever meet unless the Patriots are losing, in which case tread *very* carefully. All joking aside, Kelsey is an amazing friend who will always do right by the people she loves–a true Gryffindor at heart. I will always miss our shenanigans ranging from lounging by the pool to going rock climbing in Big Bear. Kelsey, I JUST WISH YOU WOULD RESPOND TO MY TEXTS.

My cohort is the best cohort. I would like to thank Eric Alexy, Bradley Gorsline, Carina Jette, Fa Ngamnithiporn, and Chris Reimann (relax, I'll get to you more later) for making my time at Caltech so special. I am confident that you will all go on to accomplish great things not only because you are great scientists, but also because you are amazing people.

I feel like Alexia Kim snuck into my life and I really have no idea how. We went quickly from not acknowledging each other in the hallways to hanging out almost every single day for a couple months. You're like a perfect pair of lace-up boots. There was no break-in period! The whole situation still confuses me, but I am also so thankful that it all happened. The TT club will always have a special place in my heart and I will never forget the crazy nights that were CandiPop, Polo & Pan, and AC Slater.

Speaking of the TT club, I am so thankful for Chris Lavoie. He is the glue that brings people together and without him, the TT club would've never come to fruition. Chris came into my life at the perfect time when we both needed it the most. My friendship and

interactions with Chris have helped shape me to be a more confident person. Chris, thanks for being an awesome friend and a great roommate.

Chris Reimann swears that when we first met during recruitment weekend, I didn't like him. He wasn't wrong. But, times have changed! Since day 1 at Caltech, Chris has always been an awesome friend to me, and, as time went on, I've grown to appreciate his dad jokes and snarky sense of humor. There are three distinct memories of Chris that I will always cherish: 1) our balcony rants when literally everyone and everything else sucked, 2) that time you put googly eyes all over my stuff in the office, and 3) being roommates at the GRC. I'm so glad I ended up not hating you after getting to know you.

Not in a million years would I be able to fully verbalize the love and appreciation I have for Marco Brandstätter. Marco has become one of my very best friends–a friend you really only find once in your life if ever at all. It's like we've mastered the art of telepathic communication; I can't even count on one hand the number of times we've rolled a Yahtzee for each other! Marco, despite all that is currently wrong with the world, I take comfort in knowing that I have a friend like you to weather the storm with. Thank you for always being there for me, supporting me through my last year of graduate school, and giving me one more reason to visit Switzerland.

Of course, my journey didn't begin at Caltech and I have so many people to thank for helping me get to where I am today. Thank you Professor Chris Vanderwal for allowing me to join your research group with only one quarter of sophomore organic chemistry under my belt. None of this would have been possible without your guidance and support. I would also like to thank Sam Tartakoff and Allen Hong for their patience in mentoring me as an unruly undergraduate student. From teaching me how to run my first TLC to

proofreading my graduate school applications, all that I know, I know from them. I am eternally grateful for the support of my friend and high school tutor, Andrew Fu. In the first half of my high school career, I was an unmotivated C student who was failing pre-calculus and Andrew really helped me overcome this obstacle. He instilled in me a strong work ethic that has gotten me to where I am today and for that, I am so thankful.

I would like to thank Ramsey Lee Garrett for his unconditional friendship and support. I know that I haven't always been the greatest friend to you at times, but thank you so much for always giving me the benefit of the doubt and being the kind person that you are. I appreciate all that you do for Woodson and Julep and am so glad to be co-parenting these two monkeys with you.

One real perk of being just 45 minutes away from where I grew up (east) and went to college (south) is that I always had a few friends just a short drive away. Thank you Chloe and Shannon for always being there for me even though we didn't hang out quite like we used to in high school. I am so thankful for our friendship and so glad to have you guys in my life. I'd like to thank my wombmate, Katie, for her friendship and support throughout college and graduate school. Even though we don't see each other as much as I would like, I love that we can pick up right where we left off. Gooby pls.

Never would I have guessed that my pleuromutirival would become my pleuromutifriend. I met Olivia Goethe at an antibiotics conference in Lake Annecy, France where we were two of three chemists, the third being Nick Lees AKA Steaky. What happens when you lock three chemists in a room full of biologists for 12 hours a day, 9 days straight? You form an unbreakable bond of ~everlasting friendship~. In all seriousness though, thank you for being part of my life even though we're separated by

2,868 miles. You too Steaky, but with a lot more miles. I really hope that you move to the Bay so we can be together 24/7, again.

Climbing has been a huge part of my life for the past six years. As a graduate student, most of the reactions you run don't work, and it's easy to feel like you aren't making any progress no matter how hard you try. Climbing has been an escape, allowing me to completely detach from work and focus on something that makes my psyche and my body feel good. Through climbing, I've learned that without failure, there is no progress and when you take that 20-foot whipper on what feels like a project way above your pay grade, the only way to clip the chains is to breathe, figure out the moves, and get back on the wall.

I would like to give a special thank you to all the climbing partners I've met along the way not for only keeping me sane, but also for keeping me alive on the other end of the rope. Special thanks to Michel Le Duff for believing in me more than I believe in myself, Tom Dusseault for being my first consistent partner and one of my best friends, Sophia Lin for suffering with me on climbs like Time Wave Zero, Brian Spiegel for introducing me to climbing, Peter and Kate at Stronghold for creating a safe haven for us climbers, Dan Murphy for being a great partner and friend from Red Rock to Ten Sleep, David Kingston, Cathy Nguyen, Colin Brochard, Asher Allanigue, Matt Beyer, Tung Wongwaitayakornkul, Ameera Abdelaziz, Hong Tran, and Ray Valori. Thank you all for the countless belays and for making me the climber I am today.

Thank you Eva Mendez for being the best sister I could've ever asked for. Even though we're now on opposite sides of the country, our blood runs thick and I will always look up to you as my 姊姊. I'm definitely the smarter one though.

Woodson and Julep have taught me so many lessons in patience and how to love unconditionally. They've also taught me that there's more to life than work and that it's important to make time for the things you love. Thank you for being part of my entire graduate school journey and I promise we will go on more adventures together as soon as I'm finished here. I love you both so much.

Thank you Nicholas James Race for all of the love, support, and patience you have given me this past year. From spending hours with me on Facetime going over the Baran heterocycles lectures to proofreading my proposals and my thesis, you have always been committed to my success and I am so grateful for all that you do for me. But most of all, thank you for believing in us despite the distance. You've made my last year all the sweeter, and I am so excited to see all that you will accomplish in your independent career.

Finally, I need to thank the most important people in my life, my parents. Even though it may not seem like it at times, I am so glad to have spent the past five years just a short drive away. I know I didn't go home as much as you would've liked, but I took comfort in knowing that regardless of how bad things got, I could always just go *home*. I am so grateful for all of the sacrifices you've made in providing a better life for me and Eva and for all of the home cooked meals when I was too busy to cook for myself. I love you both so much and am so proud to call you my parents.

ABSTRACT

Natural products have long stood as a rich source of biologically relevant molecules bearing highly functionalized and complex architectures. On one hand, they are a focal point for the development of new therapeutic agents owing to their inherent biological activities. On the other, they serve as an exciting testing ground for existing synthetic methodologies and provide opportunities for the development of new reactions.

Herein, we describe a modular strategy that was employed for the total synthesis of the antibiotic (+)-pleuromutilin. Key features of our synthesis include (1) the development of a highly stereoselective SmI_2-mediated ketyl radical cyclization to establish the central eight-membered ring and (2) a modular crotylation reaction to install the eight-membered ring's backbone that permits full control over the stereochemistry at C12 as desired. During our synthetic studies, a transannular [1,5]-hydrogen atom transfer reaction that affects a stereospecific redox relay to set the C10 stereocenter was serendipitously uncovered. This strategy enabled the completion of a concise total synthesis of (+)-pleuromutilin, proceeding in 18 steps. To demonstrate the modularity of our synthetic approach, the same strategy was readily applied to the synthesis of (+)-12-*epi*-pleuromutilin with no reoptimization, providing a new platform for the preparation of fully synthetic derivatives that may hold promise as broad-spectrum antibiotics.

This report also highlights the work we have conducted in the development of a synthetic strategy towards (–)-merrilactone A. We detail our investigation of a Pd-catalyzed asymmetric allylic alkylation reaction that rapidly constructs the D ring bearing the C5 and C6 vicinal quaternary centers. Potential paths forward to complete the synthesis of this neurotropic natural product leveraging this advanced intermediate will also be discussed.

PUBLISHED CONTENT AND CONTRIBUTIONS

Farney, E. P.[†]; Feng, S. S.[†]; Schäfers, F.; Reisman, S. E. *J. Am. Chem. Soc.* **2018**, *140*, 1267-1270.

DOI: 10.1021/jacs.7b13260

This article is available online at: https://pubs.acs.org/doi/10.1021/jacs.7b13260

S.S.F. contributed to the development of the synthetic strategy, conducted the experiments described herein, prepared the supporting data, and participated in writing the manuscript.

TABLE OF CONTENTS

LIST OF ABBREVIATIONS

$[\alpha]_D$	angle of optical rotation of plane-polarized light
Å	angstrom(s)
ABNO	9-azabicyclo[3.3.1]nonane *N*-oxyl
Ac	acetyl
AIBN	azobisisobutyronitrile
APCI	atmospheric-pressure chemical ionization
aq	aqueous
atm	atmosphere(s)
BBN	9-borabicyclo[3.3.1]nonane
BINAP	2,2'-*bis*(diphenylphosphino)-1,1'-binaphthyl
BINOL	1,1'-binaphthalene-2,2'-diol
Bn	benzyl
Boc	*tert*-butoxycarbonyl
bp	boiling point
bpy	2,2'-bipyridine
br	broad
brsm	based on recovered starting material
Bu	butyl
*i*Bu	*iso*-butyl
*n*Bu	butyl or *norm*-butyl
*t*Bu	*tert*-butyl

c	concentration of sample for measurement of optical rotation
^{13}C	carbon-13 isotope
/C	supported on activated carbon charcoal
°C	degrees Celsius
calc'd	calculated
cis	on the same side
cm^{-1}	wavenumber(s)
CO	carbon monoxide
cod	1,5-cyclooctadiene
conv.	conversion
COSY	homonuclear correlation spectroscopy
Δ	heat or difference
δ	chemical shift in ppm
d	doublet
d	deutero or dextrorotatory
D	deuterium
DACH	diaminocyclohexyl
dba	dibenzylideneacetone
DCC	*N,N′*-dicyclohexylcarbodiimide
DCE	1,2-dichloroethane
DDQ	2,3-dichloro-5,6-dicyano-1,4-benzoquinone
de novo	starting from the beginning; anew
DIBAL	diisobutylaluminum hydride

DMAP	4-(dimethylamino)pyridine
DMDO	dimethyldioxirane
DME	1,2-dimethoxyethane
DMF	*N*,*N*-dimethylformamide
DMP	Dess-Martin periodinane
DMSO	dimethylsulfoxide
dpm	dipivaloylmethanato
dr	diastereomeric ratio
ee	enantiomeric excess
E^+	electrophile
E	*trans* (entgegen) olefin geometry
EDCI	*N*-(3-dimethylaminopropyl)-*N*'-ethylcarbodiimide hydrochloride
e.g.	for example (Latin: *exempli gratia*)
EI	electron impact
ent	enantiomer of
epi	epimeric
equiv	equivalent(s)
ESI	electrospray ionization
Et	ethyl
et al.	and others (Latin: *et alii*)
FAB	fast atom bombardment
FTIR	fourier transform infrared spectroscopy
g	gram(s)

h	hour(s)
^{1}H	proton
HG-II	Hoveyda–Grubbs' catalyst™ 2nd generation
HMBC	heteronuclear multiple-bond correlation spectroscopy
HMDS	hexamethyldisilazide
HMPA	hexamethylphosphoramide
HMPT	hexamethylphosphorous triamide
$h\upsilon$	irradiation with light
HPLC	high performance liquid chromatography
HRMS	high resolution mass spectrometry
HSQC	heteronuclear single quantum coherence spectroscopy
Hz	hertz
i.e.	that is (Latin: *id est*)
iso	isomeric
in situ	in the reaction mixture
J	coupling constant in Hz
k	rate constant
kcal	kilocalorie(s)
kg	kilogram(s)
L	liter
L_n	ligand
l	levorotatory
LCMS	liquid chromatography–mass spectrometry

LDA	lithium diisopropylamide
m	multiplet or meter(s)
M	molar or molecular ion
m	*meta*
μ	micro
*m*CPBA	*meta*-chloroperbenzoic acid
Me	methyl
MeOH	methanol
MeCN	acetonitrile
mg	milligram(s)
MHz	megahertz
min	minute(s)
mL	milliliter(s)
mol	mole(s)
MOM	methoxymethyl
Ms	methanesulfonyl (mesyl)
MS	molecular sieves
m/z	mass-to-charge ratio
Np	naphthyl
NBS	*N*-bromosuccinimide
NCS	*N*-chlorosuccinimide
ND	not determined
nm	nanometer(s)

nM	nanomolar
NMI	1-methylimidazole
NMR	nuclear magnetic resonance
nOe	nuclear Overhauser effect
NOESY	nuclear Overhauser enhancement spectroscopy
Nu^{-}	nucleophile
o	*ortho*
p	*para*
PCC	pyridinium chlorochromate
Ph	phenyl
pH	hydrogen ion concentration in aqueous solution
PhH	benzene
PhMe	toluene
pK_a	acid dissociation constant
pm	picometer(s)
PMB	*para*-methoxybenzyl
ppm	parts per million
PPTS	pyridinium *para*-toluenesulfonate
Pr	propyl
*i*Pr	isopropyl
*n*Pr	propyl or *norm*-propyl
psi	pounds per square inch
Pyr	pyridine

q	quartet
quant.	quantitative
R	generic (alkyl) group
R_L	large group
R	rectus
RCM	ring-closing metathesis
recry.	recrystallization
ref	reference
R_f	retention factor
rgt.	Reagent
rr	regioisomeric ratio
rt	room temperature
s	singlet or seconds
S	sinister
SAR	structure-activity relationship
sat.	saturated
SFC	supercritical fluid chromatography
t	triplet
TBABr	tetra-*n*-butylammonium bromide
TBACl	tetra-*n*-butylammonium chloride
TBAF	tetra-*n*-butylammonium fluoride
TBAI	tetra-*n*-butylammonium iodide
TBDPS	*tert*-butyldiphenylsilyl

TBHP	*tert*-butyl hydroperoxide
TBS	*tert*-butyldimethylsilyl
temp	temperature
Tf	trifluoromethanesulfonyl
TFA	trifluoroacetic acid
THF	tetrahydrofuran
TLC	thin layer chromatography
TMS	trimethylsilyl
TOF	time-of-flight
Tol	tolyl
trans	on the opposite side
Ts	*para*-toluenesulfonyl (tosyl)
UV	ultraviolet
vide infra	see below
w/v	weight per volume
X	anionic ligand or halide
xs	excess
Z	*cis* (zusammen) olefin geometry

Chapter 1

An Introduction to Pleuromutilin

1.1 INTRODUCTION

"One sometimes finds what one is not looking for. When I woke up just after dawn on Sept. 28, 1928, I certainly didn't plan to revolutionize all medicine by discovering the world's first antibiotic, or bacteria killer. But I suppose that was exactly what I did." In 1928, Alexander Fleming serendipitously discovered penicillin after finding that a staphylococcus culture plate had been contaminated with mold.[1] Upon closer examination, he realized that the bacteria in close proximity to the mold colonies had stopped proliferating. He then isolated the mold and identified it as a member of the *Penicillium* genus, which he found to be effective against all Gram-positive pathogens. He noted that it was not the mold itself but rather the mold juice, or penicillin, that possessed antibiotic properties. Despite this breakthrough, there were still significant challenges in

implementing these findings for widespread use against bacteria, most notably the isolation and purification of penicillin. Fortunately, in 1940, Howard Florey and Ernst Chain reported a purification technique, leading to the mass production and distribution of penicillin in 1945.

The discovery of penicillin, as well as Ehrlich's sulfonamide antibiotics,[2] set up the paradigms for future drug discovery and small molecule research where a number of new antibiotics closely followed. The period between the 1950s and the 1970s is now considered the golden age of discovery of novel antibiotics classes; however, few have been discovered since then.[3] With the rapid emergence of pathogenic antibiotic resistance and the decline of discovery rate of new antibiotics, there has been a renaissance in the scientific community toward discovering new antibiotics.

1.2 PLEUROMUTILIN

In 1951, Kavanagh and coworkers[4,5] reported that *Pleurotus mutilus* and *P. Passeckerianus* of the genus *Pleurotus* were found to produce substances that inhibit *Staphylococcus aureus*. At the time of isolation, the full structure of (+)-pleuromutilin (**1**, Figure 1) had not yet been elucidated; however, the authors found that its antibiotic characteristics were lost by boiling the metabolite in a 0.1 N solution of sodium hydroxide, presumably removing the glycolic ester residue. This functionality was later determined to be critical for its biological activity. The antibacterial substance was isolated as a crystalline solid from culture liquids and named pleuromutilin, whose structure and biosynthetic pathway[6,7] were elucidated by Birch and Arigoni independently in the 1960s.

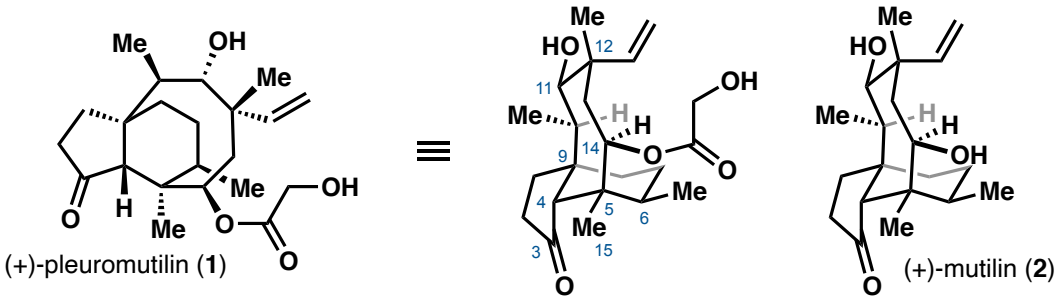

Figure 1. (+)-Pleuromutilin (**1**) and mutilin antibiotics.

1.3 PROPOSED BIOSYNTHESIS

The biosynthesis of pleuromutilin is suspected to occur through a pathway similar to other cyclic terpenes, beginning with pyrophosphate ester **3**.[6,7] Cyclization of the pyrophosphate of all-*trans* geranylgeraniol (**3**, Scheme 1) commences with protonation, which leads to a cationic polyene cyclization cascade to generate cationic *trans*-decalin **4**. A subsequent 1,2-hydride shift, 1,2-methyl shift, and second 1,2-hydride shift migrates the positive charge, resulting in a hydride induced ring contraction to afford the hydrindane framework **6**. Transannular cyclization of the isopropenyl unit in an S_N2' fashion eliminates the phosphate moiety with concomitant formation of the C11–C12 bond, forging the medium-sized ring in pleuromutilin. Addition of water and simultaneous hydride migration installs the C14 hydroxyl.

Studies done by Oikawa and coworkers[8] have shown that **8** is an intermediate in the biosynthesis of pleuromutilin. After studying the later oxidation steps of the biosynthetic pathway, it was postulated that C11 is first oxidized before introduction of the C3 carbonyl to forge mutilin (**2**). This hypothesis was later confirmed by Foster and coworkers,[9] who used stepwise heterologous expression to elucidate the full biosynthetic pathway. Addition of cytochrome p450 monooxygenase gene *pl-p450-1* resulted in C11

oxidation (**9**). Further addition of *pl-p450-1* and *pl-p450-2* led to subsequent C3 oxidation (**10**). Addition of dehydrogenase/reductase *pl-sdr* resulted in formation of the C3 ketone (**2**), where then acetylation of the C14 hydroxyl with acetyl transferase *pl-atf* and final oxidation of C22 with cytochrome P450 monooxygenase *pl-p450-3* provided pleuromutilin (**1**).

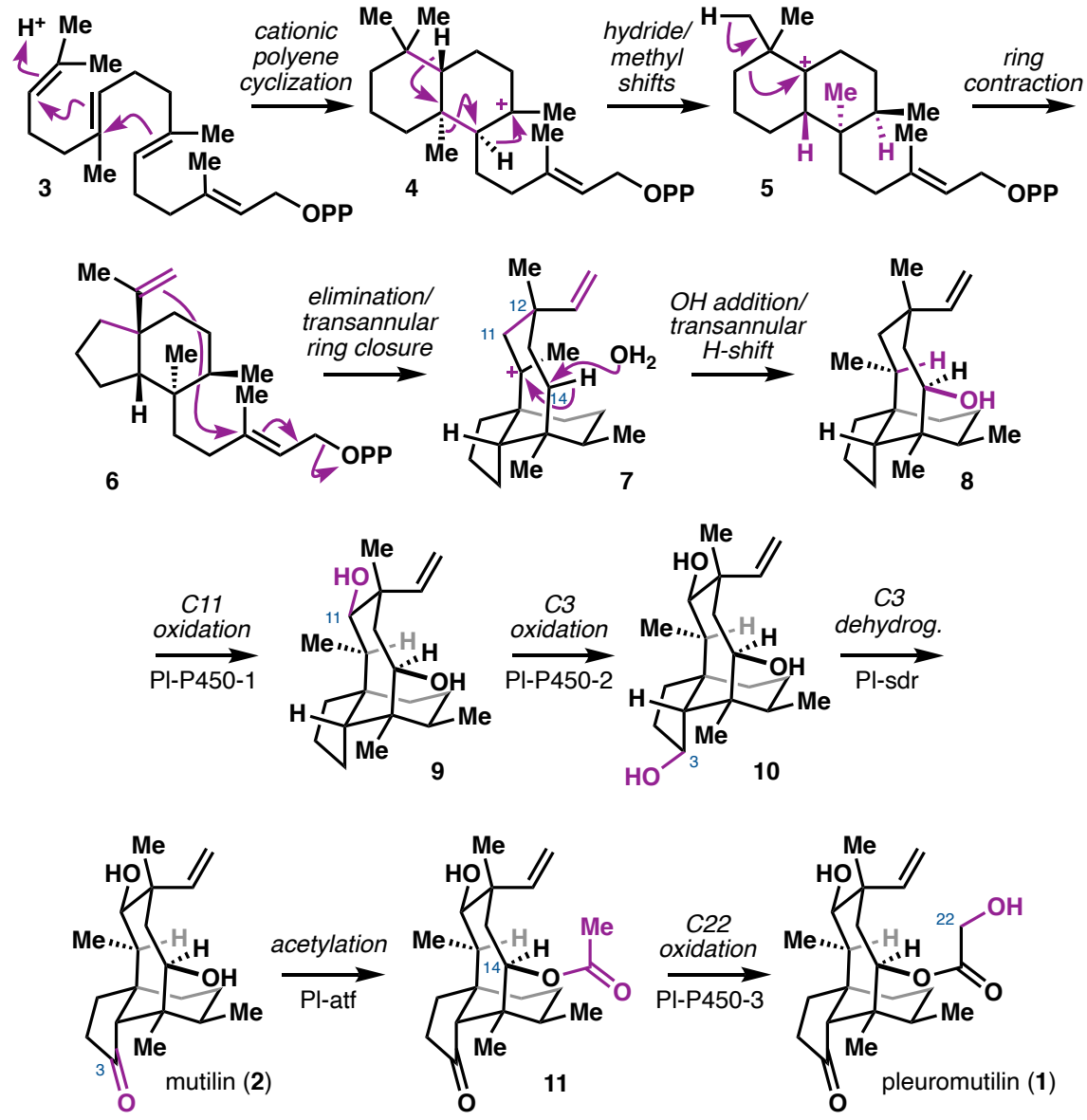

Scheme 1. Proposed biosynthesis of (+)-pleuromutilin (**1**).

1.4 BIOLOGICAL ACTIVITY

The ribosome is an organelle comprised of ribosomal proteins and ribosomal rRNA that polymerizes amino acids into proteins using information encoded in mRNA. During the elongation stage of protein synthesis, amino acid monomers are transported to the initiation complex where there are three binding sites for tRNA: the acceptor site (A site), peptidyl site (P site), and the exit site (E site). The first peptidyl tRNA binds to the P site, and the tRNA carrying the amino acid to be added enters the A site. Within the PTC, the peptide bond is formed, and the newly formed protein chain grows in the E site of the 50S subunit. The ribosome then moves down the mRNA, freeing the A site, and enabling the continuation of this process. Although many characteristics of the ribosome are conserved across all organisms, the differences that exist in rRNA sequence allow pleuromutilin antibiotics to be selective for bacterial ribosomes.

Initial studies on pleuromutilin's mode of action were carried out throughout the 1970s and 1980s first by Högenauerd[10–12] and then Cheney,[13] revealing that pleuromutilins selectively bind to the PTC within the 50S ribosomal subunit and inhibit bacterial protein synthesis.[14] Later in 2004,[15] the crystal structure of tiamulin (**19**) complexed with the 50S ribosome subunit of *Deinococcus radiodurans* was solved, providing a detailed picture of its interactions with the 23S rRNA and explaining the molecular mechanism of its antibiotic activity. The molecule's tricyclic core is situated in the A site; the peptidyl tRNA has already bound to the P site therefore disrupting the correct positioning of the second tRNA. This prevents formation of the first peptide bond, and thus protein synthesis cannot begin.[16] This discovery is further supported by previous findings that tiamulin competes with chloramaphenicol, puromycin, and carbomycin A, which also bind to the A site.[12]

Due to their mode of action in binding to functionally important nucleotides, the pleuromutilin class of antibiotics has experienced less cross-resistance than many other antibiotics, making it an exciting family of compounds to target for human use. However, these molecules suffer from low *in vivo* efficacy due to poor pharmacokinetics and rapid metabolism.[17] To combat these issues, many pleuromutilin derivatives have been synthesized in academic and industrial labs through modification of the natural product.

1.5 SYNTHETIC MODIFICATIONS OF PLEUROMUTILIN

Due to the emergence of multi-drug resistant bacteria, scientists are now focusing their research efforts on developing new antibiotics with novel modes of action and activity against resistant organisms.[18] With this goal in mind, derivatives of (+)-pleuromutilin (**1**), of which several analogs were successfully developed for veterinary medicine, have regained interest in the past few years as promising antibiotics with potential for human application. Herein, a selection of previously reported synthetic strategies toward accessing various derivatives will be discussed.

1.5.1 *Glycolic Ester (C14 and C22) Modifications*

Perhaps the most extensively derivatized position on pleuromutilin is the C22 hydroxyl due to its ease of functionalization.[19–21] Acyloxy derivatives are typically prepared through activation of the C22 hydroxyl group as a tosylate **13** or mesylate **12**, followed by substitution with a thiol, amine, or alcohol to forge the corresponding derivatives (Scheme 2). In an effort to rapidly investigate various pleuromutilin nucleoside conjugates, Nielsen and coworkers[22,23] substituted tosylpleuromutilin **13** with sodium azide

and introduced purine rings on the side chain using click chemistry and alkynyl nucleotides. However, the *in vitro* potencies of these compounds against *E. coli* were only modest.

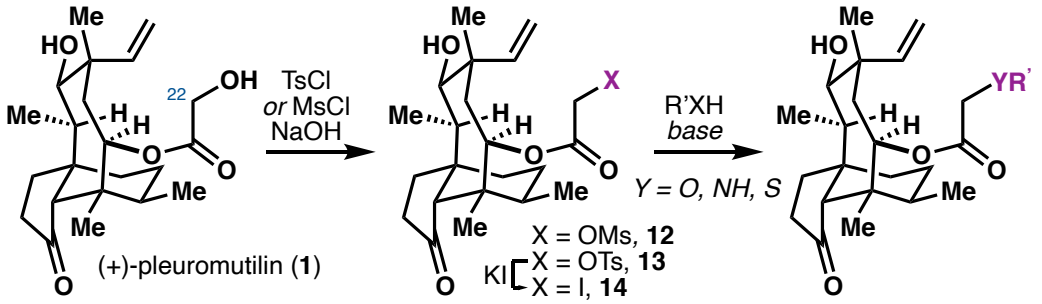

Scheme 2. C22 functionalization of (+)-pleuromutilin (**1**).

While C22-modification of pleuromutilin is facile, selective functionalization of the C14 hydroxyl of mutilin has proven to be more challenging due to the more reactive C11 hydroxyl group. Berner and coworkers[24] demonstrated that stereochemical inversion of C4 can be accomplished with a concomitant 1,5-hydride shift from C11 to C3 to forge resultant ketone **16** (Scheme 3). Because this compound now has only one hydroxyl functionality at C14, it can be selectively functionalized with the desired acid chloride to form C14 mutilin derivatives **17**. Subsequent treatment with $ZnCl_2$ and HCl restores the C4 stereochemistry, and a concomitant 1,5-hydride shift from C3 to C11 reestablishes the desired C3 carbonyl and C11 hydroxyl functionalities. Although not discussed herein, numerous alternative approaches to access C14 derivatives, specifically carbamates, have also been explored.[25,26]

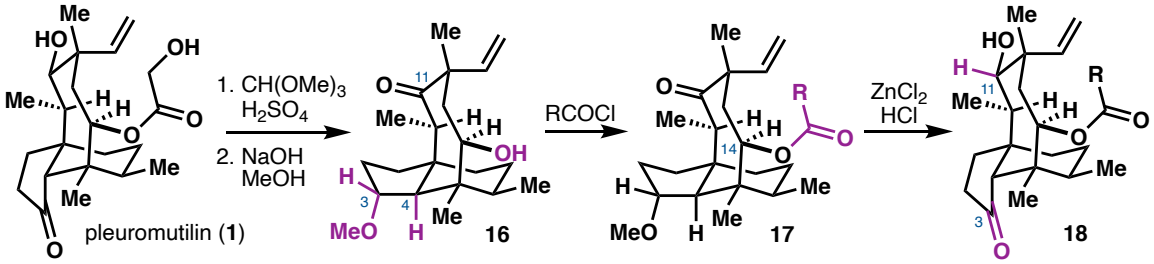

Scheme 3. C14 functionalization of (+)-pleuromutilin (**1**).

Due to the wide availability of (+)-pleuromutilin (**1**) through fermentation and ease of rapid late-stage derivatization, thousands of C14 pleuromutilin derivatives have been prepared through the methods described above. However, only sulfanylacetyl derivatives have advanced into or beyond Phase I clinical studies (Figure 2).[17,19,20]

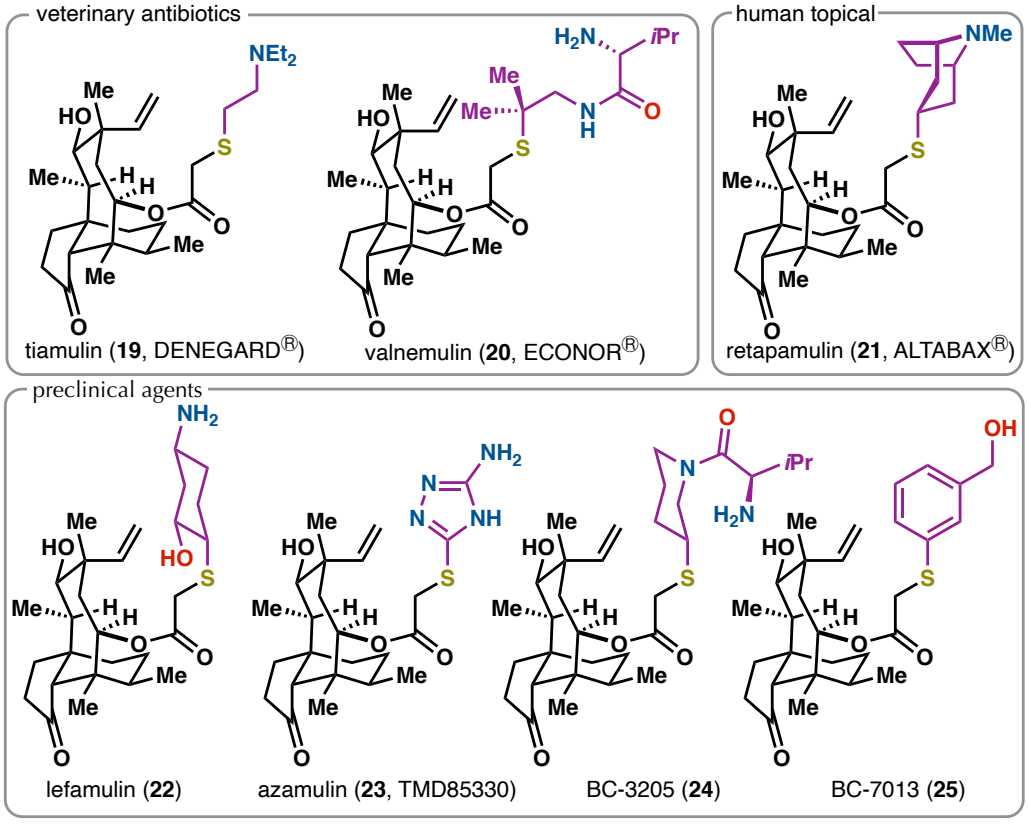

Figure 2. Clinical and preclinical pleuromutilin antibiotics.

On the other hand, the lack of general methods to functionalize the tricyclic core still remains an obstacle; as a result, the number of structural and core-modified derivatives remains relatively low.

1.5.2 *Structural Modifications*

As shown in the work described earlier by Berner and coworkers,[24] as well as that of many other groups,[24,27–30] the unique molecular structure of pleuromutilin is susceptible to alkyl and hydride shifts under forcing conditions. This can lead to stereochemical inversion, as well as ring expansion or contraction. Such structural rearrangements are often reported as undesired reaction side products.

One interesting and important finding by Berner and coworkers[31] is that the C12 quaternary center can be epimerized to a 1:1 mixture of C12 epimers through a zinc-mediated retroallylation-allylation reaction (Scheme 4). This strategy was later employed by Herzon and coworkers[32] in 2017 for the completion of their total synthesis; the only difference in the Herzon system is that C22 hydroxyl group was protected as a trityl ether.

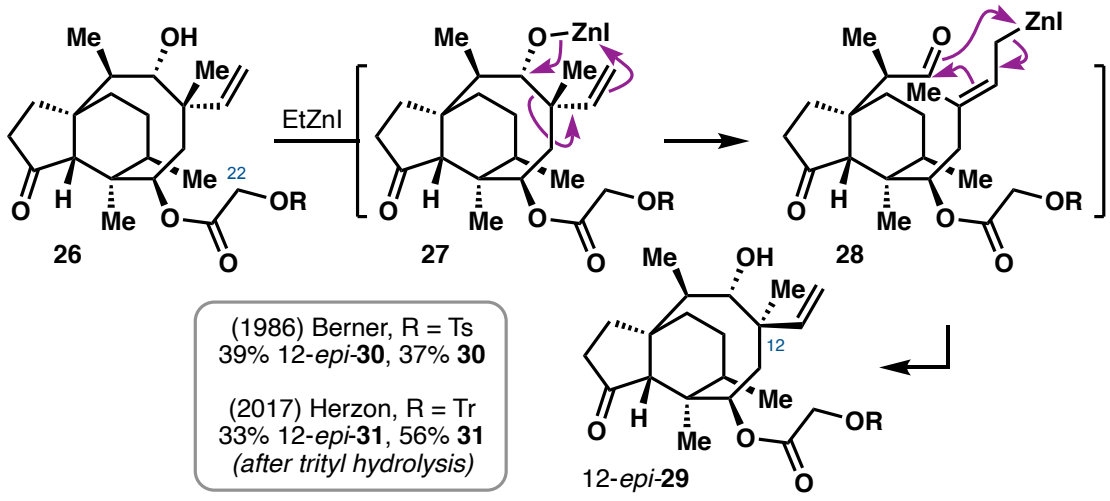

Scheme 4. Berner's zinc-mediated retroallylation-allylation for C12 epimerization.

Birch and coworkers[6] reported a ring contraction reaction that generates a novel 5-6-7 tricyclic skeleton (**33**) through treatment with PCl_5. It is suspected that this shift occurs through activation of the C11 hydroxyl as a leaving group, leading to C11–C13 bond formation. This finding has industrial relevance: as previously discussed, many pleuromutilin derivatives are accessed through activation of C22 through mesylation, followed by nucleophilic displacement (*vide supra*, Scheme 2), and it has been noted that if any competing C11-mesylation occurs, this side product readily undergoes ring contraction in the manufacturing process.[33]

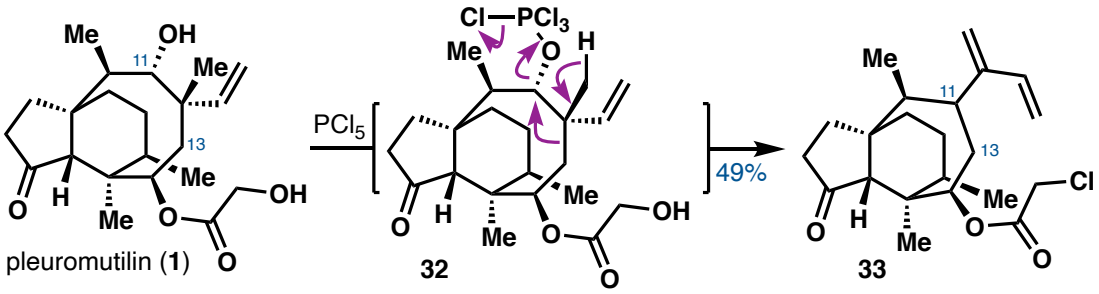

Scheme 5. PCl_5-medidated ring contraction from Birch and coworkers.

Alternatively, Springer and coworkers[27,28] reported that prolonged conditions used for methoxymethyl (MOM) protection led to formation of a tricyclic 5-6-9 ring system (**36**), where dimethoxymethane acts as a single carbon linchpin that facilitates the ring expansion reaction (Scheme 6). Furthermore, it was also reported that pleuromutilin readily undergoes oxidative cleavage of the cyclopentanone ring through a Kornblum-DeLaMare type fragmentation. Although this fragmented product no longer contains the central tricyclic core, the bicyclic system, such as that shown in **37**, has shown promising activity against *Streptococcus pneumonia* A49585.[28]

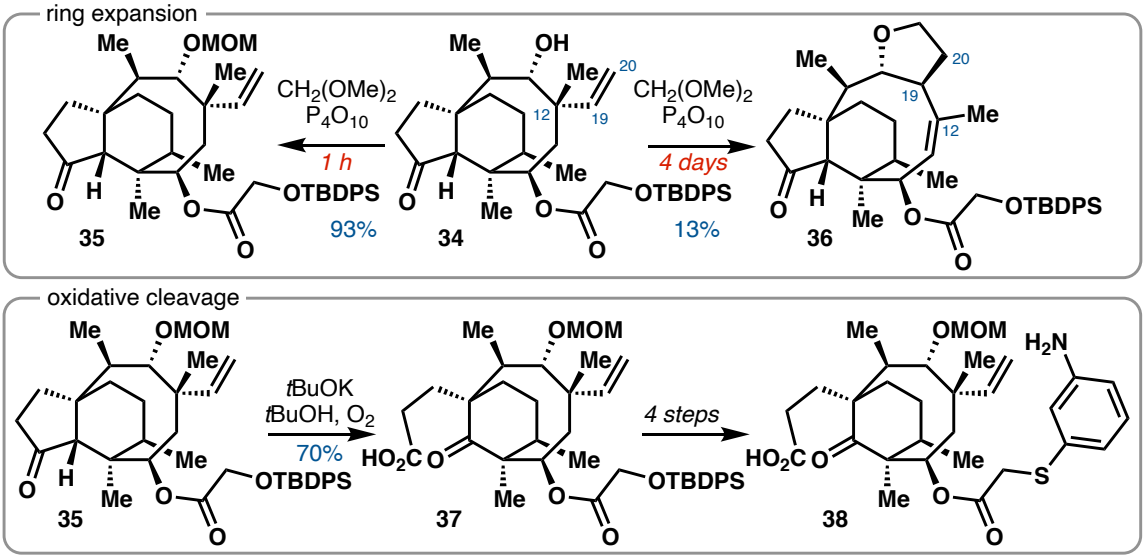

Scheme 6. Ring expansion and oxidative cleavage reports from Springer.

Currently, the vast majority of pleuromutilin derivatives are synthesized through modification of the natural product itself, primarily at C14 and C22. As a result, access to more complex structural derivatives and alternatively functionalized tricyclic cores has remained a challenge that can only be addressed with *de novo* synthesis.

1.6 PREVIOUS SYNTHESES OF PLEUROMUTILIN

The development of *de novo* syntheses of (+)-pleuromutilin (**1**) has been the focus of intense effort by the synthetic community over the past four decades.[30,34–40] Because synthetic work in this area has been extensively reviewed by Procter and coworkers in 2014,[21] this section is focused on completed total syntheses. Thus far, there have been five completed syntheses of (+)-pleuromutilin (**1**), each utilizing distinct strategies in construction of the eight-membered ring.[21,32,41–44]

1.6.1 *Gibbons' Total Synthesis of (±)-Pleuromutilin*

Gibbons' strategy commences with construction of tricyclic intermediate **41** by a double Michael addition of cyclohexenone **39** to cyclopentene **40** (Scheme 7). Elaboration of **41** through an eleven-step procedure affords key tetracyclic intermediate **42**. The initial ring expansion reaction was envisioned to proceed through a retro-aldol fragmentation; however, those efforts were unsuccessful. Ultimately, this transformation was accomplished through a bromination-induced Grob fragmentation to construct the central eight-membered ring (**43**).

In five steps, diketone **44** was reduced to the correct oxidation states present in the natural product (**1**) and MOM protection of the C14 hydroxyl, followed by ozonolysis of the C12 exocyclic olefin afforded ketone **45**. At this stage, elaboration of the ketone to the C12 quaternary center was investigated. Gibbons reported that carbanion formation at C12 resulted in elimination of the C11 hydroxyl group, and methods that relied on a carbocation at C12 also proved unsuccessful. Alternatively, a four-step route from ketone **45** to the C12-functionalized tricycle **47** was developed. Enal formation, followed by reduction afforded allylic alcohol **46**, which upon γ-alkylation with Murahashi's conditions[45] afforded **47**. Benzyl deprotection of **47**, oxidation, and MOM cleavage completed the first racemic total synthesis of mutilin (**2**), which was converted to pleuromutilin (**1**) through *bis*-glycolic ester formation and hydrolysis.

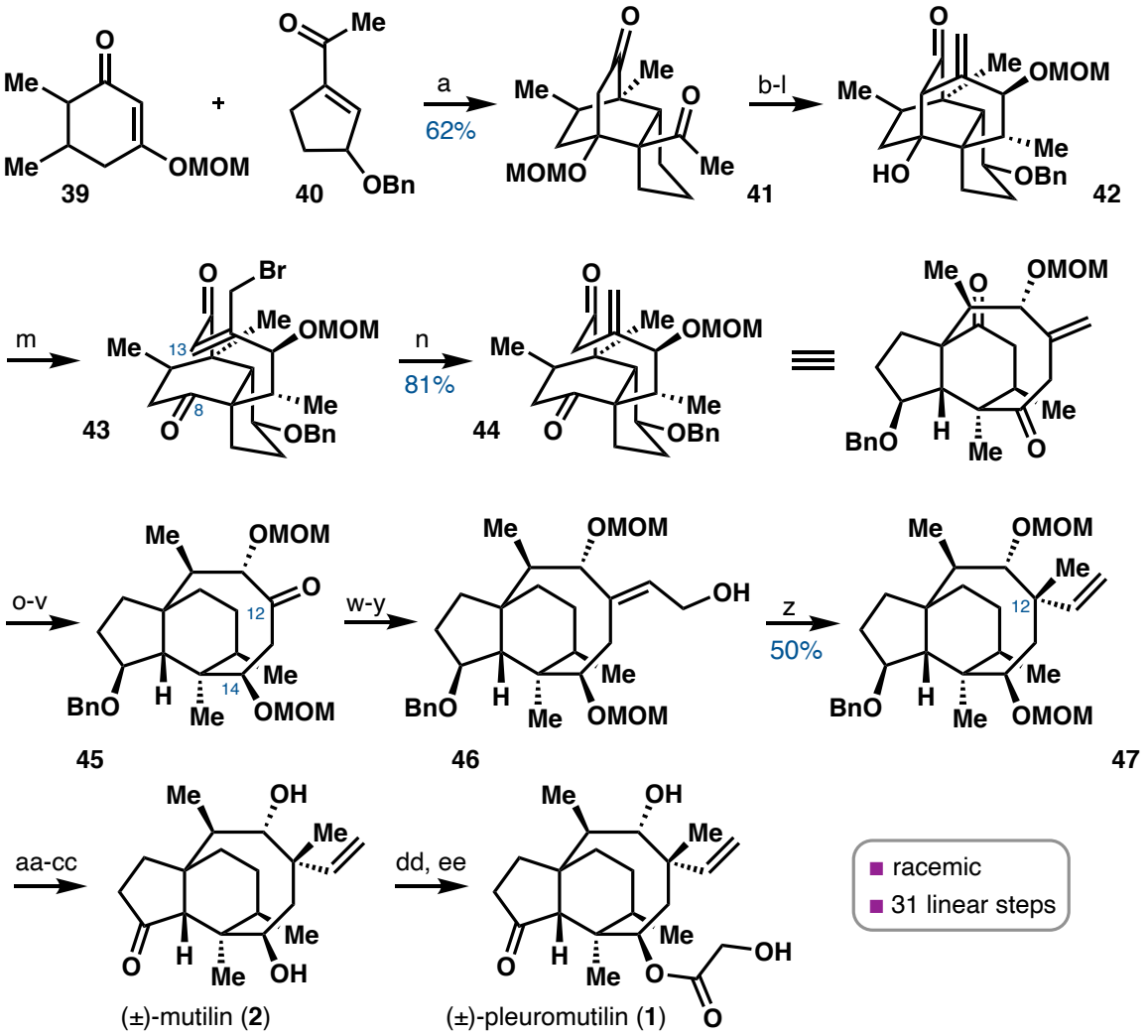

Reagents and conditions: a) LDA, 62%; **b)** CH_2CHLi, 67%; **c)** PCC, 79%; **d)** MeLi, 88%; **e)** MnO_2, 88%; **f)** H_2, 10% Pd/Al_2O_3, MgO, 61%; **g)** K_2CO_3, 92%; **h)** $POCl_3$, DMAP, py; **i)** TFA, 80% (2 steps); **j)** *t*BuOOH, $VO(acac)_2$, 97%; **k)** *t*BuOK, *t*BuOH; **l)** KH, MOMCl, 71% (2 steps); **m)** *N*-bromoacetamide, NaOAc; **n)** Zn, AcOH, 81% (2 steps); **o)** DIBAL; **p)** MsCl, py; **q)** $LiAlH_4$, 68% (3 steps); **r)** PCC; **s)** Na, Na/Hg, 88% (2 steps); **t)** MOMBr, *i*Pr_2NEt; **u)** O_3; **v)** $P(OMe)_3$, 95% (3 steps); **w)** (*Z*)-[2-ethoxyvinyl]lithium; **x)** H_2SO_4, 50% (2 steps); **y)** DIBAL, 95%; **z)** CuI, MeLi, $[Bu_3PN(Me)Ph]^+I^-$, 50%; **aa)** Li, NH_3; **bb)** PCC; **cc)** HCl, 80% (3 steps); **dd)** $AcOCH_2COOH$, MsCl, DMAP, py; **ee)** KOH, MeOH.

Scheme 7. Gibbons' total synthesis of (±)-pleuromutilin (**1**).

1.6.2 *Boeckman's Total Synthesis of (±)-Pleuromutilin*

Boeckman's synthetic route[42] towards pleuromutilin (**1**) involved early construction of the tricyclic framework devoid of functionalities with the intention of installing them at a later stage (Scheme 8). The strategic design was guided by two

hypotheses that were based on MM2 calculations: 1) all substituents on the eight-membered rings resided in equatorial-like environments in the most stable conformation. 2) The few accessible conformations available to the eight-membered ring by the bicyclic ring fusion greatly reduce the conformational complexity to only two unique low-energy conformations.

First efforts were focused on construction of vinyl carbinol **52** for investigation of the key anion oxy-Cope that would afford tricycle **53** (Scheme 8). Two-step Robinson annulation of cyclohexenone **48** and pentanone **49**, followed by deprotection and tosylation afforded dienone tosylate **50**. This intermediate was now primed for their key conjugate addition–alkylation sequence to install the C6 methyl substituent. Methyl cuprate addition resulted in complete axial selectivity, delivering methylated bicycle **51**; however, vinyl addition resulted in a 1:1 mixture of diastereomers. Resubjection of the undesired diastereomer could be performed to obtain a 70% overall yield of rearrangement precursor **52** after two cycles of equilibration. Key anionic oxy-Cope rearrangement proceeded smoothly to afford tricycle **53**.

Following construction of the carbon skeleton, investigations toward installing the functionalities on the eight-membered ring commenced. Formation of functionalized tricycle **54** occurred through a four-step procedure that involved epoxidation and rearrangement at C3, selective ketalization, C3 ketone reduction, and benzyl protection. Subsequent treatment with $Py^{+}HBr_3^{-}$ forged the equatorial bromo-ketal and *syn*-elimination delivered *E*-alkene **55**. Hydration to install the C14 hydroxyl, ketal hydrolysis, and MOM protection afforded methoxymethyl ether **56**. Initial attempts at installing the C11 hydroxyl were focused on selective silyl enol ether formation; however this strategy

always resulted in mixtures that led to a mixture of silyloxy products upon oxidation. Fortunately, Rubottom-type oxidation selectively installed the C11 hydroxyl as a single epimer, and MOM protection afforded Gibbons' intermediate **57** (*vide supra*, Scheme 7).

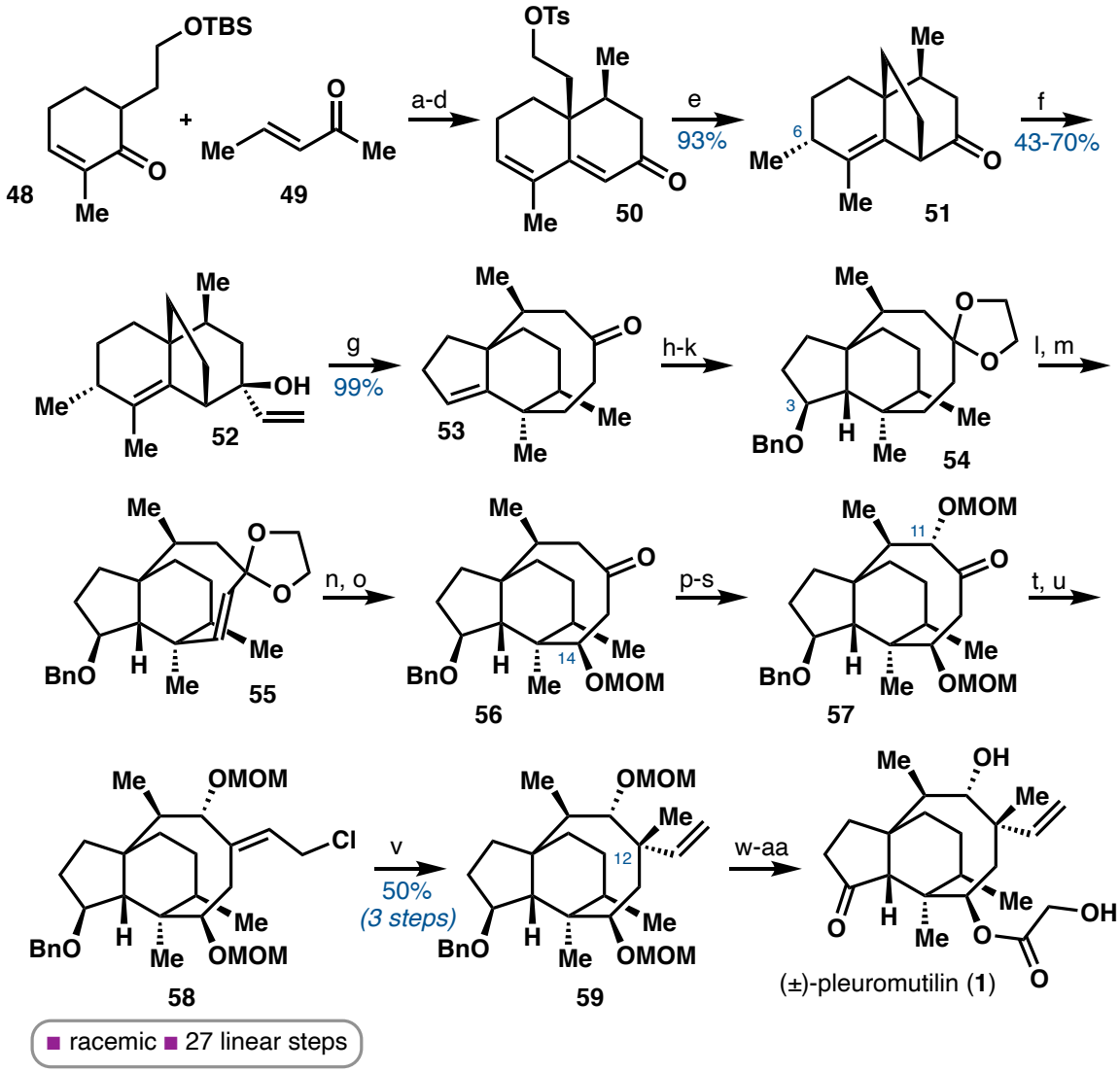

Reagents and conditions: a) LDA, 61%; **b**) pyrrolidine; AcOH, NaOH, 98%; **c)** AcOH; **d)** *p*TsCl, DMAP, py, 74% (2 steps); **e)** $(Me)_2CuLi$, HMPA, 93%; **f)** $CH_2CHMgBr$, 43%, minor epimer recycled, PhSCl, MeOH, $P(OEt)_3$, 70% after 2 cycles); **g)** KH, 18-crown-6, 99%; **h)** *m*CPBA; **i)** $BF_3{\cdot}OEt_2$ $(CH_2OH)_2$, 89% (2 steps); **j)** Li, NH_3; **k)** KH, BnBr, 69% (2 steps); **l)** $pyH^+Br_3^-$; **m)** *t*BuOK, DMSO, 67% (2 steps); **n)** *p*TsOH, H_2O, 67%; **o)** MOMCl, *i*Pr_2NEt; **p)** TMSI, HMDS; **q)** *m*CPBA, $NaHCO_3$; **r)** TBAF, 62% (4 steps); **s)** MOMCl, *i*Pr_2NEt, 90%; **t)** $CH_2CHMgBr$; **u)** $SOCl_2$; **v)** $MeCuB(Me)_3$, 50% (3 steps); **w)** Li, NH_3; **x)** PCC; **y)** HCl/EtOH, 80% (3 steps); **z)** $AcOCH_2COOMs$, DMAP; **aa)** KOH, MeOH, 39% (2 steps).

Scheme 8. Boeckman's total synthesis of (±)-pleuromutilin (**1**).

At this stage, attention was turned towards installing the C12 quaternary center. Using a strategy similar to Gibbons', vinyl addition followed by treatment of the resulting mixture of allylic alcohols with thionyl chloride and triethylamine furnished allylic chloride **58** (Scheme 8). S_N2' methyl addition afforded the C12 quaternary center as a 5:1 mixture of diastereomers, favoring the correct stereochemistry, intercepting Gibbons' intermediate **59**. Despite constructing differentially protected analogues of **59**, Boeckman ultimately found Gibbons' final steps to be the most concise, and therefore both syntheses were completed in the same manner.

1.6.3 *Procter's Total Synthesis of (+)-Pleuromutilin*

Similar to the previous two syntheses discussed, Procter's strategy towards pleuromutilin centers on early construction of the tricyclic core and late stage functionalization of the eight-membered ring. At the heart of their approach is a SmI_2-mediated cyclization cascade to construct the tricyclic core in a single step, forming both the five- and eight-membered rings and four stereocenters. Their synthesis also features the first efficient conversion of mutilin (**2**) to pleuromutilin (**1**) in 75% yield over two steps, whereas prior unselective methods gave 39% yield.

Construction of the SmI_2-cyclization precursor commenced with synthesis of dialdehyde **64** through a nine-step protocol from (+)-*trans*-dihydrocarvone (**60**), Scheme 9).[46–48] Oxidative fragmentation of the isopropenyl unit, conjugate addition, and Saegusa–Ito oxidation[49] afforded enone **61**. Conjugate addition with silylisopropenyl nucleophile installed the C9 quaternary center and proceeded to give an inseparable 2.5:1 mixture of diastereomers; subsequent trapping with Comin's reagent forged the vinyl triflate.

Palladium-catalyzed methoxycarbonylation then furnished the α,β-unsaturated ester **62** that is critical for their cascade. Cyclization precursor **64** was formed through Hosomi–Sakurai allylation of allyl silane **62** and the corresponding aldehyde to afford homo-allylic alcohol **63**. Subsequent pivalate protection, bis-desilylation, and bis-oxidation then set the stage for the key SmI_2-mediated cyclization cascade.

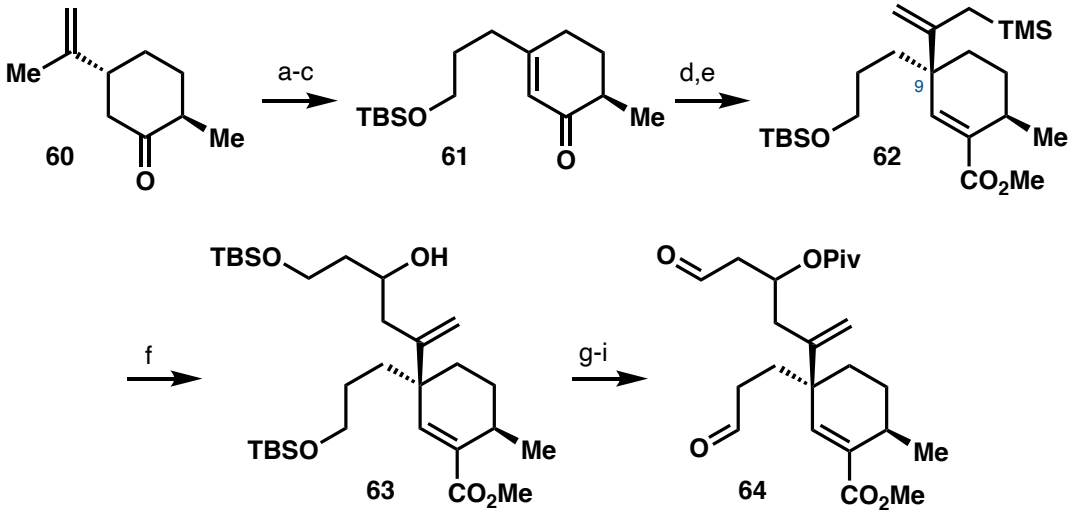

Reagents and conditions: a) O_3, MeOH, *then* $FeSO4{\cdot}7H_2O$, $CuOAc_2$, 57%; **b)** $TBSO(CH_2)_3MgBr$, $CuCN{\cdot}2LiCl$, THF, –45 ºC, 20 min; TMSCl, 10 min, 23 ºC; **c)** $Pd(OAc)_2$ (10 mol %), DMSO, O_2, 3 days, 85% (2 steps), 95% *ee* by HPLC; **d)** CuI, $TMSCH_2C(MgBr)CH_2$, THF, –78 ºC to 0 ºC, 10 min; **61**, –78 ºC, 1.5 h, Comins' reagent, –78 ºC to 23 ºC, 60 h, 85%, 2.5:1 dr; **e)** $Pd(OAc)_2$, PPh_3, Et_3N, MeOH, DMF, CO, 40 ºC, 24 h, 85%, 2.5:1 dr; **f)** $TBSOO(CH_2)_2CHO$, $BF_3{\cdot}OEt_2$, TBAT, 4 Å MS, –78 ºC, 18 h, –20 ºC, 4 h, 73%, 2.5:2.5:1:1 dr; **g)** PivCl, Py., DMAP, CH_2Cl_2, 18 h; **h)** HF, Pt. MeCN, 0 ºC to 23 ºC, 16h; **i)** DMP, CH_2Cl_2, 3 h, 88% (3 steps).

Scheme 9. Procter's synthesis of SmI_2-mediated cyclization cascade precursor **64**.

Dialdehyde **64** underwent smooth cascade cyclization to give **65** upon treatment with 2.5 equiv SmI_2 (Scheme 10). Procter proposed that the cascade commences with single-electron ketone reduction to form radical anion **66**. A 5-*exo*-trig cyclization[50] then forges the C3–C4 bond and selectively forms the (*Z*)-Sm^{III}-enolate **67**[51] due to Sm^{III} chelation of the radical anion with the ester carbonyl. The stereochemistry is consistent with the 8-membered ring formation by a chelation-controlled aldol cyclization through

transition state **68**. It is proposed that the high diastereocontrol was achieved due to pre-coordination of samarium to the carbonyl group and unsaturated ester.[52]

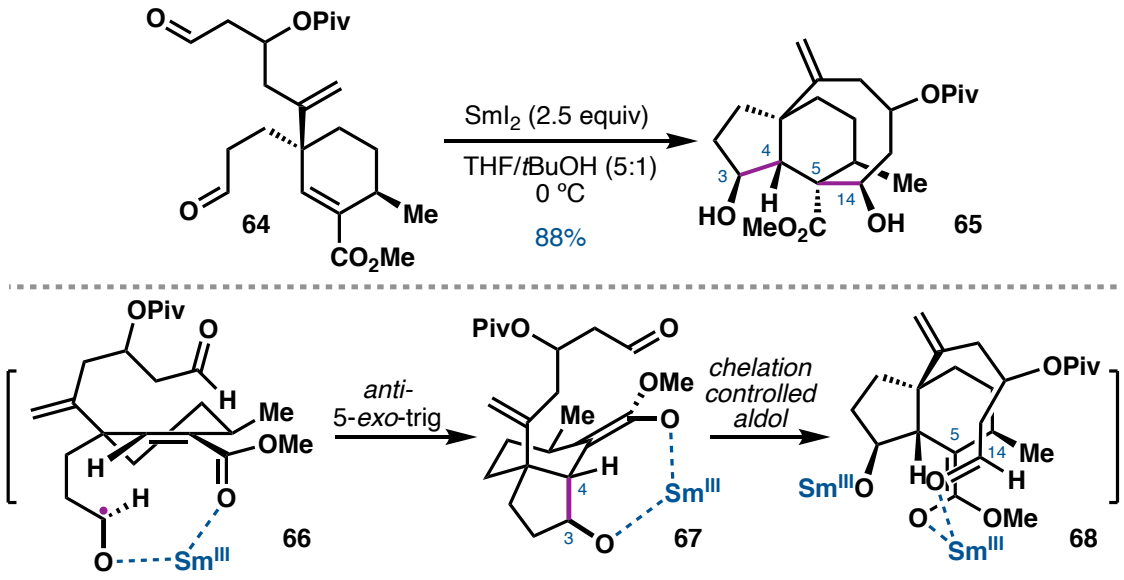

Scheme 10. Procter's key SmI_2-mediated cyclization cascade.

After validation of the key SmI_2-mediated cyclization cascade, bis-silylation, pivalate deprotection, and oxidation of the C12 hydroxyl gave a separable 2.5:1 mixture of diastereomers (**69**) that arose from conjugate addition to forge C9 (*vide supra*, Scheme 9). Subsequent Pd-catalyzed hydrogenation of alkene **70** furnished a separable 3:1 diastereomeric mixture at C10. The next key challenge of their synthesis involved reduction of the methyl ester to the C5 methyl substituent present in pleuromutilin. Initial attempts at reduction involved treatment with lithium aluminum hydride that ultimately led to an additional five steps of protecting group manipulations and reduction to access diol **71**. However, improved efforts later shortened the sequence to two steps through ketal protection with concomitant C3 desilylation, followed by methyl ester reduction with conditions utilizing SmI_2.[53–55] Final reduction of the primary hydroxyl to the desired methyl oxidation state (**72**) was accomplished in three steps: 1) protection of the C3-hydroxyl with

p-methyl benzoate (MBz), 2) conversion of the primary hydroxyl to the thioimidazolide, and 3) deoxygenation under radical conditions.

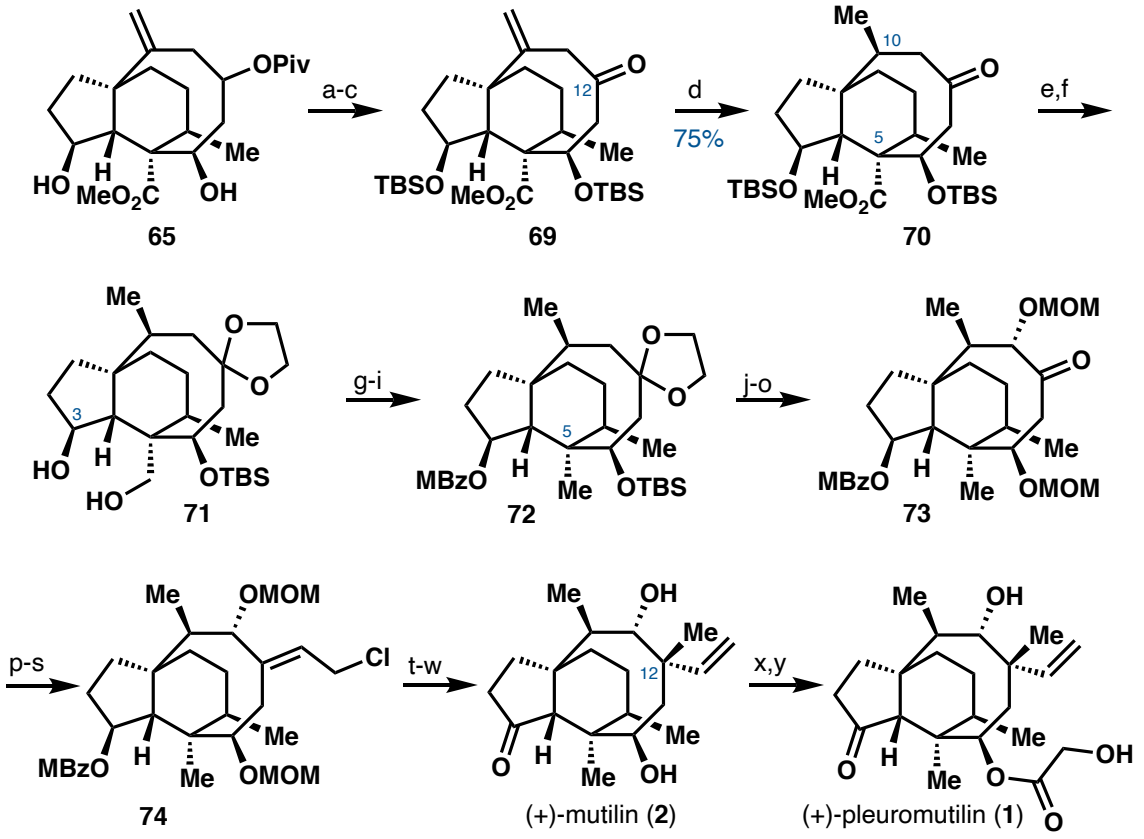

Reagents and conditions: a) Et_3N, TBSOTf, CH_2Cl_2, 0 ºC, 5 min, 23 ºC, 30 min, 76%; **b)** $LiAlH_4$, Et_2O, 30 min; **c)** DMP, CH_2Cl_2, 16 h, 63% (2 steps); **d)** H_2, 10 % Pd/C, EtOH, 12 h, 3:1 dr, 75%; **e)** 1,2-ethanediol, $HC(OCH_3)_3$, Amberlyst® 15, PhMe, MeCN, 23 ºC, 40 h, 96%; **f)** SmI_2, pyrrolidine, H_2O, THF, 23 ºC, 18 h, 95%; **g)** LDA, –78 ºC, 30 min; MBzCl, THF, –78 ºC, 30 min, 97%; **h)** TCDI, THF, 60 ºC, 5 days; **i)** nBu$_3$SnH, AIBN, PhMe, 80 ºC, 4 h, 66% (2 steps); **j)** $FeCl_3$·SiO_2, acetone, 23 ºC, 24 h, 99%; **k)** HMDS, TMSI, CH_2Cl_2, –20 ºC to 10 ºC, 3 h; **l)** $NaHCO_3$, *m*CPBA, CH_2Cl_2, 0 ºC, 10 min; **m)** TBAF, THF, 23 ºC, 3 min, 94%; **n**) $HF_{(aq)}$, MeCN, 23 ºC, 18 h, 78%; **o)** MOMCl, DIPEA (3 additions), CH_2Cl_2, 23 ºC, 2 days, 75%; **p)** EtOCHCHSnBu$_3$, nBuLi, THF, –78 ºC, 1 h, **73**, THF, –78 ºC, 15 min; **q)** $FeCl_3$·SiO_2, acetone, 23 ºC, 5 min; **r)** $NaBH_4$, THF/H_2O, 23 ºC, 30 min, 63% (3 steps); **s)** NCS, DMS, CH_2Cl_2, 0 ºC, 10 min, –20 ºC to 23 ºC, 16 h, 97%; **t)** CuCN, DMF, 23 ºC, 30 min, Me_2Zn, –20 ºC, 24 h, 71%; **u)** $LiAlH_4$, THF, 23 ºC, 90 min; **v)** DMP, CH_2Cl_2, 23 ºC, 1 h; **w)** AcCl, EtOH, 23 ºC, 3 h, 69% (3 steps); **x)** trifluoroacetylimidazole, EtOAc, –45 ºC, 30 min; **y)** 2-(2,2,2-trifluoroacetoxy)acetic acid, EDCI, DMAP, CH_2Cl_2, 23 ºC, 30 min; MeOH, Et_3N, 24 h, 75% (2 steps).

Scheme 11. Procter's completion of (+)-pleuromutilin (**1**).

Now that the final oxidation state of the C5 methyl substituent was installed, attention was turned towards functionalizing the eight-membered ring. Ketal deprotection

revealed the C12 ketone and use of Boeckman's procedure for selective α-hydroxylation (*vide supra*, Scheme 8) followed by desilylation and MOM protection furnished ketone intermediate **73**. Building off the work of Gibbons and Boeckman, conversion of the C12 ketone to the desired quaternary center was accomplished through a similar sequence. Ketone **73** was treated with a lithiated enol ether. The addition product was hydrolyzed and the intermediate enal was reduced and subjected to Corey-Kim chlorination[56] conditions to give allylic chloride **74**. S_N2' displacement of the chloride with Me_2Zn and CuCN in DMF afforded a single diastereomer at C12. Thus, benzoate deprotection, Dess-Martin oxidation, and MOM cleavage furnished (+)-mutilin (**2**) in 69% overall yield.

After identifying that existing methods for the conversion of mutilin to pleuromutilin suffered from poor yields and selectivity, Procter and coworkers turned towards methods developed in industry[57] for the conversion of mutilin to C14 analogues of pleuromutilin. Protection of (+)-mutilin (**2**) as the C10 trifluoroacetate, followed by coupling with 2-(2,2,2-trifluoroacetoxy) acetic acid and subsequent deprotection furnished (+)-pleuromutilin (**1**) in 75% overall yield, concluding the first enantiospecific total synthesis of **1**.

1.6.4 *Herzon's Total Synthesis of (+)-Pleuromutilin*

Herzon and coworkers developed a modular route to access (+)-pleuromutilin (**1**) and its stereochemical derivatives, specifically at C11 and C12. Proceeding through the intermediates that are epimeric at C12, their synthesis was made possible through known diastereomer equilibration conditions developed by Berner and coworkers in 1986 (*vide supra*, Scheme 4).

The Herzon synthesis commences with a Cu-catalyzed enantioselective conjugate addition-acylation reaction into cyclohexenone **75**, followed by methylation that proceeds in high enantio- and diastereoselectivity, respectively, to afford β-keto ester **76** (Scheme 12).[58] Deprotonation and trapping of the resultant enolate with *N*-phenyltriflimide furnished vinyl triflate **77**, which was then converted to dienone **78** via a Pd-catalyzed carbonylative coupling.[59] Cu-catalyzed Nazarov cyclization delivered hydrindanone **79** as a single olefin isomer. A Nagata hydrocyanation[60] was next performed on hydrindanone **79** to afford the C9 addition product in 3:1 dr; however, because this reaction forged the undesired *trans*-ring junction, subsequent epimerization with sodium hydroxide was necessary to access **80**. Ketal protection of ketone **80** provided **81**.

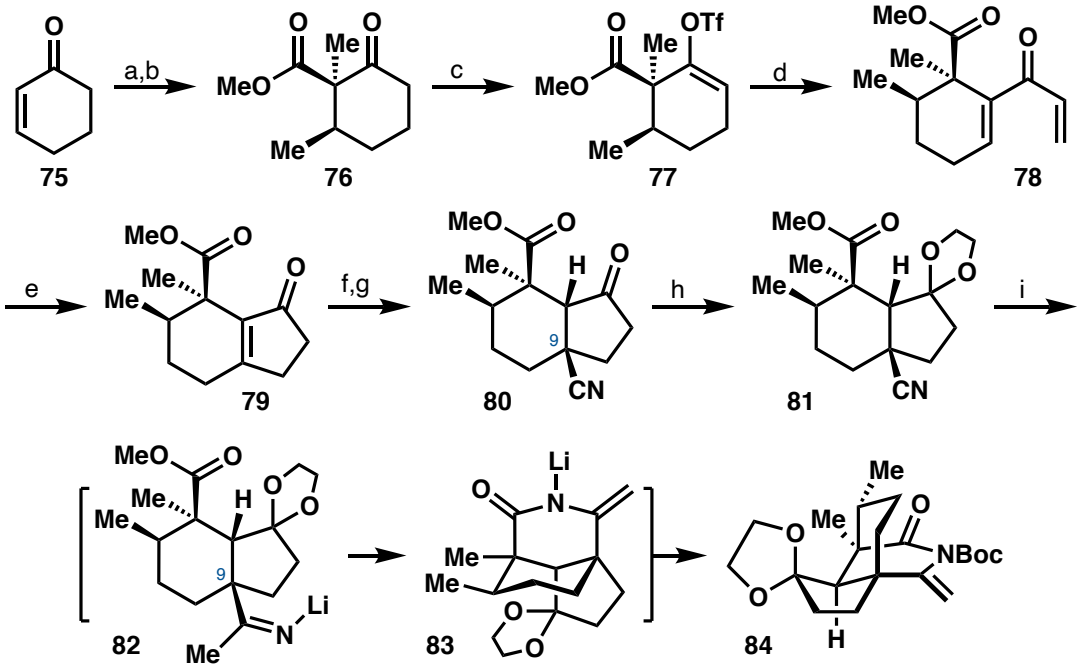

Reagents and conditions: a) $Zn(Me)_3$, $Cu(OTf)_2$ (0.5 mol %), ligand (1.0 mol %), PhMe, 0 °C, *then* MeLi, –78 °C, *then* methylcyanoformate, –78 °C; **b)** MeI, NaO*t*Bu, MeOH, 0 °C, 71%; **c)** KHMDS, $PhNTf_2$, THF, –78 °C, 88%; **d)** CO, tetravinyltin, LiCl, $Pd(PPh_3)_4$ (5 mol %), DMF, 40 °C **e)** $Cu(OTf)_2$ (5 mol %), $(CH_2Cl)_2$, 70 °C; **f)** Et_2AlCN, THF, 0 °C, *then* DIBAL, –78 °C; **g)** 0.01 M NaOH, MeOH/H_2O (5:1), 0 °C, 65%; **h)** TMSOTf, $(TMSOCH_2)_2$, CH_2Cl_2, 30 °C; **i)** MeLi, PhMe, 0 °C, *then* Boc_2O, 0 °C, 80%.

Scheme 12. Synthesis of Herzon's key enimide intermediate **84**.

It was reported that selective functionalization of the C9 nitrile was challenging due to steric congestion; however, it was ultimately found that treatment with excess methyllithium, followed by di-*tert*-butyl dicarbonate, provided cyclic enimide **84**. This cascade is likely to occur through methyllithium addition to the nitrile, followed by intramolecular cyclization onto the C5 methyl ester and deprotonation to form intermediate **83**. Final *N*-acylation would forge their key enamide intermediate **84**, setting the stage for the key two-fold neopentyl fragment coupling.

In the key sequence to form the eight-membered ring, addition of the organolithium derived from iodoether **85** to enimide **84** resulted in addition at C14; *in situ* hydrolysis of the resulting lithioenamine provided methyl ketone **86** (Scheme 13). It was noted that electronic activation of the C14 carbonyl group and minimization of nearby nonbonded interactions via the cyclic enimide was critical for the success of the reaction.

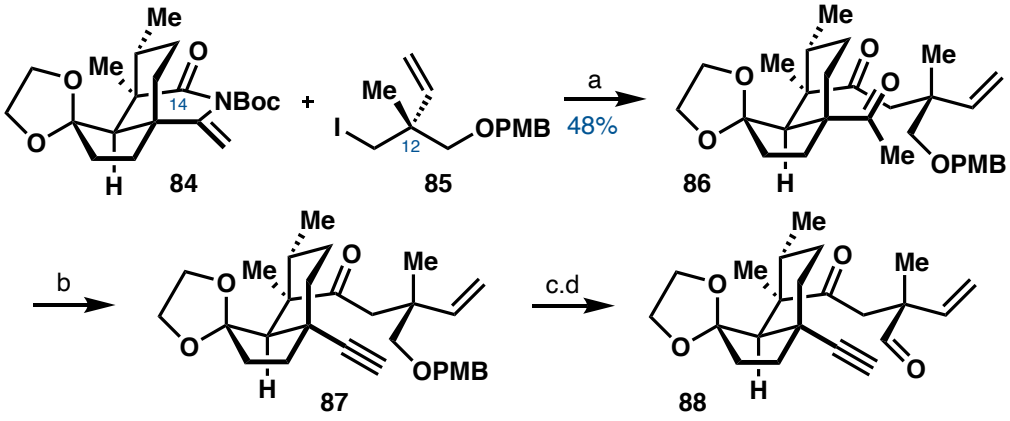

Reagents and conditions: a) *t*BuLi, **85**, Et_2O, –45 °C, *then* **84**, –45 °C, *then* HCl, THF, 0 °C, 48%; **b)** KHMDS, Comin's reagent, THF, –78 °C, 81%; **c)** DDQ, CH_2Cl_2, pH 7 buffer, 20 °C; **d)** DMP, CH_2Cl_2, 20 °C, 83% (2 steps)

Scheme 13. Herzon's synthesis of reductive cyclization precursor **88**.

Formal dehydration of methyl ketone **86** through base-induced elimination of a transiently-formed vinyl triflate provided alkyne **87**. Deprotection and Dess-Martin oxidation

furnished aldehyde **88**, setting the stage for an *exo*-selective reductive cyclization for the construction of the central eight-membered ring.

The authors envisioned that the limited number of rotatable bonds along the nascent macrocycle would lower the entropic penalty of ring closure while enhancing regio- and stereocontrol. Furthermore, it was proposed that the presence of the sp^2-hybridized carbon atoms at C10 and C14 of **88** would alleviate transannular nonbonding interactions in the eight-membered ring. Using a nickel-based catalyst, a single diastereomer of an allylic silyl ether was formed and desilylated to provide tricycle **89** in high diastereo- and regioselectivity (Scheme 14). Interestingly, their attempts to perform the Ni-catalyzed reductive cyclization on the substrate bearing the correct C12 stereochemistry resulted in tetracycle **91** formation. Thus, their strategy for accessing (+)-pleuromutilin (**1**) with the correct stereochemistry in place at C12 was thwarted, forcing them to proceed through the 12-*epi* cyclization substrate **89**.

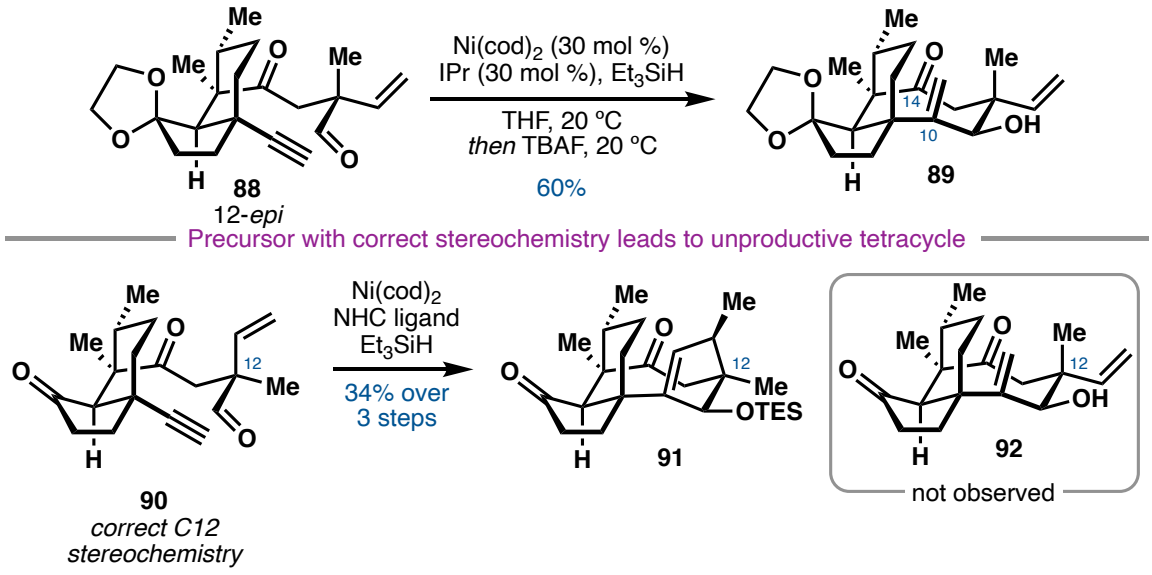

Scheme 14. Herzon's reductive cyclization reaction of **88** (12-*epi*).

Completion of their synthesis required five subsequent transformations. Dess-Martin oxidation of the C11 alcohol to the enone and conjugate reduction with SmI_2 afforded the C10 methyl with complete site- and stereoselectivity. (+)-12-*epi*-mutilin (**94**) and (+)-11,12-di-*epi*-mutilin (**95**) were then formed as a thermodynamic 3:1 mixture of diastereomers upon single-electron reduction with excess sodium; the two mutilin diastereomers were brought forward to form several stereochemical pleuromutilin derivatives (Scheme 15).

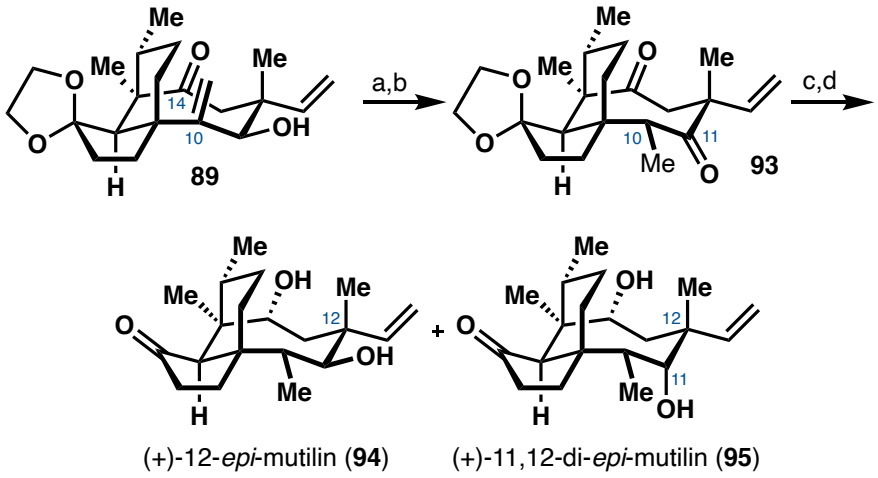

Reagents and conditions: a) DMP, CH_2Cl_2, 20 °C; **b)** SmI_2, THF, MeOH, 20 °C, 98% (2 steps); **c)** Na, EtOH, 20 °C, *then* HCl, H_2O, MeOH, THF, 20 °C, 52%; **d)** HCl, H_2O, MeOH, THF, 20 °C, 96% for **94**, 81% for **95**.

Scheme 15. Herzon's synthesis of (+)-12-*epi*-mutilin (**94**) and (+)-11,12-di-*epi*-mutilin (**95**).

Pressing forward, Herzon and coworkers found that the isolated mutilin diastereomers **94** and **95** could be elaborated to their respective pleuromutilin derivatives. It was also found that (+)-12-*epi*-mutilin (**94**) could be epimerized at C12 and advanced to (+)-pleuromutilin (**1**) through a three-step procedure (Scheme 16). Following Procter's protocol (*vide supra,* Scheme 11), trifluoroacetyl protection of C11 and *O*-acylation of C14 with trifluoroacetylglycolic acid, followed by *in situ* methanolysis of the trifluoroacetyl esters furnished (+)-12-*epi*-pleuromutilin (**94**). The same procedure was also applied to

(+)-11,12-di-*epi*-mutilin (**95**) for the synthesis of (+)-11,12-di-*epi*-pleuromutilin. Because (+)-12-*epi*-mutilin (**94**) is en route to (+)-pleuromutilin (**1**), their synthesis of the natural product was made possible by epimerization conditions developed by Berner and coworkers (*vide supra,* Scheme 4). Trifluoroacetyl protection of C11, followed by trityl-protected glycolic ester installation and methanolysis furnished trityl-protected (+)-12-*epi*-pleuromutilin derivative **97**, where treatment with zinc-mediated conditions to effect equilibration at C12 via a retro-allylation/allylation sequence afforded (+)-pleuromutilin (**1**) in 33% yield, with the major isomer formed being (+)-12-*epi*-pleuromutilin (**96**) in 56% yield. They were also able to synthesize (+)-11,12-di-*epi*-pleuromutilin through a similar reaction sequence.

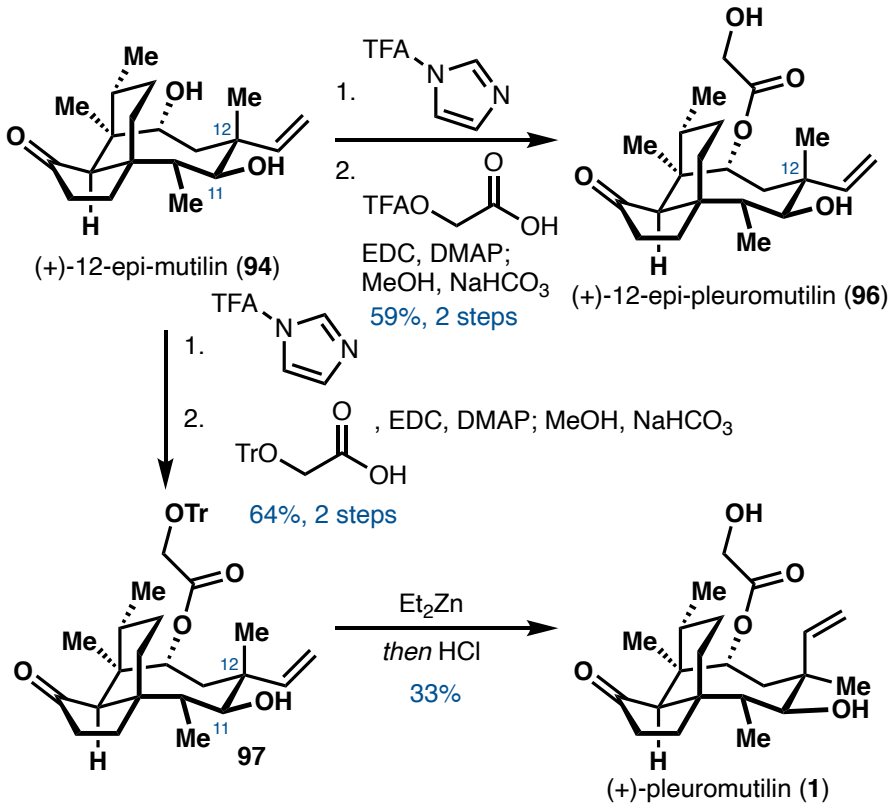

Scheme 16. Completing the synthesis of (+)-pleuromutilin (**1**).

1.7 CONCLUDING REMARKS

The mutilins are a class of antibiotics that bind to the peptidyl transferase center of the bacterial ribosome. To date, the C14 glycolic ester has served as the focal point of optimization of the antibacterial activity, with thousands of C14 analogs having been prepared through semisynthesis. However, evidence suggests that the tricyclic core has potential for further optimization. For example, epimerization of the C12 quaternary center, followed by functionalization of the primary olefin can provide extended spectrum antibiotics with activity against Gram-negative and drug-resistant pathogens.[61] Ultimately, these structural derivatives can only been accessed through development of a *de novo* synthesis of (+)-pleuromutilin. In the following chapter, we will discuss our development of a modular and enantiospecific route towards (+)-pleuromutilin (**1**) and (+)-12-*epi*-pleuromutilin.

1.8 NOTES AND REFERENCES

(1) Fleming, A. On the Antibacterial Action of Cultures of a Penicillium, with Special Reference to Their Use in the Isolation of B. Influenzæ. *Br. J. Exp. Pathol.* **1929**, *10* (3), 226–236.

(2) Williams, K. J. The Introduction of 'Chemotherapy' Using Arsphenamine – the First Magic Bullet: *J. R. Soc. Med.* **2009**.

(3) Aminov, R. I. A Brief History of the Antibiotic Era: Lessons Learned and Challenges for the Future. *Front. Microbiol.* **2010**, *1*.

(4) Kavanagh, F.; Hervey, A.; Robbins, W. J. Antibiotic Substances From Basidiomycetes: VIII. Pleurotus Multilus (Fr.) Sacc. and Pleurotus Passeckerianus Pilat. *Proc. Natl. Acad. Sci.* **1951**, *37* (9), 570–574.

(5) Kavanagh, F.; Hervey, A.; Robbins, W. J. Antibiotic Substances from Basidiomycetes: IX. Drosophila Subtarata. (Batsch Ex Fr.) Quel. *Proc. Natl. Acad. Sci.* **1952**, *38* (7), 555–560.

(6) Birch, A. J.; Holzapfel, C. W.; Rickards, R. W. The Structure and Some Aspects of the Biosynthesis of Pleuromutilin. *Tetrahedron* **1966**, *22*, 359–387.

(7) Arigoni, D. Some Studies in the Biosynthesis of Terpenes and Related Compounds. *Pure Appl. Chem.* **1968**, *17* (3–4), 331–348.

(8) Tsukagoshi, T.; Tokiwano, T.; Oikawa, H. Studies on the Later Stage of the Biosynthesis of Pleuromutilin. *Biosci. Biotechnol. Biochem.* **2007**, *71* (12), 3116–3121.

(9) Alberti, F.; Khairudin, K.; Venegas, E. R.; Davies, J. A.; Hayes, P. M.; Willis, C. L.; Bailey, A. M.; Foster, G. D. Heterologous Expression Reveals the Biosynthesis of the Antibiotic Pleuromutilin and Generates Bioactive Semi-Synthetic Derivatives. *Nat. Commun.* **2017**, *8* (1), 1–9.

(10) Dornhelm, P.; Högenauer, G. The Effects of Tiamulin, a Semisynthetic Pleuromutilin Derivative, on Bacterial Polypeptide Chain Initiation. *Eur. J. Biochem.* **1978**, *91* (2), 465–473.

(11) Högenauer, G. The Mode of Action of Pleuromutilin Derivatives. Location and Properties of the Pleuromutilin Binding Site on Escherichia Coli Ribosomes. *Eur. J. Biochem.* **1975**, *52* (1), 93–98.

(12) Hodgin, L. A.; Högenauer, G. The Mode of Action of Pleuromutilin Derivatives. *Eur. J. Biochem.* **1974**, *47* (3), 527–533.

(13) Cheney, B. V.; Miller, A. B. Structural Comparisons of Antibiotic Inhibitors of Peptidyl Transferase. *J. Mol. Struct. THEOCHEM* **1986**, *134* (3), 389–400.

(14) Högenauer, G.; Ruf, C. Ribosomal Binding Region for the Antibiotic Tiamulin: Stoichiometry, Subunit Location, and Affinity for Various Analogs. *Antimicrob. Agents Chemother.* **1981**, *19* (2), 260–265.

(15) Schlünzen, F.; Pyetan, E.; Fucini, P.; Yonath, A.; Harms, J. M. Inhibition of Peptide Bond Formation by Pleuromutilins: The Structure of the 50S Ribosomal Subunit from Deinococcus Radiodurans in Complex with Tiamulin. *Mol. Microbiol. 54* (5), 1287–1294.

(16) Poulsen, S. M.; Karlsson, M.; Johansson, L. B.; Vester, B. The Pleuromutilin Drugs Tiamulin and Valnemulin Bind to the RNA at the Peptidyl Transferase Centre on the Ribosome. *Mol. Microbiol.* **2001**, *41* (5), 1091–1099.

(17) Phillips, O. A.; Sharaf, L. H. Pleuromutilin Antibacterial Agents: Patent Review 2001 – 2006. *Expert Opin. Ther. Pat.* **2007**, *17* (4), 429–435.

(18) Aslam, B.; Wang, W.; Arshad, M. I.; Khurshid, M.; Muzammil, S.; Rasool, M. H.; Nisar, M. A.; Alvi, R. F.; Aslam, M. A.; Qamar, M. U.; et al. Antibiotic Resistance: A Rundown of a Global Crisis. *Infect. Drug Resist.* **2018**, *11*, 1645–1658.

(19) Tang, Y.-Z.; Chen, Y.-H. L. and J.-X. Pleuromutilin and its Derivatives-The Lead Compounds for Novel Antibiotics http://www.eurekaselect.com/89330/article (accessed Mar 1, 2020).

(20) Shang, R.; Wang, J.; Liang, W. G. and J. Efficient Antibacterial Agents: A Review of the Synthesis, Biological Evaluation and Mechanism of Pleuromutilin Derivatives http://www.eurekaselect.com/117585/article (accessed Mar 1, 2020).

(21) Fazakerley, N. J.; Procter, D. J. Synthesis and Synthetic Chemistry of Pleuromutilin. *Tetrahedron* **2014**, *70* (39), 6911–6930.

(22) Lolk, L.; Pøhlsgaard, J.; Jepsen, A. S.; Hansen, L. H.; Nielsen, H.; Steffansen, S. I.; Sparving, L.; Nielsen, A. B.; Vester, B.; Nielsen, P. A Click Chemistry Approach to Pleuromutilin Conjugates with Nucleosides or Acyclic Nucleoside Derivatives and Their Binding to the Bacterial Ribosome. *J. Med. Chem.* **2008**, *51* (16), 4957–4967.

(23) Dreier, I.; Kumar, S.; Søndergaard, H.; Rasmussen, M. L.; Hansen, L. H.; List, N. H.; Kongsted, J.; Vester, B.; Nielsen, P. A Click Chemistry Approach to Pleuromutilin Derivatives, Part 2: Conjugates with Acyclic Nucleosides and Their Ribosomal Binding and Antibacterial Activity. *J. Med. Chem.* **2012**, *55* (5), 2067–2077.

(24) Berner, H.; Schulz, G.; Schneider, H. Synthese ab-trans-anellierter derivate des tricyclischen diterpens pleuromutilin durch intramolekulare 1,5-hydrid-verschiebung. *Tetrahedron* **1980**, *36* (12), 1807–1811.

(25) Brooks, G.; Burgess, W.; Colthurst, D.; Hinks, J. D.; Hunt, E.; Pearson, M. J.; Shea, B.; Takle, A. K.; Wilson, J. M.; Woodnutt, G. Pleuromutilins. Part 1. The Identification of Novel Mutilin 14-Carbamates. *Bioorg. Med. Chem.* **2001**, *9* (5), 1221–1231.

(26) Fu, L.; Liu, X.; Ling, C.; Cheng, J.; Guo, X.; He, H.; Ding, S.; Yang, Y. Design, Synthesis, and Structure–Activity Relationship Studies of Conformationally Restricted Mutilin 14-Carbamates. *Bioorg. Med. Chem. Lett.* **2012**, *22* (2), 814–819.

(27) Springer, D. M.; Goodrich, J. T.; Huang, S. A Novel Ring Expansion of the Pleuromutilin Skeleton. *Tetrahedron Lett.* **2002**, *43* (27), 4857–4860.

(28) Springer, D. M.; Bunker, A.; Luh, B.-Y.; Sorenson, M. E.; Goodrich, J. T.; Bronson, J. J.; DenBleyker, K.; Dougherty, T. J.; Fung-Tomc, J. Cyclopentanone Ring-Cleaved Pleuromutilin Derivatives. *Eur. J. Med. Chem.* **2007**, *42* (1), 109–113.

(29) Berner, H.; Vyplel, H.; Schulz, G.; Stuchlik, P. Chemie Der Pleuromutiline—IV: Synthese Des 14-O-Acetyl-8α-Hydroxy-Mutilins. *Tetrahedron* **1983**, *39* (8), 1317–1321.

(30) Lotesta, S. D.; Liu, J.; Yates, E. V.; Krieger, I.; Sacchettini, J. C.; Freundlich, J. S.; Sorensen, E. J. Expanding the Pleuromutilin Class of Antibiotics by de Novo Chemical Synthesis. *Chem. Sci.* **2011**, *2* (7), 1258.

(31) Berner, H.; Vyplel, H.; Schulz, G.; Schneider, H. Chemie der Pleuromutiline, 11. Mitt.: Konfigurationsumkehr der Vinylgruppe am Kohlenstoff 12 durch reversible Retro-En-Spaltung. *Monatshefte F□r Chem. Chem. Mon.* **1986**, *117* (8–9), 1073–1080.

(32) Murphy, S. K.; Zeng, M.; Herzon, S. B. A Modular and Enantioselective Synthesis of the Pleuromutilin Antibiotics. *Science* **2017**, *356* (6341), 956–959.

(33) Choudary, B.; Giles, R. G.; Jovic, F.; Lewis, N.; Moore, S.; Urquhart, M. Synthesis of the Pleuromutilin Antibiotic SB-268091: A New Practical and Efficient Synthesis of Quinuclidine-4-Thiol. *Org. Process Res. Dev.* **2012**, *16* (12), 1927–1939.

(34) Kahn, M. Anionic Oxy-Cope Reaction of a Divinyl Cyclobutanol, Pleuromutilin Model Study. *Tetrahedron Lett.* **1980**, *21* (47), 4547–4548.

(35) Paquette, L. A.; Pansegrau, P. D.; Wiedeman, P. E.; Springer, J. P. (+)-Pleuromutilin Synthetic Studies. Examples of Intramolecular Hydrogen Abstraction by the .Beta.-Carbon of a 2-Cyclopentenone Subunit with Resultant .Alpha.-Coupling. *J. Org. Chem.* **1988**, *53* (7), 1461–1466.

(36) Paquette, L. A.; Bulman-Page, P. C.; Pansegrau, P. D.; Wiedeman, P. E. (+)-Pleuromutilin Synthetic Studies. Direct Degradation to and Independent Preparation of an Advanced Diketone Intermediate. Demonstration That Reconstruction of the Eight-Membered Ring Suffers from Serious Kinetic Retardation. *J. Org. Chem.* **1988**, *53* (7), 1450–1460.

(37) Paquette, L. A.; Wiedeman, P. E.; Bulman-Page, P. C. (+)-Pleuromutilin Synthetic Studies. Degradative and de Novo Acquisition of a Levorotatory Tricyclic Lactone Subunit. *J. Org. Chem.* **1988**, *53* (7), 1441–1450.

(38) Bacqué, E.; Pautrat, F.; Zard, S. Z. A Flexible Strategy for the Divergent Modification of Pleuromutilin. *Chem. Commun.* **2002**, No. 20, 2312–2313.

(39) Findley, T. J. K.; Sucunza, D.; Miller, L. C.; Helm, M. D.; Helliwell, M.; Davies, D. T.; Procter, D. J. A Stereoselective, Sm(II)-Mediated Approach to Decorated Cis-Hydrindanes: Synthetic Studies on Faurinone and Pleuromutilin. *Org. Biomol. Chem.* **2011**, *9* (7), 2433–2451.

(40) Liu, J.; Lotesta, S. D.; Sorensen, E. J. A Concise Synthesis of the Molecular Framework of Pleuromutilin. *Chem. Commun.* **2011**, *47* (5), 1500–1502.

(41) Gibbons, E. G. Total Synthesis of (.+-.)-Pleuromutilin. *J. Am. Chem. Soc.* **1982**, *104* (6), 1767–1769.

(42) Boeckman, R. K.; Springer, D. M.; Alessi, T. R. Synthetic Studies Directed toward Naturally Occurring Cyclooctanoids. 2. A Stereocontrolled Assembly of (.+-.)-Pleuromutilin via a Remarkable Sterically Demanding Oxy-Cope Rearrangement. *J. Am. Chem. Soc.* **1989**, *111* (21), 8284–8286.

(43) Fazakerley, N. J.; Helm, M. D.; Procter, D. J. Total Synthesis of (+)-Pleuromutilin. *Chem. – Eur. J. 19* (21), 6718–6723.

(44) Zeng, M.; Murphy, S. K.; Herzon, S. B. Development of a Modular Synthetic Route to (+)-Pleuromutilin, (+)-12-Epi-Mutilins, and Related Structures. *J. Am. Chem. Soc.* **2017**, *139* (45), 16377–16388.

(45) Tanigawa, Y.; Ohta, H.; Sonoda, A.; Murahashi, S. Regio- and Stereoselective .Gamma. Substitution of Allylic Alcohols with Alkyllithium Compounds by Using N,N-Methylphenylaminotributylphosphonium Iodide. Anti Stereochemistry of SN2' Reaction. *J. Am. Chem. Soc.* **1978**, *100* (14), 4610–4612.

(46) Schreiber, S. L. Fragmentation Reactions of .Alpha.-Alkoxy Hydroperoxides and Application to the Synthesis of the Macrolide (.+-.)-Recifeiolide. *J. Am. Chem. Soc.* **1980**, *102* (19), 6163–6165.

(47) Solladie, G.; Hutt, J. Total Synthesis of Dihydrovitamin DHV3 and Dihydrotachysterol DHT3. Application of the Low-Valent Titanium Induced Reductive Elimination. *J. Org. Chem.* **1987**, *52* (16), 3560–3566.

(48) White, J. D.; Grether, U. M.; Lee, C.-S. (R)-(+)-3,4-DIMETHYLCYCLOHEX-2-EN-1-ONE. *Org. Synth.* **2005**, *82*, 108.

(49) Ito, Y.; Hirao, T.; Saegusa, T. Synthesis of .Alpha.,.Beta.-Unsaturated Carbonyl Compounds by Palladium(II)-Catalyzed Dehydrosilylation of Silyl Enol Ethers. *J. Org. Chem.* **1978**, *43* (5), 1011–1013.

(50) Beckwith, A. L. J. Regio-Selectivity and Stereo-Selectivity in Radical Reactions. *Tetrahedron* **1981**, *37* (18), 3073–3100.

(51) Rudkin, I. M.; Miller, L. C.; Procter, D. J. Samarium Enolates and Their Application in Organic Synthesis. In *Organometallic Chemistry*; 2008; pp 19–45.

(52) Johnston, D.; Couché, E.; Edmonds, D. J.; Muir, K. W.; Procter, D. J. The First Synthetic Studies on Pestalotiopsin A. A Stereocontrolled Approach to the Functionalised Bicyclic Core. *Org. Biomol. Chem.* **2003**, *1* (2), 328–337.

(53) Szostak, M.; Spain, M.; Procter, D. J. Electron Transfer Reduction of Unactivated Esters Using SmI2–H2O. *Chem. Commun.* **2011**, *47* (37), 10254–10256.

(54) Szostak, M.; Spain, M.; Procter, D. J. Electron Transfer Reduction of Carboxylic Acids Using SmI2–H2O–Et3N. *Org. Lett.* **2012**, *14* (3), 840–843.

(55) Szostak, M.; Collins, K. D.; Fazakerley, N. J.; Spain, M.; Procter, D. J. A General Electron Transfer Reduction of Lactones Using SmI2–H2O. *Org. Biomol. Chem.* **2012**, *10* (30), 5820–5824.

(56) Corey, E. J.; Kim, C. U.; Takeda, M. A Method for Selective Conversion of Allylic and Benzylic Alcohols to Halides under Neutral Conditions. *Tetrahedron Lett.* **1972**, *13* (42), 4339–4342.

(57) Hinks, J. D.; Takle, A. K.; Hunt, E. Carbamoyloxy Derivatives of Mutiline and Their Use as Antibacterials. WO1997025309A1, July 17, 1997.

(58) Murphy, S. K.; Zeng, M.; Herzon, S. B. Stereoselective Multicomponent Reactions Using Zincate Nucleophiles: β-Dicarbonyl Synthesis and Functionalization. *Org. Lett.* **2016**, *18* (19), 4880–4883.

(59) Crisp, G. T.; Scott, W. J.; Stille, J. K. Palladium-Catalyzed Carbonylative Coupling of Vinyl Triflates with Organostannanes. A Total Synthesis of (.+-.)-.DELTA.9(12)-Capnellene. *J. Am. Chem. Soc.* **1984**, *106* (24), 7500–7506.

(60) Nagata, W.; Yoshioka, M.; Terasawa, T. Hydrocyanation. VII. Stereochemistry of Conjugate Hydrocyanation of Cyclic .Alpha.,.Beta.-Unsaturated Ketones. *J. Am. Chem. Soc.* **1972**, *94* (13), 4672–4683.

(61) Paukner, S.; Wicha, W. W.; Heilmayer, W.; Thirring, K.; Riedl, R. Extended Spectrum Pleuromutilins: Potent Translation Inhibitors with Broad-Spectrum Antibacterial Activity In Vitro and In Vivo. 1.

Chapter 2

Total Synthesis of (+)-Pleuromutilin and (+)-12-epi-Pleuromutilin

2.1 INTRODUCTION

At the outset of our studies towards developing a synthetic route to access (+)-pleuromutilin **(1)** and its derivatives, there had only been three prior syntheses reported: those of Gibbons,[1] Boeckman,[2] and Procter.[3,4] While these three prior synthetic routes were unique in their construction of the tricyclic core, they shared two common features: 1) early construction of the central eight-membered ring led to numerous functional group and redox manipulations, and 2) all were linear in fashion. In contrast, we initiated a synthetic campaign towards developing a modular and convergent total synthesis of (+)-pleuromutilin (**1**) that would feature late-stage construction of the eight-membered ring. This chapter will outline the synthetic strategies attempted that ultimately enabled an 18-step total synthesis of (+)-pleuromutilin and (+)-12-*epi*-pleuromutilin.

2.2 RETROSYNTHETIC ANALYSIS

In considering a design plan for a synthesis of (+)-pleuromutilin (**1**), we envisioned a modular approach in which a hydrindane fragment (e.g., **2** and **4**) would be annulated to form the eight-membered ring through two sequential C–C bond-forming steps. This proposed annulation could occur through two different approaches: 1) C5–C14 and C10–C11, or 2) C5–C14 and C11–C12. Either disconnection links vicinal stereogenic centers which were identified as strategic points of disconnection.

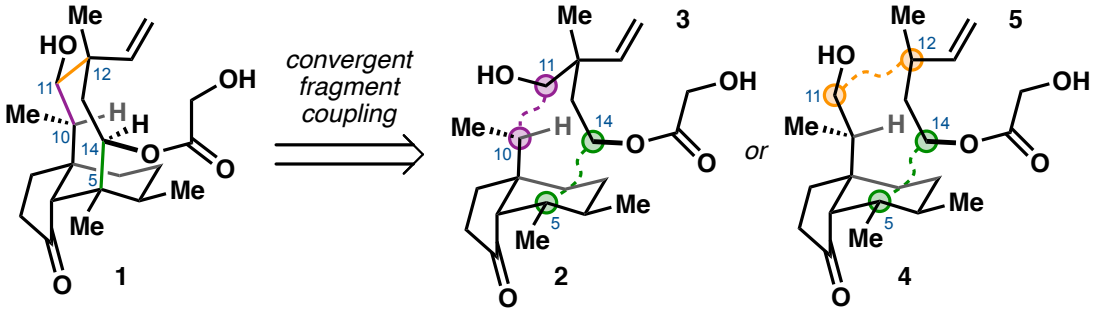

Scheme 1. Conceptual retrosynthetic analysis.

With this modular annulation strategy in mind, (+)-pleuromutilin (**1**) was first simplified to **6** via disconnecting the C14 glycolic ester (Scheme 2). Considering that the previously reported syntheses construct the tricyclic core at a very early stage, it was envisioned that C5–C14 could be forged through a diastereoselective samarium diiodide mediated cyclization reaction of aldehyde **7** to construct the eight-membered ring of pleuromutilin (**1**) at a late stage in the synthesis. This strategy would minimize the number of redox manipulations upon construction of the core, as well as leverage the constrained molecular geometry of the cyclization precursor to dictate the stereoselectivity of the cyclization reaction.

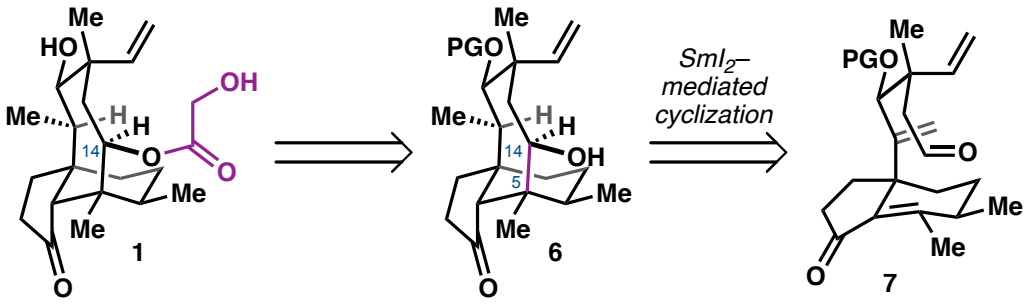

Scheme 2. Construction of eight-membered ring.

Preparation of cyclization precursor was envisioned to arise through a fragment coupling reaction between a hydrindanone fragment (e.g., **8** and **10**, Scheme 3) with its respective coupling partner (e.g., **9** and **11**). At the outset of the retrosynthetic design, two different disconnections were identified: 1) C10 and C11 could be joined through the use of hydrindanone **8** as a nucleophile (e.g. Nozaki-Hiyama-Kishi reaction)[5–7] and 2) C11 and C12 could be joined through the use of hydrindanone **10** as an electrophile (e.g. crotylation reaction)[8–10]. Both strategies would allow for diversification of the eight-membered backbone through variation of the coupling partner. As a means to investigate the feasibility of both coupling strategies, both hydrindanones could be prepared from alkyne **12.**

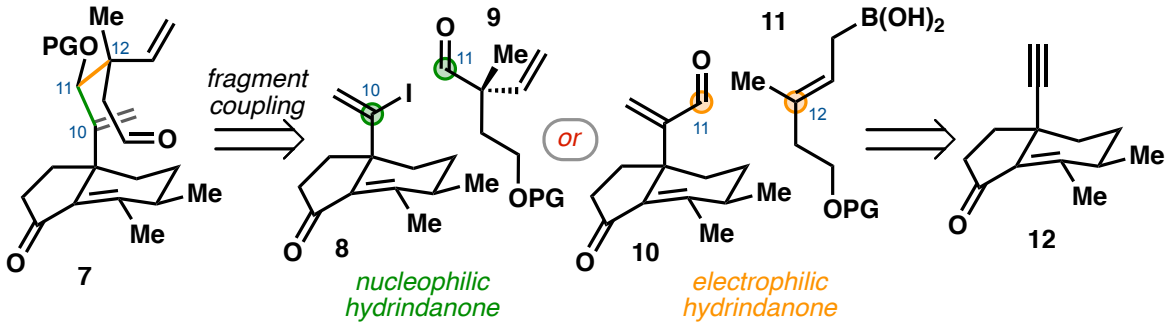

Scheme 3. Two fragment coupling approaches.

The oxidation pattern of alkyne **12** (Scheme 4) could be obtained through a methyl addition and oxidative transposition sequence from **13**. Hydrindenone **13** was then

envisioned to arise through a conjugate alkynylation and aldol cyclization from cyclohexenone **14**, which, in turn, would be accessible from chiral methyl cyclohexenone **15**.

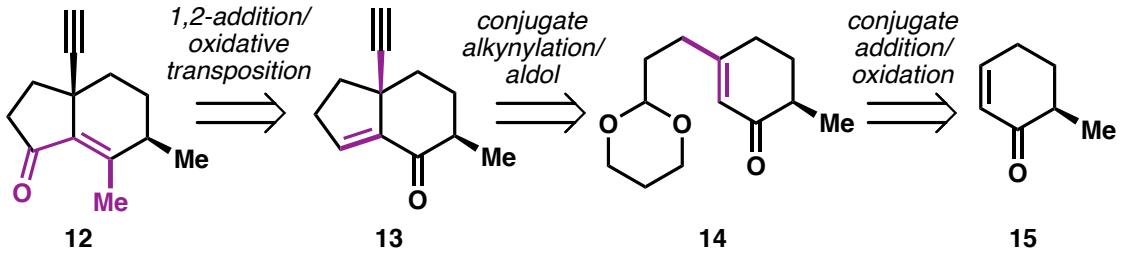

Scheme 4. Hydrindenone alkyne **12** retrosynthesis.

2.3 CYCLOOCTANE FORMATION

Medium-ring construction is a centerpiece of prior art towards (+)-pleuromutilin, perhaps best exemplified by the highly stereoselective anionic oxy-Cope rearrangement employed by Boeckman and the chelation-controlled aldol cyclization key to Proctor's Sm-ketyl radical cyclization cascade (**16**, Figure 1).[3,4] Both strategies employ *minimally-functionalized* cyclization substrates and subsequently leverage the resulting tricyclic architecture to install remaining stereocenters in laborious 18 to 25-step sequences. An important difference, however, lies in the constrained nature of Boeckman's vinyl carbinol precursor, critical for dictating the stereochemical outcome of the key anionic oxy-Cope cyclization. Proctor's cyclization substrate lacks this rigidity and instead relies on chelation control to dictate cyclization. We envisioned a hybrid, convergent strategy leveraging both the innate functionality of a *highly decorated,* geometrically constrained cyclization precursor to guide medium-ring formation as well as the propensity of ketyl radicals towards conjugate addition at a sterically-congested β-terminus.

In accordance with this logic, SmI_2 cyclization of **17** was expected to provide tricycle **6** with C3, C14, and C15 in the correct oxidation states for advancement to **1**.

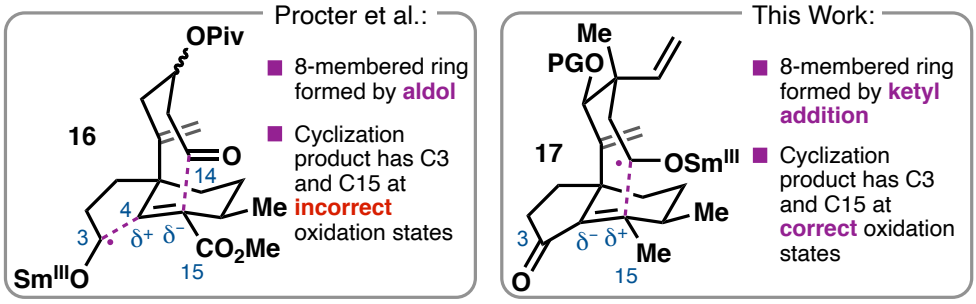

Figure 1. Comparison of SmI_2 approaches to pleuromutilin (**1**) framework.

2.4 FORWARD SYNTHETIC EFFORTS

2.4.1 *First Generation Approach Towards Hydrindanone Fragment*

Synthetic efforts towards (+)-pleuromutilin (**1**) commenced with preparation of hydrindanone alkyne **12**. Recognizing that (+)-dihydrocarvone (**18)** may serve to provide the C6 methyl stereocenter present in (+)-pleuromutilin (**1**), this material was subjected to a one-pot ozonolysis-oxidation procedure developed by Schreiber and coworkers.[11,12] Ozonolysis of the terminal alkene in methanol generated methoxy hydroperoxide **19** (Scheme 5). Single-electron transfer of an electron from iron(II) sulfate to the peroxide produced oxy radical **20**. Collapse of this tetrahedral intermediate led to formation of a carbon radical that undergoes radical combination with copper(II) acetate to yield alkyl copper intermediate **21**. Oxidative elimination from this intermediate affords a 3:1 mixture of **15** and **22**, in favor of the desired α,β-unsaturated enone.

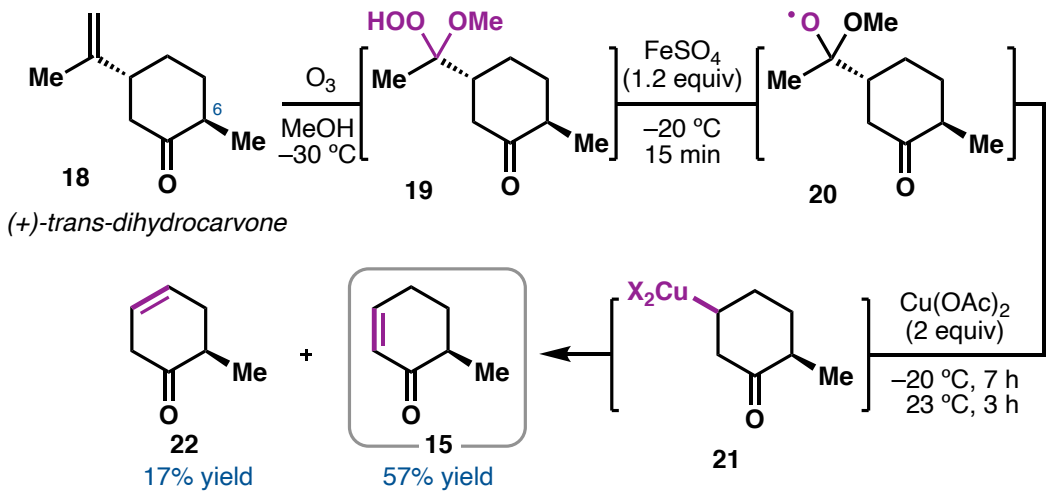

Scheme 5. Chiral enone **15** from fragmentation of (+)-*trans*-dihydrocarvone **18**.

With enone **15** in hand, investigations toward setting the C9 quaternary center commenced. Conjugate addition of the cuprate derived from **23** followed by Pd-catalyzed Saegusa-Ito oxidation furnished the trisubstituted enone **14**, setting the stage for installation of the C9 quaternary center through conjugate addition (Scheme 6).

In 1974, Corey and coworkers[13] developed a nucleophilic ethynyl group equivalent **24** and were able to perform conjugate additions into α,β-enones; subsequent treatment with lead(IV) tetraacetate unmasked the alkyne. Our initial attempts at performing this transformation with hexamethylphosphoramide as an additive resulted in no product formation; however, use of hexamethylphosphorous triamide instead greatly improved the reactivity, affording **25** as a 2.6:1 mixture of separable diastereomers in 58%. According to Corey and coworkers,[14] the insolubility of cuprous acetylides can often lead to reaction complications. This can be overcome through addition of superstoichiometric amounts of trialkyl- or triarylphosphines to the cuprate. However, tertiary phosphines are often difficult to separate from reaction products; a solution to this practical issue is the use of a

water-soluble phosphine, such as hexamethylphosphorus triamide. Pressing forward with vinyl stannane **25**, treatment with lead(IV) tetraacetate afforded alkyne **26** in 88% yield.

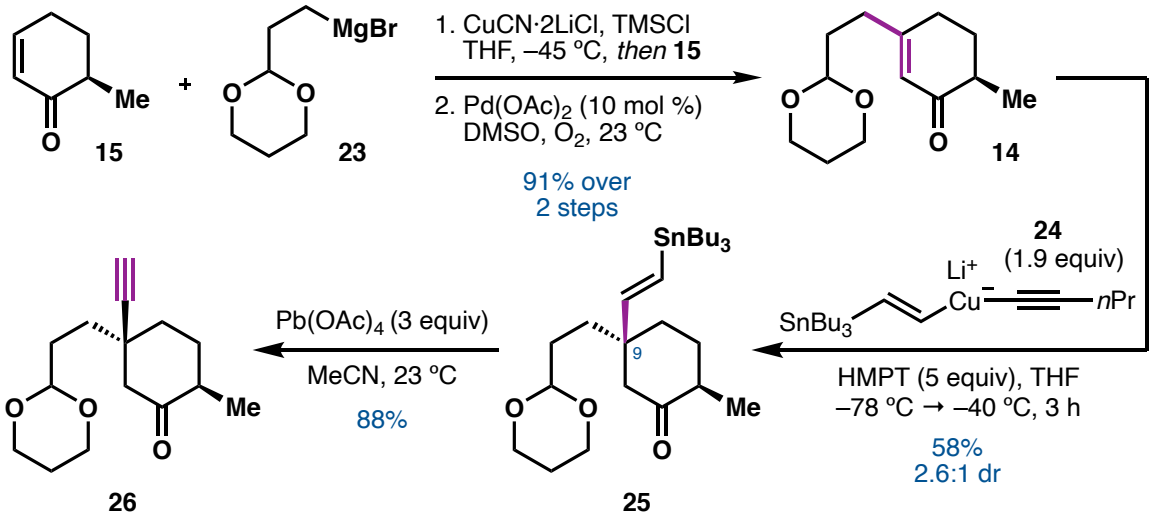

Scheme 6. Installation of the C9 quaternary center.

Alkyne **26** was elaborated to bicycle **13** through an acid-promoted intramolecular aldol condensation (Scheme 7). Treatment with 6 N HCl led to epimerization of the C6 stereocenter, giving rise to a 4:1 mixture of inseparable methyl diastereomers that were separated at the vinyl iodide (**8**) stage in the synthesis. Advancing **13** as a diastereomeric mixture, cerium-promoted 1,2-methyl addition[15] followed by Dauben oxidative transposition[16] afforded key hydrindanone alkyne **12**. Thus, fragment coupling investigations began.

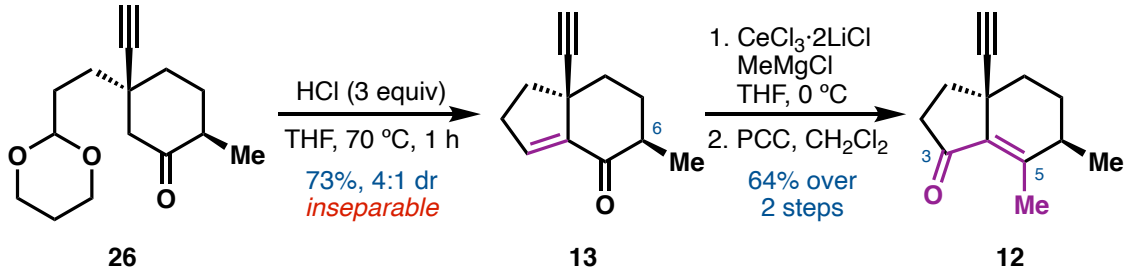

Scheme 7. Synthesis of hydrindanone alkyne **12.**

2.4.2 Fragment Coupling Investigations

Hydrindanone alkyne **12** was identified as an intermediate that would enable access to both vinyl iodide **8** and enal **10** for fragment coupling investigations. Iodoboration[17,18] followed by proto-deboration afforded vinyl iodide **8** in 94% yield. Subsequent palladium-catalyzed reductive carbonylation afforded hydrindanone enal **10** (Scheme 8). With hydrindanone coupling partners **8** and **10** in hand, the first of two key C–C bond construction required to form the bridging eight-membered ring was investigated.

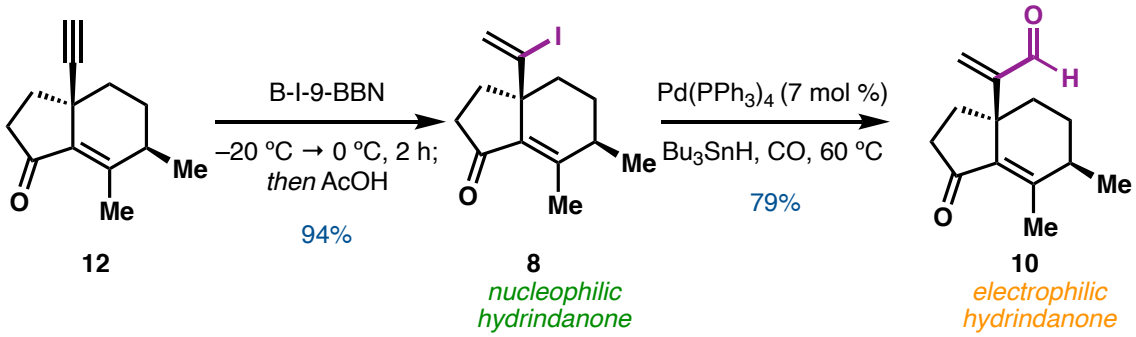

Scheme 8. Hydrindanone alkyne **12** derivatization for fragment coupling.

Preliminary Nozaki-Hiyama-Kishi reaction investigations with pentanal **27** produced none of the coupled product; instead, hydrodehalogenation **28**, homocoupled hydrindanone **29**, and starting material **8** were observed (Table 1). It appeared that vinyl iodide **8** was not amenable to NHK coupling, and investigations into this disconnection were halted.

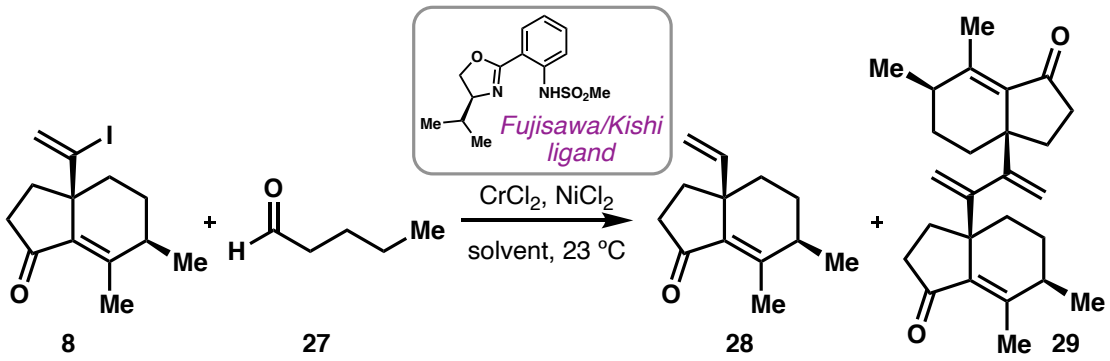

Entry	$CrCl_2$ (equiv)	$NiCl_2$ (equiv)	Ligand (equiv)	Solvent	% SM	% Yield (alkene)	% Yield (dimer)	% Yield
1	4	0.2	–	DMF (0.05 M)	–	42%	42%	–
2	4	0.02	–	DMF (0.05 M)	–	37%	35%	–
3	9	1	–	THF/DMF/4-*t*BuPy (6:3:1, 0.05 M)	–	28%	30%	–
4	3.4	0.2	3.4	THF (0.1 M)/ Et_3N (3.4 equiv)	52%	23%	–	–
5	3	1	3	THF (0.05 M)/ Et_3N (3 equiv)	91%	6%	–	–

Table 1. Nozaki-Hiyama-Kishi addition investigations.

Precedent from Szabó and coworkers[19] suggested that crotylation would be a reliable method for forming congested vicinal stereocenters. As such, attention was turned towards synthesis of crotylation fragment **35** (Scheme 9). Trityl protection of butynol **30** afforded **31** in reasonable yield. Deprotonation and nucleophilic addition into ethyl chloroformate furnished ynoate **32**, which upon conjugate addition with methyl cuprate and reduction with DIBAL-H provided allylic alcohol **34**. Treatment with palladium-catalyzed conditions for allylicboronic acid synthesis[20] afforded *Z*-allylic boronic acid **35**, the crotylation fragment.

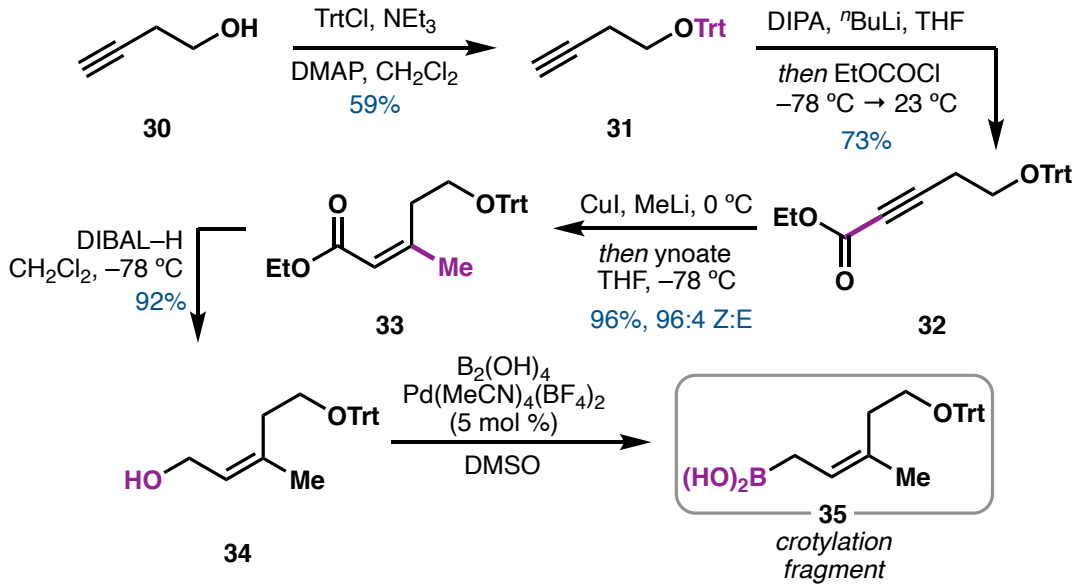

Scheme 9. Crotylation fragment **35** prepapration.

With enal **10** and *Z*-allylic boronic acid **35** in hand, use of conditions developed by Szabó and coworkers provided a mixture of separable diastereomers **36** and **37** (Scheme 10).

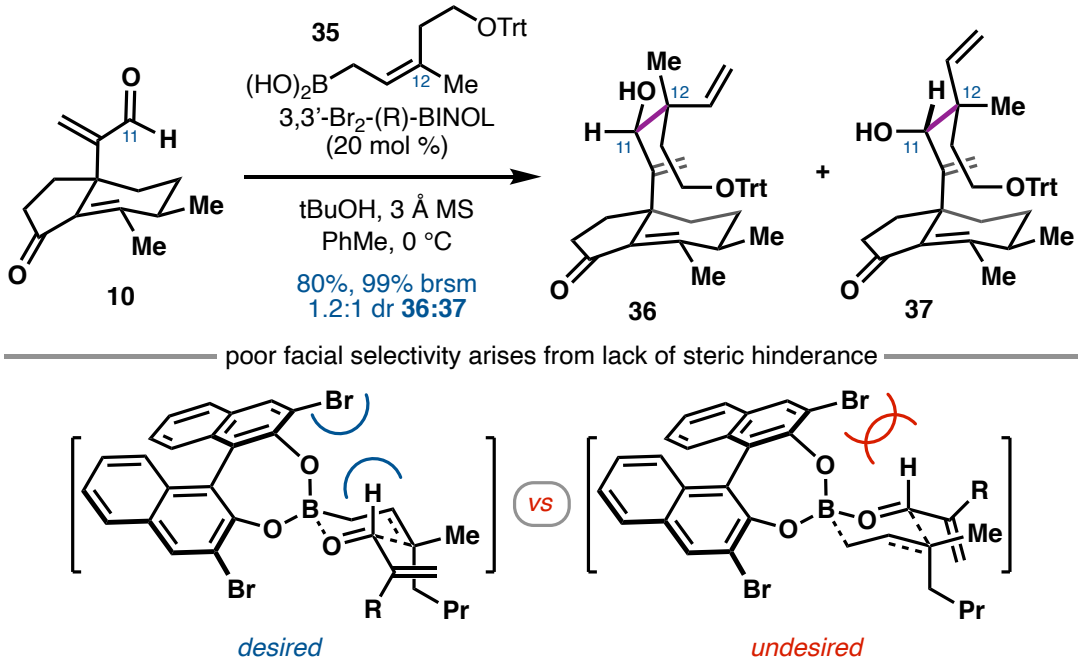

Scheme 10. Crotylation reaction and rationale for poor facial selectivity.

While the reaction proceeded with excellent selectivity for syn crotylation–consistent with a closed transition state, the catalyst did not discriminate between the faces of the aldehyde during the nucleophilic attack (Scheme 10). A brief investigation of alternative catalytic asymmetric crotylation conditions proved unfruitful (Table 2, Entries 2–4), and thus prompted further catalyst investigations. An initial survey of chiral phosphoric acids and PyBOX ligands yielded no product, and thus our efforts were focused on BINOL ligands. Use of the *S* catalyst (Table 2, Entry 5) provided a 1:1.4 mixture of **36** and **37**. It was ultimately determined that 3,3'-$(CF_3)_2$-(*R*)-BINOL (Table 2, entry 7) provided a yield comparable to that of 3,3'-Br_2-(*R*)-BINOL with slightly improved diastereoselectivity.

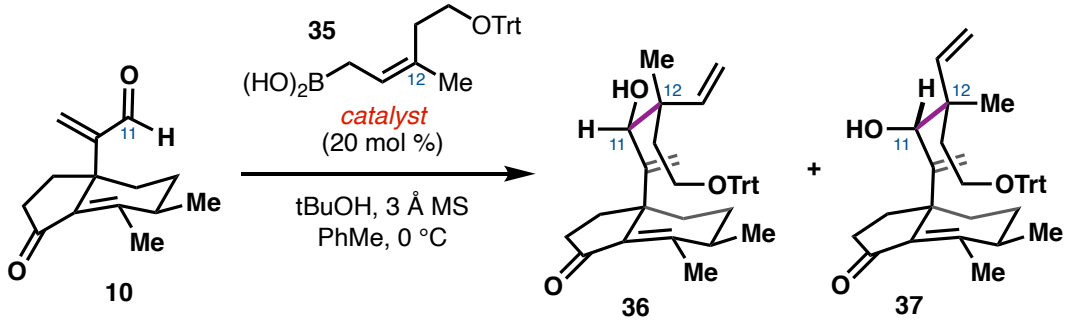

entry	catalyst	yield combined	dr
1	none	80%	1.2:1
2	**38**	–	–
3	**39**	–	–
4	**40**	–	–
5	3,3'-Br_2-(*S*)-BINOL	66%	1:1.4
6	3,3'-I_2-(*R*)-BINOL	79%	1.4:1
7	3,3'-$(CF_3)_2$-(*R*)-BINOL	77%	1.7:1

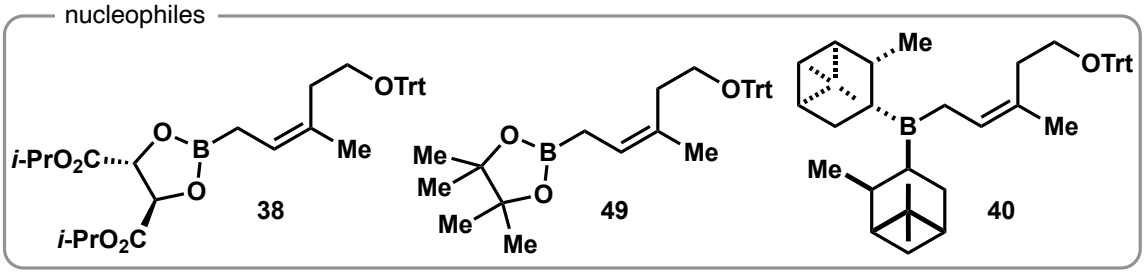

Table 2. Crotylation investigations.

In the first generation retrosynthesis, the initial motive for targeting hydrindanone alkyne **12** was to access both vinyl iodide **8** and enal **10**. Therefore, the route was optimized for hydrindanone alkyne **12**, not the desired coupling partner **10**. After determining that the key fragment coupling to forge the C11–C12 bond would proceed through a crotylation reaction between boronic acid **35** and enal **10**, attention was turned towards the development of a streamlined second generation synthesis of enal **10**. The reasons the first generation route needed to be redesigned were three-fold: 1) Conjugate addition using mixed cuprate **24** proceeded in poor 2:1 dr and necessitated the use of toxic tin reagents that were not amenable to large-scale material throughput (Scheme 11). 2) Acid-promoted aldol cyclization of **26** furnished **13** in reasonable yield; however, the reaction conditions also resulted in C6 epimerization to a mixture of inseparable diastereomers. 3) The reagent used for iodoboration (B-I-9-BBN) was not reliably available for purchase and attempts to freshly prepare the reagent led to irreproducible results. With these targeted issues in mind, attention was shifted toward developing a new route towards hydrindanone enal **10**.

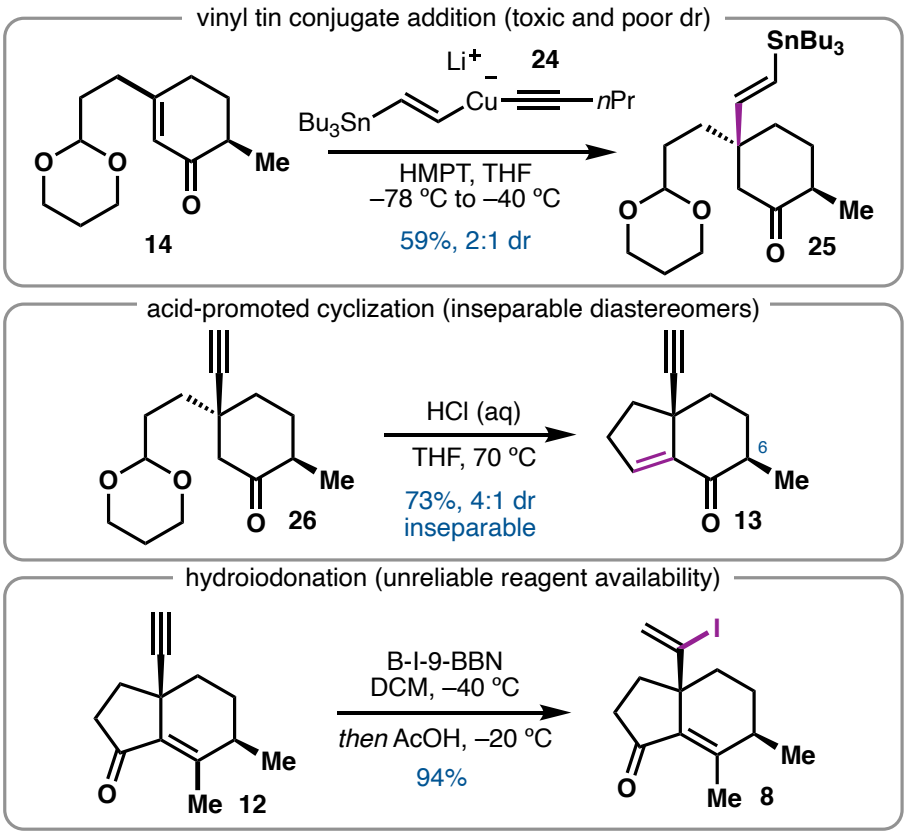

Scheme 11. Reasons for route redesign.

2.4.3 Second Generation Approach Towards Hydrindanone Fragment

After evaluating the first generation ten-step route towards hydrindanone enal **10**, it was realized that many of the issues stemmed from installation of an alkyne at C9. In the initial substrate design, it was envisioned that targeting hydrindanone alkyne 12 would give access to both vinyl iodide **8** and enal **10** for fragment coupling investigations. However, validation of the crotylation reaction with enal **10** led to designing a more efficient synthetic route towards hydrindanone enal **10**.

Beginning from trisubstituted enone **14**, conjugate addition of in situ generated vinylcuprate afforded **41** in 73% yield and 6:1 dr, a three-fold improvement from the 2:1

dr observed from vinylstannane **24** (*vide supra*, Scheme 12). This diastereoselectivity presumably arises from trans-diaxial effects to minimize the twist-boat conformation that would arise from formation of the undesired diastereomer. With this significant improvement in diastereoselectivity, a two-step procedure to elaborate **41** to alkyne **26** was developed, obviating the need to proceed through the previous route. Ozonolytic cleavage of the installed olefin furnished aldehyde **42**.

Initial attempts to convert the aldehyde to alkyne **26** resulted in a more rapid intramolecular aldol cyclization to forge [2.2.1]-bicycle **43**. It was suspected that the high concentration of methoxide in solution led to unselective reactivity for α-deprotonation. This was further supported by solvent investigations; in exchanging methanol for less acidic solvents such as ethanol and isopropanol (Scheme 12, entries 2 and 3), decreased formation of aldol product **43** was observed; however, the reaction rate also slowed considerably where the use of isopropanol as the solvent led to no formation of the desired product. Solvent mixture investigations ultimately proved fruitful, where tetrahydrofuran-methanol mixtures (Scheme 12, entries 5 and 6) significantly improved yields of the desired alkyne **26** while minimizing bicycle **43** formation.

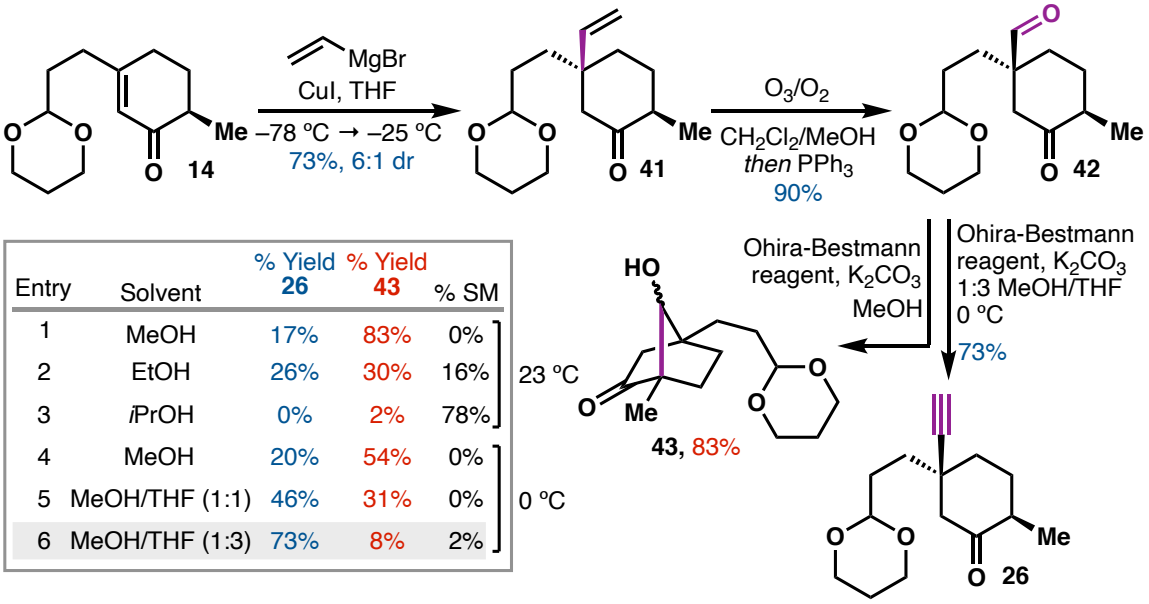

Entry	Solvent	% Yield **26**	% Yield **43**	% SM	
1	MeOH	17%	83%	0%	23 °C
2	EtOH	26%	30%	16%	
3	*i*PrOH	0%	2%	78%	
4	MeOH	20%	54%	0%	0 °C
5	MeOH/THF (1:1)	46%	31%	0%	
6	MeOH/THF (1:3)	73%	8%	2%	

Scheme 12. Intercepting alkyne **26** through vinyl conjugate addition.

Despite improving the diastereoselectivity of the conjugate addition reaction from 2:1 to 6:1 and eliminating the use of vinyl stannane **24**, the new route was unsatisfactory for three reasons: 1) obtaining the alkyne prior to cyclization would still furnish an inseparable mixture of diastereomers, 2) proceeding through the alkyne still necessitated the use of B-I-9-BBN, whose commercial availability was unreliable, and 3) utilizing the new route was one step longer than the first generation route (Scheme 13). Due to these shortcomings, additional conjugate addition investigations were pursued.

It was later envisioned that addition of an isopropenyl unit would obviate the need for homologation at a later stage by incorporating all the carbons present within the enal fragment. Initial attempts to add a hydroxyisopropenyl fragment were unfruitful. However, addition of an isopropenyl fragment proceeded smoothly in 73% yield and 4.8:1 dr (Scheme 13).

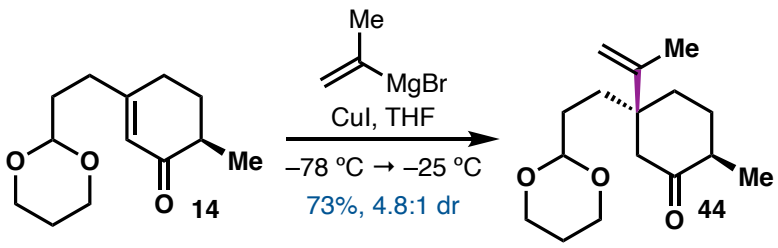

Scheme 13. Isopropenyl conjugate addition.

At this stage, acid-promoted aldol cyclization from conjugate addition product **45** was attempted but unsuccessfully due to the formation of a halo-Prins product **47** (Scheme 14). It is hypothesized that the electron-rich nature of the isopropenyl unit was the source of this undesired reactivity.

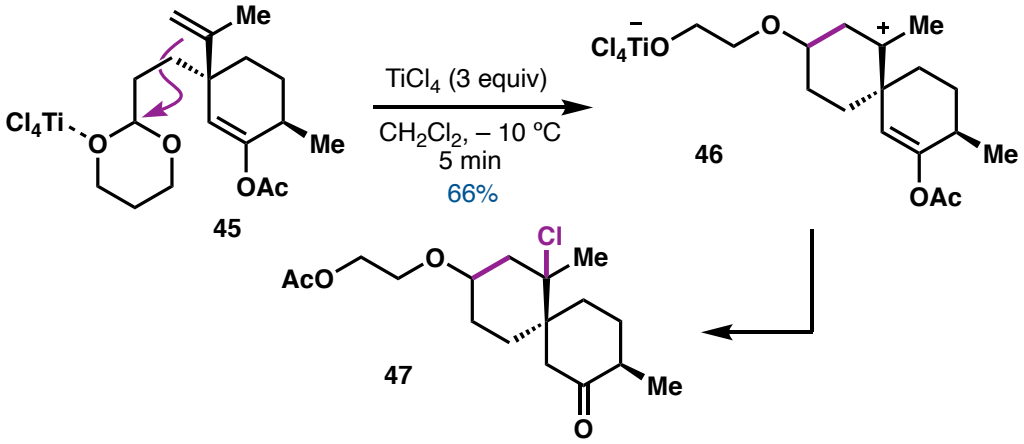

Scheme 14. Undesired halo-Prins cyclization.

Efforts were then steered towards installing an electron-withdrawing substituent at the allylic position; however, attempts to perform an allylic oxidation yielded starting material. Although hydroxyl group installation was unsuccessful, allylic chlorination with trichloroisocyanuric acid[21] proceeded smoothly, setting the stage for the previously unsuccessful acid-promoted aldol cyclization with **45** (Scheme 15). Indeed, installation of the allylic electron-withdrawing substituent deactivated the previously electron-rich olefin, and halo-Prins product formation was not observed. Incorporation of the chloroisopropenyl

unit did not minimize the amount of C6 epimerization or influence the diastereomeric ratio; however, the previously inseparable diastereomers were now separable at this stage, affording a 52% yield of the desired diastereomer **49**. Elaboration to **51** proceeded via similar conditions to those established for the first generation route.

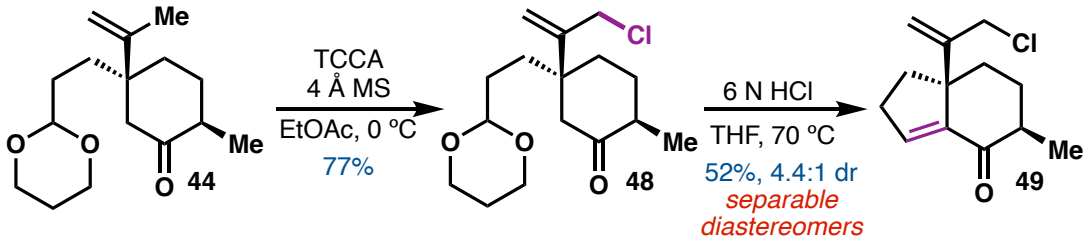

Scheme 15. Successful aldol cyclization with allylic chloride **48**.

Pressing forward, a 1,2-methyl addition assisted by the use of $CeCl_3 \cdot 2LiCl$[15] was performed to furnish tertiary allylic alcohol **50**, followed by treatment with pyridinium chlorochromate to affect a Dauben oxidative transposition[16] to reveal the desired hydrindanone oxidation pattern **51**, setting the stage for investigations of the final key oxidation to deliver hydrindanone enal **10** (Scheme 16).

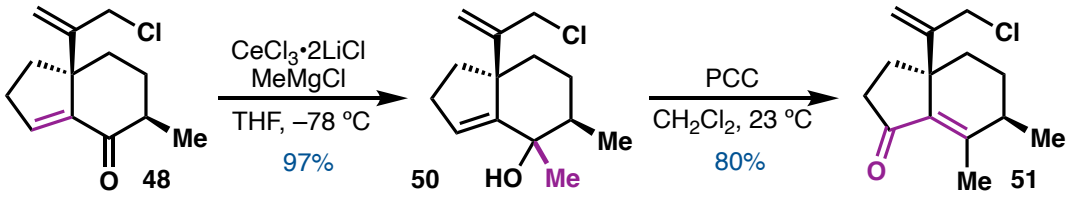

Scheme 16. Synthesis of final hydrindanone enal precursor.

Preliminary attempts to oxidize allylic chloride **51** to enal **10** via Ganem and Kornblum oxidation[22–25] conditions gave low yields. While reactions performed under microwave irradiation in the presence of silver carbonate afforded moderate yields, scaling to decagram quantities proved impractical. Further exploring Kornblum oxidation conditions that could be run in batch, it was found that use of a phosphate base with halide

salts gave modest yields (Scheme 17). It is suspected that this reaction first undergoes a Finkelstein displacement of the allylic chloride with iodide. Subsequent iodide displacement by dimethylsulfoxide and deprotonation would unveil dimethylsulfide and product. Through these new conditions that were more amenable to scale, the key coupling fragment was obtained in 69% yield. This vastly improved nine-step synthesis delivered **10** in 18% yield from commercial starting materials (compared to our first generation 10 step, 11% yielding route).

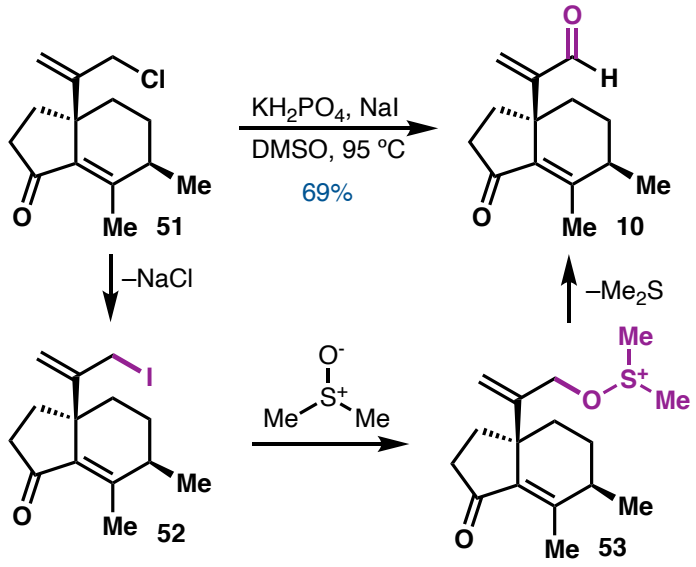

Scheme 17. Modified Kornblum oxidation.

2.4.4 Elaboration to SmI_2-Cyclization Precursor

Once a streamlined second generation route to access hydrindanone enal **10** was established and the crotylation reaction had been validated for coupling fragments **10** and **35** together, a three-step route that involved methoxymethyl protection, trityl deprotection, and Stahl oxidation[26,27] to obtain the cyclization precursor **56** was developed (Scheme 18).

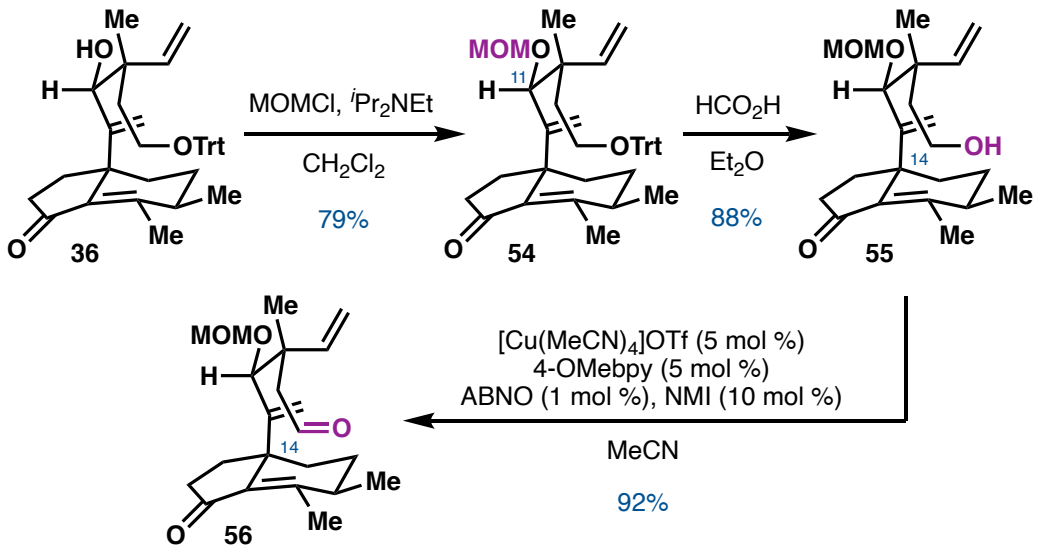

Scheme 18. Synthesis of SmI_2-cyclization precursor **56**.

2.4.5 *SmI_2-mediated Cyclization Investigations*

At this stage, attention was turned towards the second key C5–C14 bond construction step: a SmI_2-mediated cyclization to forge the central eight-membered ring. It was envisioned that this reaction would occur through generation of ketyl radical **57**, followed by cyclization onto the enone to generate samarium enolate **58**, and protonation to reveal the tricyclic core of pleuromutilin (Scheme 19).

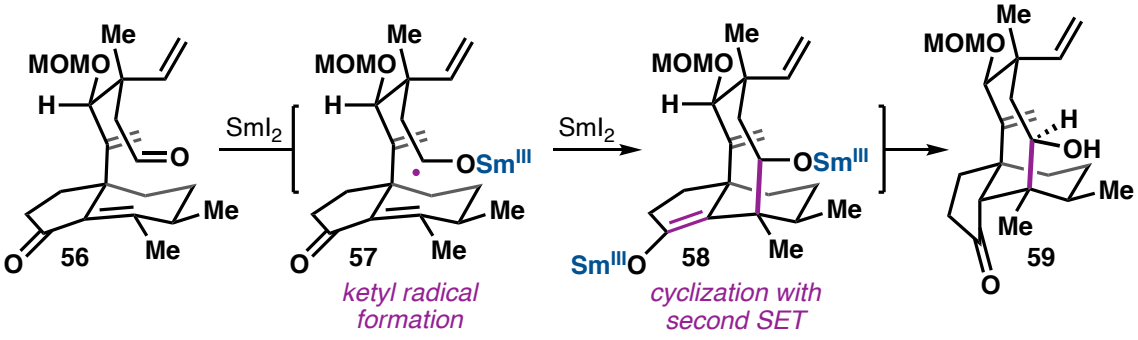

Scheme 19. SmI_2-mediated cyclization mechanism.

Initial attempts in constructing the tricyclic core resulted in ketoacid **61** (Scheme 20), the structure of which was confirmed by single-crystal X-ray diffraction. We hypothesized that this product arose from exposure of the Sm^{III}-enolate to trace oxygen in solution, resulting in hydroperoxide **60** formation and subsequent oxidative ring scission to deliver the fragmented ketoacid product. Although the ring scission was deleterious, this was nonetheless the first indicator that the desired C5–C14 bond formation had occurred with high diastereoselectivity.

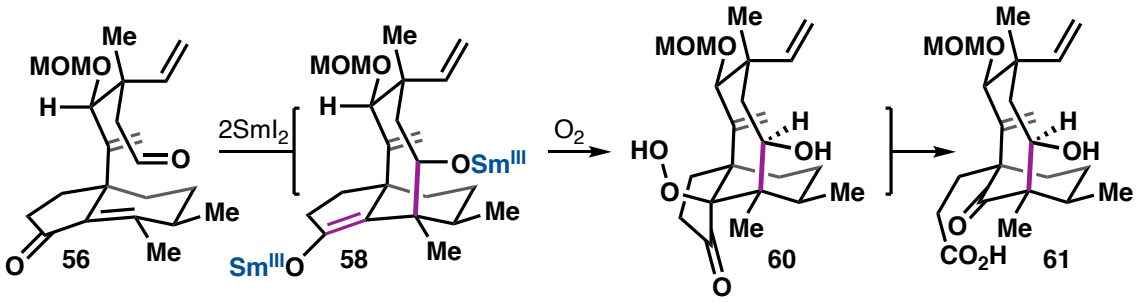

Scheme 20. C5–C14 bond formation with undesired oxidative ring scission.

To prevent unwanted formation of ketoacid **61**, a variety of conditions were evaluated. Initial optimization studies involved rigorously deoxygenating all components of the reaction mixture. Because productive C5–C14 bond formation was occurring, attention was focused on investigating alternative quenches and found that TMSCl provided a 78% yield on first pass; however, this result was highly variable and contingent upon the humidity in the air (Scheme 21). When the reaction was performed under rigorously anhydrous conditions, trace amounts of desired tricycle **59** with fragmented **61** and silylether **62** were isolated, all with 1:1 dr at C14. This observation led to the conclusion that water must be a crucial component of the reaction! Upon investigating equivalents of water, it was discovered that six equivalents were absolutely crucial for high yields and diastereoselectivity. Although there have been extensive discussions on the role of

additives in SmI_2 reactions,[28] it is postulated that in this particular case, water reacts with trimethylsilyl chloride to generate hydrochloride acid *in situ*, which can then quench the samarium enolate before it can react with residual oxygen in solution. Perhaps this is also the reason that upon addition of water, formation of silyl ether **62** was no longer observed. It is also possible that the water is necessary for an organized transition state to make this reaction highly diastereoselective.

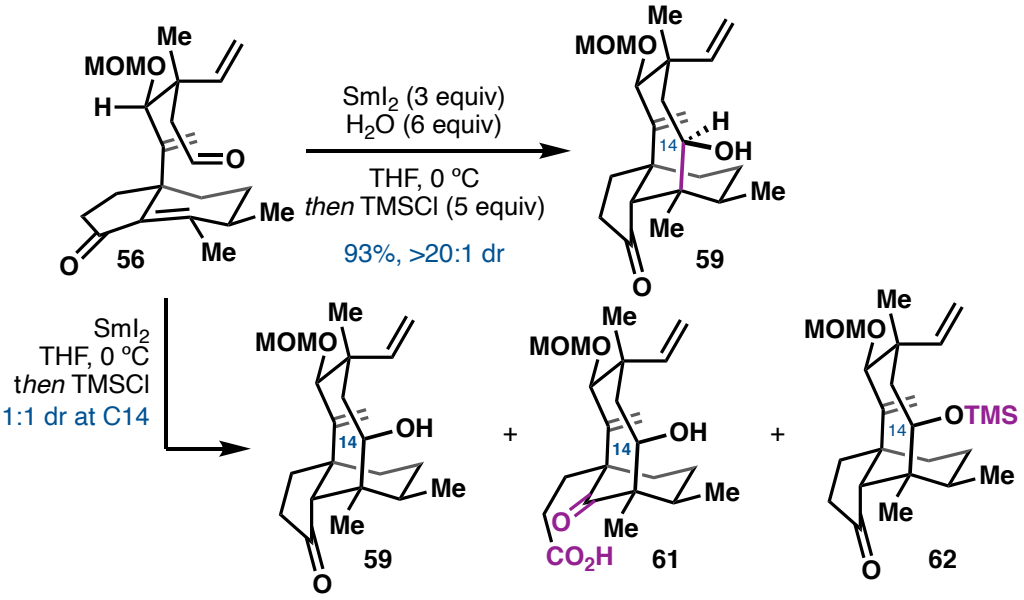

Scheme 21. Successful construction of the tricyclic core.

2.4.6 C10 Olefin Reduction

In the initial retrosynthetic analysis, it was envisioned that upon SmI_2-mediated cyclization to construct the tricyclic core, completion of the synthesis would only require two further functional group manipulations: reduction of the C10 olefin and installation of the C14 glycolic side chain (Scheme 22). It was not until the tricyclic intermediate was obtained that we realized what a challenge selective C10 reduction in the presence of the C19 olefin would pose.

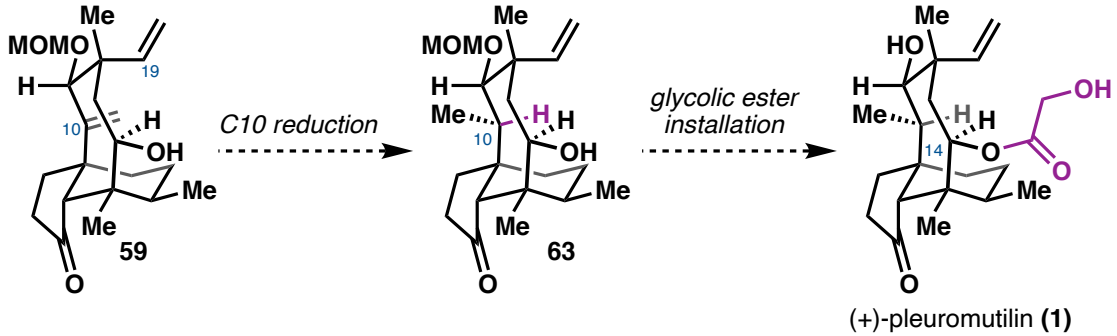

Scheme 22. Envisioned endgame for the synthesis of (+)-pleuromutilin (**1**).

Standard hydrogenation conditions employing cationic transition metal complexes[29,30] gave rapid and exclusive reduction of the more sterically accessible C19 olefin. Instead, attention was turned towards hydrogen atom transfer conditions,[31,32] seeking to leverage the thermodynamic preference for formation of a tertiary carbon-centered radical over formation of a secondary radical if C19 reduction were to occur. Using conditions developed by Shenvi and coworkers,[33] diastereoselective reduction of the C10 olefin (**59**) was observed; however, this was met with concomitant oxidation of the C14 alcohol to the undesired ketone (**65**) in a redox-relay type process (Scheme 23). Only trace products arising from competing C19–C20 vinyl reduction were observed.

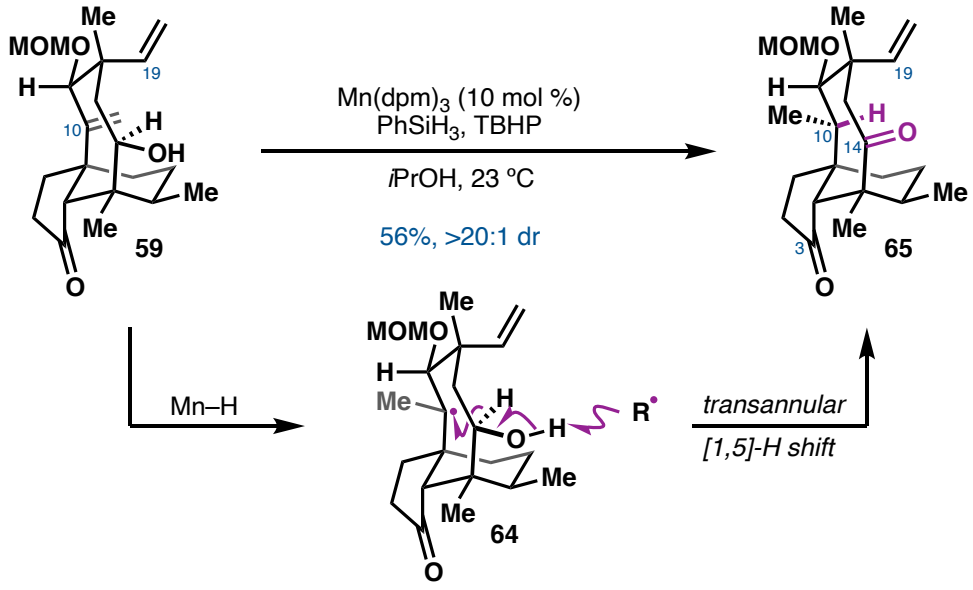

Scheme 23. Redox-relay by transannular 1,5-hydrogen atom transfer.

To test whether this reaction proceeds through a transannular [1,5]-hydrogen atom transfer process, deuterium-labeled tricycle **68** was prepared through a four-step protocol (Scheme 24). First, Pinnick oxidation[34,35] of aldehyde **56** to the carboxylic acid, followed by reduction with lithium aluminum deuteride afforded deuterated reduction product **66**. Oxidation of the alcohol using conditions developed by Stahl and coworkers[26] afforded deuterated aldehyde **67**, which was smoothly converted to deuterated tricycle **68** using the previously optimized SmI_2-mediated cyclization conditions. Exposure to the optimized 1,5-hydrogen atom transfer conditions led to formation of diketone **69** as a single diastereomer with complete transfer of the deuterium label. The observation that substrates in which the C14 alcohol is protected perform poorly under hydrogen atom transfer conditions suggests that cleavage of the O–H bond to form the C14 ketone serves as a driving force for this transformation.

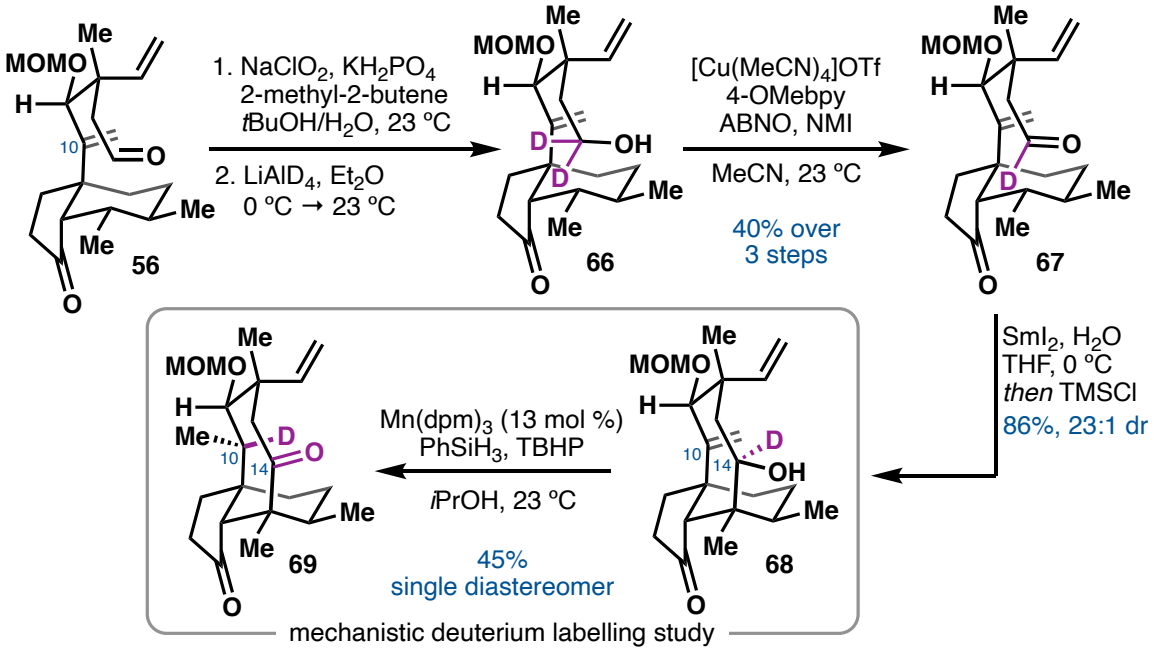

Scheme 24. Mechanistic deuterium labelling study for redox-relay process.

2.4.7 Completing the Synthesis of (+)-Pleuromutilin

Although reduction of the C10 olefin using hydrogen atom transfer conditions was successful, the resulting C14 ketone presented a new set of challenges. Ultimately, selective reduction of the C14 ketone in the presence of the C3 ketone proved to be untenable due to the more sterically encumbered nature of the C14 ketone. To circumvent performing a selective reduction, triisopropylsilyl (TIPS) enol ether **70** was prepared and submitted to the previously optimized 1,5-hydrogen atom transfer conditions to obtain ketone **71** as a single diastereomer (Scheme 25). To complete the synthesis, **71** was exposed to excess lithium in ammonia to furnish alcohol **72** as a separable 14:1 mixture of diastereomers. This selectivity arises from the alcohol being placed in the pseudoequatorial position upon reduction. Subsequent one-pot acylation with 2-(2,2,2-trifluoroacetoxy)-acetic acid[4] followed by trifluoroacetate methanolysis and acidic hydrolysis affected global deprotection to deliver (+)-pleuromutilin (**1**).

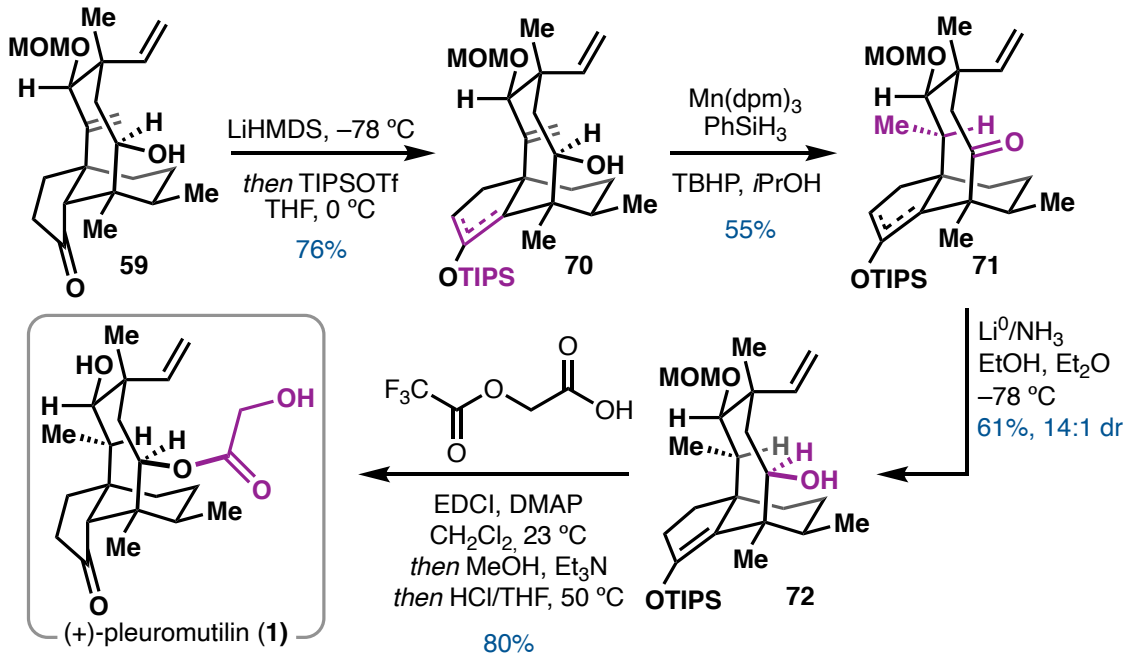

Scheme 25. Completing the synthesis of (+)-pleuromutilin (**1**).

2.5 EFFORTS TOWARD NOVEL ANALOGUES

A key design aspect of the strategy described was the ability to easily vary the stereochemistry of the cyclization substrates at C11 and C12. Given the recent interest in derivatives of C12-*epi*-mutilin as broad spectrum antibiotics,[36] it was envisioned that the 12-*epi*-mutilin framework could be prepared using our synthetic route.

When enal **10** was subjected to crotylation with *Z*-boronic acid **35,** diastereomers **36** and **37** (the 11,12-bis-*epi* variant) were observed as a 1.2:1 mixture. When enal **10** was subjected to crotylation with *E*-boronic acid **73**, diastereomers **74** (12-*epi*) and **75** (11-*epi*) were formed in 85% yield and 2:1 dr (Scheme 26).

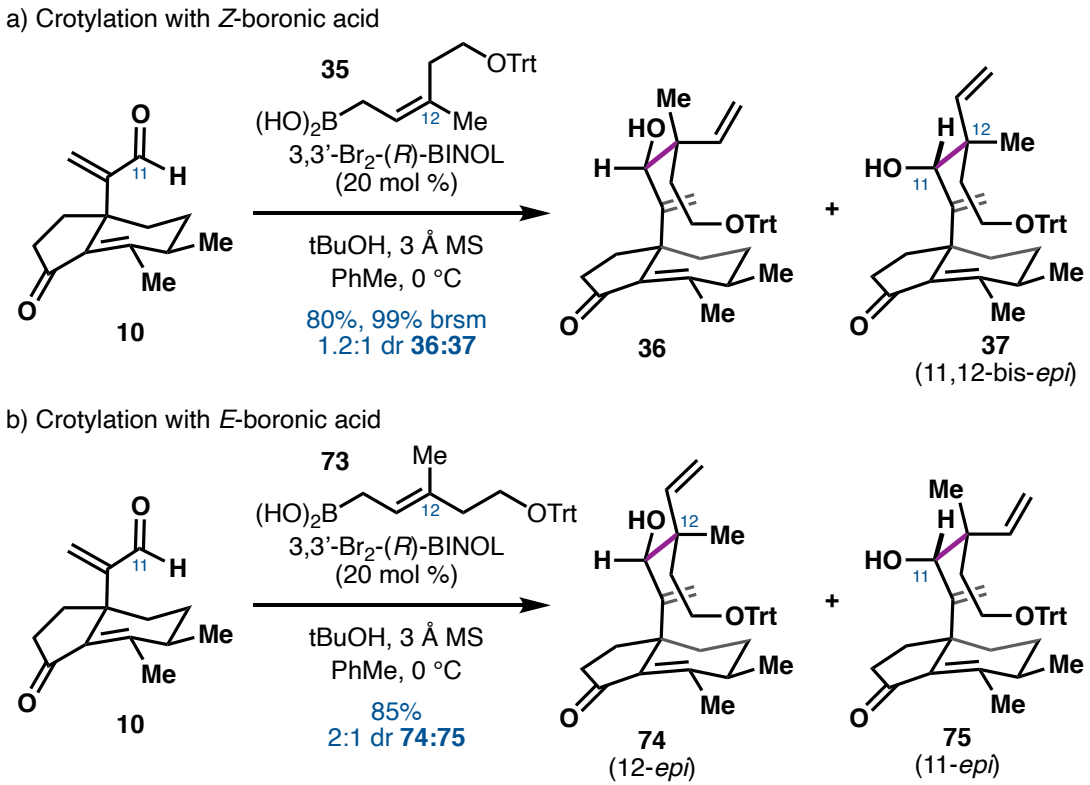

Scheme 26. Crotylation to access stereochemical analogues.

Elaboration of **74** (12-*epi*) to (+)-12-*epi*-pleuromutilin **82** was straightforward and no further optimization was required. Tricycle **79** formation proceeded in good yield and

diastereoselectivity as it did for the natural system and the 1,5-hydrogen atom transfer smoothly afforded the reduced product **81** (Scheme 27). Ketone reduction, glycolic ester installation, and global deprotection afforded (+)-12-*epi*-pleuromutilin (**82**).

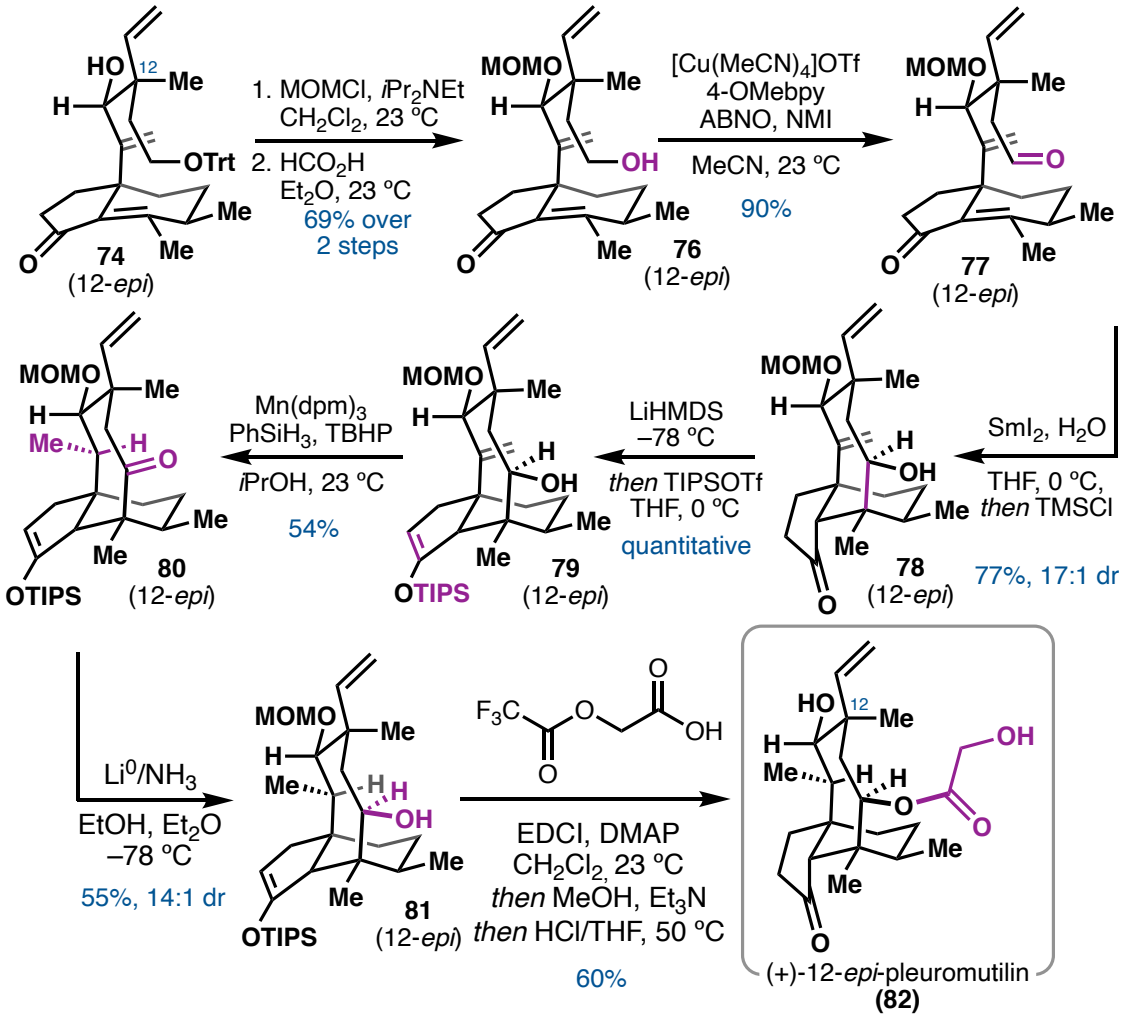

Scheme 27. Synthesis of (+)-12-*epi*-pleuromutilin.

However, attempts to cyclize any of the 11-*epi*-isomers revealed that the C11 stereochemistry exerts a pronounced effect on the reactivity. Subjection of **37** to the SmI_2-mediated cyclization conditions provided tricycle **83** as the major product in 20% yield (Scheme 28). It is suspected that conformational gearing to minimize $A_{1,2}$ strain at C11 reverses the regioselectivity of the ketyl radical addition to the enone, producing radical

84. Subsequent Dowd-Beckwith rearrangement proceeding through cyclopropane **85** delivers the product bearing a bridgehead olefin. Attempts to cyclize **75** (11-*epi*) also led to an analogous product.

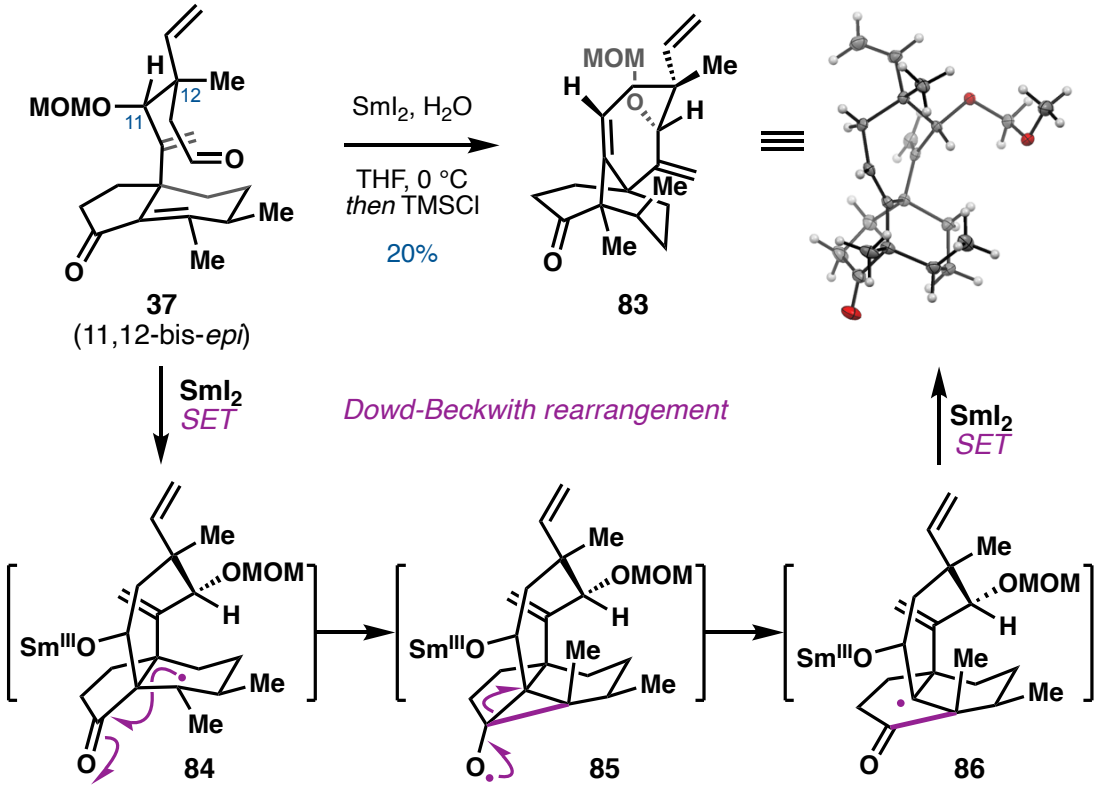

Scheme 28. Cyclization of **7** (11,12-bis-*epi*).

2.6 CONCLUDING REMARKS

Herein, a modular synthesis of (+)-pleuromutilin and (+)-12-*epi*-pleuromutilin has been disclosed and each was completed in 18 steps (longest linear sequence) from (+)-*trans*-dihydrocarvone. These syntheses were enabled by a modular approach that employed a highly diastereoselective SmI_2-mediated radical cyclization to form the eight-membered ring. In addition, a transannular [1,5]-hydrogen atom transfer that affects a stereospecific redox relay to set the C10 stereocenter was uncovered. The brevity and modularity of the

route will enable the design and synthesis of new fully synthetic variants of mutilin antibiotics.

2.7 EXPERIMENTAL SECTION

Materials and Methods

Unless otherwise stated, reactions were performed under an inert atmosphere (Ar) with freshly dried solvents utilizing standard Schlenk techniques. Glassware was oven-dried at 120 °C for a minimum of four hours, or flame-dried utilizing a Bunsen burner under high vacuum. Tetrahydrofuran (THF), methylene chloride (CH_2Cl_2), diethyl ether (Et_2O), benzene (PhH), and toluene (PhMe) were dried by passing through activated alumina columns. Absolute ethanol (200 Proof) was purchased from Koptec. Methanol (HPLC grade) was purchased from Fisher Scientific. Anhydrous ammonia (NH_3) was purchased from Matheson Tri-Gas. N,N-diisopropylethylamine (iPr$_2$NEt), triethylamine (Et_3N), methanol (MeOH), isopropanol (iPrOH), tert-butanol (tBuOH), and trimethylsilyl chloride (TMSCl) were distilled over calcium hydride prior to use. Unless otherwise stated, chemicals and reagents were used as received. All reactions were monitored by thin-layer chromatography using EMD/Merck silica gel 60 F254 pre-coated plates (0.25 mm) and were visualized by UV (254 nm), p-anisaldehyde, and/or $KMnO_4$ staining. Flash column chromatography was performed using silica gel (SiliaFlash® P60, particle size 40-63 microns [230 to 400 mesh]) purchased from Silicycle. 1H and 13C NMR spectra were recorded on a Bruker Avance III HD with Prodigy Cryoprobe (at 400 MHz and 101 MHz, respectively) or a Varian Inova 500 (at 500 MHz and 101 MHz respectively) and are reported relative to internal $CHCl_3$ (1H, δ = 7.26) and $CDCl_3$ (13C, δ = 77.0). Data for 1H

NMR spectra are reported as follows: chemical shift (δ ppm) (multiplicity, coupling constant (Hz), integration). Multiplicity and qualifier abbreviations are as follows: s = singlet, d = doublet, t = triplet, q = quartet, m = multiplet, br = broad, app = apparent. IR spectra were recorded on a Perkin Elmer Paragon 1000 spectrometer and are reported in frequency of absorption (cm–1). HRMS were acquired from the Caltech Mass Spectral Facility using fast-atom bombardment (FAB), electrospray ionization (ES+-TOF) or electron impact (EI). Optical rotations were measured on a Jasco P-2000 polarimeter using a 100 mm path-length cell at 589 nm.

Reagents were purchased from commercial vendors as follows: 2-(2-bromoethyl)-1,3-dioxane was purchased from TCI America. Palladium(II) acetate ($Pd(OAc)_2$, >99%), copper(I) iodide (CuI, 99.999%), and tetrakis(acetonitrile)palladium(II) tetrafluoroborate ($Pd(CH_3CN)_4(BF_4)_2$, >98%) were purchased from Strem Chemicals and stored in a nitrogen-filled glovebox. Tetrahydroxydiboron ($B_2(OH)_2$, 95%) and copper(I) cyanide (CuCN, 99.98%) were purchased from Sigma-Aldrich and stored in a nitrogen-filled glovebox. Samarium ingot (99.9% trace rare earth metals basis), tris(2,2,6,6-tetramethyl-3,5-heptanedionato)manganese(III) ($Mn(dpm)_3$, 97%), phenylsilane ($PhSiH_3$, 97%), lithium (wire stored in mineral oil, 99.9% trace metal basis), and tert-butyl hydroperoxide (TBHP, 5.5 M in decane over 4 Å MS) were purchased from Sigma-Aldrich.

2.7.1 Experimental Procedures

Preparation of trisubstituted enone (14):

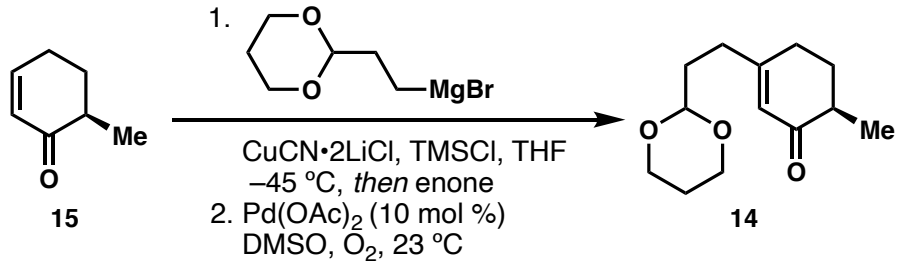

A flame-dried, 1 L, 3-necked round-bottom flask equipped with a stir bar, reflux condenser, addition funnel, and glass stopper was charged with activated magnesium turnings (8.02 g, 330.0 mmol, 3 equiv). The atmosphere was exchanged three times with argon before addition of THF (40 mL). Added to the rapidly stirred suspension was 1,2-dibromoethane (3.10 g, 16.5 mmol, 0.15 equiv) dropwise. An exothermic reaction was observed, and the suspension became grey. The reaction was cooled to ambient temperature, and subsequently, a solution of 2-(2-bromoethyl)-1,3-dioxane (42.9 g, 219.9 mmol, 2 equiv) in THF (170 mL, 0.64 M) was added dropwise via an addition funnel over 1 h. Upon completion of addition, the reaction was stirred for an additional 30 min. The resulting suspension was filtered via cannula into a flame-dried, 2 L, 2-necked round-bottom flask equipped with a large stir bar under an atmosphere of argon, and the Grignard reagent was diluted with THF (170 mL, 0.64 M). Titration against salicylaldehyde phenylhydrazone yielded the concentration of Grignard reagent as 0.38 M.

The Grignard solution was cooled to –45 °C. Subsequently, a freshly prepared solution of CuCN•2LiCl in THF was added via cannula over 20 min. CuCN•2LiCl was prepared by dissolving CuCN (9.85 g, 110.0 mmol, 1 equiv) and LiCl (9.32 g, 220.0 mmol,

2 equiv) in THF (110 mL, 1.0 M w.r.t. CuCN) and vigorously stirred at ambient temperature for 1 h. After an additional 20 min, freshly distilled TMSCl (14.3 g, 132.0 mmol, 1.2 equiv) was added. The reaction became heterogeneous, and stirring was difficult. After 10 min, a solution of (*R*)-enone[11,12] **15** (12.1 g, 110.0 mmol, 1 equiv) in THF (183 mL, 0.6 M) was added via cannula over 30 min. The reaction was stirred for 1 h and then quenched with sat. aq. $NaHCO_3$ (10 mL) at –45 °C. After warming to ambient temperature, pentane (600 mL) was added, and the suspension was filtered through Celite. The volatiles were concentrated under reduced pressure, additional pentane (500 mL) was added, and the slurry was filtered through Celite. This process was repeated an additional time to afford 38.2 g of a clear oil. ^{1}H NMR ($CDCl_3$) shows desired silyl enol ether along with 2-(2-cyanoethyl)-1,3-dioxane. The silyl enol ether was used immediately without further purification.

To a 1 L round-bottom flask equipped with a stir bar was added the silyl enol ether, anhydrous DMSO (550 mL, 0.2 M) and $Pd(OAc)_2$ (2.47 g, 11.0 mmol, 10 mol %). The mixture was sparged with O_2 for 2 h then stirred at ambient temperature for 36 h. At this time, ^{1}H NMR analysis showed the ratio of product to remaining silyl enol ether was 11:1. Water (700 mL) was added, and the product was extracted into Et_2O (4 x 400 mL). The combined organic layers were washed with brine (1 x 50 mL), dried over Na_2SO_4, and concentrated under reduced pressure to afford 38.1 g of a viscous, yellow oil.

Purification was achieved via flash column chromatography on SiO_2 [750 g SiO_2, 60 mL fractions, Et_2O/hexanes = 40% (1.5 L), 45% (500 mL), 50% (500 mL), 55% (500 mL), 65% (500 mL), 80% (500 mL)] to afford trisubstituted enone **14** (20.3 g, 90.5 mmol, 91% yield over 2 steps) as a viscous, clear oil.

TLC (25% EtOAc/hexanes): R_f = 0.23 (UV, *p*-anisaldehyde).

^{1}H NMR (400 MHz, $CDCl_3$): δ 5.84 (s, 1H, C_4), 4.53 (t, *J* = 5.0 Hz, 1H, C_3), 4.09 (ddt, *J* = 10.7, 5.1, 1.3 Hz, 2H, O***CH*****$_2$**CH_2***CH*****$_2$**O), 3.75 (m, 2H, O***CH*****$_2$**CH_2***CH*****$_2$**O), 2.31 (m, 5H, C_1, C_2, C_6, C_8), 2.05 (m, 2H, OCH_2***CH*****$_2$**, C_7), 1.78 (m, 2H, C_1, C_2), 1.68 (m, 1H, C_7), (d sept, *J* = 13.5, 1.4 Hz, 1H, OCH_2***CH*****$_2$**), 1.12 (d, *J* = 6.9 Hz, 3H, C_{16}).

^{13}C NMR (101 MHz, $CDCl_3$): δ 202.3 (*C*$_5$=O), 164.5 (C_9), 125.1 (C_4), 101.2 (C_3), 66.9 (O***C***H_2CH_2), 40.8 (C_6), 32.3 (C_1), 31.9 (C_2), 30.8 (C_7), 29.3 (C_8), 25.7 (OCH_2***C***H_2), 15.1 (C_{16}).

FTIR (AT-IR): 2857, 2249, 1662, 1375, 1211, 1146, 1079, 1046, 907, 647 cm^{-1}.

HRMS (FAB+, m/z): calc'd for $C_{13}H_{21}O_3$ $[M+H]^+$ 225.1491, found: 225.1502.

$[\alpha]_D^{23}$: +65° (*c* = 1.055, $CHCl_3$).

Preparation of vinyl stannane 25

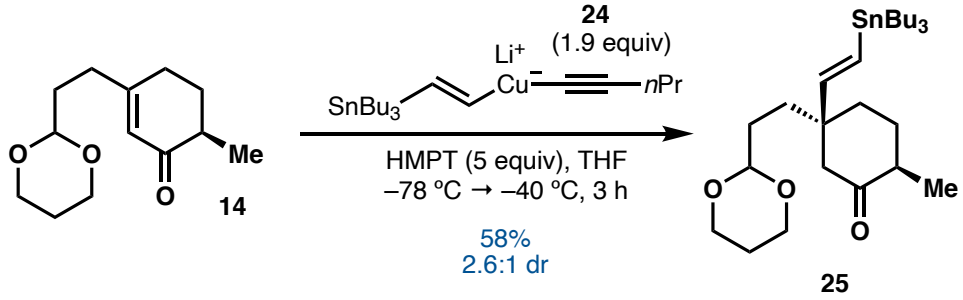

A flame-dried, argon-purged, 1 L round-bottom flask equipped with a stir bar was charged with *trans*-1,2-bis(tri-*n*-butylstannyl)ethylene (61.8 g, 102.0 mmol, 1.9 equiv) and THF (270 mL, 0.2 M). The mixture was cooled to –78 °C, and a 2.42 M solution of *n*-BuLi (44.4 mL, 107.4 mmol, 2 equiv) was added dropwise. The reaction was allowed to warm to –40 °C over 30 min.

A separate flame-dried, argon-purged, 1 L bottom flask equipped with a stir bar was charged with *n*-propylethynylcopper (13.3 g, 102.0 mmol, 1.9 equiv), hexamethylphosphorous triamide (HMPT, 43.8 g, 268.4 mmol, 5 equiv), and THF (67 mL, 0.8 M). The mixture was stirred at rt until all of the polymeric *n*-propylethynylcopper dissolved to give a homogeneous solution (approximately 10 min required). The solution was cooled to –40 °C, and the vinyl lithium-stannyl species prepared above was transferred to the *n*-propylethynylcopper solution via cannula over 30 min. The resulting mixture was cooled to –78 °C and stirred for 45 min before a solution of the chiral enone **14** (12.0 g, 53.7 mmol, 1 equiv) in THF (54 mL, 1.0 M) was added over 15 min. The reaction was stirred for 30 min then warmed to –40 °C over 15 min. While cold, the reaction was poured into ice-cold saturated aqueous $(NH_4)_2SO_4$ (100 mL), and the layers were separated. The aqueous layer was back-extracted with Et_2O (1 x 50 mL), and the combined organic layers were washed with 2% (v/v) H_2SO_4 (2 x 250 mL). A black/brown precipitate formed, and the mixture was filtered through Celite, dried over Na_2SO_4, and the volatiles were removed *in vacuo* to afford 95.3 g of a dark red/brown viscous oil.

The crude reaction was purified via flash column chromatography on silica gel [650 g SiO_2, 60 mL fractions, collected 750 mL forerun, Et_2O/hexanes = 15% (1.5 L), 20% (1 L), 30% (1 L), 40% (500 mL), 50% (1 L)] to afford Bu_4Sn, vinyltributylstannane, and HMPT (fractions 2–15), minor diastereomer (fractions 17–31), and major diastereomer **25** (fractions 31–53). The volatiles were removed *in vacuo* to afford 8.23 g of minor diastereomer and 17.93 g of major diastereomer **25**. ^1H NMR ($CDCl_3$) shows pure diasteromers. Yield: 90%. R_f (minor diastereomer) = 0.45 (Et_2O/hexanes = 30%,

visualized with $KMnO_4$). R_f (major diastereomer) = 0.35 (Et_2O/hexanes = 30%, visualized with $KMnO_4$).

^{1}H NMR (400 MHz, $CDCl_3$): δ 5.84 (d, *J* = 19.7 Hz, 1H), 5.56 (d, *J* = 19.7 Hz, 1H), 4.52 – 4.38 (m, 1H), 4.08 (ddd, *J* = 11.5, 4.9, 1.4 Hz, 2H), 3.73 (tdd, *J* = 12.1, 2.6, 1.2 Hz, 2H), 2.62 (dd, *J* = 14.1, 2.1 Hz, 1H), 2.27 – 1.98 (m, 3H), 1.84 (ddt, *J* = 13.0, 6.3, 3.3 Hz, 1H), 1.78 – 1.64 (m, 2H), 1.55 – 1.37 (m, 9H), 1.37 – 1.20 (m, 7H), 0.96 (d, *J* = 6.5 Hz, 3H), 0.92 – 0.78 (m, 13H).

^{13}C NMR (101 MHz, $CDCl_3$): δ 212.1, 152.5, 129.3, 102.5, 66.9, 48.6, 47.7, 44.7, 36.8, 36.0, 30.7, 29.5, 29.1, 27.2, 25.8, 14.4, 13.7, 9.4.

Preparation of alkyne 26

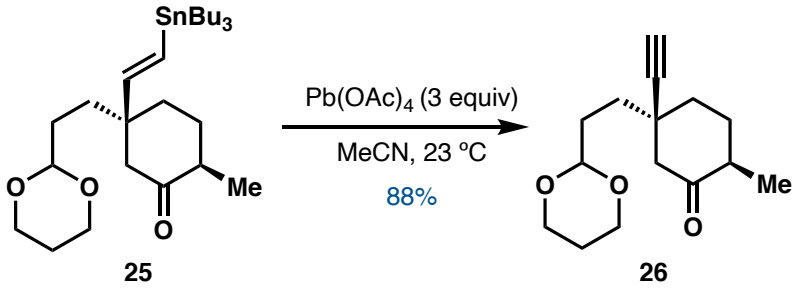

25 26

A flame-dried, 1 L bottom flask equipped with a stir bar was charged with major diastereomer **25** (17.9 g, 33.1 mmol, 1 equiv) and MeCN (330 mL, 0.1 M). Added to the homogenous solution was $Pb(OAc)_4$ (44.1 g, 99.4 mmol, 3 equiv), and the reaction was stirred at rt for 72 h, at which time ^{1}H NMR analysis showed complete conversion. The yellowish-white heterogeneous suspension was diluted with pentane (600 mL), filtered through Celite, and the volatiles were removed *in vacuo*. The oil and white solid obtained was triturated with 30% Et_2O/hexanes (250 mL), filtered through Celite, and the volatiles

were removed *in vacuo*. The process was repeated an additional time with 30% Et_2O/hexanes (100 mL).

The resulting residue was purified via flash column chromatography on silica gel [450 g SiO_2, 60 mL fractions, collected 500 mL forerun, Et_2O/hexanes = 30% (1 L), 35% (500 mL), 40% (500 mL), 50% (500 mL), 70% (1 L)] to afford Bu_3SnOAc and trace residual RSM (fractions 19–31), a faint spot staining in *p*-anisaldehyde (fractions 35-43), and product (fractions 43-68). The volatiles were removed *in vacuo* to afford 6.86 g of alkyne **26** as a viscous, colorless oil. Yield: 86%.

TLC (50% Et_2O/hexanes): R_f = 0.10 (*p*-anisaldehyde).

^{1}H NMR (400 MHz, $CDCl_3$): δ 4.58 (t, *J* = 4.9 Hz, 1H), 4.13 (ddt, *J* = 10.4, 5.0, 1.4 Hz, 2H), 3.87 – 3.71 (m, 3H), 2.52 (dd, *J* = 13.1, 2.6 Hz, 1H), 2.32 (dtd, *J* = 12.5, 6.2, 1.2 Hz, 1H), 2.24 (dd, *J* = 13.1, 1.2 Hz, 1H), 2.17 – 2.00 (m, 2H), 1.96 (dq, *J* = 12.9, 3.0 Hz, 1H), 1.89 – 1.78 (m, 3H), 1.72 – 1.62 (m, 3H), 1.37 (dtt, *J* = 13.5, 2.7, 1.4 Hz, 1H), 1.07 (d, *J* = 6.5 Hz, 3H).

^{13}C NMR (101 MHz, $CDCl_3$): δ 210.1, 102.0, 85.8, 73.2, 66.9, 52.4, 44.7, 40.8, 36.6, 36.4, 31.9, 30.3, 25.7, 14.3.

HRMS (FAB+, m/z): calc'd for $C_{15}H_{21}O_3$ [M+H]–H_2 249.1491, found: 249.1482.

$[\alpha]_D^{23}$: +23.4° (*c* = 0.92, $CHCl_3$).

Preparation of hydrindanone alkyne 13

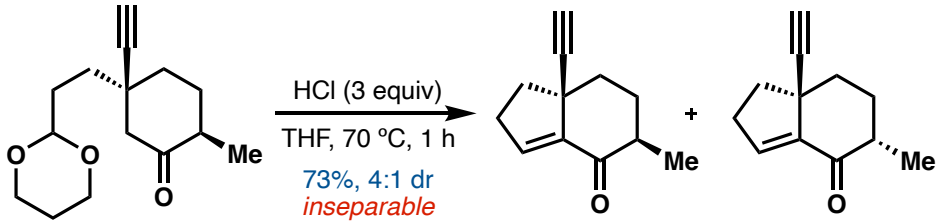

26 **13**

A flame-dried, 500 mL bottom flask equipped with a stir bar was charged with alkyne **26** (6.86 g, 27.4 mmol, 1 equiv) and THF (137 mL, 0.2 M). To the homogenous solution was added aqueous HCl (13.7 mL of a 6 M solution, 3 equiv). The system was equipped with a reflux condenser, and the reaction was heated to 70 °C. After 90 min, TLC analysis showed complete conversion. The resulting yellow solution was cooled to rt and basified via slow addition of saturated aqueous $NaHCO_3$ (100 mL). The biphasic mixture was transferred to a separatory funnel, and the layers were separated. The aqueous layer was extracted with Et_2O (3 x 50 mL), and the combined organic layers were washed with brine (1 x 50 mL), dried over Na_2SO_4, and the volatiles were removed *in vacuo* (rotovap only) to afford a yellow oil.

The resulting residue was purified via flash column chromatography on silica gel (175 g SiO_2, Et_2O/hexanes = 10%) to afford two faint UV-active spots (fractions 7–12) and product **13** (fractions 15-35). The volatiles were removed *in vacuo* (rotovap only) to afford 3.49 g of **13** as a pale yellow oil. ^1H NMR ($CDCl_3$) shows pure product as a 4.3:1 mixture of diastereomers epimeric at the α-methyl group. Yield: 73%. R_f = 0.35 (Et_2O/hexanes = 10%, visualized with UV and *p*-anisaldehyde).

Preparation of hydrindanone alkyne 12

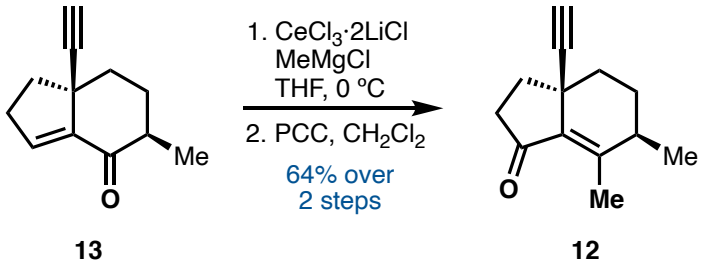

13 **12**

A flame-dried, 200 mL bottom flask equipped with a stir bar was charged with hydrindanone alkyne **13** (2.02 g, 11.6 mmol, 1 equiv). The atmosphere was exchanged with argon three times before adding a solution of $CeCl_3$•2LiCl (0.3 M in THF, 38.6 mL, 11.6 mmol, 1 equiv). Upon addition of $CeCl_3$•2LiCl, a bright yellow solution was obtained and stirred at rt for 1 h, over which time the reaction became pale yellow. The mixture was then cooled to 0 °C and allowed to equilibrate for 10 min. Subsequently, a solution of methylmagnesium chloride (3.0 M in THF (Aldrich), 7.72 mL, 23.2 mmol, 2 equiv) was added dropwise over 10 min, and the reaction was stirred at 0 °C until TLC analysis indicated complete consumption of enone **13** (10 min at this scale). (Note: the separable diastereomer has identical polarity to that of starting enone, but while the enone is UV-active, the separable diastereomer is not; thus TLC analysis may be used to monitor reaction progress).

The resulting dark yellow solution was quenched at 0 °C via slow addition of 1 M HCl (25 mL) using a vent needle to relieve excess pressure. Thereafter, the mixture was diluted with H_2O (30 mL) and Et_2O (50 mL), transferred to a separatory funnel, and the layers were separated. The aqueous layer was extracted with Et_2O (3 x 50 mL), the combined organic layers were dried over Na_2SO_4, and the volatiles were removed *in vacuo* (rotovap only) to afford a viscous yellow oil.

A flame-dried, 250 mL round-bottom flask equipped with a stir bar was charged with PCC (7.83 g, 36.3 mmol, 3 equiv) and CH_2Cl_2 (36 mL, 0.33 M). To the heterogeneous orange suspension was added a solution of crude allylic alcohol (2.30 g, 12.1 mmol, 1 equiv) in CH_2Cl_2 (47 mL, 0.25 M) over 3 min. The suspension was stirred at rt for 12 h, at which time TLC analysis indicated complete conversion.

Thereafter, the tarry mixture was diluted with Et_2O (300 mL) and transferred to a separatory funnel. Added to the tar remaining in the reaction flask was Et_2O (150 mL) and silica gel (25 g), and the mixture was stirred for 1 h before being filtered over Celite. The resulting solution was combined with the initial reaction mixture. The combined organic layers were washed with 5% NaOH (2 x 100 mL), 5% HCl (1 x 100 mL), saturated aqueous $NaHCO_3$ (1 x 100 mL), dried over Na_2SO_4, and the volatiles were removed *in vacuo* (rotovap only) to afford 1.89 g of a viscous yellow oil.

Purification was achieved via flash column chromatography on silica gel (80 g SiO_2, Et_2O/hexanes = 10%) to afford a faint UV-active spot with R_f = 0.5 (fractions 7–8) and product (fractions 9–20). The volatiles were removed *in vacuo* (rotovap only) to afford 1.51 g of the **12** as a clear, viscous oil. Yield: 64%.

TLC (10% Et_2O/hexanes): R_f = 0.4 (UV, *p*-anisaldehyde).

^{1}H NMR (400 MHz, $CDCl_3$): δ 2.63 (ddd, *J* = 18.0, 13.1, 8.3 Hz, 1H), 2.38 – 2.17 (m, 3H), 2.17 – 2.07 (m, 5H), 1.89 (ddt, *J* = 13.4, 6.6, 3.4 Hz, 1H), 1.75 (tdd, *J* = 13.7, 10.3, 3.2 Hz, 1H), 1.68 – 1.58 (m, 1H), 1.40 – 1.29 (m, 1H), 1.15 (d, *J* = 7.1 Hz, 3H).

^{13}C NMR (101 MHz, $CDCl_3$): δ 206.3, 152.1, 134.1, 88.6, 69.8, 40.5, 37.5, 36.9, 35.8, 35.5, 29.3, 19.2, 16.8.

FTIR (AT-IR): 3285, 2931.24, 2860.32, 2359.59, 1452, 1409, 1370, 1262, 1165, 967, 908

HRMS (ET+, m/z): calc'ed for $C_{13}H_{16}O$ $[M]^+$ 188.1201, found: 188.1226.

$[\alpha]_D^{23}$**:** –245.4° (*c* = 0.81, $CHCl_3$).

Preparation of vinyl iodide 8

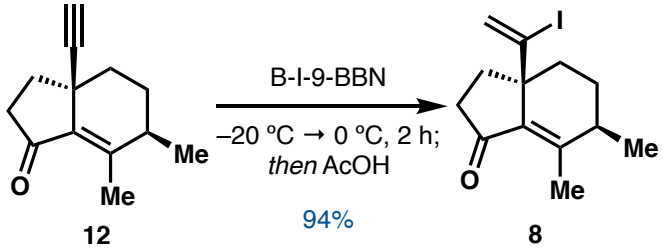

12 8

A flame-dried, 250 mL round-bottom flask equipped with a stir bar was charged with the hydrindanone alkyne **8** (645 mg, 3.43 mmol, 1 equiv). The atmosphere was exchanged three times with argon and then CH_2Cl_2 (43 mL, 0.08 M) was added. The homogenous solution was cooled to –20 °C, and a solution of B-I-9-BBN (6.85 mL of a 1.0 M solution in hexanes, 6.85 mmol, 2 equiv) was added dropwise over 15 min. The yellow solution was stirred for 1 h then warmed to 0 °C and stirred for 1 h. Added to the resulting dark red solution was glacial AcOH (2.65 mL, 46.3 mmol, 13.5 equiv) over 2 min. The reaction was stirred 30 min at 0 °C then warmed to rt and stirred for 30 min. Subsequently, 5% w/w aqueous $NaHCO_3$ (100 mL) was added slowly causing vigorous gas evolution, and the biphasic mixture was stirred for 10 min.

Thereafter, the mixture was transferred to a separatory funnel with CH_2Cl_2 (50 mL), and the layers were separated. The aqueous layer was extracted with CH_2Cl_2 (2 x 20 mL), and the combined organic layers were washed with 1 M $Na_2S_2O_3$ (1 x 100 mL), dried over Na_2SO_4, and the volatiles were removed *in vacuo* to afford a viscous oil.

Purification was achieved via flash column chromatography on silica gel (200 g SiO_2, Et_2O/hexanes = 5%) to afford minor diastereomer and bis-iodinated product (fractions 19–24) and major diastereomer **8** (fractions 23–36). The volatiles were removed *in vacuo* to afford 631 mg of the product as a clear, viscous oil. ^1H NMR analysis revealed a 9:1 mixture of diastereomers. Yield: 58%.

TLC (15% Et_2O/hexanes): R_f = 0.4 (UV).

Preparation of hydrindanone enal 10 from vinyl iodide 8

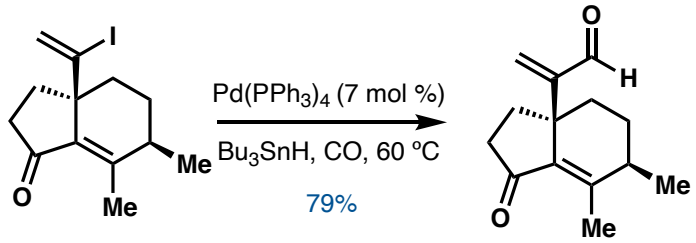

8 **10**

A flame-dried, 250 mL round-bottom flask equipped with a stir bar was charged with the hydrindanone vinyl iodide **8** (405 mg, 1.28 mmol, 1 equiv) and anhydrous PhMe (32 mL, 0.04 M). The homogeneous solution was sparged with CO (g) from a double-walled balloon for 10 min and was subsequently heated to 60 °C. Stirring and sparging was continued at 60 °C for an additional 10 min before adding a solution of $Pd(PPh_3)_4$ (104 mg, 0.0897 mmol, 7 mol %) in anhydrous PhMe (11 mL, 0.11 M) in one portion. Upon addition, the reaction turned brown/black, and sparging was continued for another 5 min. Subsequently, the purge needle was placed just above the reaction mixture, and a solution of freshly distilled Bu_3SnH (485 mg, 1.67 mmol, 1.3 equiv) in anhydrous PhMe (10 mL, 0.13 M) was added dropwise over 2 h while the reaction mixture was maintained at 60 °C.

After approximately 5 mL of the $Bu_3SnH/PhCH_3$ solution had been added, the reaction turned bright yellow and remained as such until addition was complete.

The reaction was cooled to rt and sparged with argon for 10 min before PhMe was removed by distillation under reduced pressure.

The resulting viscous brown residue was immediately purified via flash column chromatography on silica gel (50 g SiO_2, Et_2O/hexanes = 15%→25%) to afford residual [Sn] (fractions 4–7), a bright yellow band (fractions 29–57), and product (fractions 36–57). The volatiles were removed *in vacuo* to afford 293 mg of **10** contaminated with residual $Pd(PPh_3)_4$. Given that $Pd(PPh_3)_4$ is insoluble in hexanes and the product is soluble in hexanes, the yellow solid was triturated with hexanes, filtered, and the volatiles were removed to afford 226 mg of the enal **10** as an off-white solid after standing overnight in the refrigerator. Yield: 80%.

TLC (30% Et_2O/hexanes): R_f = 0.3 (UV).

Preparation of trityl protected alcohol 31.

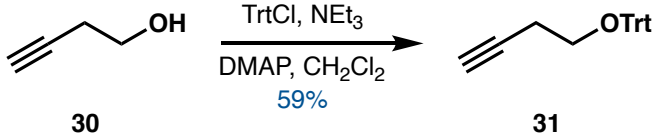

A flame-dried, 250 mL round-bottom flask equipped with a stir bar was charged with 3-butyn-1-ol **30** (7.01 g, 100.0 mmol, 7.57 mL, 1 equiv), CH_2Cl_2 (150 mL, 0.67 M), and DMAP (2.44 g, 20.0 mmol, 20 mol %). To the homogeneous solution was added Et_3N (20.2 g, 200.0 mmol, 27.9 mL, 2 equiv) and trityl chloride (27.8 g, 100.0 mmol, 1 equiv). The reaction was stirred at ambient temperature for 18 h and H_2O (225 mL) was

subsequently added. The resultant mixture was extracted with Et_2O (3 x 200 mL). The combined organic layers were washed with brine (2 x 50 mL), dried over Na_2SO_4, and concentrated under reduced pressure to afford a white solid.

The solid was dissolved in a minimal volume of CH_2Cl_2 (30 mL) and purified via flash column chromatography on SiO_2 (300 g SiO_2, Et_2O/hexanes = 5%) to afford product **31** (21.9 g, 70.1 mmol, 70% yield) as a white solid. Spectral data were in complete agreement with literature values.

TLC (20% Et_2O/hexanes): R_f = 0.73 (UV, $KMnO_4$).

Preparation of ynoate 32

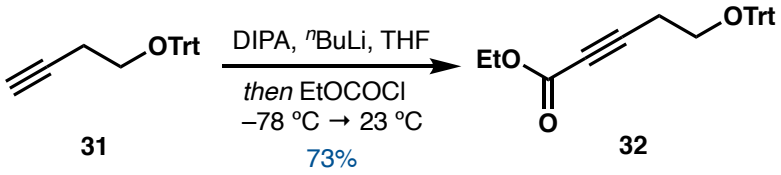

The atmosphere of a flame-dried, 1 L round-bottom flask equipped with a stir bar was exchanged three times for nitrogen, then charged with anhydrous THF (180 mL) and freshly distilled diisopropylamine (9.58 g, 94.6 mmol, 13.3 mL, 1.35 equiv). The mixture was cooled to –78 °C and ^{n}BuLi (35.9 mL of a 2.46 M solution, 88.3 mmol, 1.26 equiv) was added slowly over 15 min. The solution was stirred at –78 °C for 5 min, warmed to 0 °C, stirred 10 min, then cooled back to –78 °C. Thereafter, a solution of the trityl-protected substrate **31** (21.9 g, 70.1 mmol, 1 equiv) in anhydrous THF (70 mL) was added dropwise over 30 min, and the reaction was stirred for an additional 15 min. Ethyl chloroformate (22.8 g, 210.3 mmol, 20.1 mL, 3 equiv) was then

added over 15 min, and the reaction was stirred for an additional 10 min before being warmed to ambient temperature and stirred for 3 h.

The reaction was quenched via addition of saturated aq. NH_4Cl (150 mL) and stirred for 10 min. Thereafter, H_2O (150 ml) was added, the reaction was extracted into Et_2O (2 x 150 mL), the combined organic layers were dried over Na_2SO_4, and concentrated under reduced pressure to afford a pale yellow solid. The crude residue was suspended in hexanes (80 mL), heated to a boil, additional hexanes (100 mL) was added, and the heterogeneous suspension was filtered while hot to remove residual ammonium salts. The mixture was re-heated and slowly cooled overnight to afford product **32** (19.6 g, 51.0 mmol, 73% yield) as white crystals.

TLC (20% Et_2O/hexanes): R_f = 0.52 (UV).

^{1}H NMR (400 MHz, $CDCl_3$): δ 7.52–7.42 (m, 6H, ***Ph*$_3$CO**), 7.34–7.20 (m, 9H, ***Ph*$_3$CO**), 4.25 (q, *J* = 7.2 Hz, 2H, OC***H***$_2$CH$_3$), 3.31 (t, *J* = 6.9 Hz, 2H, C_{14}), 2.63 (t, *J* = 6.9 Hz, 2H, C_{13}), 1.34 (t, *J* = 7.1 Hz, 3H, OCH_2C***H***$_3$).

^{13}C NMR (101 MHz, $CDCl_3$): δ 153.7 (C_{20}=O), 143.7 (***Ph*$_3$CO**), 128.6 (***Ph*$_3$CO**), 127.9 (***Ph*$_3$CO**), 127.1 (***Ph*$_3$CO**), 86.9 (Ph_3***C***O), 86.5 (C_{12}), 74.0 (C_{19}), 61.9 (O***C***H_2CH_3), 61.1 (C_{14}), 20.3 (C_{13}), 14.1 (OCH_2***C***H_3).

FTIR (AT-IR): 2937, 2882, 2243, 1713, 1471, 1377, 1018 cm^{-1}.

HRMS (FAB+, m/z): calc'd for $C_{26}H_{24}O_3$ $[M]^+$ 384.1726, found 384.1739.

Melting point: 89.4–90.0 °C

Preparation of acrylate 33

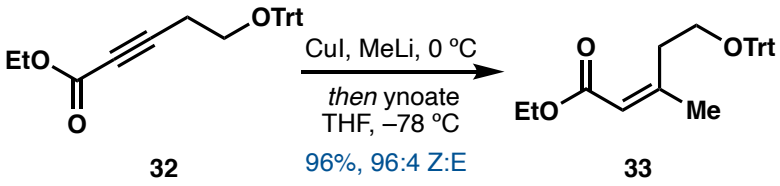

32 **33**

In a nitrogen-filled glovebox, a flame-dried 2 L flask equipped with a large stir bar was charged with CuI (9.68 g, 50.9 mmol, 1 equiv). Anhydrous THF (390 mL) was transferred to the flask via cannula, and the heterogeneous suspension was stirred at 0 °C for 20 min. Thereafter, MeLi (64.8 mL of a 1.57 M solution in Et_2O, 101.7 mmol, 2 equiv) was added dropwise over 25 min during which time the reaction went from a heterogeneous brown suspension to a nearly colorless, homogeneous solution. After an additional 5 min of stirring, the mixture was cooled to –78 °C and stirred for 20 min prior to dropwise addition of alkynoate ester **32** (19.6 g, 50.9 mmol, 1 equiv) in anhydrous THF (130 mL) via cannula over 20 min. The reaction was stirred at –78 °C for 2 h then quenched with H_2O (25 mL) at –78 °C.

After 10 min, the solution was warmed to ambient temperature, filtered through a pad of Celite, and the Celite was rinsed with Et_2O (3 x 75 mL). The combined organic layers were washed with H_2O (2 x 50 mL) and brine (1 x 50 mL), dried over Na_2SO_4, and concentrated under reduced pressure to afford acrylate **33** (19.5 g, 48.7 mmol, 96% yield, 96:4 *Z:E*) as a viscous, yellow oil.

TLC (10% Et_2O/hexanes): R_f = 0.55 (UV).

^{1}H NMR (400 MHz, $CDCl_3$): δ 7.48–7.41 (m, 6H, ***Ph***$_3$CO), 7.32–7.19 (m, 9H, ***Ph***$_3$CO), 5.74 (d, *J* = 1.4 Hz, 1H, C_{19}), 4.13 (q, *J* = 7.1 Hz, 2H, OC***H***$_2$CH$_3$), 3.26 (t, *J* = 6.4 Hz, 2H,

C_{14}), 2.97 (t, J = 6.4 Hz, 2H, C_{13}), 1.90 (d, J = 1.4 Hz, 3H, C_{18}), 1.26 (t, J = 7.1 Hz, 3H, $OCH_2C\boldsymbol{H}_3$).

^{13}C NMR (101 MHz, $CDCl_3$): δ 166.2 (C_{20}=O), 157.9 (C_{12}), 144.2 (***Ph*$_3$**CO), 128.7 (***Ph*$_3$**CO), 127.7 (***Ph*$_3$**CO), 126.8 (***Ph*$_3$**CO), 117.5 (C_{19}), 86.6 ($Ph_3\boldsymbol{C}O$), 62.4 (C_{14}), 59.5 ($O\boldsymbol{C}H_2CH_3$), 33.7 (C_{13}), 26.1 (C_{18}), 14.3 ($OCH_2\boldsymbol{C}H_3$).

FTIR (AT-IR): 2982, 2915, 2873, 1709, 1652, 1489, 1447, 1265, 1194, 1146, 779 cm^{-1}.

HRMS (FAB+, m/z): calc'd for $C_{17}H_{27}O_3[(M+H)–H_2]^+$ 399.1960, found 399.1958.

Preparation of allylic alcohol 34

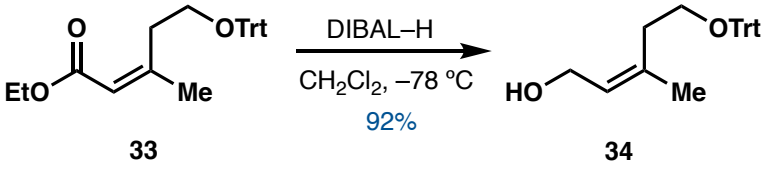

33 **34**

The atmosphere of a flame-dried, 1 L round-bottom flask equipped with a stir bar was exchanged three times for argon then charged with acrylate **33** (19.5 g, 48.7 mmol, 1 equiv) and anhydrous CH_2Cl_2 (162 mL) and cooled to –78 °C. Subsequently, a freshly-prepared solution of DIBAL-H (20.8 g, 146.2 mmol, 26.1 mL) in anhydrous hexanes (122 mL) was added via cannula over 25 min. The resulting light yellow reaction was stirred at –78 °C for 2 h.

The reaction was quenched at –78 °C via slow addition of H_2O (30 mL) followed by 2 M NaOH (30 mL), stirred 10 min at –78 °C, and warmed to 0 °C. Additional H_2O (30 mL) was added, and the suspension was transferred to a 1 L Erlenmeyer flask containing a large stir bar and cooled to 0 °C. Subsequently, anhydrous $MgSO_4$ (100 g) was added slowly, and a strongly exothermic reaction was observed. After stirring vigorously for 20

min, the slurry was filtered through Celite, the Celite was washed with Et_2O (3 x 100 mL), and concentrated under reduced pressure to afford a viscous, pale yellow oil.

Purification was achieved via flash column chromatography on SiO_2 [300 g SiO_2, Et_2O/hexanes = 30% → 50%] to afford allylic alcohol **34** (16.2 g, 45.2 mmol, 92% yield) as a viscous, colorless oil.

TLC (30% Et_2O/hexanes): R_f = 0.30 ($KMnO_4$).

^{1}H NMR (400 MHz, $CDCl_3$): δ 7.48–7.41 (m, 6H, ***Ph*$_3$CO**), 7.32–7.19 (m, 9H, ***Ph*$_3$CO**), 5.59 (t, *J* = 7.1 Hz, 1H, C_{19}), 4.14 (d, *J* = 7.1 Hz, 2H, C_{20}), 3.20 (t, *J* =6.4 Hz, 2H, C_{14}), 2.37 (t, *J* = 6.4 Hz, 2H, C_{13}), 1.66 (s, 3H, C_{18}), 1.50 (br m, 1H, O***H***).

^{13}C NMR (101 MHz, $CDCl_3$): δ 144.0 (***Ph*$_3$CO**), 137.5 (C_{12}), 128.7 (***Ph*$_3$CO**), 127.8 (***Ph*$_3$CO**), 127.0 (***Ph*$_3$CO**), 126.1 (C_{19}), 87.0 (Ph$_3$***C***O), 61.8 (C_{14}), 58.9 (C_{20}), 32.6 (C_{13}), 23.7 (C_{18}).

FTIR (AT-IR): 3361 (br), 3057, 2915, 2875, 1596, 1490, 1448, 1265, 1061, 1001 cm^{-1}.

HRMS (TOF, ES+): calc'd for $C_{25}H_{26}O_2Na$ $[M+Na]^+$ 381.1831, found 381.1843.

Preparation of *Z*-allylic boronic acid 35

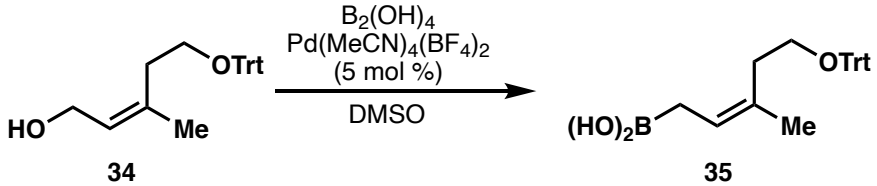

This procedure was adapted from the work of Szabó and coworkers.[5] In a nitrogen-filled glovebox, a flame-dried, 100 mL round-bottom flask equipped with a stir bar was charged with allylic alcohol **34** (2.67 g, 7.45 mmol, 1 equiv) and anhydrous, degassed DMSO (18.6

mL, 0.4 M). The mixture was stirred until the viscous allylic alcohol dissolved, at which time $Pd(MeCN)_4(BF_4)_2$ (165 mg, 0.373 mmol, 5 mol %) was added, followed by tetrahydroxydiboron (801 mg, 8.94 mmol, 1.2 equiv). The reaction was vigorously stirred and transformed from a dark orange/red solution to dark green to black within 2 min. After stirring for 90 min at ambient temperature, the black mixture was transferred via cannula to a 100 mL Schlenk flask, the atmosphere of which had been exchanged with argon three times. Degassed PhMe (37.0 mL) was added to the black mixture followed by degassed 16% aq. NaCl (15 mL). The system was sealed off, shaken, and the layers were separated. The organic layer was washed with additional degassed 16% aq. NaCl (3 x 15 mL) to afford an organic solution with a black particulate suspension. The suspension was allowed to stand for 30 min, during which time the particulates settled. The top solution was transferred via cannula to a 100 mL Schlenk tube, the atmosphere of which had been exchanged with argon three times, and the tube was pumped into the glovebox where naphthalene was added as an internal standard. A ^1H NMR sample was prepared in the glovebox using dry, degassed $CDCl_3$, and it was determined that [allylicboronic acid] = 0.18 M. Allylicboronic acid **35** was immediately used in the next reaction.

Preparation of crotylation adducts 36 and 7

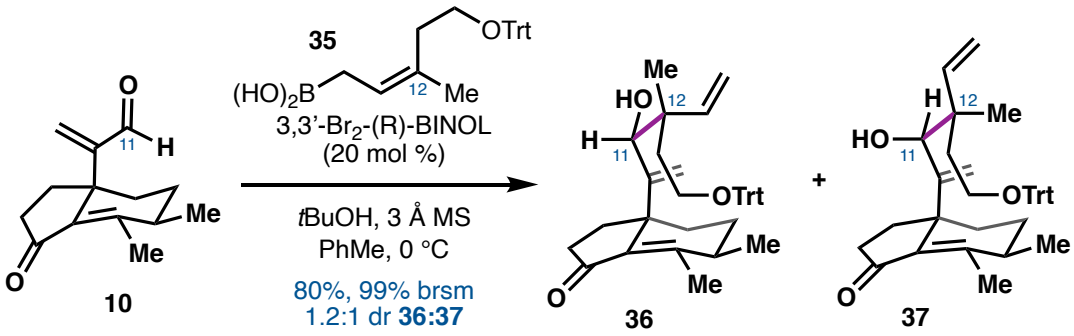

This procedure was adapted from the work of Szabó and coworkers.[10] In a nitrogen-filled glovebox, a flame-dried, 100 mL Schlenk flask equipped with a stir bar was charged with freshly activated 3 Å molecular sieves (pellets) (1.79 g), allylicboronic acid **35** (25.3 mL of a 0.18 M solution, 4.47 mmol, 1 equiv), 3,3′-Br_2-(*R*)-BINOL (397 mg, 0.894 mmol, 20 mol %), freshly distilled *t*BuOH (1.28 mL, 13.4 mmol, 3 equiv), and a solution of the enal hydrindanone **10** (976 mg, 4.47 mmol, 1 equiv) in dry, degassed PhMe (4.5 mL). The resulting heterogeneous mixture was sealed, removed from the glovebox, cooled to –30 °C for 5 min, then placed in a pre-equilibrated 0 °C bath and stirred.

After 40 h, the reaction was quenched with MeOH (5 mL), stirred for 5 min, filtered, and concentrated under reduced pressure to afford a viscous residue. Purification was achieved via flash column chromatography on SiO_2 [100 g SiO_2, Acetone/hexanes = 4%→15%] to afford remaining enal (fractions 22–31), the desired diastereomer **36** (fractions 37–70), and **37** and residual 3,3′-Br_2-(*R*)-BINOL (fractions 71–85). The volatiles were concentrated under reduced pressure to afford remaining enal (237 mg, 1.09 mmol, 24% recovered contaminated with ~5% protodeboronated nucleophile), the desired diastereomer **36** (1.03 g, 1.84 mmol, 41% yield), and the more polar diastereomer **37**/BINOL mixture respectively.

The **7**/BINOL mixture was subjected to flash column chromatography on SiO_2 [100 g SiO_2, Et_2O/hexanes = 40%] to afford 3,3′-Br_2-(*R*)-BINOL (fractions 1–3) and the more polar diastereomer **37** (fractions 23–38). 3,3′-Br_2-(*R*)-BINOL (343 mg, 0.772 mmol, 86% recovered) and the more polar diastereomer **37** (972 mg, 1.73 mmol, 39% yield) were obtained. Both diastereomers were isolated as puffy white foams.

Experimental Note: It is critical that all operations be carried out in a rigorously oxygen-free environment. Failure to do so will result in rapid decomposition of the allylicboronic acid.

Preparation of vinyl cyclohexanone 41

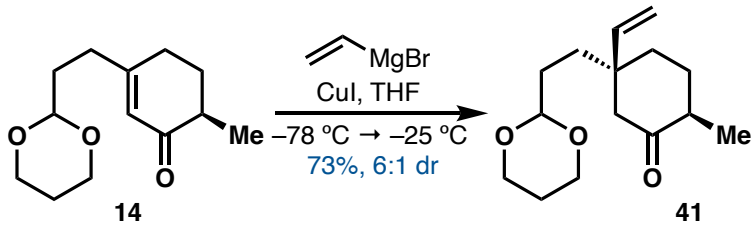

A flame-dried, 2 L, 2-necked round-bottom flask equipped with a stir bar was evacuated and backfilled with argon three times. The flask was charged with CuI (9.27 g, 48.7 mmol, 1.5 equiv) and THF (325 mL). The suspension was cooled to –78 ºC and stirred for 15 min. vinylmagnesium bromide (1.0 M in THF (Aldrich), 97.4 mL, 97.4 mmol, 3 equiv) was added dropwise via cannula transfer and the solution was stirred for 5 min. The reaction was warmed to –25 ºC and stirred for 30 min. Thereafter, the mixture was cooled back down to –78 ºC and stirred for 15 min. Trisubstituted enone **14** (7.29 g, 32.5 mmol, 1 equiv) was dissolved in THF (325 mL) and added dropwise via cannula transfer. The solution was warmed to –50 ºC and stirred until complete by TLC analysis. The reaction

mixture was quenched with sat. aq. NH_4Cl (400 mL) at –50 ºC and the biphasic solution was warmed to ambient temperature. The layers were separated and the aqueous phase was extracted with Et_2O (3 x 350 mL). The combined organic layers were washed with brine (100 mL), dried over $MgSO_4$, and concentrated under reduced pressure to afford a viscous oil.

Purification was achieved via flash column chromatography on SiO_2 [40% EtOAc/hexanes → 25% → 50%] to afford vinyl cyclohexenone **41** (4.32 g, 24.4 mmol, 73% yield) as a clear oil.

^{1}H NMR (300 MHz, $CDCl_3$): δ 5.47 (ddd, *J* = 17.7, 11.0, 0.9 Hz, 1H), 5.13 (dd, *J* = 11.0, 0.8 Hz, 1H), 4.94 (dd, *J* = 17.7, 0.8 Hz, 1H), 4.47 (dd, *J* = 5.0, 3.7 Hz, 1H), 4.11 – 4.05 (m, 2H), 3.79 – 3.68 (m, 2H), 2.60 – 2.53 (m, 1H), 2.24 (dtd, *J* = 12.4, 6.1, 1.3 Hz, 1H), 2.14 (dt, *J* = 13.9, 1.1 Hz, 1H), 2.14 – 1.97 (m, 2H), 1.87 (ddt, *J* = 13.0, 6.0, 3.4 Hz, 1H), 1.72 (ddt, *J* = 8.7, 3.6, 1.5 Hz, 2H), 1.51 (dt, *J* = 3.9, 1.3 Hz, 2H), 1.33 (dtt, *J* = 13.5, 2.7, 1.4 Hz, 1H), 0.98 (d, *J* = 6.5 Hz, 3H).

Preparation of aldehyde 42

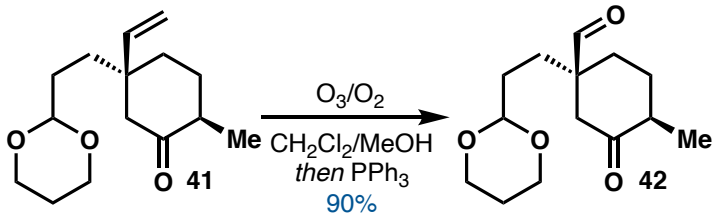

A 1 L round-bottom flask equipped with a stir bar was charged with vinyl cyclohexanone **41** (7.83 g, 31.0 mmol, 1 equiv), MeOH (62 mL), CH_2Cl_2 (155 mL), and cooled to –78 ºC. The solution was ozonolyzed for 10 min or until complete by TLC analysis. Upon completion, the solution turned light blue. The reaction mixture was

sparged with O_2 for 20 min, then Ar for 5 min, and quenched with PPh_3 (6.24 g, 23.8 mmol. 1.5 equiv). The suspension was allowed to stir for 3 hours, where it was then concentrated under reduced pressure to afford a crude white solid.

Purification was achieved via flash column chromatography on SiO_2 [40% EtOAc/hexanes → 50%] to afford aldehyde **42** (10.6 g, 42.1 mmol, 90% yield).

^{1}H NMR (400 MHz, $CDCl_3$): δ 9.37 (s, 1H), 4.47 (t, *J* = 4.8 Hz, 1H), 4.06 (ddt, *J* = 10.5, 5.0, 1.4 Hz, 2H), 3.72 (dddt, *J* = 14.2, 10.4, 2.6, 1.0 Hz, 2H), 2.69 (dd, *J* = 14.4, 2.5 Hz, 1H), 2.25 (dddd, *J* = 12.4, 6.9, 5.9, 1.2 Hz, 1H), 2.15 – 1.89 (m, 4H), 1.84 – 1.38 (m, 6H), 1.36 – 1.18 (m, 2H), 0.99 (d, *J* = 6.6 Hz, 3H).

^{13}C NMR (101 MHz, $CDCl_3$): δ 209.7, 209.7, 204.0, 204.0, 101.2, 101.2, 66.8, 66.8, 53.9, 44.9, 44.3, 30.8, 30.6, 30.3, 29.2, 25.6, 14.2.

HRMS (FAB+, m/z): calc'd for $C_{14}H_{23}O_4$

$[\alpha]_D^{23}$: +4.06° (*c* = 1.16, $CHCl_3$).

Preparation of bicycle 43

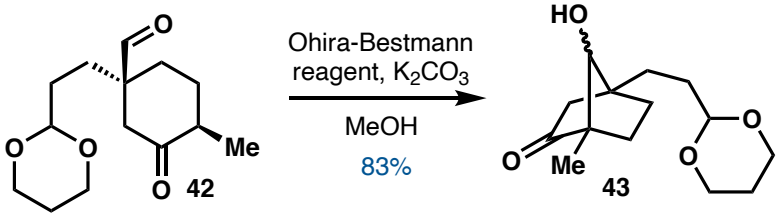

To a 1 dram vial equipped with a stir bar was charged aldehyde **42** (10 mg, 0.039 mmol, 1 equiv) and MeOH (650 µL) at 23 ºC. Ohira-Bestmann reagent was then added in MeOH (650 µL) and the reaction was allowed to stir until complete by TLC analysis. The reaction mixture was quenched with H_2O (500 µL) and the aqueous phase was extracted

with Et_2O (3 x 1 mL). The combined organic layers were washed with brine (2 mL), dried over $MgSO_4$, and concentrated under reduced pressure to afford a clear oil.

Purification was achieved via flash column chromatography on SiO_2 [70% EtOAc/hexanes to afford bicycle **43** (8.3 mg, 0.032 mmol, 83% yield).

TLC (50% EtOAc/hexanes): R_f = 0.20 (*p*-anisaldehyde).

^{1}H NMR (400 MHz, $CDCl_3$): δ 4.60 – 4.52 (m, 1H), 4.11 (ddt, *J* = 9.6, 4.4, 1.3 Hz, 2H), 3.83 – 3.71 (m, 2H), 3.48 (d, *J* = 2.4 Hz, 3H), 2.58 (d, *J* = 20.6 Hz, 1H), 2.16 – 2.00 (m, 2H), 1.95 – 1.82 (m, 2H), 1.69 – 1.52 (m, 3H), 1.51 – 1.30 (m, 3H), 1.08 (s, 3H).

^{13}C NMR (101 MHz, $CDCl_3$): δ 215.6, 102.2, 82.9, 81.3, 67.0, 58.2, 57.2, 50.9, 48.8, 47.2, 46.9, 45.4, 31.2, 30.8, 29.9, 29.1, 28.5, 27.6, 25.9, 11.3, 11.1.

Preparation of cyclohexanone 44

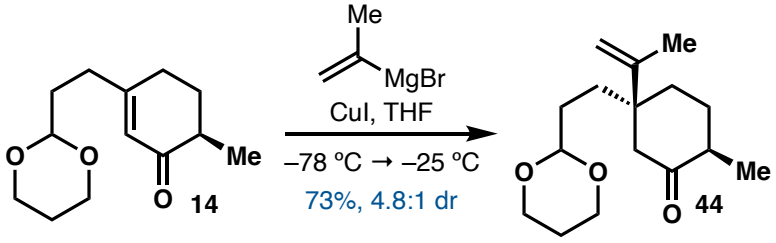

A flame-dried, 3 L, 2-necked round-bottom flask equipped with a stir bar was evacuated and backfilled with argon three times. The flask was charged with CuI (17.6 g, 92.6 mmol, 1.5 equiv) and THF (617 mL). The suspension was cooled to –78 ºC and stirred for 15 min. Isopropenylmagnesium bromide (0.5 M in THF (Aldrich), 371 mL, 185 mmol, 3 equiv) was added dropwise via cannula transfer and the solution was stirred for 5 min. The reaction was warmed to –25 ºC and stirred for 10 min. Thereafter, the mixture was cooled back down to –78 ºC and stirred for 15 min. Trisubstituted enone **14** (13.9 g, 61.8

mmol, 1 equiv) was dissolved in THF (617 mL) and added dropwise via cannula transfer. The solution was warmed to –50 ºC and stirred for 25 min or until complete by TLC analysis. The reaction mixture was quenched with sat. aq. NH_4Cl (400 mL) at –50 ºC, and the biphasic solution was warmed to ambient temperature. The layers were separated and the aqueous phase was extracted with Et_2O (3 x 350 mL). The combined organic layers were washed with brine (100 mL), dried over $MgSO_4$ and concentrated under reduced pressure to afford 18.4 g of a viscous oil.

Purification was achieved via flash column chromatography on SiO_2 [1400 g SiO_2, 20% EtOAc/hexanes] to afford isopropenyl cyclohexenone **44** (11.64 g, 43.7 mmol, 71% yield) as a white solid.

Major Diastereomer (44)

TLC (20% EtOAc/hexanes): R_f = 0.16 (*p*-anisaldehyde).

^{1}H NMR (400 MHz, $CDCl_3$): δ 4.93 (br s, 1H, C_{17}), 4.69 (s, 1H, C_{17}), 4.45 (t, *J* = 4.7 Hz, 1H, C_3), 4.07 (m, 2H, O*C**H**$_2$*CH_2), 3.72 (m, 2H, O*C**H**$_2$*CH_2), 2.73 (dd, *J* = 14.2, 3.0 Hz, 1H, C_4), 2.20 (app d of septets, *J* = 6.7, 1.2 Hz, 1H, C_6), 2.07 (dd, *J* = 14.2, 1.0 Hz, 1H, C_4), 2.04 (m, 1H, O*C*H$_2$*C**H**$_2$), 1.96 (dq, *J* = 13.8, 3.2 Hz, 1H, C_8), 1.83 (m, 1H, C_7), 1.65 (m, 1H, C_2), 1.61 (dd, *J* = 1.2, 0.5 Hz, 3H, C_{11}), 1.59 (m, 1H, C_8), 1.46 (m, 1H, C_1), 1.41 (m, 1H, C_1), 1.37 (m, 1H, C_2), 1.36 (m, 1H, C_7), 1.32 (m, 1H, O*C*H$_2$*C**H**$_2$), 0.97 (d, *J* = 6.5 Hz, 3H, C_{16}).

^{13}C NMR (101 MHz, $CDCl_3$): δ 212.2 (C_5=O), 145.7 (C_{10}), 116.0 (C_{17}), 102.3 (C_3), 66.9 (O***C***H_2CH_2), 49.8 (C_4), 47.7 (C_9), 44.8 (C_6), 34.8 (C_8), 34.5 (C_2), 30.4 (C_7), 29.5 (C_1), 25.7 (OCH_2***C***H_2), 18.9 (C_{11}), 14.5 (C_{16}).

FTIR (AT-IR): 2960, 2929, 2853, 1706, 1454, 1239, 1144, 994, 880 cm^{-1}.

HRMS (FAB+, m/z): calc'd for $C_{16}H_{27}O_3$ $[M+H]^+$ 267.1960, found: 267.1966.

$[\alpha]_D^{23}$**:** +42° (*c* = 1.16, $CHCl_3$).

Minor Diastereomer

TLC (20% EtOAc/hexanes): R_f = 0.27 (*p*-anisaldehyde).

^{1}H NMR (400 MHz, $CDCl_3$): δ 4.86 (pent, *J* = 1.2 Hz, 1H, C_{17}), 4.70 (m, 1H, C_{17}), 4.42 (m, 1H, C_3), 4.06 (ddt, *J* = 10.5, 5.0, 1.2 Hz, 2H, O*C**H₂**CH_2), 3.72 (m, 2H, O*C**H₂**CH_2), 2.40 (dd, *J* = 13.3, 2.0 Hz, 1H, C_4), 2.35 (m, 1H, C_6), 2.32 (m, 1H, C_4), 2.07 (tt, *J* = 13.3, 5.2 Hz, 1H, O*C*H_2C***H***$_2$), 1.98 (m, 1H, C_7), 1.88 (m, 1H, C_1), 1.76 (td, *J* = 11.5, 4.1 Hz, 1H, C_1), 1.68 (dd, *J* = 1.3, 0.8 Hz, 3H, C_{11}), 1.50 (m, 1H, C_7), 1.40 (m, 1H, C_2), 1.39 (m, 1H, C_2), 1.37 (m, 1H, C_8), 1.35 (m, 1H, C_8), 1.30 (m, 1H, O*C*H_2C***H***$_2$), 1.05 (d, *J* = 6.7 Hz, 3H, C_{16}).

^{13}C NMR (101 MHz, $CDCl_3$): δ 213.3 (C_5=O), 148.8 (C_{10}), 111.9 (C_{17}), 102.3 (C_3), 66.9 (O***C***H_2CH_2), 66.8 (O***C***H_2CH_2), 50.0 (C_4), 46.7 (C_9), 44.3 (C_6), 31.9 (C_1), 30.2 (C_7), 29.5 (C_8), 28.2 (C_2), 25.7 (OCH_2***C***H_2), 19.0 (C_{11}), 14.9 (C_{16}).

FTIR (AT-IR): 2961, 2930, 2850, 1708, 1635, 1452, 1377, 1143, 994, 880 cm^{-1}.

HRMS (FAB+, m/z): calc'd for $C_{16}H_{27}O_3$ $[M+H]^+$ 267.1960, found: 267.1949.

$[\alpha]_D^{23}$**:** +1.9° (*c* = 0.91, $CHCl_3$).

Preparation of allylic chloride 48

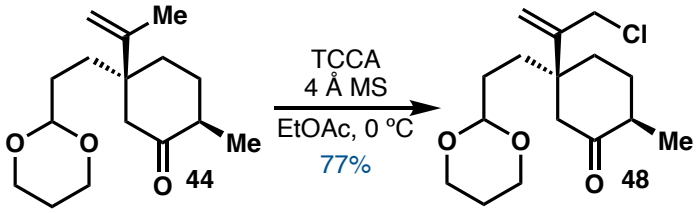

This procedure was adapted from the work of Kumar and coworkers.[21] A flame-dried, 2 L, 2-neck round-bottom flask equipped with a stir bar was charged with activated 4 Å mol sieves and cyclohexanone **44** (12.06 g, 45.28 mmol, 1 equiv). The atmosphere was exchanged three times with argon before adding EtOAc (916 mL, 0.05 M) that had been degassed with argon. The resulting colorless solution was cooled to 0 ºC and stirred for an additional 10 min. Subsequently, finely ground trichloroisocyanuric acid (TCCA) (10.52 g, 45.28 mmol, 1 equiv) was added in one portion. The reaction was stirred (900 rpm) for 10 min or until complete by TLC analysis. The reaction mixture was quenched at 0 ºC with sat. aq. $Na_2S_2O_3$ (150 mL). The biphasic solution was warmed to ambient temperature and filtered. The aqueous layer was extracted with EtOAc (4 x 100 mL). The combined organic layers were washed with H_2O (100 mL), dried over $MgSO_4$, filtered, and concentrated under reduced pressure to afford a yellow oil.

Purification was achieved via flash column chromatography on SiO_2 [1400 g SiO_2, 15% EtOAc/hexanes → 30%] to afford allylic chloride **48** (10.52 g, 39.5 mmol, 77% yield) as a white solid.

TLC (50% EtOAc/hexanes): R_f = 0.5 (*p*-anisaldehyde).

^{1}H NMR (400 MHz, $CDCl_3$): δ 5.54 (s, 1H, C_{17}), 5.15 (s, 1H, C_{17}), 4.46 (t, *J* = 4.8 Hz, 1H, C_3), 4.12 – 4.03 (m, 2H, O***CH***$_2$$CH_2$$C$***H***$_2$O), 4.01 (d, *J* = 1.0 Hz, 2H, C_{11}), 3.73 (td, *J* =

12.2, 2.4 Hz, 2H, OC***H***$_2$CH$_2$C***H***$_2$O), 2.76 (dd, *J* = 14.2, 3.0 Hz, 1H, C$_4$), 2.34 – 2.20 (m, 1H, C$_6$), 2.14 (dd, *J* = 14.2, 1.1 Hz, 1H, C$_2$), 2.04 (tdd, *J* = 17.5, 8.7, 4.2 Hz, 2H, C$_1$), 1.89 (ddt, *J* = 13.3, 6.6, 3.5 Hz, 1H, C$_7$), 1.80 – 1.65 (m, 2H, C$_8$), 1.55 – 1.28 (m, 4H, C$_1$, C$_7$, C$_2$, OCH$_2$C***H$_2$***CH$_2$O), 0.99 (d, 3H, C$_{16}$).

^{13}C NMR (101 MHz, CDCl$_3$): δ 211.7 (C$_5$=O), 145.0 (C$_{10}$), 121.0 (C$_{17}$), 101.9 (C$_3$), 66.9 (O**C**H-$_2$CH$_2$**C**H$_2$O), 50.2 (C$_4$), 48.1 (C$_9$), 44.9 (C$_6$), 44.0 (C$_{11}$), 35.0 (C$_8$), 35.0 (C$_1$), 30.6 (C$_7$), 29.5 (C$_2$), 25.7 (OCH$_2$**C**H$_2$CH$_2$O), 14.4 (C$_{16}$).

FTIR (AT-IR): 2929, 2359, 1707, 1377, 1214, 1143, 1079, 880, 730, 668 cm^{-1}.

HRMS (FAB+, m/z): calc'd for C$_{16}$H$_{26}$O$_3$Cl [M+H]$^+$ 301.1571, found: 301.1564.

$[\alpha]_D^{23}$: +49° (*c* = 0.495, CHCl$_3$).

Preparation of hydrindanone 49

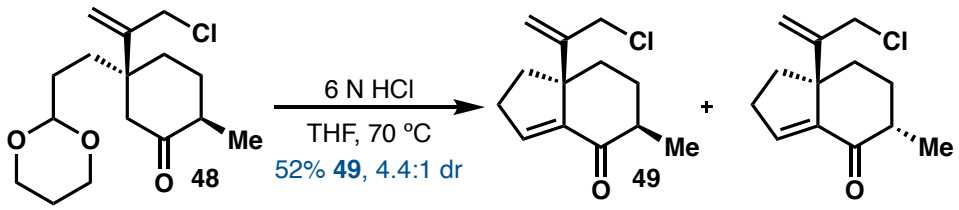

A 250 mL round-bottom flask equipped with a stir bar and reflux condenser was charged with allylic chloride **48** (10.8 g, 35.9 mmol, 1 equiv) and THF (125 mL). The homogeneous solution was vigorously stirred (960 rpm), and 6 N HCl (17.96 mL, 108 mmol, 3 equiv) was added dropwise. The reaction was heated to 70 ºC and stirred for 4 h. The reaction was quenched with sat. aq. NaHCO$_3$ (45 mL). The layers were separated and the aqueous layer was extracted with Et$_2$O (3 x 75 mL). The combined organic layers were washed with brine (25 mL) and dried over MgSO$_4$. The suspension was filtered, and concentrated under reduced pressure to afford 10.4 g of a viscous yellow oil.

Purification was achieved via flash column chromatography on SiO_2 [1400 g SiO_2, 5% Et_2O/hexanes → 10%] to afford enone **49** (4.15 g, 18.5 mmol, 52% yield) as a colorless solid.

Major Diastereomer (49)

TLC (50% Et_2O/hexanes): R_f = 0.75 (UV, *p*-anisaldehyde).

^{1}H NMR (400 MHz, $CDCl_3$): δ 6.55 (t, *J* = 2.7 Hz, 1H, C_3), 5.39 (s, 1H, C_{17}), 4.96 (s, 1H, C_{17}), 4.16 – 4.05 (m, 2H, C_{11}), 2.39 – 2.32 (m, 3H, C_1, C_2), 2.29 – 2.18 (m, 2H, C_6, C_8), 1.95 – 1.84 (m, 2H, C_7, C_8), 1.73 – 1.45 (m, 2H, C_1, C_7), 1.09 (d, *J* = 6.7 Hz, 2H, C_6).

^{13}C NMR (101 MHz, $CDCl_3$): δ 202.1 (C_5=O), 146.8 (C_4), 146.4 (C_{10}), 137.6 (C_3), 119.0 (C_{17}), 57.9 (C_9), 45.2 (C_6), 44.7 (C_{11}), 39.4 (C_8), 35.3 (C_1), 30.5 (C_7), 30.1 (C_2), 14.9 (C_{16}).

FTIR (AT-IR): 2929, 2860, 1682, 1622, 1454, 1312, 1232, 1012, 927, 757, cm^{-1}.

HRMS (FAB+, m/z): calc'd for $C_{13}H_{18}ClO$ $[M+H]^+$ 225.1046, found: 225.1061.

$[\alpha]_D^{23}$: +58.4° (*c* = 0.715, $CHCl_3$).

Minor Diastereomer

TLC (50% Et_2O/hexanes): R_f = 0.75 (UV, *p*-anisaldehyde)

^{1}H NMR (400 MHz, $CDCl_3$): δ 6.70 (t, *J* = 2.7 Hz, 1H, C_3), 5.3 (s, 1H, C_{17}), 5.00 (s, 1H, C_{17}), 4.21 – 4.01 (m, 2H, C_{11}), 2.55 – 2.44 (m, 1H, C_6), 2.42 – 2.32 (m, 2H, C_2), 2.28 (ddt, *J* = 12.6, 5.4, 2.7 Hz, 1H, C_1), 2.16 (dt, *J* = 13.8, 4.0 Hz, 1H, C_8), 2.04 – 1.83 (m, 2H, C_1, C_7), 1.74 (td, *J* = 13.4, 3.9 Hz, 1H, C_8), 1.54 (dq, *J* = 13.9, 3.9 Hz, 1H, C_7), 1.12 (d, *J* = 7.4 Hz, 3H, C_{16}).

^{13}C NMR (101 MHz, $CDCl_3$): δ 203.4 (C_5=O), 146.7 (C_4), 145.3 (C_{10}), 140.1 (C_3), 118.2 (C_{17}), 56.7 (C_9), 44.8 (C_{11}), 41.9 (C_6), 39.8 (C_{12}), 30.7 (C_8), 30.0 (C_2), 28.0 (C_7), 17.8 (C_{16}).

FTIR (AT-IR): 2925, 2855, 1687, 1620, 1456, 1376, 1262, 1175, 1098, 924 cm^{-1}.

HRMS (EI+, m/z): calc'd for $C_{13}H_{17}ClO$ $[M]^+$224.0968, found: 224.0940.

$[\alpha]_D^{23}$**:** 46.8° (*c* = 0.115, $CHCl_3$).

Preparation of allylic alcohol 50

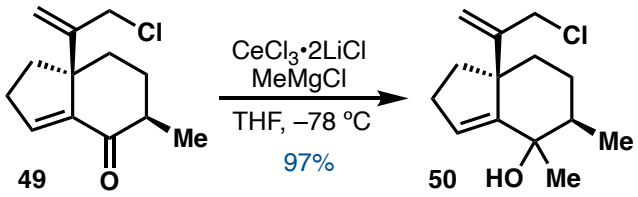

A flame-dried, 50 mL round-bottom flask equipped with a stir bar was charged with enone **49** (1.101 g, 4.9 mmol, 1 equiv). The atmosphere was exchanged with argon three times before adding a solution of $CeCl_3$•2LiCl (0.3 M in THF, 16.3 mL, 1 equiv). Upon addition of $CeCl_3$•2LiCl, a bright yellow solution was obtained and stirred for 1 h at ambient temperature. The reaction mixture was then cooled to –78 ºC and stirred for 15 min. The solution then became pale yellow slurry and stirring became difficult. A solution of methylmagnesium chloride (3.0 M in THF (Aldrich), 3.3 mL, 9.8 mmol, 2 equiv) was added dropwise over 30 min. The slurry was perturbed by hand until magnetic stirring resumed. The reaction was stirred at –78 ºC until TLC analysis indicated complete consumption of starting material (about 15 min).

The gray solution was quenched at –78 ºC via slow addition of 1 M HCl (15 mL) using a vent needle to relieve excess pressure. Thereafter, the solution was warmed to ambient temperature while the slurry slowly quenched. The mixture was then transferred to a separatory funnel and diluted with H_2O (20 mL) and Et_2O (50 mL). The layers separated, and the aqueous layer was extracted with Et_2O (3 x 20 mL). The combined

organic layers were washed with brine (40 mL) and dried over $MgSO_4$. The suspension was filtered and concentrated under reduced pressure to afford a yellow oil.

Purification was achieved via flash column chromatography on SiO_2 [100 g SiO_2, 45 mL fractions, 200 mL forerun, Et_2O/hexanes = 15% (1.2 L), 30% (250 mL), 40% (1 L)] to afford the less polar diastereomer (fractions 3–10) followed by the more polar diastereomer (fractions 17–33). The volatiles were concentrated under reduced pressure to afford an inconsequential mixture of diastereomers **50** (1.15 g, 4.78 mmol, 97% combined yield). An analytically pure sample of the less polar diastereomer was obtained and a representative spectrum of the mixture as used in the next step is also provided.

TLC (20% Et_2O/hexanes): R_f = 0.46 and 0.09 (*p*-anisaldehyde).

^{1}H NMR (400 MHz, $CDCl_3$): δ 5.79 (t, *J* = 2.4 Hz, 1H, C_3), 5.44 – 5.41 (m, 1H, C_{17}), 5.27 (s, 1H, C_{17}), 4.24 (dd, *J* = 13.1, 0.6 Hz, 1H, C_{11}), 4.08 (dd, *J* = 13.1, 1.0 Hz, 1H, C_{11}), 2.46 – 2.33 (m, 3H, C_2, C_8), 2.05 (ddd, *J* = 13.4, 7.9, 3.4 Hz, 1H, C_1), 1.76 (dt, *J* = 13.3, 9.0 Hz, 1H, C_1), 1.57 (s, 1H, OH), 1.46 – 1.38 (m, 3H, C_6, C_7, C_8), 1.37 (s, 3H, C_{15}), 0.92 (d, *J* = 6.4 Hz, 3H, C_{16}).

^{13}C NMR (101 MHz, $CDCl_3$): δ 150.1 (C_4), 149.7 (C_{10}), 126.5 (C_3), 113.8 (C_{17}), 72.1 (C_5), 54.5 (C_9), 45.7 (C_{11}), 43.1 (C_6), 41.4 (C_1), 38.2 (C_8), 30.3 (C_2), 28.3 (C_7), 24.4 (C_{15}), 14.8 (C_{16}).

FTIR (AT-IR): 3315, 2872, 2360, 1596, 1489, 1275, 1031, 1001, 899, 697 cm^{-1}.

HRMS (FAB+, m/z): calc'd for $C_{14}H_{20}ClO$ $[M+H]^+–H_2$ 239.1203, found: 239.1176.

$[\alpha]_D^{23}$: +27.0° (*c* = 0.210, $CHCl_3$).

Preparation of hydrindenone 51

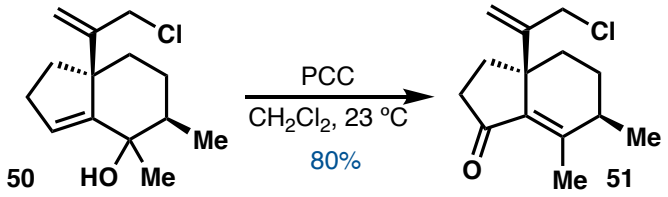

This procedure was adapted from the work of Dauben and coworkers.[16] To a 100 mL round-bottom flask equipped with a stir bar was added allylic alcohol **50** (1.15 g, 4.78 mmol, 1 equiv) and CH_2Cl_2 (32 mL). Pyridinium chlorochromate (3.09 g, 14.24 mmol. 3 equiv) was added in one portion and the reaction was stirred at ambient temperature for 12 h or until complete by aliquot NMR.

Upon complete consumption of starting material, the reaction mixture was transferred to a 500 mL separatory funnel. In the reaction flask remained a black resin, which was diluted with 20 mL Et_2O and 60 mL of 5% NaOH. The biphasic mixture was stirred until all the black resin had gone into solution, where it was then transferred into the separatory funnel. The organic layer was separated, and the aqueous layer was extracted with Et_2O (3 x 20 mL). The combined organic layers were then washed with 1 M HCl (2 x 15 mL) which gave a pale yellow organic layer. The phases were again separated, and washed with sat. aq. $NaHCO_3$. The combined organic layers were dried over $MgSO_4$, filtered, and concentrated under reduced pressure.

Purification was achieved via flash column chromatography with SiO_2 [50 g SiO_2, 10% Et_2O/hexanes] to afford enone **51** (902 mg, 3.78 mmol, 80% yield) as viscous, clear oil.

TLC (20% Et_2O/hexanes): R_f = 0.24 (UV, *p*-anisaldehyde).

^{1}H NMR (400 MHz, $CDCl_3$): δ 5.49 (s, 1H, C_{17}), 4.93 (d, J = 0.8 Hz, 1H, C_{17}), 4.10 (d, J = 0.9 Hz, 2H, C_{11}), 2.34 – 2.04 (m, 5H, C_1, C_2, C_6, C_8, C_{15}), 1.75 – 1.66 (m, 1H, C_7), 1.63 – 1.54 (m, 1H, C_1), 1.39 – 1.15 (m, 2H, C_7, C_8), 1.06 (d, J = 7.1 Hz, 3H, C_{16}).

^{13}C NMR (101 MHz, $CDCl_3$): δ 207.4 (C_3=O), 152.3 (C_4), 147.4 (C_5), 135.6 (C_{10}), 121.8 (C_{17}), 50.6 (C_9), 43.9 (C_{11}), 37.7 (C_6), 35.6 (C_2), 33.2 (C_8), 32.5 (C_1), 28.2 (C_7), 19.1 (C_{16}), 16.9 (C_{15}).

FTIR (AT-IR): 2932, 1707, 1630, 1444, 1267, 1211, 1077, 926, 801, 754, 622 cm^{-1}.

HRMS (TOF, ES+): calc'd for $C_{14}H_{19}ClONa[M+Na]^+$ 261.1022, found 261.1006.

$[\alpha]_D^{23}$: –252.8° (c = 0.66, $CHCl_3$).

Preparation of enal 10

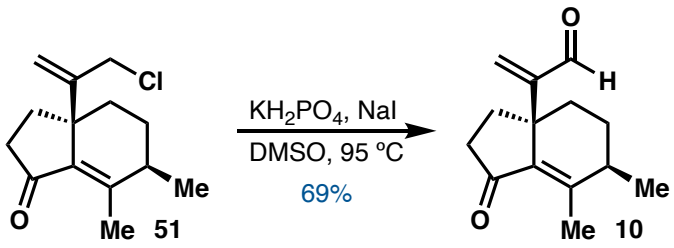

This procedure was adapted from the work of Kumar and coworkers.[2] A 20 mL scintillation vial equipped with a stir bar was charged with hydrindenone **51** (250 mg, 1.047 mmol, 1 equiv), K_2HPO_4•$3H_2O$ (595 mg, 2.62 mmol, 2.5 equiv), NaI (65 mg, 0.419 mmol, 0.4 equiv) and DMSO (10 mL). The vial was sealed with a teflon cap and the heterogeneous mixture was heated to 95 ºC with vigorous stirring (1000 rpm). After 7.5 h, aliquot NMR analysis indicated complete consumption of starting material. The heterogeneous mixture was allowed to cool to ambient temperature and sat. aq. $NaHCO_3$ (5 mL) was added. The layers were separated and the aqueous layer was extracted with Et_2O (4 x 15 mL). The combined organic layers were washed with H_2O (10 mL), and dried over $MgSO_4$. The suspension was filtered and concentrated under reduced pressure to afford a yellow oil.

Purification was achieved via flash column chromatography on SiO_2 [75 g SiO_2, Et_2O/hexanes = 20%] to afford enal **10** (157 mg, 0.719 mmol, 69% yield) as a white solid.

TLC (30% Et_2O/hexanes): R_f = 0.30 (UV, *p*-anisaldehyde).

^{1}H NMR (400 MHz, $CDCl_3$): δ 9.57 (s, 3H, C_{11}), 6.17 (s, 1H, C_{17}), 6.06 (s, 1H, C_{17}), 2.58 (ddd, *J* = 12.9, 7.9, 1.2 Hz, 1H, C_2), 2.48 (dt, *J* = 13.1, 3.4 Hz, 1H, C_8), 2.17 (m, 1H, C_6), 2.16 (s, 3H, C_{15}), 2.12 (ddd, *J* = 18.5, 8.6, 1.1 Hz, 1H, C_1) 2.06 (ddd, *J* = 18.5, 12.6, 7.9 Hz, 1H, C_1), 1.70 (m, 1H, C_7), 1.64 (dd, *J* = 12.6, 8.7, Hz, 1H, C_2), 1.34 (td, *J* = 14.0, 2.7 Hz, 1H, C_8), 1.04 (s, 3H, C_{16}), 0.97 (m, 1H, C_7).

^{13}C NMR (101 MHz, $CDCl_3$): δ 207.9 (C_3=O), 193.8 (C_{11}=O), 153.5 (C_5), 152.8 (C_{10}), 140.5 (C_{17}), 135.1 (C_4), 48.1 (C_9), 37.5 (C_6), 35.9 (C_1), 32.3 (C_8), 31.8 (C_2), 28.5 (C_7), 19.3 (C_{16}) 17.0 (C_{15}).

FTIR (AT-IR): 2950, 2931, 1705, 1629, 1080, 907, 878, 764, 702, 647 cm^{-1}.

HRMS (FAB+, m/z): calc'd for $C_{14}H_{19}O_2$ $[M+H]^+$ 219.1385, found 219.1387.

$[\alpha]_D^{23}$: –215° (*c* = 1.01, $CHCl_3$).

Preparation of MOM protected crotylation adduct 54

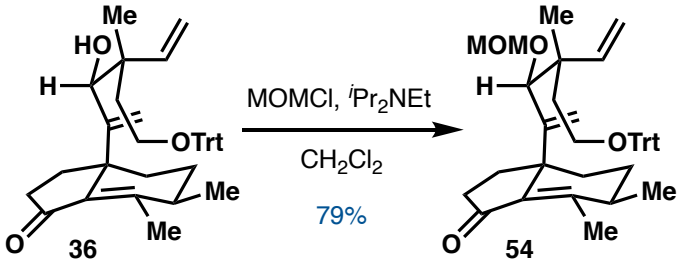

A flame-dried, 25 mL round-bottom flask equipped with a stir bar was charged with alcohol **36** (300 mg, 0.535 mmol, 1 equiv), CH_2Cl_2 (8.7 mL), and freshly distilled ^{i}Pr$_2$NEt

(2.42 mL, 13.9 mmol, 26 equiv). To the homogeneous solution was added chloromethyl methyl ether (1.02 mL, 7.80 mmol, 25 equiv) dropwise over 10 min, taking care to vent HCl fumes formed via the use of a needle. The reaction was stirred at ambient temperature for 36 h. The resulting viscous, orange mixture was quenched via addition of sat. aq. $NaHCO_3$ (20 mL) and stirred at ambient temperature for 30 min. The aqueous layer was extracted with CH_2Cl_2 (3 x 10 mL). The combined organic layers were washed with H_2O (1 x 10 mL), brine (1 x 10 mL), dried over Na_2SO_4, and concentrated via distillation to afford a viscous, dark orange residue.

Purification was achieved via flash column chromatography on SiO_2 [35 g SiO_2, Et_2O/hexanes = 16% → 35%] to afford MOM ether **54** (281 mg, 0.465 mmol, 79% yield) as a puffy white solid. Starting material **36** was also isolated (38.0 mg, 0.0678 mmol, 13% recovered).

TLC (40% Et_2O/hexanes): R_f = 0.71 (UV, *p*-anisaldehyde).

^{1}H NMR (400 MHz, $CDCl_3$): δ 7.46–7.38 (m, 6H, ***Ph*$_3$**CO), 7.32–7.19 (m, 9H, ***Ph*$_3$**CO), 5.77 (dd, *J* = 16.9, 9.9 Hz, 1H, C_{19}), 5.42 (d, *J* = 1.1 Hz, 1H, C_{17}), 4.93 (br m, 1H, C_{17}), 4.84 (dd, *J* = 9.9, 2.4 Hz, 1H, C_{20}), 4.80 (dd, *J* = 16.9, 2.4 Hz, 1H, C_{20}), 4.52 (d, *J* = 6.7 Hz, 1H, OC***H*$_2$**OMe), 4.46 (d, *J* = 6.7 Hz, 1H, OC***H*$_2$**OMe), 3.87 (br s, 1H, C_{11}), 3.37 (s, 3H, OCH_2OC***H*$_3$**), 3.10 (m, m, 2H, C_{14}), 2.17 (app dt, *J* = 12.0, 7.9 Hz, 1H, C_2), 2.15 (m 1H, C_1), 2.11 (m, 1H, C_6), 2.10 (s, 3H, C_{15}), 2.08 (m, 1H, C_8), 1.98 (m, 1H, C_{13}), 1.93 (m, 1H, C_2), 1.86 (m, 1H, C_{13}), 1.62 (m, 1H, C_7), 1.44 (m, 1H, C_1), 1.25 (m, 1H, C_7), 1.23 (m, 1H, C_8), 1.05 (d, *J* = 7.0 Hz, 3H, C_{16}), 0.99 (s, 3H, C_{18}).

^{13}C NMR (101 MHz, $CDCl_3$): δ 208.4 (C_3=O), 151.1 (C_5), 149.7 (C_{10}), 144.4 (***Ph*$_3$**CO), 142.6 (C_{19}), 136.4 (C_4), 128.7 (***Ph*$_3$**CO), 127.7 (***Ph*$_3$**CO), 126.8 (***Ph*$_3$**CO), 122.3 (C_{17}), 113.9 (C_{20}), 95.1 (O***C***H_2OCH_3), 86.7 (Ph$_3$***C***O), 80.2 (C_{11}), 60.7 (C_{14}), 56.4 (OCH_2O***C***H_3), 50.8 (C_9), 45.2 (C_{12}), 38.3 (C_{13}), 37.5 (C_6), 35.9 (C_2), 33.2 (C_8), 32.7 (C_1), 28.2 (C_7), 19.1 (C_{16}), 17.9 (C_{18}), 17.0 (C_{15}).

FTIR (AT-IR): 2930, 1703, 1627, 1448, 1213, 1034, 919, 735 cm^{-1}.

HRMS (TOF, ES+): calc'd for $C_{41}H_{48}O_4Na$ $[M+Na]^+$ 627.3450, found 627.3419.

$[\alpha]_D^{23}$: –39° (*c* = 1.06, $CHCl_3$).

Melting point: 62.0–63.3 °C

Preparation of alcohol 55

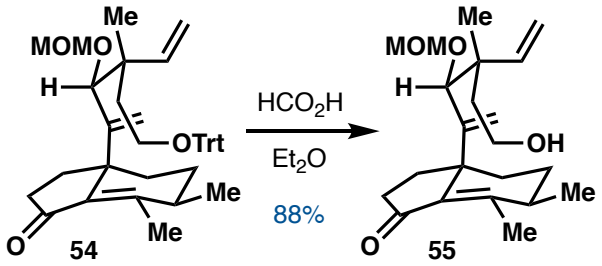

A flame-dried, 250 mL round-bottom flask equipped with a stir bar was charged with MOM ether **54** (431 mg, 0.713 mmol, 1 equiv). Thereafter, a freshly prepared solution of formic acid (98%, 4.8 mL) and Et_2O (4.8 mL) was rapidly added, and within 5 min, the reaction was judged to be complete by TLC analysis. We found it critical to stop this reaction immediately after full conversion was achieved. Prolonged times afforded copious quantities of formate ester product. The reaction was diluted with Et_2O (10 mL) and quenched via slow addition of $NaHCO_3$ (100 mL). The aqueous layer was extracted with Et_2O (4 x 25 mL) and washed with H_2O (1 x 10 mL). The combined organic layers were

washed with brine (1 x 5 mL), dried over Na_2SO_4, and concentrated under reduced pressure to afford a viscous yellow residue.

Purification was achieved via flash column chromatography on SiO_2 [15 g SiO_2, Et_2O/hexanes = 70%] to afford alcohol **55** (225 mg, 0.621 mmol, 88% yield) as a viscous, colorless oil.

TLC (70% Et_2O/hexanes): R_f = 0.20 (UV, *p*-anisaldehyde).

^{1}H NMR (400 MHz, $CDCl_3$): δ 5.99 (dd, *J* = 16.9, 9.9 Hz, 1H, C_{19}), 5.49 (d, *J* = 1.1 Hz, 1H, C_{17}), 5.05 (dd, *J*= 9.9, 2.4 Hz, 1H, C_{20}), 5.01 (br m, 1H, C_{17}), 4.99 (dd, *J* = 16.9, 2.4 Hz, 1H, C_{20}), 4.58 (d, *J* = 6.7 Hz, 1H, OC***H***$_2$OMe), 4.50 (d, *J* = 6.7 Hz, 1H, OC***H***$_2$OMe), 4.01 (br s, 1H, C_{11}), 3.66 (m, 2H, C_{14}), 3.41 (s, 3H, $OCH_2OC\boldsymbol{H_3}$), 2.24 (m, 1H, C_2), 2.22 (m 1H, C_1), 2.13 (m, 1H, C_6), 2.11 (m, 1H, C_8), 2.10 (s, 3H, C_{15}), 1.99 (m, 1H, C_2), 1.95 (m, 1H, C_{13}), 1.88 (m, 1H, C_{13}), 1.63 (m, 1H, C_7), 1.50 (m, 1H, C_1), 1.27 (m, 1H, C_8), 1.25 (m, 1H, C_7), 1.12 (s, 3H, C_{18}), 1.05 (d, *J* = 7.0 Hz, 3H, C_{16}).

^{13}C NMR (101 MHz, $CDCl_3$): δ 208.3 (C_3=O), 151.2 (C_5), 149.7 (C_{10}), 143.1 (C_{19}), 136.4 (C_4), 122.5 (C_{17}), 114.1 (C_{20}), 95.0 (O***C***H_2OCH_3), 80.0 (C_{11}), 59.8 (C_{14}), 56.4 ($OCH_2O\boldsymbol{C}H_3$), 50.7 (C_9), 45.3 (C_{12}), 41.5 (C_{13}), 37.5 (C_6), 35.9 (C_2), 33.2 (C_8), 32.8 (C_1), 28.2 (C_7), 19.1 (C_{16}), 17.7 (C_{18}), 17.0 (C_{15}).

FTIR (AT-IR): 3397, 2930, 1701, 1625, 1456, 1371, 1212, 1145, 1035, 917, 734 cm^{-1}.

HRMS (TOF, ES+): calc'd for $C_{22}H_{34}O_4Na$ $[M+Na]^+$ 385.2355, found 385.2371.

$[\alpha]_D^{23}$: –53° (*c* = 0.475, $CHCl_3$).

Preparation of aldehyde 56

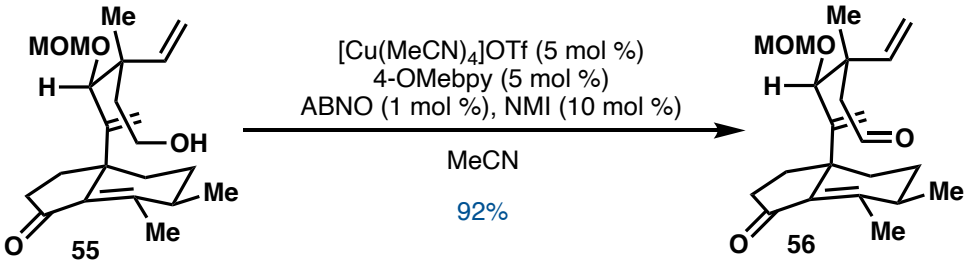

A flame-dried, 2 dram vial equipped with a stir bar was charged with alcohol **55** (165 mg, 0.455 mmol, 1 equiv) and MeCN (2.0 mL). Thereafter, added 860 μL of the [Cu]/bpy stock solution, 860 μL of the NMI stock solution, and 860 μL of the ABNO stock solution, in that order. The orange reaction was stirred at 960 rpm open to the atmosphere for 90 min. Subsequently, the resulting light blue solution was diluted with Et_2O (10 mL), passed through a short pad of SiO_2 using Et_2O as the eluent and concentrated under reduced pressure to afford a pale yellow oil.

Purification was achieved via flash column chromatography on SiO_2 [8 g SiO_2, Et_2O/hexanes = 30%→60%] to afford aldehyde **56** (151 mg, 0.419 mmol, 92% yield) as a viscous, colorless oil that solidified to a white solid upon standing in the freezer.

Preparation of stock solutions: $[Cu(MeCN)_4]OTf$ (30.0 mg) and 4,4′-dimethoxy-2,2′-bipyridyl (4-OMebpy) (17.0 mg) were suspended in MeCN (3.0 mL) and stirred for 5 min resulting in a homogeneous, green solution. ABNO (2.5 mg) was dissolved in MeCN (3.0 mL). *N*-methylimidazole (13.4 mg) was dissolved in MeCN (3.0 mL).

TLC (80% Et_2O/hexanes): R_f = 0.65 (UV, *p*-anisaldehyde).

^{1}H NMR (400 MHz, $CDCl_3$): δ 9.74 (t, *J* = 2.8 Hz, 1H, C_{14}), 6.07 (dd, *J* = 16.9, 9.9 Hz, 1H, C_{19}), 5.48 (d, *J* = 0.7 Hz, 1H, C_{17}), 5.13 (dd, *J* = 9.9, 2.4 Hz, 1H, C_{20}), 5.09 (dd, *J* = 16.9, 2.4 Hz, 1H, C_{20}), 5.05 (br m, 1H, C_{17}), 4.54 (d, *J* = 6.7 Hz, 1H, OC***H***$_2$OMe), 4.42 (d, *J* = 6.7 Hz, 1H, OC***H***$_2$OMe), 4.12 (br s, 1H, C_{11}), 3.36 (s, 3H, $OCH_2OC\boldsymbol{H_3}$), 2.56 (m, 2H, C_{13}), 2.26 (m, 1H, C_1), 2.19 (m, 1H, C_8), 2.17 (m, 1H, C_2), 2.14 (m 1H, C_6), 2.11 (s, 3H, C_{15}), 2.00 (dd, *J* = 17.0, 7.6 Hz, 1H, C_2), 1.65 (m, 1H, C_7), 1.52 (m, 1H, C_1), 1.27 (s, 3H, C_{18}), 1.25 (m, 1H, C_8), 1.23 (m, 1H, C_7), 1.07 (d, *J* = 7.0 Hz, 3H, C_{16}).

^{13}C NMR (101 MHz, $CDCl_3$): δ 208.1 (C_3=O), 202.2 (C_{14}=O), 151.4 (C_5), 149.0 (C_{10}), 142.4 (C_{19}), 136.2 (C_4), 122.7 (C_{17}), 114.5 (C_{20}), 94.2 (O***C***H_2OCH_3), 78.2 (C_{11}), 56.6 ($OCH_2O\boldsymbol{C}H_3$), 52.4 (C_{13}), 50.5 (C_9), 45.5 (C_{12}), 37.4 (C_6), 35.9 (C_2), 33.1 (C_8), 32.7 (C_1), 28.2 (C_7), 19.1 (C_{16}), 18.9 (C_{18}), 17.0 (C_{15}).

FTIR (AT-IR): 2931, 1704, 1627, 1456, 1212, 1146, 1032, 919, 708 cm^{-1}.

HRMS (TOF, ES+): calc'd for $C_{22}H_{32}O_4$[M+Na]$^+$ 383.2198, found 383.2189.

$[\alpha]_D^{23}$: –56° (*c* = 0.475, $CHCl_3$).

Preparation of tricycle 59

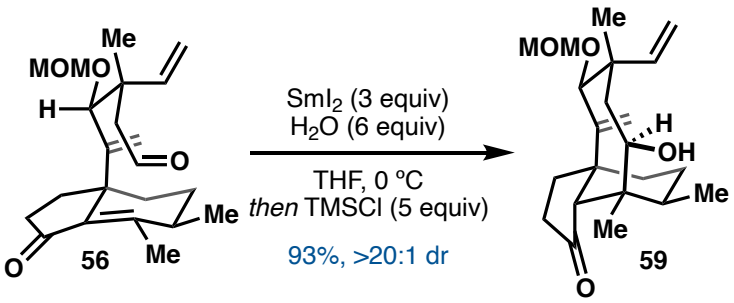

A 100 mL Schlenk flask equipped with a stir bar was charged with aldehyde **56** (108 mg, 0.300 mmol, 1 equiv), deionized H_2O (32 µL, 1.80 mmol, 6 equiv), and THF (15.0 mL) and submitted to five freeze-pump-thaw cycles. The solution was cooled to 0 °C

and stirred at this temperature for 15 min. Thereafter, SmI_2/THF (9.0 mL, 0.900 mmol, 3 equiv) was added dropwise over 8 min. The deep blue color of SmI_2 was immediately quenched upon addition of each drop. The first drop afforded a yellow solution, fading to pale yellow and almost clear by the time 1.6 equiv SmI_2 had been added. When 2.2 equiv SmI_2 had been added, the blue color became increasingly persistent and upon addition of 2.6 equiv SmI_2, the reaction was dark blue/green. After stirring an additional 10 min at 0 °C, TMSCl/THF (1.5 mL, 1.50 mmol, 5 equiv TMSCl) was added dropwise over 2 min, and the reaction was stirred an additional 10 min. Throughout this time, the deep blue color was quenched to yellow. Thereafter, the reaction was removed from the ice bath and stirred open to the atmosphere for 5 min.

The resulting pale yellow solution was diluted with Et_2O (75 mL), and washed with H_2O (2 x 15 mL). The aqueous layer was back-extracted with Et_2O (2 x 15 mL), and the combined organic layers were dried over Na_2SO_4, filtered, and concentrated under reduced pressure to afford a dark orange oil.

Purification was achieved via flash column chromatography on SiO_2 [12 g SiO_2, Et_2O/hexanes = 30%] to afford tricycle **59** (100 mg, 0.276 mmol, 92% yield) as a crystalline white solid.

Preparation of SmI_2: A 100 mL Schlenk flask containing a stir bar was charged with freshly filed Sm metal (650 mg). The system was flame-dried under high vacuum then cooled to ambient temperature before adding freshly purified 1,2-diiodoethane (700 mg). 1,2-diiodoethane (1.6 g) was dissolved in Et_2O (50 mL) and washed with sat. aq. $Na_2S_2O_3$ (3 x 10 mL) and deionized water (2 x 10 mL), dried over Na_2SO_4, filtered, and dried to

1.41 g of a white solid. The atmosphere was exchanged three times for argon. Subsequently, the flask was charged with anhydrous THF (25 mL) that had been submitted to five freeze-pump-thaw cycles. Note: The THF used for the synthesis of SmI_2 must contain <50 ppm H_2O; THF containing greater quantities of water resulted in excessive induction times for the synthesis of SmI_2. Further, residual oxygen results in formation of oxidative fragmentation products in the radical cyclization. The suspension was stirred for 2 min and the flask was cautiously and briefly (5 s) placed under partial high vacuum, then purged with argon. This process was repeated two additional times to remove ethylene gas formed from insertion of Sm metal into 1,2-diiodoethane. The resulting heterogeneous suspension was rapidly (930 rpm) stirred; after 5 min, the reaction turned dark green, and within 10 min, a dark blue color was observed. After stirring under argon for 3 h at ambient temperature, the system was cautiously and briefly placed under high vacuum, then purged with argon. This process was repeated two additional times, then stirring was halted. The mixture was allowed to settle for 15 min prior to use.

Stock solution of TMSCl: TMSCl was freshly distilled from CaH_2 (5% w/w) under argon, collecting a 15% forerun then taking the middle fraction. A solution of TMSCl (350 μL) in THF (5.0 mL) was submitted to five freeze-pump-thaw cycles.

TLC (50% Et_2O/hexanes): R_f = 0.55 (*p*-anisaldehyde).

^{1}H NMR (400 MHz, $CDCl_3$): δ 6.35 (dd, *J* = 17.8, 11.3 Hz, 1H, C_{19}), 5.33 (dd, *J* = 17.8, 1.4 Hz, 1H, C_{20}), 5.34 (s, 1H, C_{17}), 5.28 (s, 1H, C_{17}), 5.19 (dd, *J* = 11.2, 1.4 Hz, 1H, C_{20}), 4.54 (d, *J* = 7.1 Hz, 1H, OC***H***$_2$OMe), 4.40 (d, *J* = 6.7 Hz, 1H, OC***H***$_2$OMe), 4.13 (d, *J* = 5.9

Hz, 1H, C_{14}), 3.95 (s, 1H, C_{11}), 3.38 (s, 3H, $OCH_2OC\boldsymbol{H_3}$), 2.33 (m, 1H, C_2), 2.29 (m, 1H, C_2), 2.24 (m, 1H, C_4), 2.06 (m, 1H, C_1), 2.03 (m, 1H, C_8), 1.92 (dd, J = 16.1, 6.5 Hz, 1H, C_{13}), 1.70 (m, 1H, C_6), 1.60 (dt, J = 13.3, 3.4 Hz, 1H, C_7), 1.50 (dd, J = 16.1, 0.9 Hz, 1H, C_{13}), 1.39 (ddt, J = 13.3, 6.5, 3.4 Hz, 1H, C_7), 1.33 (m, 1H, C_1), 1.30 (s, 3H, C_{15}), 1.28 (m, 1H, C_8), 1.24 (s, 3H, C_{18}), 0.96 (d, J = 7.0 Hz, 3H, C_{16}).

^{13}C NMR (101 MHz, $CDCl_3$): δ 216.8 (C_3=O), 148.3 (C_{10}), 139.9 (C_{19}), 114.2 (C_{20}), 112.2 (C_{17}), 92.1 ($O\boldsymbol{C}H_2OCH_3$), 77.2 (C_{11}), 67.2 (C_{14}), 59.6 (C_4), 56.0 ($OCH_2O\boldsymbol{C}H_3$), 46.5 (C_9), 45.2 (C_{13}), 44.7 (C_{12}), 42.1 (C_5), 37.3 (C_6), 34.9 (C_2), 31.0 (C_8), 29.7 (C_1), 28.8 (C_{18}), 26.8 (C_7), 18.2 (C_{16}), 13.4 (C_{15}).

FTIR (AT-IR): 3508 (br), 2926, 1735, 1628, 1458, 1264, 1144, 1093, 1024, 907, 738 cm^{-1}.

HRMS (TOF, ES+): calc'd for $C_{22}H_{35}O_4$ $[M+H]^+$ 363.2535, found 363.2536.

$[\alpha]_D^{23}$: +155° (c = 0.330, $CHCl_3$).

Melting point: 142.0–143.4 °C

Preparation of diketone 65

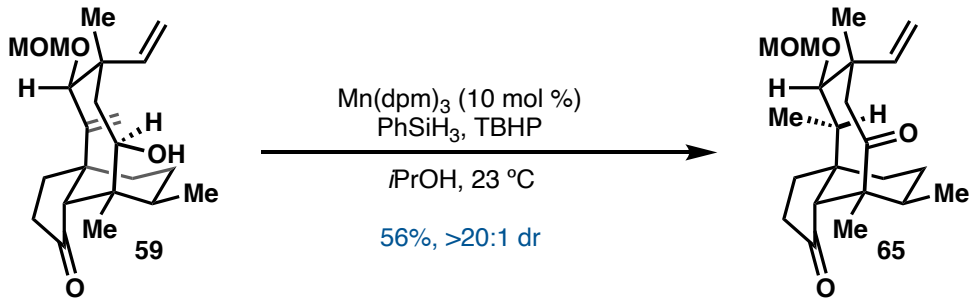

This procedure was adapted from work by Shenvi and coworkers.[33] A flame-dried 1 dram vial was charged with tricycle **59** (30.0 mg, 0.0828 mmol, 1 equiv) and adventitious water was removed via azeotropic drying with PhMe (3 x 400 μL) under high vacuum. An

oven-dried stir bar was added, and the atmosphere was exchanged three times for argon. Thereafter, ^{i}PrOH (830 μL), $PhSiH_3$ (13.4 mg, 0.124 mmol, 15.2 μL, 1.5 equiv), and *tert*-butyl hydroperoxide (33.1 μL of a 5.0 M solution in nonane, 0.166 mmol, 2 equiv) were added. The heterogeneous mixture was sparged with argon for 10 min. Subsequently, tris(2,2,6,6-tetramethyl-3,5-heptanedionato)manganese(III) (5.0 mg, 0.00828 mmol, 10 mol %) was added as a solid, sparging was continued for an additional 20 sec, and the reaction was stirred at ambient temperature. After 10 min, the reaction was diluted with Et_2O/hexanes = 50%, passed through a plug of SiO_2 (eluting with Et_2O/hexanes = 50%), and concentrated under reduced pressure to afford a dark orange oil.

Purification was achieved via flash column chromatography on SiO_2 [15 g SiO_2, Et_2O/hexanes = 20% → 35%] to afford ketone **65** (16.9 mg, 0.047 mmol, 56% yield) as a clear residue. Isolated starting material (12.1 mg, 0.033 mmol, 40%).

Experimental Notes: This reaction exhibits a pronounced sensitivity to both residual oxygen and water. In addition, we found it critical to perform this reaction at 23 °C, as higher temperatures promoted over-reduction and lower temperatures slowed catalysis. ^{i}PrOH was stored over activated 4 Å molecular sieves (pellets) overnight then was distilled from CaH_2 (10% w/v) in a flame-dried, argon-filled apparatus immediately prior to use.

TLC (40% Et_2O/hexanes): R_f = 0.24 (*p*-anisaldehyde).

^{1}H NMR (400 MHz, $CDCl_3$): δ 6.18 (dd, *J* = 17.8, 11.3 Hz, 1H, C_{19}), 5.36 (dd, *J* = 17.8, 1.5 Hz, 1H, C_{20}), 5.27 (dd, *J* = 11.2, 1.5 Hz, 1H, C_{20}), 4.67 (ABq, *J* = 6.8 Hz, 2H, OC***H***$_2$OMe), 3.54 (d, *J* = 5.2 Hz, 1H, C_{11}), 3.42 (s, 3H, $OCH_2OC\boldsymbol{H_3}$), 2.70 (d, *J* = 12.4 Hz,

1H, C_{13}), 2.57 (d, J = 2.3 Hz, 1H, C_4), 2.27 (m, 2H, C_2), 2.07 (d, J = 12.4 Hz, 1H, C_{13}), 1.99 (dq, J = 7.2, 5.2 Hz, 1H, C_{10}), 1.83 (dd, J = 12.9, 9.6 Hz, 1H, C_1), 1.74 (dq, J = 14.3, 2.9 Hz, C_8), 1.63 (dt, J = 12.9, 3.3 Hz, 1H, C_7), 1.56 (m, 1H, C_6), 1.53 (m, 1H, C_1), 1.46 (s, 3H, C_{15}), 1.29 (m, 1H, C_7), 1.21 (s, 3H, C_{18}), 1.18 (d, J = 6.8 Hz, 3H, C_{16}), 1.17 (m, 1H, C_8), 0.89 (d, J = 7.2 Hz, 3H, C_{17}).

^{13}C NMR (101 MHz, $CDCl_3$): δ 216.9 (C_3=O), 212.5 (C_{14}=O), 138.5 (C_{19}), 116.1 (C_{20}), 98.1 (O***C***H_2OCH$_3$), 81.9 (C_{11}), 57.9 (C_4), 56.8 (OCH$_2$O***C***H$_3$), 50.6 (C_5), 48.1 (C_{12}), 47.5 (C_{13}), 45.6 (C_9), 36.5 (C_6), 35.5 (C_{10}), 34.6 (C_2), 31.0 (C_8), 27.9 (C_{18}), 26.1 (C_7), 24.7 (C_1), 21.0 (C_{15}), 16.2 (C_{16}), 11.1 (C_{17}).

FTIR (AT-IR): 2957, 1734, 1698, 1455, 1089, 1035, 916 cm^{-1}.

HRMS (TOF, ES+): calc'd $C_{22}H_{34}O_4$ $[(M+H)–H_2]^+$ 361.2379, found 361.2396.

$[\alpha]_D^{23}$: +34.0° (c = 0.951, $CHCl_3$).

Preparation of deuterium-labeled aldehyde 67

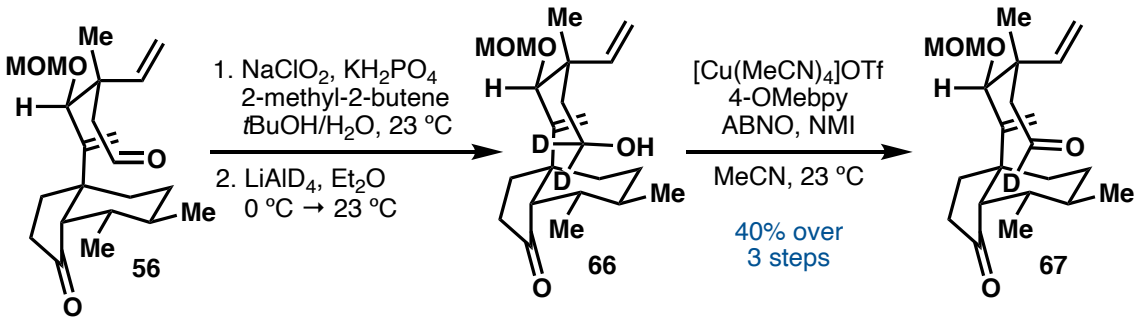

A 25 mL round-bottom flask equipped with a stir bar was charged with aldehyde **56** (32.2 mg, 0.0894 mmol, 1 equiv) and ^{t}BuOH (4.5 mL) followed by deionized water (3.2 mL) and 2-methyl-2-butene (163 mg, 2.32 mmol, 246 µL, 26 equiv). Thereafter, a solution of KH_2PO_4 (42.6 mg, 0.313 mmol, 3.5 equiv) in H_2O (650 µL) was added followed by a

solution of $NaClO_2$ (8.9 mg, 0.0983 mmol, 1.1 equiv) in H_2O (650 μL). The mixture was rapidly stirred at ambient temperature for 6 h, at which time the reaction was extracted into Et_2O (4 x 2 mL). The combined organic layers were dried over Na_2SO_4, filtered, and concentrated under reduced pressure to afford 25.8 mg of a clear oil that was used in the next step without further purification.

A flame-dried 2 dram vial equipped with a stir bar was charged with $LiAlD_4$ (11.5 mg, 0.274 mmol, 4 equiv) and the atmosphere was exchanged three times for argon. Subsequently, anhydrous Et_2O (1.7 mL) was added followed by dropwise addition of carboxylic acid in Et_2O (1.7 mL) over 5 min. The resulting light grey suspension was rapidly stirred at ambient temperature for 45 min, at which time H_2O (1 mL) was cautiously added, using a vent needle to aid in expulsion of gas. The slurry was extracted into Et_2O (4 x 2 mL), the combined organic layers were dried over Na_2SO_4, and concentrated under reduced pressure to afford 14.1 mg of a viscous oil that was used in the next step without further purification.

Stahl Oxidation:

A flame-dried, 2 dram vial equipped with a stir bar was charged with alcohol **66** and MeCN (100 μL). Thereafter, added 140 μL of the [Cu]/bpy stock solution, 140 μL of the NMI stock solution, and 140 μL of the ABNO stock solution, in that order. The orange reaction was stirred at 960 rpm open to the atmosphere. Within 15 min, TLC analysis (Et_2O/hexanes = 70%, UV and anisaldehyde) indicated complete conversion to aldehyde **67** (R_f = 0.57, stains deep blue), and after 2 h, complete conversion to the desired enone-aldehyde product (R_f = 0.66, stains brown) was observed. Subsequently, the resulting light

blue solution was diluted with Et_2O (2 mL), passed through a short pad of SiO_2 using Et_2O as the eluent, and concentrated under reduced pressure to afford a pale yellow oil.

Purification was achieved via flash column chromatography on SiO_2 [1.5 g SiO_2, Et_2O/hexanes = 30%→45%] to afford deuterated aldehyde **67** (9.8 mg, 0.027 mmol, 40% yield over 3 steps) as a viscous, colorless oil. It should be noted that this compound was isolated as a 9:1 mixture of C_6-epimers, separable after the reductive radical cyclization. ^{1}H NMR indicates 94% deuterium incorporation at C_{14}.

Preparation of stock solutions: See page **101.**

TLC (80% Et_2O/hexanes): R_f = 0.65 (UV).

^{1}H NMR (400 MHz, $CDCl_3$): δ 6.07 (dd, *J* = 16.9, 9.9 Hz, 1H, C_{19}), 5.48 (d, *J* = 0.7 Hz, 1H, C_{17}), 5.13 (dd, *J* = 9.9, 2.4 Hz, 1H, C_{20}), 5.09 (dd, *J* = 16.9, 2.4 Hz, 1H, C_{20}), 5.05 (br m, 1H, C_{17}), 4.54 (d, *J* = 6.7 Hz, 1H, OC***H***$_2$OMe), 4.42 (d, *J* = 6.7 Hz, 1H, OC***H***$_2$OMe), 4.12 (br s, 1H, C_{11}), 3.36 (s, 3H, $OCH_2OC\boldsymbol{H_3}$), 2.56 (m, 2H, C_{13}), 2.26 (m, 1H, C_1), 2.19 (m, 1H, C_8), 2.17 (m, 1H, C_2), 2.14 (m 1H, C_6), 2.11 (s, 3H, C_{15}), 2.00 (dd, *J* = 17.0, 7.6 Hz, 1H, C_2), 1.65 (m, 1H, C_7), 1.52 (m, 1H, C_1), 1.27 (s, 3H, C_{18}), 1.25 (m, 1H, C_8), 1.23 (m, 1H, C_7), 1.07 (d, *J* = 7.0 Hz, 3H, C_{16}).

^{13}C NMR (101 MHz, $CDCl_3$): δ 208.1 (C_3=O), 202.2 (C_{14}=O) (1:1:1 triplet) (coupling of *I* = ½ ^{13}C nucleus to quadrupolar ^{2}H nucleus also causes T_2 broadening), 151.4 (C_5), 149.0 (C_{10}), 142.4 (C_{19}), 136.2 (C_4), 122.7 (C_{17}), 114.5 (C_{20}), 94.2 ($O\boldsymbol{C}H_2OCH_3$), 78.2 (C_{11}), 56.6 ($OCH_2O\boldsymbol{C}H_3$), 52.4 (C_{13}) (reduced intensity due to ^{2}H coupling), 50.5 (C_9), 45.5 (C_{12}), 37.4 (C_6), 35.9 (C_2), 33.1 (C_8), 32.7 (C_1), 28.2 (C_7), 19.1 (C_{16}), 18.9 (C_{18}), 17.0 (C_{15}).

FTIR (AT-IR): 2931, 2359, 2323, 1704, 1628, 1456, 1212, 1148, 1036, 919 cm^{-1}.

HRMS (TOF, ES+): calc'd for $C_{22}H_{31}DO_4Na$ $[M+Na]^+$ 384.2261, found 384.2270.

$[\alpha]_D^{23}$**:** –43.2° (*c* = 0.455, $CHCl_3$).

Preparation of deuterium-labeled tricycle 68

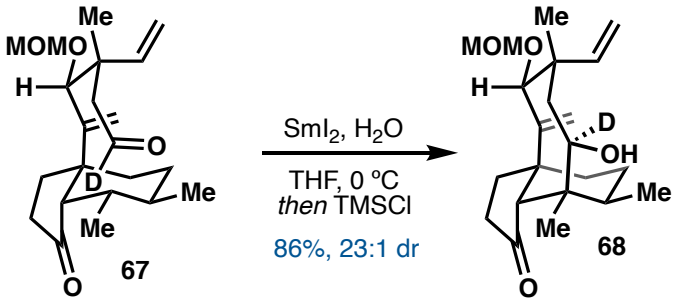

A 25 mL Schlenk flask equipped with a stir bar was charged with deuterated aldehyde **67** (7.3 mg, 0.0202 mmol, 1 equiv), THF (1.0 mL), and a solution of deionized H_2O (2.2 μL, 0.121 mmol, 6 equiv) in THF (184 μL) and submitted to five freeze-pump-thaw cycles. The solution was cooled to 0 °C and stirred at this temperature for 15 min. Thereafter, SmI_2/THF (606 μL, 0.0606 mmol, 3 equiv) was added dropwise over 8 min. After stirring an additional 10 min at 0 °C, TMSCl/THF (195 μL, 0.101 mmol, 5 equiv TMSCl) was added dropwise over 2 min, and the reaction was stirred an additional 10 min. Throughout this time, the deep blue color was quenched to yellow. Thereafter, the reaction was removed from the ice bath and stirred open to the atmosphere for 5 min. The resulting pale yellow solution was diluted with Et_2O (5 mL), and washed with H_2O (2 x 2 mL). The aqueous layer was back-extracted with Et_2O (2 x 2 mL), and the combined organic layers were dried over Na_2SO_4, filtered, and concentrated under reduced pressure to afford a dark orange oil.

Purification was achieved via flash column chromatography on SiO_2 [1.5 g SiO_2, Et_2O/hexanes = 30% → 40%] to afford deuterated tricycle **68** (6.3 mg, 0.017 mmol, 84% yield) as a clear residue.

Preparation of SmI_2: See page **103.**

Stock solution of TMSCl: See page **104.**

TLC (50% Et_2O/hexanes): R_f = 0.55 (*p*-anisaldehyde, $KMnO_4$).

^{1}H NMR (400 MHz, $CDCl_3$): δ 6.35 (dd, *J* = 17.8, 11.3 Hz, 1H, C_{19}), 5.33 (dd, *J* = 17.8, 1.4 Hz, 1H, C_{20}), 5.34 (s, 1H, C_{17}), 5.28 (s, 1H, C_{17}), 5.19 (dd, *J* = 11.2, 1.4 Hz, 1H, C_{20}), 4.54 (d, *J* = 7.1 Hz, 1H, OC***H***$_2$OMe), 4.40 (d, *J* = 6.7 Hz, 1H, OC***H***$_2$OMe), 3.95 (s, 1H, C_{11}), 3.38 (s, 3H, OCH_2OC***H***$_3$), 2.33 (m, 1H, C_2), 2.29 (m, 1H, C_2), 2.24 (m, 1H, C_4), 2.06 (m, 1H, C_1), 2.03 (m, 1H, C_8), 1.92 (dd, *J* = 16.1, 6.5 Hz, 1H, C_{13}), 1.70 (m, 1H, C_6), 1.60 (dt, *J* = 13.3, 3.4 Hz, 1H, C_7), 1.50 (dd, *J* = 16.1, 0.9 Hz, 1H, C_{13}), 1.39 (ddt, *J* = 13.3, 6.5, 3.4 Hz, 1H, C_7), 1.33 (m, 1H, C_1), 1.30 (s, 3H, C_{15}), 1.28 (m, 1H, C_8), 1.24 (s, 3H, C_{18}), 0.96 (d, *J* = 7.0 Hz, 3H, C_{16}).

^{13}C NMR (101 MHz, $CDCl_3$): δ 216.8 (*C*$_3$=O), 148.3 (C_{10}), 139.9 (C_{19}), 114.2 (C_{20}), 112.2 (C_{17}), 92.1 (O***C***H_2OCH_3), 77.2 (C_{11}), 67.2 (C_{14}) (1:1:1 triplet) (coupling of *I*= ½ ^{13}C nucleus to quadrupolar ^{2}H nucleus also causes T_2 broadening), 59.6 (C_4), 56.0 (OCH_2O***C***H_3), 46.5 (C_9), 45.2 (C_{13}) (reduced intensity due to ^{2}H coupling), 44.7 (C_{12}), 42.1 (C_5), 37.3 (C_6), 34.9 (C_2), 31.0 (C_8), 29.7 (C_1), 28.8 (C_{18}), 26.8 (C_7), 18.2 (C_{16}), 13.4 (C_{15}).

FTIR (AT-IR): 3508, 2926, 1735, 1628, 1458, 1264, 1144, 1093, 1024, 907, 738 cm^{-1}.

HRMS (TOF, ES+): calc'd for $C_{22}H_{34}DO_4$ $[M+H]^+$ 364.2598, found 364.2595.

$[\alpha]_D^{23}$**:** +123.5° (*c* = 0.235, $CHCl_3$).

Redox relay by transannular 1,5-HAT is confirmed by deuterium-labeling

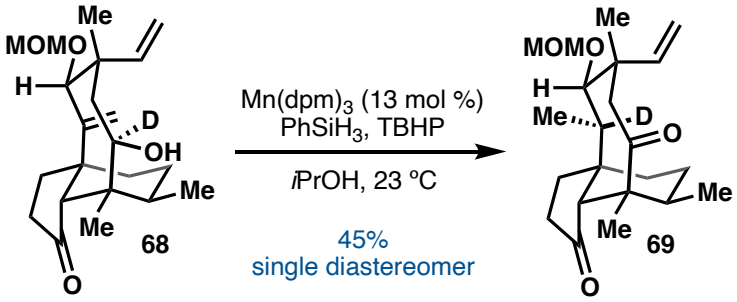

mechanistic deuterium labelling study

This procedure was adapted from work by Shenvi and coworkers.[33] A flame-dried 0.5 dram vial was charged with deuterated tricycle **68** (3.0 mg, 0.00825 mmol, 1 equiv) and adventitious water was removed via azeotropic drying with PhMe (3 x 200 µL) under high vacuum. An oven-dried stir bar was added, and the atmosphere was exchanged three times for argon. Thereafter, a stock solution of $PhSiH_3$ (0.89 mg, 0.00825 mmol, 1.0 µL, 1.5 equiv) and *tert*-butyl hydroperoxide (2.5 µL of a 5.0 M solution in nonane, 0.0124 mmol, 2 equiv) in ^{i}PrOH (96 µL) were added. Additional ^{i}PrOH (100 µL) was added, and the mixture was sparged with argon for 10 min. Subsequently, tris(2,2,6,6-tetramethyl-3,5-heptanedionato)manganese(III) (0.50 mg, 0.000825 mmol, 10 mol %) was added as a solid, sparging was continued for an additional 20 sec, and the reaction was stirred at ambient temperature. After 10 min, the reaction was diluted with Et_2O/hexanes = 50%, passed through a plug of SiO_2 (eluting with Et_2O/hexanes = 50%), and concentrated under reduced pressure to afford a dark orange oil.

Purification was achieved via flash column chromatography on SiO_2 [750 mg SiO_2, Et_2O/hexanes = 20%→30%] to afford ketone **69** (1.4 mg, 0.00385 mmol, 47%) as a clear residue. Isolated starting material (1.4 mg, 0.00385 mmol, 47%).

Experimental Notes: This reaction exhibits a pronounced sensitivity to both residual oxygen and water. In addition, we found it critical to perform this reaction at 23 °C, as higher temperatures promoted over-reduction and lower temperatures slowed catalysis. ^{i}PrOH was stored over activated 4 Å molecular sieves (pellets) overnight then was distilled from CaH_2 (10% w/v) in a flame-dried, argon-filled apparatus immediately prior to use.

Preparation of Stock Solutions: A stock solution of $PhSiH_3$ (20 μL) and *tert*-butyl hydroperoxide (50 μL of a 5.0 M solution in nonane) in ^{i}PrOH (1.6 mL) was prepared under an atmosphere of argon, and 100 μL of this stock solution was added to substrate, as described below.

TLC (40% Et_2O/hexanes): R_f = 0.24 (*p*-anisaldehyde).

^{1}H NMR (400 MHz, $CDCl_3$): δ 6.18 (dd, *J* = 17.8, 11.3 Hz, 1H, C_{19}), 5.36 (dd, *J* = 17.8, 1.5 Hz, 1H, C_{20}), 5.27 (dd, *J* = 11.2, 1.5 Hz, 1H, C_{20}), 4.67 (ABq, *J* = 6.8 Hz, 2H, OC***H***$_2$OMe), 3.54 (d, *J* = 5.2 Hz, 1H, C_{11}), 3.42 (s, 3H, $OCH_2OC\boldsymbol{H_3}$), 2.70 (d, *J* = 12.4 Hz, 1H, C_{13}), 2.57 (d, *J* = 2.3 Hz, 1H, C_4), 2.27 (m, 2H, C_2), 2.07 (d, *J* = 12.4 Hz, 1H, C_{13}), [1.99 (C_{10}) (dq signal absent)], 1.83 (dd, *J* = 12.9, 9.6 Hz, 1H, C_1), 1.74 (dq, *J* = 14.3, 2.9 Hz, C_8), 1.63 (dt, *J* = 12.9, 3.3 Hz, 1H, C_7), 1.56 (m, 1H, C_6), 1.53 (m, 1H, C_1), 1.46 (s,

3H, C_{15}), 1.29 (m, 1H, C_7), 1.21 (s, 3H, C_{18}), 1.18 (d, J = 6.8 Hz, 3H, C_{16}), 1.17 (m, 1H, C_8), 0.89 (d, J = 7.2 Hz, 3H, C_{17}).

^{13}C NMR (101 MHz, $CDCl_3$): δ 216.9 (C_3=O), 212.5 (C_{14}=O), 138.5 (C_{19}), 116.1 (C_{20}), 98.1 (O***C***H_2OCH_3), 81.9 (C_{11}) (reduced intensity due to ^{2}H coupling), 57.9 (C_4), 56.8 (OCH_2O***C***H_3), 50.6 (C_5), 48.1 (C_{12}), 47.5 (C_{13}), 45.6 (C_9), 36.5 (C_6), 35.5 (C_{10}) (signal absent), 34.6 (C_2), 31.0 (C_8), 27.9 (C_{18}), 26.1 (C_7), 24.7 (C_1), 21.0 (C_{15}), 16.2 (C_{16}), 11.1 (C_{17}).

FTIR (AT-IR): 2930, 1733, 1698, 1455, 1089, 1035 cm^{-1}.

HRMS (TOF, ES+): calc'd for $C_{22}H_{34}DO_4$ $[M+H]^+$ 364.2598, found 364.2600.

$[\boldsymbol{\alpha}]_{\boldsymbol{D}}^{\boldsymbol{23}}$**:** +24.3° (*c* = 0.065, $CHCl_3$).

Preparation of silyl enol ether 70

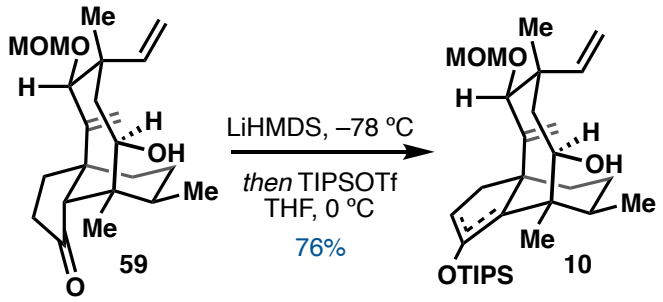

A flame-dried 25 mL round-bottom flask equipped with a stir bar was charged with tricycle **59** (129 mg, 0.356 mmol, 1 equiv) and anhydrous THF (7.1 mL) under an atmosphere of argon. The mixture was cooled to –78 °C and stirred for 5 min prior to dropwise addition of LiHMDS in THF (1.07 mL of a 1.0 M solution, 1.07 mmol, 3 equiv) over 5 min. The resulting yellow solution was stirred at –78 °C for 5 min and was then placed in an ice bath and stirred for 5 min. Subsequently, TIPSOTf (191 μL, 0.712 mmol, 2 equiv) was added rapidly. After 3 min, the reaction was quenched at 0 °C via rapid

addition of sat. aq. $NaHCO_3$ (3 mL) and vigorously stirred at 0 °C for 10 min. Thereafter, the mixture was extracted into Et_2O (3 x 20 mL) and the combined organic layers were washed with sat. aq. $NaHCO_3$ (3 x 10 mL) (note: failure to quench residual TIPSOTf in this manner resulted in extensive decomposition of product upon concentration). The combined organic layers were dried over Na_2SO_4, filtered, and concentrated under reduced pressure to afford a pale yellow oil.

Purification was achieved via flash column chromatography on SiO_2 [15 g SiO_2, Et_2O/hexanes = 8%] to afford silyl enol ether **70** (141 mg, 0.272 mmol, 76% yield) as a puffy, viscous, colorless oil that formed a white solid upon standing in the freezer overnight.

TLC (15% Et_2O/hexanes): R_f = 0.48 (*p*-anisaldehyde).

^{1}H NMR (400 MHz, $CDCl_3$): δ 6.39 (dd, *J* = 17.8, 11.3 Hz, 1H, C_{19}), 5.28 (dd, *J* = 17.8, 1.4 Hz, 1H, C_{20}), 5.17 (dd, *J* = 11.2, 1.4 Hz, 1H, C_{20}), 5.13 (s, 1H, C_{17}), 5.05 (s, 1H, C_{17}), 4.68 (d, *J* = 7.1 Hz, 1H, OC***H***$_2$OMe), 4.40 (d, *J* = 6.7 Hz, 1H, OC***H***$_2$OMe), 4.06 (m, 1H, C_{14}), 3.64 (s, 1H, C_{11}), 3.34 (s, 3H, $OCH_2OC\boldsymbol{H_3}$), 2.53 (ddd, *J* = 15.6, 10.2, 7.5 Hz, 1H, C_2), 2.37 (dd, *J* = 15.6, 11.0, 3.8 Hz, 1H, C_2), 2.32 (dd, *J* = 10.9, 3.6 Hz, 1H, C_8), 2.11 (dd, *J* = 15.0, 6.0 Hz, 1H, C_{13}), 1.78 (ddd, *J* = 13.9, 10.2, 3.8 Hz, 1H, C_1), 1.64 (m, 1H, C_7), 1.51 (m, 1H, C_6), 1.46 (ddd, *J* = 13.9, 6.3, 3.8 Hz, 1H, C_1), 1.41 (m, 1H, C_{13}), 1.40 (m, 1H, C_7), 1.39 (m, 1H, C_8), (s, 3H, C_{15}), 1.17 (s, 3H, C_{18}), 1.15 (m, 3H, $OSi(C\boldsymbol{H}(CH_3)_2)_3$), 1.12 (m, 18H, $OSi(CH(C\boldsymbol{H}_3)_2)_3$), 0.97 (d, *J* = 7.0 Hz, 3H, C_{16}).

^{13}C NMR (101 MHz, $CDCl_3$): δ 151.8 (C_{10}), 147.8 (C_3), 140.7 (C_{19}), 119.2 (C_4), 113.9 (C_{20}), 108.9 (C_{17}), 92.2 ($O\boldsymbol{C}H_2OCH_3$), 79.0 (C_{11}), 67.6 (C_{14}), 55.6 ($OCH_2O\boldsymbol{C}H_3$), 51.5 (C_9),

46.9 (C_{13}), 46.6 (C_5), 44.8 (C_{12}), 44.1 (C_6), 38.8 (C_8), 34.9 (C_1), 34.4 (C_2), 28.9 (C_{18}), 28.7 (C_7), 18.19 (OSi(***C***H(CH_3)$_2$)$_3$), 18.15 (OSi(***C***H(CH_3)$_2$)$_3$), 18.1 (C_{16}), 16.4 (C_{15}), 13.6 (OSi(CH(***C***H_3)$_2$)$_3$).

FTIR (AT-IR): 3495 (br), 2941, 2866, 2359, 2323, 1627, 1462, 1327, 1040, 1002, 882 cm^{-1}.

HRMS (TOF, ES+): calc'd for $C_{31}H_{54}O_4SiNa$ $[M+Na]^+$ 541.3689, found 541.3711.

$[\boldsymbol{\alpha}]_{\boldsymbol{D}}^{\mathbf{23}}$**:** +42.2° (*c* = 0.490, $CHCl_3$).

Melting point: 99.8–101.1°C

Preparation of ketone 71

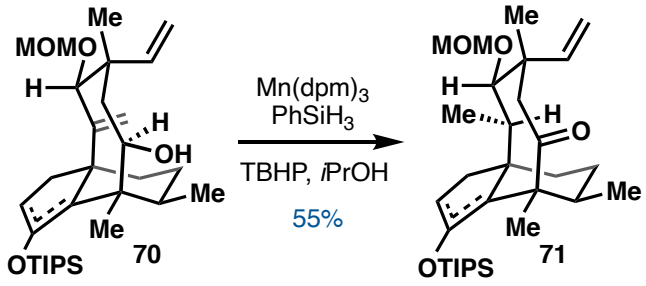

This procedure was adapted from the work of Shenvi and coworkers.[33] A flame-dried 25 mL Schlenk tube was charged with silyl enol ether **70** (116 mg, 0.224 mmol, 1 equiv) and adventitious water was removed via azeotropic drying with PhH (3 x 1 mL) under high vacuum. An oven-dried stir bar was added, and the atmosphere was exchanged three times for argon. Thereafter, ^{i}PrOH (3.4 mL), $PhSiH_3$ (36.3 mg, 0.336 mmol, 41.4 µL, 1.5 equiv), and *tert*-butyl hydroperoxide (89.5 µL of a 5.0 M solution in nonane, 0.448 mmol, 2 equiv) were added. The mixture was subjected to three freeze-pump-thaw cycles. Another Schlenk tube was charged with tris(2,2,6,6-tetramethyl-3,5-heptanedionato)manganese(III) (17.5 mg), and the atmosphere was exchanged three times

for argon before adding ^{i}PrOH (1.4 mL). This solution was subjected to three freeze-pump-thaw cycles then purged with argon. A portion of this stock solution (1.1 mL, equating to 13.5 mg $Mn(dpm)_3$, 0.0224 mmol, 10 mol %) was added to the substrate solution, and the reaction was stirred at ambient temperature. The reaction began as a dark orange solution but became light yellow within 10 min. After 30 min, an additional portion (300 μL) of the $Mn(dpm)_3$ stock solution was added.

After 1 h, the reaction was passed through a plug of SiO_2 (eluting with Et_2O/hexanes = 10%), and concentrated under reduced pressure to afford a dark orange oil that was immediately purified via flash column chromatography on SiO_2 [15 g SiO_2, Et_2O/hexanes = 7%→11%] to afford ketone **71** (63.9 mg, 0.123 mmol, 55% yield) as a viscous, colorless oil.

In addition, the following were isolated: C19–C20 reduced product (9.9 mg, 0.0190 mmol, 8% yield) (15% Et_2O/hexanes, R_f = 0.70 [*p*-anisaldehyde, stains green]), fully reduced product (4.4 mg, 0.00842 mmol, 4% yield, 1:1 dr) (15% Et_2O/hexanes, R_f = 0.53 [*p*-anisaldehyde, stains dark blue]), and remaining starting material (26.6 mg, 0.0513 mmol, 23% recovered).

Experimental Notes: This reaction exhibits a pronounced sensitivity to both residual oxygen and water. In addition, we found it critical to perform this reaction at 23 °C, as higher temperatures promoted over-reduction and lower temperatures slowed catalysis. ^{i}PrOH was stored over activated 4 Å molecular sieves (pellets) overnight then was distilled from CaH_2 (10% w/v) in a flame-dried, argon-filled apparatus immediately prior to use.

TLC (15% Et_2O/hexanes): R_f = 0.60 (*p*-anisaldehyde).

^{1}H NMR (500 MHz, $CDCl_3$): δ 6.15 (dd, *J* = 17.6, 11.1 Hz, 1H, C_{19}), 5.28 (dd, *J* = 17.6, 1.6 Hz, 1H, C_{20}), 5.23 (dd, *J* = 11.1, 1.6 Hz, 1H, C_{20}), 4.69 (d, *J* = 7.0 Hz, 1H, OC***H***$_2$OMe), 4.62 (d, *J* = 7.0 Hz, 1H, OC***H***$_2$OMe), 3.40 (s, 3H, $OCH_2OC\boldsymbol{H_3}$), 3.29 (d, *J* = 4.6 Hz, 1H, C_{11}), 2.80 (d, *J* = 11.4 Hz, 1H, C_{13}), 2.47 (m, 2H, C_2), 2.04 (ddd, *J* = 13.8, 10.2, 5.1 Hz, 1H, C_1), 1.98 (dt, *J* = 13.1, 3.0 Hz, 1H, C_8), 1.95 (d, *J* = 11.4 Hz, 1H, C_{13}), 1.91 (dq, *J* = 7.1, 4.6 Hz, 1H, C_{10}), 1.65 (qd, *J* = 13.8, 3.4 Hz, 1H, C_7), 1.57 (s, 3H, C_{15}), 1.43 (m, 1H, C_6), 1.34 (m, 1H, C_7), 1.31 (m, 1H, C_1), 1.26 (m, 1H, C_8), 1.24 (d, *J* = 7.0 Hz, 3H, C_{16}), 1.18 (m, 3H, $OSi(C\boldsymbol{H}(CH_3)_2)_3$), 1.13 (m, 18H, $OSi(CH(C\boldsymbol{H}_3)_2)_3$), 1.10 (s, 3H, C_{18}), 0.83 (d, *J* = 7.1 Hz, 3H, C_{17}).

^{13}C NMR (125 MHz, $CDCl_3$): δ 215.1 (C_{14}=O), 148.2 (C_3), 139.0 (C_{19}), 117.8 (C_4), 115.5 (C_{20}), 99.3 ($O\boldsymbol{C}H_2OCH_3$), 85.2 (C_{11}), 56.4 ($OCH_2O\boldsymbol{C}H_3$), 54.8 (C_5), 51.5 (C_9), 49.3 (C_{13}), 48.3 (C_{12}), 43.8 (C_6), 39.4 (C_8), 37.1 (C_{10}), 34.0 (C_2), 27.8 (C_7), 27.5 (C_1), 27.3 (C_{18}), 22.2 (C_{15}), 18.15 ($OSi(\boldsymbol{C}H(CH_3)_2)_3$), 18.11 ($OSi(\boldsymbol{C}H(CH_3)_2)_3$), 16.5 ($C_{16}$), 13.6 ($OSi(CH(\boldsymbol{C}H_3)_2)_3$), 11.5 ($C_{17}$).

FTIR (AT-IR): 2944, 2867, 1698, 1650, 1463, 1331, 1206, 1038, 1004 cm^{-1}.

HRMS (TOF, ES+): calc'd for $C_{31}H_{54}O_4SiNa$ $[M+Na]^+$ 541.3689, found 541.3701.

$[\boldsymbol{\alpha}]_{\boldsymbol{D}}^{\boldsymbol{23}}$: –204.8° (*c* = 1.48, $CHCl_3$).

Preparation of alcohol 72

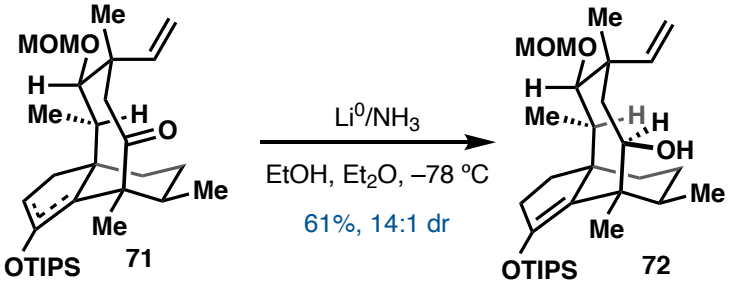

A 250 mL 3-necked flask equipped with a stir bar was equipped with a cold finger connected to a two-way valve, and the entire apparatus was flame-dried under high vacuum. After cooling to ambient temperature, the atmosphere was exchanged three times for argon, and anhydrous EtOH (13.3 mL) and Et_2O (7.3 mL) were added. The mixture was cooled to –78 °C, and ammonia (53 mL) was condensed into the vessel. Subsequently, a solution of ketone **71** (41.4 mg, 0.0798 mmol, 1 equiv) in Et_2O (8.3 mL) was added. After allowing the system to equilibrate for 5 min, Li^0 wire (124 mg, 17.9 mmol, 224 equiv) that had been freshly washed with hexanes and cut into ~5 mg pieces was added. Within 3 min, a deep blue color developed, and after 30 min, the reaction was colorless.

The apparatus was removed from the cooling bath, and ammonia was boiled off over 2 h. The resulting slurry was extracted into Et_2O (100 mL), washed with sat. aq. $NaHCO_3$ (1 x 15 mL), dried over Na_2SO_4, filtered, and concentrated under reduced pressure to afford an oil. Purification was achieved via flash column chromatography on SiO_2 [3 g SiO_2, Et_2O/hexanes = 7%] to afford alcohol **72** (25.2 mg, 0.0487 mmol, 61% yield) as a viscous, colorless oil.

TLC (15% Et_2O/hexanes): R_f = 0.41 (*p*-anisaldehyde).

^{1}H NMR (400 MHz, $CDCl_3$): δ 6.07 (ddd, *J* = 17.9, 11.2 Hz, 0.7 Hz, 1H, C_{19}), 5.28 (dd, *J* = 17.9, 1.6 Hz, 1H, C_{20}), 5.23 (dd, *J* = 11.2, 1.6 Hz, 1H, C_{20}), 4.64 (d, *J* = 6.7 Hz, 1H, $OC\boldsymbol{H}_2OMe$), 4.62 (d, *J* = 6.7 Hz, 1H, $OC\boldsymbol{H}_2OMe$), 4.16 (dd, *J* = 7.1, 2.6 Hz, 1H, C_{14}), 3.40 (s, 3H, $OCH_2OC\boldsymbol{H}_3$), 3.01 (d, *J* = 5.6 Hz, 1H, C_{11}), 2.46–2.34 (m, 2H, C_2), 2.04 (ddd, *J* = 14.9, 7.8, 0.8 Hz, 1H, C_{13}), 1.99 (m, 1H, C_{10}), 1.96 (dt, *J* = 9.4, 3.4 Hz, 1H, C_1), 1.60 (d, *J* = 14.9 Hz, 1H, C_{13}), 1.46 (m, 1H, C_7), 1.41 (m, 1H, C_6), 1.40 (s, 3H, C_{15}), 1.35 (m, 1H, C_7), 1.23 (m, 1H, C_8), 1.21 (m, 1H, C_8), 1.17 (m, 1H, C_1), 1.15 (m, 3H, $OSi(C\boldsymbol{H}(CH_3)_2)_3$), 1.13 (m, 18H, $OSi(CH(C\boldsymbol{H}_3)_2)_3$), 1.01 (s, 3H, C_{18}), 0.99 (d, *J* = 6.3 Hz, 3H, C_{16}), 0.85 (d, *J* = 7.1 Hz, 3H, C_{17}).

^{13}C NMR (101 MHz, $CDCl_3$): δ 147.0 (C_3=O), 141.3 (C_{19}), 120.5 (C_4), 114.4 (C_{20}), 99.2 ($O\boldsymbol{C}H_2OCH_3$), 84.6 (C_{11}), 68.6 (C_{14}), 56.5 ($OCH_2O\boldsymbol{C}H_3$), 50.7 (C_9), 46.5 (C_{12}), 46.1 (C_{13}), 46.0 (C_5), 43.3 (C_6), 39.3 (C_1), 38.2 (C_{10}), 34.3 (C_2), 30.0 (C_{18}), 28.5 (C_8), 28.3 (C_7), 18.3 (C_{15}), 18.24 ($OSi(\boldsymbol{C}H(CH_3)_2)_3$), 18.18 ($OSi(\boldsymbol{C}H(CH_3)_2)_3$), 17.8 ($C_{16}$), 13.8 ($OSi(CH(\boldsymbol{C}H_3)_2)_3$), 11.8 ($C_{17}$).

FTIR (AT-IR): 3493 (br), 2944, 2866, 2359, 2341, 1637, 1461, 1218, 1038, 1002 cm^{-1}.

HRMS (TOF, ES+): calc'd for $C_{31}H_{55}O_4Si$ $[(M+H)–H_2]^+$ 519.3870, found 519.3873.

$[\boldsymbol{\alpha}]_{\boldsymbol{D}}^{\boldsymbol{23}}$: –52.3° (*c* = 0.342, $CHCl_3$).

Preparation of (+)-pleuromutilin (1)

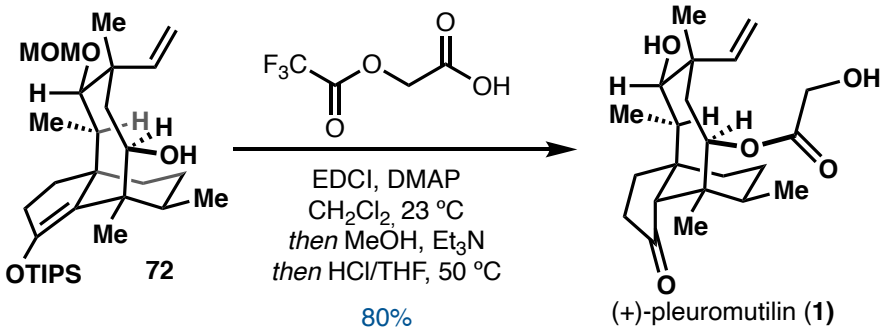

This procedure was adapted from the work of Procter and coworkers.[4] A flame-dried 2 dram vial equipped with a stir bar was charged with alcohol **72** (20.2 mg, 0.0388 mmol, 1 equiv), EDCI•HCl (44.6 mg, 0.233 mmol, 6 equiv), and DMAP (28.4 mg, 0.233 mmol, 6 equiv), and the atmosphere was exchanged three times for argon. Subsequently, the vessel was charged with anhydrous CH_2Cl_2 (1.9 mL) and 2-(2,2,2-trifluoroacetoxy)acetic acid (40.0 mg, 0.230 mmol, 6 equiv), and the reaction was stirred at ambient temperature. After 10 min, a light yellow color developed, and after 30 min, the reaction was complete by TLC analysis (30% Et_2O/hexanes, R_f = 0.77 [*p*-anisaldehyde, stains dark blue/purple], R_f (starting material) = 0.70). Thereafter, a solution of anhydrous MeOH (31 μL, 0.776 mmol, 20 equiv) in freshly distilled Et_3N (107 μL, 0.768 mmol, 20 equiv) was added, and the reaction immediately turned bright yellow. After 5 min, the reaction was judged was complete by TLC analysis (30% Et_2O/hexanes, R_f = 0.35 [*p*-anisaldehyde, stains dark blue/purple]). A solution of HCl in THF (1.16 mL of a 2.0 M solution, 1.92 mmol) was added, and the reaction was heated to 50 °C. After 30 min, an additional portion of HCl in THF (500 uL) was added. At this time, hydrolysis of the methoxymethyl group was judged complete by TLC analysis (70% Et_2O/hexanes, R_f = 0.42 [*p*-anisaldehyde, stains dark blue/black]), and after 2 h global hydrolysis was complete.

The reaction was cooled to 0 °C and was cautiously quenched with sat. aq. $NaHCO_3$ (3 mL). After warming to ambient temperature, the crude mixture was extracted into Et_2O (3 x 5 mL), dried over Na_2SO_4, filtered, and concentrated under reduced pressure to afford an orange oil. Purification was achieved via flash column chromatography on SiO_2 [1.5 g SiO_2, Et_2O/hexanes = 50%→70%] to afford (+)-pleuromutilin (**1**) (11.8 mg, 0.0312 mmol, 80% yield) as a white solid.

TLC (70% Et_2O/hexanes): R_f = 0.22 (*p*-anisaldehyde).

^{1}H NMR (500 MHz, $CDCl_3$): δ 6.50 (dd, *J* = 17.4, 11.0 Hz, 1H, C_{19}), 5.85 (d, *J* = 8.6 Hz, 1H, C_{14}), 5.37 (dd, *J* = 11.0, 1.3 Hz, 1H, C_{20}), 5.22 (dd, *J* = 17.4, 1.4 Hz, 1H, C_{20}), 4.05 (qd, *J* = 17.1, 5.4 Hz, 2H, C_{22}), 3.34 (dd, *J* = 10.8, 6.6 Hz, 1H, C_{11}), 2.35 (t, *J* = 5.5 Hz, 1H, C_{22}–O*H*), 2.33 (m, 1H, C_{10}), 2.25 (m, 1H, C_2), 2.22 (m, 1H, C_2), 2.11 (br s, 1H, C_4), 2.10 (dd, *J* = 16.0, 8.7 Hz, 1H, C_{13}), 1.79 (dq, *J* = 14.5, 3.1 Hz, 1H, C_8), 1.68 (m, 1H, C_6), 1.66 (m, 1H, C_1), 1.55 (dd, *J* = 13.8, 2.7 Hz, 1H, C_7), 1.51 (m, 1H, C_1), 1.46 (br m, 1H, C_{12}–O*H*), 1.44 (s, 3H, C_{15}), 1.40 (ddd, *J* = 13.8, 6.0, 2.7 Hz, 1H, C_7), 1.33 (d, *J* = 16.0 Hz, 1H, C_{13}), 1.19 (s, 3H, C_{18}), 1.15 (td, *J* = 14.3, 4.4 Hz, 1H, C_8), 0.91 (d, *J* = 7.1 Hz, 3H, C_{17}), 0.72 (d, *J* = 7.1 Hz, 3H, C_{16}).

^{13}C NMR (126 MHz, $CDCl_3$): δ 216.8 (C_3=O), 172.1 (C_{21}=O), 138.8 (C_{19}), 117.4 (C_{20}), 74.5 (C_{11}), 69.8 (C_{14}), 61.3 (C_{22}), 58.0 (C_4), 45.4 (C_9), 44.7 (C_{13}), 44.0 (C_{12}), 41.8 (C_5), 36.6 (C_6), 36.0 (C_{10}), 34.4 (C_2), 30.4 (C_8), 26.8 (C_7), 26.3 (C_{18}), 24.8 (C_1), 16.6 (C_{16}), 14.7 (C_{15}), 11.5 (C_{17}).

FTIR (AT-IR): 3437 (br), 2931, 1728, 1454, 1374, 1267, 1215, 1153, 1094, 1015, 915, 858, 734 cm^{-1}.

HRMS (TOF, ES+): calc'd for $C_{22}H_{34}O_5Na$ $[M+Na]^+$ 401.2304, found 401.2296.

$\boldsymbol{[\alpha]_D^{23}}$**:** +33.4° (*c* = 0.252, $CHCl_3$).

Comparison of ^{1}H NMR data for (+)-pleuromutilin (1)

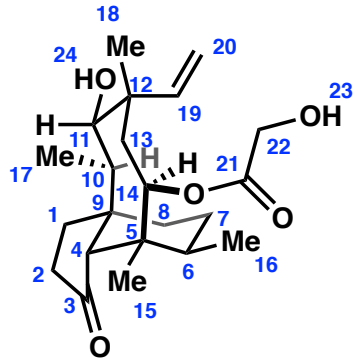

Proton Number	Natural (+)-Pleuromutilin[§] ^{1}H NMR, 500 MHz, $CDCl_3$ ^{1}H [δ, multi, *J* (Hz)]	This Work, Synthetic (+)-Pleuromutilin ^{1}H NMR, 500 MHz, $CDCl_3$ ^{1}H [δ, multi, *J* (Hz)]
1α	1.41–1.53 (m)	1.41–1.52 (m)
1β	1.61–1.73 (m)	1.61–1.73 (m)
2α	2.16–2.30 (m)	2.16–2.30 (m)
2β	2.16–2.30 (m)	2.16–2.30 (m)
3		
4	2.11 (s)	2.11 (s)
5		
6	1.61–1.73 (m)	1.61–1.73 (m)
7α	1.55 (dd, *J* = 13.8, 2.7 Hz)	1.55 (dd, *J* = 13.8, 2.7 Hz)
7β	1.40 (ddd, *J* = 13.8, 6.0, 2.7 Hz)	1.40 (ddd, *J* = 13.8, 6.0, 2.7 Hz)
8α	1.79 (dq, *J* = 14.5, 3.1 Hz)	1.79 (dq, *J* = 14.5, 3.1 Hz)
8β	1.15 (td, *J* = 14.3, 4.4 Hz)	1.15 (td, *J* = 14.3, 4.4 Hz)
9		
10	2.29–2.40 (m)	2.29–2.40 (m)
11	3.34 (dd, *J* = 10.8, 6.6 Hz)	3.34 (dd, *J* = 10.8, 6.6 Hz)
12		
13α	2.10 (dd, *J* = 16.0, 8.7 Hz)	2.10 (dd, *J* = 16.0, 8.7 Hz)
13β	1.33 (d, *J* = 16.0 Hz)	1.33 (d, *J* = 16.0 Hz)
14	5.85 (d, *J* = 8.6 Hz)	5.85 (d, *J* = 8.6 Hz)
15	1.44 (s)	1.44 (s)
16	0.71 (d, *J* = 7.1 Hz)	0.71 (d, *J* = 7.1 Hz)
17	0.90 (d, *J* = 7.1 Hz)	0.90 (d, *J* = 7.1 Hz)
18	1.18 (s)	1.18 (s)
19	6.50 (dd, *J* = 17.4, 11.0 Hz)	6.50 (dd, *J* = 17.4, 11.0 Hz)
20α	5.37 (dd, *J* = 11.0, 1.4 Hz)	5.37 (dd, *J* = 11.0, 1.3 Hz)
20β	5.22 (dd, *J* = 17.4, 1.4 Hz)	5.22 (dd, *J* = 17.4, 1.4 Hz)
21		
22	4.05 (qd, *J* = 17.1, 5.4 Hz)	4.05 (qd, *J* = 17.1, 5.4 Hz)
23	2.30–2.40 (br)*	2.30–2.40 (br)*
24	1.44–1.52 (br)*	1.44–1.52 (br)*

*Signals disappeared upon D_2O quench

[§]Spectrum acquired using a sample of natural (+)-pleuromutilin purchased from Sigma-Aldrich (SML0285-5MG, Lot# 032M4709V)

Comparison of ^{13}C NMR data for (+)-pleuromutilin (1)

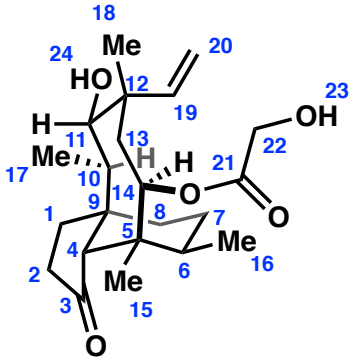

Carbon Number	Schulz and Berner Report[37], Natural (+)-Pleuromutilin ^{13}C NMR, 90 MHz, $CDCl_3$ ^{13}C (δ) ppm	This Work, Synthetic (+)-Pleuromutilin ^{13}C NMR, 126 MHz, $CDCl_3$ ^{13}C (δ) ppm	Chemical Shift Difference
1	24.9	24.8	0.1
2	34.5	34.4	0.1
3	216.8	216.8	0
4	58.2	58.0	0.2
5	41.9	41.8	0.1
6	36.7	36.6	0.1
7	26.9	26.8	0.1
8	30.4	30.4	0
9	45.5	45.4	0.1
10	36.1	36.0	0.1
11	74.7	74.5	0.2
12	44.1	44.0	0.1
13	44.9	44.7	0.2
14	69.9	69.8	0.1
15	14.8	14.7	0
16	16.6	16.6	0
17	11.5	11.5	0
18	26.5	26.3	0.2
19	138.9	138.8	0.1
20	117.3	117.4	0.1
21	172.2	172.1	0.1
22	61.4	61.3	0.1

Preparation of 12-*epi* crotylation adducts 74 and 75

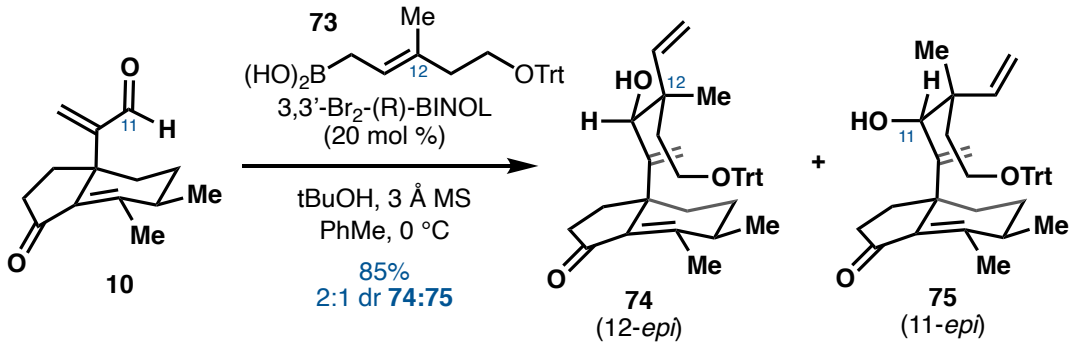

This procedure was adapted from the work of Szabó and coworkers.[10] In a nitrogen-filled glovebox, a flame-dried, 50 mL Schlenk flask equipped with a stir bar was charged with freshly activated 3 Å molecular sieves (pellets) (613 mg), allylboronic acid **73** (11.5 mL of a 0.15 M solution, 1.68 mmol, 1 equiv), 3,3′-Br_2-(*R*)-BINOL (149 mg, 0.336 mmol, 20 mol %), freshly distilled ^{t}BuOH (483 μL, 5.09 mmol, 3 equiv), and a solution of the enal hydrindanone **10** (367 mg, 1.68 mmol, 1 equiv) in dry, degassed PhMe (1.68 mL). The resulting heterogeneous mixture was sealed, removed from the glovebox, then placed in a pre-equilibrated 0 °C bath and stirred.

After 40 h, the reaction was quenched with MeOH (5 mL), stirred for 5 min, filtered, and concentrated under reduced pressure to afford a viscous residue. Purification was achieved via flash column chromatography on SiO_2 [100 g SiO_2, Acetone/hexanes = 4%→15%] to afford **74** and a mixture of **75** and residual 3,3′-Br_2-(*R*)-BINOL (fractions 71–85). The volatiles were concentrated under reduced pressure to afford **74** (566 mg, 1.01 mmol, 60% yield) as a puffy white solid and the **75**/BINOL mixture, respectively.

The **75**/BINOL mixture was subjected to flash column chromatography on SiO_2 [100 g SiO_2, Et_2O/hexanes = 40%] to afford 3,3′-Br_2-(*R*)-BINOL and **75** (237 mg, 0.423 mmol, 25% yield) as a puffy white solid.

Experimental Note: It is critical that all operations be carried out in a rigorously oxygen-free environment. Failure to do so will result in rapid decomposition of the allylboronic acid.

12-*epi* crotylation adduct (74)

TLC (20% acetone/hexanes): R_f = 0.54 (UV, *p*-anisaldehyde).

^{1}H NMR (400 MHz, $CDCl_3$): δ 7.43 (dd, *J* = 8.4, 1.3 Hz, 6H, OC***Ph*$_3$**), 7.34 – 7.19 (m, 9H, OC***Ph*$_3$**), 6.15 (dd, *J* = 17.8, 10.9 Hz, 1H, C_{19}), 5.59 (s, 1H, C_{17}), 5.04 (dd, *J* = 10.9, 1.2 Hz, 1H, C_{20}), 4.92 (dd, *J* = 17.8, 1.3 Hz, 1H, C_{20}), 4.76 (s, 1H, C_{17}), 4.01 (d, *J* = 6.7 Hz, 1H, C_{11}), 3.21 (dt, *J* = 10.0, 6.3 Hz, 1H, C_{14}), 3.11 (ddd, *J* = 9.9, 7.4, 5.4 Hz, 1H, C_{14}), 2.54 (d, *J* = 7.0 Hz, 1H, O***H***), 2.22 – 2.05 (m, 8H, C_1, C_2, C_6, C_8), 1.92 (dd, *J* = 13.5, 6.2 Hz, 1H, C_{13}), 1.80 (dd, *J* = 12.9, 6.9 Hz, 1H, C_{13}), 1.64 (dtd, *J* = 15.5, 6.1, 5.1, 3.5 Hz, 1H, C_7), 1.57 – 1.46 (m, 1H, C_1), 1.36 – 1.13 (m, 3H, C_7, C_8), 1.05 (d, *J* = 7.1 Hz, 3H, C_{16}), 0.88 (s, 3H, C_{18}).

^{13}C NMR (101 MHz, $CDCl_3$): δ 208.0 (C_3=*O*), 152.8 (C_{10}), 152.5 (C_5), 143.9 (OC***Ph*$_3$**), 142.8 (C_{19}), 135.7 (C_4), 128.6 (OC***Ph*$_3$**), 127.8 (OC***Ph*$_3$**), 127.0 (OC***Ph*$_3$**), 118.4 (C_{17}), 113.9 (C_{20}), 87.4 (O***C***Ph_3), 74.4 (C_{11}), 60.7 (C_{14}), 52.0 (C_9), 44.5 (C_{12}), 40.0 (C_{13}), 38.0 (C_6), 35.5 (C_2), 33.2 (C_8), 32.4 (C_1), 28.4 (C_7), 19.9 (C_{18}), 19.1 (C_{16}), 17.0 (C_{15}).

FTIR (thin film, NaCl): 3416, 2930, 1702, 1627, 1448, 1213, 1032, 758, 632 cm^{-1}.

HRMS (TOF, ES+): calc'd for $C_{39}H_{44}O_3Na$ $[M+Na]^+$ 583.3188, found 583.3174.

$[\alpha]_D^{23}$: –72.0° (*c* = 0.41, $CHCl_3$).

11-*epi* crotylation adduct (75)

TLC (40% Et_2O/hexanes): R_f = 0.14 (UV, *p*-anisaldehyde).

^{1}H NMR (400 MHz, $CDCl_3$): δ 7.46 – 7.39 (m, 6H, OC***Ph₃***), 7.33 – 7.20 (m, 9H, OC***Ph₃***), 6.15 (dd, *J* = 17.8, 10.9 Hz, 1H, C_{19}), 5.62 (s, 1H, C_{17}), 5.04 (dd, *J* = 10.9, 1.3 Hz, 1H, C_{20}), 4.95 (dd, *J* = 17.8, 1.4 Hz, 1H, C_{20}), 4.77 (s, 1H, C_{17}), 3.95 (d, *J* = 7.3 Hz, 1H, C_{11}), 3.26 – 3.16 (m, 1H, C_{14}), 3.15 – 3.05 (m, 1H, C_{14}), 2.62 (d, *J* = 7.4 Hz, 1H, O***H***), 2.47 (dd, *J* = 12.2, 7.9 Hz, 1H, C_2), 2.32 – 2.17 (m, 1H, C_8), 2.15 (d, *J* = 5.9 Hz, 1H, C_6), 2.12 (s, 3H, C_{15}), 2.04 (dd, *J* = 18.4, 7.6 Hz, 1H, C_8), 1.95 (dd, *J* = 12.5, 7.2 Hz, 1H, C_{13}), 1.89 (d, *J* = 13.2 Hz, 1H, C_1), 1.85 – 1.76 (m, 1H, C_{13}), 1.65 – 1.56 (m, 1H, C_7), 1.42 (td, *J* = 12.5, 7.9 Hz, 1H, C_2), 1.33 – 1.11 (m, 3H, C_1, C_7), 1.06 (d, *J* = 7.1 Hz, 3H, C_{16}), 0.89 (s, 3H, C_{18}).

^{13}C NMR (101 MHz, $CDCl_3$): δ 208.4 (C_3=*O*), 152.2 (C_{10}), 151.0 (C_5), 143.9 (OC***Ph₃***), 142.9 (C_{19}), 136.3 (C_4), 128.6 (OC***Ph₃***), 127.8 (OC***Ph₃***), 127.0 (OC***Ph₃***), 118.7 (C_{17}), 113.9 (C_{20}), 87.5 (O***C***Ph_3), 74.7 (C_{11}), 60.7 (C_{14}), 52.0 (C_9), 44.3 (C_{12}), 40.2 (C_{13}), 37.5 (C_6), 35.8 (C_8), 32.7 (C_1), 32.5 (C_2), 28.2 (C_7), 20.4 (C_{18}), 19.2 (C_{16}), 16.8 (C_{15}).

FTIR (thin film, NaCl): 3451, 2930, 1702, 1630, 1449, 1214, 1066, 923, 759, 705 cm^{-1}.

HRMS (TOF, ES+): calc'd for $C_{39}H_{44}O_3Na$ $[M+Na]^+$ 583.3188, found 583.3178.

$[\alpha]_D^{23}$: –53.4° (*c* = 0.585, $CHCl_3$).

Preparation of MOM protected crotylation adduct (12-*epi*)

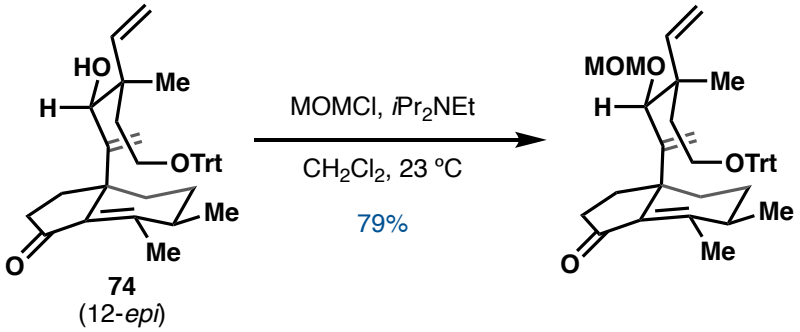

A flame-dried, 50 mL round-bottom flask equipped with a stir bar was charged with alcohol **74** (535 mg, 0.954 mmol, 1 equiv), CH_2Cl_2 (4.8 mL), and freshly distilled ^{i}Pr$_2$NEt

(4.3 mL, 24.7 mmol, 26 equiv). To the homogeneous solution was added chloromethyl methyl ether (1.8 mL. 23.8 mmol, 25 equiv) dropwise over 10 min, taking care to vent HCl fumes formed via the use of a needle. The reaction was stirred at ambient temperature for 20 h. The resulting viscous, orange mixture was quenched via addition of sat. aq. $NaHCO_3$ (20 mL) and stirred at ambient temperature for 30 min. The aqueous layer was extracted with CH_2Cl_2 (3 x 10 mL) and washed with H_2O (1 x 10 mL). The combined organic layers were washed with brine (1 x 10 mL), dried over Na_2SO_4, and concentrated via distillation to afford a viscous, dark orange residue.

Purification was achieved via flash column chromatography on SiO_2 [50 g SiO_2, Et_2O/hexanes = 20%] to afford MOM ether (455 mg, 0.75 mmol, 79% yield) as a puffy white solid.

TLC (40% Et_2O/hexanes): R_f = 0.56 (UV, *p*-anisaldehyde).

^{1}H NMR (400 MHz, $CDCl_3$): δ 7.42 (m, 6H, OC***Ph*$_3$**), 7.32 – 7.17 (m, 9H, OC***Ph*$_3$**), 5.88 (dd, *J* = 17.7, 10.9 Hz, 1H, C_{19}), 5.49 (s, 1H, C_{17}), 4.93 (dd, *J* = 10.9, 1.2 Hz, 1H, C_{20}), 4.86 (s, 1H, C_{17}), 4.79 (dd, *J* = 17.7, 1.2 Hz, 1H, C_{20}), 4.59 (d, *J* = 6.7 Hz, 1H, OC***H*$_2$**OCH_3), 4.55 (d, *J* = 6.7 Hz, 1H, OC***H*$_2$**OCH_3), 3.84 (s, 1H, C_{11}), 3.38 (s, 3H, OCH_2OC***H*$_3$**), 3.14 – 3.00 (m, 2H, C_{14}), 2.22 – 2.04 (m, 8H, C_1, C_2, C_6, C_7, C_{15}), 1.98 – 1.81 (m, 2H, C_{13}), 1.67 – 1.57 (m, 1H, C_8), 1.56 – 1.40 (m, 1H, C_1), 1.28 – 1.20 (m, 2H, C_7, C_8), 1.06 (d, *J* = 7.1 Hz, 3H, C_{16}), 0.93 (s, 3H, C_{18}).

^{13}C NMR (101 MHz, $CDCl_3$): δ 208.1 (C_3=*O*), 151.8 (C_5), 149.8 (C_{10}), 144.4 (OC***Ph*$_3$**), 143.2 (C_{19}), 136.2 (C_4), 128.7 (OC***Ph*$_3$**), 127.7 (OC***Ph*$_3$**), 126.8 (OC***Ph*$_3$**), 121.4 (C_{17}), 113.8 (C_{20}), 96.4 (O***C***H_2OCH_3), 86.8 (O***C***Ph_3), 82.1 (C_{11}), 60.7 (C_{14}), 56.4 (OCH_2O***C***H_3), 51.0 (C_9), 45.3 (C_{12}), 37.7 (C_6), 36.9 (C_{13}), 35.9 (C_2), 33.4 (C_7), 32.5 (C_1), 28.2 (C_8), 19.7 (C_{19}), 19.1 (C_{16}), 17.1 (C_{15}).

FTIR (thin film, NaCl): 3418, 2931, 2071, 1704, 1628, 1449, 1214, 1036, 920, 760 cm^{-1}.

HRMS (TOF, ES+): calc'd for $C_{41}H_{48}O_4Na$ $[M+Na]^+$ 627.3450, found 627.3444.

$[\alpha]_D^{23}$**:** –52.6° (*c* = 0.965, $CHCl_3$).

Preparation of alcohol 76 (12-*epi*)

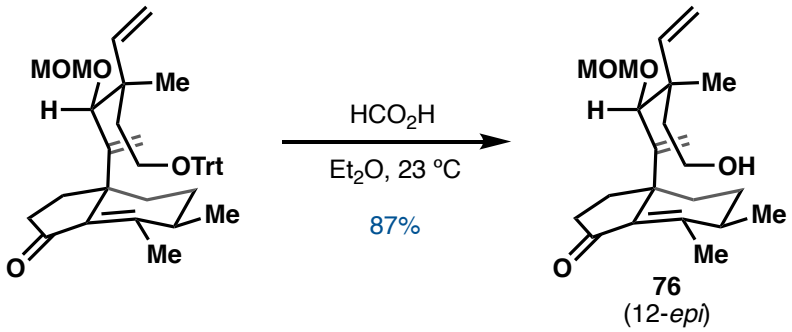

A flame-dried, 250 mL round-bottom flask equipped with a stir bar was charged with MOM ether (332 mg, 0.549 mmol, 1 equiv). Thereafter, a freshly prepared solution of formic acid (98%, 3.4 mL) and Et_2O (3.4 mL) was rapidly added, and within 5 min, the reaction was judged to be complete by TLC analysis. We found it critical to stop this reaction immediately after full conversion was achieved. Prolonged times afforded copious quantities of formate ester product. The reaction was diluted with Et_2O (15 mL) and quenched via slow addition of $NaHCO_3$ (100 mL). The aqueous layer was extracted with Et_2O (4 x 25 mL) and washed with H_2O (1 x 10 mL). The combined organic layers were washed with brine (1 x 25 mL), dried over Na_2SO_4, and concentrated under reduced pressure to afford a viscous yellow residue.

Purification was achieved via flash column chromatography on SiO_2 [7 g SiO_2, Et_2O/hexanes = 70%] to afford alcohol **76** (173 mg, 0.477 mmol, 87% yield) as a viscous, colorless oil.

TLC (40% Et_2O/hexanes): R_f = 0.13 (UV, *p*-anisaldehyde).

^{1}H NMR (400 MHz, $CDCl_3$): δ 6.07 (dd, *J* = 17.8, 10.9 Hz, 1H, C_{19}), 5.58 (s, 1H, C_{17}), 5.11 (dd, *J* = 10.9, 1.1 Hz, 1H, C_{20}), 5.03 (dd, *J* = 17.8, 1.2 Hz, 1H, C_{20}), 4.92 (s, 1H, C_{17}), 4.65 (d, *J* = 6.8 Hz, 1H, OC***H*₂**OCH_3), 4.59 (d, *J* = 6.8 Hz, 1H, OC***H*₂**OCH_3), 3.94 (s, 1H, C_{11}), 3.66 (td, *J* = 6.9, 3.0 Hz, 2H, C_{14}), 3.42 (s, 3H, OCH_2OC***H*₃**), 2.30 – 2.11 (m, 8H, C_1, C_2, C_6, C_8, C_{15}), 1.89 (td, *J* = 6.8, 4.1 Hz, 2H, C_{13}), 1.66 – 1.54 (m, 2H, C_1, C_7), 1.31 – 1.23 (m, 2H, C_7, C_8), 1.11 (s, 3H), 1.07 (d, *J* = 7.0 Hz, 3H).

^{13}C NMR (101 MHz, $CDCl_3$): δ 207.9 (C_3=*O*), 151.9 (C_5), 149.8 (C_{10}), 143.7 (C_{19}), 136.1 (C_4), 121.7 (C_{17}), 114.0 (C_{20}), 96.2 (O***C***H_2OCH_3), 82.1 (C_{11}), 59.7 (C_{14}), 56.4 (OCH_2O***C***H_3), 50.9 (C_9), 45.4 (C_{12}), 39.9 (C_{13}), 37.7 (C_7), 35.8 (C_2), 33.4 (C_8), 32.5 (C_1), 28.1 (C_7), 19.8 (C_{18}), 19.0 (C_{16}), 17.0 (C_{15}).

FTIR (thin film, NaCl): 3417, 2931, 1704, 1627, 1455, 1212, 1152, 1036, 918, 731 cm^{-1}.

HRMS (TOF, ES+): calc'd for $C_{22}H_{34}O_4Na$ $[M+Na]^+$ 385.2355, found 385.2344.

$[\alpha]_D^{23}$: –43.8° (*c* = 0.230, $CHCl_3$).

Preparation of aldehyde 77 (12-*epi*)

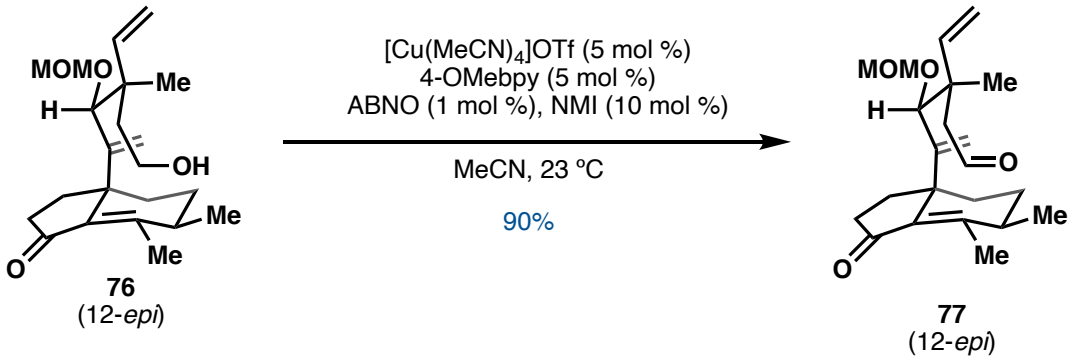

Stahl Oxidation:

A flame-dried, 2 dram vial equipped with a stir bar was charged with alcohol **76** (164 mg, 0.452 mmol, 1 equiv) and MeCN (2.0 mL). Thereafter, added 860 μL of the

[Cu]/bpy stock solution, 860 μL of the NMI stock solution, and 860 μL of the ABNO stock solution, in that order. The orange reaction was stirred at 960 rpm open to the atmosphere for 90 min. Subsequently, the resulting light blue solution was diluted with Et_2O (3 mL), passed through a short pad of SiO_2 using Et_2O as the eluent, and concentrated under reduced pressure to afford a pale yellow oil.

Purification was achieved via flash column chromatography on SiO_2 [8 g SiO_2, Et_2O/hexanes = 30%→60%] to afford aldehyde **77** (148 mg, 0.411 mmol, 90% yield) as a viscous, colorless oil that solidified to a white solid upon standing in the freezer.

Preparation of stock solutions: See page **101**.

TLC (70% Et_2O/hexanes): R_f = 0.57 (UV, *p*-anisaldehyde).

^{1}H NMR (400 MHz, $CDCl_3$): δ 9.73 (dd, *J* = 4.1, 1.8 Hz, 1H, C_{14}), 6.08 (dd, *J* = 17.7, 10.9 Hz, 1H, C_{19}), 5.51 (s, 1H, C_{17}), 5.16 (dd, *J* = 10.9, 0.7 Hz, 1H, C_{20}), 5.10 (dd, *J* = 17.7, 0.7 Hz, 1H, C_{20}), 4.99 – 4.97 (m, 1H, C_{17}), 4.58 (d, *J* = 6.9 Hz, 1H, $OC\boldsymbol{H_2}OCH_3$), 4.51 (d, *J* = 6.9 Hz, 1H, $OC\boldsymbol{H_2}OCH_3$), 4.00 (d, *J* = 1.2 Hz, 1H, C_{11}), 3.40 (s, 3H, $OCH_2OC\boldsymbol{H_3}$), 2.66 (dd, *J* = 15.1, 4.1 Hz, 1H, C_{13}), 2.49 (dd, *J* = 15.1, 1.7 Hz, 1H, C_{13}), 2.29 – 2.05 (m, 8H, C_1, C_2, C_6, C_8, C_{15}), 1.68 – 1.49 (m, 2H, C_1, C_7), 1.32 (s, 3H, C_{18}), 1.30 – 1.21 (m, 2H, C_7, C_8), 1.06 (d, *J* = 7.1 Hz, 3H, C_{16}).

^{13}C NMR (101 MHz, $CDCl_3$): δ 207.8 (C_{14}=*O*), 202.6 (C_3=*O*), 141.8 (C_5), 122.0 (C_{10}), 114.8 (C_{19}), 95.3 ($O\boldsymbol{C}H_2OCH_3$), 80.4 (C_{11}), 56.5 ($OCH_2O\boldsymbol{C}H_3$), 50.7 (C_9), 50.2 (C_{13}), 45.7 (C_{12}), 37.6 (C_6), 35.9 (C_2), 33.4 (C_8), 32.5 (C_1), 28.1 (C_7), 21.8 (C_{18}), 19.1 (C_{16}), 17.1 (C_{15}).

FTIR (thin film, NaCl): 2932, 1714, 1628, 1456, 1413, 1373, 1212, 1151, 1035, 921 cm^{-1}.

HRMS (TOF, ES+): calc'd for $C_{22}H_{32}O_4Na$ $[M+Na]^+$ 383.2198, found 383.2182.

$[\alpha]_D^{23}$: –67.3° (*c* = 0.095, $CHCl_3$).

Preparation of tricycle 78 (12-*epi*)

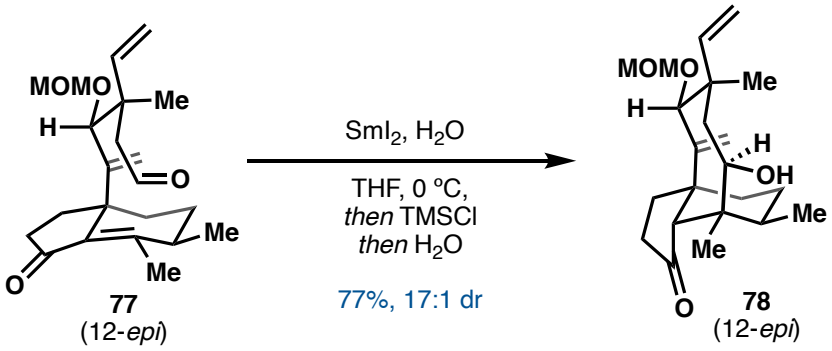

A 25 mL Schlenk tube equipped with a stir bar was charged with a solution of aldehyde **77** (75 mg, 0.208 mmol, 1 equiv) in 10.3 mL of THF that had been submitted to five freeze-pump-thaw cycles and H_2O/THF (1.88 mL). The solution was cooled to 0 ºC and stirred at this temperature for 5 min. Thereafter, SmI_2/THF (6.3 mL, 0.63 mmol, 3 equiv) was added dropwise over 8 min. The deep blue color of SmI_2 was immediately quenched upon addition of each drop. The first drop afforded a yellow solution, fading to a pale yellow and almost clear by the time 1.6 equiv SmI_2 had been added. When 2.2 equiv SmI_2 had been added, the blue color became increasingly persistent and upon addition of 2.6 equiv SmI_2, the reaction was dark blue/green. After stirring an additional 10 min at 0 ºC, TMSCl/THF (1.9 mL, 1.05 mmol, 5 equiv TMSCl) was added dropwise over 2 min, and the reaction was stirred an additional 10 min. Throughout this time, the deep blue color was quenched to yellow. Thereafter, the reaction was removed from the ice bath and stirred open to the atmosphere for 5 min.

The resulting pale yellow solution was diluted with Et_2O (50 mL), and washed with H_2O (2 x 10 mL). The aqueous layer was back-extracted with Et_2O (2 x 10 mL), and the

combined organic layers were dried over Na_2SO_4, filtered, and concentrated under reduced pressure to afford a dark orange oil. Purification was achieved via flash column chromatography on SiO_2 [10 g SiO_2, Et_2O/hexanes = 30%] to afford tricycle **78** (62 mg, 0.172 mmol, 77% yield) as a white solid.

Preparation of SmI_2: See page **103.**

Stock solution of TMSCl: See page **104.**

Stock solution of H_2O/THF: A solution of H_2O (60 μL) in THF (5.0 mL) was submitted to five freeze-pump-thaw cycles.

TLC (50% Et_2O/hexanes): R_f = 0.50 (*p*-anisaldehyde).

^{1}H NMR (400 MHz, $CDCl_3$): δ 5.98 (dd, *J* = 17.5, 10.8 Hz, 1H, C_{19}), 5.42 (d, *J* = 0.9 Hz, 1H, C_{17}), 5.32 (t, *J* = 0.7 Hz, 1H, C_{17}), 5.09 (dd, *J* = 17.5, 1.0 Hz, 1H, C_{20}), 5.03 (dd, *J* = 10.8, 1.0 Hz, 1H, C_{20}), 4.54 (d, *J* = 7.1 Hz, 1H, OC***H*****$_2$**OCH_3), 4.34 (dd, *J* = 7.1, 0.5 Hz, 1H, OC***H*****$_2$**OCH_3), 4.12 (d, *J* = 6.2 Hz, 1H, C_{14}), 4.00 (s, 1H, C_{11}), 3.34 (s, 3H, OCH_2OC***H*****$_3$**), 2.39 – 2.16 (m, 3H, C_2, C_4), 2.13 – 1.96 (m, 3H, C_1, C_8, C_{13}), 1.72 (dtt, *J* = 15.9, 6.2, 2.9 Hz, 1H, C_6), 1.63 (dd, *J* = 13.1, 3.3 Hz, 1H, C_7), 1.46 – 1.37 (m, 1H, C_7), 1.29 (s, 4H, C_1, C_{15}), 1.24 (d, *J* = 0.8 Hz, 3H, C_{18}), 1.08 (dd, *J* = 15.8, 1.2 Hz, 1H, C_8), 0.98 (d, *J* = 6.8 Hz, 3H, C_{16}).

^{13}C NMR (101 MHz, $CDCl_3$): δ 216.6 (C_3=*O*), 148.1 (C_{19}), 147.9 (C_{10}), 112.8 (C_{17}), 111.3 (C_{20}), 92.3 (O***C***H_2OCH_3), 76.2 (C_{11}), 67.0 (C_{14}), 59.5 (C_4), 55.9 (OCH_2O***C***H_3), 46.5 (C_9), 45.7 (C_8), 43.6 (C_{12}), 42.1 (C_5), 37.4 (C_6), 34.9 (C_2), 31.2 (C_{13}), 29.8 (C_1), 26.8 (C_7), 18.2 (C_{16}), 15.1 (C_{18}), 13.4 (C_{15}).

FTIR (thin film, NaCl): 3521, 2937, 1738, 1456, 1376, 1147, 1095, 1032, 967 cm $^{-1}$.

HRMS (FAB+) calc'd for $C_{22}H_{35}O_4$ $[M+H]^+$ 363.2535, found 363.2556.

$[\alpha]_D^{23}$**:** +161.6° (*c* = 0.09, $CHCl_3$).

Preparation of silyl enol ether 79 (12-*epi*)

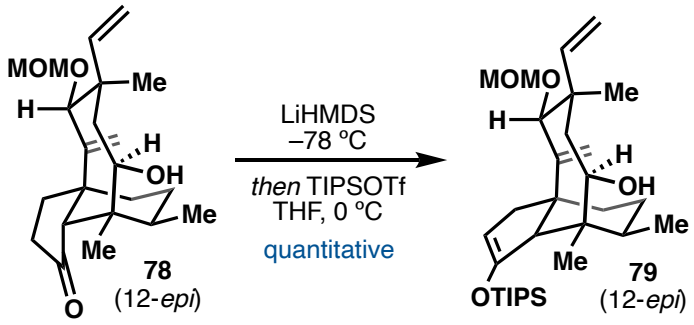

A flame-dried 1 dram vial equipped with a stir bar was charged with tricycle **78** (13.1 mg, 0.036 mmol, 1 equiv) and anhydrous THF (720 µL) under an atmosphere of argon. The mixture was cooled to –78 °C and stirred for 5 min prior to dropwise addition of LiHMDS in THF (108 µL of a 1.0 M solution, 0.108 mmol, 3 equiv) over 5 min. The resulting yellow solution was stirred at –78 °C for 5 min and was then placed in an ice bath and stirred for 5 min. Subsequently, TIPSOTf (22 µL, 0.072 mmol, 2 equiv) was added rapidly. After 3 min, the reaction was quenched at 0 °C via rapid addition of sat. aq. $NaHCO_3$ (1 mL) and vigorously stirred at 0 °C for 10 min. Thereafter, the mixture was extracted into Et_2O (3 x 1 mL) and the combined organic layers were washed with sat. aq. $NaHCO_3$ (3 x 1 mL) (note: failure to quench residual TIPSOTf in this manner resulted in extensive decomposition of product upon concentration). The combined organic layers were dried over Na_2SO_4, filtered, and concentrated under reduced pressure to afford a pale yellow oil.

Purification was achieved via flash column chromatography on SiO_2 [3 g SiO_2, Et_2O/hexanes = 8%] to afford silyl enol ether **79** (19.1 mg, 0.036 mmol, quantitative yield)

as a puffy, viscous, colorless oil that formed a white solid upon standing in the freezer overnight.

TLC (30% Et_2O/hexanes): R_f = 0.56 (*p*-anisaldehyde).

^{1}H NMR (400 MHz, $CDCl_3$): δ 6.02 (dd, *J* = 17.5, 10.8 Hz, 1H, C_{19}), 5.39 (s, 1H, C_{17}), 5.23 (s, 1H, C_{17}), 5.09 (dd, *J* = 17.5, 1.1 Hz, 1H, C_{20}), 5.01 (dd, *J* = 10.8, 1.1 Hz, 1H, C_{20}), 4.50 (d, *J* = 6.9 Hz, 1H, OC***H*₂**OCH_3), 4.42 (q, *J* = 2.8 Hz, 2H, C_2), 4.33 (d, *J* = 6.9 Hz, 1H, OC***H*₂**OCH_3), 4.24 – 4.15 (m, 2H, C_{11}, C_{14}), 3.33 (s, 3H, OCH_2OC***H*₃**), 2.81 (s, 1H, C_4), 2.33 (ddd, *J* = 14.2, 3.2, 1.7 Hz, 1H, C_1), 2.21 – 1.95 (m, 3H, C_8, C_{13}), 1.77 (ddq, *J* = 14.3, 7.1, 3.8 Hz, 1H, C_6), 1.65 – 1.53 (m, 1H, C_7), 1.45 – 1.32 (m, 2H, C_1, C_7), 1.32 – 1.18 (m, 6H, C_{18}, $OSi(C$***H***$(CH_3)_2)_3$), 1.15 (s, 3H, C_{15}), 1.12 (dd, *J* = 7.2, 5.1 Hz, 18H, $OSi(CH(C$***H***$_3)_2)_3$), 1.04 – 0.95 (m, 4H, C_{13}, C_{16}).

^{13}C NMR (101 MHz, $CDCl_3$) δ 157.5 (C_3), 149.5 (C_{10}), 148.6 (C_{19}), 112.0 (C_{17}), 110.9 (C_{20}), 98.6 (C_2), 92.7 (O***C***H_2OCH_3), 77.2 (C_{11}), 67.7 (C_{14}), 55.9 (OCH_2O***C***H_3), 53.2 (C_4), 48.9 (C_9), 46.3 (C_{13}), 43.8 (C_{12}), 41.3 (C_5), 40.9 (C_1), 38.4 (C_6), 30.1 (C_8), 27.2 (C_7), 18.3 (C_{16}), 18.1 ($OSi(CH($***C***$H_3)_2)_3$), 17.7 ($OSi(CH($***C***$H_3)_2)_3$), 15.6 (C_{18}), 15.3 (C_{15}), 12.9 ($OSi($***C***$H(CH_3)_2)_3$).

FTIR (thin film, NaCl): 2928, 1636, 1465, 1298, 1140, 1026, 906, 689 cm^{-1}.

HRMS (FAB+) calc'd for $C_{31}H_{54}O_4Si$ $[M+H]^+$ 518.3791, found 518.3798.

$[\alpha]_D^{23}$: +31.1° (*c* = 0.15, $CHCl_3$).

Preparation of ketone 80 (12-*epi*)

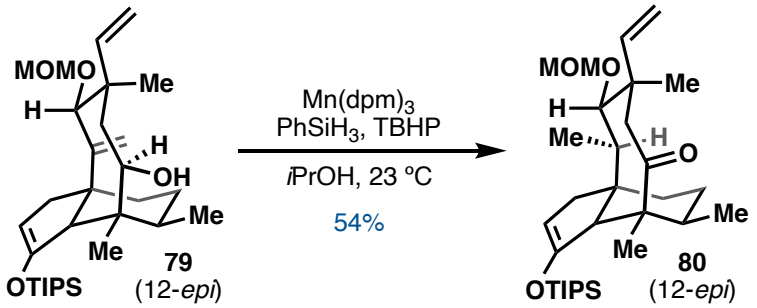

This procedure was adapted from the work of Shenvi and coworkers.[33] To a 1 dram vial was added TIPS enol ether **79** (25.6 mg, 0.049 mmol, 1 equiv) and adventitious water was removed via azeotropic drying with PhH (3 x 1 mL) under high vacuum (70 mTorr). An oven dried stir bar was added, and the atmosphere was exchanged three times with argon. Thereafter, 775 µL of a stock solution containing $PhSiH_3$ (9.3 µL, 0.075 mmol, 1.5 equiv) and TBHP (20 µL, 0.100 mmol, 2 equiv) in ^{i}PrOH was added, followed by 175 µL of a stock solution containing $Mn(dpm)_3$ (3.0 mg, 0.00506 mmol, 0.1 equiv) in ^{i}PrOH. The reaction was stirred for 30 min at ambient temperature and another 50 µL of the $Mn(dpm)_3$ (0.9 mg, 0.00144 mmol, 0.03 equiv) was added. After 1 h, the reaction was passed through a plug of SiO_2 (eluting with Et_2O/hexanes = 10%), and concentrated under reduced pressure to afford a dark orange oil.

Purification was achieved via flash column chromatography on SiO_2 [3 g SiO_2, Et_2O/hexanes = 7%→11%] to afford ketone **80** (13.7 mg, 0.0251 mmol, 54% yield) as a viscous, colorless oil.

Experimental Notes: This reaction exhibits a pronounced sensitivity to both residual oxygen and water. In addition, we found it critical to perform this reaction at 23 °C, as higher temperatures promoted over-reduction and lower temperatures slowed catalysis.

^{i}PrOH was stored over activated 4 Å molecular sieves (pellets) overnight then was distilled from CaH_2 (10% w/v) in a flame-dried, argon-filled apparatus immediately prior to use.

Preparation of stock solutions: $PhSiH_3$ (30 μL) and *tert*-butyl hydroperoxide (65 μL of a 5.0 M solution in nonane) were dissolved in ^{i}PrOH (2.5 mL) and the homogeneous solution was submitted to three freeze-pump-thaw cycles. $Mn(dpm)_3$ (17.3 mg) was dissolved in 1 mL ^{i}PrOH and the dark brown homogeneous solution was submitted to three freeze-pump-thaw cycles.

TLC (30% Et_2O/hexanes): R_f = 0.72 (*p*-anisaldehyde).

^{1}H NMR (400 MHz, $CDCl_3$): δ 5.96 (dd, *J* = 17.4, 10.7 Hz, 1H, C_{19}), 5.09 – 4.97 (m, 2H, C_{20}), 4.55 (d, *J* = 7.0 Hz, 1H, O***CH*$_2$**OCH$_3$), 4.53 (d, *J* = 7.0 Hz, 1H, OC***H*$_2$**OCH$_3$), 4.44 (s, 1H, C_2), 3.81 (d, *J* = 5.8 Hz, 1H, C_{11}), 3.37 (s, 3H, OCH$_2$OC***H*$_3$**), 3.22 (s, 1H, C_4), 2.92 (d, *J* = 12.0 Hz, 1H, C_{13}), 2.15 (ddd, *J* = 14.1, 3.2, 1.6 Hz, 1H, C_1), 1.95 – 1.66 (m, 4H, C_7, C_8, C_{10}, C_{13}), 1.66 – 1.50 (m, 3H, C_1, C_6, C_7), 1.34 (s, 3H, C_{15}), 1.27 – 1.22 (m, 4H, C_8, OSi(C***H***(CH$_3$)$_2$)$_3$), 1.19 (s, 3H, C_{18}), 1.17 (d, *J* = 7.0 Hz, 3H, C_{16}), 1.13 (d, *J* = 2.9 Hz, 9H, OSi(CH(C***H*$_3$**)$_2$)$_3$), 1.11 (d, J = 2.9 Hz, 9H, OSi(CH(C***H*$_3$**)$_2$)$_3$).

^{13}C NMR (101 MHz, $CDCl_3$): δ 214.4 (C_{14}=*O*), 156.8 (C_3), 147.7 (C_{19}), 111.4 (C_{20}), 98.6 (C_2), 98.1 (O***C***H$_2$OCH$_3$), 81.5 (C_{11}), 56.6 (OCH$_2$O***C***H$_3$), 51.5 (C_4), 50.6 (C_5), 48.1 (C_9), 47.9 (C_{12}), 46.6 (C_{13}), 37.2 (C_6), 34.5 (C_1), 34.4 (C_{10}), 32.0 (C_7), 26.7 (C_8), 23.2 (C_{15}), 18.1 (OSi(CH(***C***H$_3$)$_2$)$_3$), 16.2 (C_{16}), 15.0 (C_{18}), 12.9 (OSi(***C***H(CH$_3$)$_2$)$_3$), 12.0 (C_{17}).

FTIR (thin film, NaCl): 2946, 2868, 1698, 1634, 1463, 1300, 1129, 1086, 882, 692 cm^{-1}.

HRMS (FAB+): calc'd for $C_{31}H_{54}O_4Si$ $[M]^+$ 518.3791, found 518.3797.

$[\alpha]_D^{23}$: –18.5° (*c* = 0.195, $CHCl_3$).

Preparation of alcohol 81 (12-*epi*)

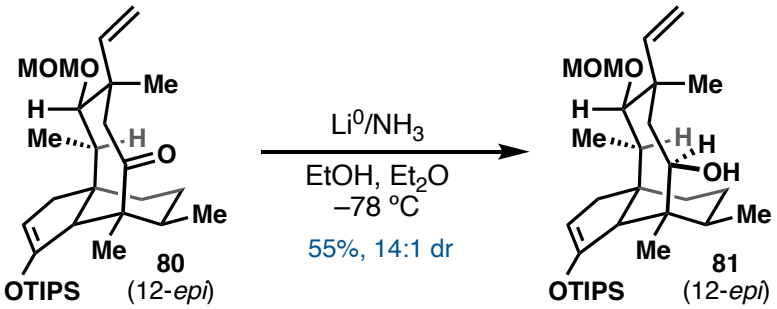

A 100 mL 3-necked flask equipped with a stir bar was equipped with a cold finger connected to a two-way valve, and the entire apparatus was flame-dried under high vacuum. After cooling to ambient temperature, the atmosphere was exchanged three times for argon, and anhydrous EtOH (7.3 mL) and Et_2O (4 mL) were added. The mixture was cooled to –78 °C, and ammonia (30 mL) was condensed into the vessel. Subsequently, a solution of ketone **80** (23 mg, 0.0443 mmol, 1 equiv) in Et_2O (5.3 mL) was added. After allowing the system to equilibrate for 5 min, Li^0 wire (69 mg, 9.9 mmol, 223 equiv) that had been freshly washed with hexanes and cut into ~10 mg pieces was added. Within 3 min, a deep blue color developed, and after 30 min, the reaction was colorless.

The apparatus was removed from the cooling bath, and ammonia was boiled off over 1 h. The resulting slurry was extracted into Et_2O (50 mL), washed with sat. aq. $NaHCO_3$ (10 mL), dried over Na_2SO_4, filtered, and concentrated under reduced pressure to afford an oil.

Purification was achieved via flash column chromatography on SiO_2 [3 g SiO_2, Et_2O/hexanes = 7%] to afford alcohol **81** (12.7 mg, 0.0244 mmol, 55% yield) as a viscous, colorless oil.

TLC (15% Et_2O/hexanes): R_f = 0.36 (*p*-anisaldehyde).

^{1}H NMR (400 MHz, $CDCl_3$): δ 5.76 (dd, *J* = 17.6, 10.8 Hz, 1H, C_{19}), 4.97 (dd, *J* = 17.6, 1.2 Hz, 1H, C_{20}), 4.90 (dd, *J* = 10.8, 1.2 Hz, 1H, C_{20}), 4.50 (d, *J* = 6.9 Hz, 1H, $OC\boldsymbol{H_2}OCH_3$), 4.47 (d, *J* = 6.8 Hz, 1H, $OC\boldsymbol{H_2}OCH_3$), 4.20 (t, *J* = 7.5, 6.7 Hz, 1H, C_{14}), 3.35 (s, 3H, $OCH_2OC\boldsymbol{H_3}$), 3.08 (d, *J* = 5.6 Hz, 1H, C_{11}), 2.47 – 2.28 (m, 2H, C_2), 2.22 – 2.07 (m, 2H, C_{10}, C_{13}), 1.98 (d, *J* = 15.3 Hz, 2H, C_1, C_7), 1.40 (m, 5H, C_6, C_7, C_{15}), 1.26 – 1.08 (m, 27H, C_1, C_8, C_{13}, C_{18}, $OSi(C\boldsymbol{H}(C\boldsymbol{H_3})_2)_3$), 1.01 (d, *J* = 6.6 Hz, 3H, C_{16}), 0.84 (d, *J* = 7.2 Hz, 3H, C_{17}).

^{13}C NMR (101 MHz, $CDCl_3$): δ 149.1 (C_{19}), 147.2 (C_3), 120.3 (C_4), 110.5 (C_{20}), 99.0 ($O\boldsymbol{C}H_2OCH_3$), 83.5 (C_{11}), 68.2 (C_{14}), 56.5 ($OCH_2O\boldsymbol{C}H_3$), 50.6 (C_9), 47.1 (C_{13}), 46.2 (C_5), 44.9 (C_{12}), 43.2 (C_6), 39.4 (C_1), 36.3 (C_{10}), 34.4 (C_2), 28.4 (C_7), 28.3 (C_8), 18.33 (C_{15}), 18.26 ($OSi(CH(\boldsymbol{C}H_3)_2)_3$), 18.2 ($OSi(CH(\boldsymbol{C}H_3)_2)_3$), 17.8 ($C_{16}$) 14.4 ($C_{18}$), 13.8 ($OSi(\boldsymbol{C}H(CH_3)_2)_3$), 11.4 ($C_{17}$).

FTIR (thin film, NaCl): 2921, 2866, 1635, 1463, 1328, 1218, 1030, 1002, 913, 797 cm^{-1}.

HRMS (FAB+): calc'd for $C_{31}H_{56}O_4Si$ $[M]^+$ 520.3948, found 520.3932.

$[\boldsymbol{\alpha}]_{\boldsymbol{D}}^{\boldsymbol{23}}$: –46.3° (*c* = 0.14, $CHCl_3$).

Preparation of (+)-12-*epi*-pleuromutilin 82 (12-*epi*)

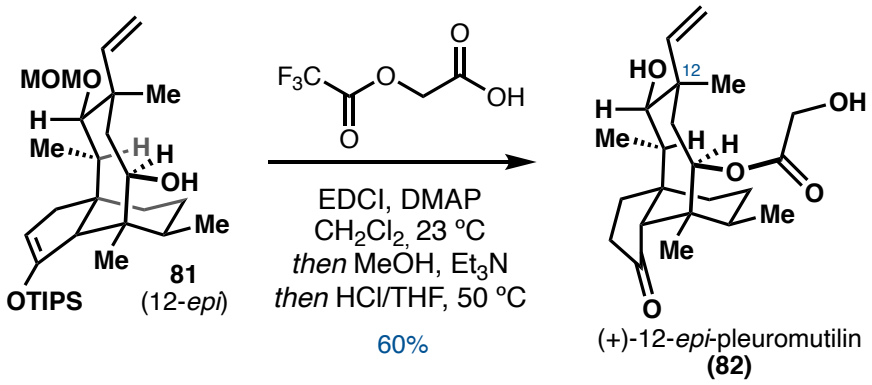

This procedure was adapted from the work of Procter and coworkers.[4] A flame-dried 2 dram vial equipped with a stir bar was charged with alcohol **81** (12.7 mg, 0.0244 mmol, 1 equiv), EDCI•HCl (28.0 mg, 0.146 mmol, 6 equiv), and DMAP (17.8 mg, 0.146 mmol, 6 equiv), and the atmosphere was exchanged three times for argon. Subsequently, the vessel was charged with anhydrous CH_2Cl_2 (1.2 mL) and 2-(2,2,2-trifluoroacetoxy)acetic acid (25.0 mg, 0.146 mmol, 6 equiv), and the reaction was stirred at ambient temperature. After 10 min, a light yellow color developed, and after 30 min, the reaction was complete by TLC analysis (30% Et_2O/hexanes, R_f = 0.77 [*p*-anisaldehyde], R_f (starting material) = 0.70). Thereafter, a solution of anhydrous MeOH (19 µL, 0.480 mmol, 20 equiv) in freshly distilled Et_3N (67 µL, 0.480 mmol, 20 equiv) was added, and the reaction immediately turned bright yellow. After 5 min, the reaction was judged was complete by TLC analysis (30% Et_2O/hexanes, R_f = 0.35 [*p*-anisaldehyde]). A solution of HCl in THF (600 µL of a 2.0 M solution, 1.2 mmol) was added, and the reaction was heated to 50 °C. After 30 min, an additional portion of HCl in THF (260 uL) was added. At this time, hydrolysis of the methoxymethyl group was judged complete by TLC analysis (70% Et_2O/hexanes, R_f = 0.42 [*p*-anisaldehyde]), and after 2 h global hydrolysis was complete.

The reaction was cooled to 0 °C and was cautiously quenched with sat. aq. $NaHCO_3$ (3 mL). After warming to ambient temperature, the crude mixture was extracted into Et_2O (3 x 5 mL), dried over Na_2SO_4, filtered, and concentrated under reduced pressure to afford an orange oil.

Purification was achieved via flash column chromatography on SiO_2 [1.5 g SiO_2, Et_2O/hexanes = 50%→70%] to afford (+)-12-*epi*-pleuromutilin **82** (5.4 mg, 0.0143 mmol, 60% yield) as a white solid.

TLC (70% Et_2O/hexanes): R_f = 0.26 (*p*-anisaldehyde).

^{1}H NMR (400 MHz, $CDCl_3$): δ 5.81 – 5.65 (m, 2H, C_{14}, C_{19}), 5.27 – 5.17 (m, 2H, C_{20}), 4.07 (dd, *J* = 17.1, 5.6 Hz, 1H, C_{22}), 4.01 (dd, *J* = 17.1, 5.2 Hz, 1H, C_{22}), 3.45 (d, *J* = 6.4 Hz, 1H, C_{11}), 2.45 – 2.00 (m, 6H, C_2, C_4, C_{10}, C_{13}, $C_{22}O\boldsymbol{H}$,), 1.81 (dq, *J* = 13.9, 2.7 Hz, 1H, C_8), 1.73 – 1.58 (m, 2H, C_1, C_6), 1.58 – 1.45 (m, 3H, C_1, C_7, $C_{11}O\boldsymbol{H}$), 1.44 (s, 3H, C_{15}), 1.42 – 1.36 (m, 1H, C_7), 1.25 (s, 3H, C_{18}), 1.18 – 1.04 (m, 2H, C_8, C_{13}), 0.97 (d, *J* = 7.1 Hz, 3H, C_{17}), 0.70 (d, *J* = 7.0 Hz, 3H, C_{16}).

^{13}C NMR (101 MHz, $CDCl_3$): δ 217.0 (C_3=*O*), 172.1 (C_{21}), 146.8 (C_{19}), 115.4 (C_{20}), 71.9 (C_{11}), 70.1 (C_{14}), 61.3 (C_{22}), 58.2 (C_4), 45.4 (C_9), 45.3 (C_{12}), 43.6 (C_{13}), 41.8 (C_5), 36.6 (C_6), 34.5 (C_2), 34.4 (C_{10}), 30.1 (C_8), 26.9 (C_7), 25.0 (C_1), 16.7 (C_{16}), 14.8 (C_{15}), 14.1 (C_{18}), 10.8 (C_{17}).

FTIR (thin film, NaCl): 3437, 2927, 1728, 1603, 1444, 1382, 1232, 1098, 1011, 755 cm^{-1}.

HRMS (FAB+): calc'd for $C_{22}H_{33}O_5$ $[M+H]^+–H_2$ 377.2328, found 377.2329

$[\boldsymbol{\alpha}]_{\boldsymbol{D}}^{\boldsymbol{23}}$: +9.12° (*c* = 0.125, $CHCl_3$).

Preparation of 11,12-bis-*epi*-Dowd-Beckwith rearrangement tricycle 83

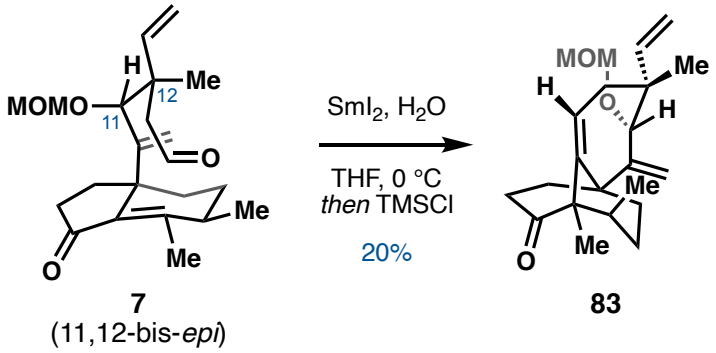

7
(11,12-bis-*epi*)

83

A 2 dram vial equipped with a stir bar was charged with a solution of aldehyde **7** (35 mg, 0.097 mmol, 1 equiv) in 4.8 mL of THF that had been submitted to five freeze-pump-thaw cycles and H_2O/THF (2.7 mL). The solution was cooled to 0 ºC and stirred at this temperature for 5 min. Thereafter, SmI_2/THF (2.9 mL, 0.294 mmol, 3 equiv) was added dropwise over 8 min. The deep blue color of SmI_2 was immediately quenched upon addition of each drop. The first drop afforded a yellow solution, fading to a pale yellow and almost clear by the time 1.6 equiv SmI_2 had been added. When 2.2 equiv SmI_2 had been added, the blue color became increasingly persistent and upon addition of 2.6 equiv SmI_2, the reaction was dark blue/green. After stirring an additional 10 min at 0 ºC, TMSCl/THF (889 µL, 0.490 mmol, 5 equiv TMSCl) was added dropwise over 2 min, and the reaction was stirred an additional 10 min. Throughout this time, the deep blue color was quenched to yellow. Thereafter, the reaction was removed from the ice bath and stirred open to the atmosphere for 5 min.

The resulting pale yellow solution was diluted with Et_2O (2 mL), and washed with H_2O (2 x 1 mL). The aqueous layer was back-extracted with Et_2O (2 x 1 mL), and the combined organic layers were dried over Na_2SO_4, filtered, and concentrated under reduced pressure to afford a dark orange oil.

Purification was achieved via flash column chromatography on SiO_2 [3 g SiO_2, Et_2O/hexanes = 20%] to afford tricycle **83** (7 mg, 0.020 mmol, 21% yield) as a white solid.

Preparation of SmI_2: See page **103.**

Stock solution of TMSCl: See page **104.**

Stock solution of H_2O/THF: See page **133.**

TLC (30% Et_2O/hexanes): R_f = 0.33 (*p*-anisaldehyde).

^{1}H NMR (400 MHz, $CDCl_3$): δ 6.11 (dd, *J* = 17.6, 10.9 Hz, 1H, C_{19}), 5.53 (dd, *J* = 9.0, 5.5 Hz, 1H, C_{14}), 5.10 (dd, *J* = 11.0, 1.4 Hz, 1H, C_{20}), 5.07 (d, *J* = 0.8 Hz, 1H, C_{17}), 5.03 (d, *J* = 0.8 Hz, 1H, C_{17}), 5.00 (dd, *J* = 17.7, 1.5 Hz, 1H, C_{20}), 4.63 (d, *J* = 6.8 Hz, 1H, $OC\boldsymbol{H_2}OCH_3$), 4.49 (d, *J* = 6.7 Hz, 1H, $OC\boldsymbol{H_2}OCH_3$), 4.21 (s, 1H, C_{11}), 3.38 (s, 3H, $OCH_2OC\boldsymbol{H_3}$), 2.49 – 2.36 (m, 3H, C_1, C_2), 2.35 – 2.18 (m, 2H, C_8, C_{13}), 2.02 (tq, *J* = 9.4, 3.6, 2.4 Hz, 1H, C_6), 1.92 (ddd, *J* = 11.7, 9.0, 6.1 Hz, 1H, C_2), 1.81 – 1.65 (m, 1H, C_7), 1.61 (dd, *J* = 13.6, 9.0 Hz, 1H, C_{13}), 1.45 – 1.36 (m, 1H, C_7), 1.26 (d, *J* = 0.9 Hz, 3H, C_{18}), 1.10 (s, 3H, C_{15}), 1.10 – 1.01 (m, 1H, C_8), 0.92 (d, *J* = 7.0 Hz, 3H, C_{16}).

^{13}C NMR (101 MHz, $CDCl_3$): δ 219.1 (C_3=*O*), 155.2 (C_{10}), 142.3 (C_{19}), 141.8 (C_{10}), 119.8 (C_{17}), 112.3 (C_{20}), 106.7 (C_{14}), 93.1 ($O\boldsymbol{C}H_2OCH_3$), 79.9 (C_{11}), 56.9 (C_5), 55.4 ($OCH_2O\boldsymbol{C}H_3$), 45.1 (C_9), 45.0 (C_{12}), 38.7 (C_6), 38.5 (C_1), 37.1 (C_8), 35.6 (C_{13}), 29.6 (C_2), 27.8 (C_7), 23.1 (C_{18}), 19.8 (C_{15}), 13.7 (C_{16}).

FTIR (thin film, NaCl): 2923, 2853, 1711, 1461, 1378, 1261, 1142, 1101, 1040 cm^{-1}.

HRMS (TOF, ES+): calc'd for $C_{22}H_{33}O_3$ $[M+H]^+$ 345.2430, found 345.2409.

$[\alpha]_D^{23}$: –78.7° (*c* = 0.045, $CHCl_3$).

2.8 NOTES AND REFERENCES

(1) Gibbons, E. G. Total Synthesis of (.+-.)-Pleuromutilin. *J. Am. Chem. Soc.* **1982**, *104* (6), 1767–1769.

(2) Boeckman, R. K.; Springer, D. M.; Alessi, T. R. Synthetic Studies Directed toward Naturally Occurring Cyclooctanoids. 2. A Stereocontrolled Assembly of (.+-.)-Pleuromutilin via a Remarkable Sterically Demanding Oxy-Cope Rearrangement. *J. Am. Chem. Soc.* **1989**, *111* (21), 8284–8286.

(3) Fazakerley, N. J.; Procter, D. J. Synthesis and Synthetic Chemistry of Pleuromutilin. *Tetrahedron* **2014**, *70* (39), 6911–6930.

(4) Fazakerley, N. J.; Helm, M. D.; Procter, D. J. Total Synthesis of (+)-Pleuromutilin. *Chemistry – A European Journal 19* (21), 6718–6723.

(5) Jin, Haolun.; Uenishi, Junichi.; Christ, W. J.; Kishi, Yoshito. Catalytic Effect of Nickel(II) Chloride and Palladium(II) Acetate on Chromium(II)-Mediated Coupling Reaction of Iodo Olefins with Aldehydes. *J. Am. Chem. Soc.* **1986**, *108* (18), 5644–5646.

(6) Takai, K.; Tagashira, M.; Kuroda, T.; Oshima, K.; Utimoto, K.; Nozaki, H. Reactions of Alkenylchromium Reagents Prepared from Alkenyl Trifluoromethanesulfonates (Triflates) with Chromium(II) Chloride under Nickel Catalysis. *J. Am. Chem. Soc.* **1986**, *108* (19), 6048–6050.

(7) Fürstner, A. Carbon−Carbon Bond Formations Involving Organochromium(III) Reagents. *Chem. Rev.* **1999**, *99* (4), 991–1046.

(8) Lou, S.; Moquist, P. N.; Schaus, S. E. Asymmetric Allylboration of Ketones Catalyzed by Chiral Diols. *J. Am. Chem. Soc.* **2006**, *128* (39), 12660–12661.

(9) Nowrouzi, F.; Thadani, A. N.; Batey, R. A. Allylation and Crotylation of Ketones and Aldehydes Using Potassium Organotrifluoroborate Salts under Lewis Acid and Montmorillonite K10 Catalyzed Conditions. *Org. Lett.* **2009**, *11* (12), 2631–2634.

(10) Diner, C.; Szabó, K. J. Recent Advances in the Preparation and Application of Allylboron Species in Organic Synthesis. *J. Am. Chem. Soc.* **2017**, *139* (1), 2–14.

(11) Schreiber, S. L. Fragmentation Reactions of .Alpha.-Alkoxy Hydroperoxides and Application to the Synthesis of the Macrolide (.+-.)-Recifeiolide. *J. Am. Chem. Soc.* **1980**, *102* (19), 6163–6165.

(12) White, J. D.; Grether, U. M.; Lee, C.-S. (R)-(+)-3,4-DIMETHYLCYCLOHEX-2-EN-1-ONE. *Org. Synth.* **2005**, *82*, 108.

(13) Corey, E. J.; Wollenberg, R. H. Nucleophilic Ethynyl Group Equivalent and Its Use in Conjugate Addition to .Alpha.,.Beta.-Enones. *J. Am. Chem. Soc.* **1974**, *96* (17), 5581–5583.

(14) Corey, E. J.; Beames, D. J. Mixed Cuprate Reagents of Type R1R2CuLi Which Allow Selective Group Transfer. *J. Am. Chem. Soc.* **1972**, *94* (20), 7210–7211.

(15) Krasovskiy, A.; Kopp, F.; Knochel, P. Soluble Lanthanide Salts (LnCl3·2 LiCl) for the Improved Addition of Organomagnesium Reagents to Carbonyl Compounds. *Angewandte Chemie International Edition* **2006**, *45* (3), 497–500.

(16) Dauben, W. G.; Michno, D. M. Direct Oxidation of Tertiary Allylic Alcohols. A Simple and Effective Method for Alkylative Carbonyl Transposition. *J. Org. Chem.* **1977**, *42* (4), 682–685.

(17) Hara, S.; Dojo, H.; Takinami, S.; Suzuki, A. ORGANIC SYNTHESIS USING HALOBORATION REACTION. I. A SIMPLE AND SELECTIVE SYNTHESIS OF Z-BROMO- AND Z-IODO-l-ALKENES. 4.

(18) Hodgson, D. M.; Foley, A. M.; Lovell, P. J. Alkene Chemoselectivity in Ring-Closing Metathesis: A Formal Synthesis of (-)-Periplanone-B. *Synlett* **1999**, *6* (6), 744–746.

(19) Alam, R.; Vollgraff, T.; Eriksson, L.; Szabó, K. J. Synthesis of Adjacent Quaternary Stereocenters by Catalytic Asymmetric Allylboration. *J. Am. Chem. Soc.* **2015**, *137* (35), 11262–11265.

(20) Raducan, M.; Alam, R.; Szabó, K. J. Palladium-Catalyzed Synthesis and Isolation of Functionalized Allylboronic Acids: Selective, Direct Allylboration of Ketones. *Angewandte Chemie International Edition* **2012**, *51* (52), 13050–13053.

(21) Singh, D.; McPhee, D.; Paddon, C. J.; Cherry, J.; Maurya, G.; Mahale, G.; Patel, Y.; Kumar, N.; Singh, S.; Sharma, B.; et al. Amalgamation of Synthetic Biology and Chemistry for High-Throughput Nonconventional Synthesis of the Antimalarial Drug Artemisinin. *Org. Process Res. Dev.* **2017**, *21* (4), 551–558.

(22) G. Godfrey, A.; Ganem, B. Ready Oxidation of Halides to Aldehydes Using Trimethylamine N-Oxide in Dimethylsulfoxide. *Tetrahedron Letters* **1990**, *31* (34), 4825–4826.

(23) Kornblum, N.; Jones, W. J.; Anderson, G. J. A NEW AND SELECTIVE METHOD OF OXIDATION. THE CONVERSION OF ALKYL HALIDES AND ALKYL TOSYLATES TO ALDEHYDES. *J. Am. Chem. Soc.* **1959**, *81* (15), 4113–4114.

(24) Kornblum, N.; Powers, J. W.; Anderson, G. J.; Jones, W. J.; Larson, H. O.; Levand, O.; Weaver, W. M. A NEW AND SELECTIVE METHOD OF OXIDATION. *J. Am. Chem. Soc.* **1957**, *79* (24), 6562–6562.

(25) Dave, P.; Byun, H.-S.; Engel, R. An Improved Direct Oxidation of Alkyl Halides to Aldehydes. *Synthetic Communications* **1986**, *16* (11), 1343–1346.

(26) Hoover, J. M.; Stahl, S. S. Highly Practical Copper(I)/TEMPO Catalyst System for Chemoselective Aerobic Oxidation of Primary Alcohols. *J. Am. Chem. Soc.* **2011**, *133* (42), 16901–16910.

(27) Hoover, J. M.; Ryland, B. L.; Stahl, S. S. Mechanism of Copper(I)/TEMPO-Catalyzed Aerobic Alcohol Oxidation. *J. Am. Chem. Soc.* **2013**, *135* (6), 2357–2367.

(28) Chapter 3:Mechanisms of SmI2-Mediated Reactions – the Basics. In *Organic Synthesis using Samarium Diiodide*; 2009; pp 20–35.

(29) Verendel, J. J.; Pàmies, O.; Diéguez, M.; Andersson, P. G. Asymmetric Hydrogenation of Olefins Using Chiral Crabtree-Type Catalysts: Scope and Limitations. *Chem. Rev.* **2014**, *114* (4), 2130–2169.

(30) Hoveyda, A. H.; Evans, D. A.; Fu, G. C. Substrate-Directable Chemical Reactions. *Chem. Rev.* **1993**, *93* (4), 1307–1370.

(31) Wang, D.; Astruc, D. The Golden Age of Transfer Hydrogenation. *Chem. Rev.* **2015**, *115* (13), 6621–6686.

(32) Crossley, S. W. M.; Obradors, C.; Martinez, R. M.; Shenvi, R. A. Mn-, Fe-, and Co-Catalyzed Radical Hydrofunctionalizations of Olefins. *Chem. Rev.* **2016**, *116* (15), 8912–9000.

(33) Iwasaki, K.; Wan, K. K.; Oppedisano, A.; Crossley, S. W. M.; Shenvi, R. A. Simple, Chemoselective Hydrogenation with Thermodynamic Stereocontrol. *J. Am. Chem. Soc.* **2014**, *136* (4), 1300–1303.

(34) Lindgren, B. O.; Nilsson, T.; Husebye, S.; Mikalsen, Ø.; Leander, K.; Swahn, C.-G. Preparation of Carboxylic Acids from Aldehydes (Including Hydroxylated Benzaldehydes) by Oxidation with Chlorite. *Acta Chem. Scand.* **1973**, *27*, 888–890.

(35) Bal, B. S.; Childers, W. E.; Pinnick, H. W. Oxidation of α,β-Un Saturated Aldehydes. *Tetrahedron* **1981**, *37* (11), 2091–2096.

(36) Thirring, K.; Heilmayer, W.; Riedl, R.; Kollmann, H.; IVEZIC-SCHOENFELD, Z.; WICHA, W.; Paukner, S.; Strickmann, D. 12-Epi-Pleuromutilins. WO2015110481A1, July 30, 2015.

(37) Berner, H.; Vyplel, H.; Schulz, G.; Stuchlik, P. Chemie der pleuromutiline-VIII: Funktionalisierung des C-atoms 13 durch intramolekulare nitreninsertion. Synthese des 14-o-[(3-amino-1,2,4-triazol-5yl)thioacetyl]-13-amino-19,20- dihydromutilin-hydrochlorid. *Tetrahedron* **1984**, *40* (5), 919–923.

Appendix 1

Spectra Relevant to Chapter 2:
Total Synthesis of (+)-Pleuromutilin and (+)-12-epi-Pleuromutilin

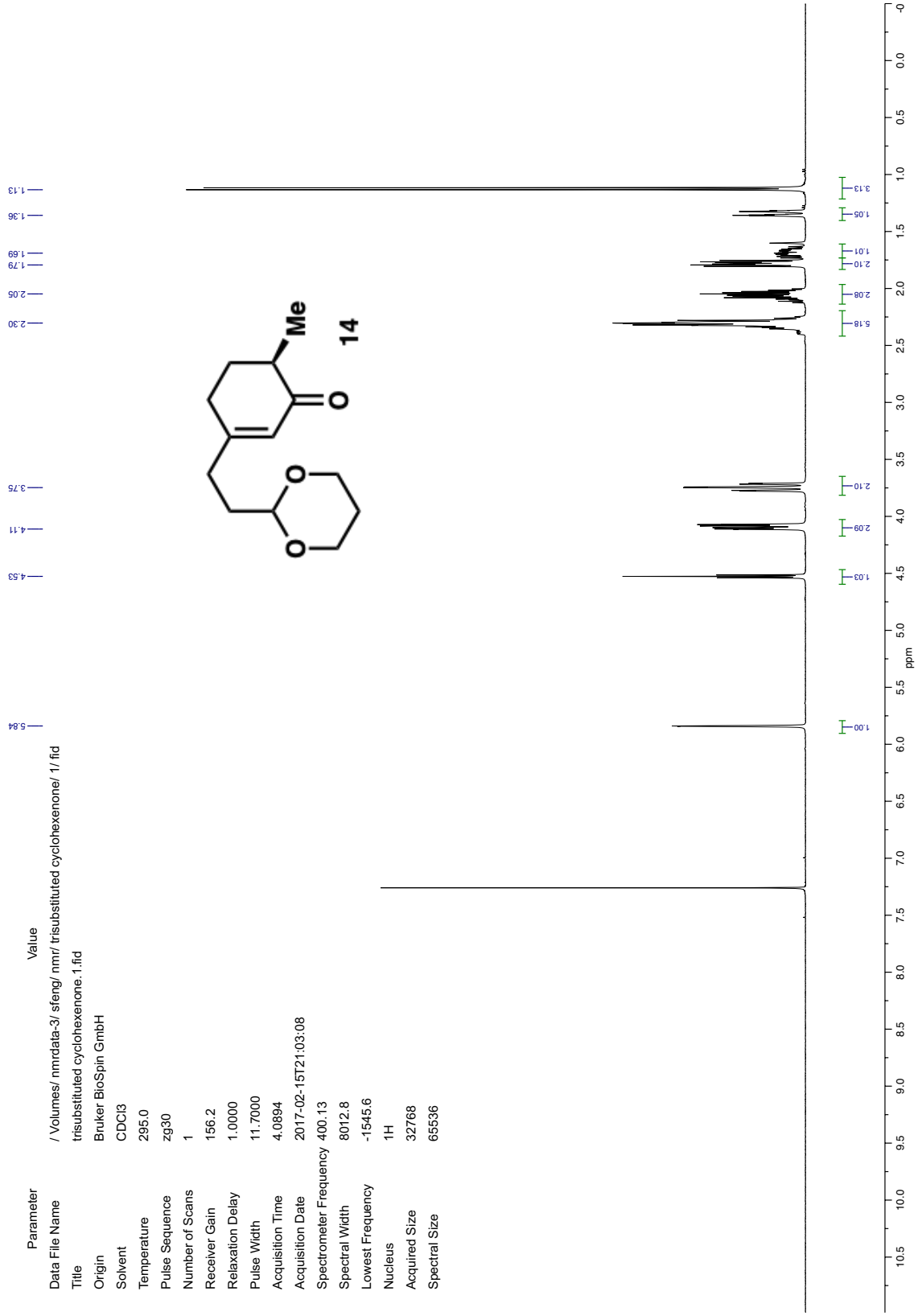

Parameter	Value
Data File Name	/ Volumes/ nmrdata-3/ sfeng/ nmr/ trisubstituted cyclohexenone/ 1/ fid
Title	trisubstituted cyclohexenone.1.fid
Origin	Bruker BioSpin GmbH
Solvent	CDCl3
Temperature	295.0
Pulse Sequence	zg30
Number of Scans	1
Receiver Gain	156.2
Relaxation Delay	1.0000
Pulse Width	11.7000
Acquisition Time	4.0894
Acquisition Date	2017-02-15T21:03:08
Spectrometer Frequency	400.13
Spectral Width	8012.8
Lowest Frequency	-1545.6
Nucleus	1H
Acquired Size	32768
Spectral Size	65536

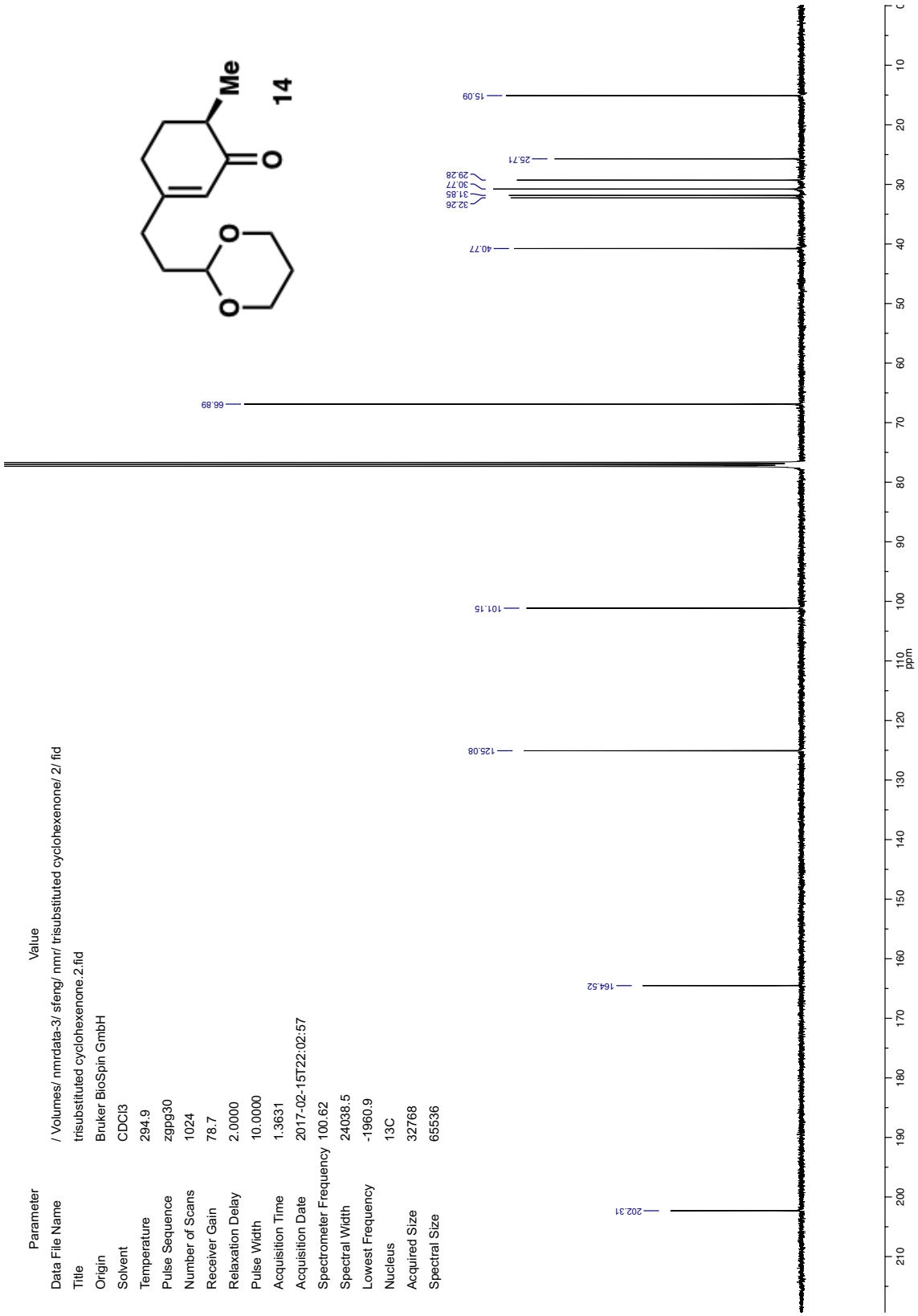

Parameter	Value
Data File Name	/ Volumes/ nmrdata-3/ sfeng/ nmr/ trisubstituted cyclohexenone/ 2/ fid
Title	trisubstituted cyclohexenone.2.fid
Origin	Bruker BioSpin GmbH
Solvent	CDCl3
Temperature	294.9
Pulse Sequence	zgpg30
Number of Scans	1024
Receiver Gain	78.7
Relaxation Delay	2.0000
Pulse Width	10.0000
Acquisition Time	1.3631
Acquisition Date	2017-02-15T22:02:57
Spectrometer Frequency	100.62
Spectral Width	24038.5
Lowest Frequency	-1960.9
Nucleus	13C
Acquired Size	32768
Spectral Size	65536

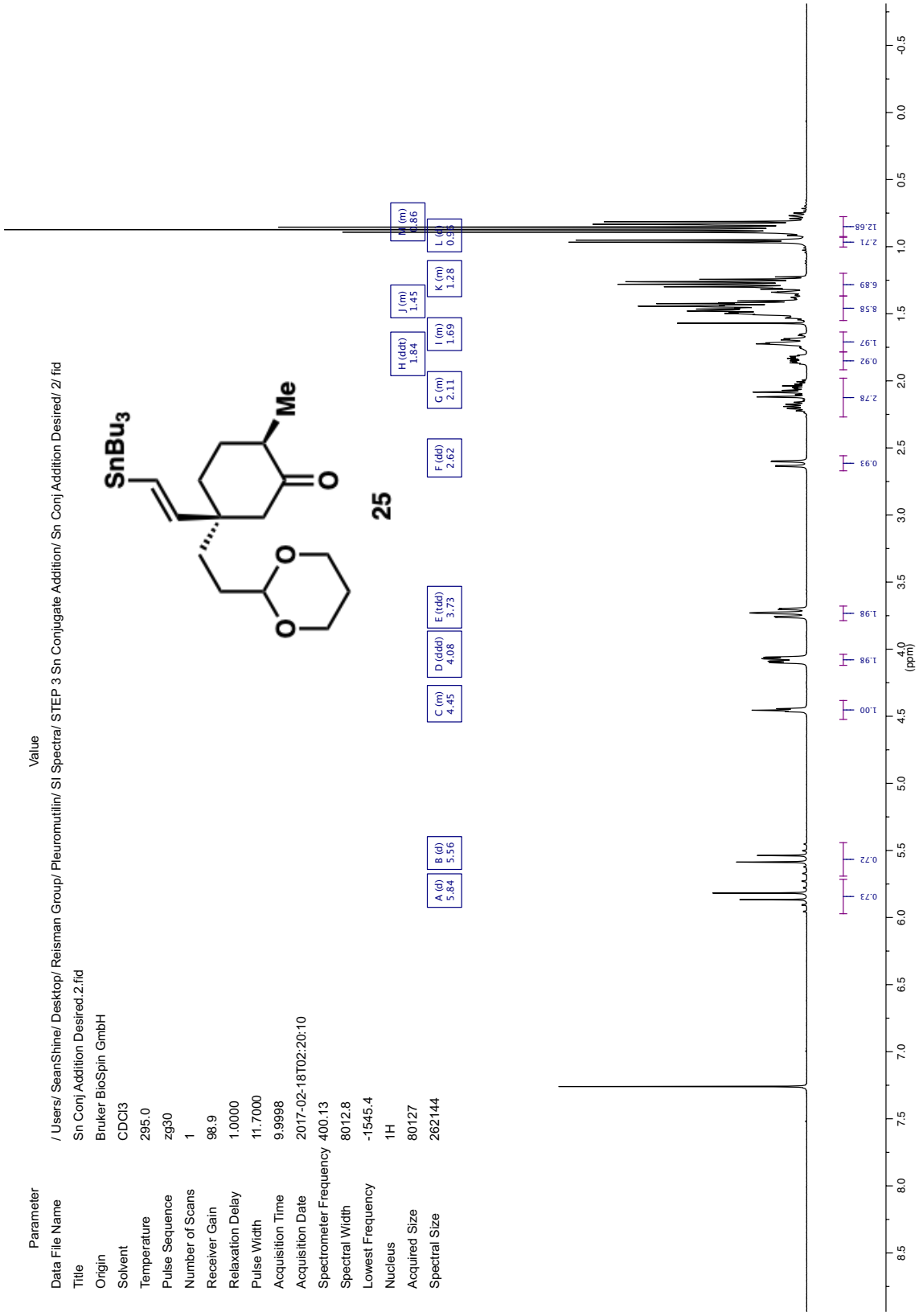
Parameter
Value
Data File Name / Users/ SeanShine/ Desktop/ Reisman Group/ Pleuromutilin/ SI Spectra/ STEP 3 Sn Conjugate Addition/ Sn Conj Addition Desired/ 2/ fid
Title Sn Conj Addition Desired.2.fid
Origin Bruker BioSpin GmbH
Solvent CDCl3
Temperature 295.0
Pulse Sequence zg30
Number of Scans 1
Receiver Gain 98.9
Relaxation Delay 1.0000
Pulse Width 11.7000
Acquisition Time 9.9998
Acquisition Date 2017-02-18T02:20:10
Spectrometer Frequency 400.13
Spectral Width 8012.8
Lowest Frequency -1545.4
Nucleus 1H
Acquired Size 80127
Spectral Size 262144
SnBu3
Me
O
O
O
25
A (d) 5.84
B (d) 5.56
C (m) 4.45
D (ddd) 4.08
E (tdd) 3.73
F (dd) 2.62
G (m) 2.11
H (ddt) 1.84
I (m) 1.69
J (m) 1.45
K (m) 1.28
L (q) 0.93
M (m) 0.86
0.73
0.72
1.00
1.98
1.98
0.93
2.78
0.92
1.97
8.58
6.89
2.71
12.68
8.5
8.0
7.5
7.0
6.5
6.0
5.5
5.0
4.5
4.0
3.5
3.0
2.5
2.0
1.5
1.0
0.5
0.0
-0.5
(ppm)

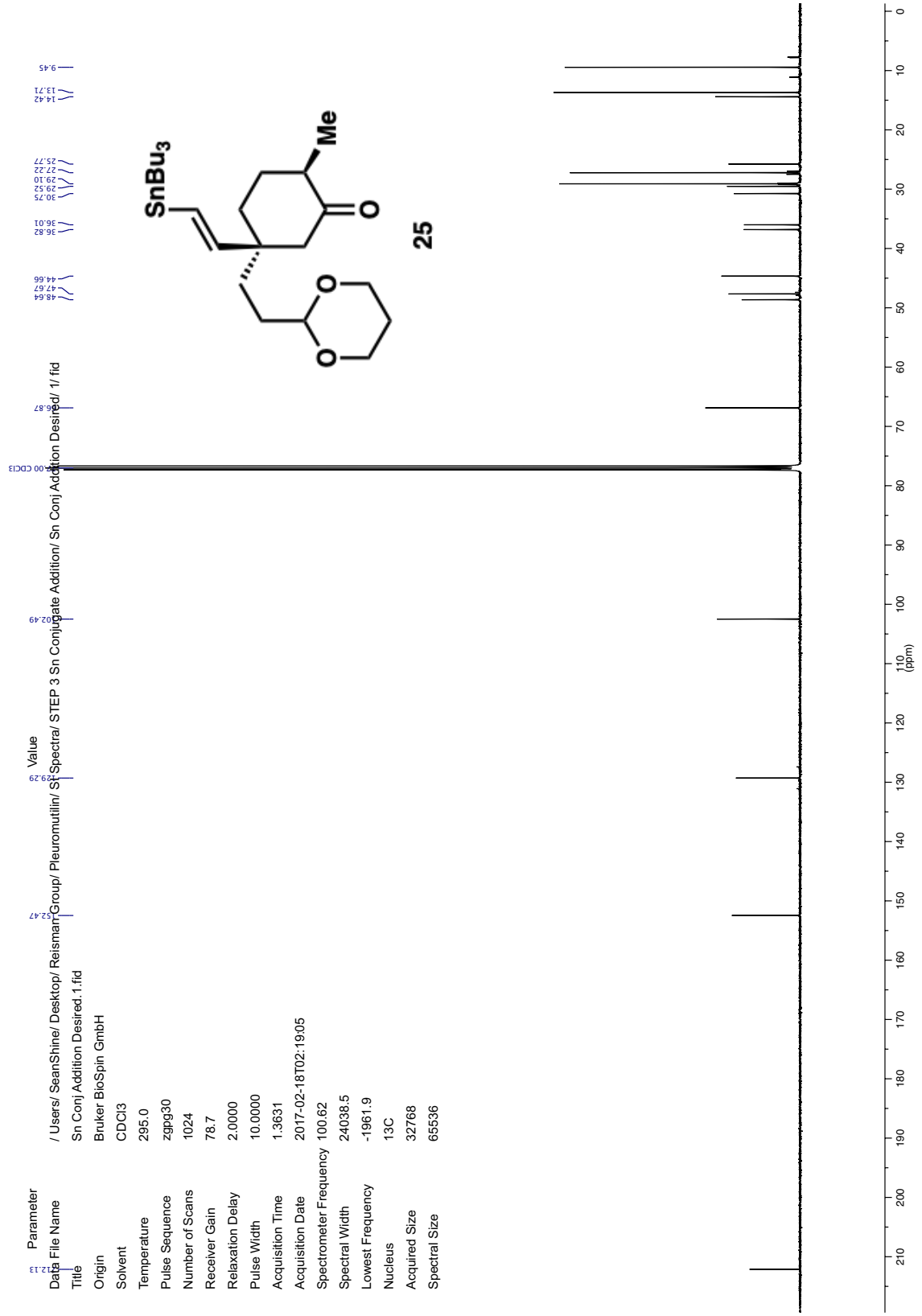
SnBu3
Me
O
O
O
25
Parameter Value
Data File Name / Users/ SeanShine/ Desktop/ Reisman Group/ Pleuromutilin/ St Spectra/ STEP 3 Sn Conjugate Addition/ Sn Conj Addition Desired/ 1/ fid
Title Sn Conj Addition Desired.1.fid
Origin Bruker BioSpin GmbH
Solvent CDCl3
Temperature 295.0
Pulse Sequence zgpg30
Number of Scans 1024
Receiver Gain 78.7
Relaxation Delay 2.0000
Pulse Width 10.0000
Acquisition Time 1.3631
Acquisition Date 2017-02-18T02:19:05
Spectrometer Frequency 100.62
Spectral Width 24038.5
Lowest Frequency -1961.9
Nucleus 13C
Acquired Size 32768
Spectral Size 65536
9.45
13.71
14.42
25.77
27.22
29.10
29.52
30.75
36.01
36.82
44.66
47.67
48.64
68.87
77.00 CDCl3
102.49
129.29
152.47
212.13
(ppm)

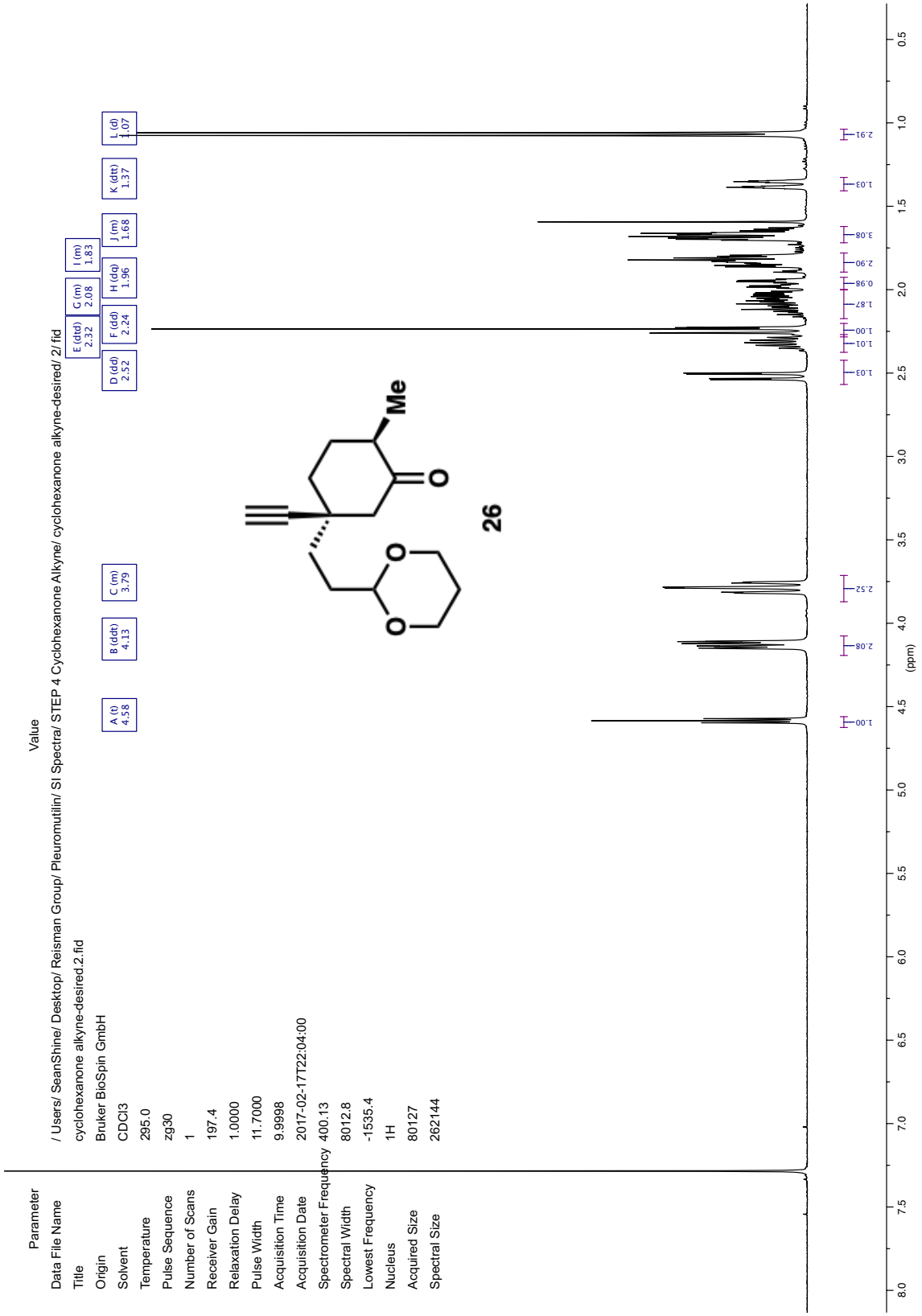
Parameter
Value
Data File Name
/ Users/ SeanShine/ Desktop/ Reisman Group/ Pleuromutilin/ SI Spectra/ STEP 4 Cyclohexanone Alkyne/ cyclohexanone alkyne-desired/ 2/ fid
Title
cyclohexanone alkyne-desired.2.fid
Origin
Bruker BioSpin GmbH
Solvent
CDCl3
Temperature
295.0
Pulse Sequence
zg30
Number of Scans
1
Receiver Gain
197.4
Relaxation Delay
1.0000
Pulse Width
11.7000
Acquisition Time
9.9998
Acquisition Date
2017-02-17T22:04:00
Spectrometer Frequency
400.13
Spectral Width
8012.8
Lowest Frequency
-1535.4
Nucleus
1H
Acquired Size
80127
Spectral Size
262144
A (t) 4.58
B (ddt) 4.13
C (m) 3.79
D (dd) 2.52
E (dtd) 2.32
F (dd) 2.24
G (m) 2.08
H (dq) 1.96
I (m) 1.83
J (m) 1.68
K (dtt) 1.37
L (d) 1.07
Me
O
O
O
26
1.00
2.08
2.52
1.03
1.01
1.00
1.87
0.98
2.90
3.08
1.03
2.91
(ppm)

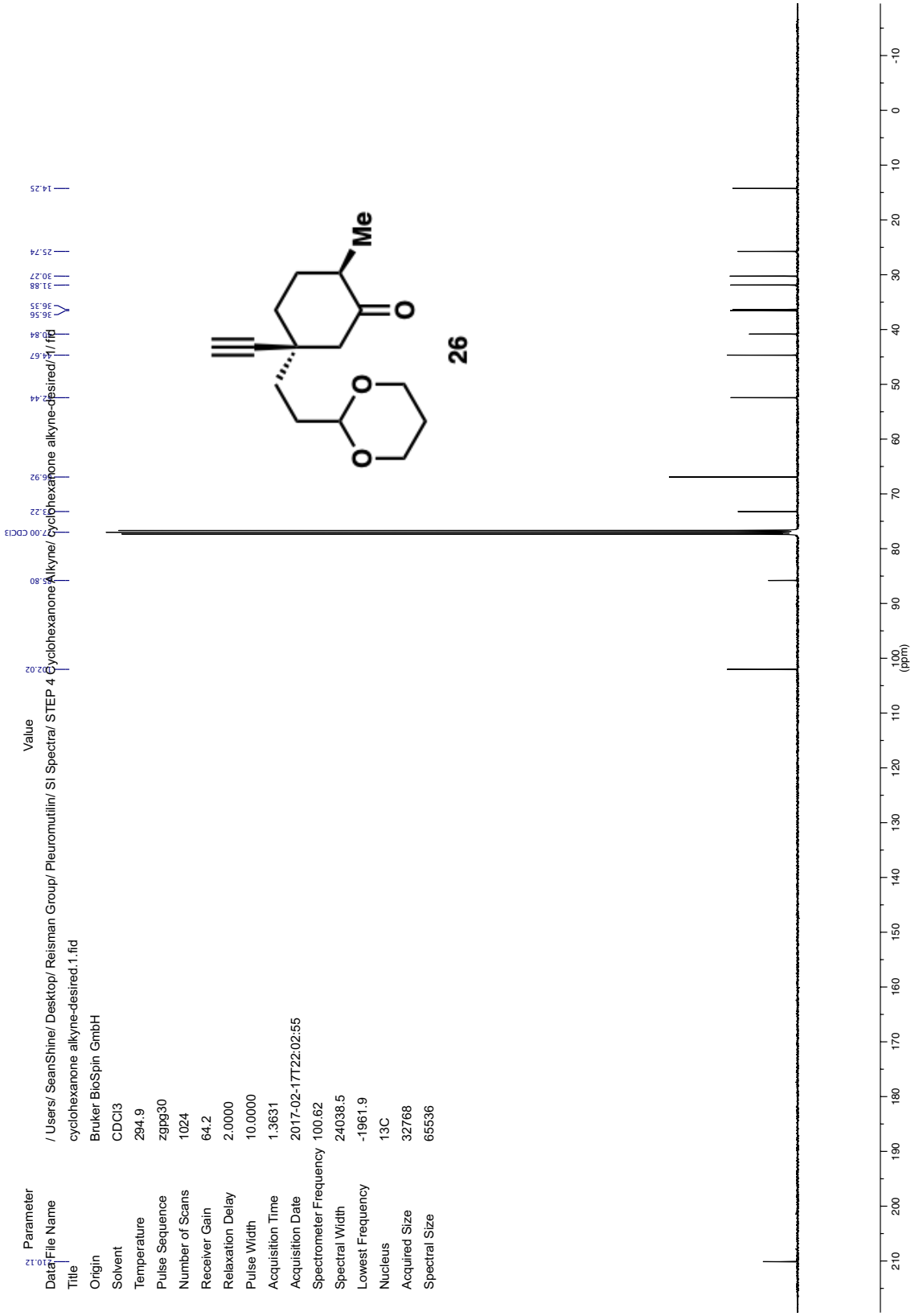
Me
O
O
O
26
Parameter
Value
Data File Name / Users/ SeanShine/ Desktop/ Reisman Group/ Pleuromutilin/ SI Spectra/ STEP 4 Cyclohexanone Alkyne/ Cyclohexanone alkyne-desired/1/ fid
Title cyclohexanone alkyne-desired.1.fid
Origin Bruker BioSpin GmbH
Solvent CDCl3
Temperature 294.9
Pulse Sequence zgpg30
Number of Scans 1024
Receiver Gain 64.2
Relaxation Delay 2.0000
Pulse Width 10.0000
Acquisition Time 1.3631
Acquisition Date 2017-02-17T22:02:55
Spectrometer Frequency 100.62
Spectral Width 24038.5
Lowest Frequency -1961.9
Nucleus 13C
Acquired Size 32768
Spectral Size 65536
10.12
25.74
30.27
31.88
36.56
36.35
40.84
44.67
52.44
76.92
77.22
77.00 CDCl3
95.80
202.02
14.25
(ppm)

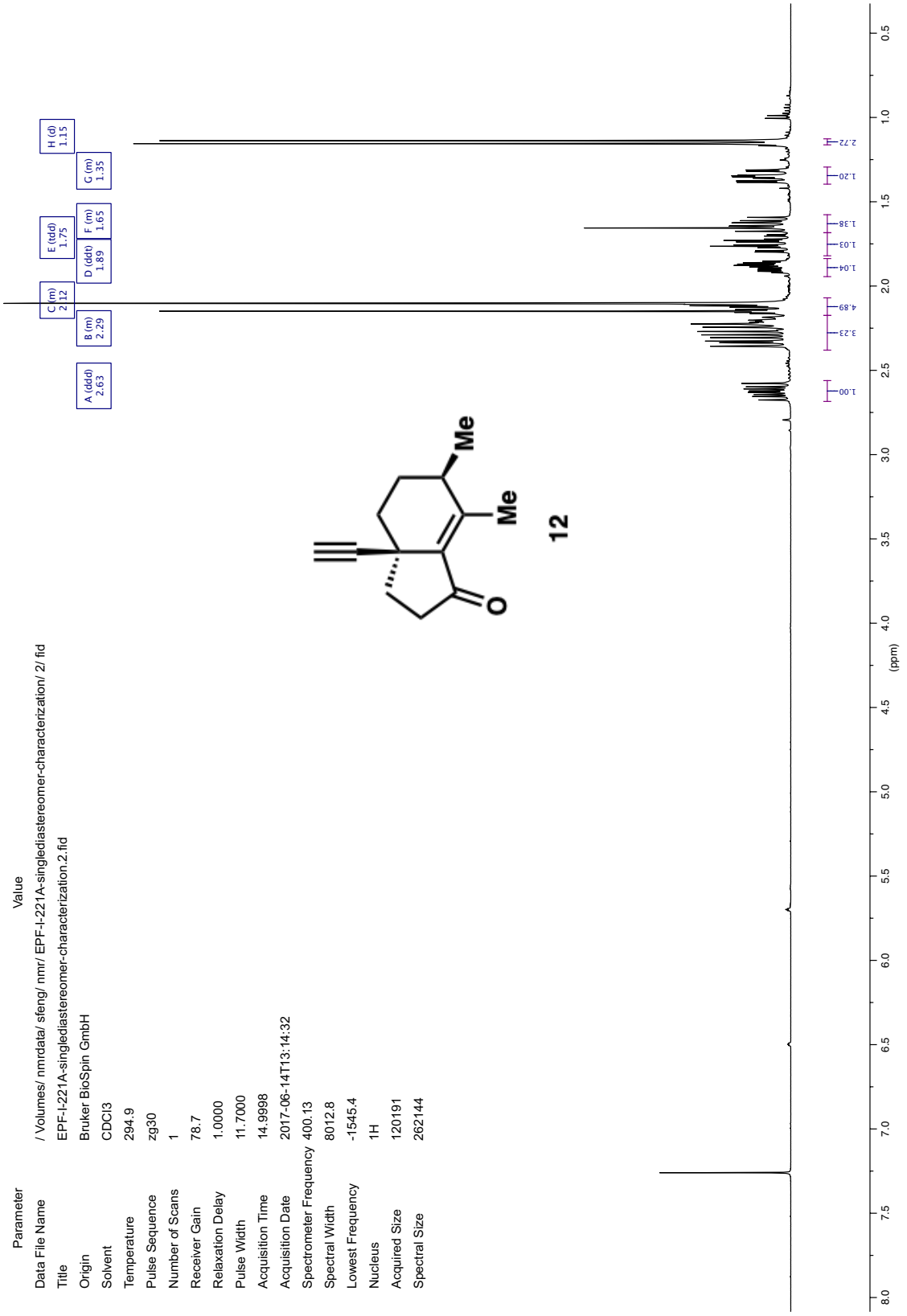
Parameter
Value
Data File Name / Volumes/ nmrdata/ sfeng/ nmr/ EPF-I-221A-singlediastereomer-characterization/ 2/ fid
Title EPF-I-221A-singlediastereomer-characterization.2.fid
Origin Bruker BioSpin GmbH
Solvent CDCl3
Temperature 294.9
Pulse Sequence zg30
Number of Scans 1
Receiver Gain 78.7
Relaxation Delay 1.0000
Pulse Width 11.7000
Acquisition Time 14.9998
Acquisition Date 2017-06-14T13:14:32
Spectrometer Frequency 400.13
Spectral Width 8012.8
Lowest Frequency -1545.4
Nucleus 1H
Acquired Size 120191
Spectral Size 262144
A (ddd) 2.63
B (m) 2.29
C (m) 2.12
D (ddt) 1.89
E (tdd) 1.75
F (m) 1.65
G (m) 1.35
H (d) 1.15
Me
Me
O
12
1.00
3.23
4.89
1.04
1.03
1.38
1.20
2.22
(ppm)

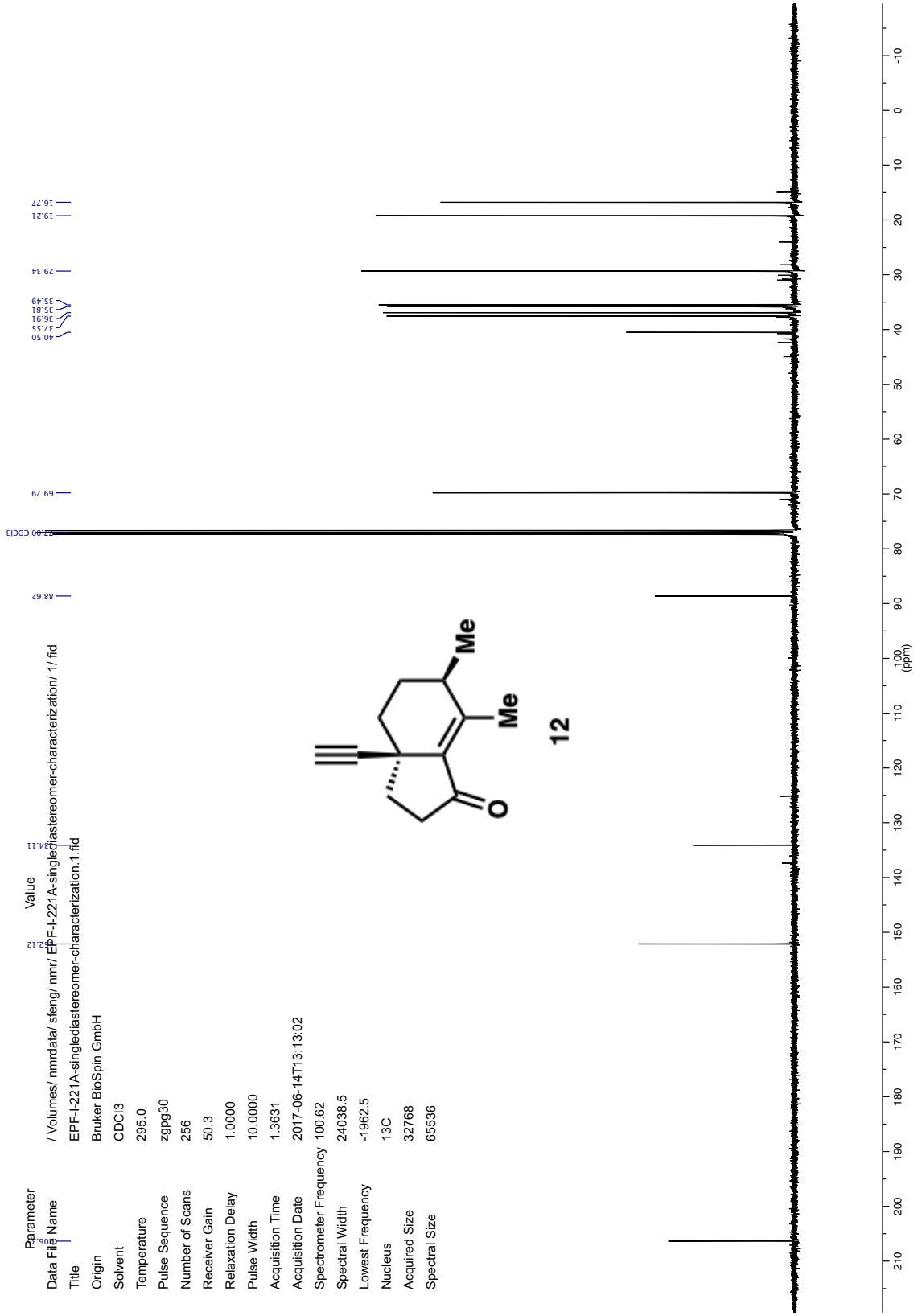
Parameter Value
Data File Name / Volumes/ nmrdata/ sfeng/ nmr/ EPF-I-221A-singlediastereomer-characterization/ 1/ fid
Title EPF-I-221A-singlediastereomer-characterization.1.fid
Origin Bruker BioSpin GmbH
Solvent CDCl3
Temperature 295.0
Pulse Sequence zgpg30
Number of Scans 256
Receiver Gain 50.3
Relaxation Delay 1.0000
Pulse Width 10.0000
Acquisition Time 1.3631
Acquisition Date 2017-06-14T13:13:02
Spectrometer Frequency 100.62
Spectral Width 24038.5
Lowest Frequency -1962.5
Nucleus 13C
Acquired Size 32768
Spectral Size 65536
Me
Me
O
12
CDCl3
16.77
19.21
29.34
35.49
35.81
36.91
37.55
40.50
69.79
88.62
134.11
152.12
100
(ppm)

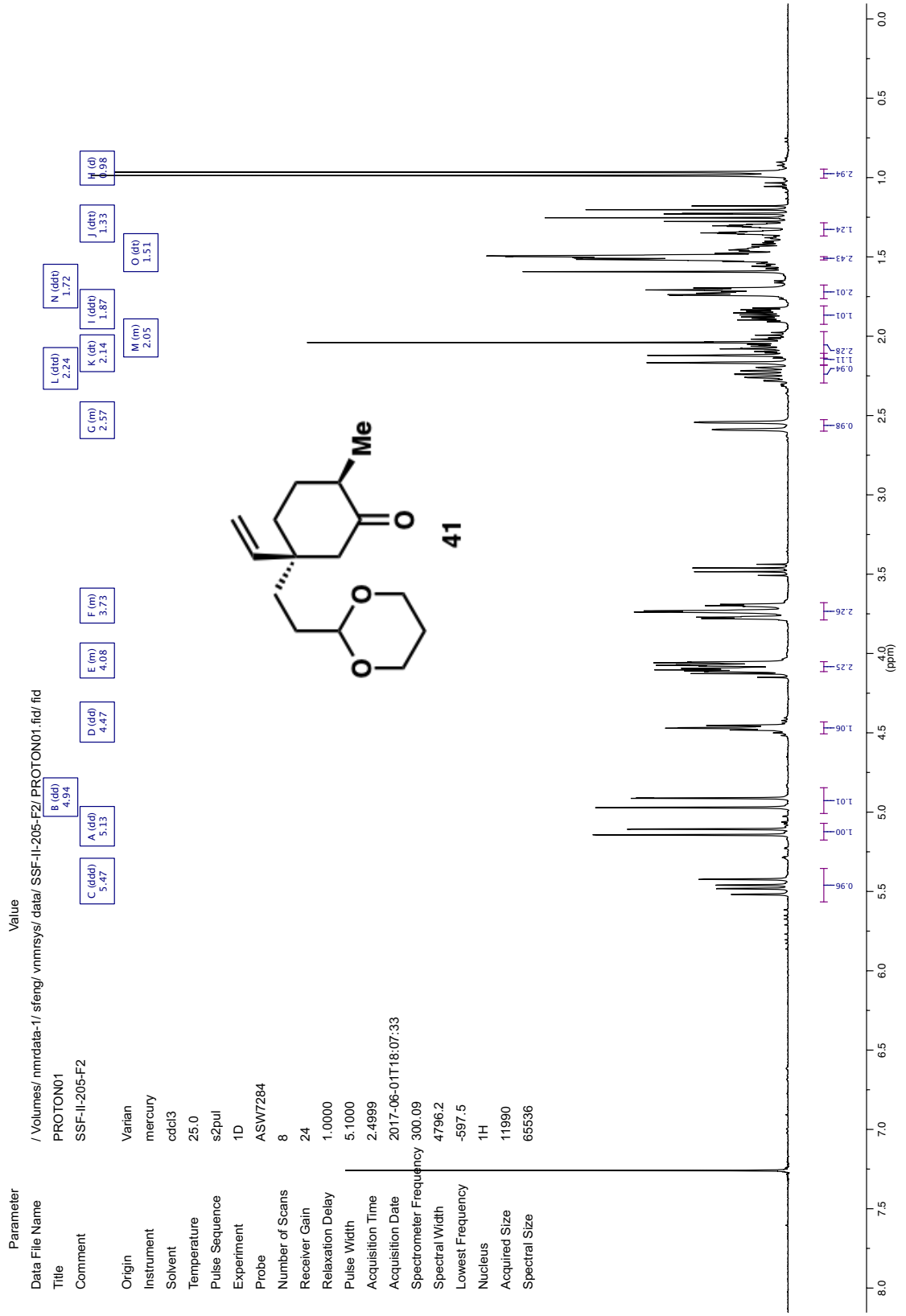
Parameter
Value
Data File Name / Volumes/ nmrdata-1/ sfeng/ vnmrsys/ data/ SSF-II-205-F2/ PROTON01.fid/ fid
Title PROTON01
Comment SSF-II-205-F2
Origin Varian
Instrument mercury
Solvent cdcl3
Temperature 25.0
Pulse Sequence s2pul
Experiment 1D
Probe ASW7284
Number of Scans 8
Receiver Gain 24
Relaxation Delay 1.0000
Pulse Width 5.1000
Acquisition Time 2.4999
Acquisition Date 2017-06-01T18:07:33
Spectrometer Frequency 300.09
Spectral Width 4796.2
Lowest Frequency -597.5
Nucleus 1H
Acquired Size 11990
Spectral Size 65536
C (ddd) 5.47
A (dd) 5.13
B (dd) 4.94
D (dd) 4.47
E (m) 4.08
F (m) 3.73
G (m) 2.57
L (dtd) 2.24
K (dt) 2.14
M (m) 2.05
I (ddt) 1.87
N (ddt) 1.72
O (dt) 1.51
J (dtt) 1.33
H (d) 0.98
Me
O
O
O
41
0.96
1.00
1.01
1.06
2.25
2.26
0.98
0.94
1.11
2.28
2.01
1.01
2.43
1.24
2.94
8.0
7.5
7.0
6.5
6.0
5.5
5.0
4.5
4.0
3.5
3.0
2.5
2.0
1.5
1.0
0.5
0.0
(ppm)

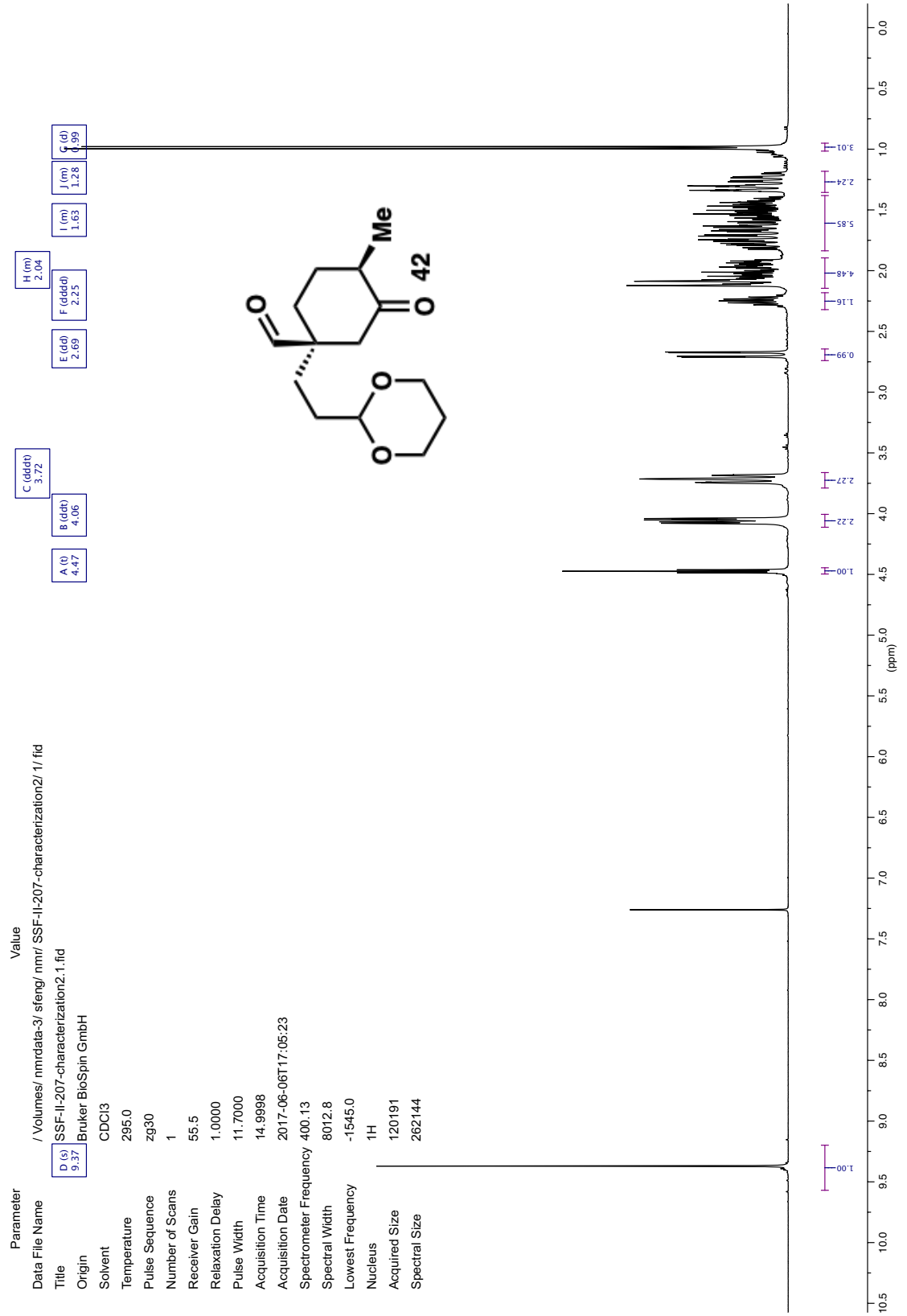
Parameter
Value
Data File Name / Volumes/ nmrdata-3/ sfeng/ nmr/ SSF-II-207-characterization2/ 1/ fid
Title SSF-II-207-characterization2.1.fid
Origin Bruker BioSpin GmbH
Solvent CDCl3
Temperature 295.0
Pulse Sequence zg30
Number of Scans 1
Receiver Gain 55.5
Relaxation Delay 1.0000
Pulse Width 11.7000
Acquisition Time 14.9998
Acquisition Date 2017-06-06T17:05:23
Spectrometer Frequency 400.13
Spectral Width 8012.8
Lowest Frequency -1545.0
Nucleus 1H
Acquired Size 120191
Spectral Size 262144
D (s) 9.37
A (t) 4.47
B (ddt) 4.06
C (dddt) 3.72
E (dd) 2.69
F (dddd) 2.25
H (m) 2.04
I (m) 1.63
J (m) 1.28
G (d) 0.99
Me
O
O
O
42
1.00
2.22
2.27
0.99
1.16
4.48
5.85
2.24
3.01
(ppm)

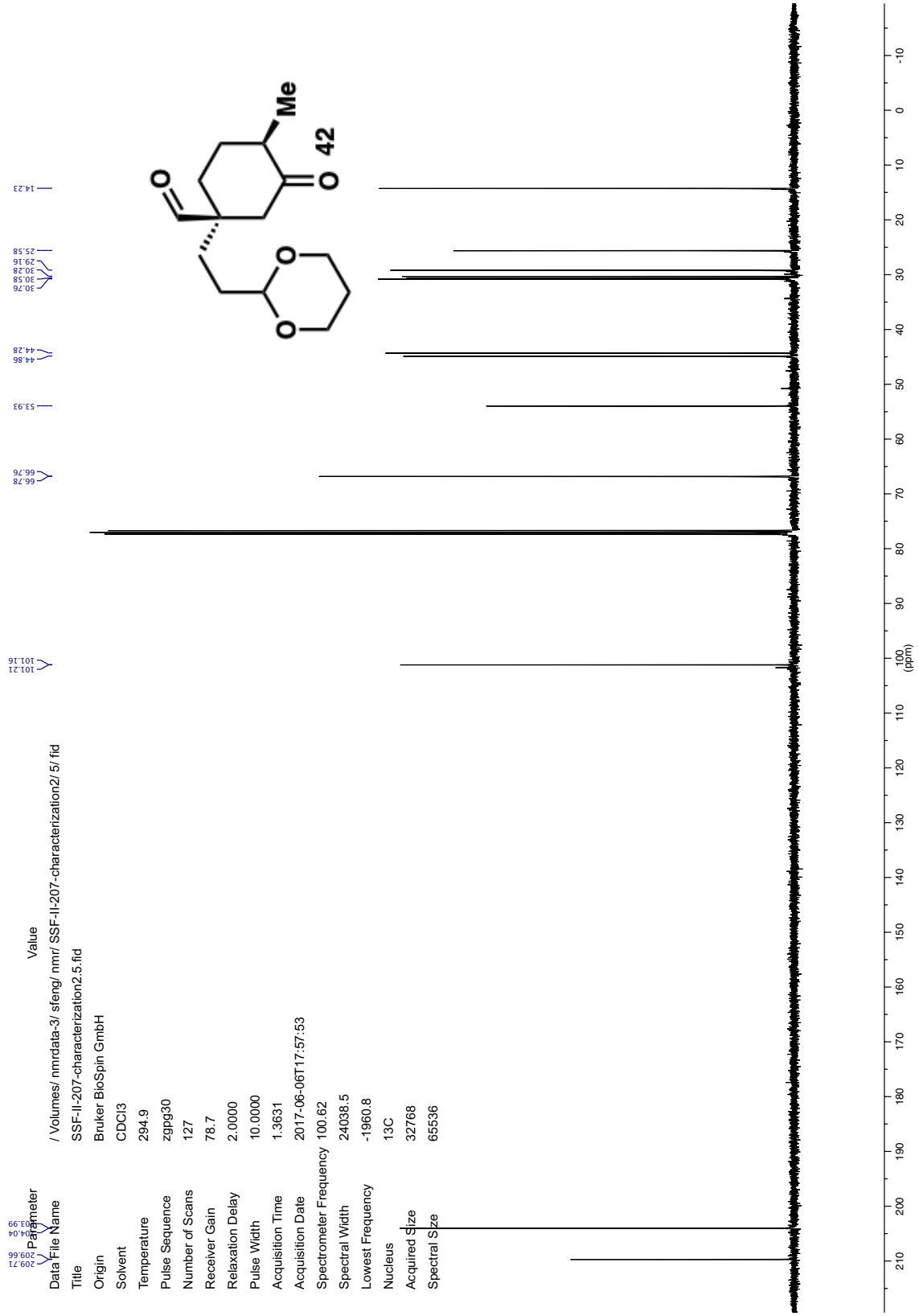

Parameter	Value
Data File Name	/ Volumes/ nmrdata-3/ sfeng/ nmr/ SSF-II-207-characterization2/ 5/ fid
Title	SSF-II-207-characterization2.5.fid
Origin	Bruker BioSpin GmbH
Solvent	CDCl3
Temperature	294.9
Pulse Sequence	zgpg30
Number of Scans	127
Receiver Gain	78.7
Relaxation Delay	2.0000
Pulse Width	10.0000
Acquisition Time	1.3631
Acquisition Date	2017-06-06T17:57:53
Spectrometer Frequency	100.62
Spectral Width	24038.5
Lowest Frequency	-1960.8
Nucleus	13C
Acquired Size	32768
Spectral Size	65536

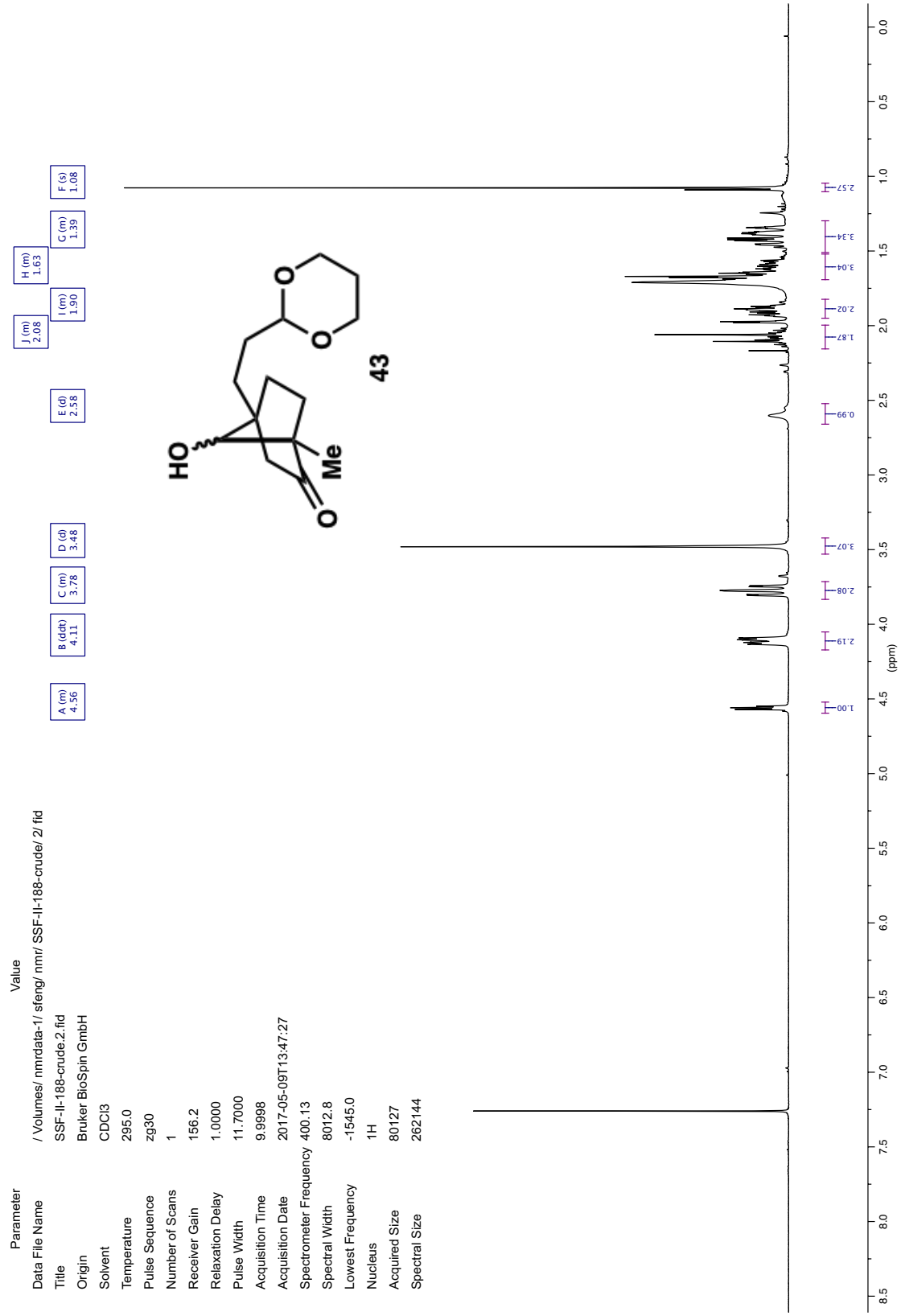
Parameter
Value
Data File Name / Volumes/ nmrdata-1/ sfeng/ nmr/ SSF-II-188-crude/ 2/ fid
Title SSF-II-188-crude.2.fid
Origin Bruker BioSpin GmbH
Solvent CDCl3
Temperature 295.0
Pulse Sequence zg30
Number of Scans 1
Receiver Gain 156.2
Relaxation Delay 1.0000
Pulse Width 11.7000
Acquisition Time 9.9998
Acquisition Date 2017-05-09T13:47:27
Spectrometer Frequency 400.13
Spectral Width 8012.8
Lowest Frequency -1545.0
Nucleus 1H
Acquired Size 80127
Spectral Size 262144
A (m) 4.56
B (ddt) 4.11
C (m) 3.78
D (d) 3.48
E (d) 2.58
I (m) 1.90
J (m) 2.08
H (m) 1.63
G (m) 1.39
F (s) 1.08
HO
Me
O
O
O
43
1.00
2.19
2.08
3.07
0.99
1.87
2.02
3.04
3.34
2.57
(ppm)

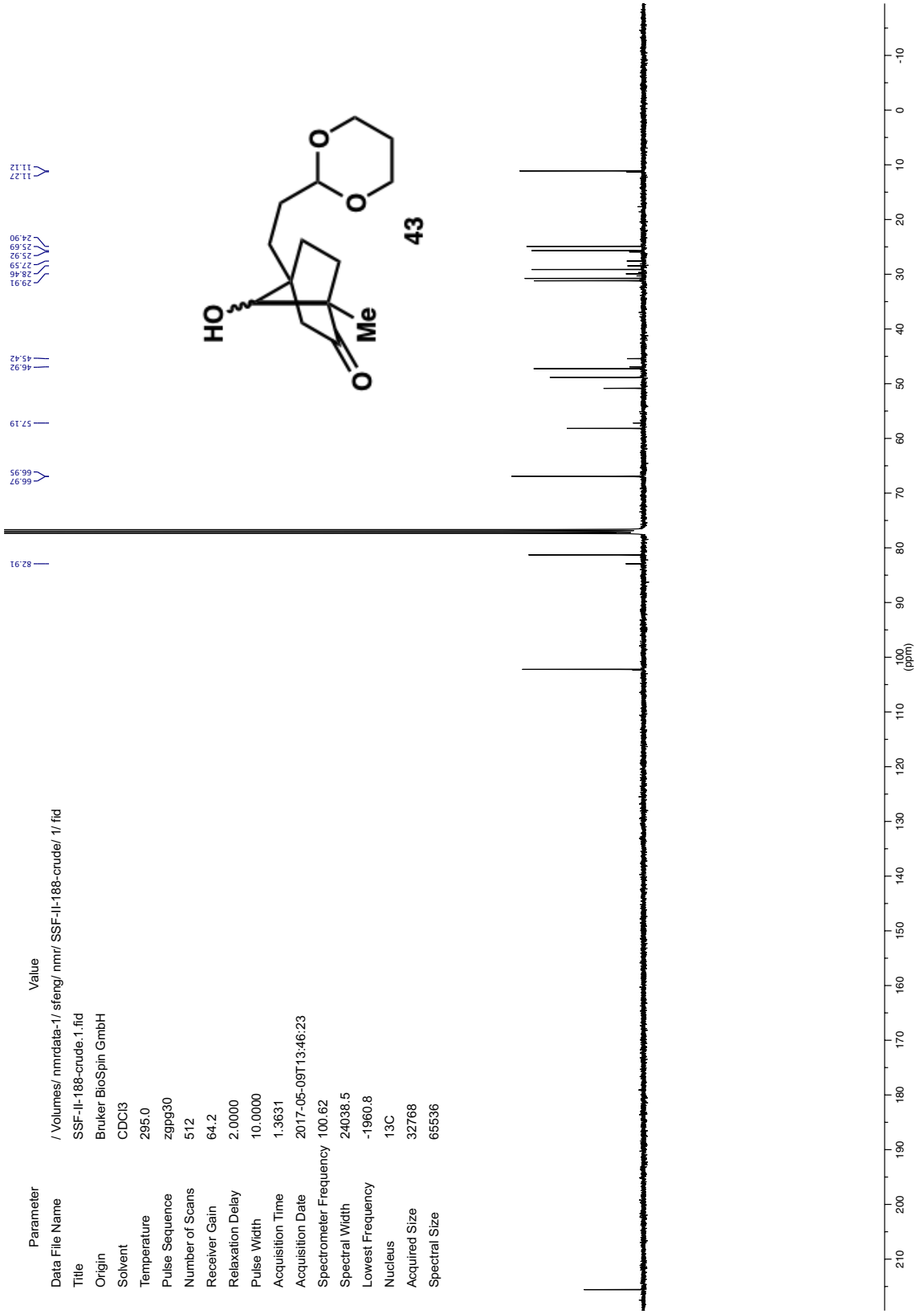
Parameter Value
Data File Name / Volumes/ nmrdata-1/ sfeng/ nmr/ SSF-II-188-crude/ 1/ fid
Title SSF-II-188-crude.1.fid
Origin Bruker BioSpin GmbH
Solvent CDCl3
Temperature 295.0
Pulse Sequence zgpg30
Number of Scans 512
Receiver Gain 64.2
Relaxation Delay 2.0000
Pulse Width 10.0000
Acquisition Time 1.3631
Acquisition Date 2017-05-09T13:46:23
Spectrometer Frequency 100.62
Spectral Width 24038.5
Lowest Frequency -1960.8
Nucleus 13C
Acquired Size 32768
Spectral Size 65536
11.27
11.12
24.90
25.69
25.92
27.59
28.46
29.91
45.42
46.92
57.19
66.95
66.97
82.91
HO
Me
O
O
O
43
210 200 190 180 170 160 150 140 130 120 110 100 90 80 70 60 50 40 30 20 10 0 -10
(ppm)

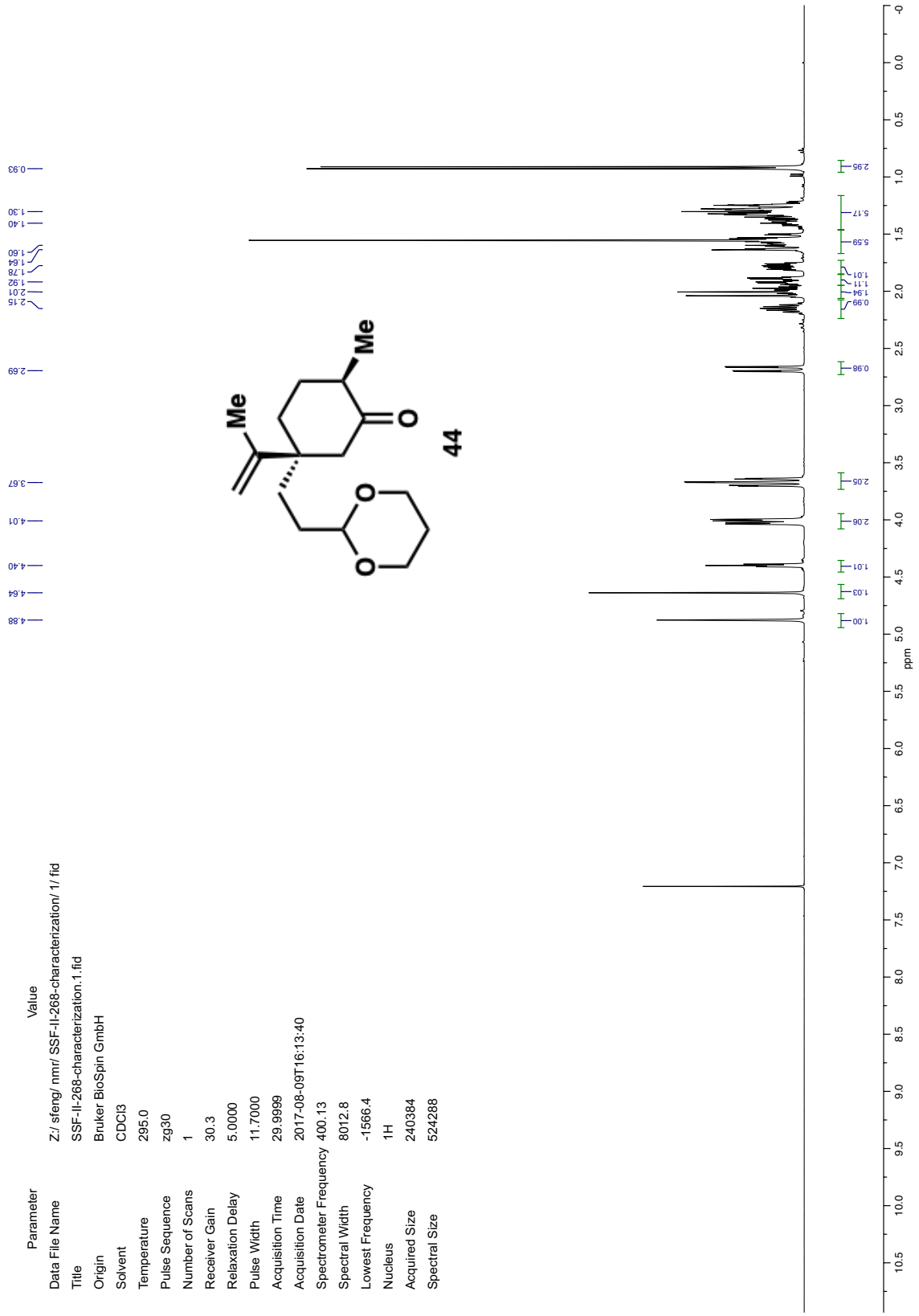

Parameter	Value
Data File Name	Z:/ sfeng/ nmr/ SSF-II-268-characterization/ 1/ fid
Title	SSF-II-268-characterization.1.fid
Origin	Bruker BioSpin GmbH
Solvent	CDCl3
Temperature	295.0
Pulse Sequence	zg30
Number of Scans	1
Receiver Gain	30.3
Relaxation Delay	5.0000
Pulse Width	11.7000
Acquisition Time	29.9999
Acquisition Date	2017-08-09T16:13:40
Spectrometer Frequency	400.13
Spectral Width	8012.8
Lowest Frequency	-1566.4
Nucleus	1H
Acquired Size	240384
Spectral Size	524288

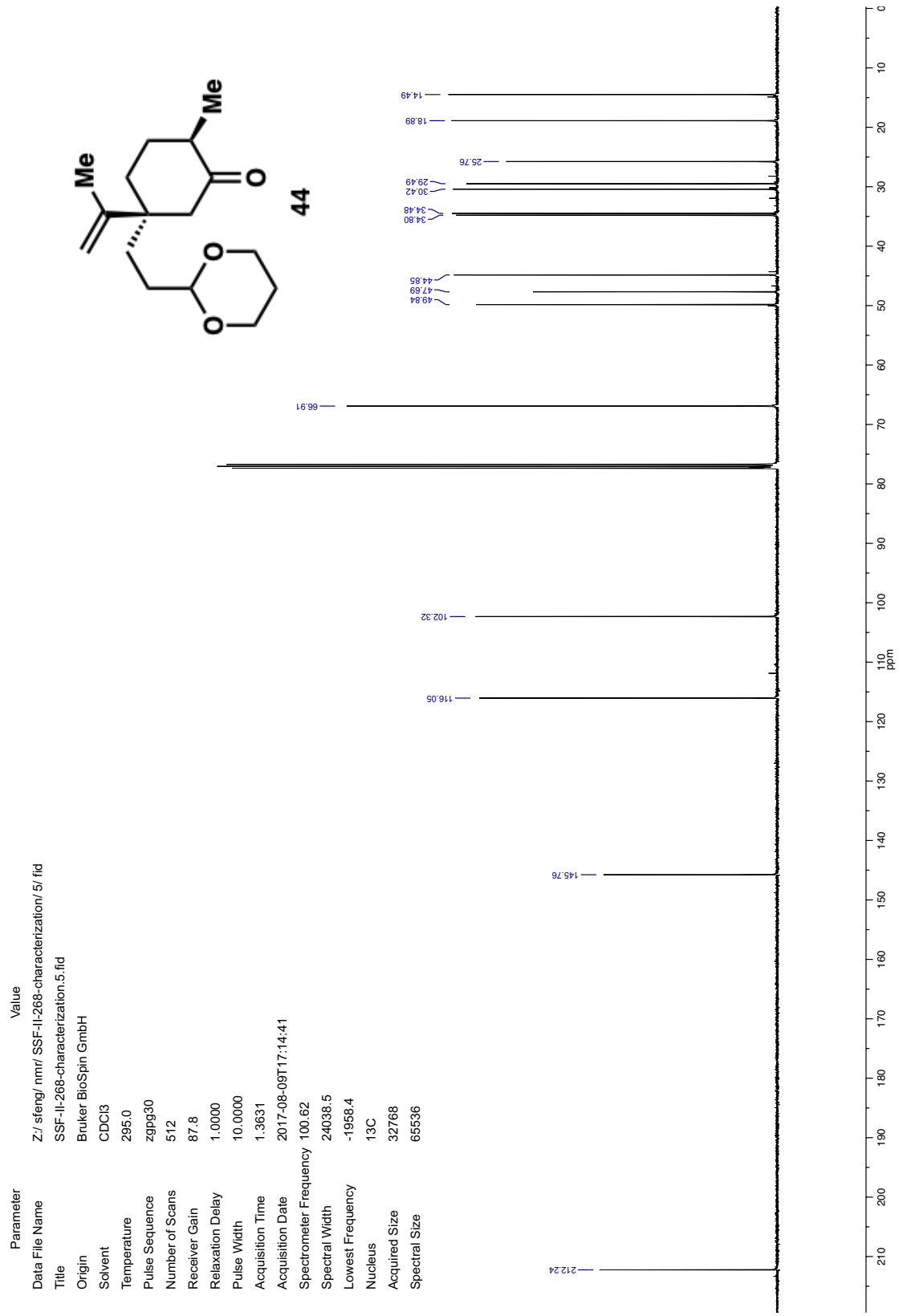

Parameter	Value
Data File Name	Z:/ sfeng/ nmr/ SSF-II-268-characterization/ 5/ fid
Title	SSF-II-268-characterization.5.fid
Origin	Bruker BioSpin GmbH
Solvent	CDCl3
Temperature	295.0
Pulse Sequence	zgpg30
Number of Scans	512
Receiver Gain	87.8
Relaxation Delay	1.0000
Pulse Width	10.0000
Acquisition Time	1.3631
Acquisition Date	2017-08-09T17:14:41
Spectrometer Frequency	100.62
Spectral Width	24038.5
Lowest Frequency	-1958.4
Nucleus	13C
Acquired Size	32768
Spectral Size	65536

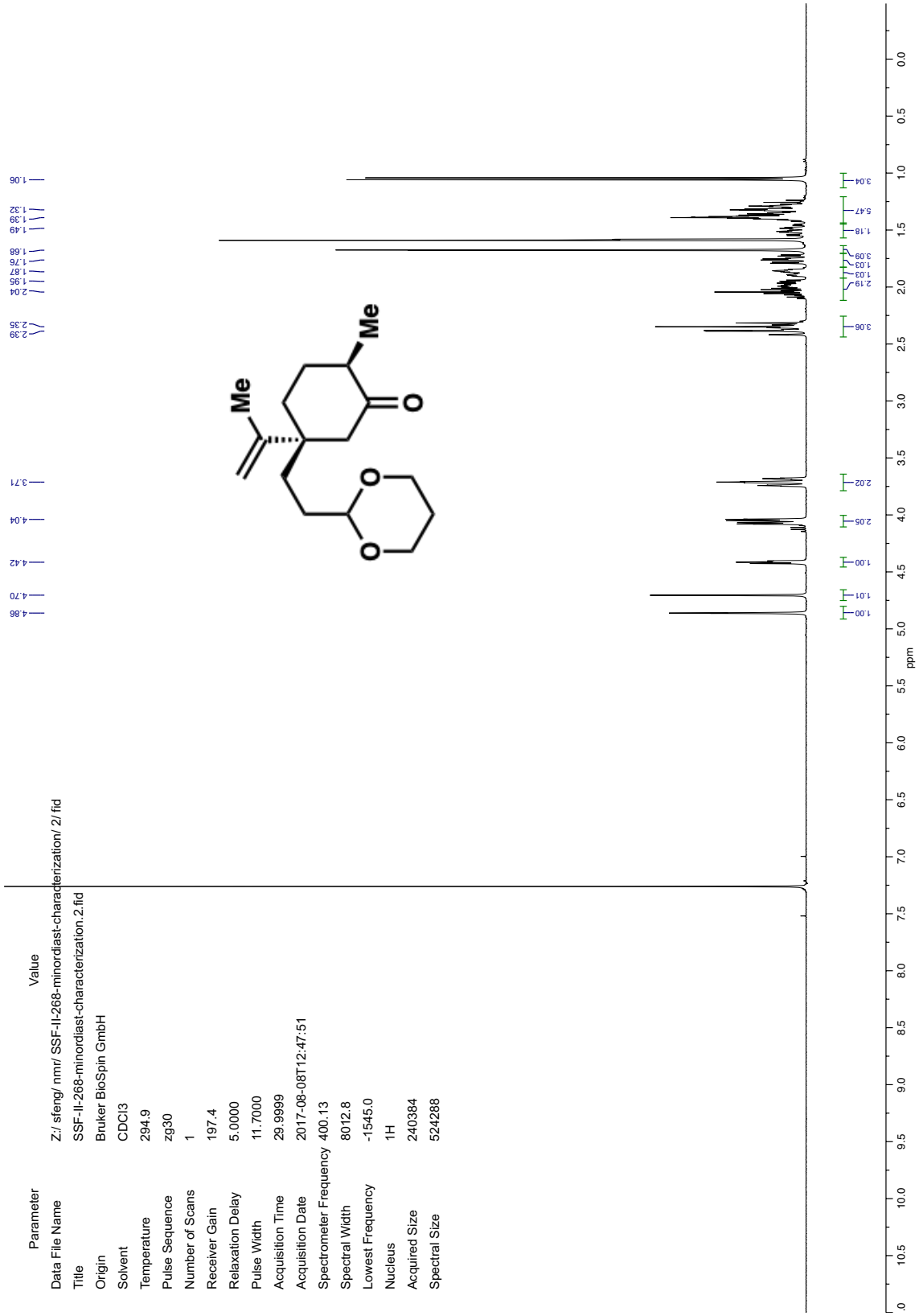

Parameter	Value
Data File Name	Z:/ sfeng/ nmr/ SSF-II-268-minordiast-characterization/ 2/ fid
Title	SSF-II-268-minordiast-characterization.2.fid
Origin	Bruker BioSpin GmbH
Solvent	CDCl3
Temperature	294.9
Pulse Sequence	zg30
Number of Scans	1
Receiver Gain	197.4
Relaxation Delay	5.0000
Pulse Width	11.7000
Acquisition Time	29.9999
Acquisition Date	2017-08-08T12:47:51
Spectrometer Frequency	400.13
Spectral Width	8012.8
Lowest Frequency	-1545.0
Nucleus	1H
Acquired Size	240384
Spectral Size	524288

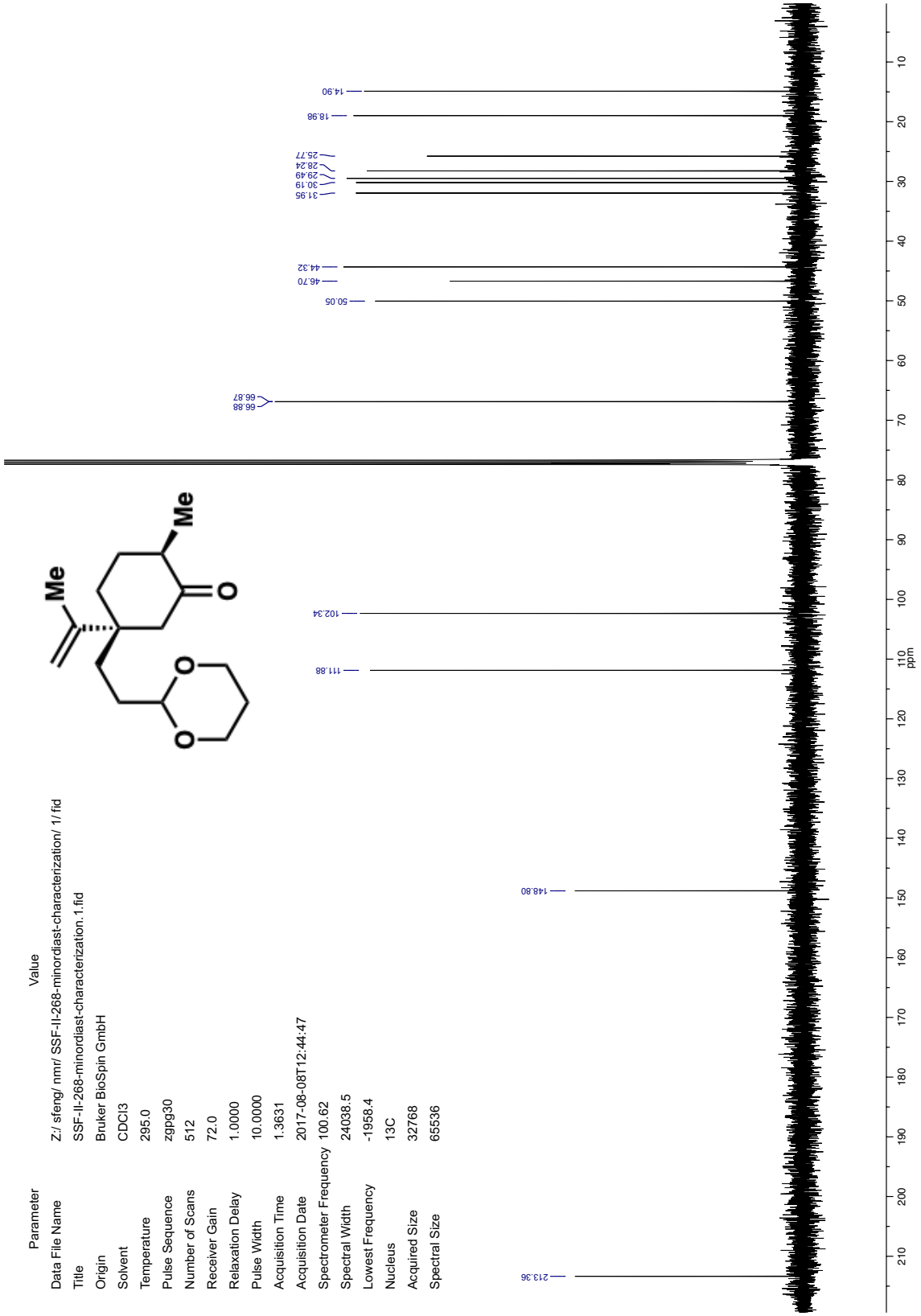

Parameter	Value
Data File Name	Z:/ sfeng/ nmr/ SSF-II-268-minordiast-characterization/ 1/ fid
Title	SSF-II-268-minordiast-characterization.1.fid
Origin	Bruker BioSpin GmbH
Solvent	CDCl3
Temperature	295.0
Pulse Sequence	zgpg30
Number of Scans	512
Receiver Gain	72.0
Relaxation Delay	1.0000
Pulse Width	10.0000
Acquisition Time	1.3631
Acquisition Date	2017-08-08T12:44:47
Spectrometer Frequency	100.62
Spectral Width	24038.5
Lowest Frequency	-1958.4
Nucleus	13C
Acquired Size	32768
Spectral Size	65536

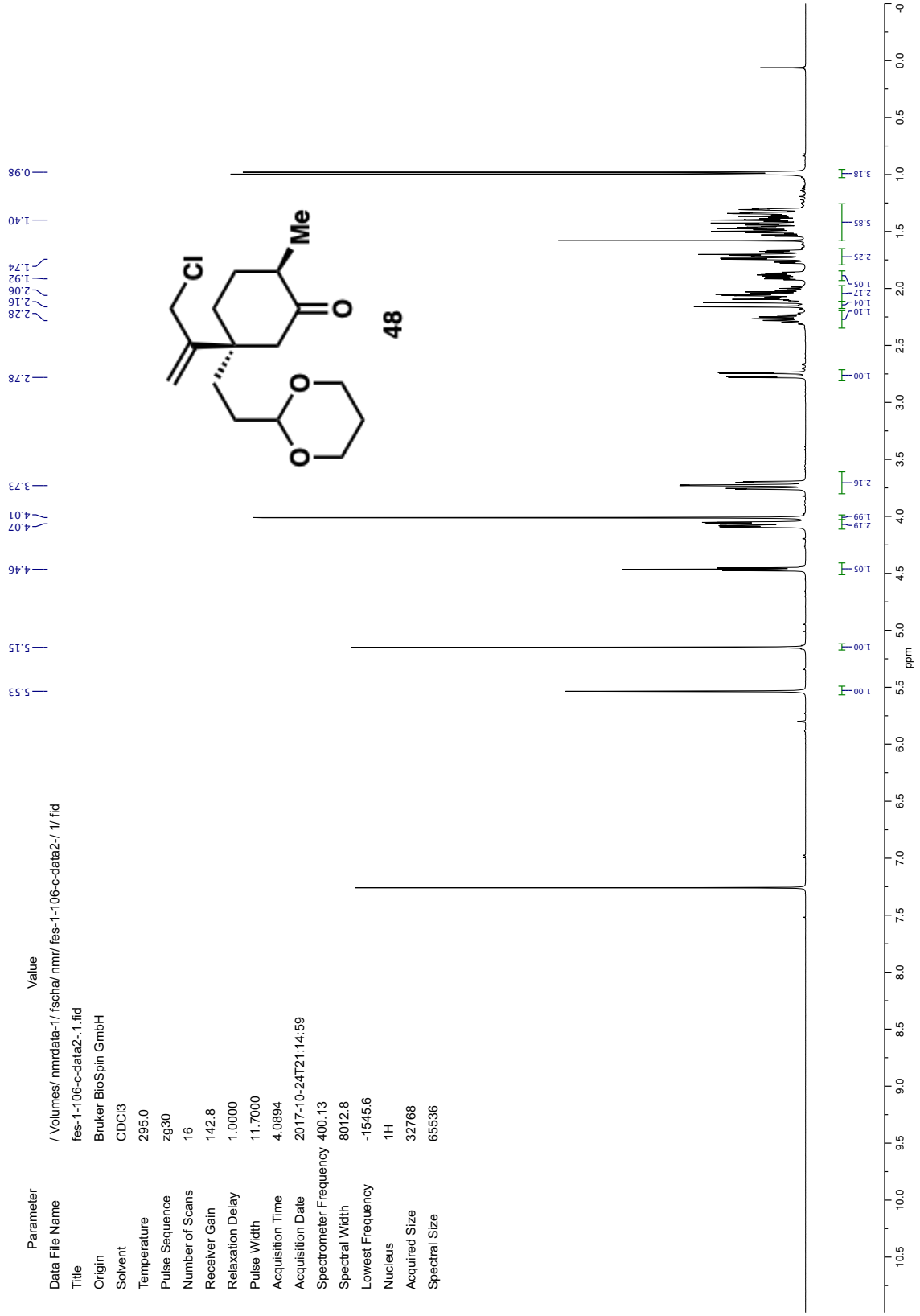

Parameter	Value
Data File Name	/ Volumes/ nmrdata-1/ fscha/ nmr/ fes-1-106-c-data2-/ 1/ fid
Title	fes-1-106-c-data2-.1.fid
Origin	Bruker BioSpin GmbH
Solvent	CDCl3
Temperature	295.0
Pulse Sequence	zg30
Number of Scans	16
Receiver Gain	142.8
Relaxation Delay	1.0000
Pulse Width	11.7000
Acquisition Time	4.0894
Acquisition Date	2017-10-24T21:14:59
Spectrometer Frequency	400.13
Spectral Width	8012.8
Lowest Frequency	-1545.6
Nucleus	1H
Acquired Size	32768
Spectral Size	65536

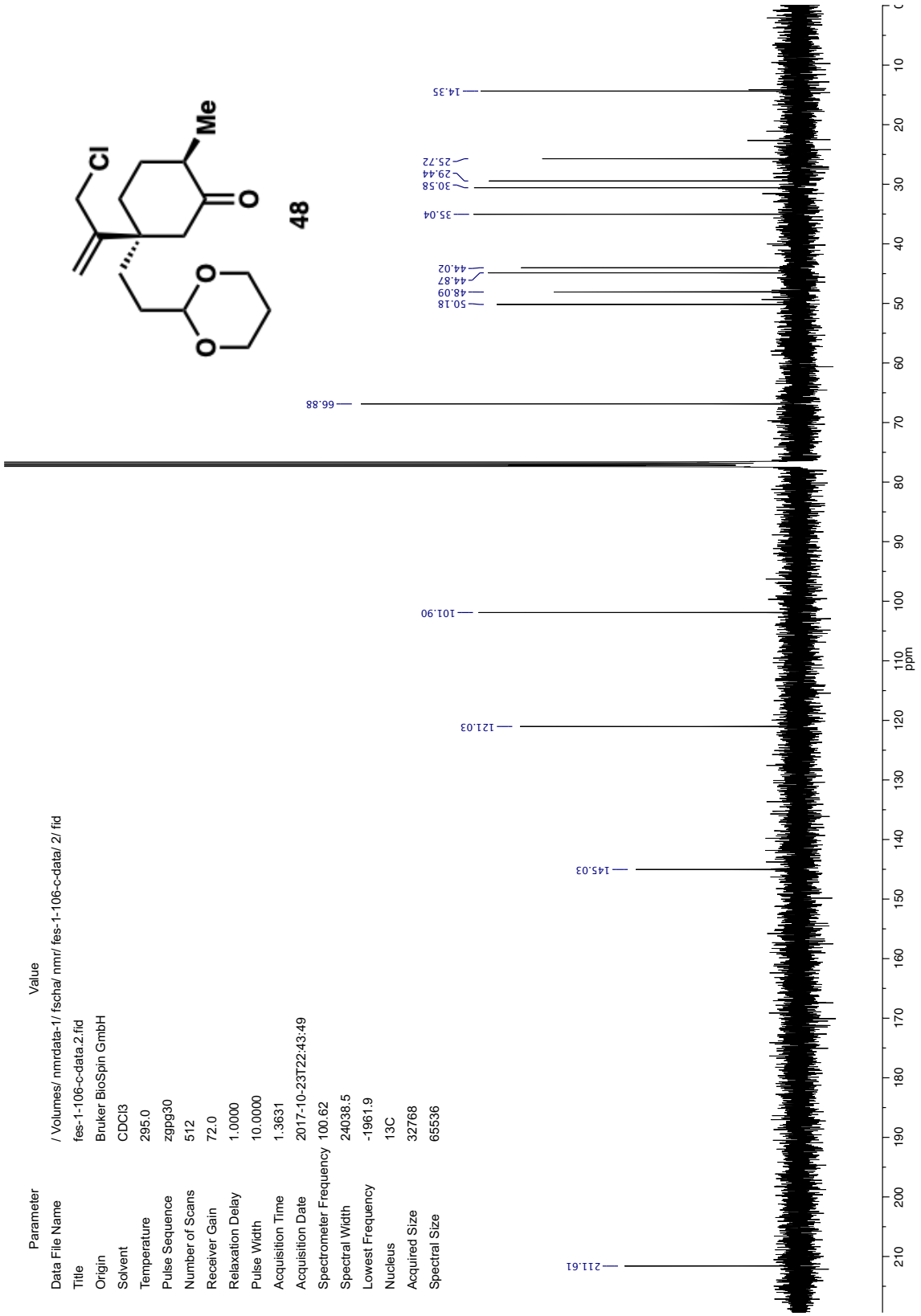

Parameter	Value
Data File Name	/ Volumes/ nmrdata-1/ fscha/ nmr/ fes-1-106-c-data/ 2/ fid
Title	fes-1-106-c-data.2.fid
Origin	Bruker BioSpin GmbH
Solvent	CDCl3
Temperature	295.0
Pulse Sequence	zgpg30
Number of Scans	512
Receiver Gain	72.0
Relaxation Delay	1.0000
Pulse Width	10.0000
Acquisition Time	1.3631
Acquisition Date	2017-10-23T22:43:49
Spectrometer Frequency	100.62
Spectral Width	24038.5
Lowest Frequency	-1961.9
Nucleus	13C
Acquired Size	32768
Spectral Size	65536

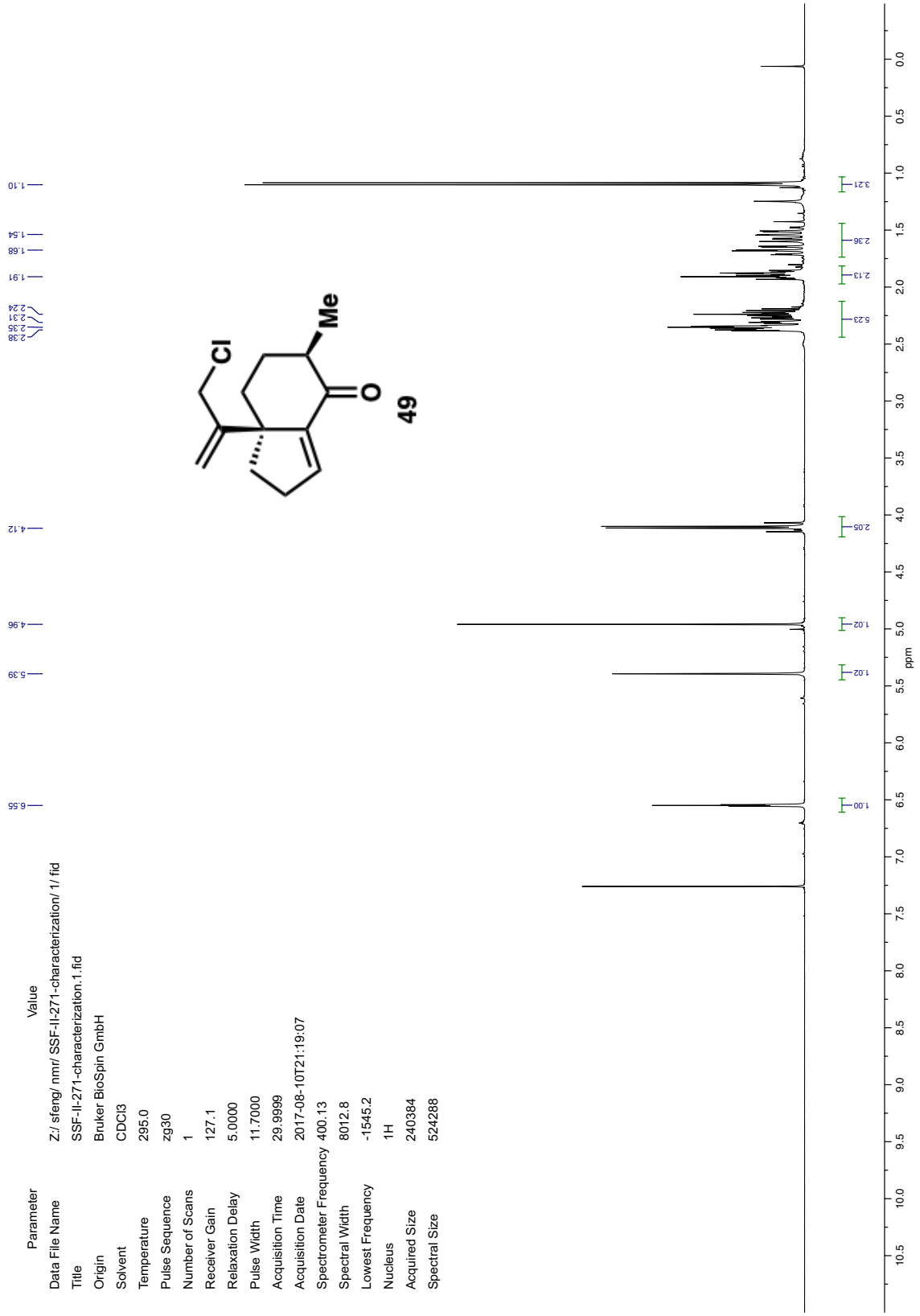
Cl
Me
O
49
Parameter Value
Data File Name Z:/ sfeng/ nmr/ SSF-II-271-characterization/ 1/ fid
Title SSF-II-271-characterization.1.fid
Origin Bruker BioSpin GmbH
Solvent CDCl3
Temperature 295.0
Pulse Sequence zg30
Number of Scans 1
Receiver Gain 127.1
Relaxation Delay 5.0000
Pulse Width 11.7000
Acquisition Time 29.9999
Acquisition Date 2017-08-10T21:19:07
Spectrometer Frequency 400.13
Spectral Width 8012.8
Lowest Frequency -1545.2
Nucleus 1H
Acquired Size 240384
Spectral Size 524288
6.55
5.39
4.96
4.12
2.38
2.35
2.31
2.24
1.91
1.68
1.54
1.10
1.00
1.02
1.02
2.05
5.23
2.13
2.36
3.21
ppm

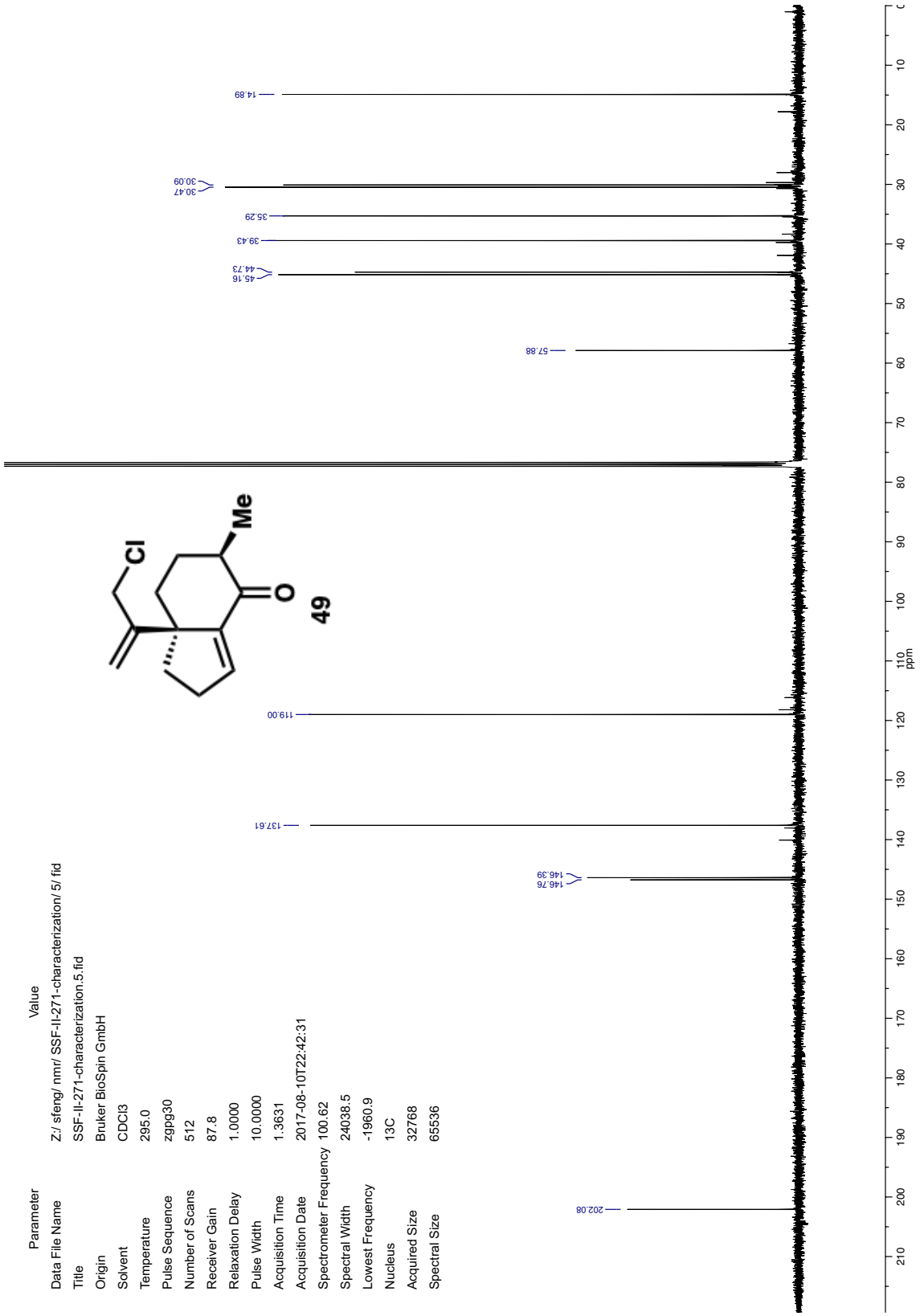
Parameter Value
Data File Name Z:/ sfeng/ nmr/ SSF-II-271-characterization/ 5/ fid
Title SSF-II-271-characterization.5.fid
Origin Bruker BioSpin GmbH
Solvent CDCl3
Temperature 295.0
Pulse Sequence zgpg30
Number of Scans 512
Receiver Gain 87.8
Relaxation Delay 1.0000
Pulse Width 10.0000
Acquisition Time 1.3631
Acquisition Date 2017-08-10T22:42:31
Spectrometer Frequency 100.62
Spectral Width 24038.5
Lowest Frequency -1960.9
Nucleus 13C
Acquired Size 32768
Spectral Size 65536
14.89
30.47
30.09
35.29
39.43
45.16
44.73
57.88
77.00
119.00
137.61
146.76
146.39
202.08
Cl
Me
O
49
ppm

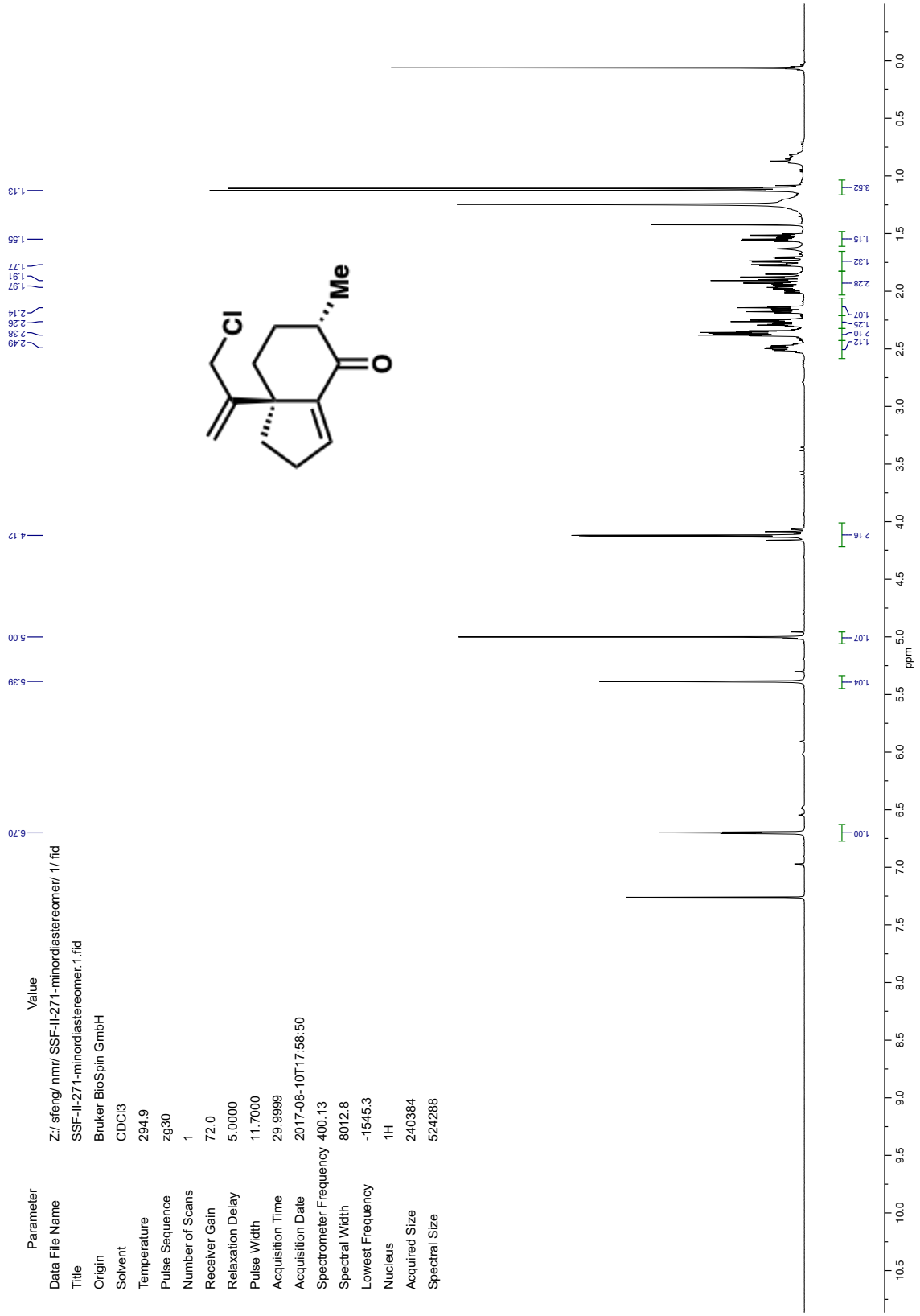

Parameter	Value
Data File Name	Z:/ sfeng/ nmr/ SSF-II-271-minordiastereomer/ 1/ fid
Title	SSF-II-271-minordiastereomer.1.fid
Origin	Bruker BioSpin GmbH
Solvent	CDCl3
Temperature	294.9
Pulse Sequence	zg30
Number of Scans	1
Receiver Gain	72.0
Relaxation Delay	5.0000
Pulse Width	11.7000
Acquisition Time	29.9999
Acquisition Date	2017-08-10T17:58:50
Spectrometer Frequency	400.13
Spectral Width	8012.8
Lowest Frequency	-1545.3
Nucleus	1H
Acquired Size	240384
Spectral Size	524288

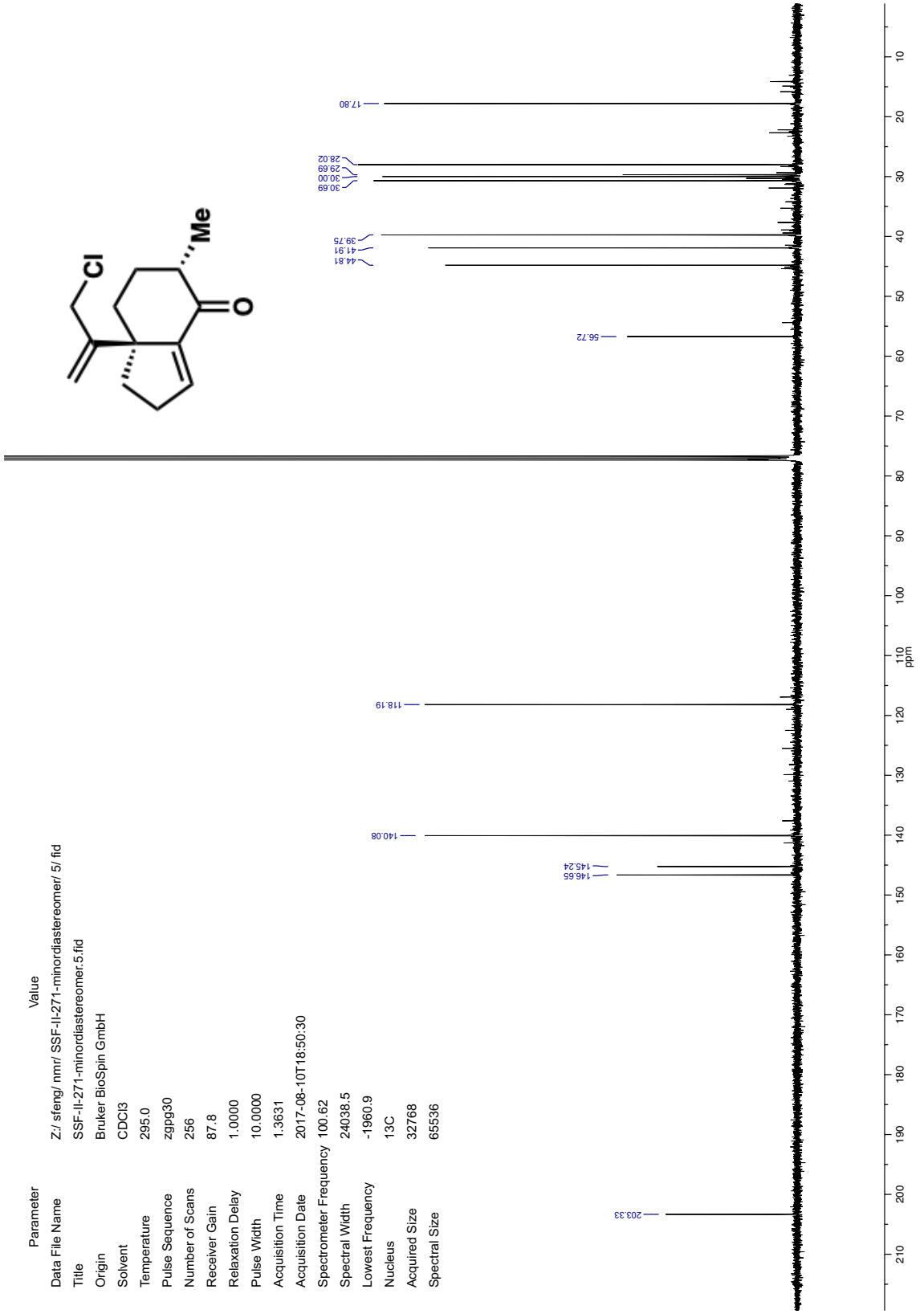

Parameter	Value
Data File Name	Z:/ sfeng/ nmr/ SSF-II-271-minordiastereomer/ 5/ fid
Title	SSF-II-271-minordiastereomer.5.fid
Origin	Bruker BioSpin GmbH
Solvent	CDCl3
Temperature	295.0
Pulse Sequence	zgpg30
Number of Scans	256
Receiver Gain	87.8
Relaxation Delay	1.0000
Pulse Width	10.0000
Acquisition Time	1.3631
Acquisition Date	2017-08-10T18:50:30
Spectrometer Frequency	100.62
Spectral Width	24038.5
Lowest Frequency	-1960.9
Nucleus	13C
Acquired Size	32768
Spectral Size	65536

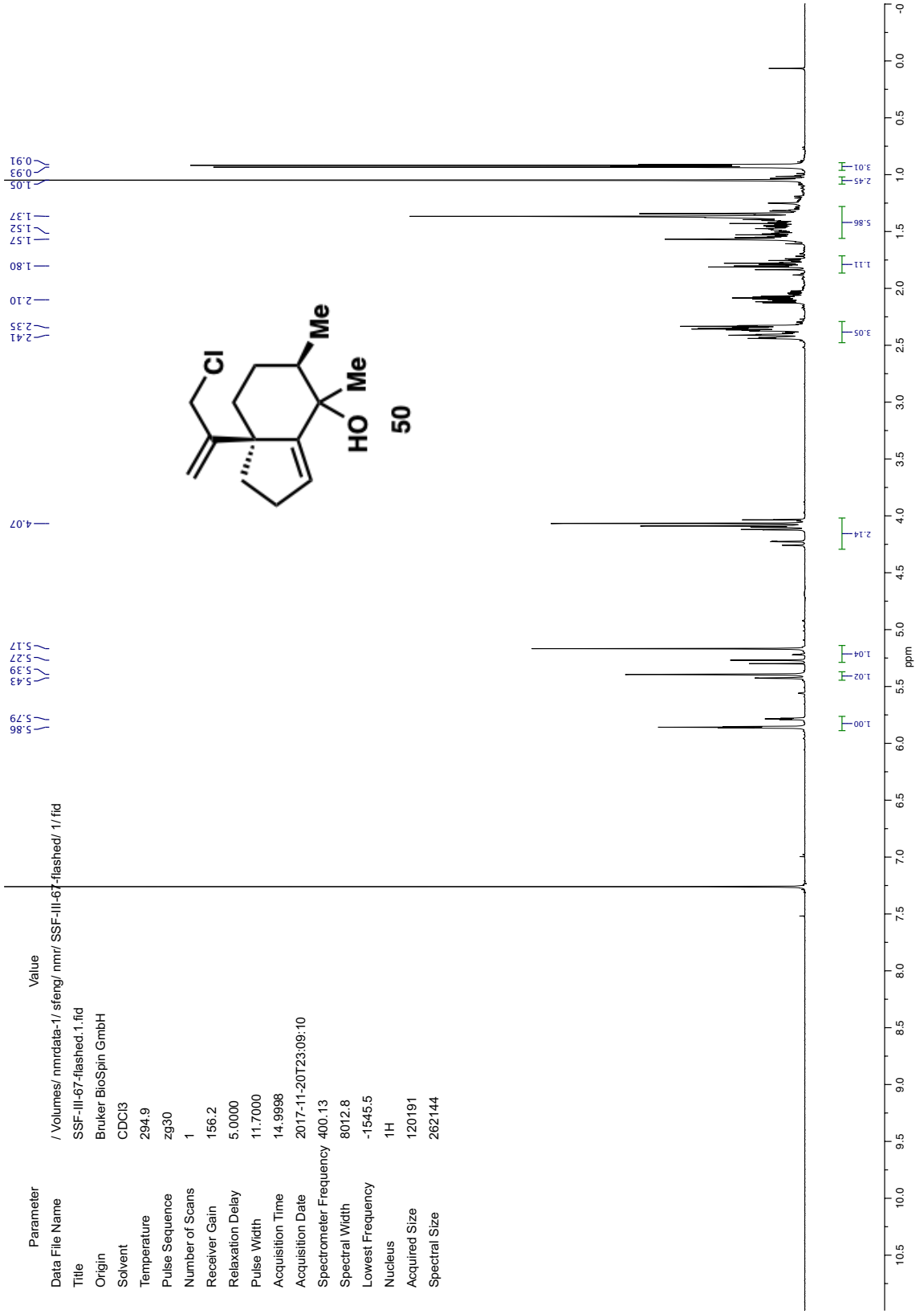

Parameter	Value
Data File Name	/ Volumes/ nmrdata-1/ sfeng/ nmr/ SSF-III-67-flashed/ 1/ fid
Title	SSF-III-67-flashed.1.fid
Origin	Bruker BioSpin GmbH
Solvent	CDCl3
Temperature	294.9
Pulse Sequence	zg30
Number of Scans	1
Receiver Gain	156.2
Relaxation Delay	5.0000
Pulse Width	11.7000
Acquisition Time	14.9998
Acquisition Date	2017-11-20T23:09:10
Spectrometer Frequency	400.13
Spectral Width	8012.8
Lowest Frequency	-1545.5
Nucleus	1H
Acquired Size	120191
Spectral Size	262144

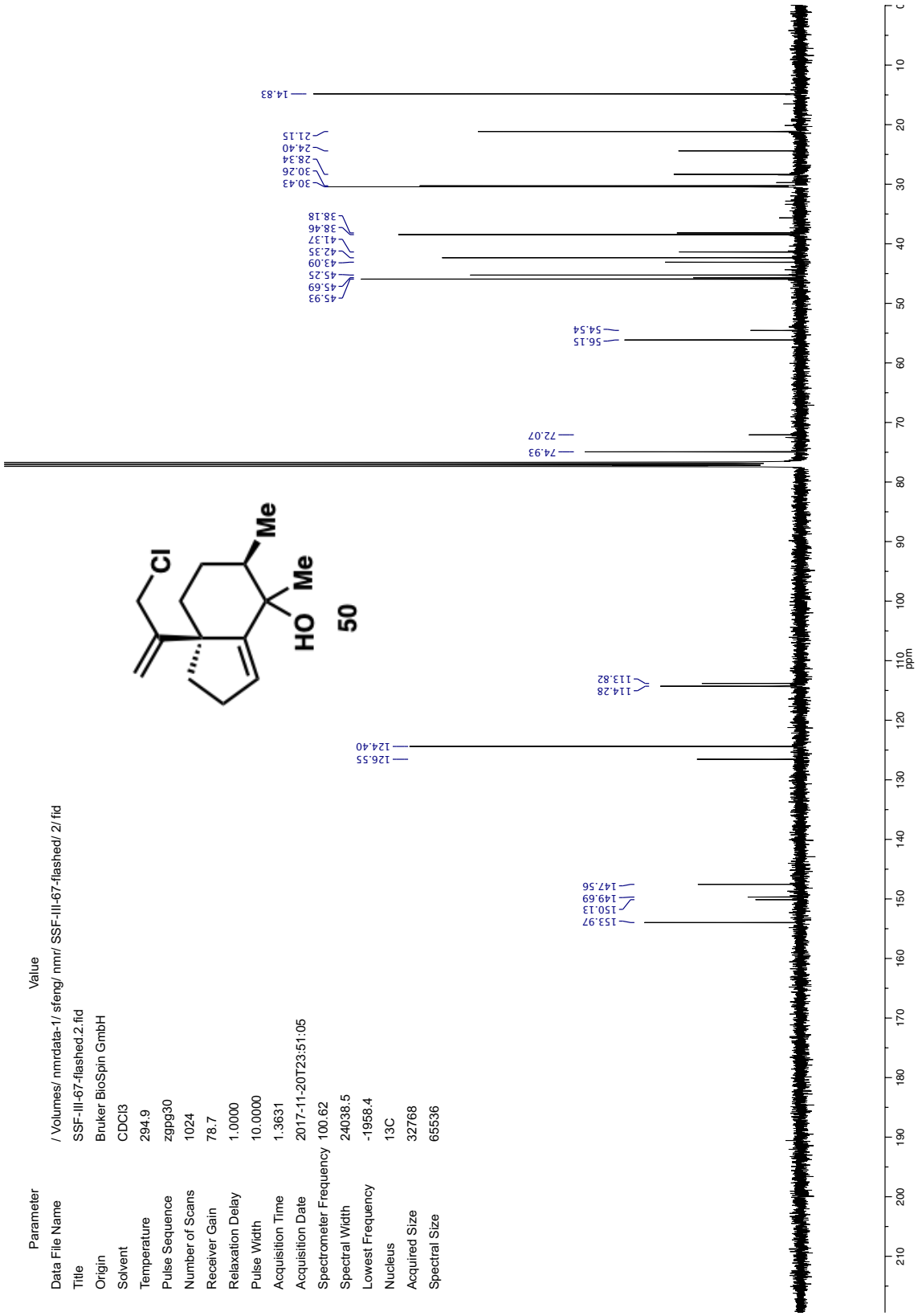

Parameter	Value
Data File Name	/ Volumes/ nmrdata-1/ sfeng/ nmr/ SSF-III-67-flashed/ 2/ fid
Title	SSF-III-67-flashed.2.fid
Origin	Bruker BioSpin GmbH
Solvent	CDCl3
Temperature	294.9
Pulse Sequence	zgpg30
Number of Scans	1024
Receiver Gain	78.7
Relaxation Delay	1.0000
Pulse Width	10.0000
Acquisition Time	1.3631
Acquisition Date	2017-11-20T23:51:05
Spectrometer Frequency	100.62
Spectral Width	24038.5
Lowest Frequency	-1958.4
Nucleus	13C
Acquired Size	32768
Spectral Size	65536

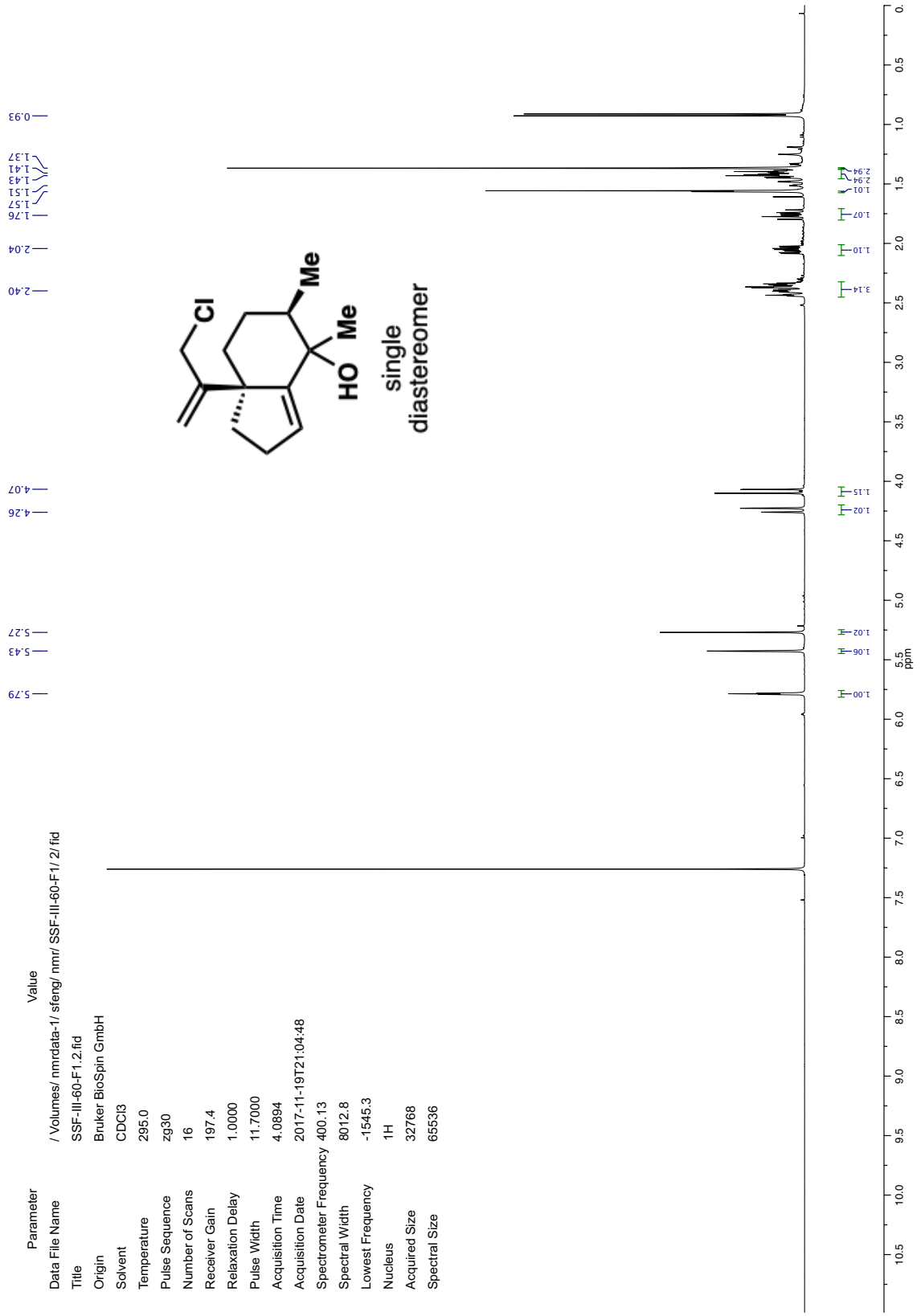
Parameter
Value
Data File Name / Volumes/ nmrdata-1/ sfeng/ nmr/ SSF-III-60-F1/ 2/ fid
Title SSF-III-60-F1.2.fid
Origin Bruker BioSpin GmbH
Solvent CDCl3
Temperature 295.0
Pulse Sequence zg30
Number of Scans 16
Receiver Gain 197.4
Relaxation Delay 1.0000
Pulse Width 11.7000
Acquisition Time 4.0894
Acquisition Date 2017-11-19T21:04:48
Spectrometer Frequency 400.13
Spectral Width 8012.8
Lowest Frequency -1545.3
Nucleus 1H
Acquired Size 32768
Spectral Size 65536
Cl
Me
HO
Me
single
diastereomer
0.93
1.37
1.41
1.43
1.51
1.57
1.76
2.04
2.40
4.07
4.26
5.27
5.43
5.79
1.00
1.06
1.02
1.02
1.15
1.02
3.14
1.10
1.07
1.01
2.94
2.94
ppm

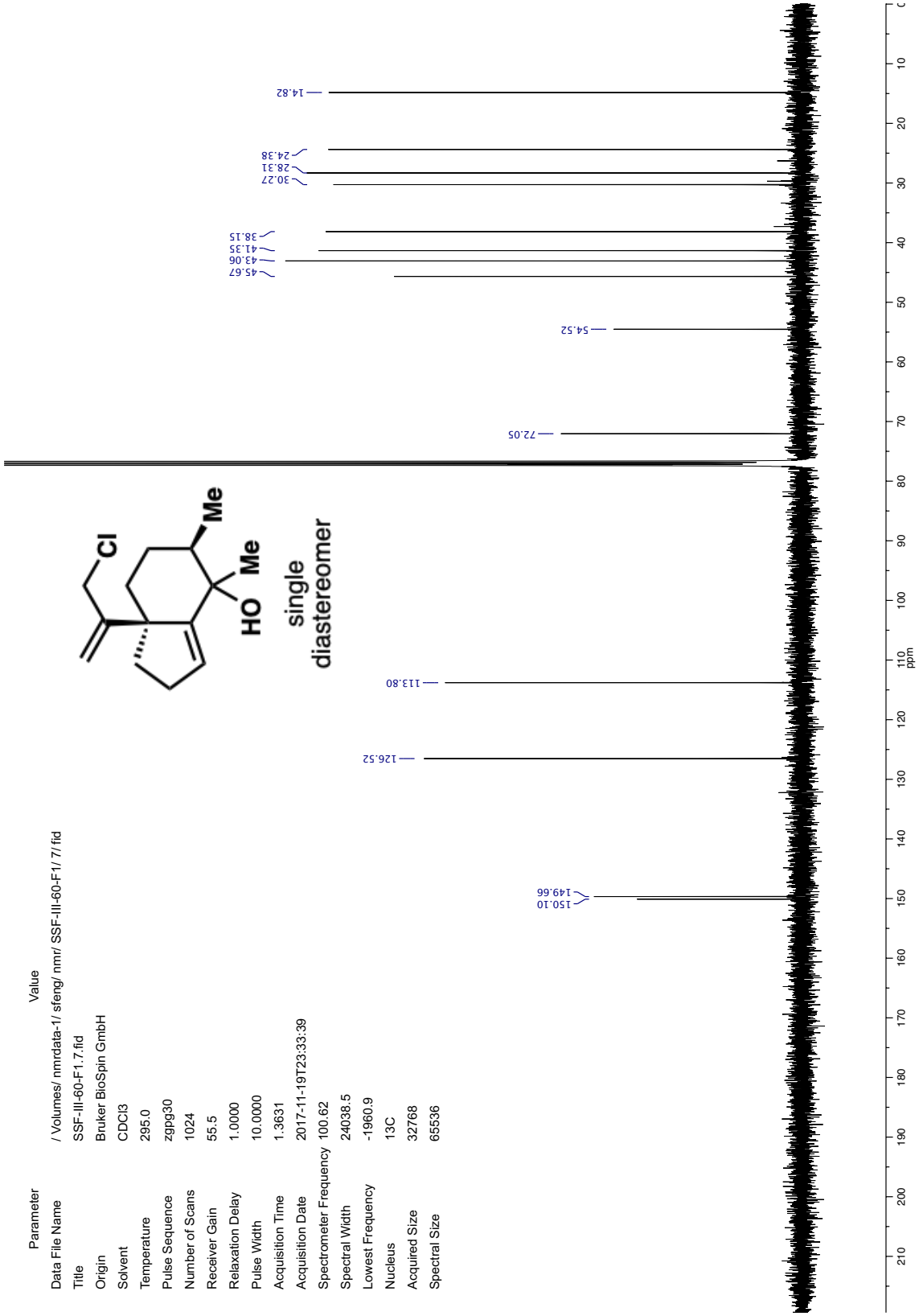

Parameter	Value
Data File Name	/ Volumes/ nmrdata-1/ sfeng/ nmr/ SSF-III-60-F1/ 7/ fid
Title	SSF-III-60-F1.7.fid
Origin	Bruker BioSpin GmbH
Solvent	CDCl3
Temperature	295.0
Pulse Sequence	zgpg30
Number of Scans	1024
Receiver Gain	55.5
Relaxation Delay	1.0000
Pulse Width	10.0000
Acquisition Time	1.3631
Acquisition Date	2017-11-19T23:33:39
Spectrometer Frequency	100.62
Spectral Width	24038.5
Lowest Frequency	-1960.9
Nucleus	13C
Acquired Size	32768
Spectral Size	65536

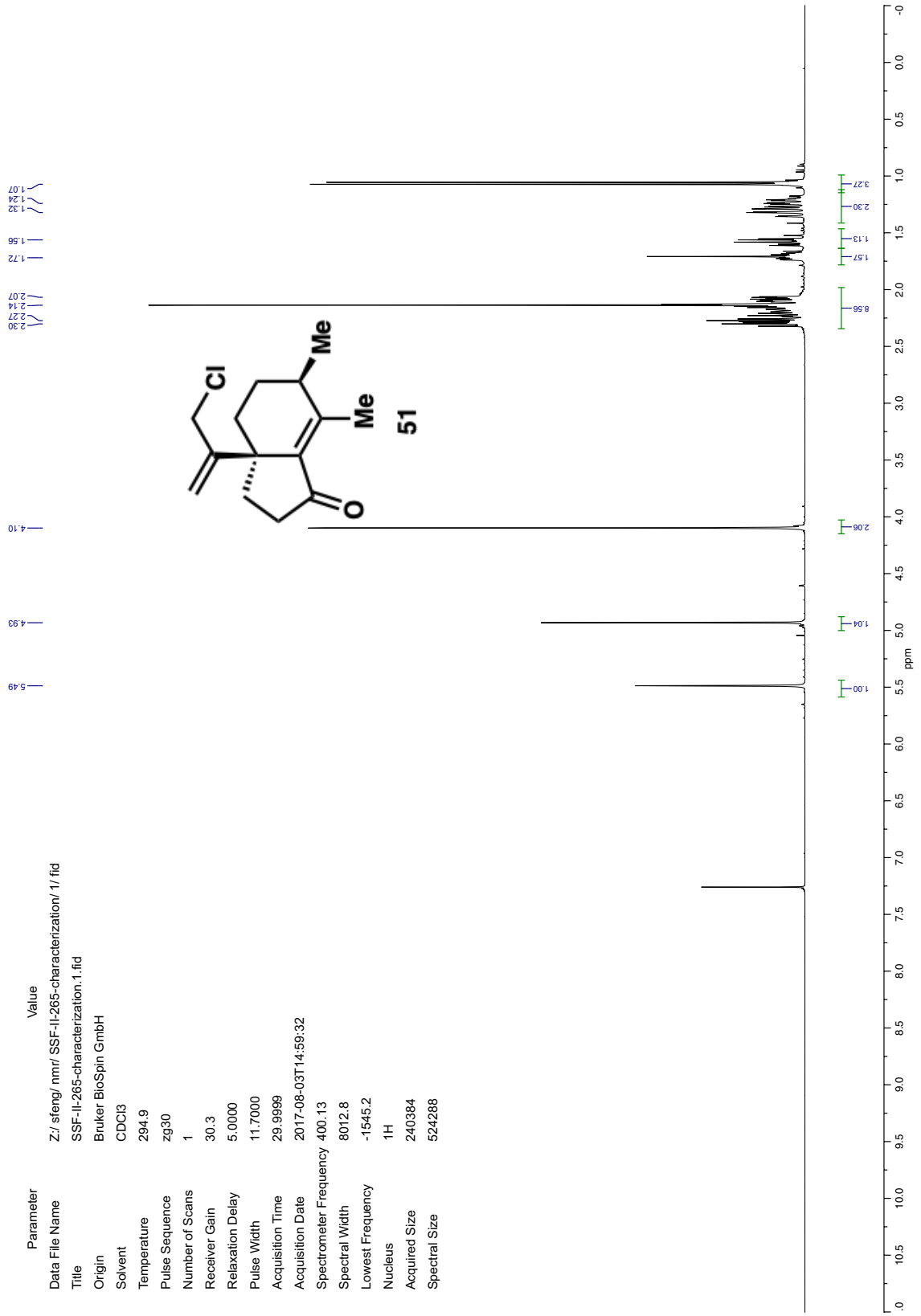
Parameter
Value
Data File Name
Z:/ sfeng/ nmr/ SSF-II-265-characterization/ 1/ fid
Title
SSF-II-265-characterization.1.fid
Origin
Bruker BioSpin GmbH
Solvent
CDCl3
Temperature
294.9
Pulse Sequence
zg30
Number of Scans
1
Receiver Gain
30.3
Relaxation Delay
5.0000
Pulse Width
11.7000
Acquisition Time
29.9999
Acquisition Date
2017-08-03T14:59:32
Spectrometer Frequency
400.13
Spectral Width
8012.8
Lowest Frequency
-1545.2
Nucleus
1H
Acquired Size
240384
Spectral Size
524288
Cl
Me
Me
O
51
ppm

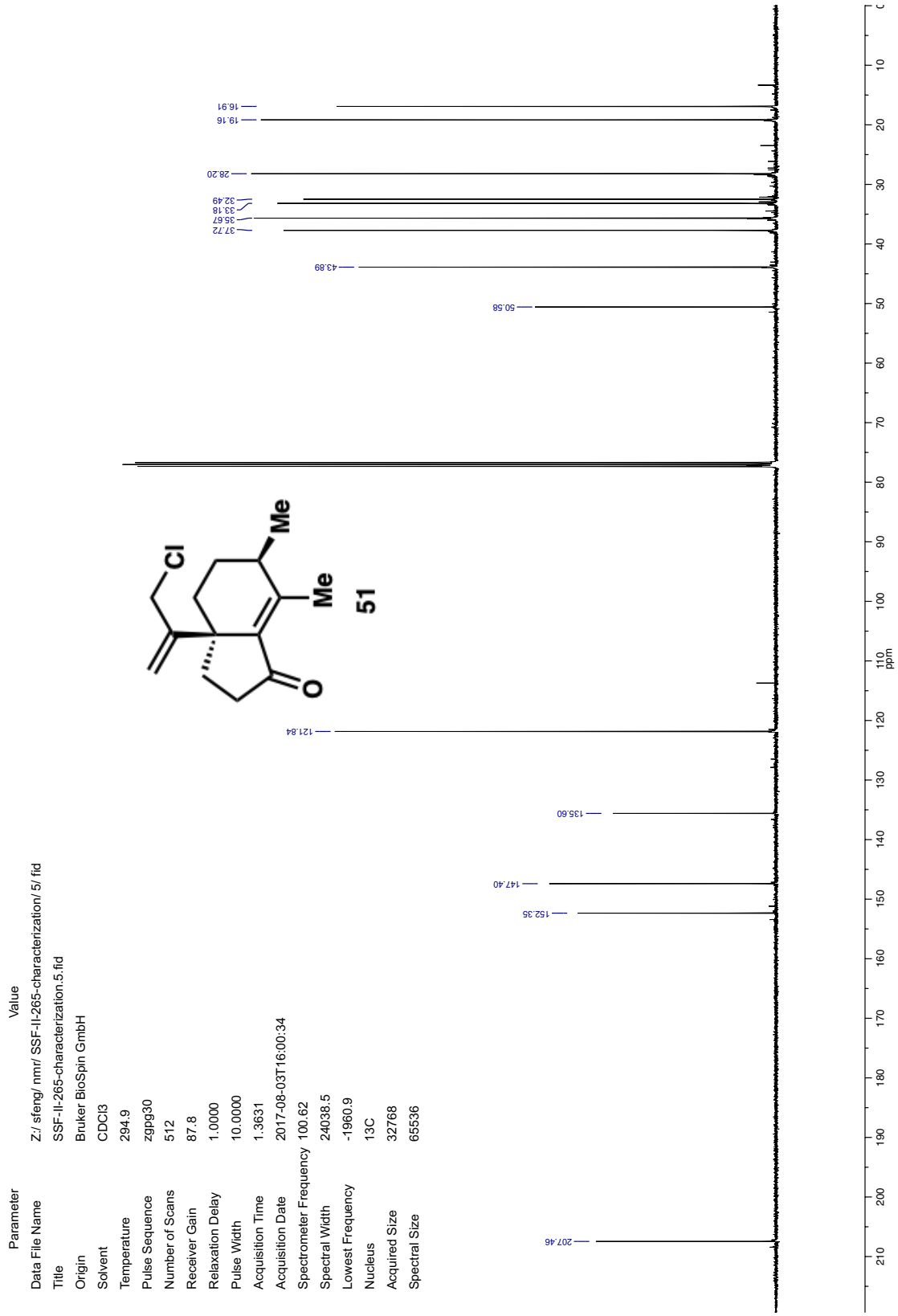
Parameter
Value
Data File Name
Z:/ sfeng/ nmr/ SSF-II-265-characterization/ 5/ fid
Title
SSF-II-265-characterization.5.fid
Origin
Bruker BioSpin GmbH
Solvent
CDCl3
Temperature
294.9
Pulse Sequence
zgpg30
Number of Scans
512
Receiver Gain
87.8
Relaxation Delay
1.0000
Pulse Width
10.0000
Acquisition Time
1.3631
Acquisition Date
2017-08-03T16:00:34
Spectrometer Frequency
100.62
Spectral Width
24038.5
Lowest Frequency
-1960.9
Nucleus
13C
Acquired Size
32768
Spectral Size
65536
16.91
19.16
28.20
32.49
33.18
35.67
37.72
43.89
50.58
121.84
135.60
147.40
152.35
207.46
Cl
Me
Me
O
51
ppm

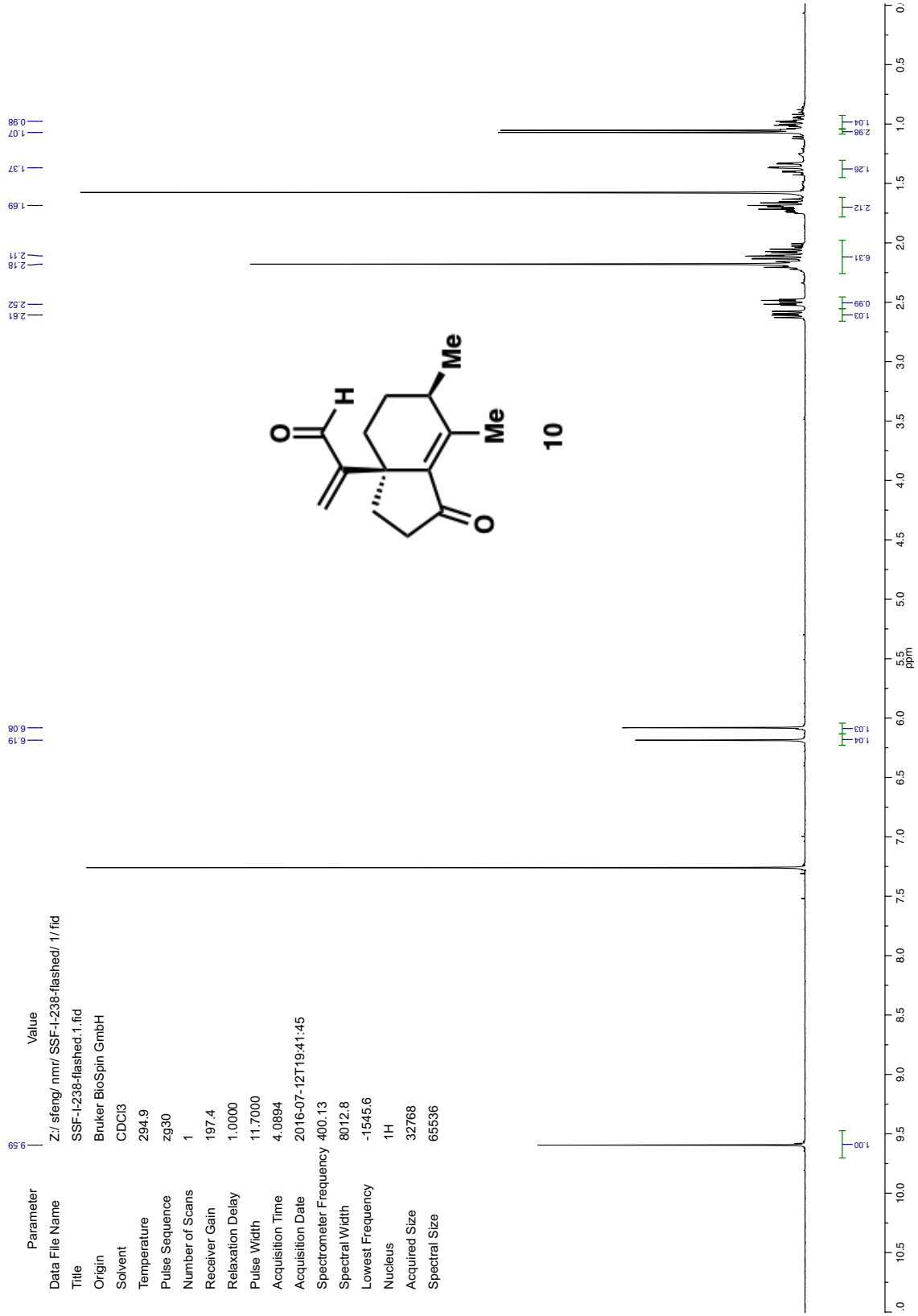
Parameter Value
Data File Name Z:/ sfeng/ nmr/ SSF-I-238-flashed/ 1/ fid
Title SSF-I-238-flashed.1.fid
Origin Bruker BioSpin GmbH
Solvent CDCl3
Temperature 294.9
Pulse Sequence zg30
Number of Scans 1
Receiver Gain 197.4
Relaxation Delay 1.0000
Pulse Width 11.7000
Acquisition Time 4.0894
Acquisition Date 2016-07-12T19:41:45
Spectrometer Frequency 400.13
Spectral Width 8012.8
Lowest Frequency -1545.6
Nucleus 1H
Acquired Size 32768
Spectral Size 65536
9.59
6.19
6.08
2.61
2.52
2.18
2.11
1.69
1.37
1.07
0.98
1.00
1.03
1.04
0.99
1.03
6.31
2.12
1.26
2.98
1.04
O
H
Me
Me
O
10
ppm

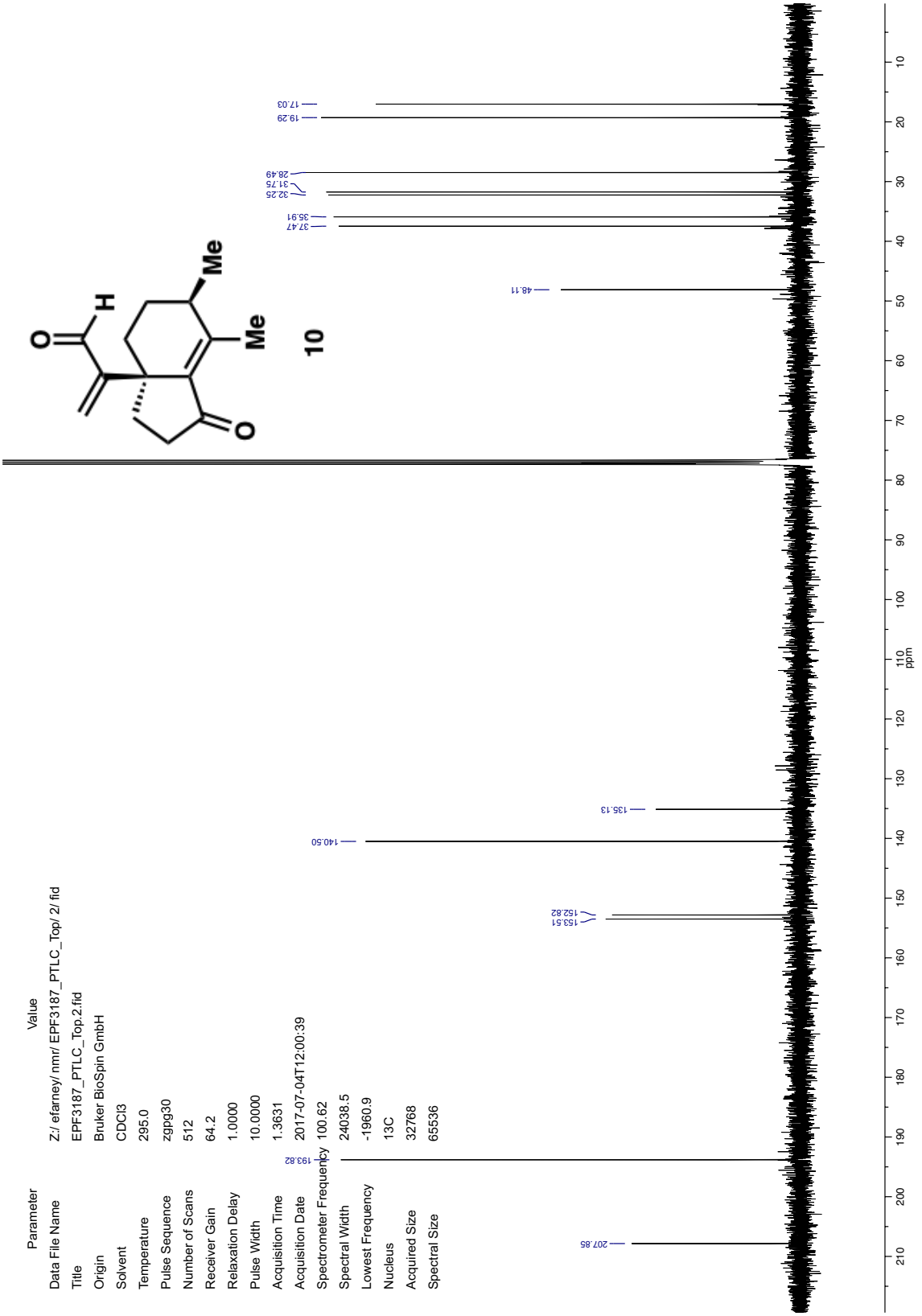
Parameter
Value
Data File Name
Z:/ efarney/ nmr/ EPF3187_PTLC_Top/ 2/ fid
Title
EPF3187_PTLC_Top.2.fid
Origin
Bruker BioSpin GmbH
Solvent
CDCl3
Temperature
295.0
Pulse Sequence
zgpg30
Number of Scans
512
Receiver Gain
64.2
Relaxation Delay
1.0000
Pulse Width
10.0000
Acquisition Time
1.3631
Acquisition Date
2017-07-04T12:00:39
Spectrometer Frequency
100.62
Spectral Width
24038.5
Lowest Frequency
-1960.9
Nucleus
13C
Acquired Size
32768
Spectral Size
65536
10
O
H
Me
Me
O
17.03
19.29
28.49
31.75
32.25
35.91
37.47
48.11
135.13
140.50
152.82
153.51
193.82
207.85
10
20
30
40
50
60
70
80
90
100
110
120
130
140
150
160
170
180
190
200
210
ppm

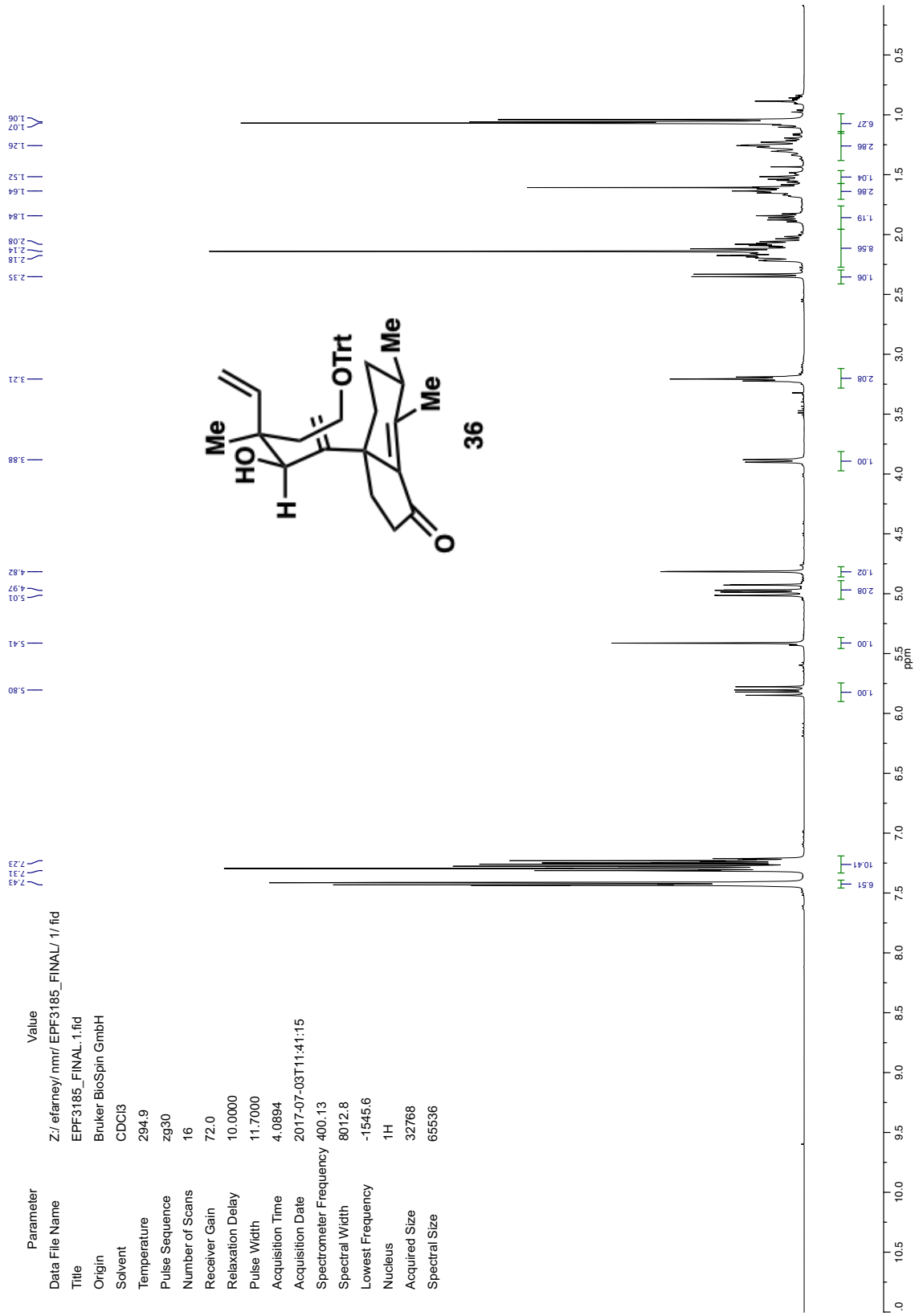

Parameter	Value
Data File Name	Z:/ efarney/ nmr/ EPF3185_FINAL/ 1/ fid
Title	EPF3185_FINAL.1.fid
Origin	Bruker BioSpin GmbH
Solvent	CDCl3
Temperature	294.9
Pulse Sequence	zg30
Number of Scans	16
Receiver Gain	72.0
Relaxation Delay	10.0000
Pulse Width	11.7000
Acquisition Time	4.0894
Acquisition Date	2017-07-03T11:41:15
Spectrometer Frequency	400.13
Spectral Width	8012.8
Lowest Frequency	-1545.6
Nucleus	1H
Acquired Size	32768
Spectral Size	65536

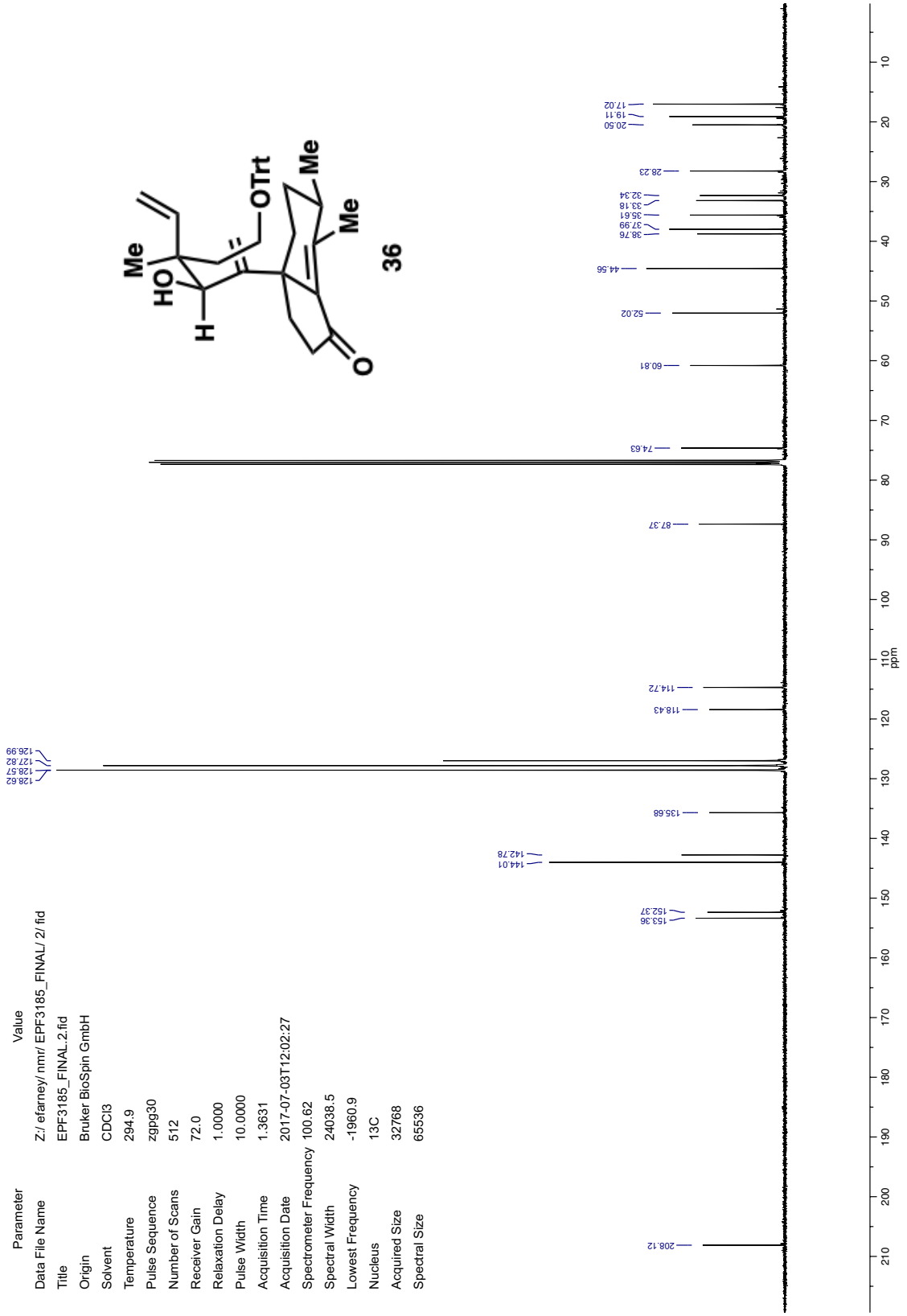
Me
HO
H
OTrt
Me
Me
O
36
Parameter
Value
Data File Name
Z:/ efarney/ nmr/ EPF3185_FINAL/ 2/ fid
Title
EPF3185_FINAL.2.fid
Origin
Bruker BioSpin GmbH
Solvent
CDCl3
Temperature
294.9
Pulse Sequence
zgpg30
Number of Scans
512
Receiver Gain
72.0
Relaxation Delay
1.0000
Pulse Width
10.0000
Acquisition Time
1.3631
Acquisition Date
2017-07-03T12:02:27
Spectrometer Frequency
100.62
Spectral Width
24038.5
Lowest Frequency
-1960.9
Nucleus
13C
Acquired Size
32768
Spectral Size
65536
208.12
153.36
152.37
144.01
142.78
135.68
128.62
128.57
127.82
126.99
118.43
114.72
87.37
74.63
60.81
52.02
44.56
38.76
37.99
35.61
33.18
32.34
28.23
20.50
19.11
17.02
ppm

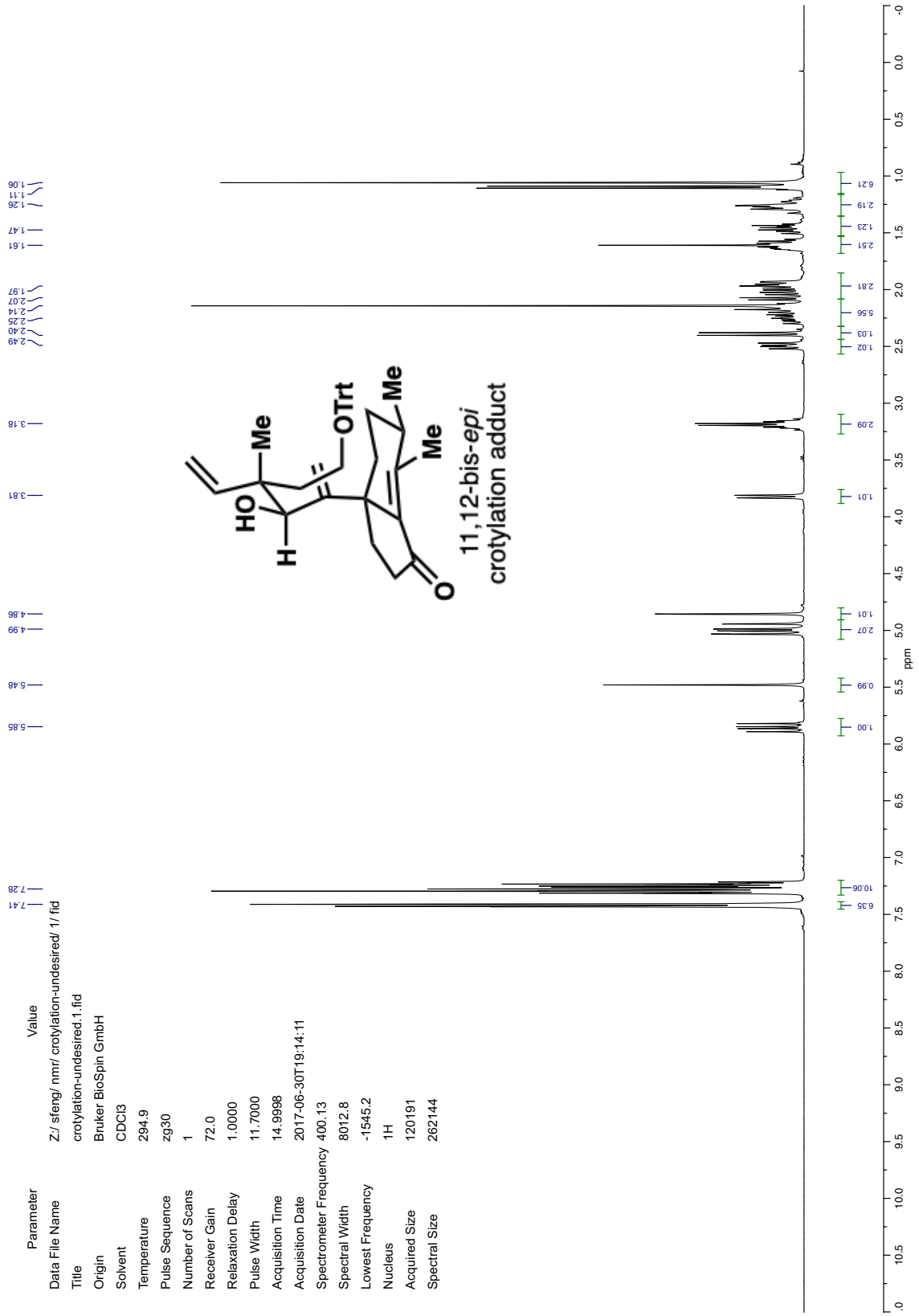
Parameter Value
Data File Name Z:/ sfeng/ nmr/ crotylation-undesired/ 1/ fid
Title crotylation-undesired.1.fid
Origin Bruker BioSpin GmbH
Solvent CDCl3
Temperature 294.9
Pulse Sequence zg30
Number of Scans 1
Receiver Gain 72.0
Relaxation Delay 1.0000
Pulse Width 11.7000
Acquisition Time 14.9998
Acquisition Date 2017-06-30T19:14:11
Spectrometer Frequency 400.13
Spectral Width 8012.8
Lowest Frequency -1545.2
Nucleus 1H
Acquired Size 120191
Spectral Size 262144
HO
Me
H
OTrt
Me
Me
O
11,12-bis-epi
crotylation adduct
ppm

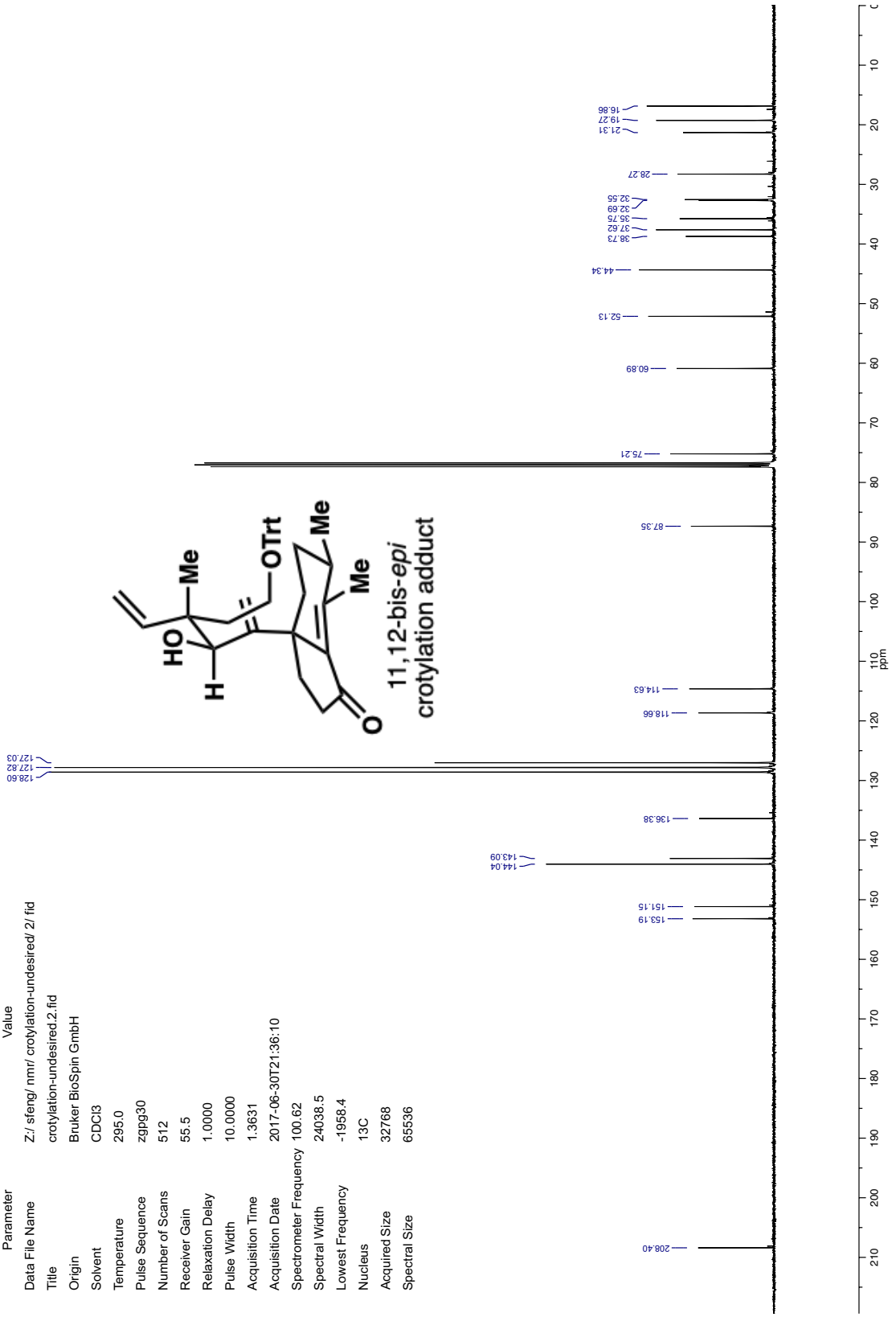
Parameter
Value
Data File Name
Z:/ sfeng/ nmr/ crotylation-undesired/ 2/ fid
Title
crotylation-undesired.2.fid
Origin
Bruker BioSpin GmbH
Solvent
CDCl3
Temperature
295.0
Pulse Sequence
zgpg30
Number of Scans
512
Receiver Gain
55.5
Relaxation Delay
1.0000
Pulse Width
10.0000
Acquisition Time
1.3631
Acquisition Date
2017-06-30T21:36:10
Spectrometer Frequency
100.62
Spectral Width
24038.5
Lowest Frequency
-1958.4
Nucleus
13C
Acquired Size
32768
Spectral Size
65536
HO
Me
OTrt
Me
Me
H
O
11,12-bis-epi
crotylation adduct
208.40
153.19
151.15
144.04
143.09
136.38
128.60
127.82
127.03
114.63
118.66
87.35
75.21
60.89
52.13
44.34
38.73
37.62
35.75
32.69
32.55
28.27
21.31
19.27
16.86
ppm

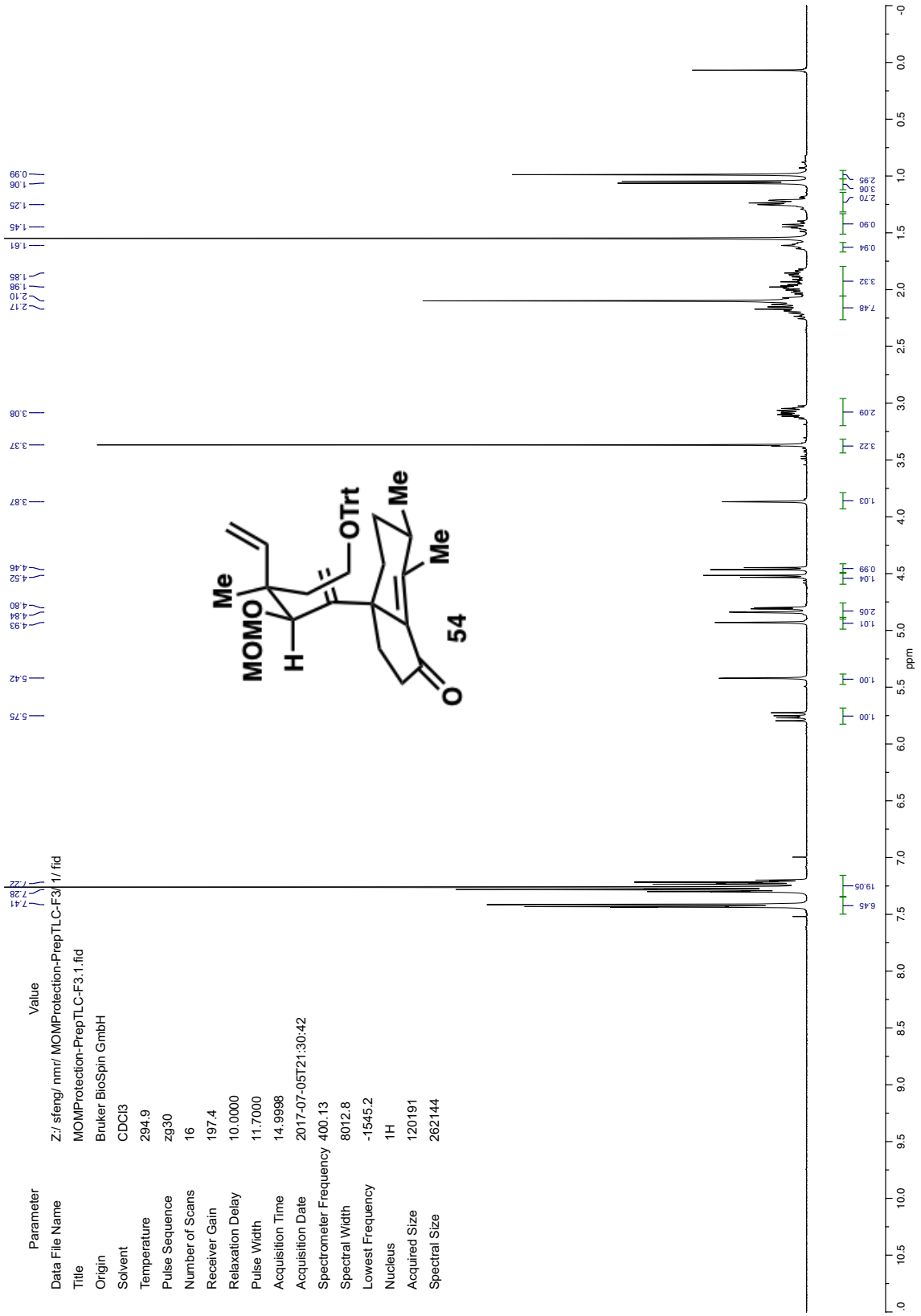

Parameter	Value
Data File Name	Z:/ sfeng/ nmr/ MOMProtection-PrepTLC-F3/ 1/ fid
Title	MOMProtection-PrepTLC-F3.1.fid
Origin	Bruker BioSpin GmbH
Solvent	CDCl3
Temperature	294.9
Pulse Sequence	zg30
Number of Scans	16
Receiver Gain	197.4
Relaxation Delay	10.0000
Pulse Width	11.7000
Acquisition Time	14.9998
Acquisition Date	2017-07-05T21:30:42
Spectrometer Frequency	400.13
Spectral Width	8012.8
Lowest Frequency	-1545.2
Nucleus	1H
Acquired Size	120191
Spectral Size	262144

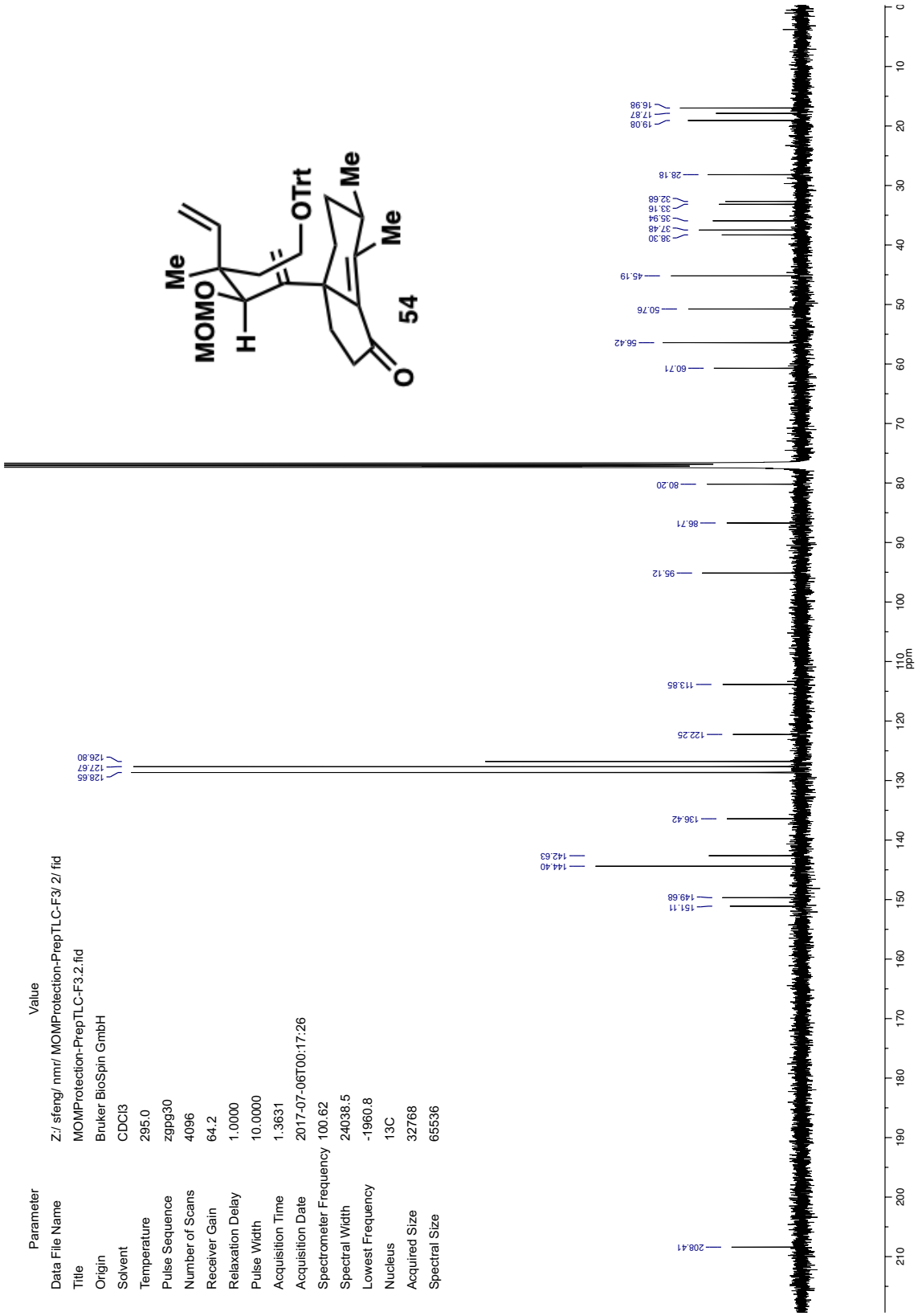

Parameter	Value
Data File Name	Z:/ sfeng/ nmr/ MOMProtection-PrepTLC-F3/ 2/ fid
Title	MOMProtection-PrepTLC-F3.2.fid
Origin	Bruker BioSpin GmbH
Solvent	CDCl3
Temperature	295.0
Pulse Sequence	zgpg30
Number of Scans	4096
Receiver Gain	64.2
Relaxation Delay	1.0000
Pulse Width	10.0000
Acquisition Time	1.3631
Acquisition Date	2017-07-06T00:17:26
Spectrometer Frequency	100.62
Spectral Width	24038.5
Lowest Frequency	-1960.8
Nucleus	13C
Acquired Size	32768
Spectral Size	65536

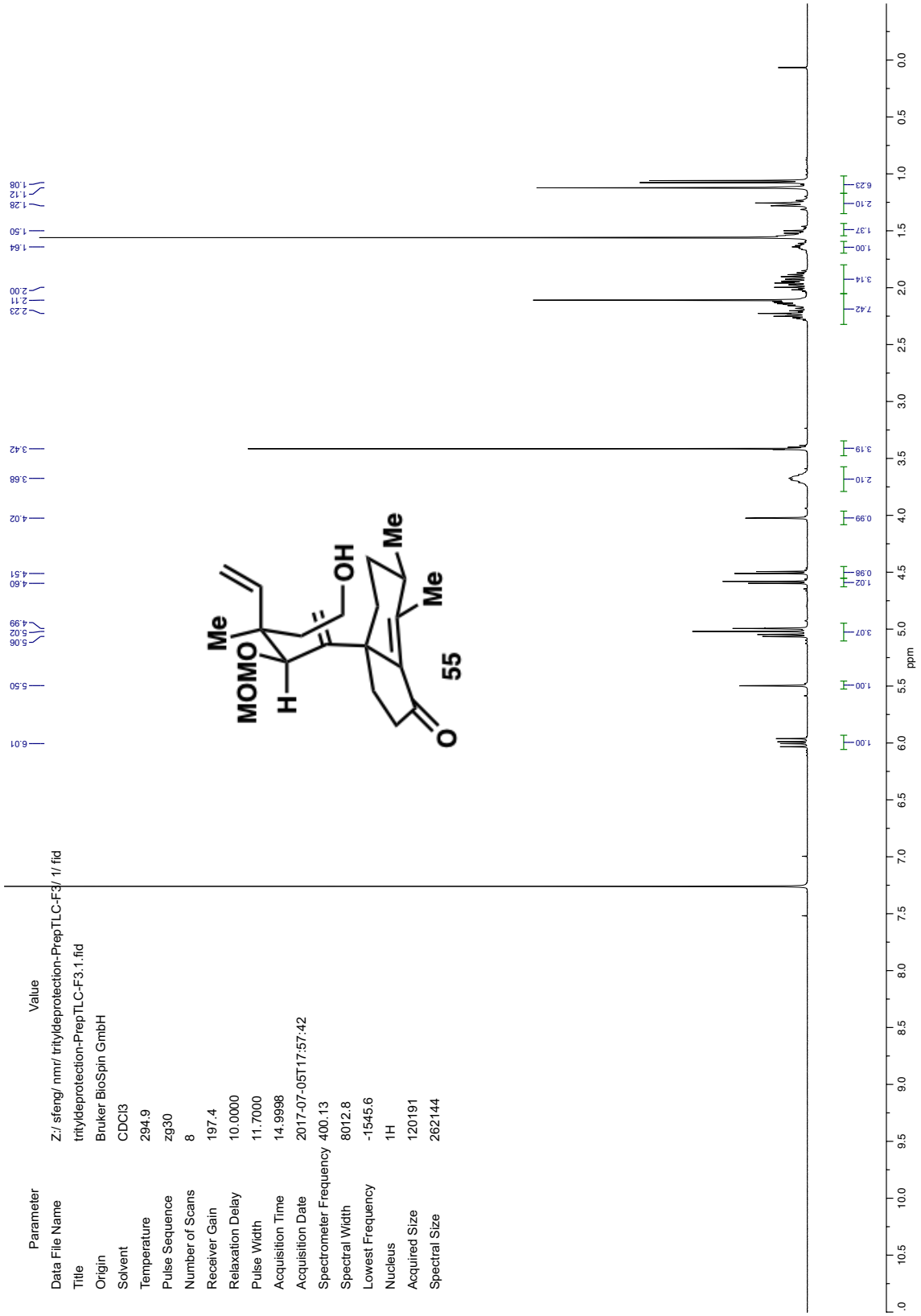
Parameter
Value
Data File Name
Z:/ sfeng/ nmr/ trityldeprotection-PrepTLC-F3/ 1/ fid
Title
trityldeprotection-PrepTLC-F3.1.fid
Origin
Bruker BioSpin GmbH
Solvent
CDCl3
Temperature
294.9
Pulse Sequence
zg30
Number of Scans
8
Receiver Gain
197.4
Relaxation Delay
10.0000
Pulse Width
11.7000
Acquisition Time
14.9998
Acquisition Date
2017-07-05T17:57:42
Spectrometer Frequency
400.13
Spectral Width
8012.8
Lowest Frequency
-1545.6
Nucleus
1H
Acquired Size
120191
Spectral Size
262144
Me
MOMO
H
OH
Me
Me
O
55
ppm

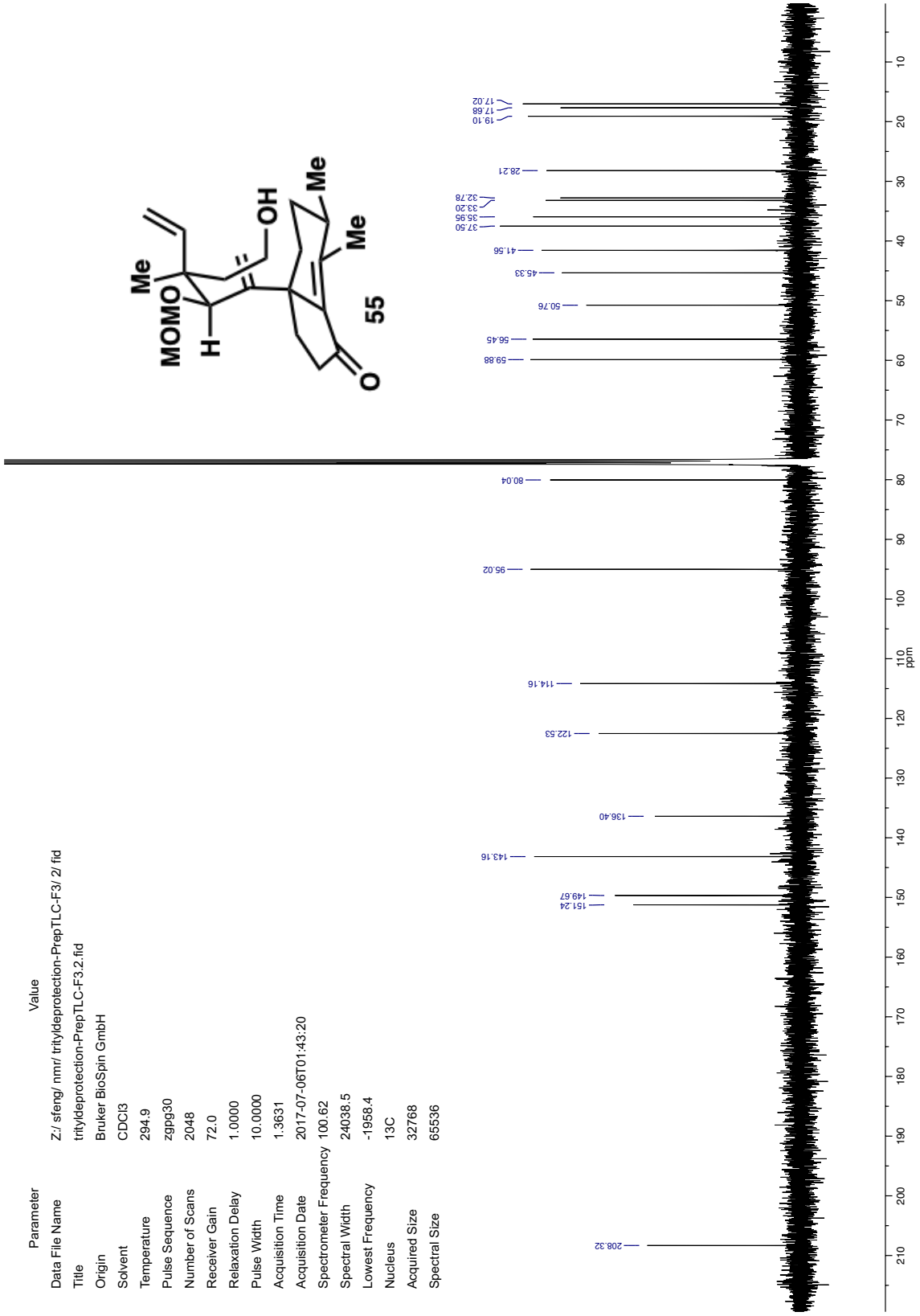

Parameter	Value
Data File Name	Z:/ sfeng/ nmr/ tritydeprotection-PrepTLC-F3/ 2/ fid
Title	tritydeprotection-PrepTLC-F3.2.fid
Origin	Bruker BioSpin GmbH
Solvent	CDCl3
Temperature	294.9
Pulse Sequence	zgpg30
Number of Scans	2048
Receiver Gain	72.0
Relaxation Delay	1.0000
Pulse Width	10.0000
Acquisition Time	1.3631
Acquisition Date	2017-07-06T01:43:20
Spectrometer Frequency	100.62
Spectral Width	24038.5
Lowest Frequency	-1958.4
Nucleus	13C
Acquired Size	32768
Spectral Size	65536

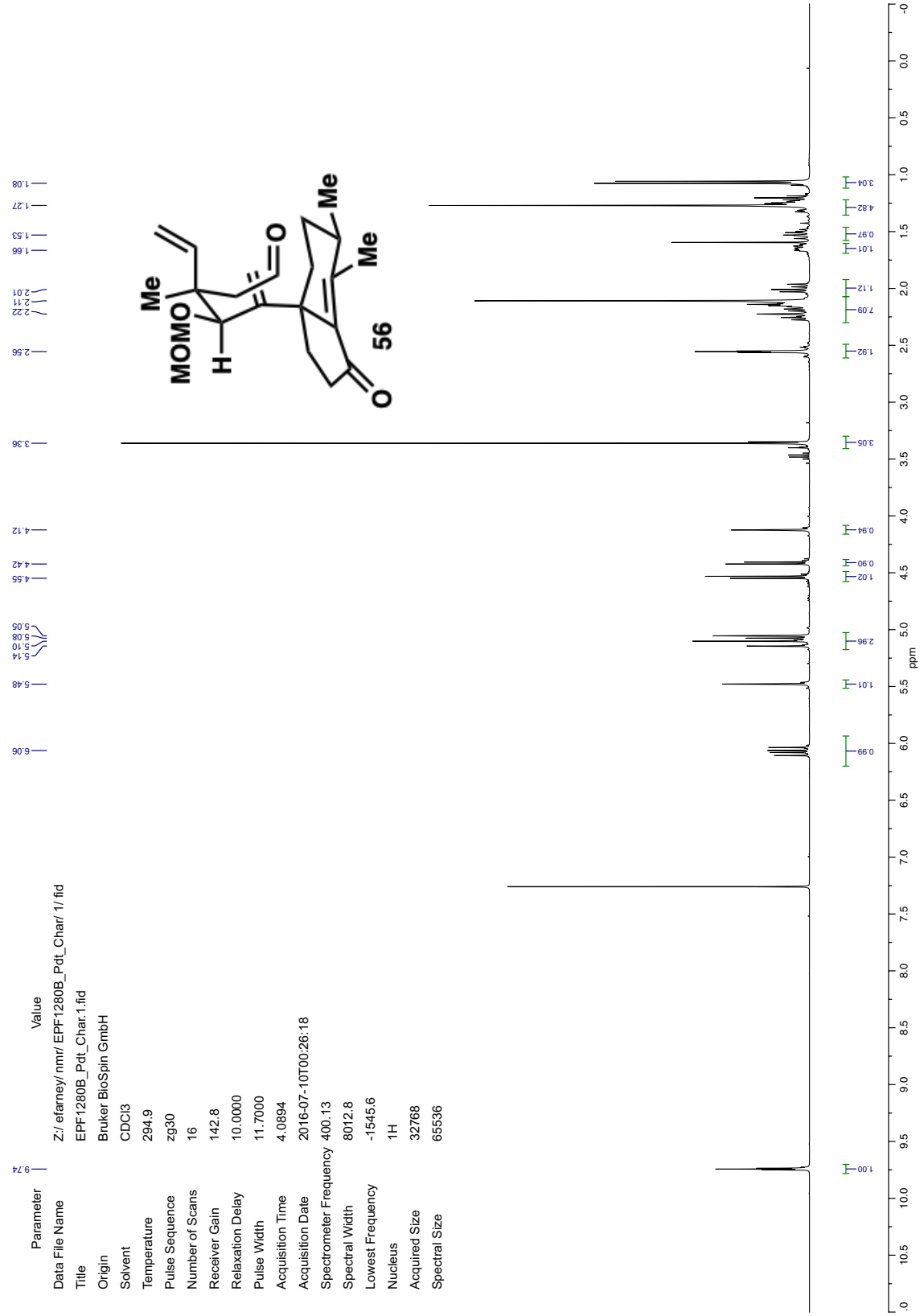

Parameter	Value
Data File Name	Z:/ efarney/ nmr/ EPF1280B_Pdt_Char/ 1/ fid
Title	EPF1280B_Pdt_Char.1.fid
Origin	Bruker BioSpin GmbH
Solvent	CDCl3
Temperature	294.9
Pulse Sequence	zg30
Number of Scans	16
Receiver Gain	142.8
Relaxation Delay	10.0000
Pulse Width	11.7000
Acquisition Time	4.0894
Acquisition Date	2016-07-10T00:26:18
Spectrometer Frequency	400.13
Spectral Width	8012.8
Lowest Frequency	-1545.6
Nucleus	1H
Acquired Size	32768
Spectral Size	65536

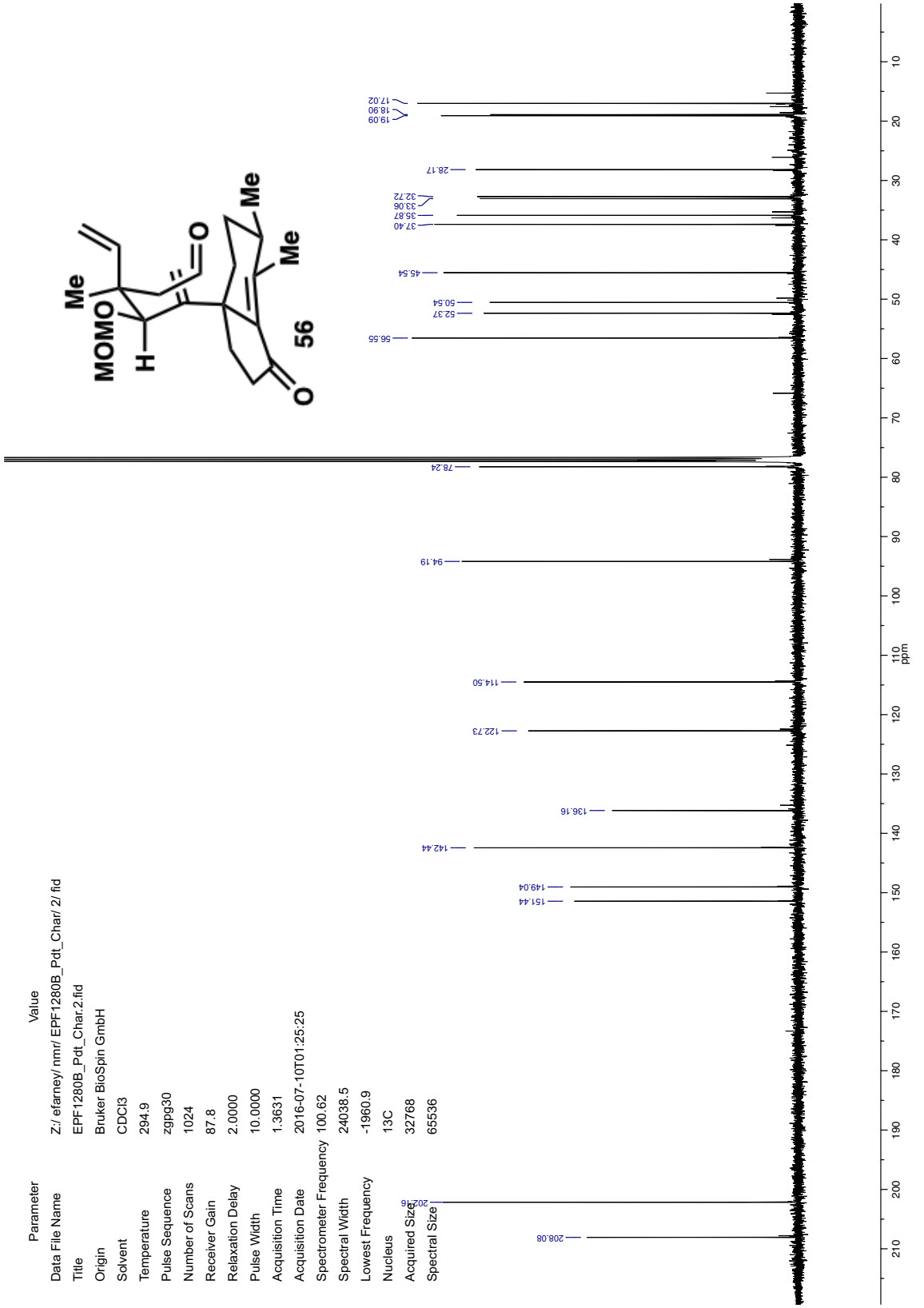

Parameter	Value
Data File Name	Z:/ efarney/ nmr/ EPF1280B_Pdt_Char/ 2/ fid
Title	EPF1280B_Pdt_Char.2.fid
Origin	Bruker BioSpin GmbH
Solvent	CDCl3
Temperature	294.9
Pulse Sequence	zgpg30
Number of Scans	1024
Receiver Gain	87.8
Relaxation Delay	2.0000
Pulse Width	10.0000
Acquisition Time	1.3631
Acquisition Date	2016-07-10T01:25:25
Spectrometer Frequency	100.62
Spectral Width	24038.5
Lowest Frequency	-1960.9
Nucleus	13C
Acquired Size	32768
Spectral Size	65536

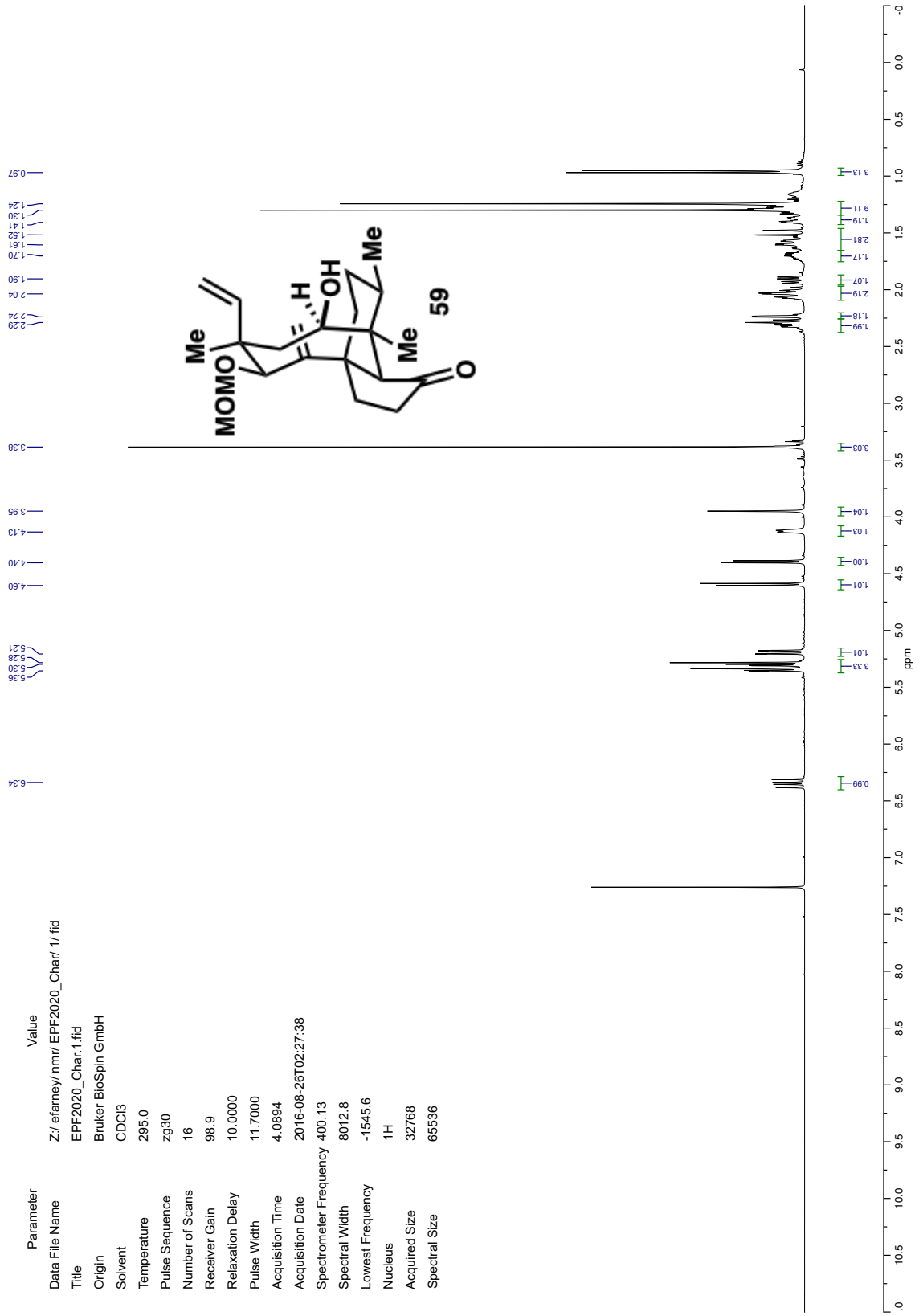

Parameter	Value
Data File Name	Z:/ efarney/ nmr/ EPF2020_Char/ 1/ fid
Title	EPF2020_Char.1.fid
Origin	Bruker BioSpin GmbH
Solvent	CDCl3
Temperature	295.0
Pulse Sequence	zg30
Number of Scans	16
Receiver Gain	98.9
Relaxation Delay	10.0000
Pulse Width	11.7000
Acquisition Time	4.0894
Acquisition Date	2016-08-26T02:27:38
Spectrometer Frequency	400.13
Spectral Width	8012.8
Lowest Frequency	-1545.6
Nucleus	1H
Acquired Size	32768
Spectral Size	65536

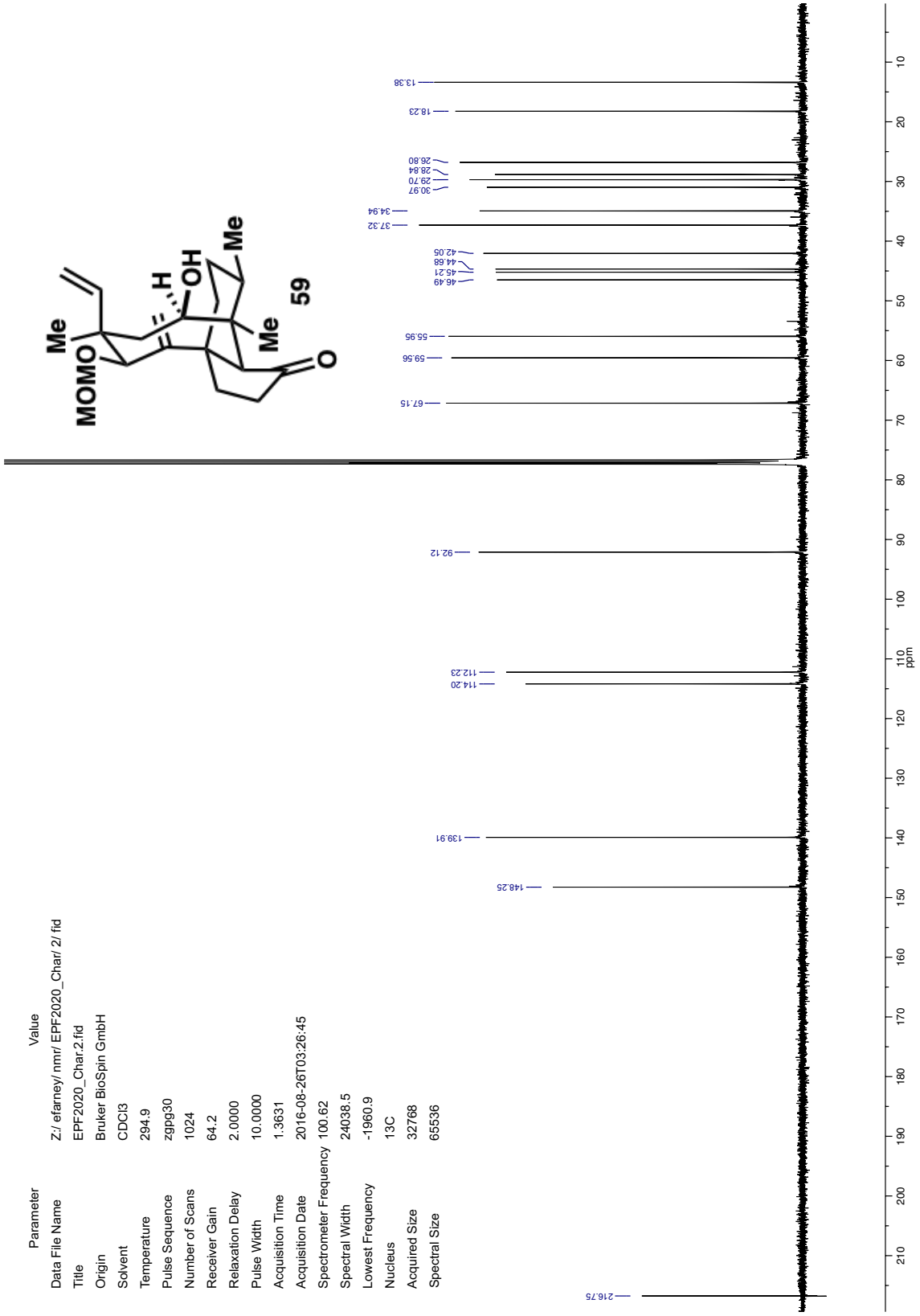

Parameter	Value
Data File Name	Z:/ efarney/ nmr/ EPF2020_Char/ 2/ fid
Title	EPF2020_Char.2.fid
Origin	Bruker BioSpin GmbH
Solvent	CDCl3
Temperature	294.9
Pulse Sequence	zgpg30
Number of Scans	1024
Receiver Gain	64.2
Relaxation Delay	2.0000
Pulse Width	10.0000
Acquisition Time	1.3631
Acquisition Date	2016-08-26T03:26:45
Spectrometer Frequency	100.62
Spectral Width	24038.5
Lowest Frequency	-1960.9
Nucleus	13C
Acquired Size	32768
Spectral Size	65536

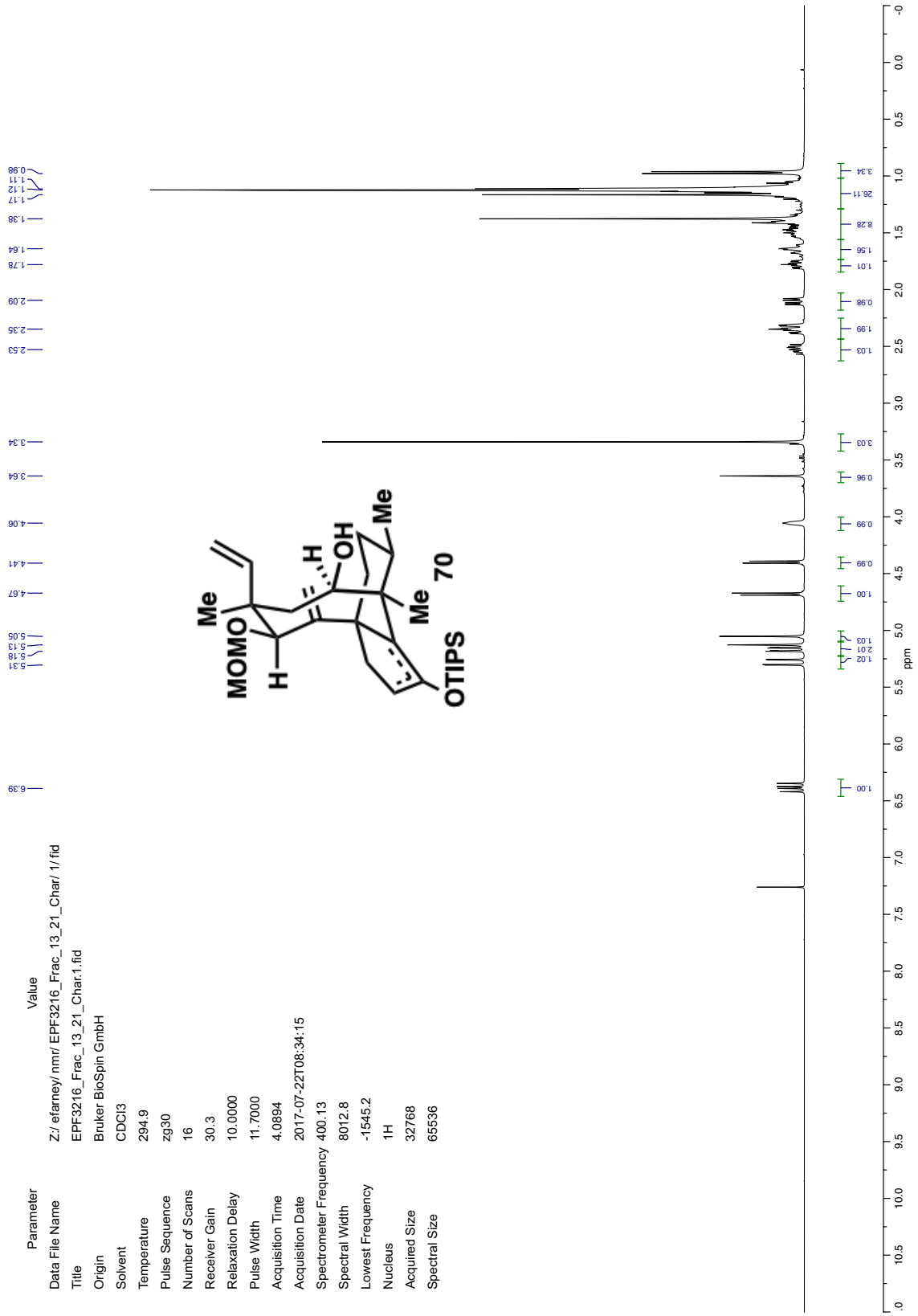
Parameter
Value
Data File Name
Z:/ efarney/ nmr/ EPF3216_Frac_13_21_Char/ 1/ fid
Title
EPF3216_Frac_13_21_Char.1.fid
Origin
Bruker BioSpin GmbH
Solvent
CDCl3
Temperature
294.9
Pulse Sequence
zg30
Number of Scans
16
Receiver Gain
30.3
Relaxation Delay
10.0000
Pulse Width
11.7000
Acquisition Time
4.0894
Acquisition Date
2017-07-22T08:34:15
Spectrometer Frequency
400.13
Spectral Width
8012.8
Lowest Frequency
-1545.2
Nucleus
1H
Acquired Size
32768
Spectral Size
65536
Me
MOMO
H
H
OH
Me
Me
OTIPS
70
ppm

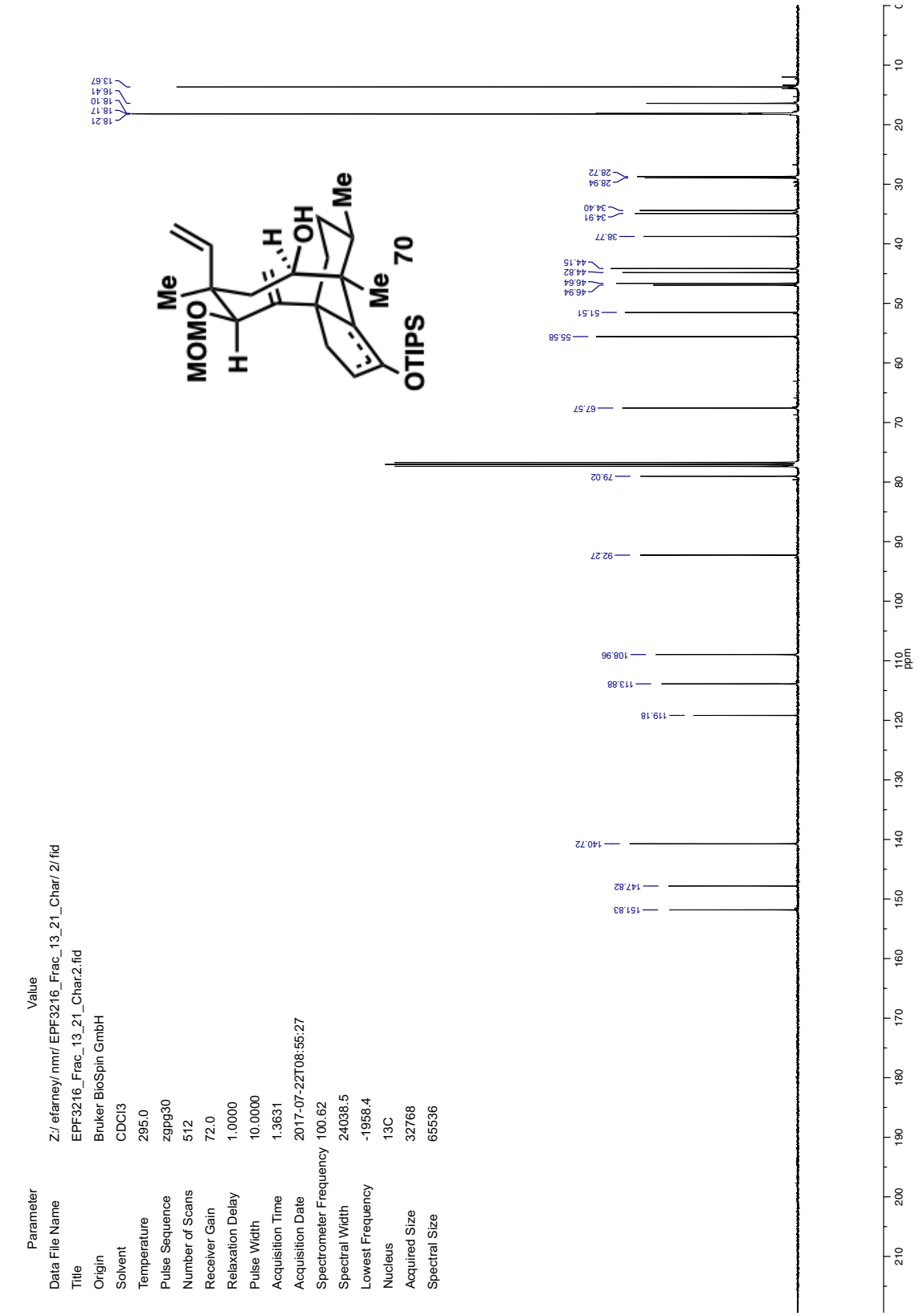

Parameter	Value
Data File Name	Z:/ efarney/ nmr/ EPF3216_Frac_13_21_Char/ 2/ fid
Title	EPF3216_Frac_13_21_Char.2.fid
Origin	Bruker BioSpin GmbH
Solvent	CDCl3
Temperature	295.0
Pulse Sequence	zgpg30
Number of Scans	512
Receiver Gain	72.0
Relaxation Delay	1.0000
Pulse Width	10.0000
Acquisition Time	1.3631
Acquisition Date	2017-07-22T08:55:27
Spectrometer Frequency	100.62
Spectral Width	24038.5
Lowest Frequency	-1958.4
Nucleus	13C
Acquired Size	32768
Spectral Size	65536

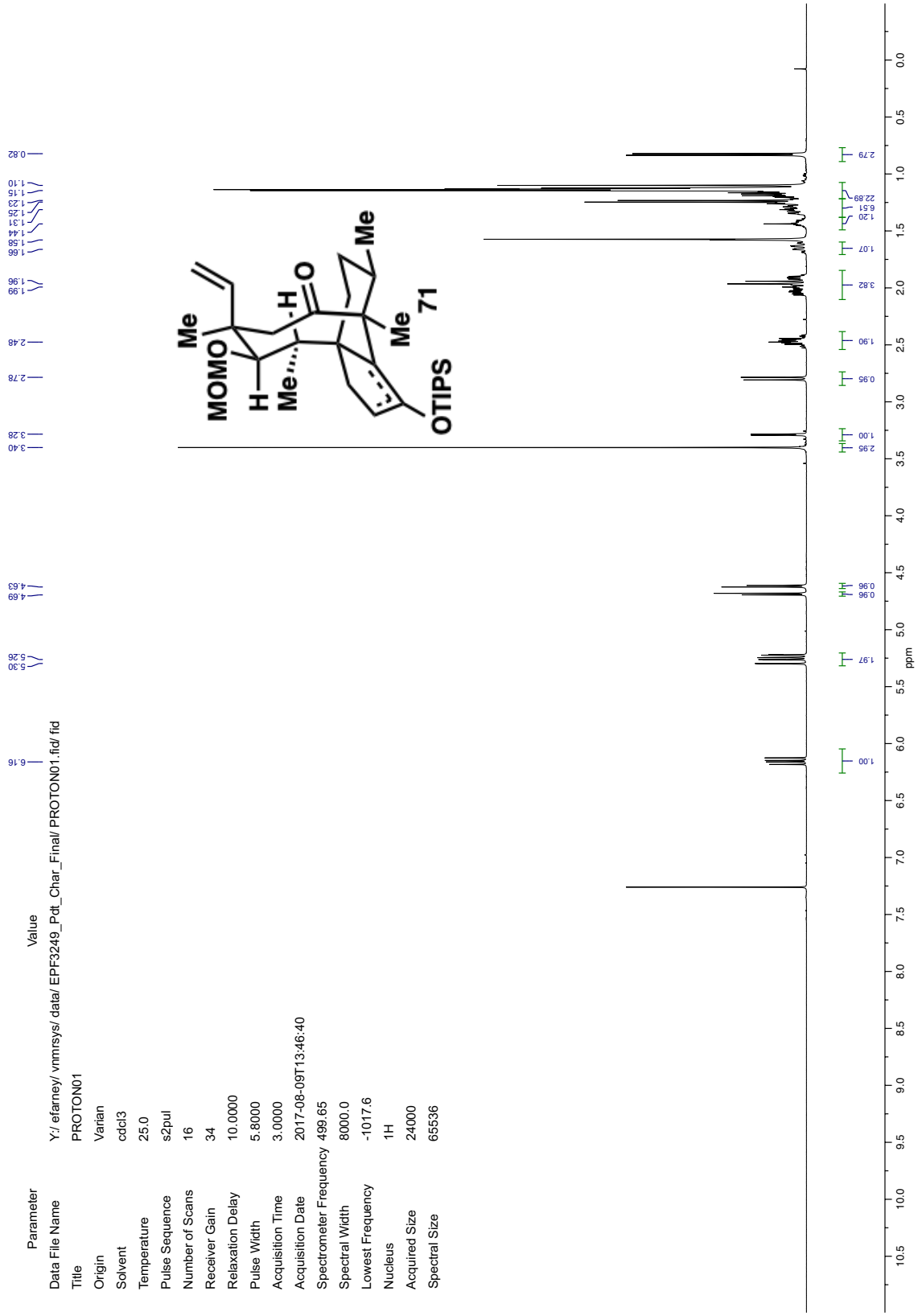

Parameter	Value
Data File Name	Y:/ efarney/ vnmrsys/ data/ EPF3249_Pdt_Char_Final/ PROTON01.fid/ fid
Title	PROTON01
Origin	Varian
Solvent	cdcl3
Temperature	25.0
Pulse Sequence	s2pul
Number of Scans	16
Receiver Gain	34
Relaxation Delay	10.0000
Pulse Width	5.8000
Acquisition Time	3.0000
Acquisition Date	2017-08-09T13:46:40
Spectrometer Frequency	499.65
Spectral Width	8000.0
Lowest Frequency	-1017.6
Nucleus	1H
Acquired Size	24000
Spectral Size	65536

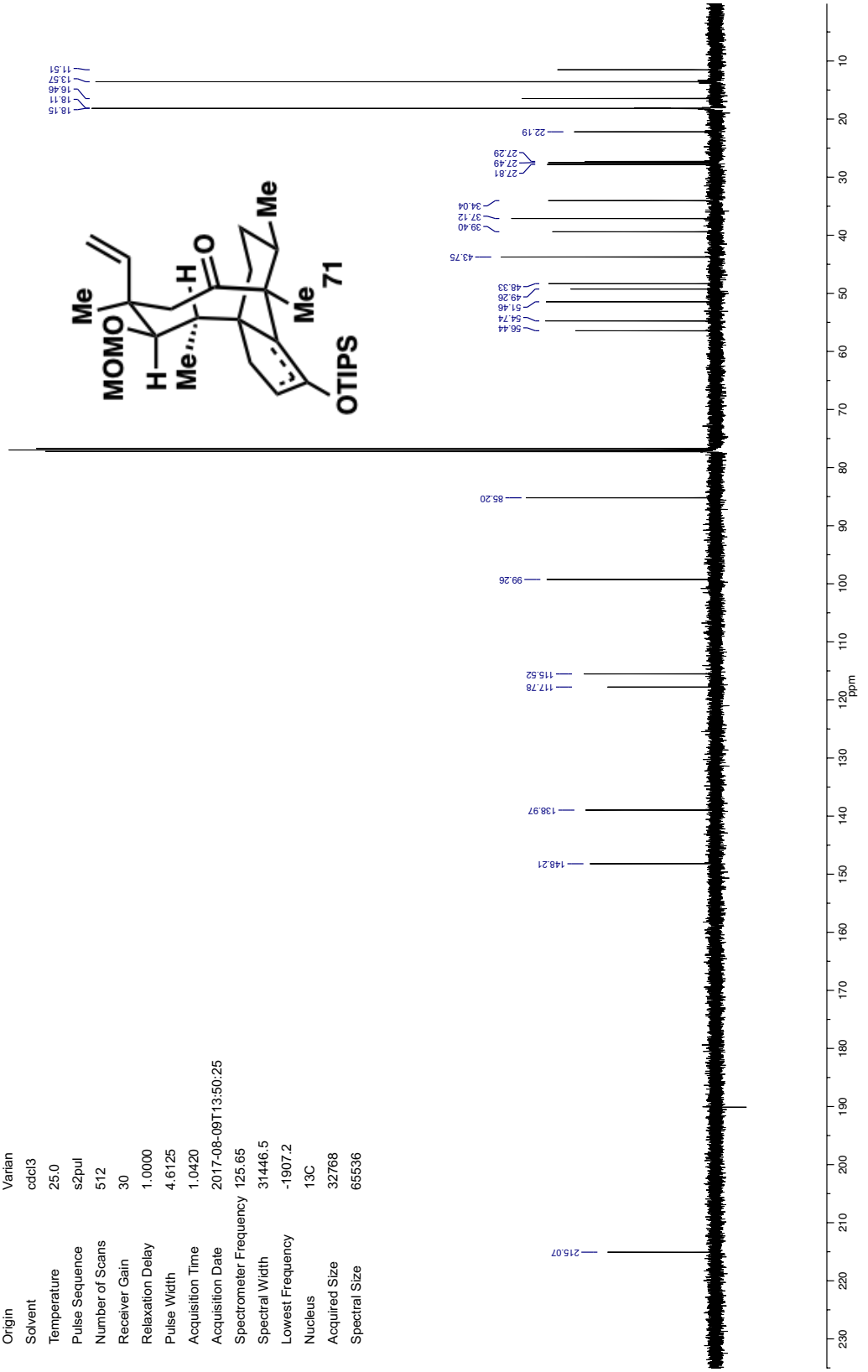

Parameter	Value
Data File Name	Y:/ efarney/ vnmrsys/ data/ EPF3249_Pdt_Char_Final/ CARBON01.fid/ fid
Title	CARBON01
Origin	Varian
Solvent	cdcl3
Temperature	25.0
Pulse Sequence	s2pul
Number of Scans	512
Receiver Gain	30
Relaxation Delay	1.0000
Pulse Width	4.6125
Acquisition Time	1.0420
Acquisition Date	2017-08-09T13:50:25
Spectrometer Frequency	125.65
Spectral Width	31446.5
Lowest Frequency	-1907.2
Nucleus	13C
Acquired Size	32768
Spectral Size	65536

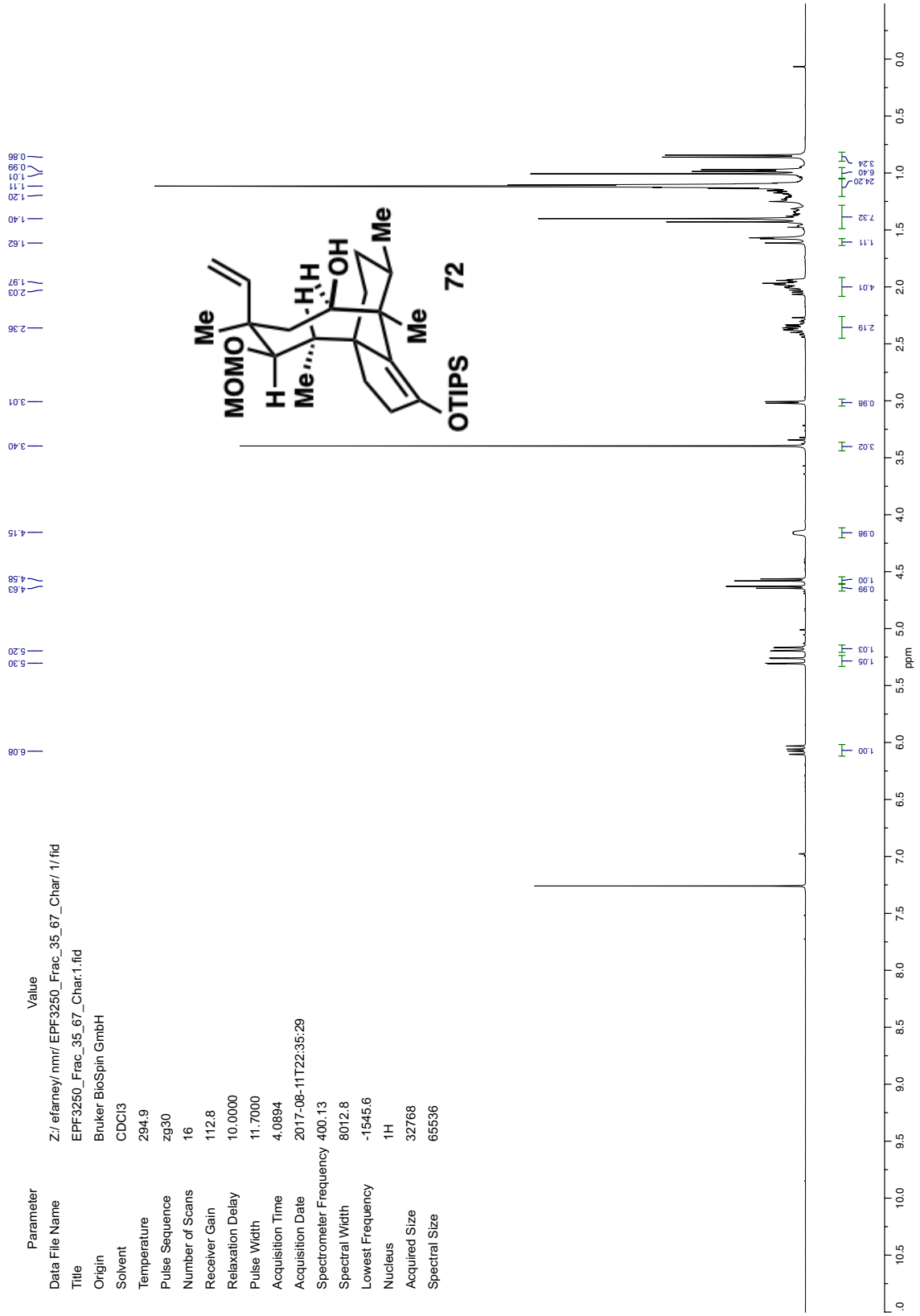
Parameter
Value
Data File Name
Z:/ efarney/ nmr/ EPF3250_Frac_35_67_Char/ 1/ fid
Title
EPF3250_Frac_35_67_Char.1.fid
Origin
Bruker BioSpin GmbH
Solvent
CDCl3
Temperature
294.9
Pulse Sequence
zg30
Number of Scans
16
Receiver Gain
112.8
Relaxation Delay
10.0000
Pulse Width
11.7000
Acquisition Time
4.0894
Acquisition Date
2017-08-11T22:35:29
Spectrometer Frequency
400.13
Spectral Width
8012.8
Lowest Frequency
-1545.6
Nucleus
1H
Acquired Size
32768
Spectral Size
65536
Me
MOMO
H
Me
H
OH
Me
Me
OTIPS
72
ppm

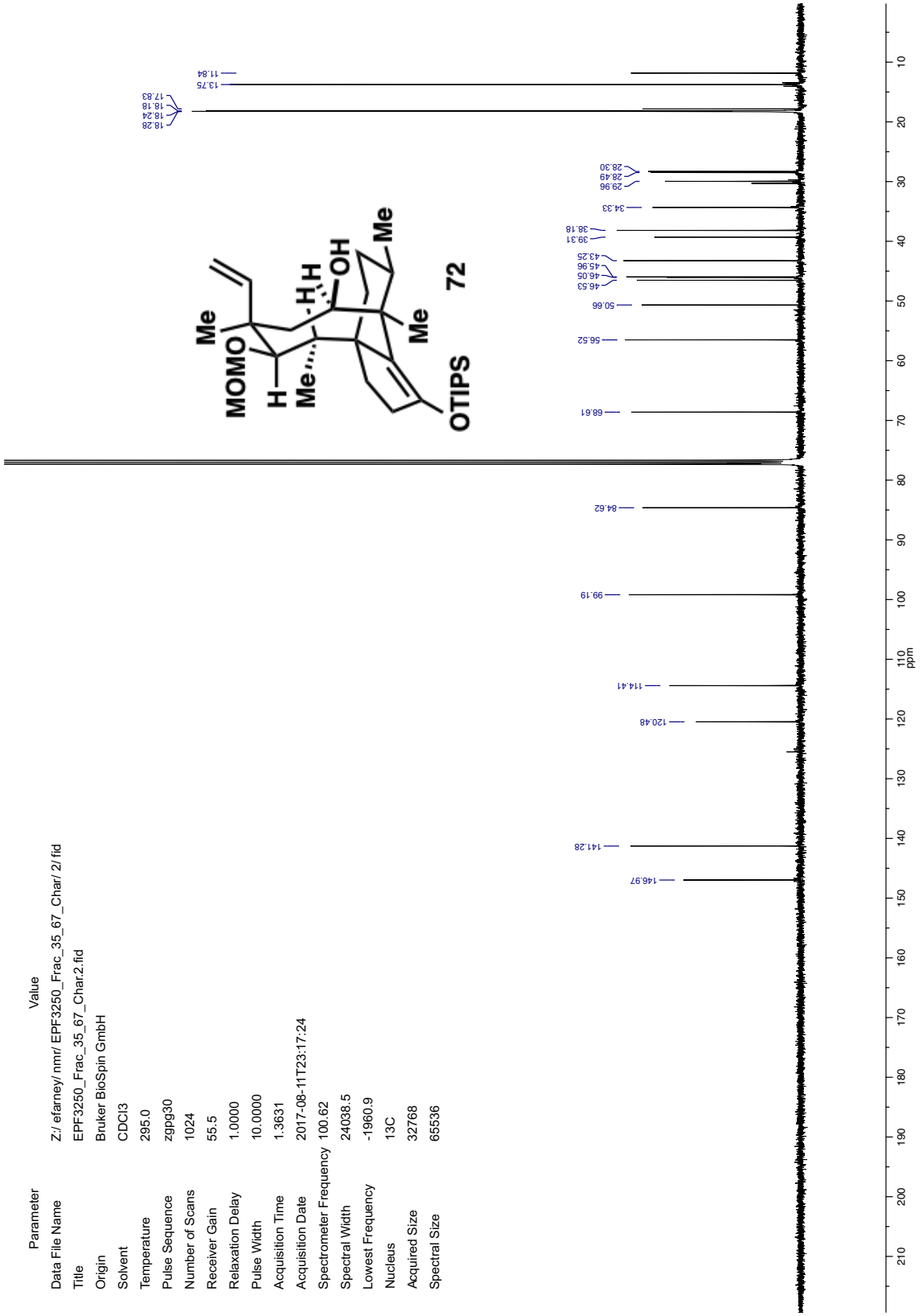

Parameter	Value
Data File Name	Z:/ efarney/ nmr/ EPF3250_Frac_35_67_Char/ 2/ fid
Title	EPF3250_Frac_35_67_Char.2.fid
Origin	Bruker BioSpin GmbH
Solvent	CDCl3
Temperature	295.0
Pulse Sequence	zgpg30
Number of Scans	1024
Receiver Gain	55.5
Relaxation Delay	1.0000
Pulse Width	10.0000
Acquisition Time	1.3631
Acquisition Date	2017-08-11T23:17:24
Spectrometer Frequency	100.62
Spectral Width	24038.5
Lowest Frequency	-1960.9
Nucleus	13C
Acquired Size	32768
Spectral Size	65536

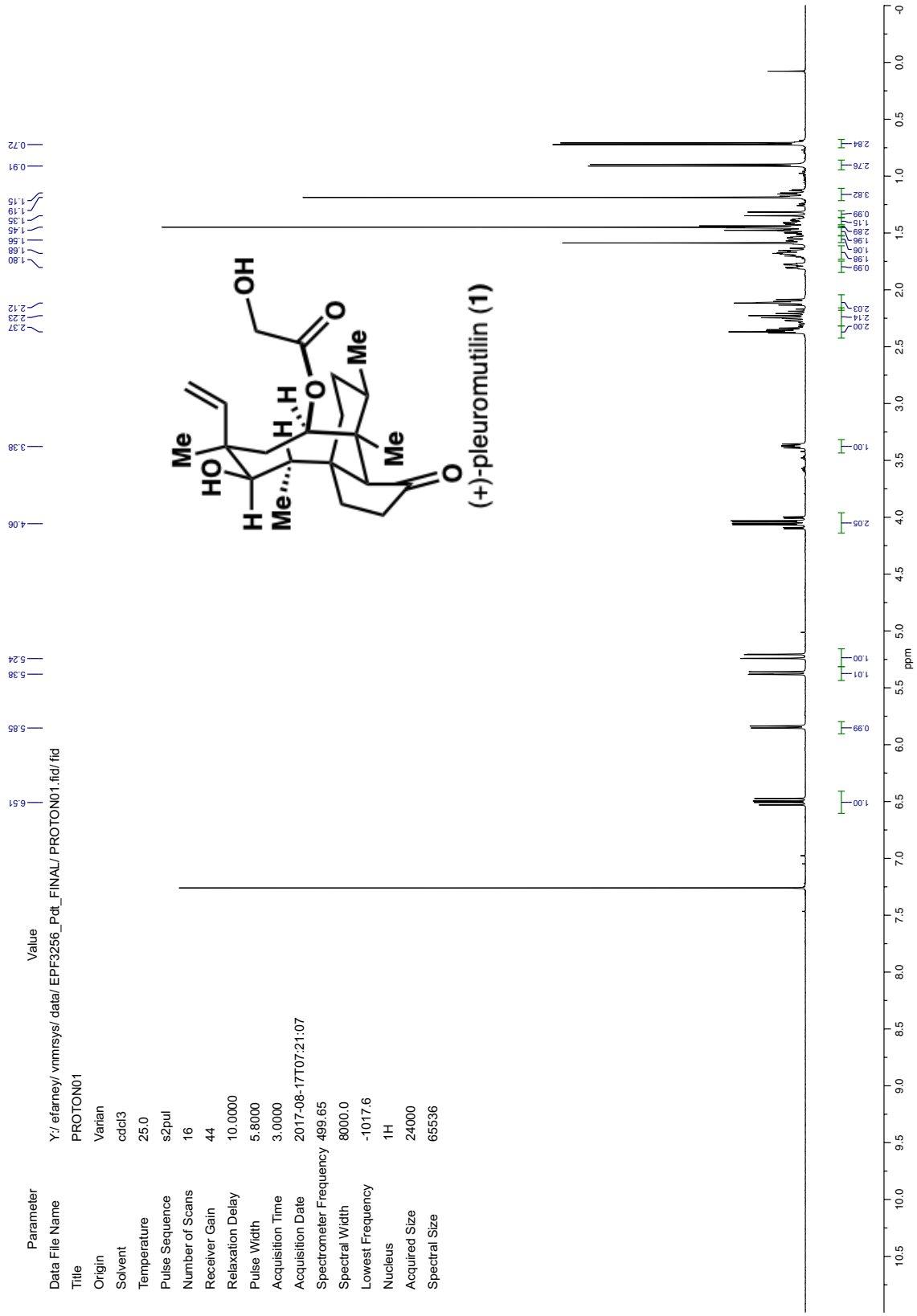
Parameter
Value
Data File Name
Y:/ efarney/ vnmrsys/ data/ EPF3256_Pdt_FINAL/ PROTON01.fid/ fid
Title
PROTON01
Origin
Varian
Solvent
cdcl3
Temperature
25.0
Pulse Sequence
s2pul
Number of Scans
16
Receiver Gain
44
Relaxation Delay
10.0000
Pulse Width
5.8000
Acquisition Time
3.0000
Acquisition Date
2017-08-17T07:21:07
Spectrometer Frequency
499.65
Spectral Width
8000.0
Lowest Frequency
-1017.6
Nucleus
1H
Acquired Size
24000
Spectral Size
65536
(+)-pleuromutilin (1)
ppm

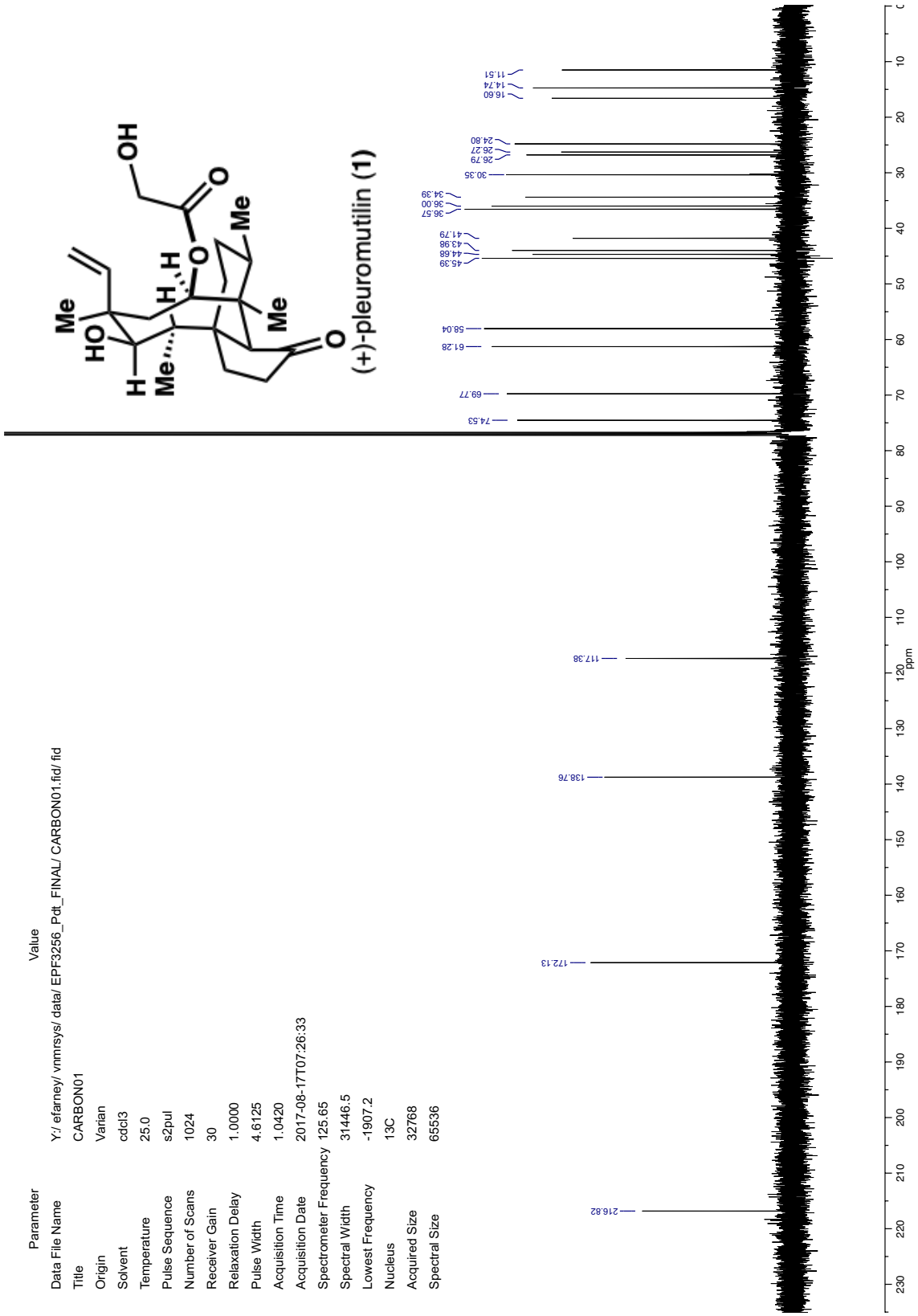

Parameter	Value
Data File Name	Y:/ efarney/ vnmrsys/ data/ EPF3256_Pdt_FINAL/ CARBON01.fid/ fid
Title	CARBON01
Origin	Varian
Solvent	cdcl3
Temperature	25.0
Pulse Sequence	s2pul
Number of Scans	1024
Receiver Gain	30
Relaxation Delay	1.0000
Pulse Width	4.6125
Acquisition Time	1.0420
Acquisition Date	2017-08-17T07:26:33
Spectrometer Frequency	125.65
Spectral Width	31446.5
Lowest Frequency	-1907.2
Nucleus	13C
Acquired Size	32768
Spectral Size	65536

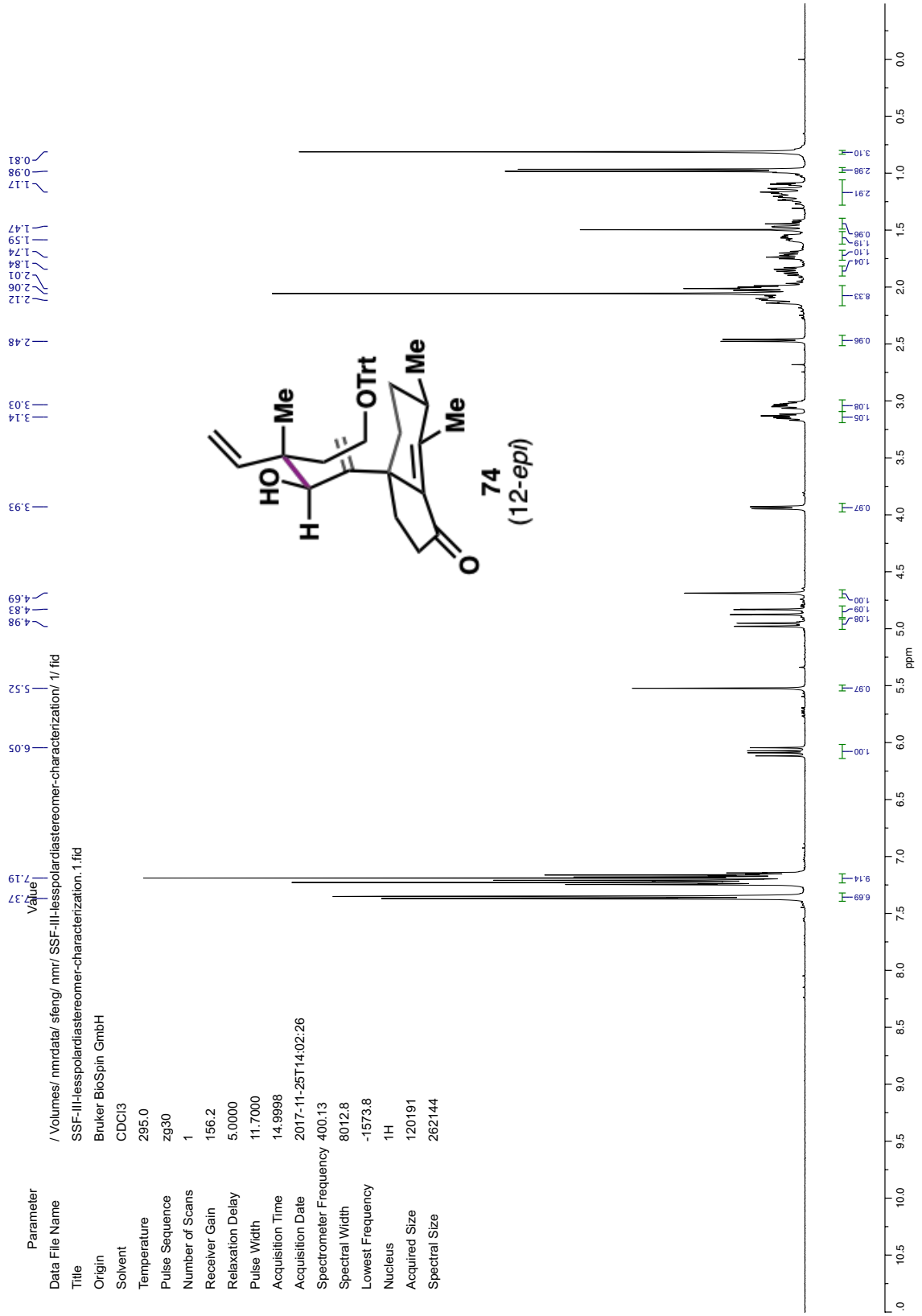
Parameter
Value
Data File Name / Volumes/ nmrdata/ sfeng/ nmr/ SSF-III-lesspolardiastereomer-characterization/ 1/ fid
Title SSF-III-lesspolardiastereomer-characterization.1.fid
Origin Bruker BioSpin GmbH
Solvent CDCl3
Temperature 295.0
Pulse Sequence zg30
Number of Scans 1
Receiver Gain 156.2
Relaxation Delay 5.0000
Pulse Width 11.7000
Acquisition Time 14.9998
Acquisition Date 2017-11-25T14:02:26
Spectrometer Frequency 400.13
Spectral Width 8012.8
Lowest Frequency -1573.8
Nucleus 1H
Acquired Size 120191
Spectral Size 262144
HO
Me
OTrt
Me
Me
H
O
74
(12-epi)
ppm

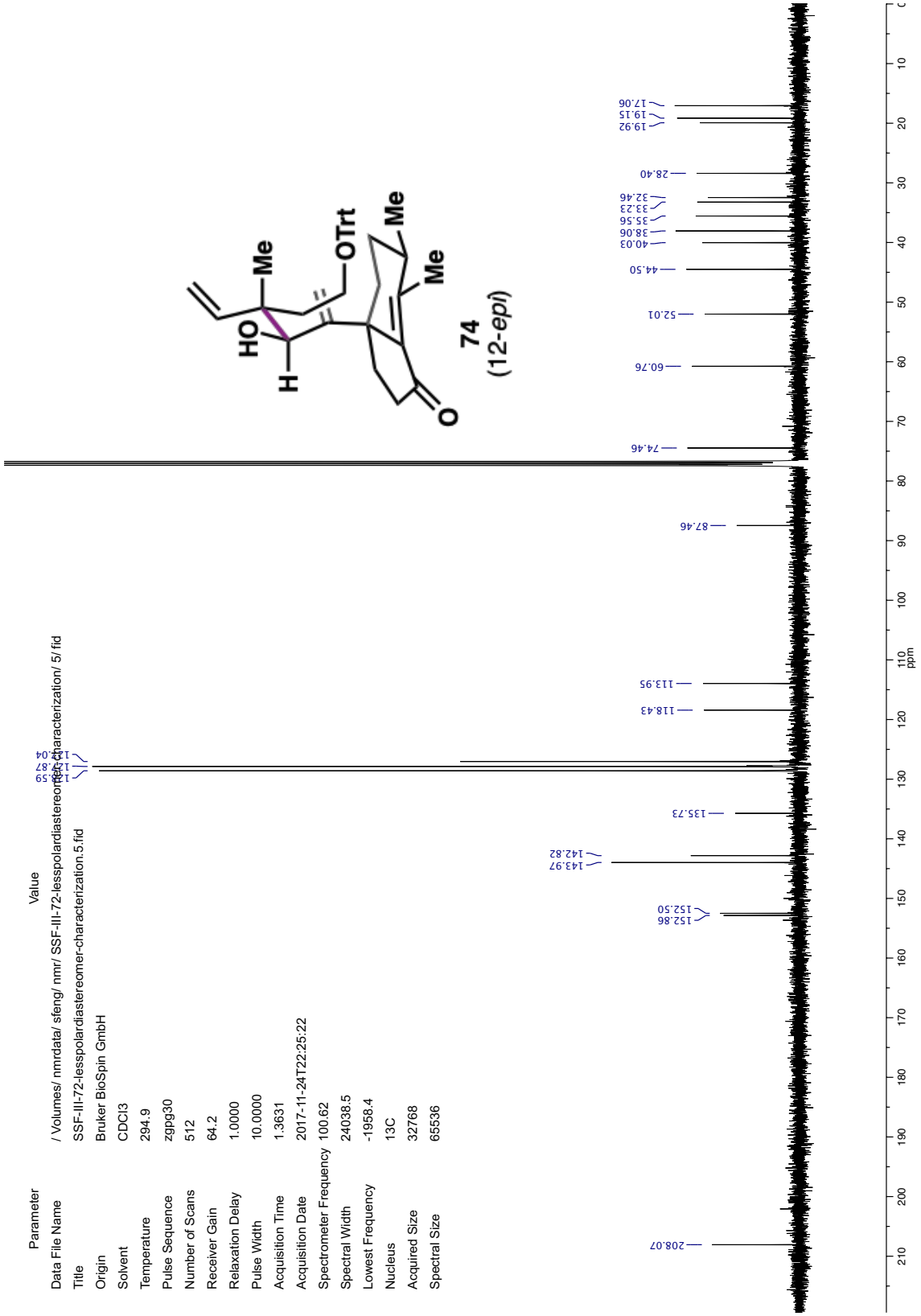
Parameter
Value
Data File Name / Volumes/ nmrdata/ sfeng/ nmr/ SSF-III-72-lesspolardiastereomer-characterization/ 5/ fid
Title SSF-III-72-lesspolardiastereomer-characterization.5.fid
Origin Bruker BioSpin GmbH
Solvent CDCl3
Temperature 294.9
Pulse Sequence zgpg30
Number of Scans 512
Receiver Gain 64.2
Relaxation Delay 1.0000
Pulse Width 10.0000
Acquisition Time 1.3631
Acquisition Date 2017-11-24T22:25:22
Spectrometer Frequency 100.62
Spectral Width 24038.5
Lowest Frequency -1958.4
Nucleus 13C
Acquired Size 32768
Spectral Size 65536
HO
Me
H
OTrt
Me
Me
O
74
(12-epi)
208.07
152.86
152.50
143.97
142.82
135.73
118.43
113.95
87.46
74.46
60.76
52.01
44.50
40.03
38.06
35.56
33.23
32.46
28.40
19.92
19.15
17.06
ppm

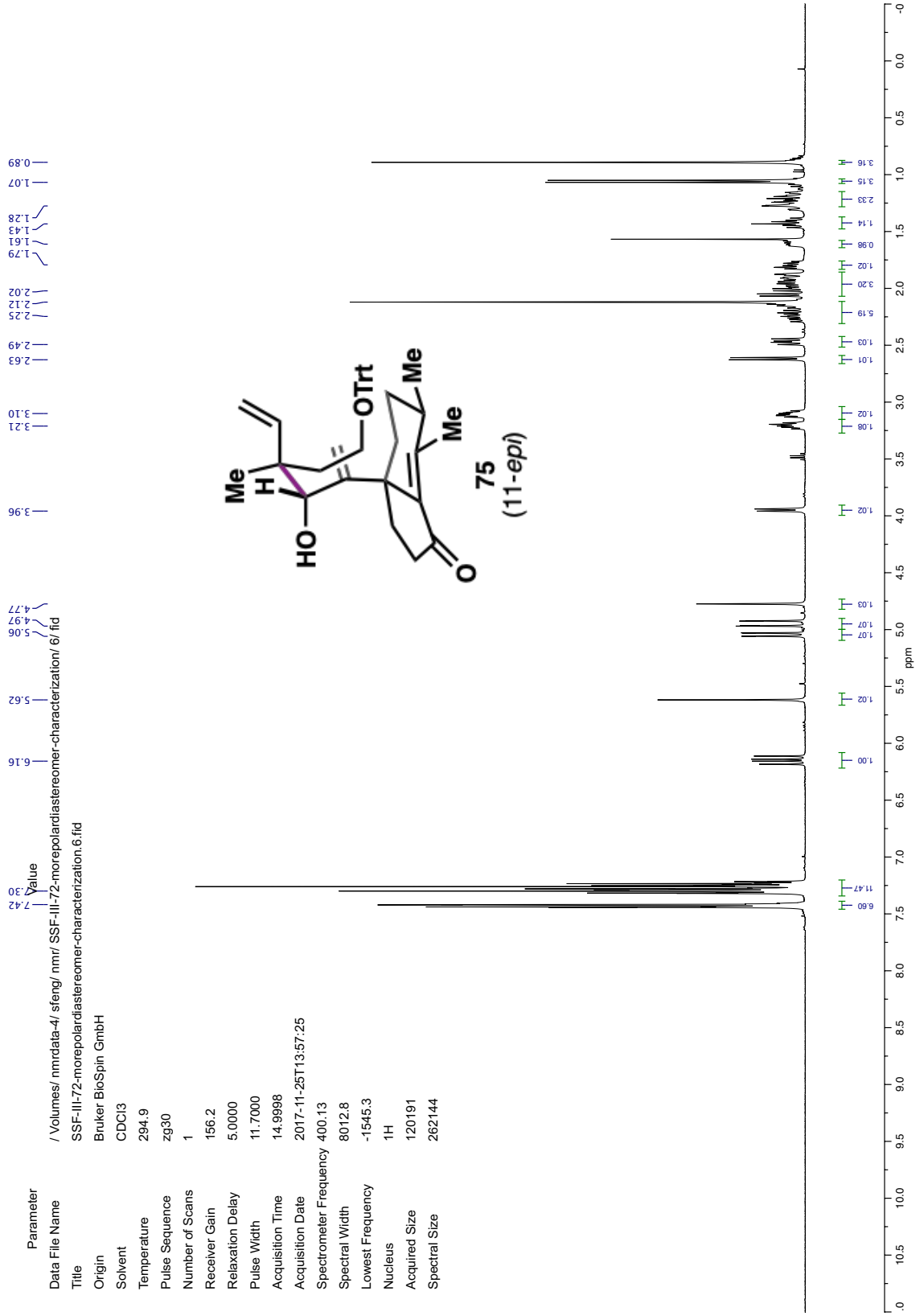
Parameter Value
Data File Name / Volumes/ nmrdata-4/ sfeng/ nmr/ SSF-III-72-morepolardiastereomer-characterization/ 6/ fid
Title SSF-III-72-morepolardiastereomer-characterization.6.fid
Origin Bruker BioSpin GmbH
Solvent CDCl3
Temperature 294.9
Pulse Sequence zg30
Number of Scans 1
Receiver Gain 156.2
Relaxation Delay 5.0000
Pulse Width 11.7000
Acquisition Time 14.9998
Acquisition Date 2017-11-25T13:57:25
Spectrometer Frequency 400.13
Spectral Width 8012.8
Lowest Frequency -1545.3
Nucleus 1H
Acquired Size 120191
Spectral Size 262144
Me
H
HO
OTrt
Me
Me
O
75
(11-epi)
ppm

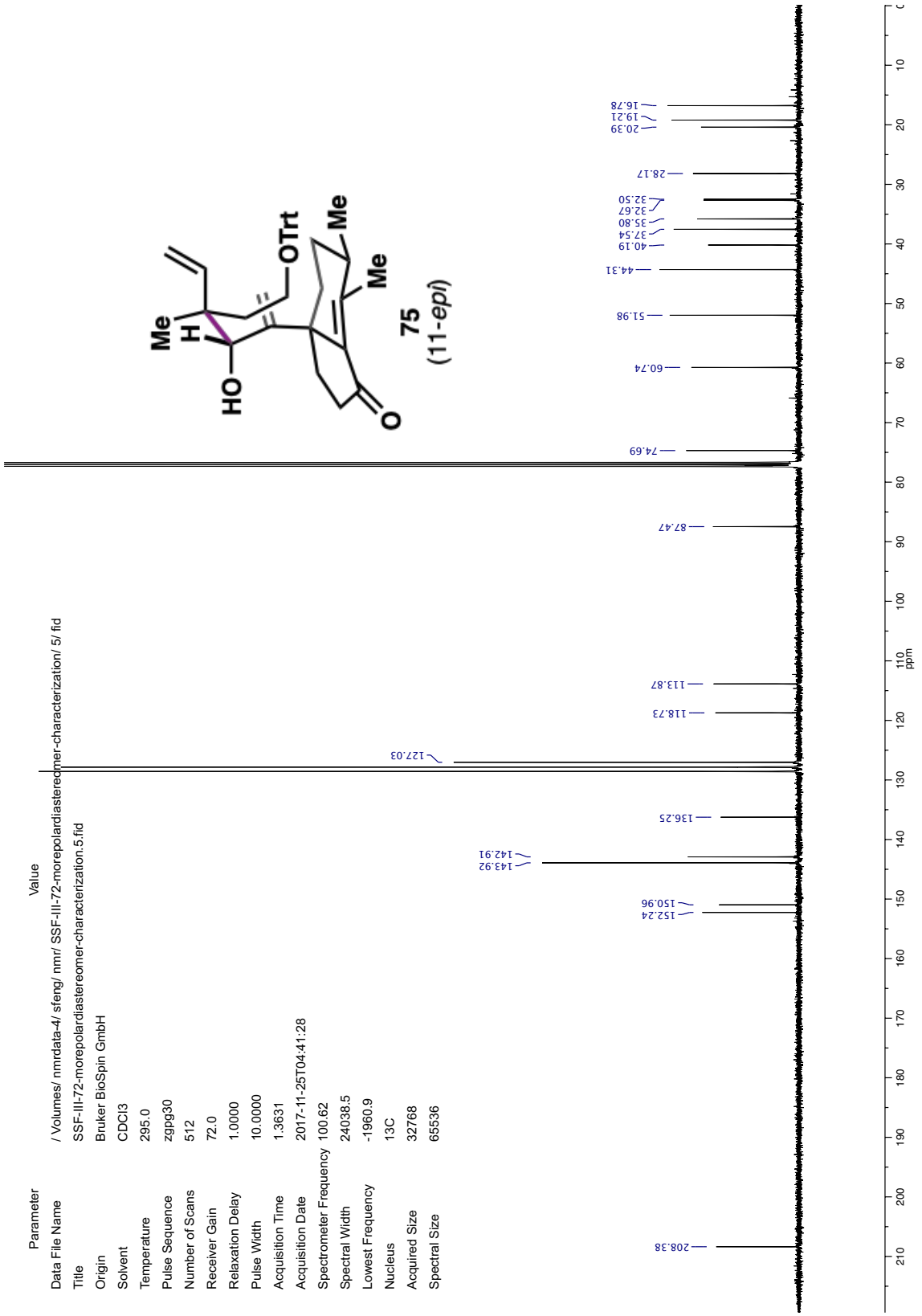
Me
H
HO
OTrt
Me
Me
O
75
(11-epi)
Parameter Value
Data File Name / Volumes/ nmrdata-4/ sfeng/ nmr/ SSF-III-72-morepolardiastereomer-characterization/ 5/ fid
Title SSF-III-72-morepolardiastereomer-characterization.5.fid
Origin Bruker BioSpin GmbH
Solvent CDCl3
Temperature 295.0
Pulse Sequence zgpg30
Number of Scans 512
Receiver Gain 72.0
Relaxation Delay 1.0000
Pulse Width 10.0000
Acquisition Time 1.3631
Acquisition Date 2017-11-25T04:41:28
Spectrometer Frequency 100.62
Spectral Width 24038.5
Lowest Frequency -1960.9
Nucleus 13C
Acquired Size 32768
Spectral Size 65536
208.38
152.24
150.96
143.92
142.91
136.25
127.03
118.73
113.87
87.47
74.69
60.74
51.98
44.31
40.19
37.54
35.80
32.67
32.50
28.17
20.39
19.21
16.78
ppm

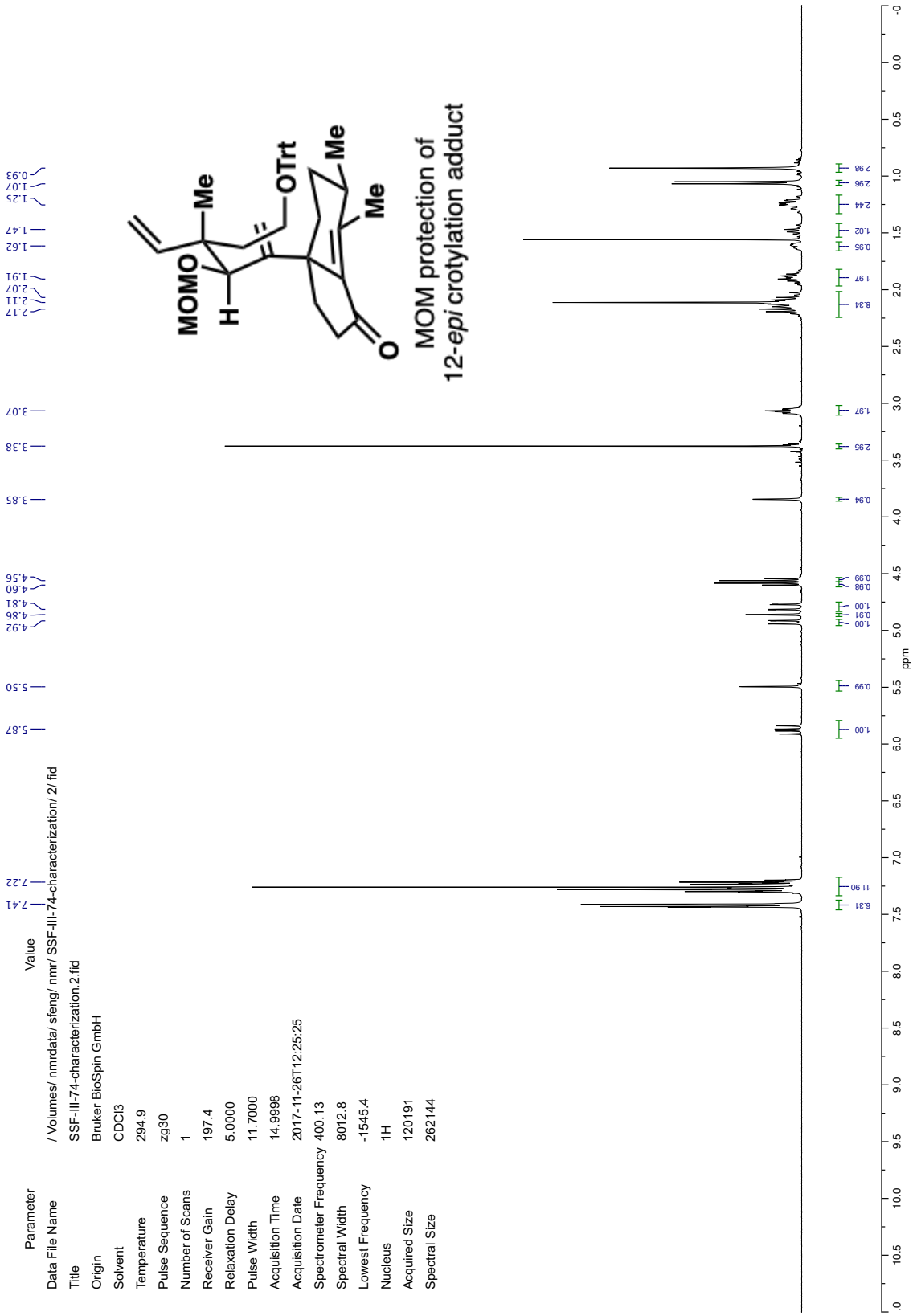
MOM protection of
12-*epi* crotylation adduct
MOMO
Me
H
OTrt
Me
Me
O
Parameter
Value
Data File Name / Volumes/ nmrdata/ sfeng/ nmr/ SSF-III-74-characterization/ 2/ fid
Title SSF-III-74-characterization.2.fid
Origin Bruker BioSpin GmbH
Solvent CDCl3
Temperature 294.9
Pulse Sequence zg30
Number of Scans 1
Receiver Gain 197.4
Relaxation Delay 5.0000
Pulse Width 11.7000
Acquisition Time 14.9998
Acquisition Date 2017-11-26T12:25:25
Spectrometer Frequency 400.13
Spectral Width 8012.8
Lowest Frequency -1545.4
Nucleus 1H
Acquired Size 120191
Spectral Size 262144
7.41
7.22
5.87
5.50
4.92
4.86
4.81
4.60
4.56
3.85
3.38
3.07
2.17
2.11
2.07
1.91
1.62
1.47
1.25
1.07
0.93
6.31
11.90
1.00
0.99
1.00
0.91
1.00
0.98
0.99
0.94
2.95
1.97
8.34
1.97
0.95
1.02
2.44
2.96
2.98
ppm

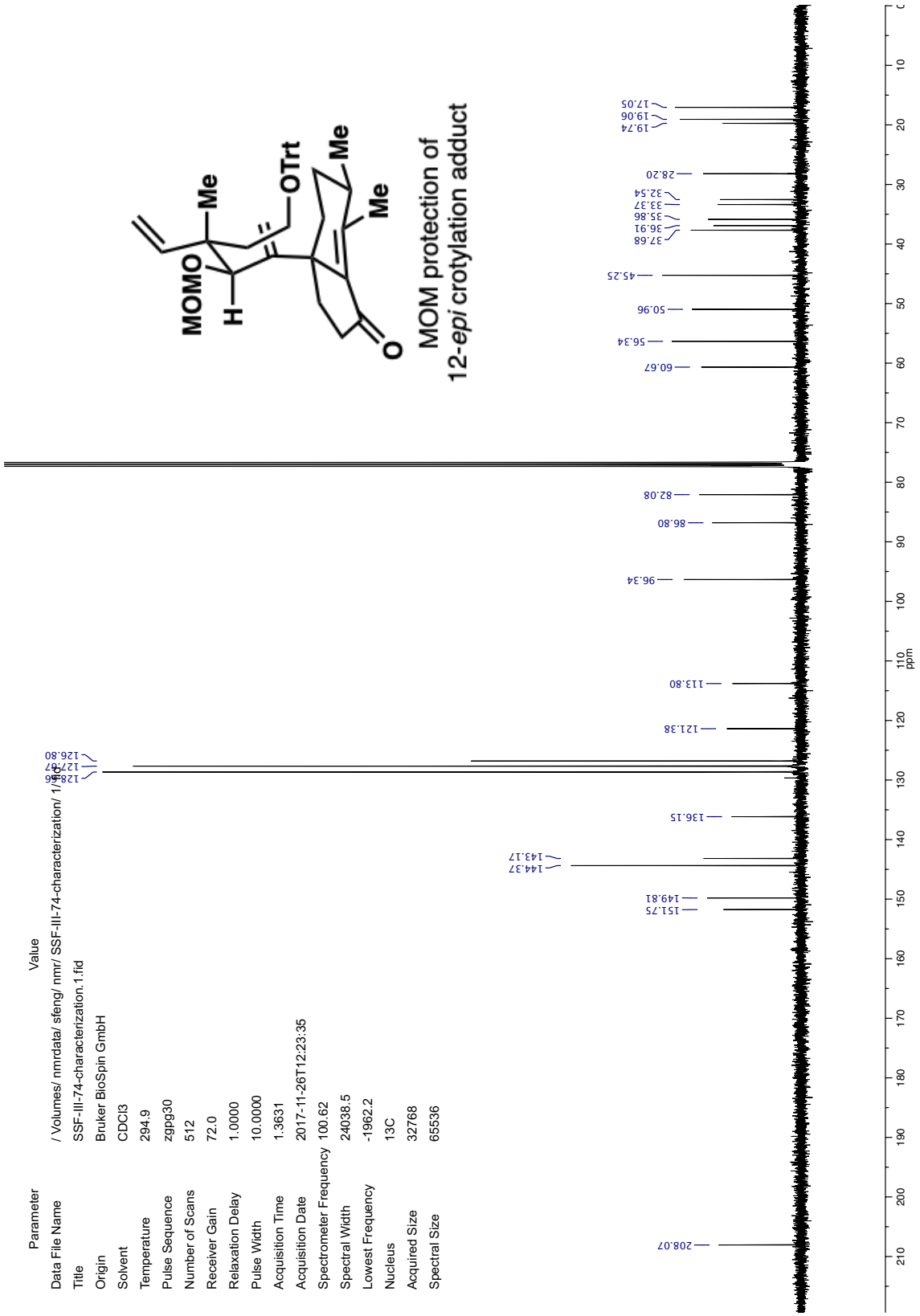
MOM protection of
12-epi crotylation adduct
MOMO
Me
H
OTrt
Me
Me
O
Parameter
Value
Data File Name / Volumes/ nmrdata/ sfeng/ nmr/ SSF-III-74-characterization/ 1/fid
Title SSF-III-74-characterization.1.fid
Origin Bruker BioSpin GmbH
Solvent CDCl3
Temperature 294.9
Pulse Sequence zgpg30
Number of Scans 512
Receiver Gain 72.0
Relaxation Delay 1.0000
Pulse Width 10.0000
Acquisition Time 1.3631
Acquisition Date 2017-11-26T12:23:35
Spectrometer Frequency 100.62
Spectral Width 24038.5
Lowest Frequency -1962.2
Nucleus 13C
Acquired Size 32768
Spectral Size 65536
208.07
151.75
149.81
144.37
143.17
136.15
128.56
127.87
126.80
121.38
113.80
96.34
86.80
82.08
60.67
56.34
50.96
45.25
37.68
36.91
35.86
33.37
32.54
28.20
19.74
19.06
17.05
ppm

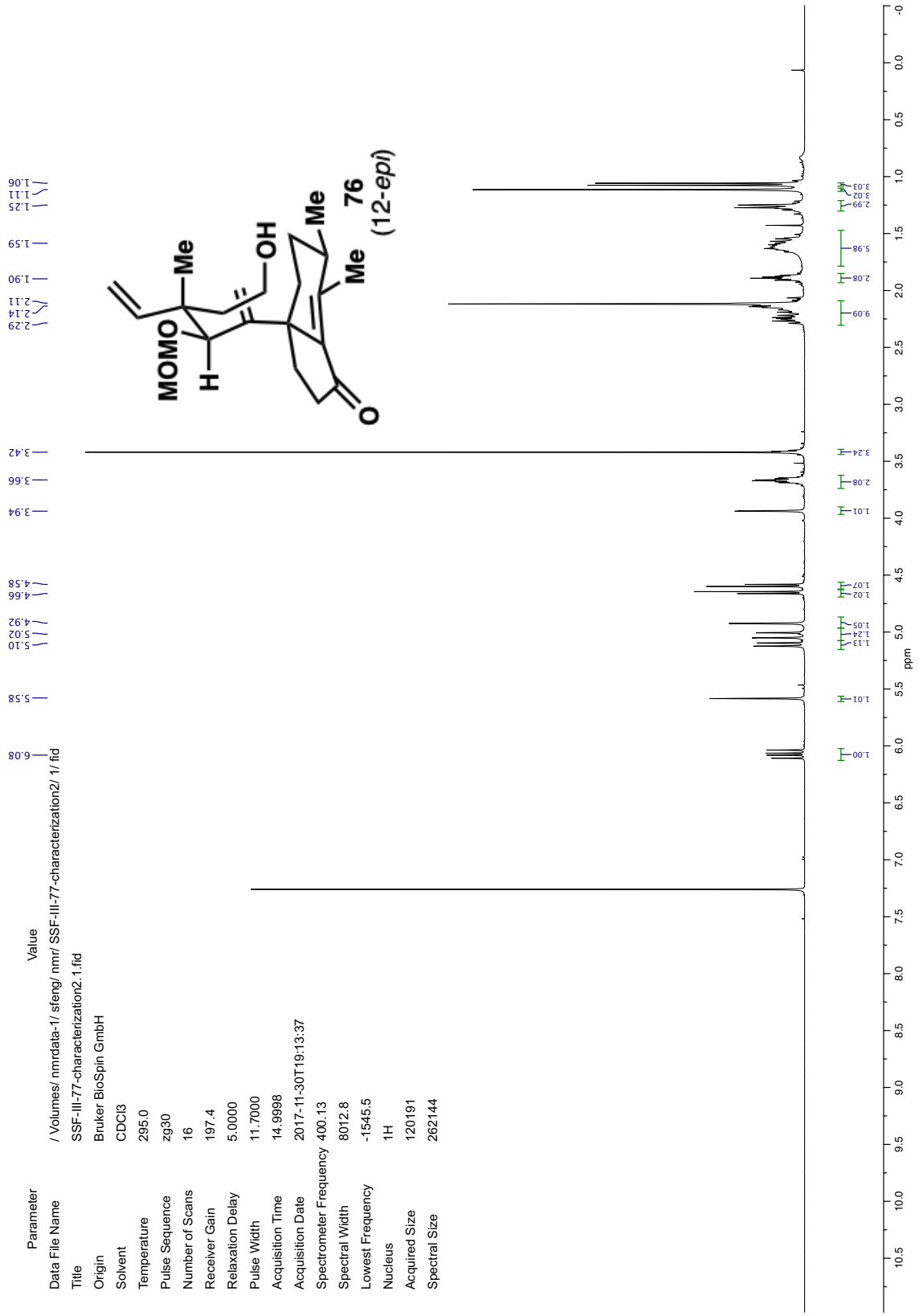
Parameter
Value
Data File Name / Volumes/ nmrdata-1/ sfeng/ nmr/ SSF-III-77-characterization2/ 1/ fid
Title SSF-III-77-characterization2.1.fid
Origin Bruker BioSpin GmbH
Solvent CDCl3
Temperature 295.0
Pulse Sequence zg30
Number of Scans 16
Receiver Gain 197.4
Relaxation Delay 5.0000
Pulse Width 11.7000
Acquisition Time 14.9998
Acquisition Date 2017-11-30T19:13:37
Spectrometer Frequency 400.13
Spectral Width 8012.8
Lowest Frequency -1545.5
Nucleus 1H
Acquired Size 120191
Spectral Size 262144
MOMO
H
Me
OH
Me
Me
76
(12-epi)
O
ppm

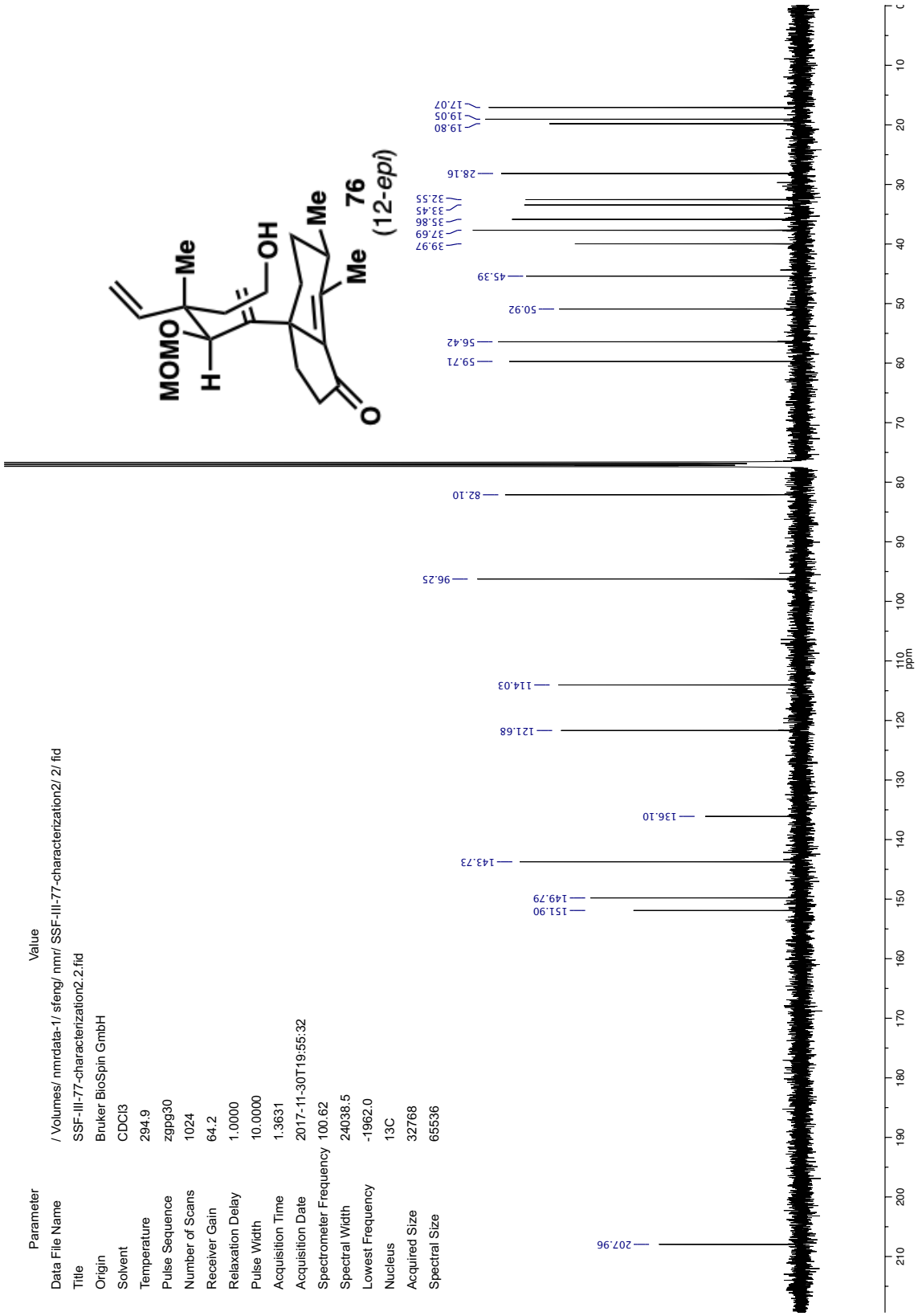

Parameter	Value
Data File Name	/ Volumes/ nmrdata-1/ sfeng/ nmr/ SSF-III-77-characterization2/ 2/ fid
Title	SSF-III-77-characterization2.2.fid
Origin	Bruker BioSpin GmbH
Solvent	CDCl3
Temperature	294.9
Pulse Sequence	zgpg30
Number of Scans	1024
Receiver Gain	64.2
Relaxation Delay	1.0000
Pulse Width	10.0000
Acquisition Time	1.3631
Acquisition Date	2017-11-30T19:55:32
Spectrometer Frequency	100.62
Spectral Width	24038.5
Lowest Frequency	-1962.0
Nucleus	13C
Acquired Size	32768
Spectral Size	65536

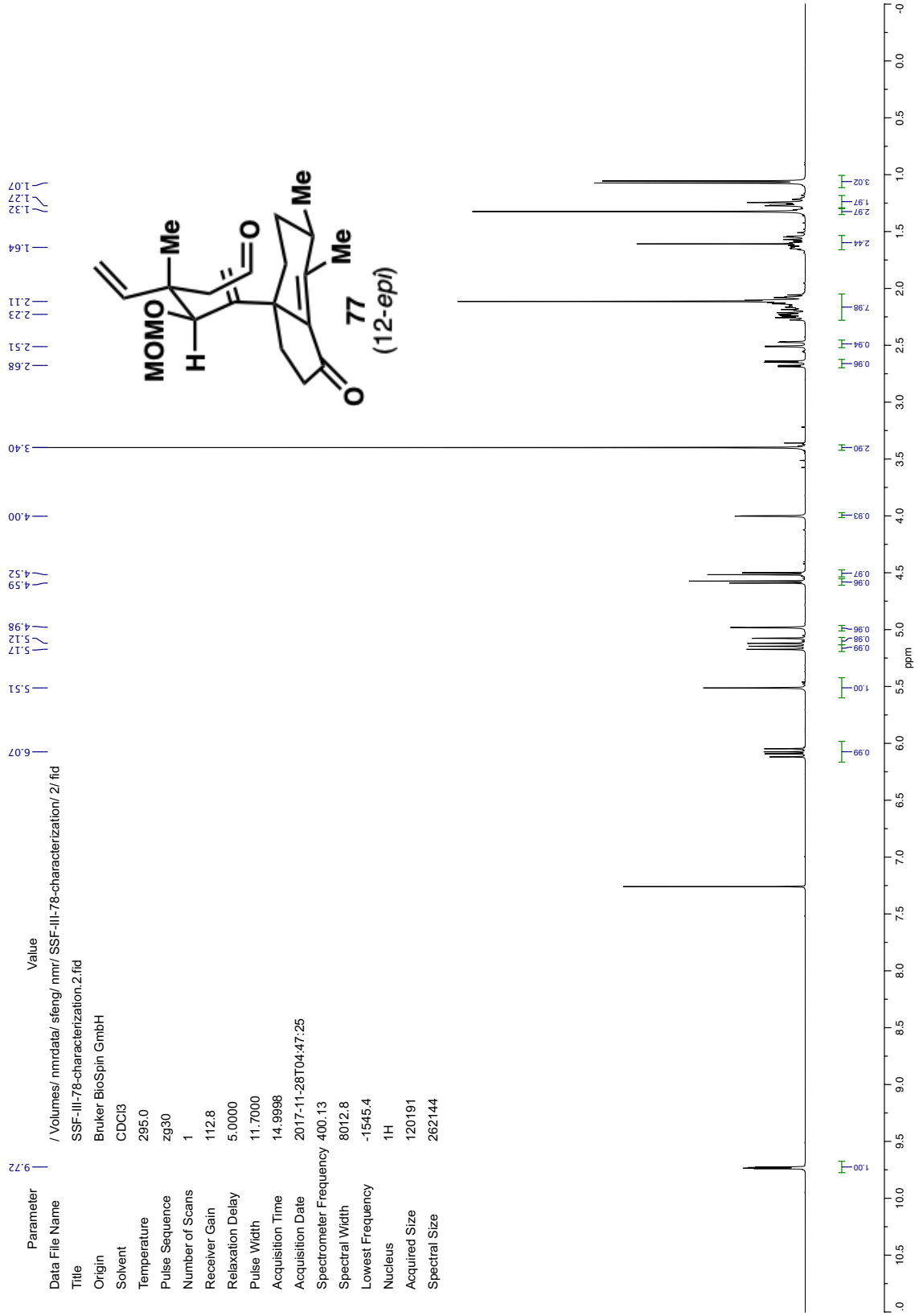
Parameter
Value
Data File Name / Volumes/ nmrdata/ sfeng/ nmr/ SSF-III-78-characterization/ 2/ fid
Title SSF-III-78-characterization.2.fid
Origin Bruker BioSpin GmbH
Solvent CDCl3
Temperature 295.0
Pulse Sequence zg30
Number of Scans 1
Receiver Gain 112.8
Relaxation Delay 5.0000
Pulse Width 11.7000
Acquisition Time 14.9998
Acquisition Date 2017-11-28T04:47:25
Spectrometer Frequency 400.13
Spectral Width 8012.8
Lowest Frequency -1545.4
Nucleus 1H
Acquired Size 120191
Spectral Size 262144
MOMO
Me
H
O
Me
Me
O
77
(12-epi)
ppm

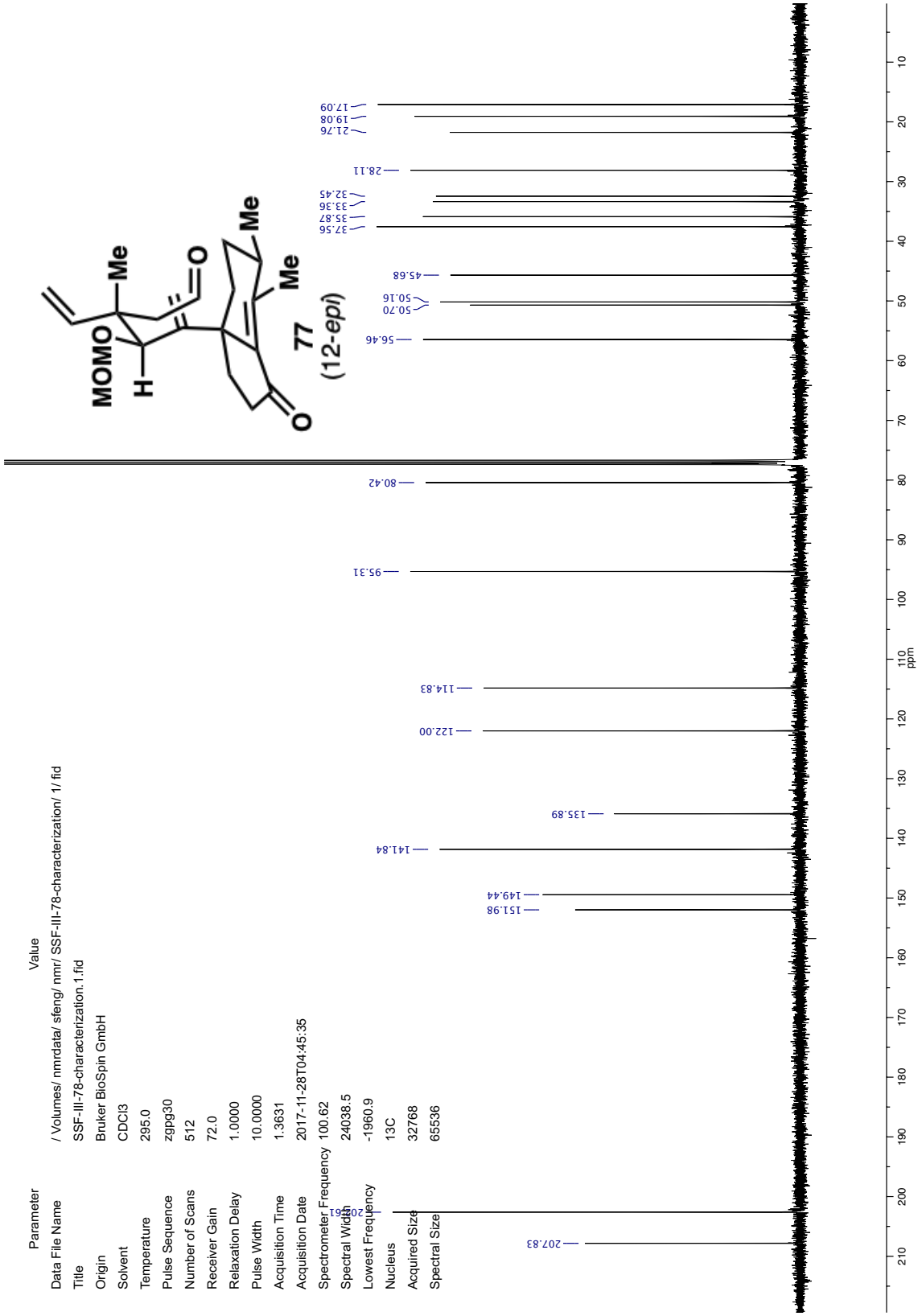
MOMO
H
Me
O
Me
Me
O
77
(12-epi)
17.09
19.08
21.76
28.11
32.45
33.36
35.87
37.56
45.68
50.16
50.70
56.46
80.42
95.31
114.83
122.00
135.89
141.84
149.44
151.98
207.83
Parameter
Value
Data File Name / Volumes/ nmrdata/ sfeng/ nmr/ SSF-III-78-characterization/ 1/ fid
Title SSF-III-78-characterization.1.fid
Origin Bruker BioSpin GmbH
Solvent CDCl3
Temperature 295.0
Pulse Sequence zgpg30
Number of Scans 512
Receiver Gain 72.0
Relaxation Delay 1.0000
Pulse Width 10.0000
Acquisition Time 1.3631
Acquisition Date 2017-11-28T04:45:35
Spectrometer Frequency 100.62
Spectral Width 24038.5
Lowest Frequency -1960.9
Nucleus 13C
Acquired Size 32768
Spectral Size 65536
ppm

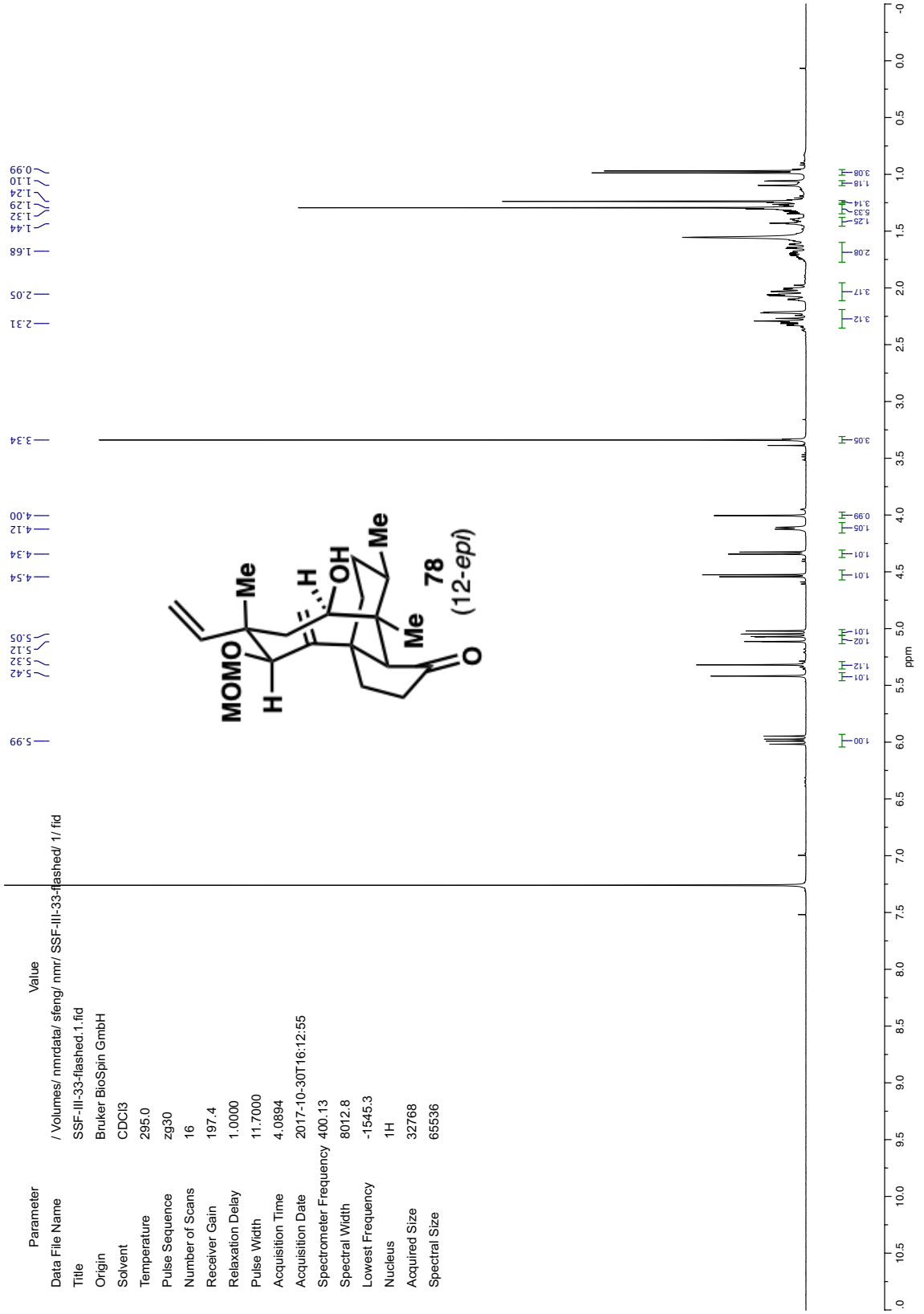
Parameter
Value
Data File Name / Volumes/ nmrdata/ sfeng/ nmr/ SSF-III-33-flashed/ 1/ fid
Title SSF-III-33-flashed.1.fid
Origin Bruker BioSpin GmbH
Solvent CDCl3
Temperature 295.0
Pulse Sequence zg30
Number of Scans 16
Receiver Gain 197.4
Relaxation Delay 1.0000
Pulse Width 11.7000
Acquisition Time 4.0894
Acquisition Date 2017-10-30T16:12:55
Spectrometer Frequency 400.13
Spectral Width 8012.8
Lowest Frequency -1545.3
Nucleus 1H
Acquired Size 32768
Spectral Size 65536
MOMO
Me
H
OH
H
Me
Me
O
78
(12-epi)
ppm

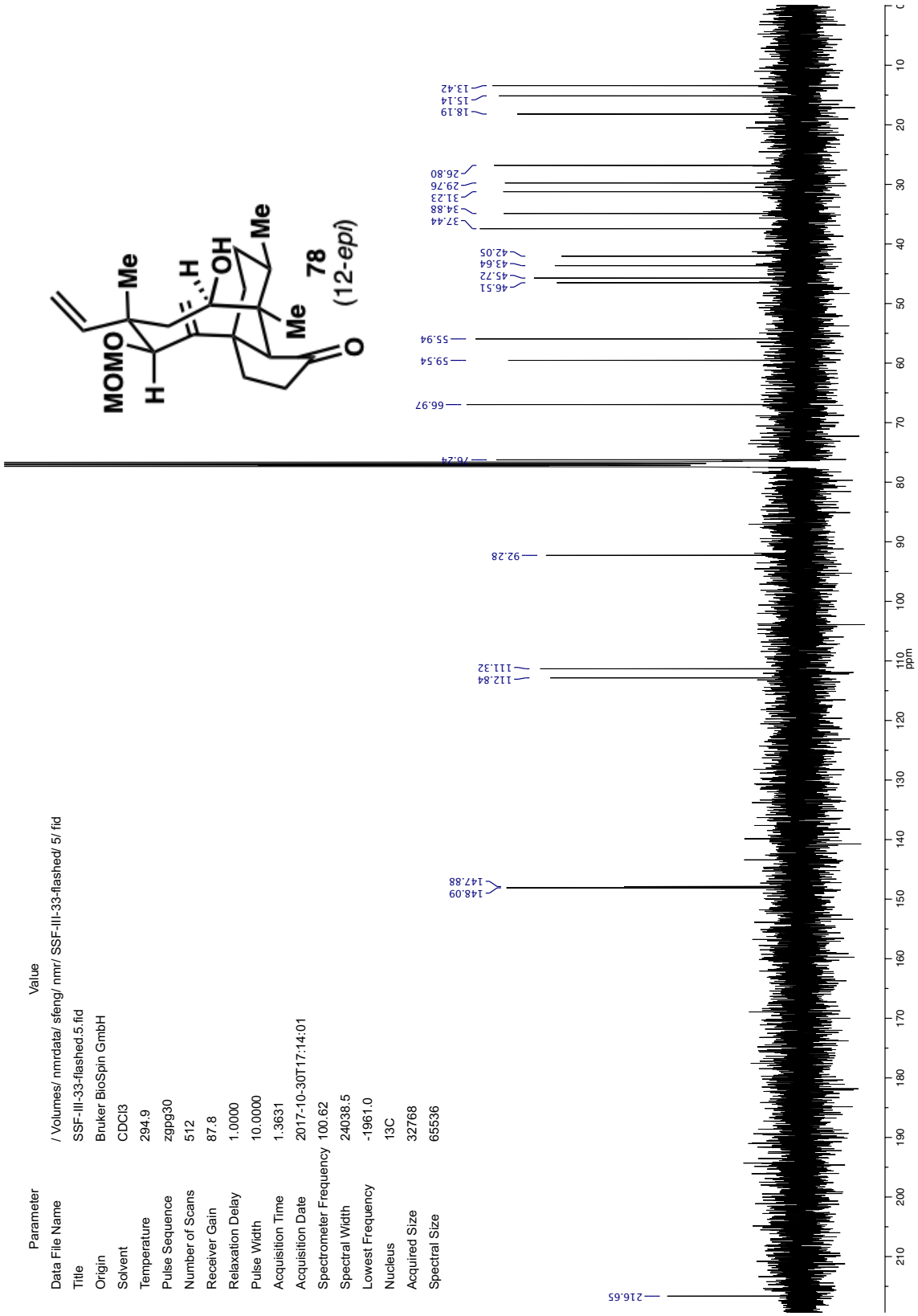

Parameter	Value
Data File Name	/ Volumes/ nmrdata/ sfeng/ nmr/ SSF-III-33-flashed/ 5/ fid
Title	SSF-III-33-flashed.5.fid
Origin	Bruker BioSpin GmbH
Solvent	CDCl3
Temperature	294.9
Pulse Sequence	zgpg30
Number of Scans	512
Receiver Gain	87.8
Relaxation Delay	1.0000
Pulse Width	10.0000
Acquisition Time	1.3631
Acquisition Date	2017-10-30T17:14:01
Spectrometer Frequency	100.62
Spectral Width	24038.5
Lowest Frequency	-1961.0
Nucleus	13C
Acquired Size	32768
Spectral Size	65536

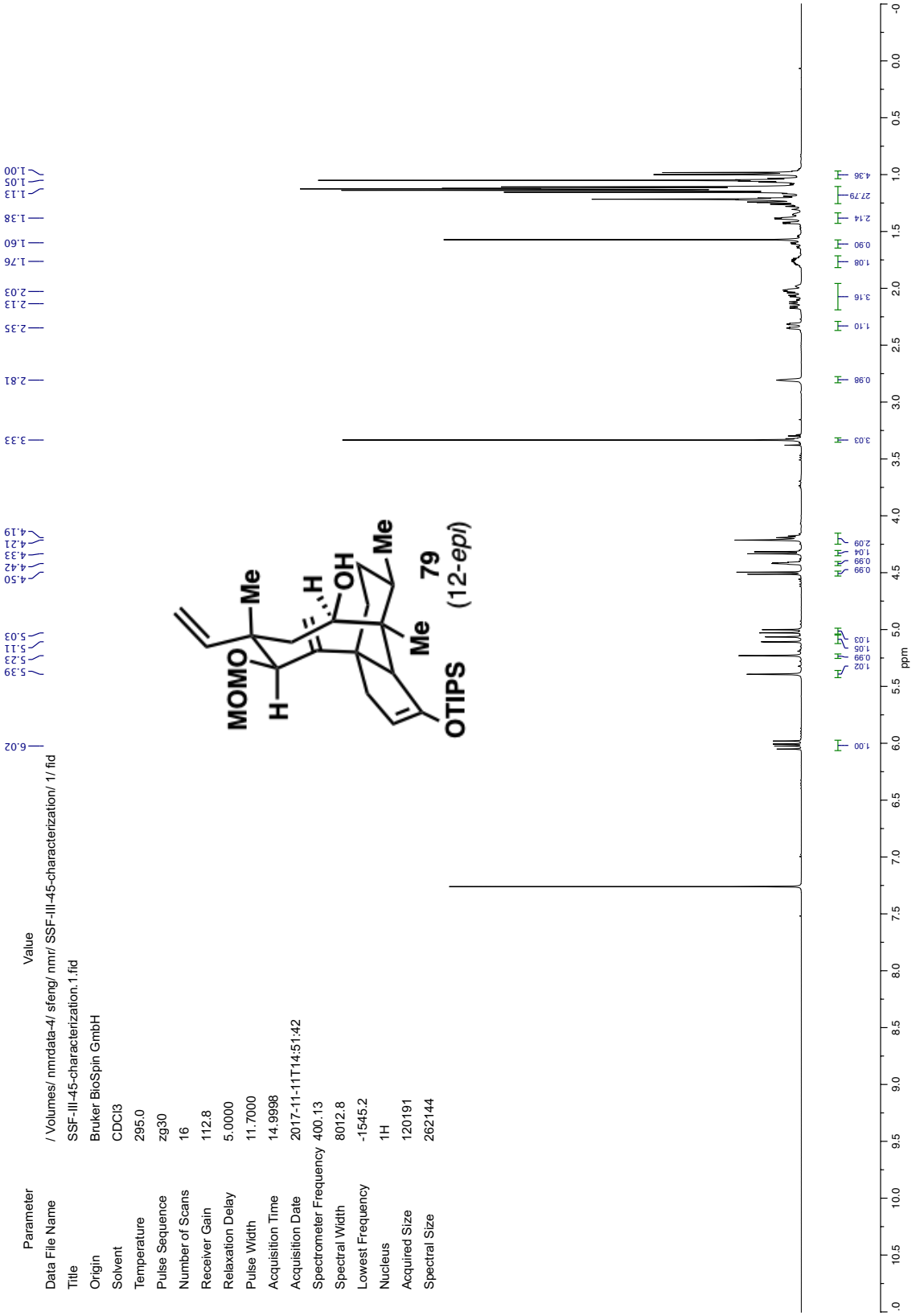
Parameter
Value
Data File Name / Volumes/ nmrdata-4/ sfeng/ nmr/ SSF-III-45-characterization/ 1/ fid
Title SSF-III-45-characterization.1.fid
Origin Bruker BioSpin GmbH
Solvent CDCl3
Temperature 295.0
Pulse Sequence zg30
Number of Scans 16
Receiver Gain 112.8
Relaxation Delay 5.0000
Pulse Width 11.7000
Acquisition Time 14.9998
Acquisition Date 2017-11-11T14:51:42
Spectrometer Frequency 400.13
Spectral Width 8012.8
Lowest Frequency -1545.2
Nucleus 1H
Acquired Size 120191
Spectral Size 262144
MOMO
Me
H
H
OH
Me
Me
79
OTIPS
(12-epi)
ppm

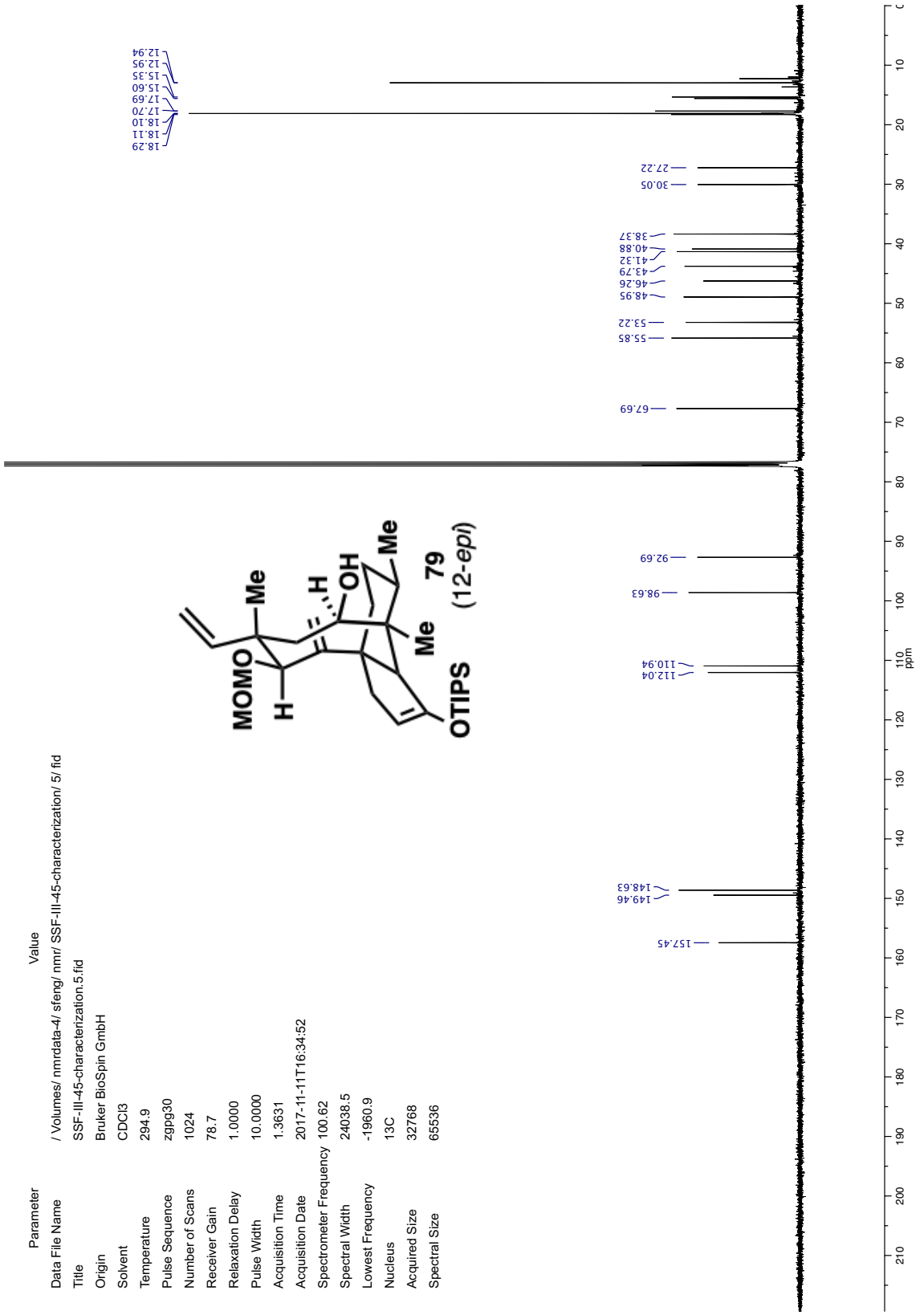

Parameter	Value
Data File Name	/ Volumes/ nmrdata-4/ sfeng/ nmr/ SSF-III-45-characterization/ 5/ fid
Title	SSF-III-45-characterization.5.fid
Origin	Bruker BioSpin GmbH
Solvent	CDCl3
Temperature	294.9
Pulse Sequence	zgpg30
Number of Scans	1024
Receiver Gain	78.7
Relaxation Delay	1.0000
Pulse Width	10.0000
Acquisition Time	1.3631
Acquisition Date	2017-11-11T16:34:52
Spectrometer Frequency	100.62
Spectral Width	24038.5
Lowest Frequency	-1960.9
Nucleus	13C
Acquired Size	32768
Spectral Size	65536

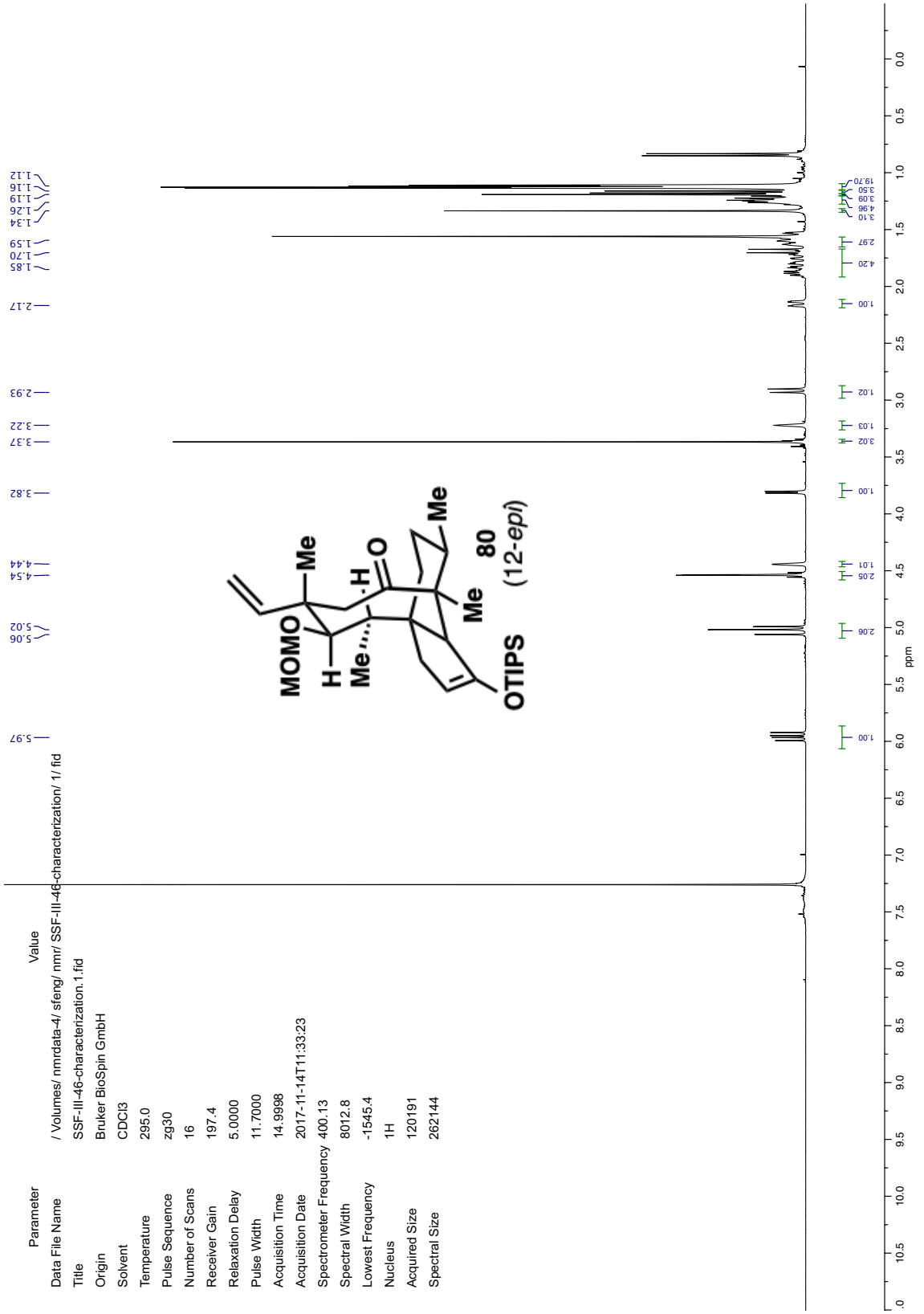
Parameter
Value
Data File Name / Volumes/ nmrdata-4/ sfeng/ nmr/ SSF-III-46-characterization/ 1/ fid
Title SSF-III-46-characterization.1.fid
Origin Bruker BioSpin GmbH
Solvent CDCl3
Temperature 295.0
Pulse Sequence zg30
Number of Scans 16
Receiver Gain 197.4
Relaxation Delay 5.0000
Pulse Width 11.7000
Acquisition Time 14.9998
Acquisition Date 2017-11-14T11:33:23
Spectrometer Frequency 400.13
Spectral Width 8012.8
Lowest Frequency -1545.4
Nucleus 1H
Acquired Size 120191
Spectral Size 262144
MOMO
Me
H
Me
O
Me
Me
80
OTIPS
(12-epi)
ppm

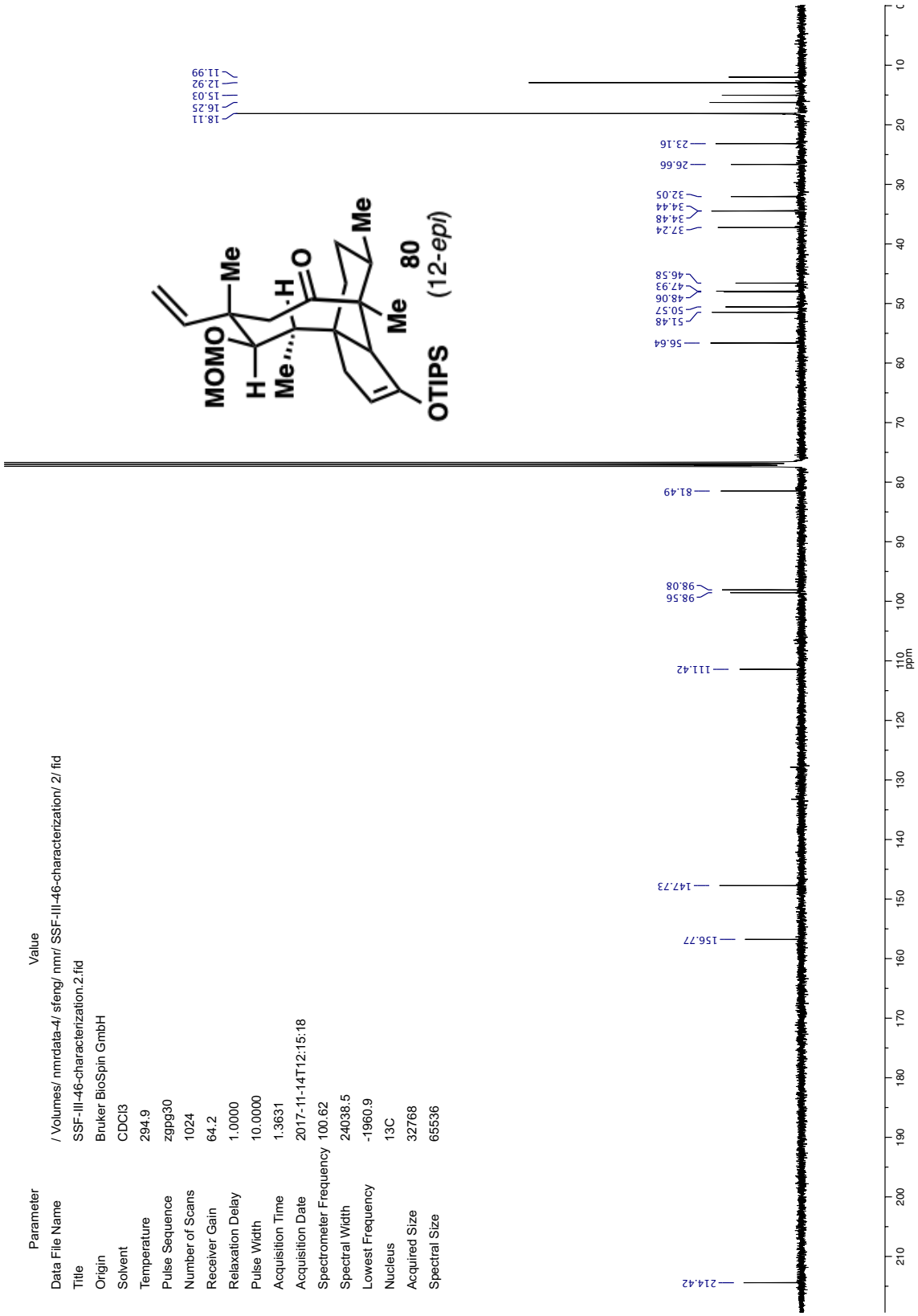
Parameter Value
Data File Name / Volumes/ nmrdata-4/ sfeng/ nmr/ SSF-III-46-characterization/ 2/ fid
Title SSF-III-46-characterization.2.fid
Origin Bruker BioSpin GmbH
Solvent CDCl3
Temperature 294.9
Pulse Sequence zgpg30
Number of Scans 1024
Receiver Gain 64.2
Relaxation Delay 1.0000
Pulse Width 10.0000
Acquisition Time 1.3631
Acquisition Date 2017-11-14T12:15:18
Spectrometer Frequency 100.62
Spectral Width 24038.5
Lowest Frequency -1960.9
Nucleus 13C
Acquired Size 32768
Spectral Size 65536
MOMO
H
Me
Me
O
H
Me
Me
80
OTIPS
(12-epi)
214.42
156.77
147.73
111.42
98.56
98.08
81.49
56.64
51.48
50.57
48.06
47.93
46.58
37.24
34.48
34.44
32.05
26.66
23.16
18.11
16.25
15.03
12.92
11.99
ppm

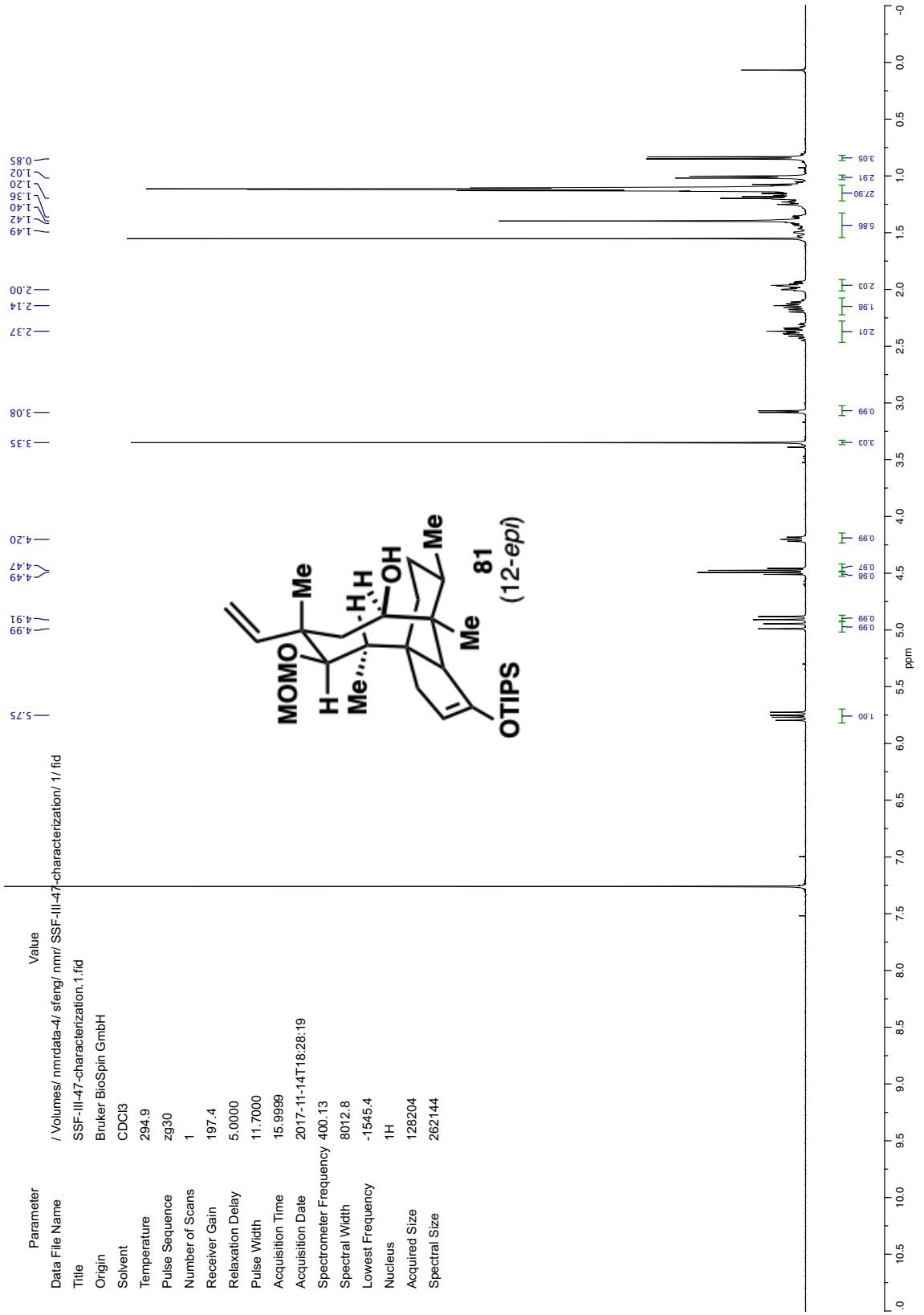
Parameter
Value
Data File Name / Volumes/ nmrdata-4/ sfeng/ nmr/ SSF-III-47-characterization/ 1/ fid
Title SSF-III-47-characterization.1.fid
Origin Bruker BioSpin GmbH
Solvent CDCl3
Temperature 294.9
Pulse Sequence zg30
Number of Scans 1
Receiver Gain 197.4
Relaxation Delay 5.0000
Pulse Width 11.7000
Acquisition Time 15.9999
Acquisition Date 2017-11-14T18:28:19
Spectrometer Frequency 400.13
Spectral Width 8012.8
Lowest Frequency -1545.4
Nucleus 1H
Acquired Size 128204
Spectral Size 262144
MOMO
Me
H
Me
OH
Me
Me
OTIPS
81
(12-epi)
ppm

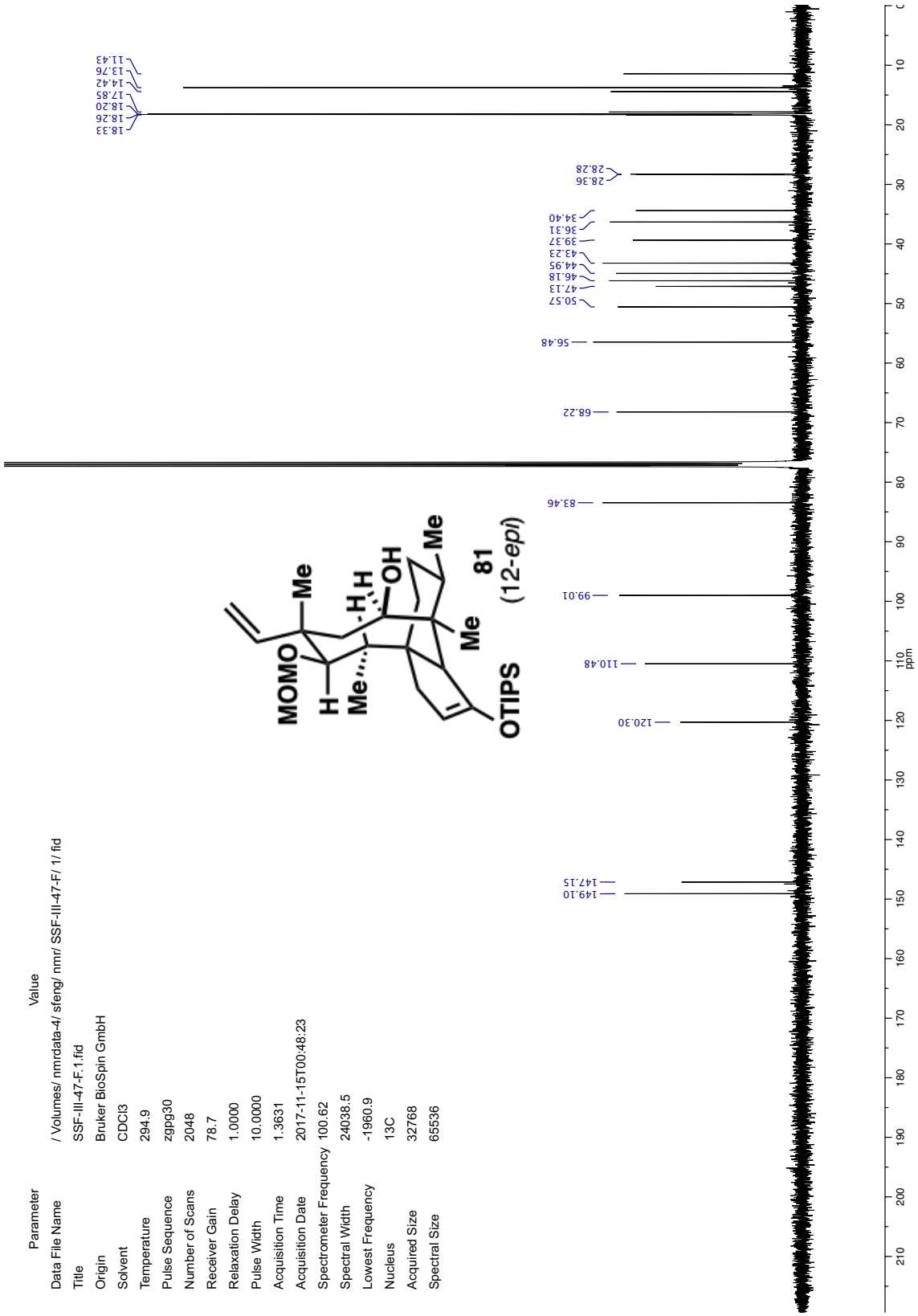
Parameter Value
Data File Name / Volumes/ nmrdata-4/ sfeng/ nmr/ SSF-III-47-F/ 1/ fid
Title SSF-III-47-F.1.fid
Origin Bruker BioSpin GmbH
Solvent CDCl3
Temperature 294.9
Pulse Sequence zgpg30
Number of Scans 2048
Receiver Gain 78.7
Relaxation Delay 1.0000
Pulse Width 10.0000
Acquisition Time 1.3631
Acquisition Date 2017-11-15T00:48:23
Spectrometer Frequency 100.62
Spectral Width 24038.5
Lowest Frequency -1960.9
Nucleus 13C
Acquired Size 32768
Spectral Size 65536
MOMO
Me
H
Me
OH
Me
Me
OTIPS
81
(12-epi)
11.43
13.76
14.42
17.85
18.20
18.26
18.33
28.28
28.36
34.40
36.31
39.37
43.23
44.95
46.18
47.13
50.57
56.48
68.22
83.46
99.01
110.48
120.30
147.15
149.10
ppm

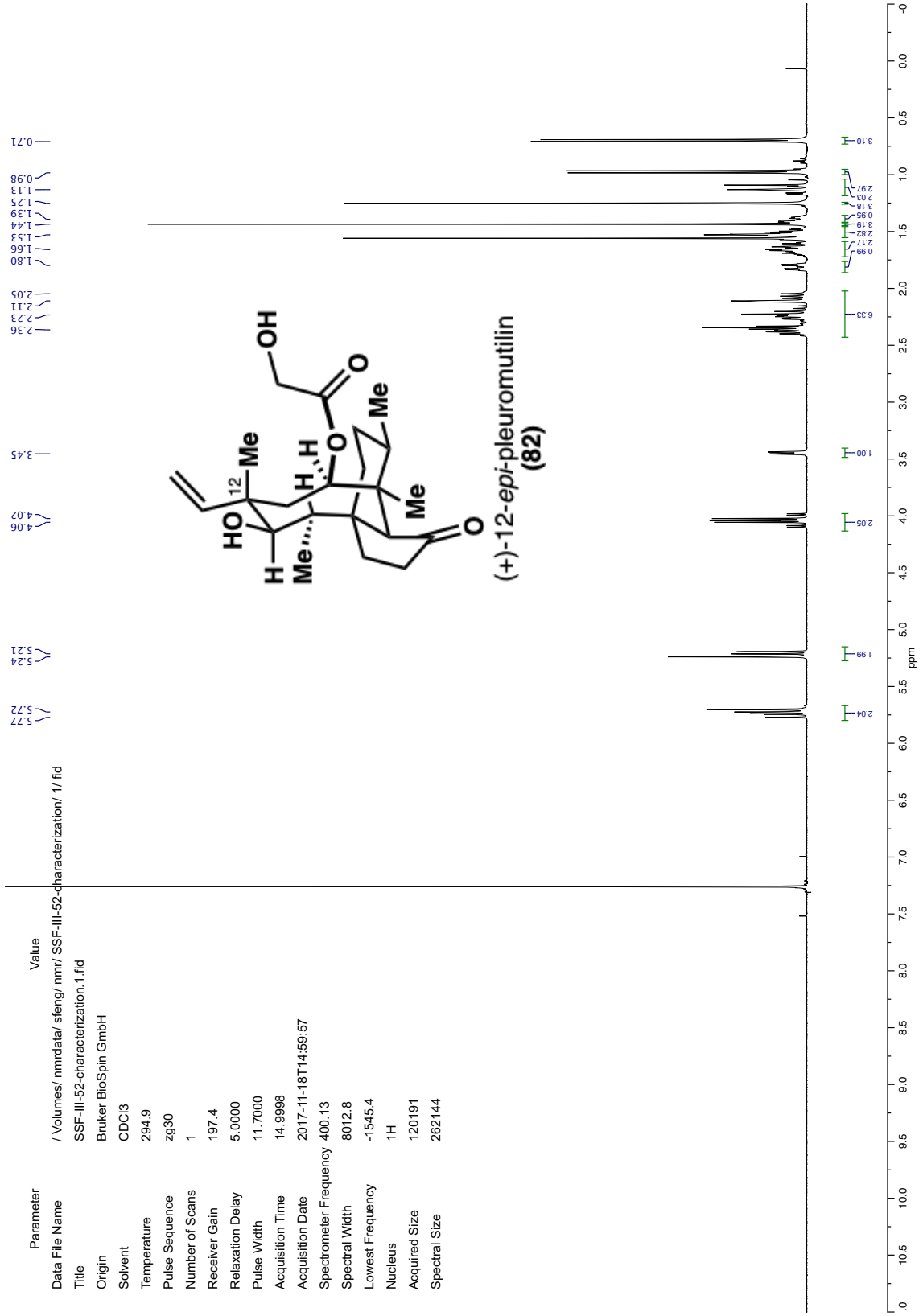
(+)-12-epi-pleuromutilin
(82)
Parameter
Value
Data File Name / Volumes/ nmrdata/ sfeng/ nmr/ SSF-III-52-characterization/ 1/ fid
Title SSF-III-52-characterization.1.fid
Origin Bruker BioSpin GmbH
Solvent CDCl3
Temperature 294.9
Pulse Sequence zg30
Number of Scans 1
Receiver Gain 197.4
Relaxation Delay 5.0000
Pulse Width 11.7000
Acquisition Time 14.9998
Acquisition Date 2017-11-18T14:59:57
Spectrometer Frequency 400.13
Spectral Width 8012.8
Lowest Frequency -1545.4
Nucleus 1H
Acquired Size 120191
Spectral Size 262144
ppm

Parameter	Value
Data File Name	/ Volumes/ nmrdata/ sfeng/ nmr/ SSF-III-52-characterization/ 2/ fid
Title	SSF-III-52-characterization.2.fid
Origin	Bruker BioSpin GmbH
Solvent	CDCl3
Temperature	295.0
Pulse Sequence	zgpg30
Number of Scans	2048
Receiver Gain	87.8
Relaxation Delay	1.0000
Pulse Width	10.0000
Acquisition Time	1.3631
Acquisition Date	2017-11-19T00:01:06
Spectrometer Frequency	100.62
Spectral Width	24038.5
Lowest Frequency	-1960.9
Nucleus	13C
Acquired Size	32768
Spectral Size	65536

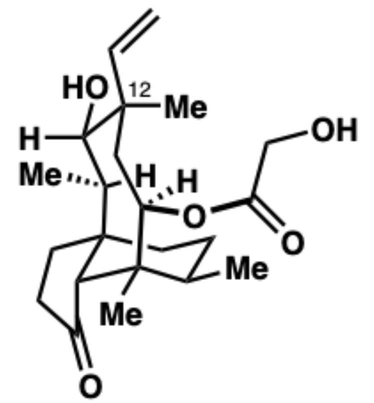

(+)-12-*epi*-pleuromutilin
(82)

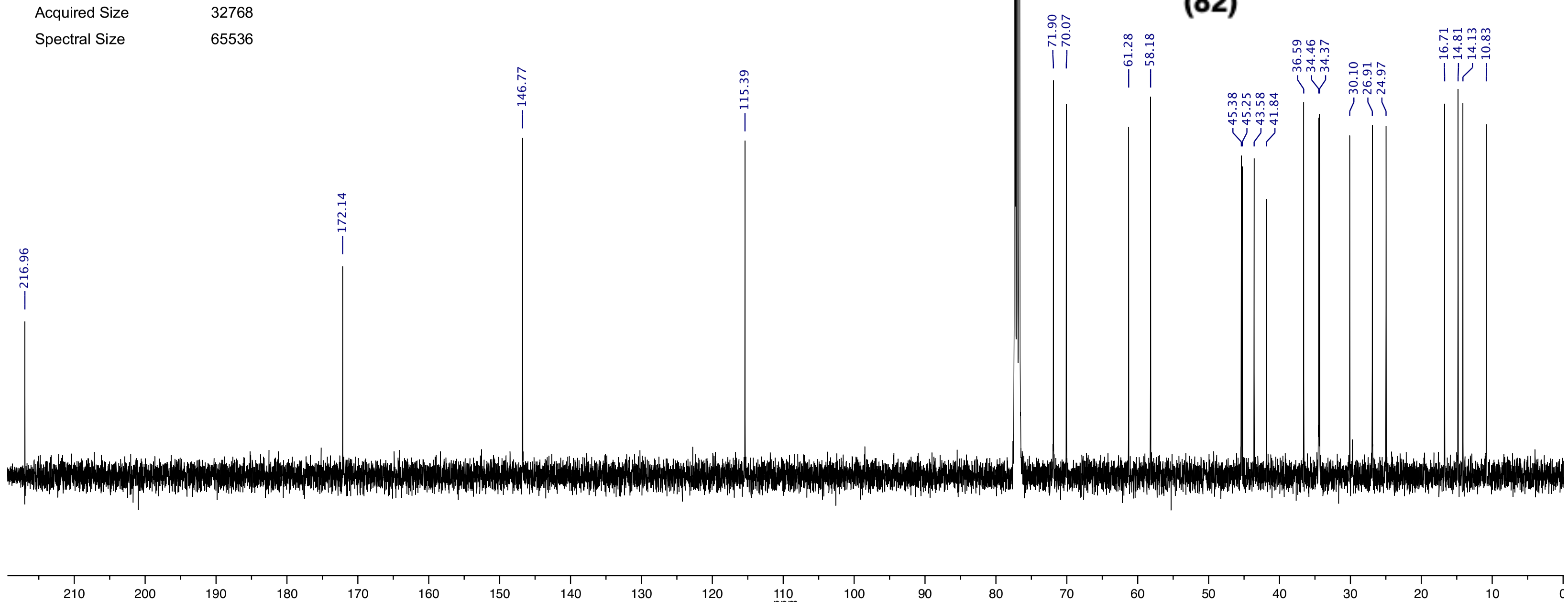

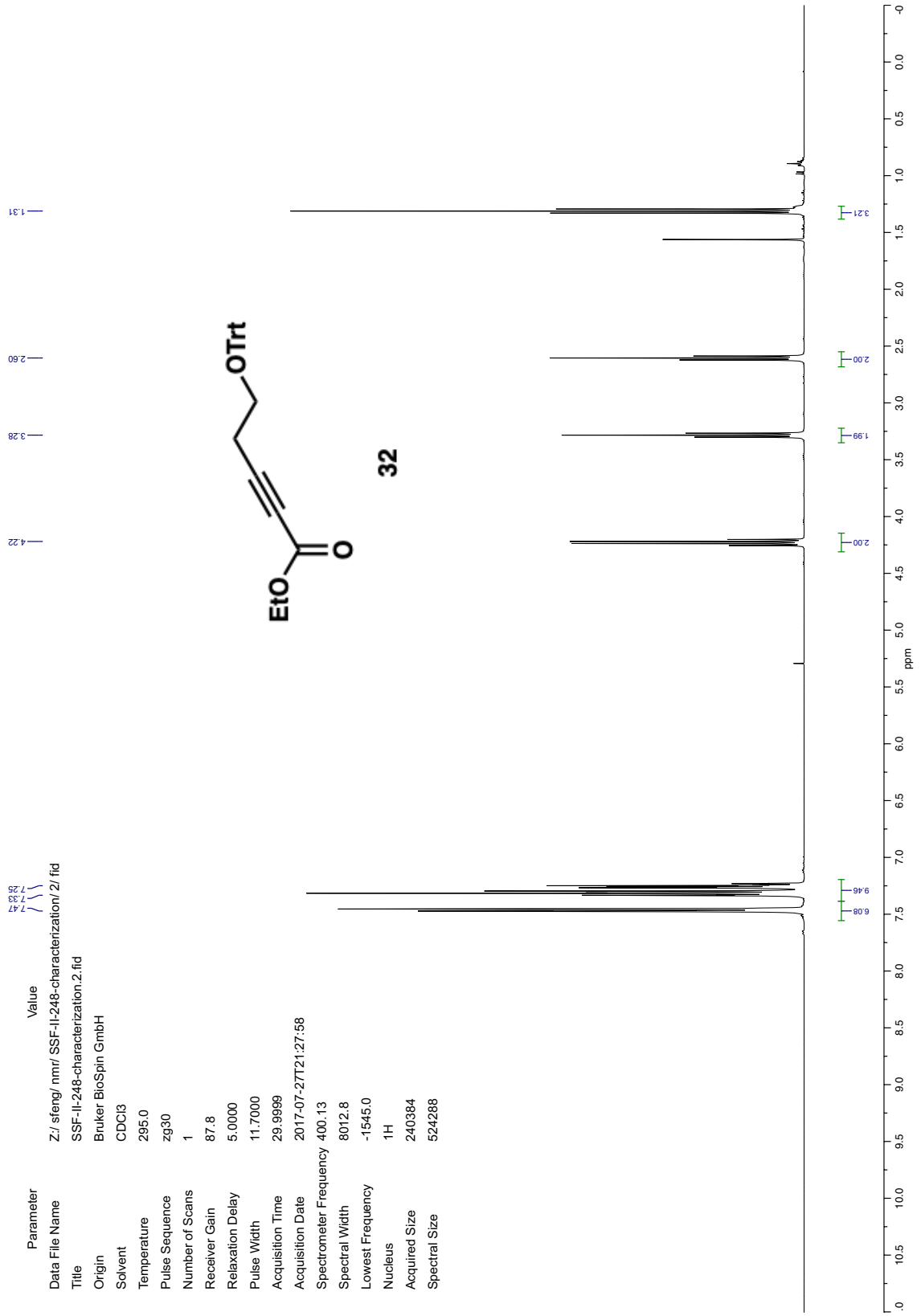
Parameter
Value
Data File Name
Z:/ sfeng/ nmr/ SSF-II-248-characterization/ 2/ fid
Title
SSF-II-248-characterization.2.fid
Origin
Bruker BioSpin GmbH
Solvent
CDCl3
Temperature
295.0
Pulse Sequence
zg30
Number of Scans
1
Receiver Gain
87.8
Relaxation Delay
5.0000
Pulse Width
11.7000
Acquisition Time
29.9999
Acquisition Date
2017-07-27T21:27:58
Spectrometer Frequency
400.13
Spectral Width
8012.8
Lowest Frequency
-1545.0
Nucleus
1H
Acquired Size
240384
Spectral Size
524288
7.47
7.33
7.25
4.22
3.28
2.60
1.31
9.46
6.08
2.00
1.99
2.00
3.21
EtO
O
OTrt
32
ppm

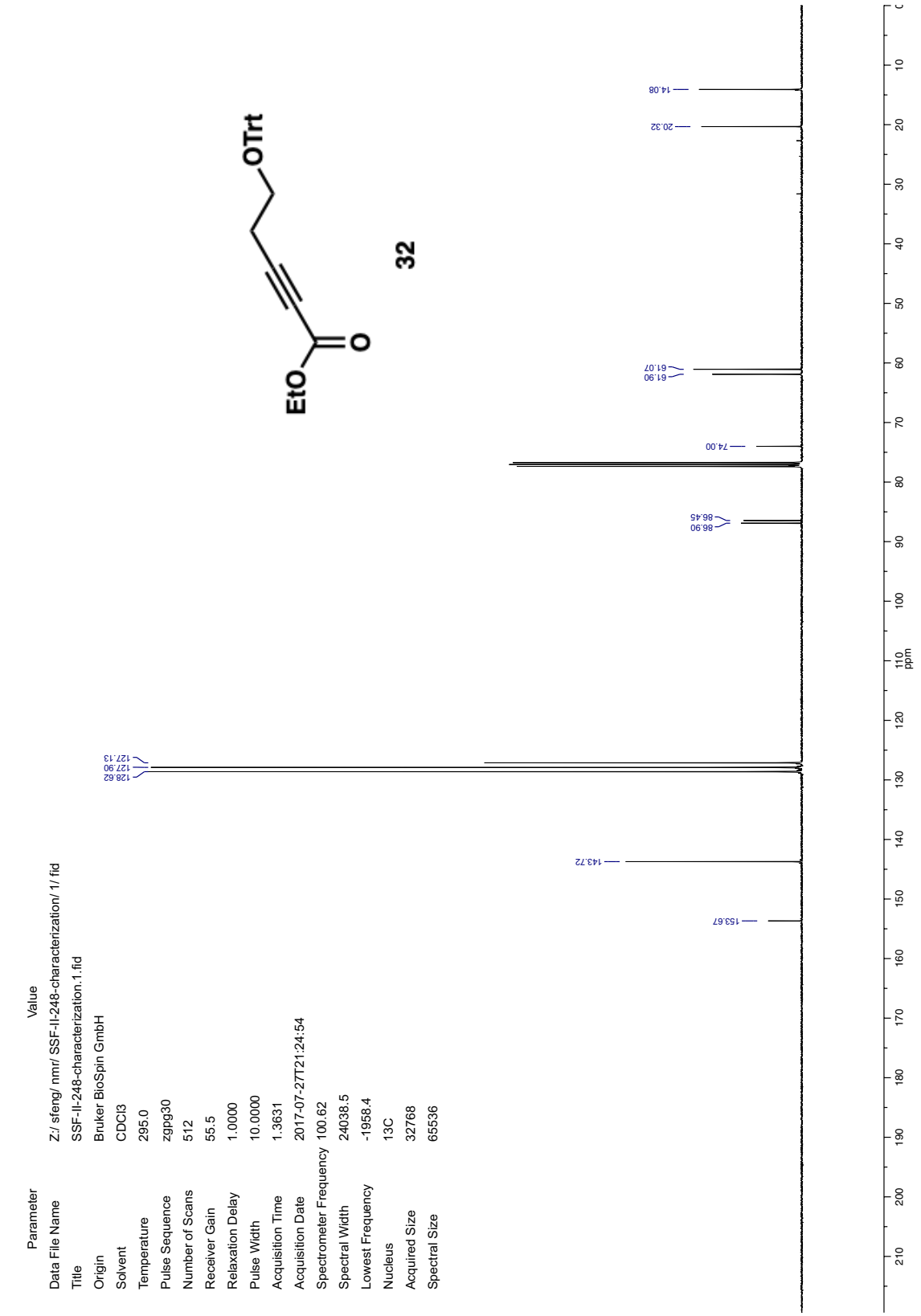

Parameter	Value
Data File Name	Z:/ sfeng/ nmr/ SSF-II-248-characterization/ 1/ fid
Title	SSF-II-248-characterization.1.fid
Origin	Bruker BioSpin GmbH
Solvent	CDCl3
Temperature	295.0
Pulse Sequence	zgpg30
Number of Scans	512
Receiver Gain	55.5
Relaxation Delay	1.0000
Pulse Width	10.0000
Acquisition Time	1.3631
Acquisition Date	2017-07-27T21:24:54
Spectrometer Frequency	100.62
Spectral Width	24038.5
Lowest Frequency	-1958.4
Nucleus	13C
Acquired Size	32768
Spectral Size	65536

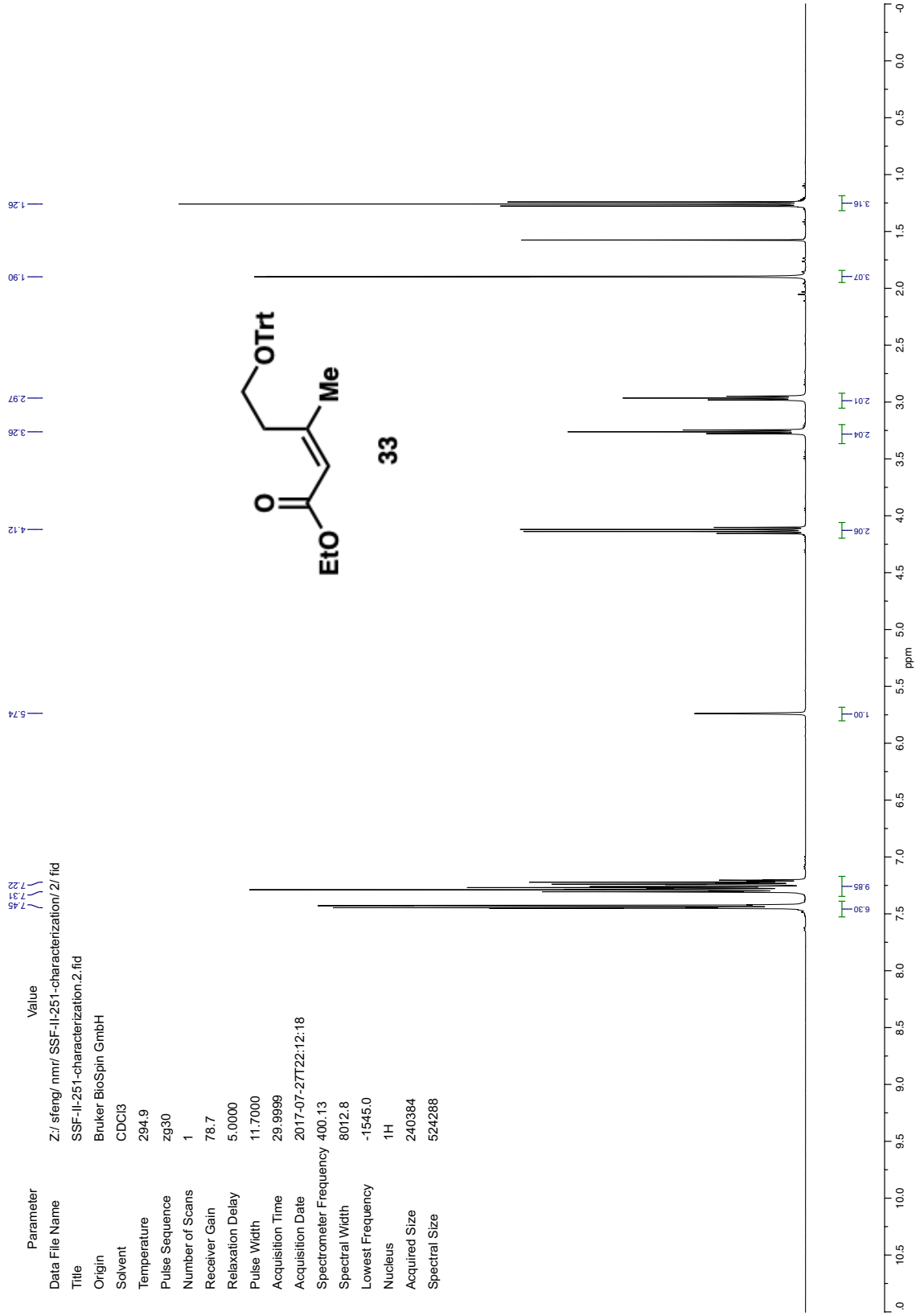

Parameter	Value
Data File Name	Z:/ sfeng/ nmr/ SSF-II-251-characterization/ 2/ fid
Title	SSF-II-251-characterization.2.fid
Origin	Bruker BioSpin GmbH
Solvent	CDCl3
Temperature	294.9
Pulse Sequence	zg30
Number of Scans	1
Receiver Gain	78.7
Relaxation Delay	5.0000
Pulse Width	11.7000
Acquisition Time	29.9999
Acquisition Date	2017-07-27T22:12:18
Spectrometer Frequency	400.13
Spectral Width	8012.8
Lowest Frequency	-1545.0
Nucleus	1H
Acquired Size	240384
Spectral Size	524288

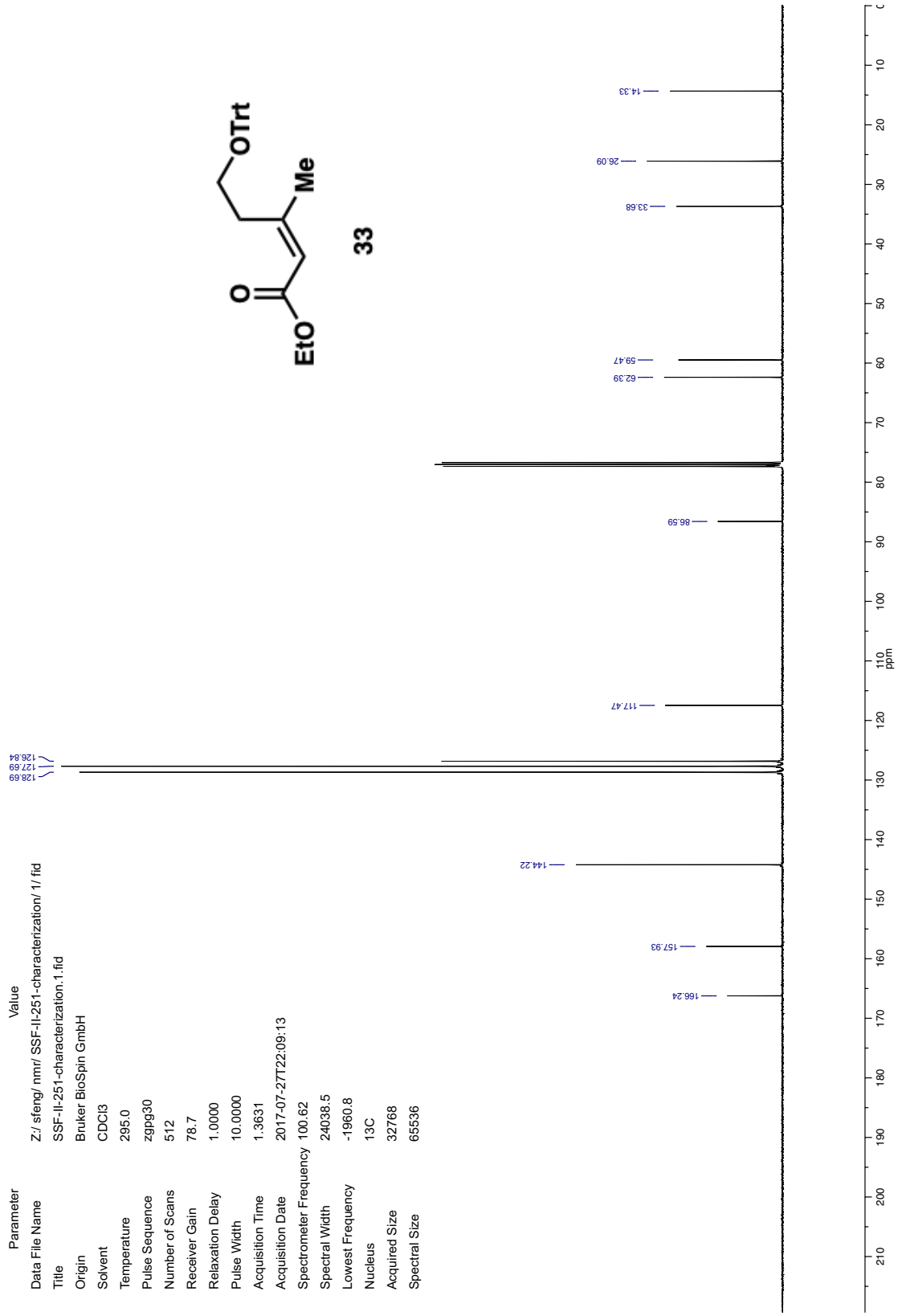

Parameter	Value
Data File Name	Z:/ sfeng/ nmr/ SSF-II-251-characterization/ 1/ fid
Title	SSF-II-251-characterization.1.fid
Origin	Bruker BioSpin GmbH
Solvent	CDCl3
Temperature	295.0
Pulse Sequence	zgpg30
Number of Scans	512
Receiver Gain	78.7
Relaxation Delay	1.0000
Pulse Width	10.0000
Acquisition Time	1.3631
Acquisition Date	2017-07-27T22:09:13
Spectrometer Frequency	100.62
Spectral Width	24038.5
Lowest Frequency	-1960.8
Nucleus	13C
Acquired Size	32768
Spectral Size	65536

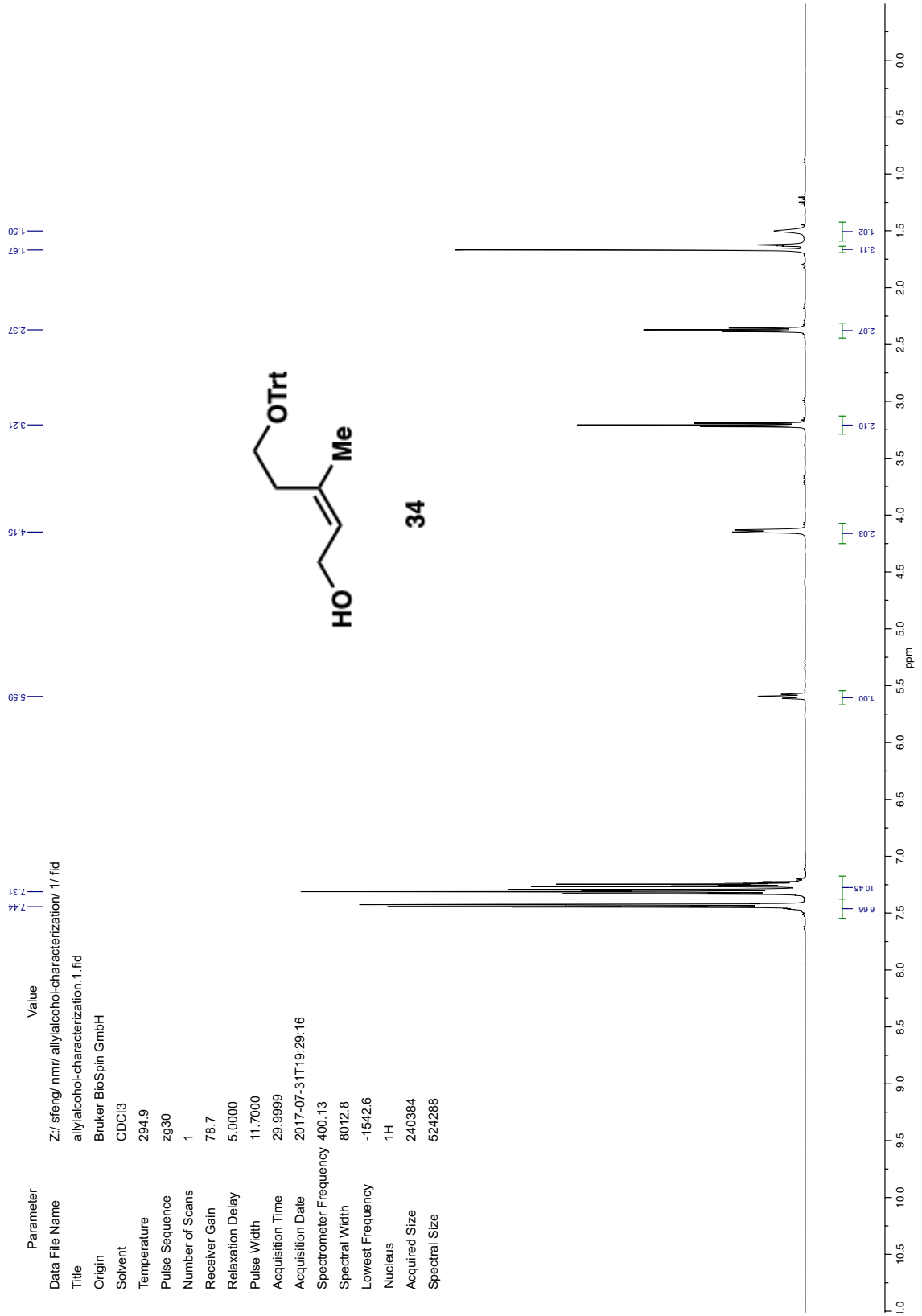
Parameter
Value
Data File Name
Z:/ sfeng/ nmr/ allylalcohol-characterization/ 1/ fid
Title
allylalcohol-characterization.1.fid
Origin
Bruker BioSpin GmbH
Solvent
CDCl3
Temperature
294.9
Pulse Sequence
zg30
Number of Scans
1
Receiver Gain
78.7
Relaxation Delay
5.0000
Pulse Width
11.7000
Acquisition Time
29.9999
Acquisition Date
2017-07-31T19:29:16
Spectrometer Frequency
400.13
Spectral Width
8012.8
Lowest Frequency
-1542.6
Nucleus
1H
Acquired Size
240384
Spectral Size
524288
OTrt
Me
HO
34
ppm

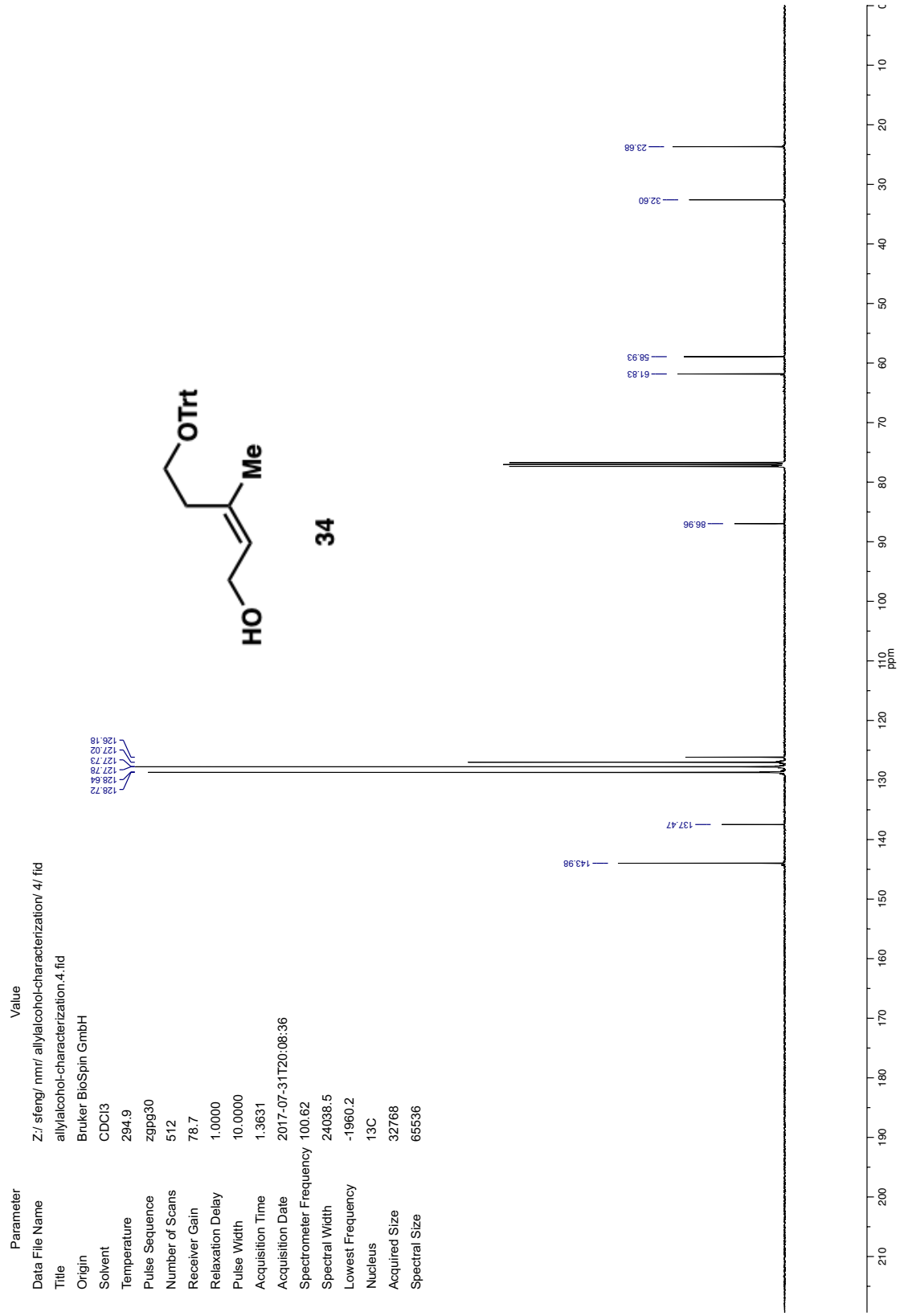

Parameter	Value
Data File Name	Z:/ sfeng/ nmr/ allylalcohol-characterization/ 4/ fid
Title	allylalcohol-characterization.4.fid
Origin	Bruker BioSpin GmbH
Solvent	CDCl3
Temperature	294.9
Pulse Sequence	zgpg30
Number of Scans	512
Receiver Gain	78.7
Relaxation Delay	1.0000
Pulse Width	10.0000
Acquisition Time	1.3631
Acquisition Date	2017-07-31T20:08:36
Spectrometer Frequency	100.62
Spectral Width	24038.5
Lowest Frequency	-1960.2
Nucleus	13C
Acquired Size	32768
Spectral Size	65536

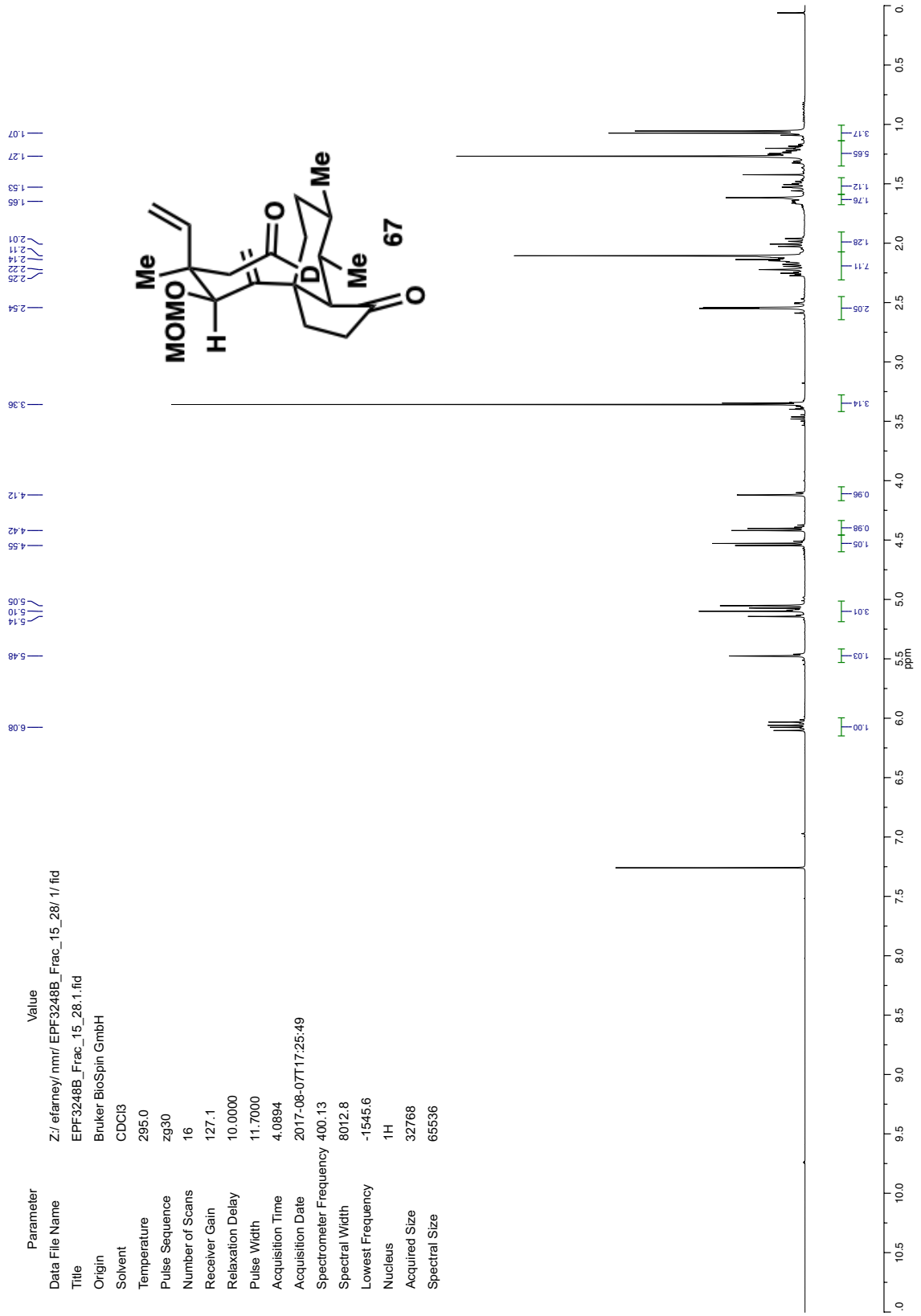
Me
MOMO
H
O
D
Me
Me
O
67
Parameter
Value
Data File Name
Z:/ efarney/ nmr/ EPF3248B_Frac_15_28/ 1/ fid
Title
EPF3248B_Frac_15_28.1.fid
Origin
Bruker BioSpin GmbH
Solvent
CDCl3
Temperature
295.0
Pulse Sequence
zg30
Number of Scans
16
Receiver Gain
127.1
Relaxation Delay
10.0000
Pulse Width
11.7000
Acquisition Time
4.0894
Acquisition Date
2017-08-07T17:25:49
Spectrometer Frequency
400.13
Spectral Width
8012.8
Lowest Frequency
-1545.6
Nucleus
1H
Acquired Size
32768
Spectral Size
65536
ppm

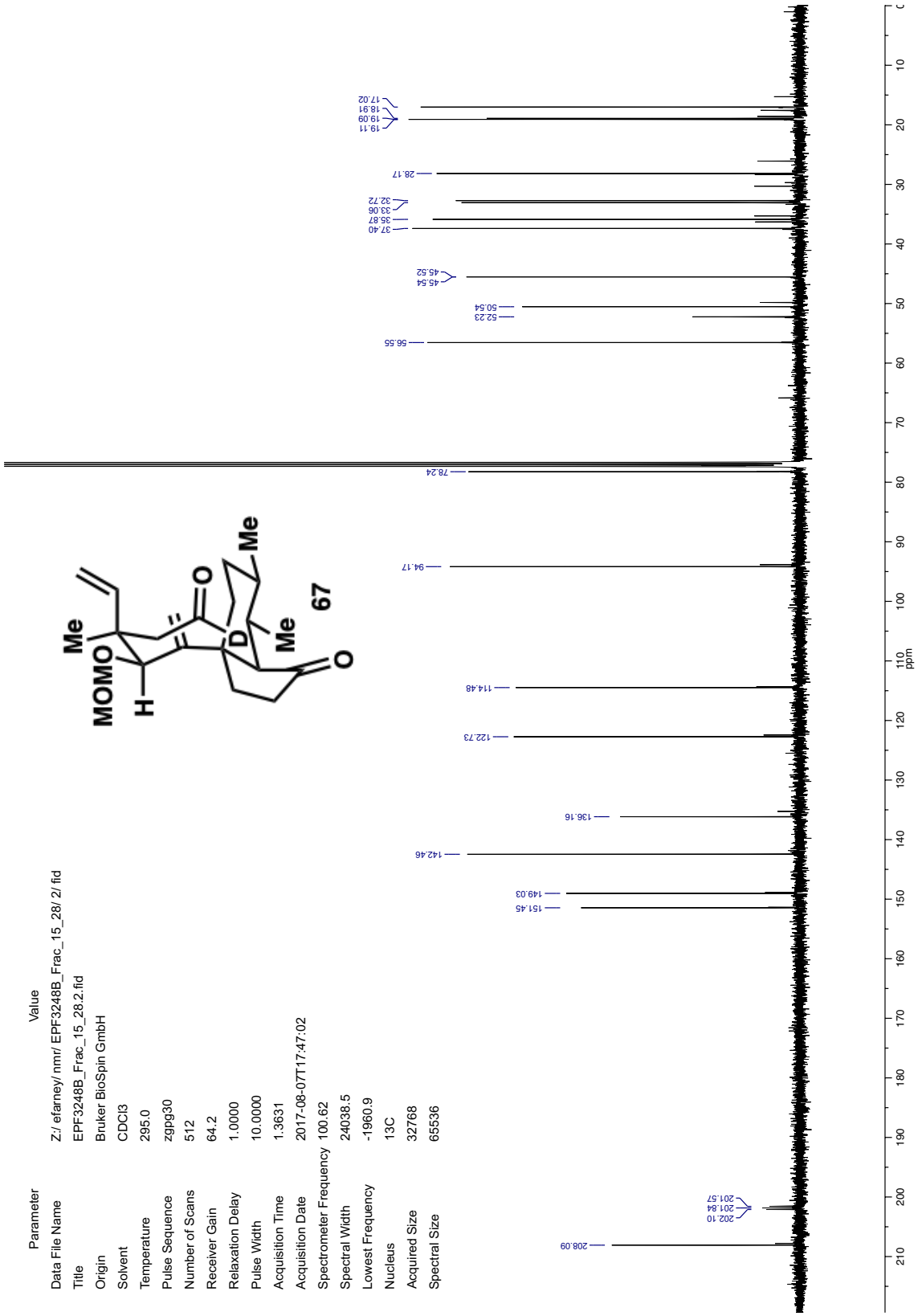
Parameter Value
Data File Name Z:/ efarney/ nmr/ EPF3248B_Frac_15_28/ 2/ fid
Title EPF3248B_Frac_15_28.2.fid
Origin Bruker BioSpin GmbH
Solvent CDCl3
Temperature 295.0
Pulse Sequence zgpg30
Number of Scans 512
Receiver Gain 64.2
Relaxation Delay 1.0000
Pulse Width 10.0000
Acquisition Time 1.3631
Acquisition Date 2017-08-07T17:47:02
Spectrometer Frequency 100.62
Spectral Width 24038.5
Lowest Frequency -1960.9
Nucleus 13C
Acquired Size 32768
Spectral Size 65536
Me
MOMO
H
O
D
Me
Me
O
67
17.02
18.91
19.09
19.11
28.17
32.72
33.06
35.87
37.40
45.52
45.54
50.54
52.23
56.55
78.24
94.17
114.48
122.73
136.16
142.46
149.03
151.45
201.57
201.84
202.10
208.09
ppm

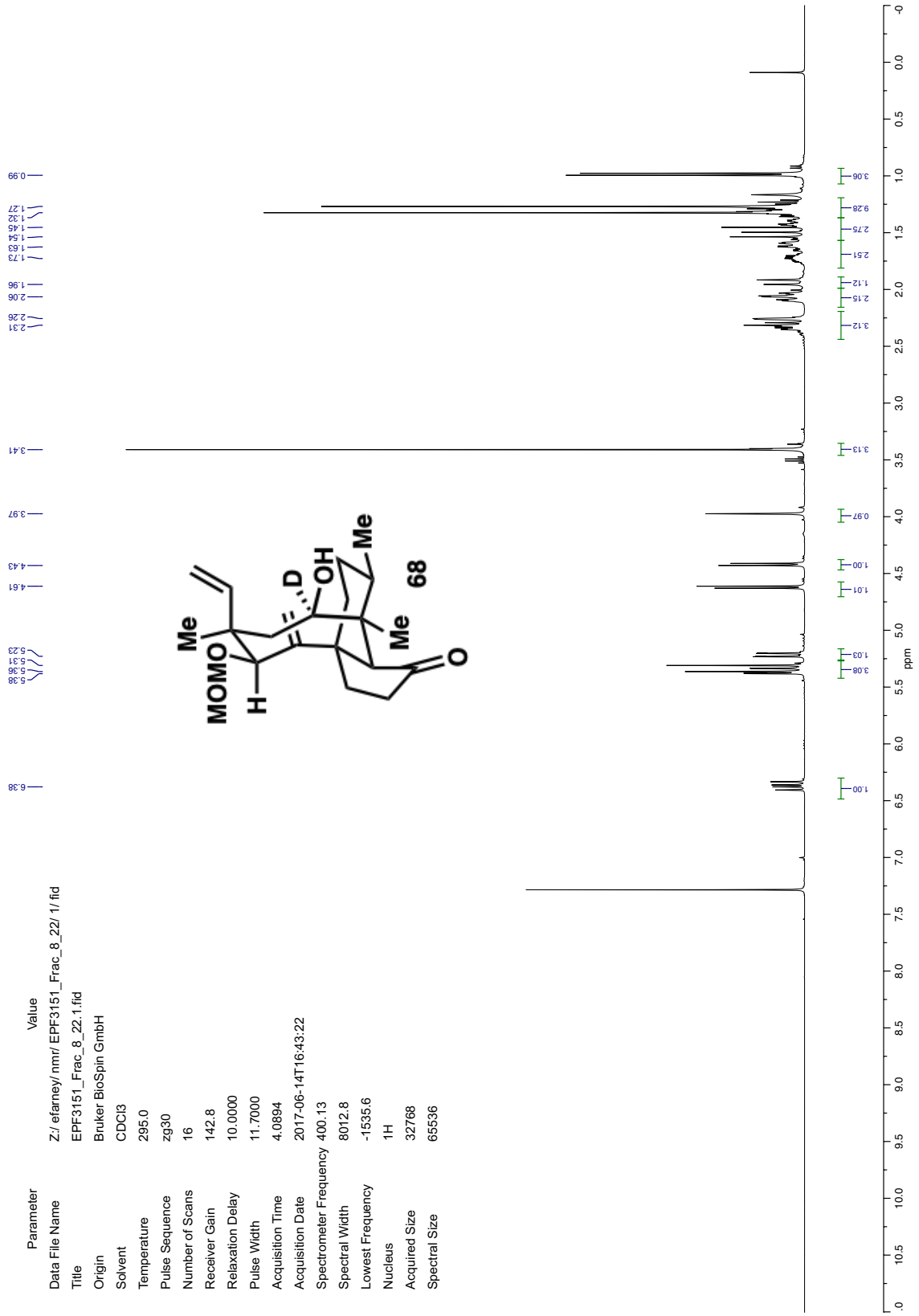
Parameter
Value
Data File Name
Z:/ efarney/ nmr/ EPF3151_Frac_8_22/ 1/ fid
Title
EPF3151_Frac_8_22.1.fid
Origin
Bruker BioSpin GmbH
Solvent
CDCl3
Temperature
295.0
Pulse Sequence
zg30
Number of Scans
16
Receiver Gain
142.8
Relaxation Delay
10.0000
Pulse Width
11.7000
Acquisition Time
4.0894
Acquisition Date
2017-06-14T16:43:22
Spectrometer Frequency
400.13
Spectral Width
8012.8
Lowest Frequency
-1535.6
Nucleus
1H
Acquired Size
32768
Spectral Size
65536
Me
MOMO
H
D
OH
Me
Me
O
68
ppm

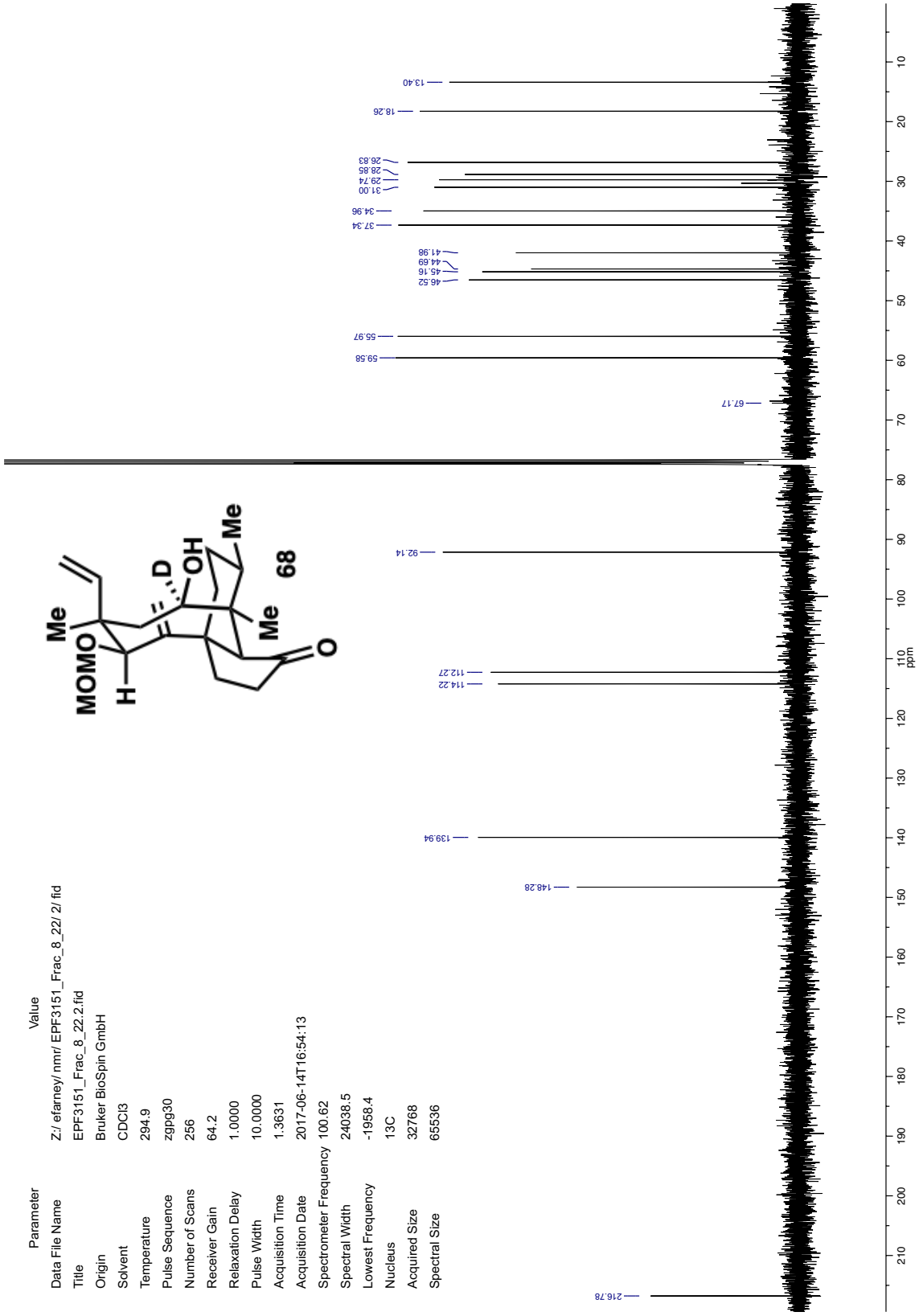
Parameter
Value
Data File Name
Z:/ efarney/ nmr/ EPF3151_Frac_8_22/ 2/ fid
Title
EPF3151_Frac_8_22.2.fid
Origin
Bruker BioSpin GmbH
Solvent
CDCl3
Temperature
294.9
Pulse Sequence
zgpg30
Number of Scans
256
Receiver Gain
64.2
Relaxation Delay
1.0000
Pulse Width
10.0000
Acquisition Time
1.3631
Acquisition Date
2017-06-14T16:54:13
Spectrometer Frequency
100.62
Spectral Width
24038.5
Lowest Frequency
-1958.4
Nucleus
13C
Acquired Size
32768
Spectral Size
65536
Me
MOMO
H
D
OH
Me
Me
O
68
216.78
148.28
139.94
114.22
112.27
92.14
67.17
59.58
55.97
46.52
45.16
44.69
41.98
37.34
34.96
31.00
29.74
28.85
26.83
18.26
13.40
ppm

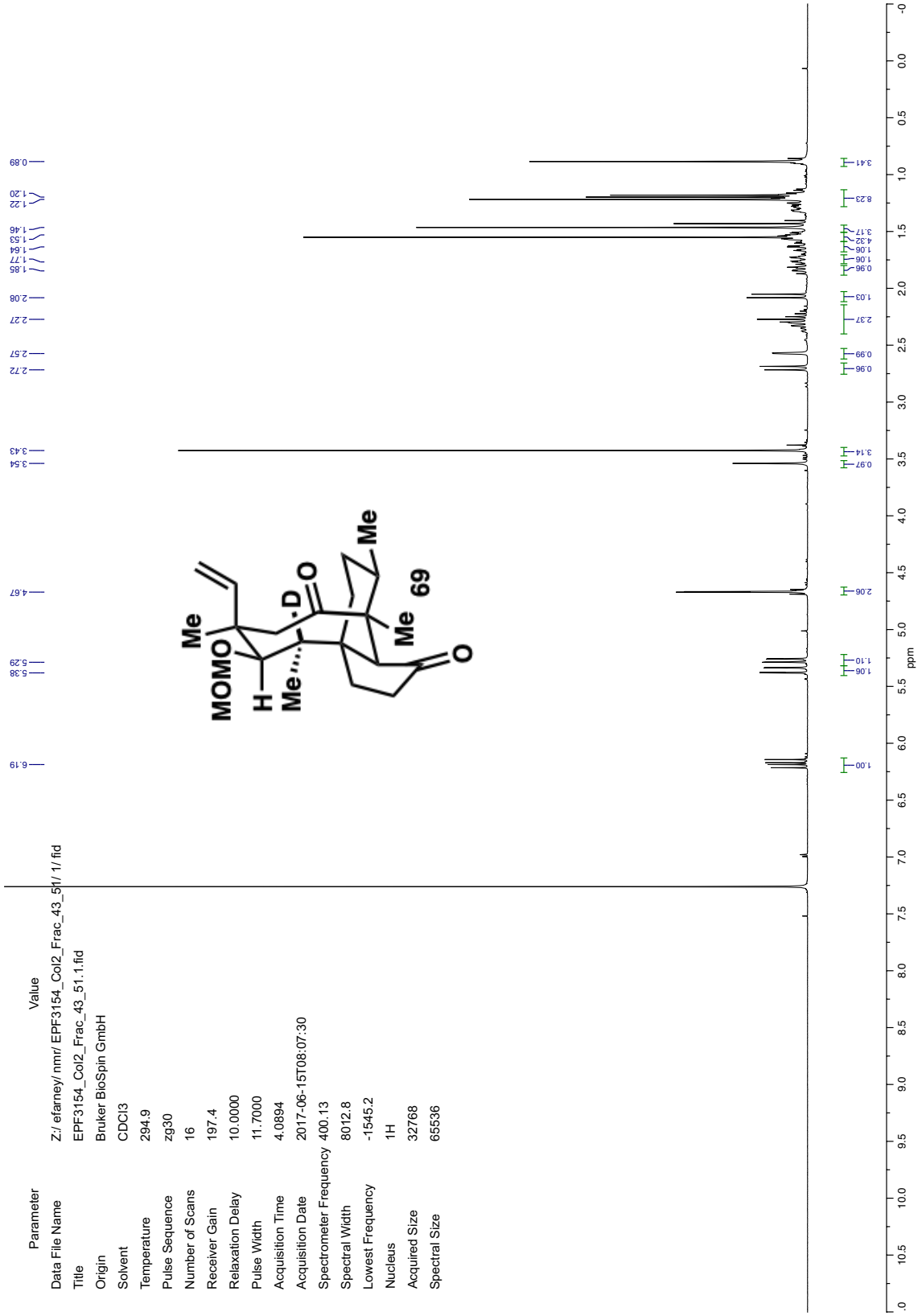
Parameter Value
Data File Name Z:/ efarney/ nmr/ EPF3154_Col2_Frac_43_51/ 1/ fid
Title EPF3154_Col2_Frac_43_51.1.fid
Origin Bruker BioSpin GmbH
Solvent CDCl3
Temperature 294.9
Pulse Sequence zg30
Number of Scans 16
Receiver Gain 197.4
Relaxation Delay 10.0000
Pulse Width 11.7000
Acquisition Time 4.0894
Acquisition Date 2017-06-15T08:07:30
Spectrometer Frequency 400.13
Spectral Width 8012.8
Lowest Frequency -1545.2
Nucleus 1H
Acquired Size 32768
Spectral Size 65536
MOMO
Me
H
Me
D
O
Me
Me
O
69
ppm

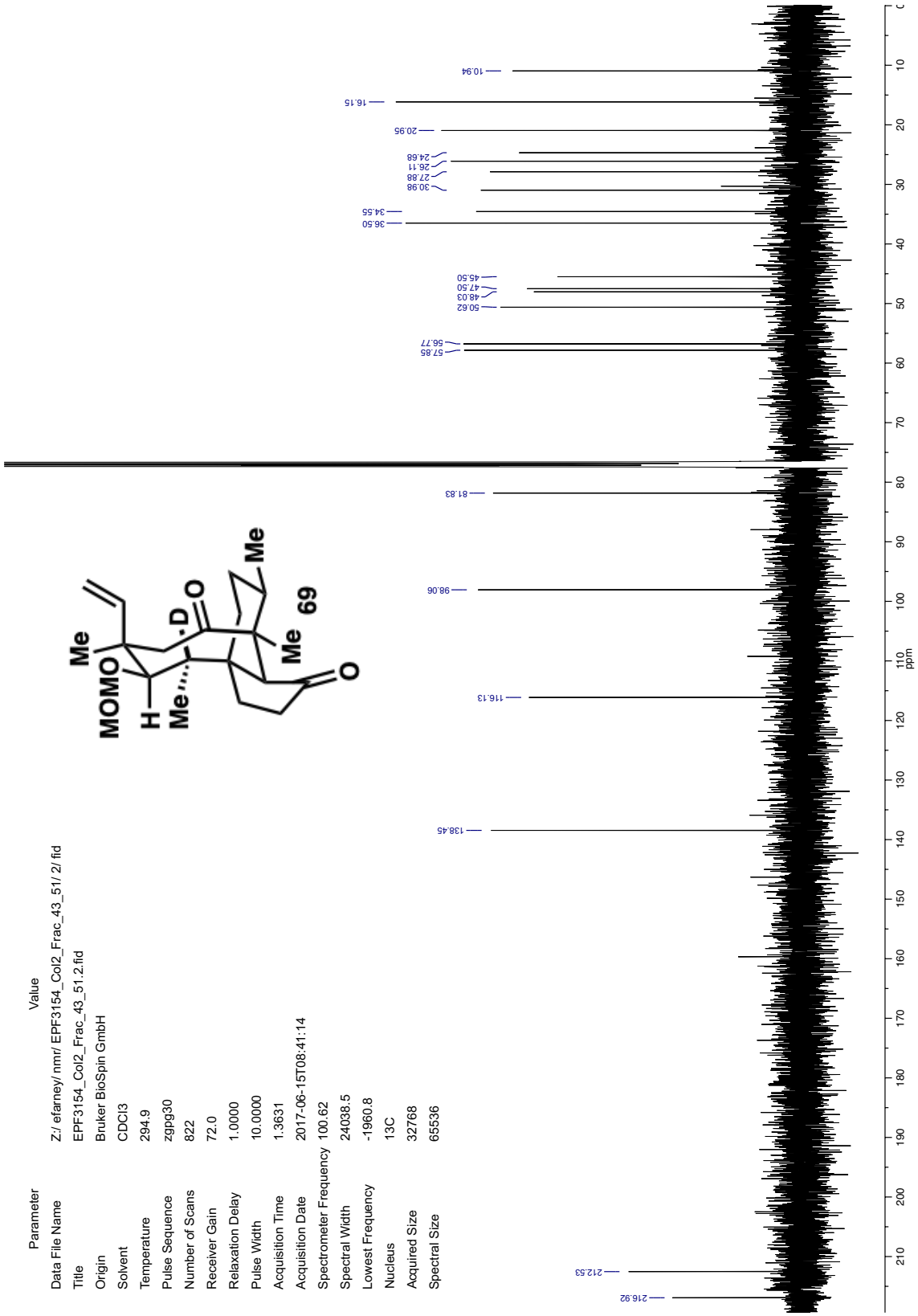
Parameter
Value
Data File Name
Z:/ efarney/ nmr/ EPF3154_Col2_Frac_43_51/ 2/ fid
Title
EPF3154_Col2_Frac_43_51.2.fid
Origin
Bruker BioSpin GmbH
Solvent
CDCl3
Temperature
294.9
Pulse Sequence
zgpg30
Number of Scans
822
Receiver Gain
72.0
Relaxation Delay
1.0000
Pulse Width
10.0000
Acquisition Time
1.3631
Acquisition Date
2017-06-15T08:41:14
Spectrometer Frequency
100.62
Spectral Width
24038.5
Lowest Frequency
-1960.8
Nucleus
13C
Acquired Size
32768
Spectral Size
65536
MOMO
Me
H
Me
D
O
Me
Me
69
O
10.94
16.15
20.95
24.68
26.11
27.88
30.98
34.55
36.50
45.50
47.50
48.03
50.62
56.77
57.85
81.83
98.06
116.13
138.45
212.53
216.92
ppm

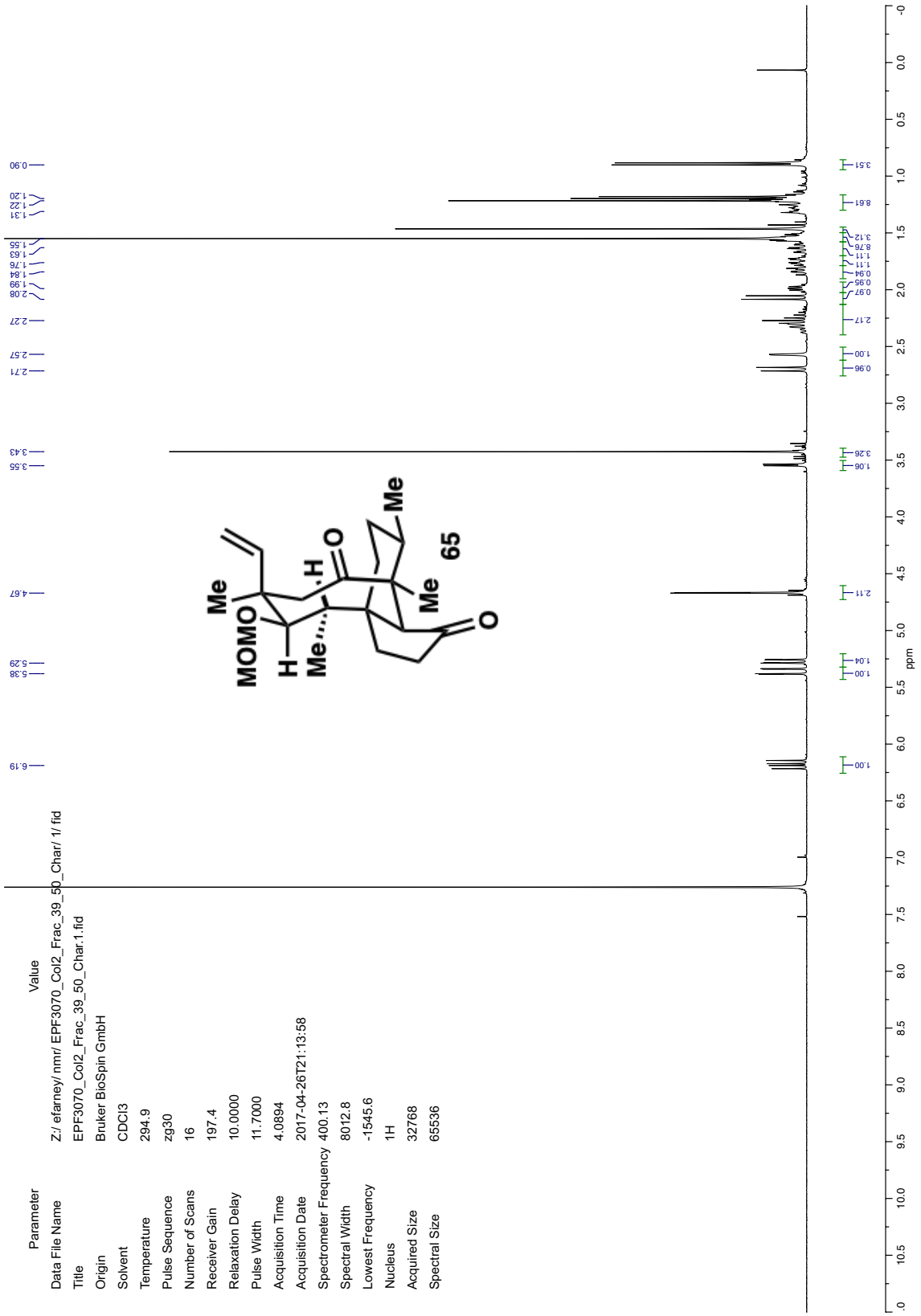
Parameter
Value
Data File Name
Z:/ efarney/ nmr/ EPF3070_Col2_Frac_39_50_Char/ 1/ fid
Title
EPF3070_Col2_Frac_39_50_Char.1.fid
Origin
Bruker BioSpin GmbH
Solvent
CDCl3
Temperature
294.9
Pulse Sequence
zg30
Number of Scans
16
Receiver Gain
197.4
Relaxation Delay
10.0000
Pulse Width
11.7000
Acquisition Time
4.0894
Acquisition Date
2017-04-26T21:13:58
Spectrometer Frequency
400.13
Spectral Width
8012.8
Lowest Frequency
-1545.6
Nucleus
1H
Acquired Size
32768
Spectral Size
65536
Me
MOMO
H
Me
H
O
Me
Me
O
65
ppm

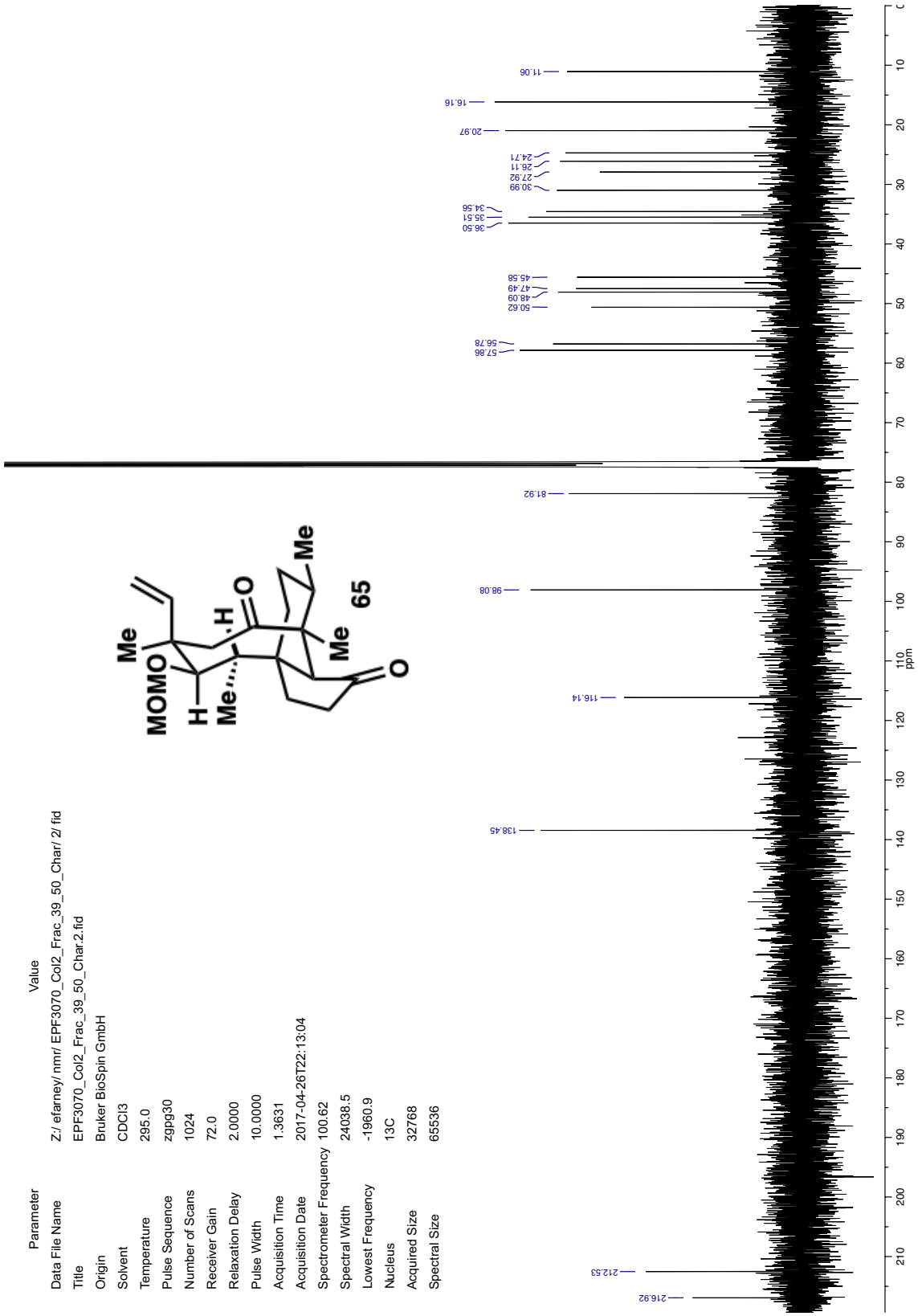
Parameter
Value
Data File Name
Z:/ efarney/ nmr/ EPF3070_Col2_Frac_39_50_Char/ 2/ fid
Title
EPF3070_Col2_Frac_39_50_Char.2.fid
Origin
Bruker BioSpin GmbH
Solvent
CDCl3
Temperature
295.0
Pulse Sequence
zgpg30
Number of Scans
1024
Receiver Gain
72.0
Relaxation Delay
2.0000
Pulse Width
10.0000
Acquisition Time
1.3631
Acquisition Date
2017-04-26T22:13:04
Spectrometer Frequency
100.62
Spectral Width
24038.5
Lowest Frequency
-1960.9
Nucleus
13C
Acquired Size
32768
Spectral Size
65536
MOMO
Me
H
Me
O
H
Me
Me
O
65
11.06
16.16
20.97
24.71
26.11
27.92
30.99
34.56
35.51
36.50
45.58
47.49
48.09
50.62
56.78
57.86
81.92
98.08
116.14
138.45
212.53
216.92
ppm

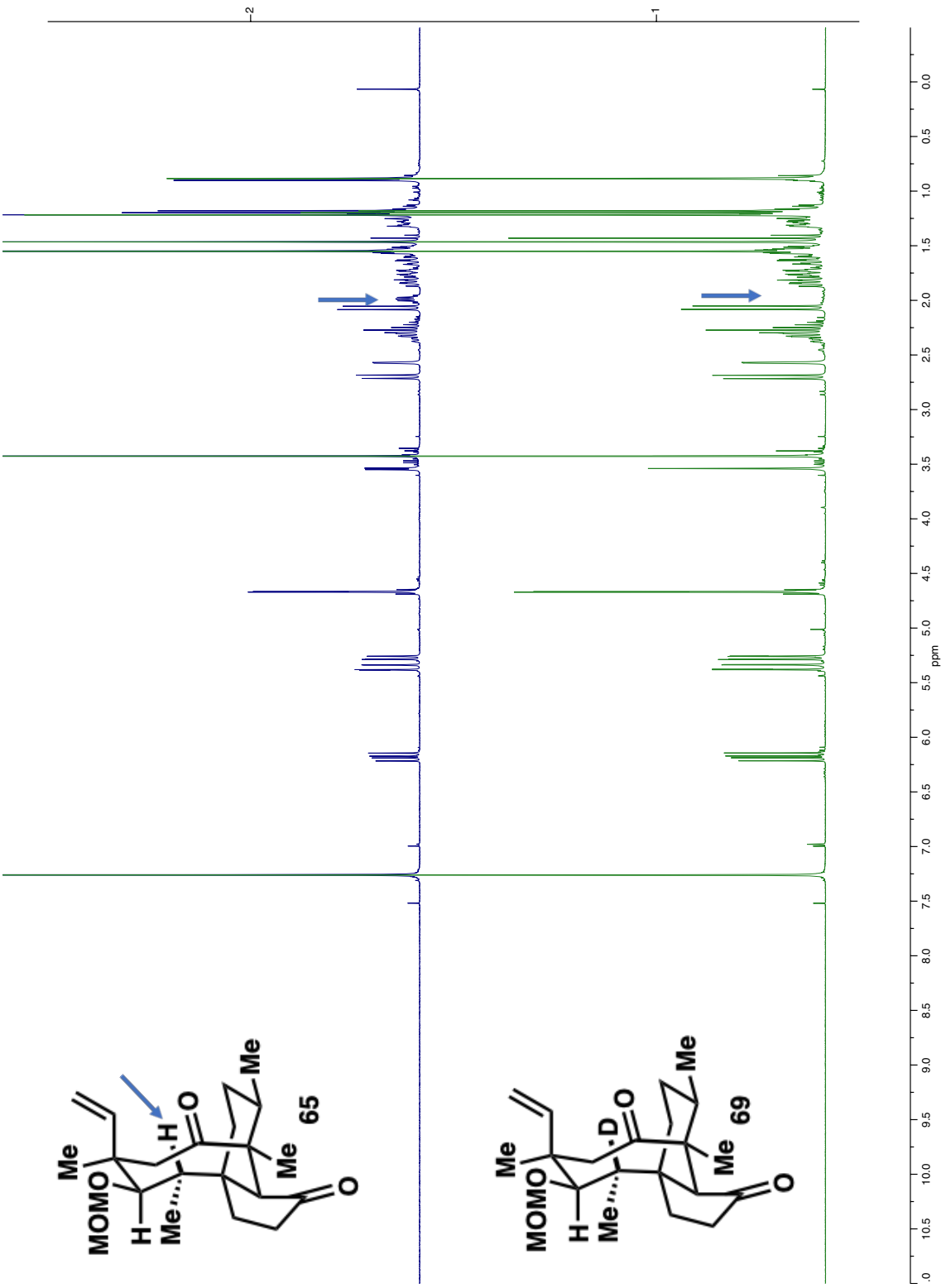
2
1
Me
MOMO
H
Me
H
O
Me
Me
O
65
Me
MOMO
H
Me
D
O
Me
Me
O
69
ppm

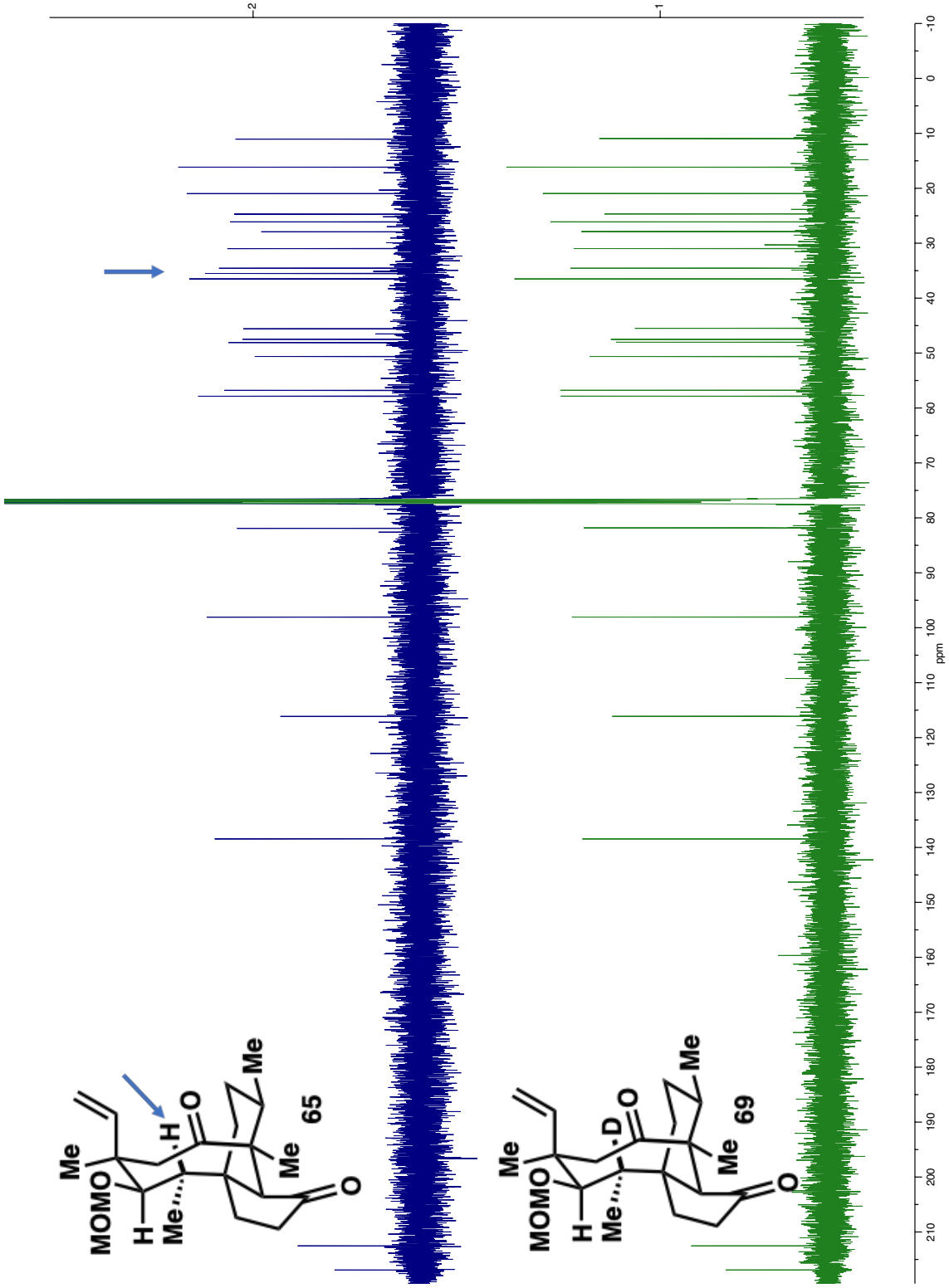
Me
MOMO
H
Me
H
O
Me
Me
O
65
Me
MOMO
H
Me
D
O
Me
Me
O
69
ppm

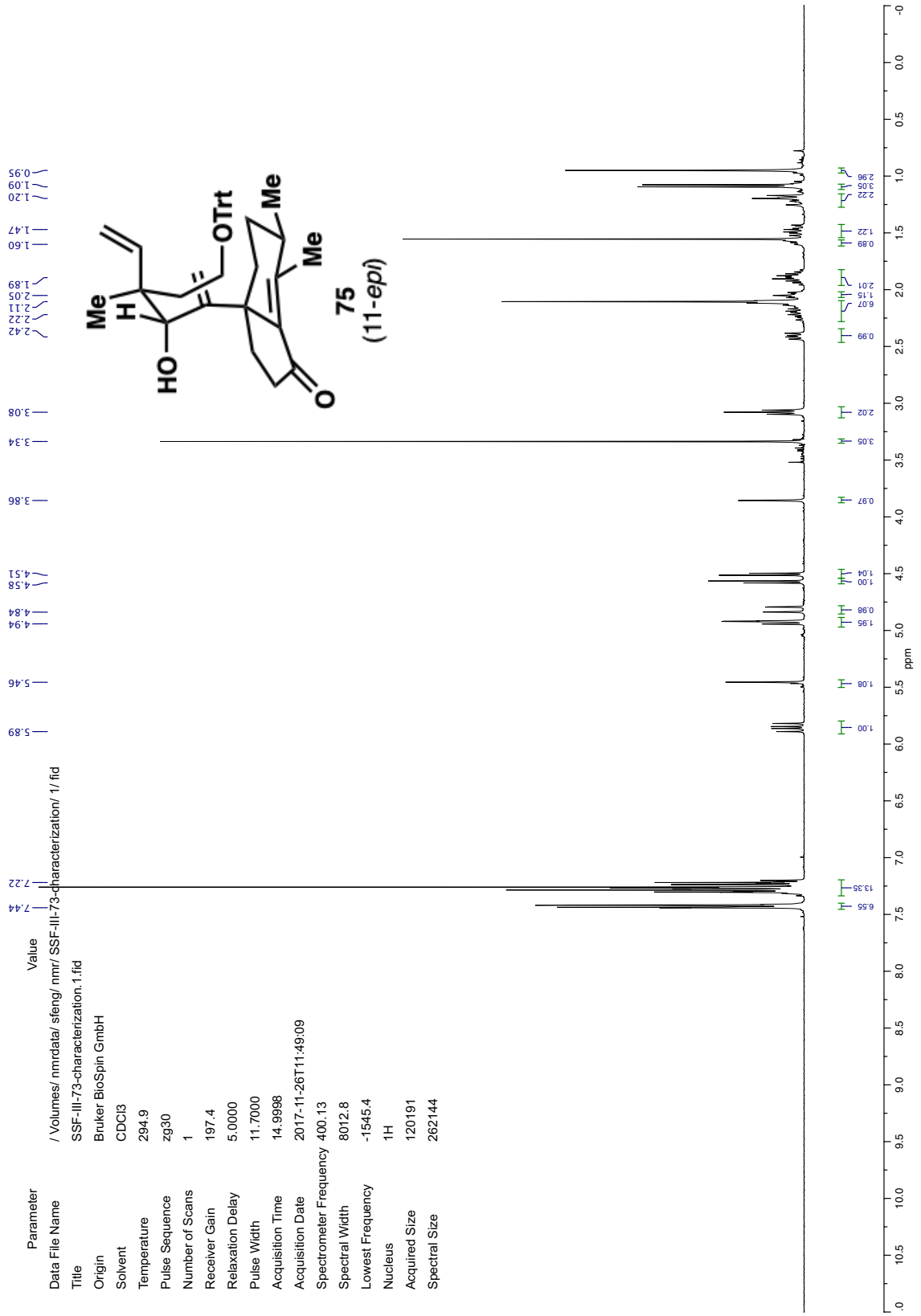
Me
H
HO
OTrt
Me
Me
O
75
(11-epi)
Parameter Value
Data File Name / Volumes/ nmrdata/ sfeng/ nmr/ SSF-III-73-characterization/ 1/ fid
Title SSF-III-73-characterization.1.fid
Origin Bruker BioSpin GmbH
Solvent CDCl3
Temperature 294.9
Pulse Sequence zg30
Number of Scans 1
Receiver Gain 197.4
Relaxation Delay 5.0000
Pulse Width 11.7000
Acquisition Time 14.9998
Acquisition Date 2017-11-26T11:49:09
Spectrometer Frequency 400.13
Spectral Width 8012.8
Lowest Frequency -1545.4
Nucleus 1H
Acquired Size 120191
Spectral Size 262144
ppm

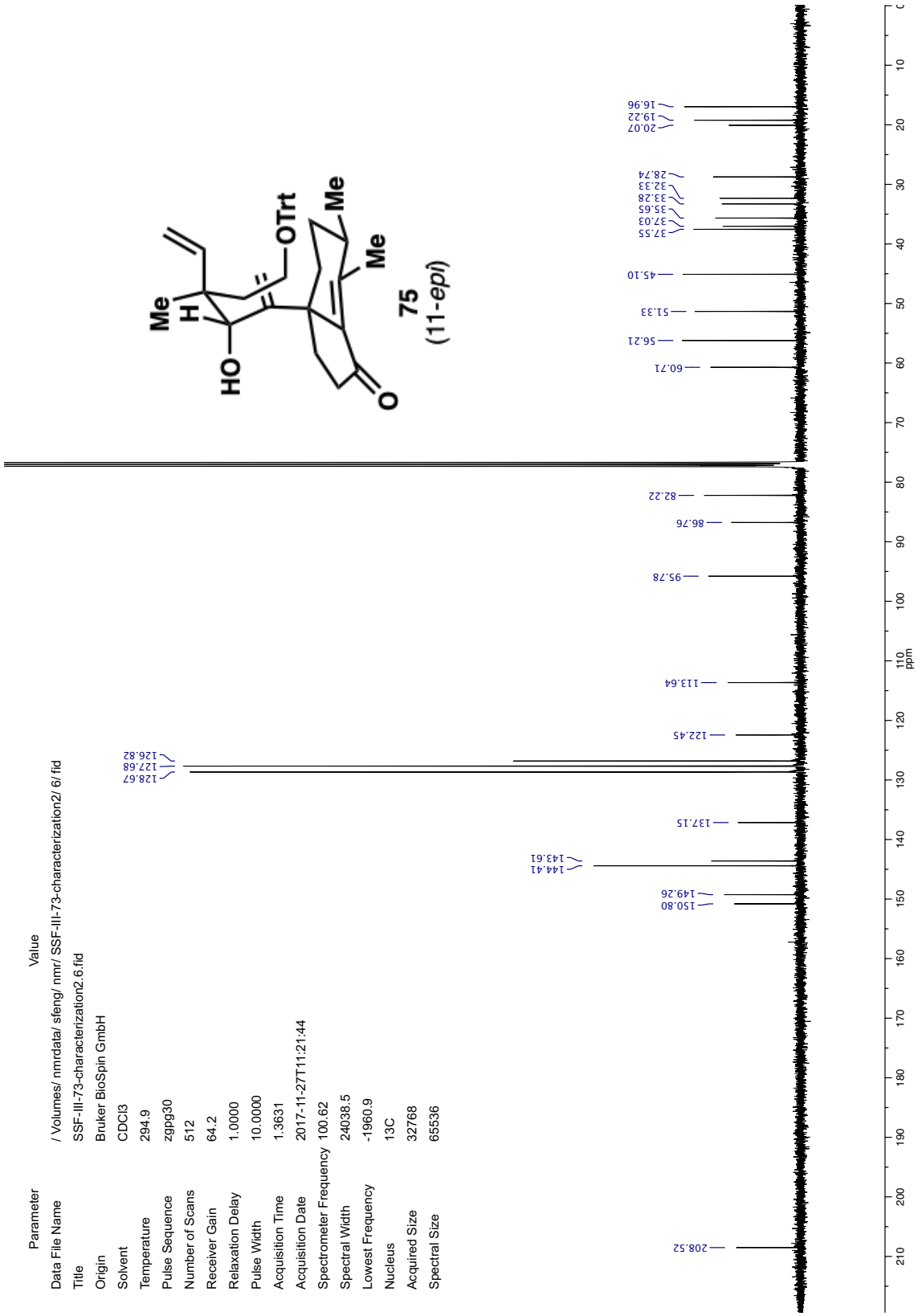

Parameter	Value
Data File Name	/ Volumes/ nmrdata/ sfeng/ nmr/ SSF-III-73-characterization2/ 6/ fid
Title	SSF-III-73-characterization2.6.fid
Origin	Bruker BioSpin GmbH
Solvent	CDCl3
Temperature	294.9
Pulse Sequence	zgpg30
Number of Scans	512
Receiver Gain	64.2
Relaxation Delay	1.0000
Pulse Width	10.0000
Acquisition Time	1.3631
Acquisition Date	2017-11-27T11:21:44
Spectrometer Frequency	100.62
Spectral Width	24038.5
Lowest Frequency	-1960.9
Nucleus	13C
Acquired Size	32768
Spectral Size	65536

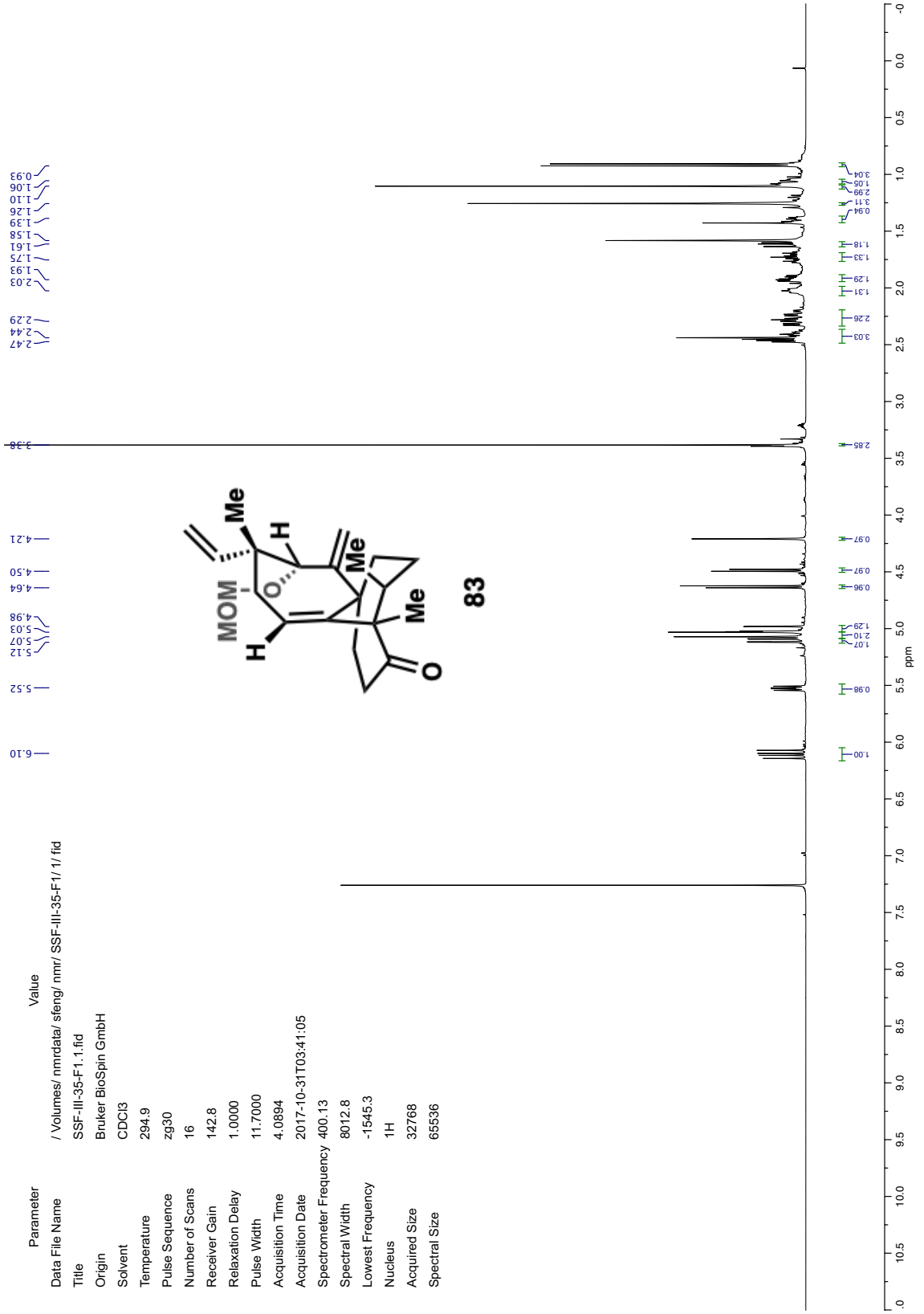
Parameter
Value
Data File Name / Volumes/ nmrdata/ sfeng/ nmr/ SSF-III-35-F1/ 1/ fid
Title SSF-III-35-F1.1.fid
Origin Bruker BioSpin GmbH
Solvent CDCl3
Temperature 294.9
Pulse Sequence zg30
Number of Scans 16
Receiver Gain 142.8
Relaxation Delay 1.0000
Pulse Width 11.7000
Acquisition Time 4.0894
Acquisition Date 2017-10-31T03:41:05
Spectrometer Frequency 400.13
Spectral Width 8012.8
Lowest Frequency -1545.3
Nucleus 1H
Acquired Size 32768
Spectral Size 65536
MOM
Me
H
Me
Me
O
O
H
83
ppm

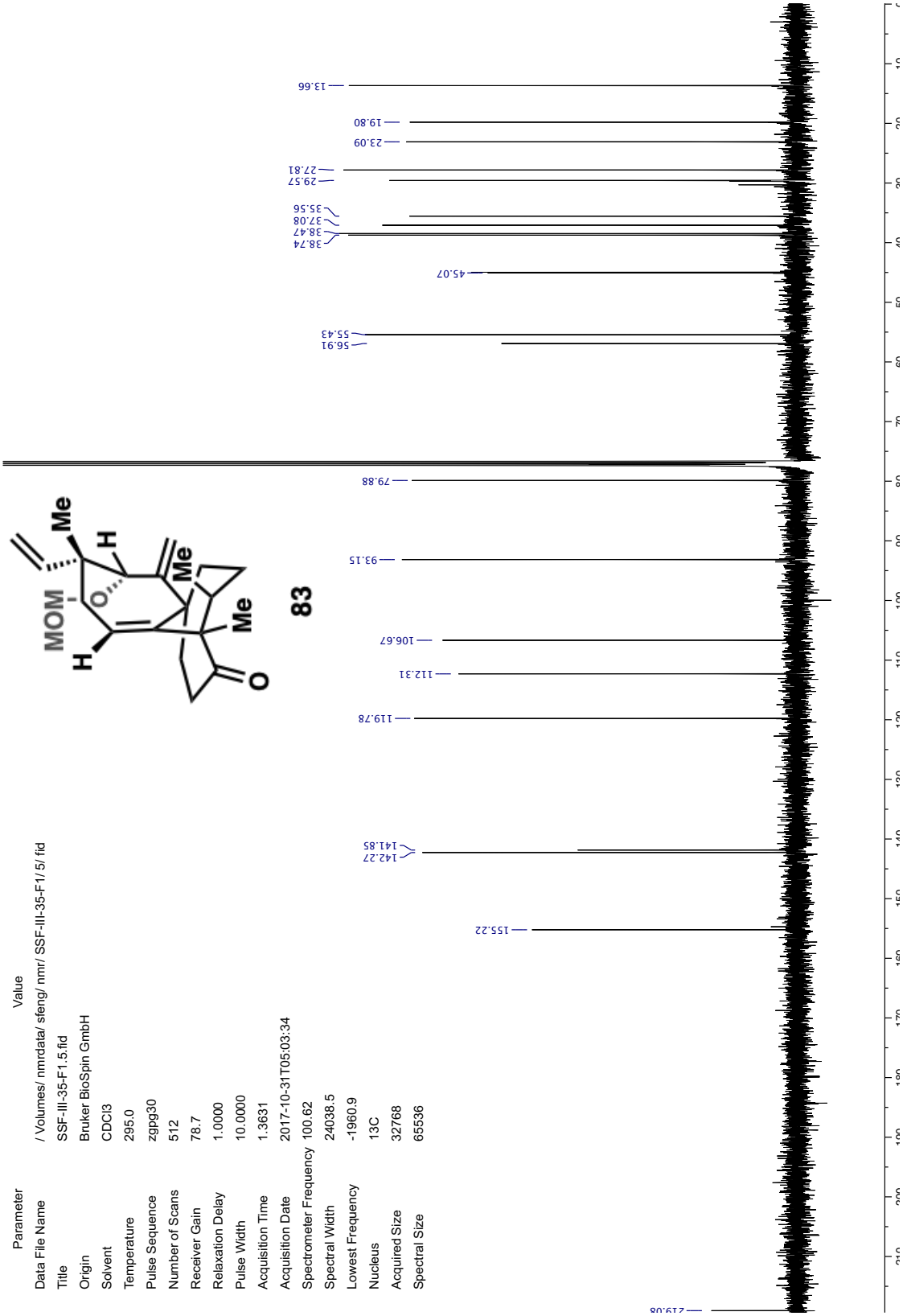
Parameter
Value
Data File Name / Volumes/ nmrdata/ sfeng/ nmr/ SSF-III-35-F1/ 5/ fid
Title SSF-III-35-F1.5.fid
Origin Bruker BioSpin GmbH
Solvent CDCl3
Temperature 295.0
Pulse Sequence zgpg30
Number of Scans 512
Receiver Gain 78.7
Relaxation Delay 1.0000
Pulse Width 10.0000
Acquisition Time 1.3631
Acquisition Date 2017-10-31T05:03:34
Spectrometer Frequency 100.62
Spectral Width 24038.5
Lowest Frequency -1960.9
Nucleus 13C
Acquired Size 32768
Spectral Size 65536
MOM
Me
Me
Me
H
H
O
O
83
219.08
155.22
142.27
141.85
119.78
112.31
106.67
93.15
79.88
56.91
55.43
45.07
38.74
38.47
37.08
35.56
29.57
27.81
23.09
19.80
13.66

Appendix 2

X-Ray Crystallography Reports Relevant to Chapter 2:
Total Synthesis of (+)-Pleuromutilin and (+)-12-epi-Pleuromutilin

Single Crystal X-ray Diffraction Data

Low-temperature diffraction data (φ- and ω-scans) were collected on a Bruker AXS D8 VENTURE KAPPA diffractometer coupled to a PHOTON 100 CMOS detector with Cu-K_α radiation (λ = 1.54178 Å) from a $I_\mu S$ HB micro-focus sealed X-ray tube. All diffractometer manipulations, including data collection, integration, and scaling were carried out using the Bruker APEXII software.[1] Absorption corrections were applied using SADABS.[2] The structure was solved by intrinsic phasing using SHELXT[3] and refined against F^2 on all data by full-matrix least squares with SHELXL-2014[4] using established refinement techniques.[5] All non-hydrogen atoms were refined anisotropically. Unless otherwise noted, all hydrogen atoms were included into the model at geometrically calculated positions and refined using a riding model. The isotropic displacement parameters of all hydrogen atoms were fixed to 1.2 times the *U* value of the atoms they are linked to (1.5 times for methyl and hydroxyl groups). Crystallographic data for **61**, **59**, and **83** can be obtained free of charge from The Cambridge Crystallographic Data Centre (CCDC) via www.ccdc.cam.ac.uk/data_request/cif under CCDC deposition numbers 1589653-1589655. Graphical representation of the structure with 50% probability thermal ellipsoids was generated using Mercury visualization software.[6]

Table 1: Crystal and refinement data for compounds 61, 59, and 83.

	61	**59**	**83**
CCDC Number	1589655	1589654	1589653
Empirical formula	$C_{22}H_{34}O_6$	$C_{22}H_{34}O_4$	$C_{22}H_{32}O_3$
Formula weight	394.49	362.49	344.47
T (K)	100	100	100
Crystal system	Orthorhombic	Orthorhombic	Orthorhombic
Space group	$P2_12_12_1$	$P2_12_12_1$	$P2_12_12_1$
a, Å	7.2336(4)	8.8601(3)	7.4344(9)
b, Å	16.5583(8)	11.6560(4)	11.7916(15)
c, Å	34.6198(18)	37.8871(14)	21.810(3)
α, °	90	90	90
β, °	90	90	90
γ, °	90	90	90
Volume, $Å^3$	4146.6(4)	3912.7(2)	1912.0(4)
Z	8	8	4
d_{calc}, g/cm^3	1.264	1.231	1.197
Abs. coeff. (mm^{-1})	0.738	0.658	0.609
θ range, °	2.552 to 79.430	3.968 to 79.461	4.054 to 78.898
Abs. correction	Semi-empirical	Semi-empirical	Semi-empirical
GOF	1.066	1.097	1.064
R_1,[a] wR_2,[b] [I>2σ(I)]	0.0345, 0.0897	0.0339, 0.0877	0.0291, 0.0764
Flack parameter	0.04(3)	0.06(2)	0.00(4)
Extinction coefficient	n/a	0.00096(12)	0.0103(7)

[a] $R_1 = \Sigma||F_o|-|F_c||/\Sigma|F_o|$. [b] $wR_2 = [\Sigma[w(F_o^2-F_c^2)^2]/\Sigma[w(F_o^2)^2]]^{1/2}$.

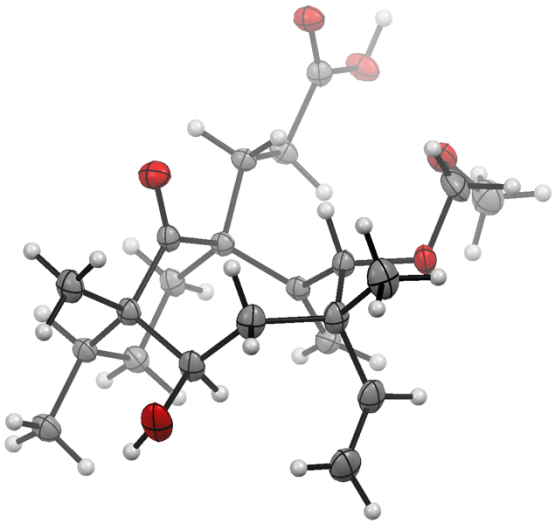

Figure 1: Structure of **61** with 50% probability anisotropic displacement ellipsoids. The second molecule of **16** is omitted for clarity.

Special Refinement Details for 61

Compound **61** crystallizes in the orthorhombic space group $P2_12_12_1$ with two molecules in the asymmetric unit. The coordinates for the hydrogen atoms bound to O2A, O4A, O2B, and O4B were located in the difference Fourier synthesis and refined using a riding model. No hydrogen bond acceptor was found for O2B. Absolute configuration was determined by anomalous dispersion (Flack = 0.04(3)).[6]

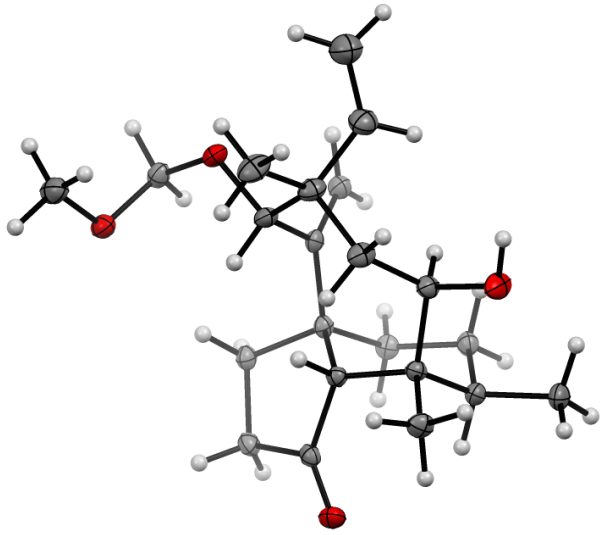

Figure 2: Structure of **59** with 50% probability anisotropic displacement ellipsoids. The second molecule of **17** is omitted for clarity.

Special Refinement Details for 59

Compound **59** crystallizes in the orthorhombic space group $P2_12_12_1$ with two molecules in the asymmetric unit. The coordinates for the hydrogen atoms bound to O2A and O2B were located in the difference Fourier synthesis and refined using a riding model. Absolute configuration was determined by anomalous dispersion (Flack = 0.06(2)).[6]

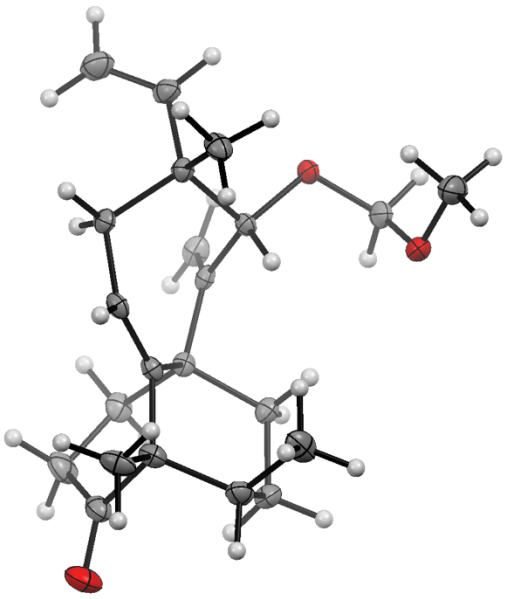

Figure 3: Structure of **83** with 50% probability anisotropic displacement ellipsoids.

Special Refinement Details for 83

Compound **83** crystallizes in the orthorhombic space group $P2_12_12_1$ with one molecule in the asymmetric unit. Absolute configuration was determined by anomalous dispersion (Flack = 0.00(4)).[6]

1. APEX2, Version 2 User Manual, M86-E01078, Bruker Analytical X-ray Systems, Madison, WI, **June 2006**.
2. Sheldrick, G.M. *"SADABS (version 2008/1): Program for Absorption Correction for Data from Area Detector Frames"*, University of Göttingen, **2008**.
3. Sheldrick, G. *Acta Crystallogr., Sect. A: Found. Crystallogr*. **2008**, *64*, 112.
4. Müller, P. *Crystallogr. Rev.* **2009**, *15*, 57.
5. Macrae, C. F.; Edgington, P. R.; McCabe, P.; Pidcock, E.; Shields, G. P.; Taylor, R.; Towler M.; van de Streek, J. *J. Appl. Cryst.* **2006**, *39*, 453.
6. Parsons, S; Flack, H. D; Wagner, T. *Acta Crystallogr*. **2013**, *B69*, 249.

Chapter 3

Progress Towards the Total Synthesis of (–)-Merrilactone A

3.1 INTRODUCTION

The *Illicium* family of neurotrophic natural products has received remarkable attention from the synthetic community not only for their challenging chemical structures but also for their promising biological activities. Since their discovery as small molecules that are capable of promoting outgrowth in neuronal cultures, synthetic chemists across the field have sought to develop novel synthetic routes to access these natural products.[1–25]

Amongst the *Illicium* natural products, comprehensive biological investigation of merrilactone A has been limited, as the *Illicium* genus only produces it in quantities of parts-per-million. Structurally, merrilactone A is a complex cage-shaped pentacyclic sesquiterpene that contains a highly strained oxetane moiety. Its lack of natural availability, coupled with its densely functionalized and complex architectural framework has attracted

considerable attention from the synthetic community. However, the syntheses to date do not address the shortage of material needed for biological studies. Recognizing this quandary as an opportunity for the development of a concise synthesis with the prospect of new reaction development, a synthetic campaign towards (–)-merrilactone A was initiated. This chapter will outline the development of a novel Pd-catalyzed asymmetric allylic alkylation reaction for the synthesis of vicinal quaternary centers that will enable our synthetic studies towards (–)-merrilactone A.

3.2 NEUROTROPHINS AND CURRENT LIMITATIONS

Neurodegeneration poses a serious threat to human health and is the hallmark of many diseases including Alzheimer's disease, Parkinson's disease, motor neuron diseases, Huntington's disease, spinocerebellar ataxia, spinal muscular atrophy, and amyotrophic lateral sclerosis. Individuals diagnosed with neurological disorders have few treatment options, which leaves them to endure poor quality of life and ultimately results in death. The prevalence of neurodegenerative brain disorders increases dramatically with advanced age, and with the increasing average life expectancy, the projected financial, societal, and emotional costs of treating these disorders are expected to be staggering.[26,27] Thus, uncovering novel treatments or preventative interventions for brain related neurodegenerative disorders is paramount to reducing these growing health threats.

Neurotrophic factors present a compelling opportunity for treating neurological disorders. Studies have demonstrated that under conditions of neurodegeneration, supra-physiological (i.e., biopharmaceutical) application of neurotrophic factors can activate neuronal repair genes.[28] Induction of these repair genes by neurotrophins is reported to

produce morphological and functional restoration of the degenerating neurons, preventing further neurodegeneration while also protecting against cell death.[29] Since the discovery of the first neurotrophin, NGF (**1**, Figure 1), neurotrophic factors have become the focus of substantial interdisciplinary research due to their therapeutic potential; however efforts to translate this potential to the clinic has been unsatisfactory, as *in vivo* evaluation requires direct microinjection of the peptides into the brain.[29] Currently, most well-characterized neurotrophins are naturally occurring polypeptidic or protein based biomolecules (NGF, BDNF, GDNF, NT4/5, NT6) which are too large to cross the blood–brain barrier. These suboptimal pharmacological properties are a serious impediment to future development and applications as treatment for neurodegeneration in humans.[30] In contrast to protein neurotrophins such as NGF, small-molecule neurotrophins are of considerable interest because of their desirable pharmacokinetic properties and pharmacological advantages: low molecular weight, high serum stability, and most importantly, blood–brain barrier permeability.

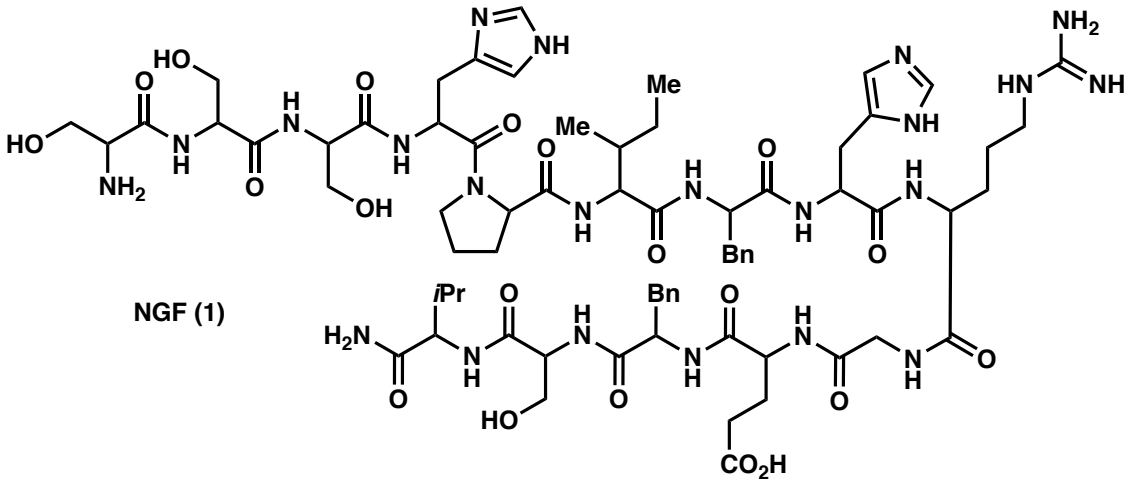

Figure 1. Known polypeptide neurotrophic factor, NGF, **1**.

3.3 OVERVIEW OF ILLICIUM SESQUITERPENES AND PROPOSED BIOSYNTHETIC PATHWAY

To date, over 100 sesquiterpene lactones have been isolated from the *Illicium* genus of plants. Collectively known as *Illicium* sesquiterpenes, these natural products share a common ring system that have varying oxidation patterns. Initial isolations, for example of anisatin **(2)** and pseudoanisatin (**3**), were guided by their potent neurotoxic activities (Figure 2).[31,32] More recently, Fukuyama and coworkers have demonstrated that a number of natural products of the same family, such as jiadifenolide (**4**) and merrilactone A (**5**), do not share this same toxicity profile but instead stimulate neurite outgrowth at low nanomolar to low micromolar concentrations in primary cultures of fetal rat cortical neurons.[33] Such results have drastic implications in the study of neurodegenerative diseases such as Alzheimer's and Parkinson's[28,34] and this difference in activity truly highlights how slight oxidation state changes in this family of natural products leads to profoundly different biological activities.

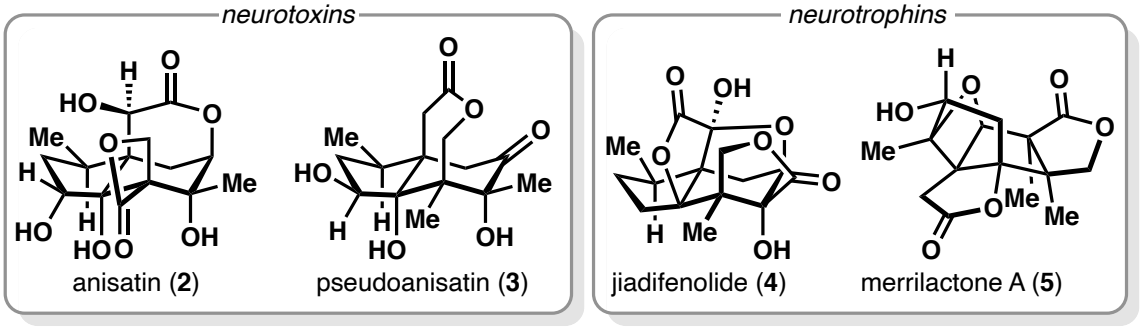

Figure 2. Neurotoxic and neurotophic *Illicium* sesquiterpenes.

The *Illicium* sesquiterpene family member subtypes are ultimately categorized by two things: their differing lactonization patterns that are established through rearrangement

during the cyclase phase of the biosynthesis and their differing oxidation patterns. (Figure 3).

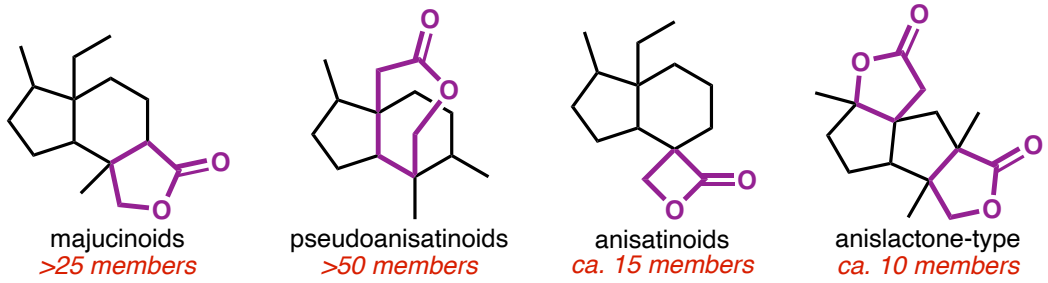

Figure 3. *Illicium* sesquiterpene subtypes based on lactonization pattern.

The proposed biosynthesis of this class of natural product commences with cyclization of farnesyl pyrophosphate **6** to give bisabolyl cation **7** (Scheme 1). A subsequent series of hydride shifts and cyclizations give rise to the polycyclic *allo*-cedrane skeleton **12**.[33] At this stage, a series of oxidations can lead to the *allo*-cedrane sesquiterpenes, such as 11-*O*-debenzoyl-tashironin (**17**). Alternatively, C–C bond cleavages would forge the *seco*-prezizaane **13** or anislactone-type **16** skeletons. Subsequent selective enzymatic oxidations can then afford *Illicium* members such as majucin (**14**) and merrilactone A (**5**).

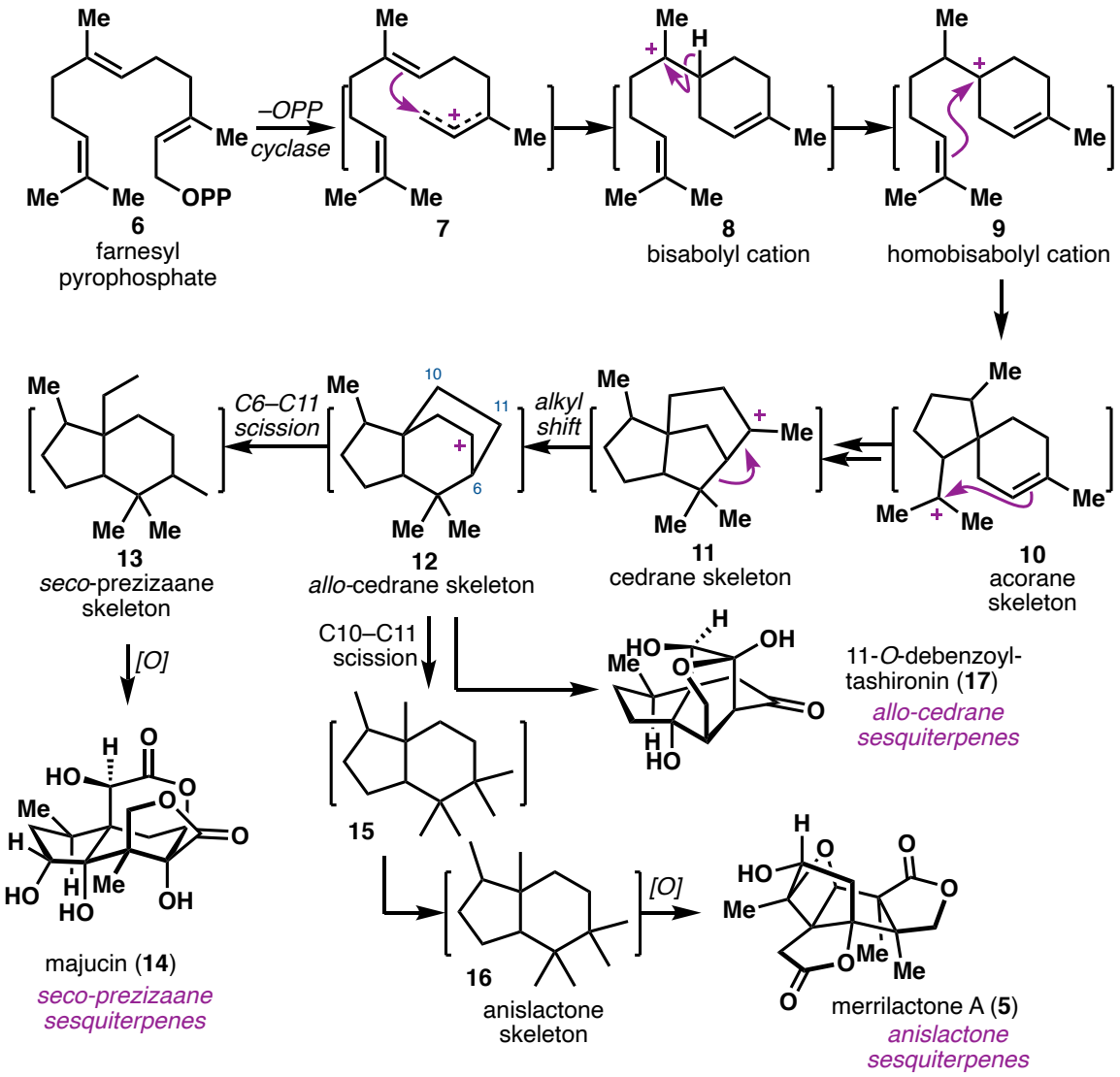

Scheme 1. Proposed biosynthesis of *Illicium* sesquiterpenoids.

3.4 (–)-MERRILACTONE A

Merrilactone A (**5**) is a pentacyclic sesquiterpene dilactone isolated from *Illicium merrillianum* by Fukuyama and coworkers in 2000 (Figure 4). It was identified as a nonpeptidal neurotrophic factor that promotes neurite outgrowth in the culture of fetal rat cortical neurons at potent concentrations of 0.1 μmol/L.[1,30]

In addition to its interesting bioactivity, the dense triquinane-like carbon skeleton has garnered much interest from the synthetic community due to its oxygenation pattern and structural complexity. Merrilactone A (**5**) contains seven contiguous stereocenters, three of which are quaternary and two of which are vicinal. It also bears an oxetane linkage bridging the β-faces of C7 and C1, making the overall structure highly compact and caged.

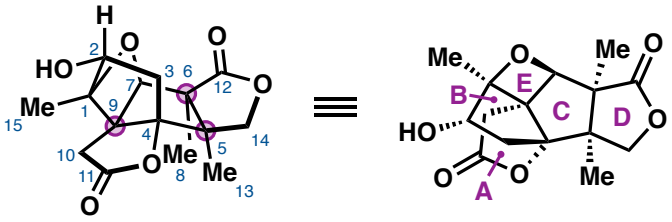

(–)-merrilactone A (**5**)

Figure 4. Structure and numbering of (–)-merrilactone A (**5**).

3.5 PREVIOUS SYNTHESES OF MERRILACTONE A

Over the past two decades, there have been numerous efforts throughout the synthetic community toward developing *de novo* syntheses of (–)-merrilactone A (**5**).[2–8,11,12,14,16,17] Because synthetic work in this area is quite extensive, this section will be focused on a selection of completed syntheses of merrilactone A (**5**), highlighting distinct strategies used in constructing this natural product as well as common features.

3.5.1 *Fukuyama's Semisynthesis*

Structurally, merrilactone A (**5**) is related to anislactone A and B (**18**), a pair of epimeric sesquiterpene dilactones discovered ten years prior by Kouno and coworkers from the plant *Illicium anistatum*.[35] Fukuyama was able to convert anislactone B (**18**) to merrilactone A (**5**) using a three-step sequence, suggesting that the anislactones may be

biogenetic precursors to merrilactone A (**5**).[1] The two-step sequence from Fukuyama's intermediate involves 1) epoxidation and 2) homo-Payne rearrangement, and has been adopted by many groups for the construction of the oxetane E ring in order to access merrilactone A (**5**).

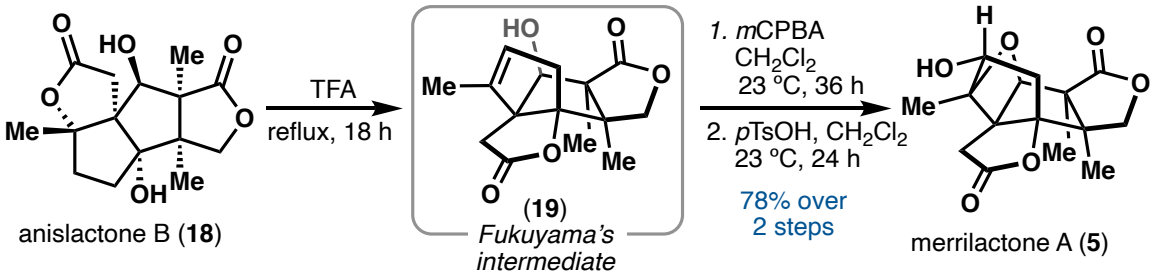

Scheme 1. Conversion of anislactone B (**18**) to merrilactone A (**5**).

3.5.2 *Danishefsky's Racemic Synthesis*

Danishefsky and coworkers developed the first racemic synthesis of merrilactone A (**5**) in 2002, and later translated this strategy into an asymmetric synthesis.[2,6] Their racemic synthesis commenced with a Diels-Alder reaction between 2,3-dimethylmaleic anhydride **21** and diene **20** to afford bicycle **22** (Scheme 2). In five steps, they were able to elaborate the cyclic anhydride **22** to bicyclic lactone **23**, completing the D ring.

Initial efforts to accomplish this transformation in a single step using conventional borohydride reagents led to complex mixtures, where ultimately a five-step protocol was developed that involved opening of the anhydride, converting to a diester, reduction, and saponification to afford the desired lactone **23**. At this stage, conversion to **24** was accomplished through a three-step procedure that involved ozonolysis, enamine-promoted aldol cyclization, and borohydride reduction to afford the C ring **24**. Installation of the C9 methylene carboxylic acid fragment was performed through a Johnson–Claisen

rearrangement, followed by saponification to produce a mixture of carboxylic acids **25** in 1.8:1 dr that were inseparable until iodolactonization was performed to forge the A ring **26**. Construction of the final B ring was accomplished in six steps through a radical cyclization reaction to afford Fukuyama's intermediate **19**, which was then epoxidized and subjected to an acid-promoted homo-Payne rearrangement to afford merrilactone A (**5**) in 20 linear steps.

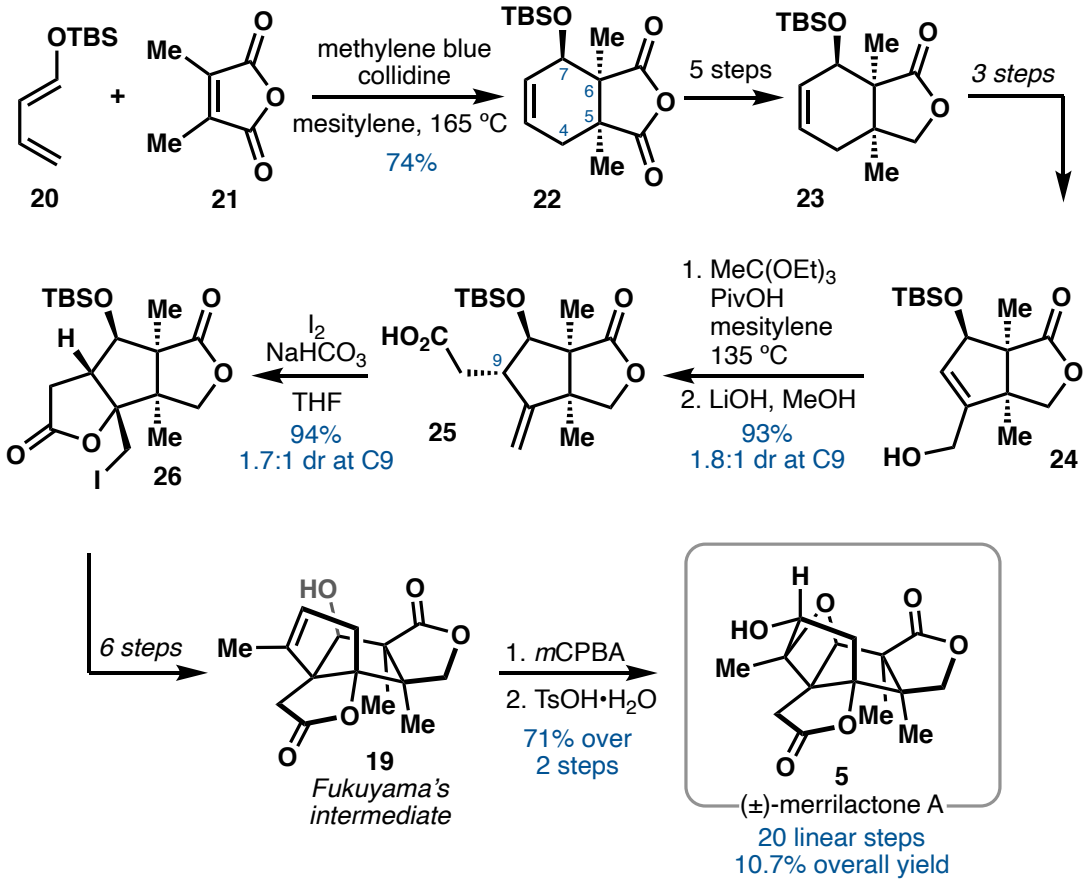

Scheme 2. Danishefsky's racemic synthesis of merrilactone A (**5**).

3.5.3 *Frontier's Racemic Synthesis*

Frontier and coworkers developed a concise racemic synthesis of merrilactone A (**5**) featuring a key Nazarov cyclization to establish the C ring of the natural product.[11]

Their synthesis commenced with conversion of ynol **27** to substituted furan **28** that later served as the A ring lactone (Scheme 3). Lithium-halogen exchange of **28** and treatment with Weinreb amide **29** afforded coupled product **30**, which was poised for their key Nazarov cyclization reaction. As planned, Nazarov cyclization of **30** proceeded smoothly using a dicationic iridium catalyst to afford a single diastereomer of bicycle **31**. Initial attempts to cyclize protected alkyne **31** failed to provide tricycle **33**. However, desilylation to afford **32** allowed smooth radical cyclization to **33**.

To forge the final D ring, a three-step protocol was developed. **33** was subjected to fluoride-mediated silyl deprotection conditions, converted to the carbonate, and intramolecularly lactonized upon treatment with base to afford tetracycle **34**. The C6 vicinal quaternary center was installed through α-methylation in near quantitative yield and complete diastereoselectivity. Reduction of ketone **35** with sodium borohydride afforded a 1.2:1 mixture of diastereomers **36** at the resultant alcohol which could be reoxidized and resubjected to increase product yield. Exocyclic olefin **19** was isomerized under acidic conditions to afford Fukuyama's intermediate **19**. Epoxidation and homo-Payne rearrangement afforded merrilactone A (**5**) in 17 linear steps from ynol **27**.

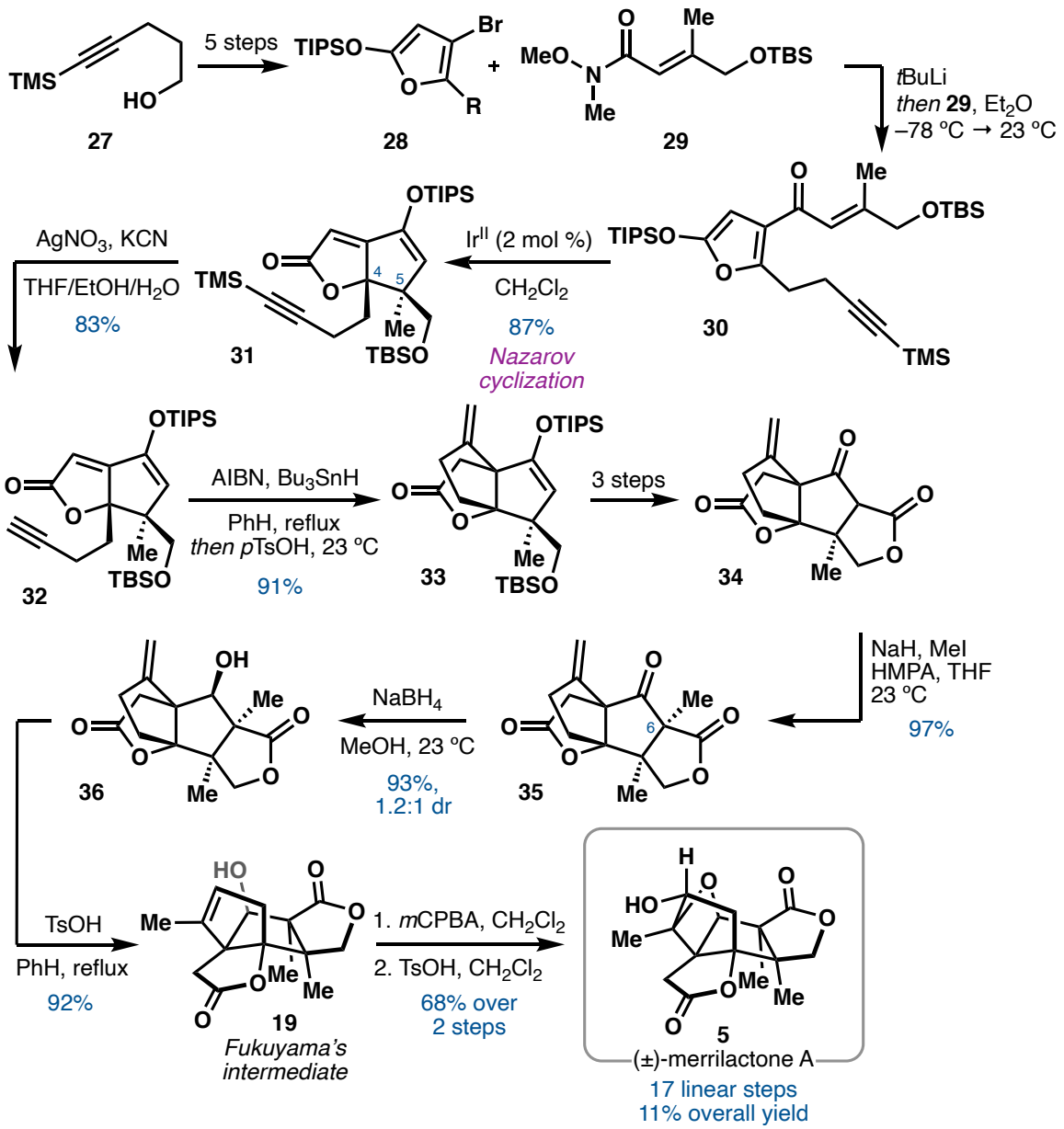

Scheme 3. Frontier's racemic synthesis of merrilactone A (**5**).

3.5.4 *Inoue's Asymmetric Synthesis*

In 2003, Inoue and coworkers developed a racemic[3] synthesis of merrilactone A (**5**) prior to their asymmetric[7,12] synthesis in 2006. Lactone **38**, which is available in five steps from 2,3-dimethylmaleinic anhydride, underwent a [2+2] photocycloaddition with cis-2,3-dichloroethylene **37** to afford bicycle **39** (Scheme 4). A subsequent eight steps afforded

key intermediate **40** where a bis(trifluoromethyl)benzyl (BTB) group was installed as a bulky protecting group to differentiate C5 from C6. **40** was then subjected to a ring-closing metathesis reaction to produce a bicyclo[4.2.0]octyl system, which was then subjected *in situ* to lead(IV) tetraacetate-promoted oxidative ring expansion to yield the substituted eight-membered ring **41**. At this stage, the key transannular aldol reaction was performed and site-selective deprotonation and diastereoselective C4–C9 bond formation was observed to afford bicycle **42**. In 13 steps, the A and D rings were installed to afford Fukuyama's intermediate, which could be elaborated to (–)-merrilactone A (**5**) in two steps making their asymmetric synthesis 31 linear steps.

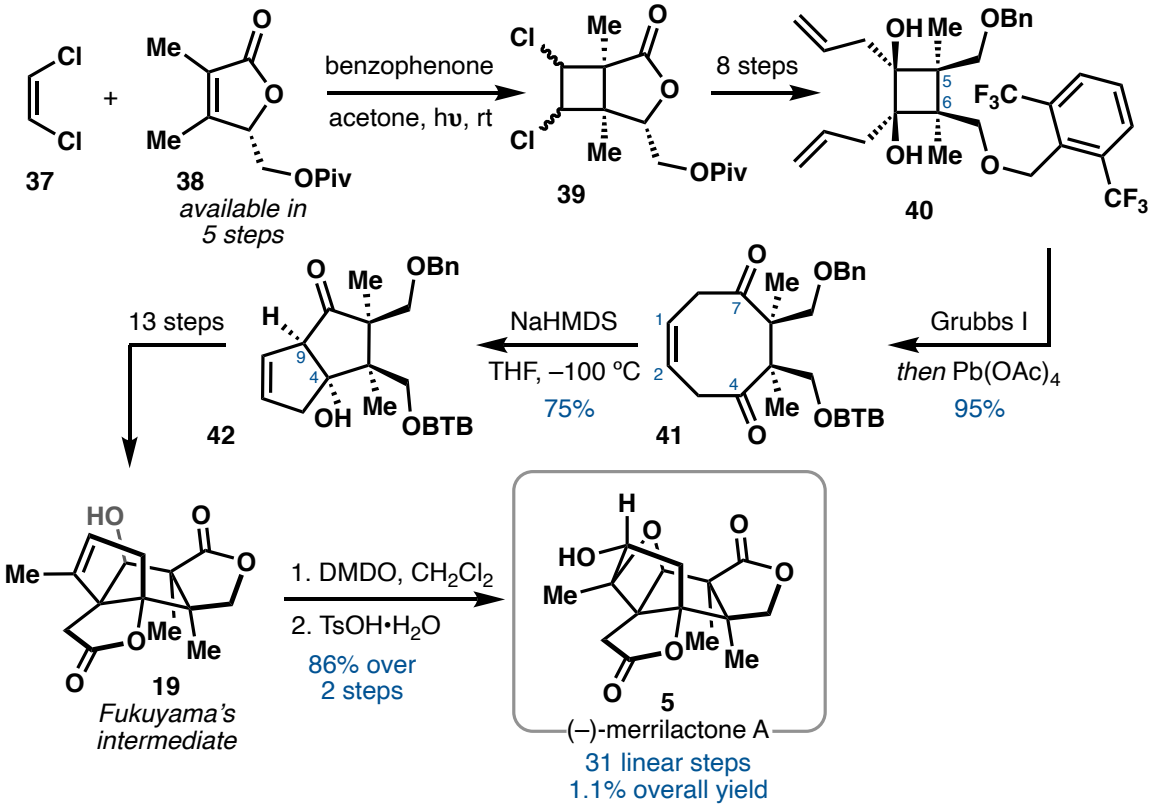

Scheme 4. Inoue's asymmetric synthesis of (–)-merrilactone A (**5**).

In summary, there have been numerous different approaches towards merrilactone A (**5**); however, none have suitably addressed the material demand for thorough biological

studies of this natural product (Table 1). Structurally, the C5 and C6 vicinal quaternary centers within such a compact and densely functionalized scaffold also present a unique challenge and are an opportunity for the development of new methodologies to access this type of structural motif. For the aforementioned reasons, efforts towards an asymmetric synthesis were initiated. It was envisioned that our synthesis would allow investigators to design analogues through elaboration of key intermediates to address questions surrounding the biological target, its ability to cross the blood-brain barrier, and the rational design of potent synthetic neurotrophic small molecules.

Entry	Laboratory (year)	C5/C6	Longest Linear Sequence	Yield (%)	Series (±)
1	Danishefsky (2001)	[4+2]	20 steps	11	(±)
2	Inoue & Hirama (2006)	[2+2]	31 steps	1.1	(–)
3	Inoue (2007)	[2+2]	23 steps	1.7	(+)
4	Mehta (2006)	[2+2]	21 steps	0.0042	(±)
5	Greaney (2010)	[2+2]	25 steps	4	(±)
6	Frontier (2006)	Nazarov/Enolate	17 steps	3.7	(±)
7	Zhai (2012)	[3,3]/Enolate	18 steps	3.7	(±)
8	Wang (2018)	–	15 steps	1.5	(±)

Table 1. Summary of prior syntheses of merrilactone A (**5**).

3.6 RETROSYNTHETIC ANALYSIS

Retrosynthetically, it was envisioned that (–)-merrilactone A (**5**) would arise from Fukuyama's intermediate (**19**) through epoxidation and Payne rearrangements as reported by many other prior syntheses (Scheme 5). The A ring of **19** could then be accessed through lactonization of acetylated **43**, which could be obtained through a selenium(II) oxide mediated allylic C–H oxidation[36] from tricycle **44**. The B ring of tricycle **44** could be forged

through an intramolecular Pauson–Khand reaction from enyne **45**. Enyne **45** could then be synthesized from **46** through a nucleophilic propynyl addition.

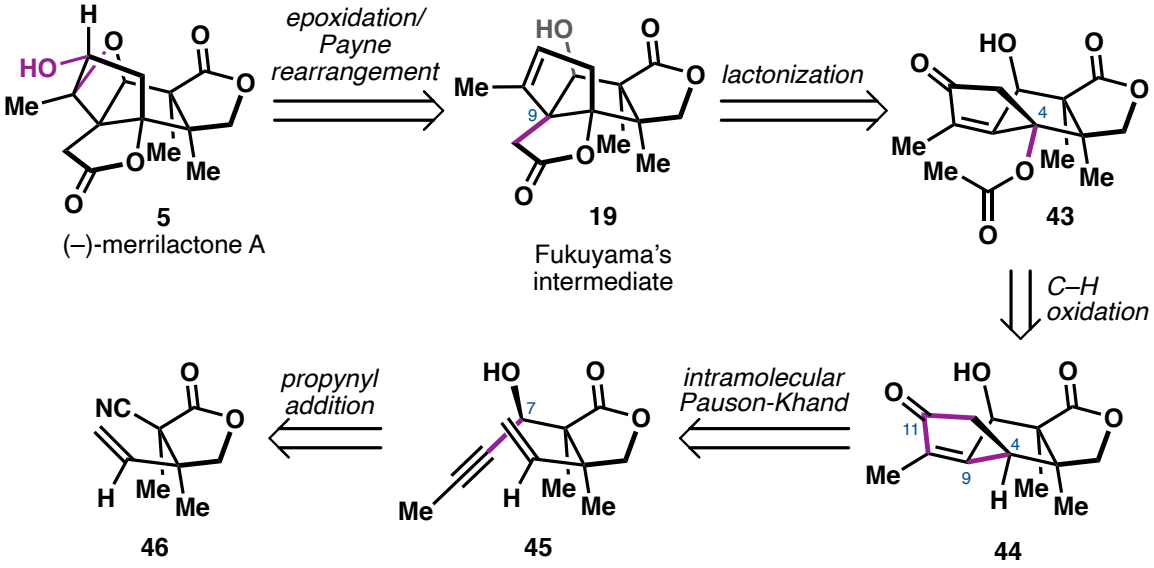

Scheme 5. Retrosynthesis of (–)-merrilactone A (**5**).

It was hypothesized that Pauson–Khand reaction could possibly favor the desired diastereomer **47** due to conformational analysis shown in Scheme 6. Upon coordination of the rhodium catalyst, there are two possible conformations leading to either product, **44** or **47**. Evaluation of these two conformers reveals a steric interaction between the C4–H atom and the propargyl hydroxyl group in the conformation leading to diastereomer **47**. By contrast, coordination of the rhodium catalyst to the desired conformation in which the C4–H is pointing downwards minimizes this sterically destabilizing interaction.

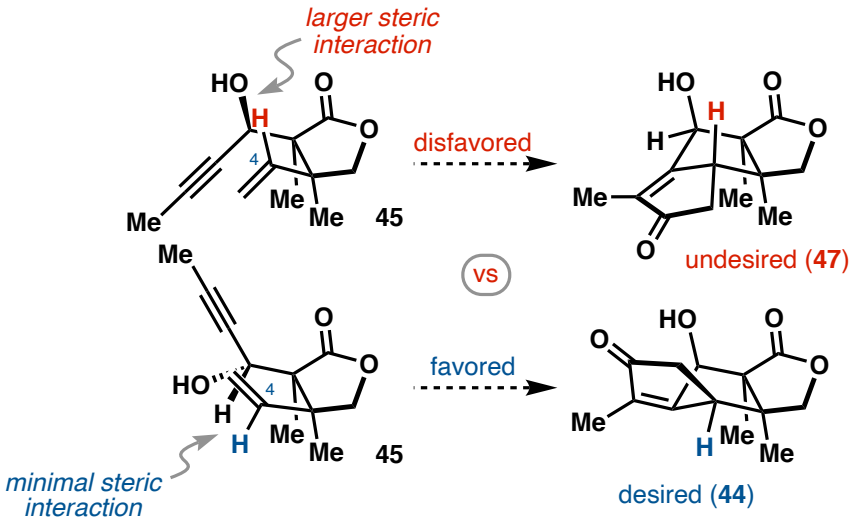

Scheme 6. Pauson–Khand reaction stereochemical rationale.

It was then envisioned that the vicinal quaternary centers at C5 and C6 could be constructed through a palladium-catalyzed asymmetric allylic alkylation reaction from commercially available materials **48** and **49** (Scheme 7).

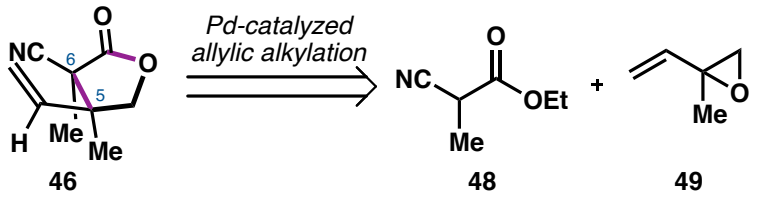

Scheme 7. Pd-catalyzed asymmetric allylic alkylation to set vicinal quaternary centers.

Similar reactions employing epoxide **49** under Tsuji-Trost conditions have been successfully used to rapidly build complexity in a single step. For example, in Xie's total synthesis of hyperolactone C and (–)-biyouyanagin A,[37] malonate derivative **50** was used to asymmetrically construct the fully substituted vicinal stereocenters with excellent diastereo- and enantioselectivity to furnish the desired branched product **51** (Scheme 8). Hence, it was reasoned that the reaction of vinyl epoxide **49** and a malonate derivative such

as α-cyano ester **48** under conditions adapted from Xie's synthesis, could provide enantioselective access to lactone **46**.

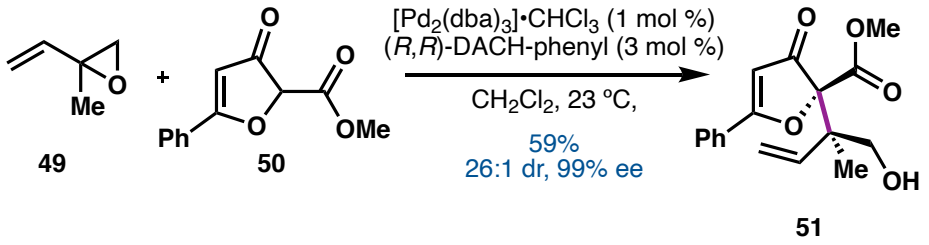

Scheme 8. Xie's allylic alkylation en route to hyperolactone C.

3.7 FORWARD SYNTHETIC EFFORTS

3.7.1 *Development of a Pd-catalyzed Asymmetric Allylic Alkylation*

Synthetic efforts towards (–)-merrilactone A (**5**) began with the development of an asymmetric Pd-catalyzed asymmetric allylic alkylation reaction for the synthesis of the D-ring lactone. It was envisioned that the catalytic cycle would commence with coordination of palladium(0) to the alkene of vinyl epoxide **49**, resulting in epoxide ionization and formation of the intermediate Pd-π-allyl complex (**52**, Scheme 9). Nucleophile **53** can then trap the π-allyl complex, affording the branched product **55**. Subsequent lactonization affords the desired lactone **46** bearing the vicinal quaternary centers.

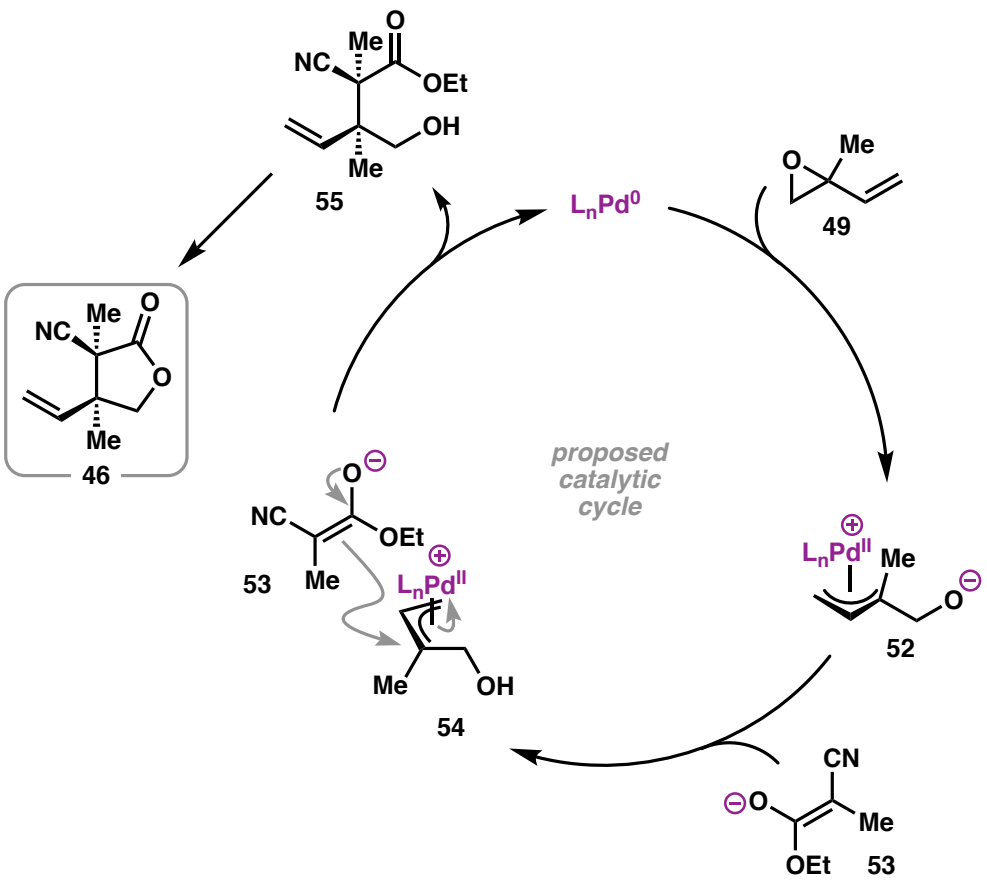

Scheme 9. Proposed catalytic cycle.

With this catalytic cycle in mind, investigations of this reaction were initiated (Scheme 10). Thus, treatment of vinyl epoxide **49** and α-cyano ester **48** with $Pd_2(dba)_3$ (1 mol %) and (*R*,*R*)-DACH-naphthyl ligand **69** (3 mol %, *vide infra,* Table 2) in anhydrous benzene afforded a diastereomeric mixture of lactones **56**, branched uncyclized product **55**, and linear product **57** in 35%, 8%, and 17%, respectively, as a mixture of diastereomers in all cases. With these initial results in hand, it was apparent that the primary challenge in developing this reaction would be the regioselectivity of nucleophilic addition. Thus, various parameters were investigated that would maximize selective formation of branched lactone **56** in high enantiomeric excess and minimize uncyclized **55** and linear product **57**.

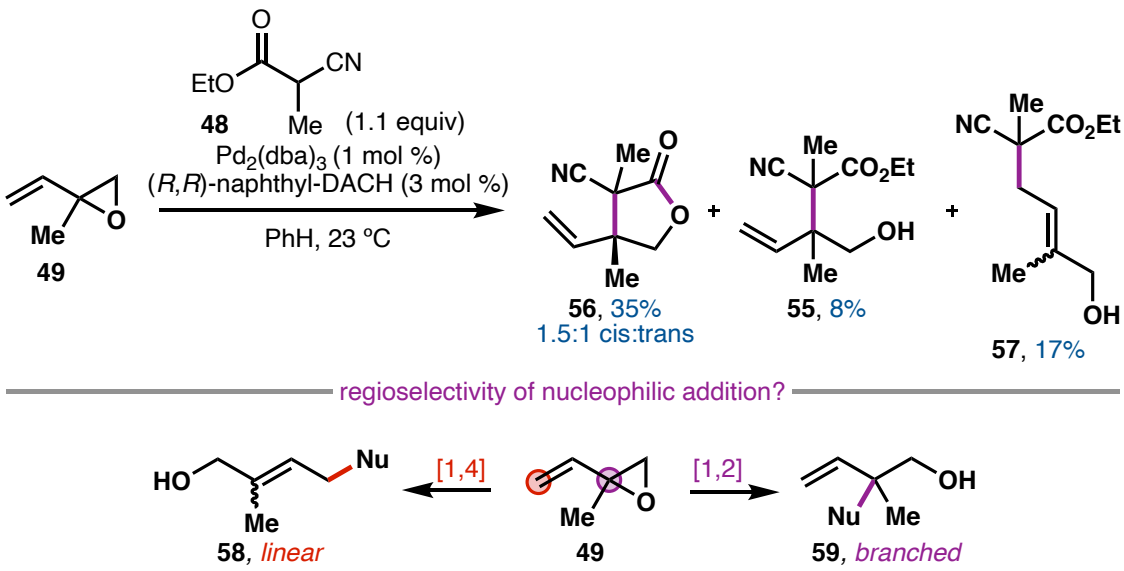

Scheme 10. Initial result for the formation of lactone **56** and anticipated challenges.

Optimization commenced with investigations of alternative nucleophiles. It was ultimately found that nucleophiles that did not contain an α-cyano ester component (Table 2, entries 1 and 2) fared poorly in the reaction and delivered trace product. Variation of the alkyl substituent on the ester (entries 4 and 5) led to diminished yields. Interestingly, the phenyl variant **66** furnished more linear product than the lactone and branched product combined; however, this was not the case with the *tert*-butyl nucleophile **65**. From this study, the initial nucleophile **48** was determined to be optimal for this reaction.

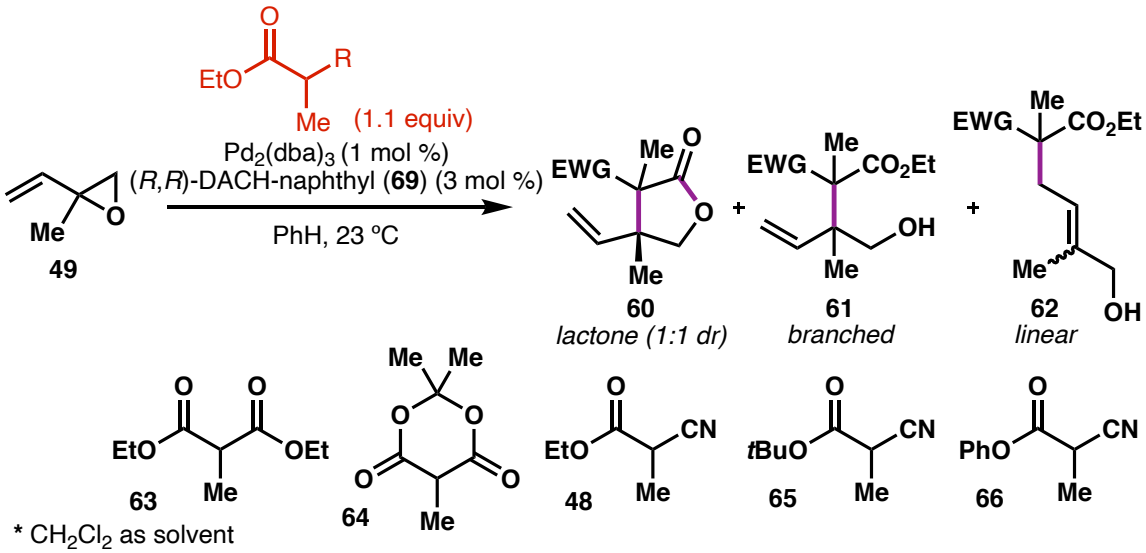

Entry	1	2	3	4*	5*
% lactone	2%	3%	35%	33%	0%
% branched	–	–	8%	10%	12%
% linear	–	–	17%	21%	26%

Table 2. Evaluation of alternative nucleophiles.

Next, a ligand evaluation was conducted in an effort to improve the yield and diastereoselectivity. Efforts with non-diaminocyclohexyl (DACH) ligands (Table 3, entries 1 and 2) furnished high yields of the undesired linear products; however, little lactone and branched products were observed. Therefore, ligand investigations were continued with DACH ligands, where nearly all (entries 4–6) yielded some productive reactivity with the exception of (*R*,*R*)-DACH-pyridyl **67**, which mainly resulted in recovered starting ester **48**. In summary, most of the ligands employed facilitated successful nucleophilic addition; however, the previously established conditions with (*R*,*R*)-DACH-naphthyl **69** were still superior in branched-to-linear selectivity.

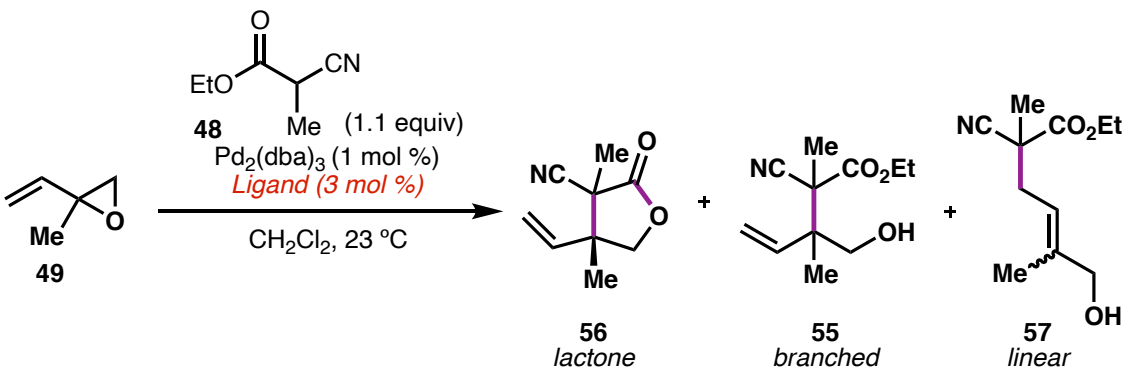

Entry	Ligand	% SM (ester)	% lactone	(cis:trans)	% branched	% linear
1	(*R*)-BINAP	0%	3%	1:1	4%	78%
2	(*S*)-*t*Bu-Bn-PHOX	0%	0%	–	0%	99%
3	(*R*,*R*)-DACH-pyridyl **67**	60%	0%	–	0%	0%
4	(*R*,*R*)-DACH-phenyl **70**	0%	0%	–	51%	43%
5	(*R*,*R*)-DACH-naphthyl **69**	0%	30%	1:1	15%	56%
6	(*R*,*R*)-DAPh-phenyl **68**	0%	35%	1:1	–	43%

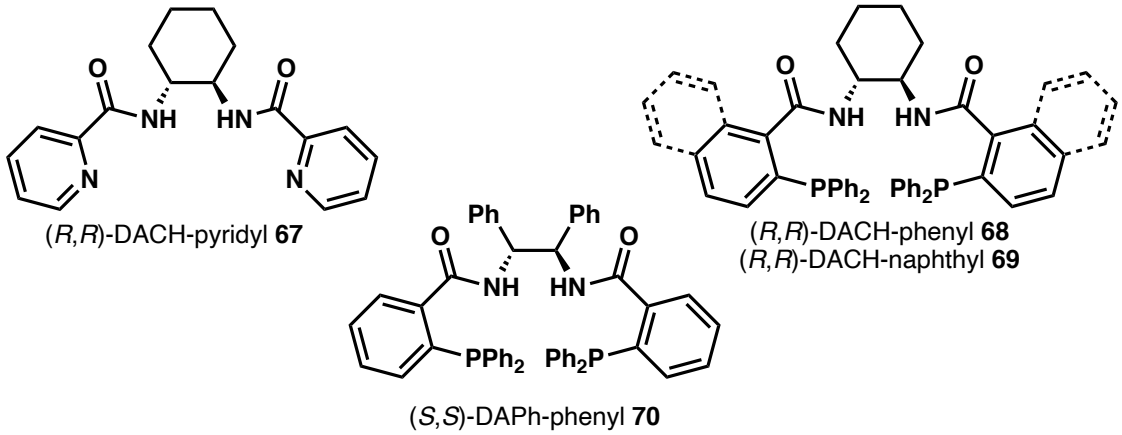

Table 3. Ligand evaluations.

Upon establishing the optimal nucleophile and ligand for the reaction, attention was turned towards additive investigations. Efforts were focused on tetrabutylammonium salts due to their low cost and reasonable solubility in most organic solvents. A survey of tetrabutylammonium halides led to a prominent increase in lactone (**56**, Table 4, entries 1–3) formation and a decrease in linear product **57** formation. Interestingly, softer anions led

to higher lactone **56** yields. A notable increase in yield occurred when 15 mol % of tetrabutylammonium difluorotriphenylsilicate (TBAT) was used (entries 5–7).

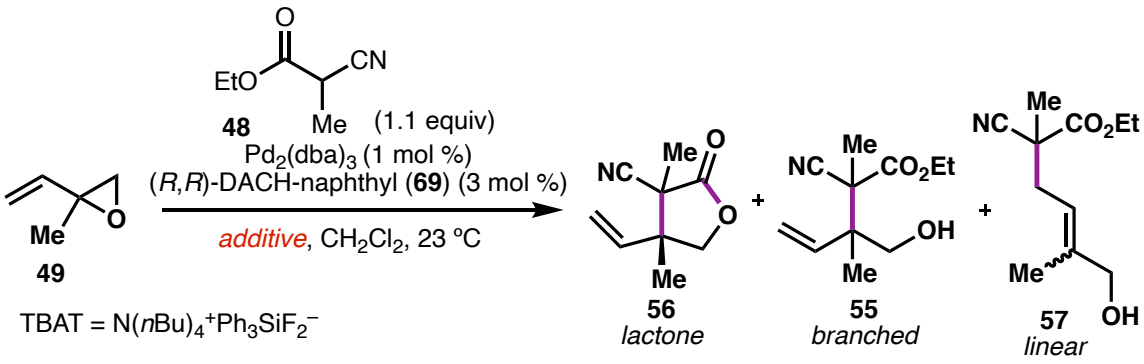

Entry	additive (60 mol %)	% SM (ester)	% lactone	(cis:trans)	% branched	% linear
1	TBACl	0%	17%	1:1.5	57%	11%
2	TBABr	0%	58%	1:1.7	26%	16%
3	TBAI	0%	61%	1:1.5	12%	18%
4	TBACN	48%	5%	–	–	6%
5	TBAT (30 mol %)	0%	66%	1:1.3	10%	33%
6	TBAT (15 mol %)	0%	71%	1:1.5	3%	14%
7	TBAT (10 mol %)	0%	63%	1:1	0%	30%

Table 4. Additive investigations.

The use of TBAT in Pd-catalyzed asymmetric allylic alkylation reactions and its effects on regioselectivity have been studied extensively.[38–44] It is hypothesized that, in the absence of TBAT, the initial ionization of racemic epoxide **49** results in a kinetically determined ratio of the two diastereomeric π-allylpalladium species: one that favors the formation of the branched product and the other that favors the formation of the linear product (Figure 4). If interconversion between the two diastereomers is sluggish, the initial diastereomeric ratio dictates the branched-to-linear selectivity. It is proposed that the addition of TBAT increases the rate of equilibration of the diastereomeric π-allylpalladium complexes, which can then lead to better regioselectivity.[44]

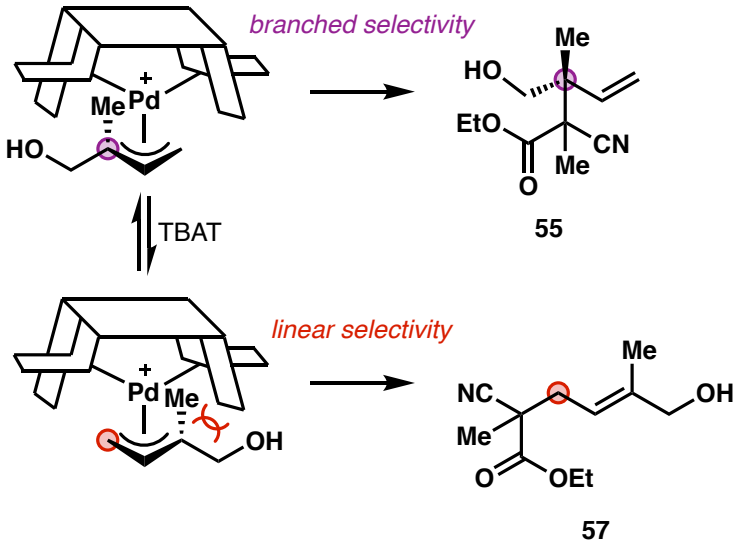

Figure 4. Cartoon adapted from Trost and coworkers[44] rationalizing regioselectivity.

Further improvement of the yield of the reaction was achieved by changing the solvent, where 2-methyltetrahydrofuran at 0.2 M concentration was found to be best (Table 5, entry 8). At this stage, the enantiomeric excess of each product (cis and trans) was also determined. It was found that across all solvents, both diastereomers were formed in high enantiomeric excess; however, the diastereoselectivity remained poor (Table 5). It is hypothesized that this poor diastereoselectivity arises from poor facial selectivity of the enolate nucleophile. It is also possible that reaction though a mixture of enolate geometries is responsible for the poor dr.

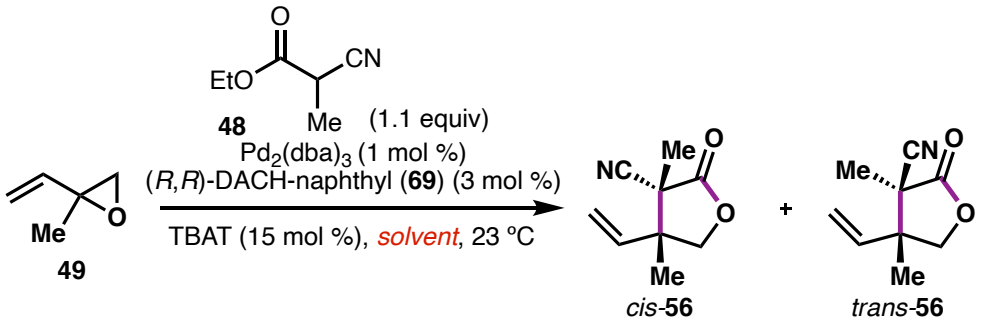

Entry	solvent (1.0 M)	% lactone	(cis:trans)	%ee (cis)	% ee (trans)
1	CH_2Cl_2	51%	1:1.6	87%	84%
2	1,2-DCE	40%	1:1.3	93%	95%
3	PhMe	60%	1:1.5	90%	91%
4	THF	47%	1:1	95%	95%
5	2-Me-THF	62%	1:1	90%	92%
6	1,4-dioxane	61%	1:1	93%	96%
7	MeCN	44%	1:1.2	92%	92%
8	2-Me-THF (0.2 M)	69%	1:1	96%	93%

Table 5. Solvent evaluation.

After the reaction parameters were optimized, it was critical that the scalability of the reaction be investigated if it were to be used as the first step in total synthesis investigations. During the small-scale optimization stage, reactions were performed in a nitrogen-filled glovebox in one dram vials. However, this setup was impractical on larger scales. Fortunately, this reaction scaled considerably well after slight procedural modifications on the benchtop, and the yield increased to 73% (Scheme 11). It was determined during optimization that slight variations in the glovebox temperature greatly influenced the yield of the reaction mixture. Therefore, it is hypothesized that slow addition and more consistent temperatures on the benchtop contributed to the yield increase.

Although reaction optimization was carried out with (*R*,*R*)-DACH-naphthyl (**69**) ligand, it was later determined that this enantiomer resulted in formation of the undesired

enantiomers *cis*-**56** and *trans*-**56**. This was discovered once semisolid *cis*-**56** was converted to crystalline dimethylamide **72**. Scale up studies were therefore conducted using the (*S*,*S*)-DACH-naphthyl, allowing a mixture of *cis*-**73** and *trans*-**73** to be prepared in 73% yield on 94 mmol scale.

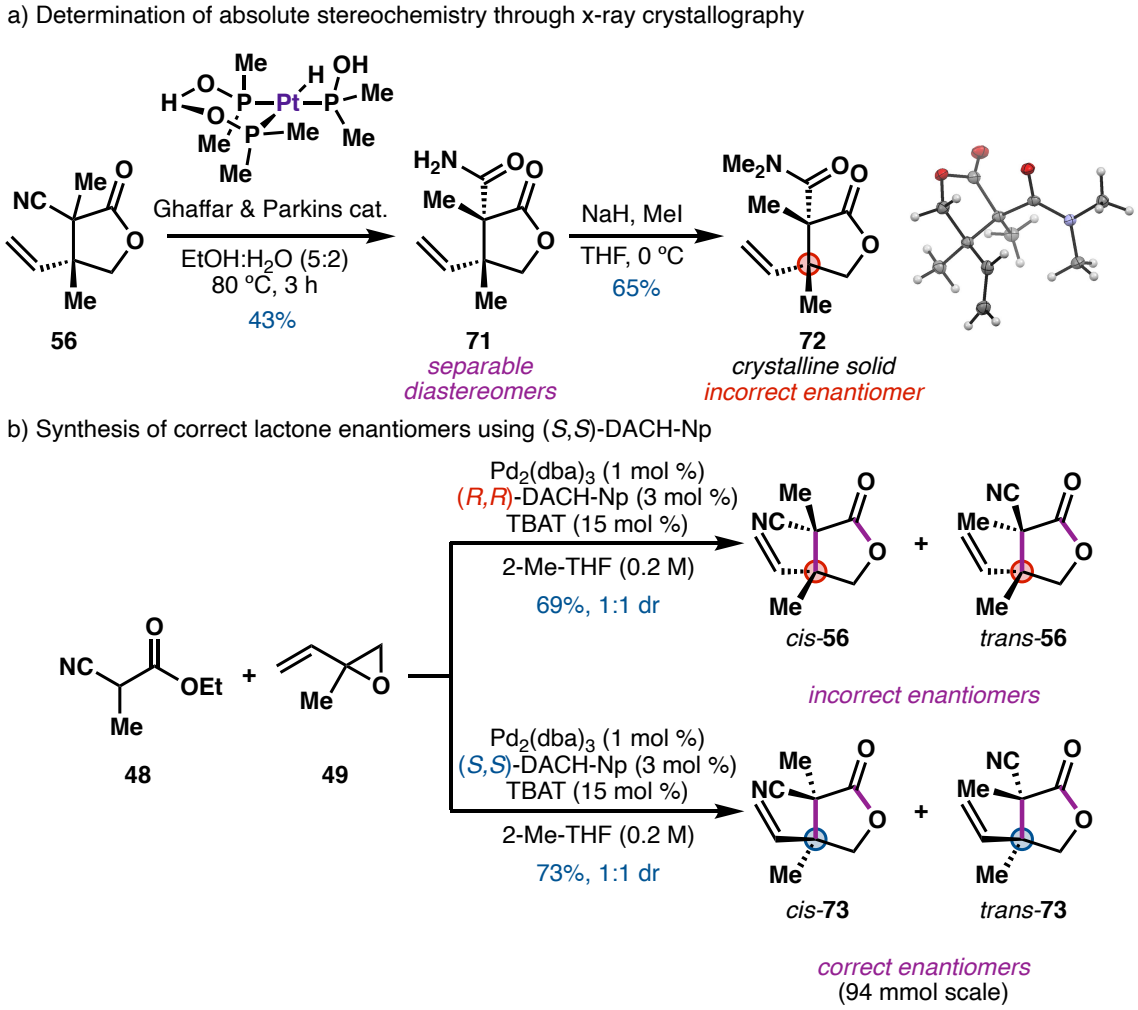

Scheme 12. Determination of absolute stereochemistry and successful upscale.

3.7.2 *Proposed Path Forward*

Although the Pd-catalyzed asymmetric allylic alkylation delivers a 1:1 mixture of diastereomers *cis*-**73** and *trans*-**73**, it was determined that the pseudosymmetrical nature of

both diastereomers would be useful for these synthetic efforts (Scheme 13). If propynyl addition were to occur preferentially into the nitrile, *cis*-**73** would be used to afford ynone **74**. Reduction of the carbonyl would then afford propargyl alcohol **45**, the Pauson–Khand precursor.

If propynyl addition were to occur preferentially into the lactone, the *trans*-**73** would be used to afford resultant alkoxide **75**. Alkoxide **75** could then lactonize onto the nitrile, and upon reduction, would afford propargyl alcohol **45**. Therefore, both diastereomers could potentially be elaborated to the Pauson–Khand precursor.

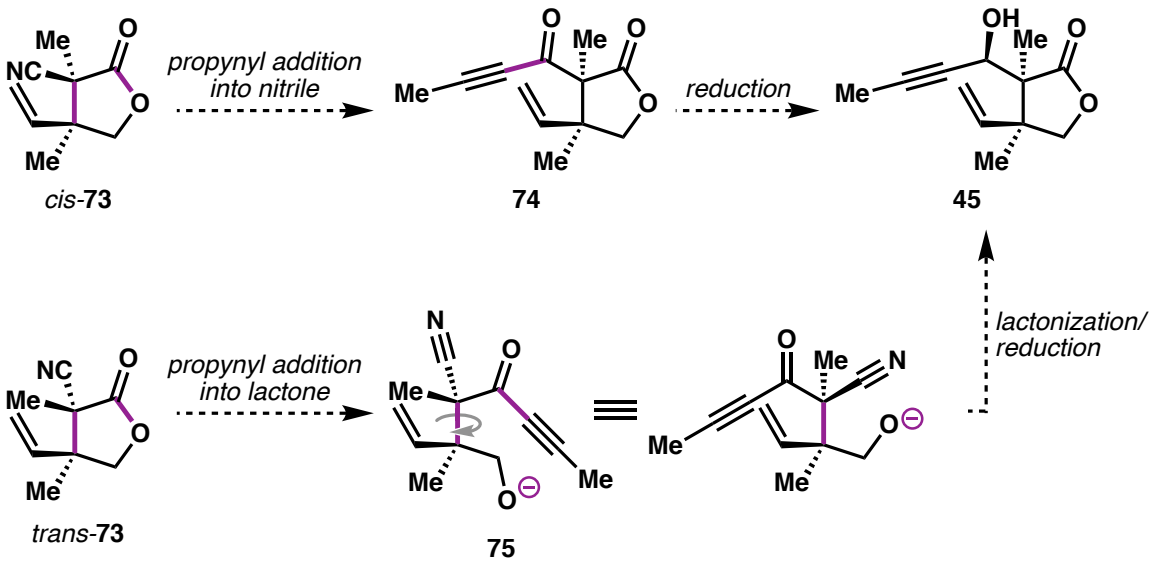

Scheme 13. PKR precursor **45** is accessible to both diastereomers.

3.8 CONCLUDING REMARKS

Herein is described a proposed strategy toward the synthesis of (–)-merrilactone A featuring a late-stage allylic C–H oxidation, Pauson–Khand reaction to construct the B and C rings, and a Pd-catalyzed asymmetric allylic alkylation reaction for D-ring construction to set the C5 and C6 vicinal quaternary centers. The development of the key Pd-catalyzed

asymmetric allylic alkylation reaction was accomplished and should enable future synthetic efforts toward this structurally complex and biologically active natural product.

3.9 EXPERIMENTAL SECTION

3.9.1 *Materials and Methods*

Unless otherwise stated, reactions were performed under an inert atmosphere (Ar) with freshly dried solvents utilizing standard Schlenk techniques. Glassware was oven-dried at 120 °C for a minimum of four hours, or flame-dried utilizing a Bunsen burner under high vacuum. Tetrahydrofuran (THF), methylene chloride (CH_2Cl_2), diethyl ether (Et_2O), benzene (PhH), and toluene (PhMe) were dried by passing through activated alumina columns. Absolute ethanol (200 Proof) was purchased from Koptec. Methanol (HPLC grade) was purchased from Fisher Scientific. Anhydrous ammonia (NH_3) was purchased from Matheson Tri-Gas. N,N-diisopropylethylamine (iPr$_2$NEt), triethylamine (Et_3N), methanol (MeOH), isopropanol (iPrOH), tert-butanol (tBuOH), and trimethylsilyl chloride (TMSCl) were distilled over calcium hydride prior to use. Unless otherwise stated, chemicals and reagents were used as received. All reactions were monitored by thin-layer chromatography using EMD/Merck silica gel 60 F254 pre-coated plates (0.25 mm) and were visualized by UV (254 nm), p-anisaldehyde, and/or $KMnO_4$ staining. Flash column chromatography was performed using silica gel (SiliaFlash® P60, particle size 40-63 microns [230 to 400 mesh]) purchased from Silicycle. 1H and 13C NMR spectra were recorded on a Bruker Avance III HD with Prodigy Cryoprobe (at 400 MHz and 101 MHz, respectively) or a Varian Inova 500 (at 500 MHz and 101 MHz respectively) and are reported relative to internal $CHCl_3$ (1H, δ = 7.26) and $CDCl_3$ (13C, δ = 77.0). Data for 1H

NMR spectra are reported as follows: chemical shift (δ ppm) (multiplicity, coupling constant (Hz), integration). Multiplicity and qualifier abbreviations are as follows: s = singlet, d = doublet, t = triplet, q = quartet, m = multiplet, br = broad, app = apparent. IR spectra were recorded on a Perkin Elmer Paragon 1000 spectrometer and are reported in frequency of absorption (cm–1).

3.9.2 *Experimental Procedures*

Preparation of lactones *cis*-73 and *trans*-73

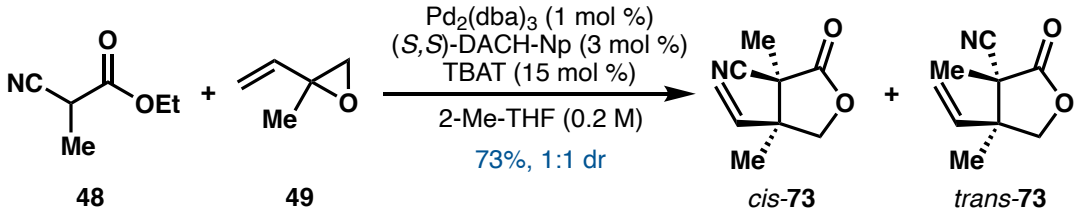

48 **49** *cis*-**73** *trans*-**73**

To an oven-dried 3-neck round-bottom flask equipped with a stir bar was added Pd_2dba_3 (0.862 g, 0.94 mmol, 1 mol %), (*S*,*S*)-DACH-Np (2.61 g, 3.30 mmol, 3.4 mol %), and TBAT (7.63 g, 14.1 mmol, 15 mol %) under a steady stream of argon. The flask was evacuated and backfilled with Ar three times. 157 mL of 2-Me-THF was added and the maroon solution was stirred for 30 min. at ambient temperature. The solution became dark orange after 40 minutes. A solution of ethyl 2-cyanopropanoate **48** (11.84 mL, 94 mmol, 1 equiv) in 157 mL 2-Me-THF was added in one portion (stirring was set to 500 rpm). Isoprene monoxide **49** (15.28 mL, 155 mmol, 1.65 equiv) was added in 157 mL 2-Me-THF via addition funnel over 30 minutes, where the solution began to turn dark yellow/green over the course of epoxide addition. Once two-thirds of the solution had been added, the temperature of the solution had risen to 23 ºC and began to steadily decrease back to ambient temperature thereafter. The slightly heterogeneous solution was stirred (110 rpm)

at ambient temperature for 5 h. Upon completion by TLC analysis, the reaction was filtered through 65 g of SiO_2 below a pad of celite. ^{1}H NMR analysis of the crude mixture showed a 1:1 diastereomeric mixture.

Purification was achieved via flash column chromatography on SiO_2 [0% EtOAc/hexanes → 25%] afforded a mixture of the diastereomers *cis*-**73** and *trans*-**73** as a white solid (11.3 g, 68.6 mmol, 73%).

^{1}H NMR (500 MHz, $CDCl_3$): δ 6.08 (dd, *J* = 17.3, 10.8 Hz, 1H), 5.77 (dd, *J* = 17.5, 10.9 Hz, 1H), 5.47 (d, *J* = 10.9 Hz, 1H), 5.40 (d, *J* = 10.9 Hz, 1H), 5.36 (d, *J* = 17.3 Hz, 1H), 5.28 (d, *J* = 17.5 Hz, 1H), 4.45 – 4.41 (m, 1H), 4.33 (d, *J* = 9.3 Hz, 1H), 4.21 (d, *J* = 9.3 Hz, 1H), 4.08 (d, *J* = 9.4 Hz, 1H), 1.52 (s, 3H), 1.52 (s, 3H), 1.50 (d, *J* = 0.4 Hz, 2H), 1.24 (d, *J* = 0.6 Hz, 3H).

Preparation of amide 71

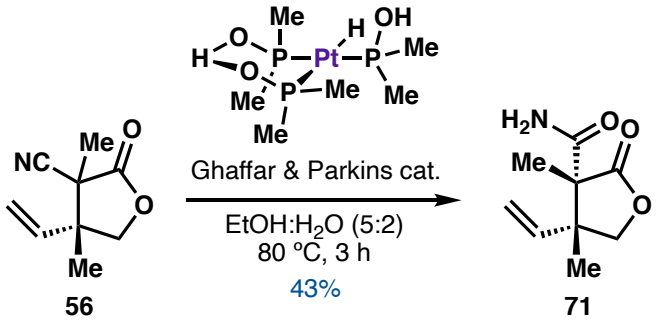

A 150 mL pressure flask was charged with lactone **56** (8.5 g, 51.5 mmol) and suspended in EtOH:H_2O (5:2, 85 mL, 0.6 M) after which Ghaffar-Parkins catalyst was added (100 mg, 0.233 mmol, 0.0045 mol %). The vessel was sealed and placed in a preheated oil bath at 80 °C and monitored by TLC and LCMS. After 5 hours, the reaction

was removed from heating and allowed to cool to ambient temperature. The crude reaction mixture was then poured into a 500 mL separatory funnel, diluted with water (100 mL), and extracted with 10% DCM in EtOAc (150 mL x 5), dried over Na_2SO_4, filtered, and concentrated under reduced pressure to yield a mixture of diastereomers as a white solid (8.76 g, 47.8 mmol, 87% combined yield).

^{1}H NMR analysis of the crude mixture shows a 1:1 diastereomeric mixture. The diastereomers were separated by flash column chromatography on SiO_2 [15% Et_2O/15% acetone/70% hexanes] to yield the *cis*-diastereomer **71** (4.5 g, 24.7 mmol, 43% yield) as a white solid.

TLC (50% EtOAc/Hexanes): R_f = 0.40 (UV, p-anisaldehyde).

^{1}H NMR (400 MHz, $CDCl_3$): δ 7.32 (dd, J = 7.7, 0.8 Hz, 1H), 7.19 (d, J = 7.7 Hz, 1H), 3.77 (s, 3H), 3.20 (ddq, J = 6.7, 4.5, 2.2 Hz, 1H), 2.63 (dd, J = 17.8, 4.5 Hz, 1H), 2.55 (dd, J = 17.8, 6.6 Hz, 1H), 2.34 (d, J = 0.7 Hz, 3H), 2.08 (d, J = 2.2 Hz, 3H), 1.69 (s, 3H).

^{13}C NMR (101 MHz, $CDCl_3$): δ 210.3, 168.8, 155.1, 152.0, 134.7, 133.8, 132.3, 128.1, 118.8, 75.6, 60.8, 55.7, 35.2, 24.6, 15.9, 9.9.

FTIR (NaCl, thin film): 3389, 2963, 2919, 1690, 1639, 1320, 1227, 1091, 1018 cm^{-1}.

HRMS (MM:ESI–APCI): calc'd for [M+Na]+ 259.1334, found 259.1347.

Preparation of dimethylamide 72

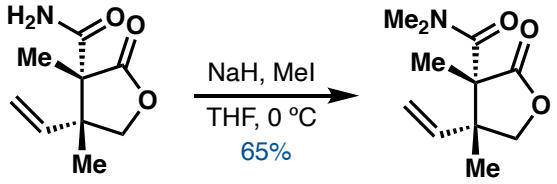

71 **72**

An oven-dried 500 mL round-bottom flask equipped with a stir bar was charged with NaH (2.06 g, 86.3 mmol, 3.5 equiv) and THF (100 mL). An oven-dried addition funnel was quickly attached to the reaction flask and filled with a solution of *cis*-amide **71** (4.5 g, 24.7 mmol, 1.0 equiv) in THF (100 mL). The flask was then cooled to 0 ºC. After cooling for 15 min, a solution of the *cis*-amide **71** was added dropwise over 30 min at 0 ºC. The solution was warmed to ambient temperature over 30 min. The flask was cooled to 0 ºC and stirred for 15 min before a solution of MeI (6.14 mL, 98.7 mmol, 4.0 equiv) in THF (50 mL) was added dropwise over 30 min at 0 ºC, after which the reaction was warmed to ambient temperature and stirred for 24 h. The reaction was then cooled to 0 ºC and 1 N HCl (10 mL) was slowly added. The solution was diluted with H_2O (100 mL). The crude reaction mixture was extracted with 10% DCM/EtOAc (120 mL x 5), dried over Na_2SO_4, filtered, and concentrated under reduced pressure.

Purification was achieved through flash column chromatography on SiO_2 [10% EtOAc/hexanes → 60%] to afford dimethylamide **72** as an off-white solid (3.4 g, 16.1 mmol, 65% yield).

TLC (50% EtOAc/Hexanes): R_f = 0.40 (UV, p-anisaldehyde).

^{1}H NMR (400 MHz, $CDCl_3$): δ 7.32 (dd, J = 7.7, 0.8 Hz, 1H), 7.19 (d, J = 7.7 Hz, 1H), 3.77 (s, 3H), 3.20 (ddq, J = 6.7, 4.5, 2.2 Hz, 1H), 2.63 (dd, J = 17.8, 4.5 Hz, 1H), 2.55 (dd, J = 17.8, 6.6 Hz, 1H), 2.34 (d, J = 0.7 Hz, 3H), 2.08 (d, J = 2.2 Hz, 3H), 1.69 (s, 3H).

^{13}C NMR (101 MHz, $CDCl_3$): δ 210.3, 168.8, 155.1, 152.0, 134.7, 133.8, 132.3, 128.1, 118.8, 75.6, 60.8, 55.7, 35.2, 24.6, 15.9, 9.9.

FTIR (NaCl, thin film): 3389, 2963, 2919, 1690, 1639, 1320, 1227, 1091, 1018, 921 cm-

HRMS (MM:ESI–APCI): calc'd for [M+Na]+ 259.1334, found 259.1347.

3.9.3 *Proof of Enantiopurity*

Due to COVID-19, this data at the present moment is not obtainable.

3.10 NOTES AND REFERENCES

(1) Huang, J.-M.; Yang, C.-S.; Tanaka, M.; Fukuyama, Y. Structures of Merrilactones B and C, Novel Anislactone-Type Sesquiterpenes from Illicium Merrillianum, and Chemical Conversion of Anislactone B to Merrilactone A. *Tetrahedron* **2001**, *57* (22), 4691–4698.

(2) Birman, V. B.; Danishefsky, S. J. The Total Synthesis of (±)-Merrilactone A. *J. Am. Chem. Soc.* **2002**, *124* (10), 2080–2081.

(3) Inoue, M.; Sato, T.; Hirama, M. Total Synthesis of Merrilactone A. *J. Am. Chem. Soc.* **2003**, *125* (36), 10772–10773.

(4) Harada, K.; Kato, H.; Fukuyama, Y. Synthetic Studies toward Merrilactone A: A Short Synthesis of AB Ring Motif. *Tetrahedron Letters* **2005**, *46* (43), 7407–7410.

(5) Iriondo-Alberdi, J.; Perea-Buceta, J. E.; Greaney, M. F. A Paternò−Büchi Approach to the Synthesis of Merrilactone A. *Org. Lett.* **2005**, *7* (18), 3969–3971.

(6) Meng, Z.; Danishefsky, S. J. A Synthetic Pathway to Either Enantiomer of Merrilactone A. *Angewandte Chemie International Edition* **2005**, *44* (10), 1511–1513.

(7) Inoue, M.; Sato, T.; Hirama, M. Asymmetric Total Synthesis of (−)-Merrilactone A: Use of a Bulky Protecting Group as Long-Range Stereocontrolling Element. *Angewandte Chemie International Edition* **2006**, *45* (29), 4843–4848.

(8) Mehta, G.; Singh, S. R. Toward a Total Synthesis of the Novel Neurotrophic Sesquiterpene Merrilactone A: A RCM and [2+2]-Photocycloaddition Based Approach to Framework Construction. *Tetrahedron Letters* **2005**, *46* (12), 2079–2082.

(9) Mehta, G.; Singh, S. R. Total Synthesis of (±)-Merrilactone A. *Angewandte Chemie International Edition* **2006**, *45* (6), 953–955.

(10) Harada, K.; Ito, H.; Hioki, H.; Fukuyama, Y. An Efficient Synthesis of the CD Rings Model for Merrilactone A. *Tetrahedron Letters* **2007**, *48* (35), 6105–6108.

(11) He, W.; Huang, J.; Sun, X.; Frontier, A. J. Total Synthesis of (±)-Merrilactone A via Catalytic Nazarov Cyclization. *J. Am. Chem. Soc.* **2007**, *129* (3), 498–499.

(12) Inoue, M.; Lee, N.; Kasuya, S.; Sato, T.; Hirama, M.; Moriyama, M.; Fukuyama, Y. Total Synthesis and Bioactivity of an Unnatural Enantiomer of Merrilactone A: Development of an Enantioselective Desymmetrization Strategy. *J. Org. Chem.* **2007**, *72* (8), 3065–3075.

(13) He, W.; Huang, J.; Sun, X.; Frontier, A. J. Total Synthesis of (±)-Merrilactone A. *J. Am. Chem. Soc.* **2008**, *130* (1), 300–308.

(14) Shi, L.; Meyer, K.; Greaney, M. F. Synthesis of (±)-Merrilactone A and (±)-Anislactone A. *Angewandte Chemie International Edition* **2010**, *49* (48), 9250–9253.

(15) Xu, J.; Trzoss, L.; Chang, W. K.; Theodorakis, E. A. Enantioselective Total Synthesis of (−)-Jiadifenolide. *Angewandte Chemie International Edition* **2011**, *50* (16), 3672–3676.

(16) Nazef, N.; Davies, R. D. M.; Greaney, M. F. Formal Synthesis of Merrilactone A Using a Domino Cyanide 1,4-Addition–Aldol Cyclization. *Org. Lett.* **2012**, *14* (14), 3720–3723.

(17) Chen, J.; Gao, P.; Yu, F.; Yang, Y.; Zhu, S.; Zhai, H. Total Synthesis of (±)-Merrilactone A. *Angewandte Chemie International Edition* **2012**, *51* (24), 5897–5899.

(18) Trzoss, L.; Xu, J.; Lacoske, M. H.; Theodorakis, E. A. Synthesis of the Tetracyclic Core of Illicium Sesquiterpenes Using an Organocatalyzed Asymmetric Robinson Annulation. *Beilstein J. Org. Chem.* **2013**, *9* (1), 1135–1140.

(19) Siler, D. A.; Mighion, J. D.; Sorensen, E. J. An Enantiospecific Synthesis of Jiadifenolide. *Angewandte Chemie International Edition* **2014**, *53* (21), 5332–5335.

(20) Paterson, I.; Xuan, M.; Dalby, S. M. Total Synthesis of Jiadifenolide. *Angewandte Chemie International Edition* **2014**, *53* (28), 7286–7289.

(21) Shen, Y.; Li, L.; Pan, Z.; Wang, Y.; Li, J.; Wang, K.; Wang, X.; Zhang, Y.; Hu, T.; Zhang, Y. Protecting-Group-Free Total Synthesis of (−)-Jiadifenolide: Development

of a [4 + 1] Annulation toward Multisubstituted Tetrahydrofurans. *Org. Lett.* **2015**, *17* (21), 5480–5483.

(22) Lu, H.-H.; Martinez, M. D.; Shenvi, R. A. An Eight-Step Gram-Scale Synthesis of (−)-Jiadifenolide. *Nature Chemistry* **2015**, *7* (7), 604–607.

(23) Gomes, J.; Daeppen, C.; Liffert, R.; Roesslein, J.; Kaufmann, E.; Heikinheimo, A.; Neuburger, M.; Gademann, K. Formal Total Synthesis of (−)-Jiadifenolide and Synthetic Studies toward Seco-Prezizaane-Type Sesquiterpenes. *J. Org. Chem.* **2016**, *81* (22), 11017–11034.

(24) Condakes, M. L.; Hung, K.; Harwood, S. J.; Maimone, T. J. Total Syntheses of (−)-Majucin and (−)-Jiadifenoxolane A, Complex Majucin-Type Illicium Sesquiterpenes. *J. Am. Chem. Soc.* **2017**, *139* (49), 17783–17786.

(25) Hung, K.; Condakes, M. L.; Novaes, L. F. T.; Harwood, S. J.; Morikawa, T.; Yang, Z.; Maimone, T. J. Development of a Terpene Feedstock-Based Oxidative Synthetic Approach to the Illicium Sesquiterpenes. *J. Am. Chem. Soc.* **2019**, *141* (7), 3083–3099.

(26) Forman, M. S.; Trojanowski, J. Q.; Lee, V. M.-Y. Neurodegenerative Diseases: A Decade of Discoveries Paves the Way for Therapeutic Breakthroughs. *Nat. Med.* **2004**, *10* (10), 1055–1063.

(27) Hebert, L. E.; Scherr, P. A.; Bienias, J. L.; Bennett, D. A.; Evans, D. A. Alzheimer Disease in the US Population: Prevalence Estimates Using the 2000 Census. *Arch. Neurol.* **2003**, *60* (8), 1119–1122.

(28) Xu, J.; Lacoske, M. H.; Theodorakis, E. A. Neurotrophic Natural Products: Chemistry and Biology. *Angewandte Chemie International Edition* **2014**, *53* (4), 956–987.

(29) Bartus, R. T. Translating the Therapeutic Potential of Neurotrophic Factors to Clinical 'Proof of Concept': A Personal Saga Achieving a Career-Long Quest. *Neurobiology of Disease* **2012**, *48* (2), 153–178.

(30) Huang, J.; Yokoyama, R.; Yang, C.; Fukuyama, Y. Merrilactone A, a Novel Neurotrophic Sesquiterpene Dilactone from Illicium Merrillianum. *Tetrahedron Letters* **2000**, *41* (32), 6111–6114.

(31) Yamada, K.; Takada, S.; Nakamura, S.; Hirata, Y. The Structures of Anisatin and Neoanisatin: Toxic Sesquiterpenes from Illicium Anisatum L. *Tetrahedron* **1968**, *24* (1), 199–229.

(32) Lane, J. F.; Koch, W. T.; Leeds, N. S.; Gorin, G. On the Toxin of Illicium Anisatum. I. The Isolation and Characterization of a Convulsant Principle: Anisatin1. *J. Am. Chem. Soc.* **1952**, *74* (13), 3211–3215.

(33) Fukuyama, Y.; Huang, J.-M. Chemistry and Neurotrophic Activity of Seco-Prezizaane- and Anislactone-Type Sesquiterpenes from Illicium Species. In *Studies in Natural Products Chemistry*; Atta-ur-Rahman, Ed.; Bioactive Natural Products (Part L); Elsevier, 2005; Vol. 32, pp 395–427.

(34) Shenvi, R. A. Neurite Outgrowth Enhancement by Jiadifenolide: Possible Targets. *Nat. Prod. Rep.* **2016**, *33* (4), 535–539.

(35) Kouno, I.; Mori, K.; Kawano, N. Structure of Anislactone A; a New Skeletal Type of Sesquiterpene from the Pericaps of Illicium Anisatum. *Tetrahedron Letters* **1990**, *31* (26), 3658.

(36) Dibrell, S. E.; Maser, M.; Reisman, S. E. SeO2-Mediated Oxidative Transposition of Pauson–Khand Products. *J. Am. Chem. Soc.* **2020**.

(37) Du, C.; Li, L.; Li, Y.; Xie, Z. Construction of Two Vicinal Quaternary Carbons by Asymmetric Allylic Alkylation: Total Synthesis of Hyperolactone C and (−)-Biyouyanagin A. *Angewandte Chemie International Edition* **2009**, *48* (42), 7853–7856.

(38) Simpkins, N. S.; Nytko, F. E.; DeShong, P. Tetrabutylammonium Difluorotriphenylsilicate. In *Encyclopedia of Reagents for Organic Synthesis*; American Cancer Society, 2011.

(39) Trost, B. M.; Brennan, M. K. Palladium-Catalyzed Regio- and Enantioselective Allylic Alkylation of Bis Allylic Carbonates Derived from Morita−Baylis−Hillman Adducts. *Org. Lett.* **2007**, *9* (20), 3961–3964.

(40) Trost, B. M.; Brennan, M. K. Palladium Asymmetric Allylic Alkylation of Prochiral Nucleophiles: Horsfiline. *Org. Lett.* **2006**, *8* (10), 2027–2030.

(41) Bélanger, É.; Cantin, K.; Messe, O.; Tremblay, M.; Paquin, J.-F. Enantioselective Pd-Catalyzed Allylation Reaction of Fluorinated Silyl Enol Ethers. *J. Am. Chem. Soc.* **2007**, *129* (5), 1034–1035.

(42) Trost, B. M.; Toste, F. D. Regio- and Enantioselective Allylic Alkylation of an Unsymmetrical Substrate: A Working Model. *J. Am. Chem. Soc.* **1999**, *121* (19), 4545–4554.

(43) Burckhardt, U.; Baumann, M.; Togni, A. A Remarkable Anion Effect on the Enantioselectivity of the Pd-Catalyzed Allylic Amination Using Ferrocenyl Ligands. *Tetrahedron: Asymmetry* **1997**, *8* (1), 155–159.

(44) Trost, B. M.; Jiang, C. Atom Economic Asymmetric Creation of Quaternary Carbon: Regio- and Enantioselective Reactions of a Vinylepoxide with a Carbon Nucleophile. *J. Am. Chem. Soc.* **2001**, *123* (51), 12907–12908.

Appendix 3

Spectra Relevant to Chapter 3:

Progress Towards the Total Synthesis of (–)-Merrilactone A


Parameter
Value
Data File Name
/ Volumes/ nmrdata/ sfeng/ vnmrsys/ data/ SSF-III-267-flashed/ PROTON01.fid/ fid
Title
PROTON01
Comment
SSF-III-267-flashed
Origin
Varian
Instrument
inova
Solvent
cdcl3
Temperature
3.0
Pulse Sequence
s2pul
Experiment
1D
Probe
autox7991
Number of Scans
8
Receiver Gain
58
Relaxation Delay
5.0000
Pulse Width
5.8000
Acquisition Time
15.0000
Acquisition Date
2019-01-16T14:19:54
Spectrometer Frequency
499.63
Spectral Width
8000.0
Lowest Frequency
-1029.7
Nucleus
1H
Acquired Size
120000
Spectral Size
262144
A (dd) 6.08
B (dd) 5.77
C (d) 5.47
D (d) 5.40
E (d) 5.36
F (d) 5.28
G (m) 4.43
H (d) 4.33
I (d) 4.21
J (d) 4.08
K (s) 1.52
L (s) 1.52
M (d) 1.50
N (d) 1.24
Me
NC
O
cis-73
trans-73
+
ppm

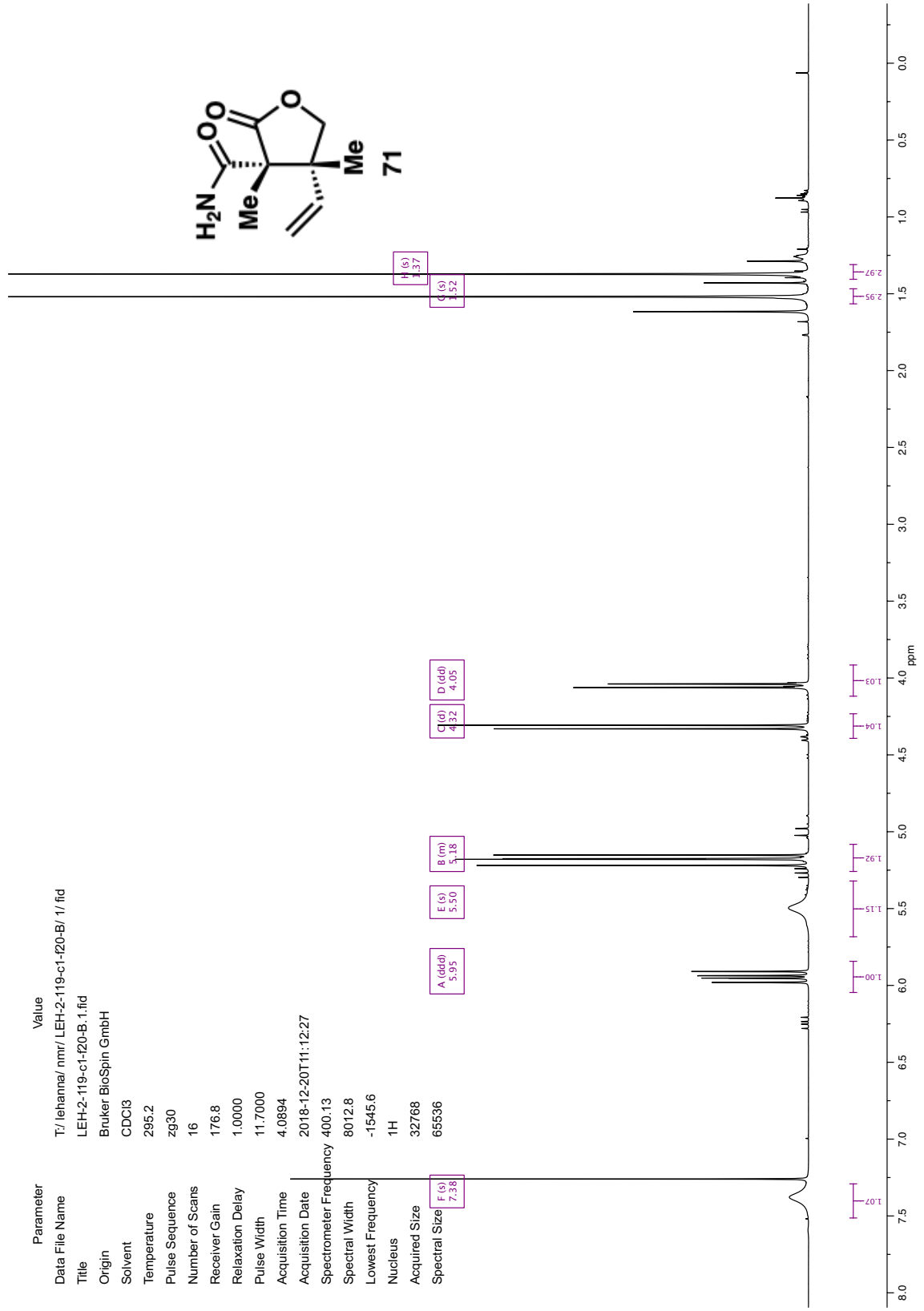
Parameter
Value
Data File Name T:/ lehanna/ nmr/ LEH-2-119-c1-f20-B/ 1/ fid
Title LEH-2-119-c1-f20-B.1.fid
Origin Bruker BioSpin GmbH
Solvent CDCl3
Temperature 295.2
Pulse Sequence zg30
Number of Scans 16
Receiver Gain 176.8
Relaxation Delay 1.0000
Pulse Width 11.7000
Acquisition Time 4.0894
Acquisition Date 2018-12-20T11:12:27
Spectrometer Frequency 400.13
Spectral Width 8012.8
Lowest Frequency -1545.6
Nucleus 1H
Acquired Size 32768
Spectral Size 65536
F (s) 7.38
A (ddd) 5.95
E (s) 5.50
B (m) 5.18
C (d) 4.32
D (dd) 4.05
H (s) 1.37
G (s) 1.52
1.07
1.00
1.15
1.92
1.04
1.03
2.97
2.95
ppm
H_2N
Me
Me
71

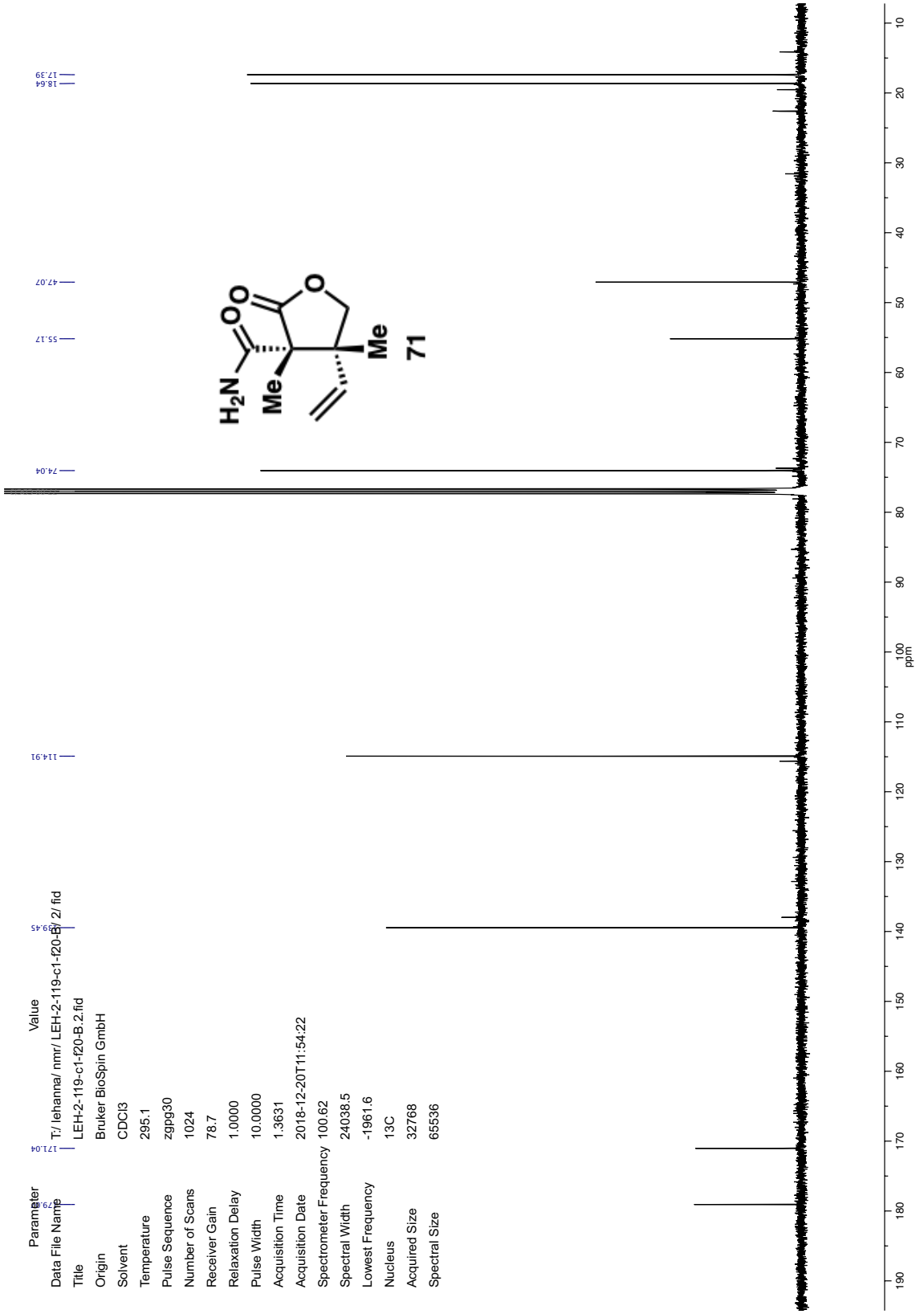
Parameter Value
Data File Name T:/ lehanna/ nmr/ LEH-2-119-c1-f20-B/ 2/ fid
Title LEH-2-119-c1-f20-B.2.fid
Origin Bruker BioSpin GmbH
Solvent CDCl3
Temperature 295.1
Pulse Sequence zgpg30
Number of Scans 1024
Receiver Gain 78.7
Relaxation Delay 1.0000
Pulse Width 10.0000
Acquisition Time 1.3631
Acquisition Date 2018-12-20T11:54:22
Spectrometer Frequency 100.62
Spectral Width 24038.5
Lowest Frequency -1961.6
Nucleus 13C
Acquired Size 32768
Spectral Size 65536
17.39
18.64
47.07
55.17
74.04
114.91
139.45
171.04
179.79
H2N
O
O
Me
Me
71
ppm

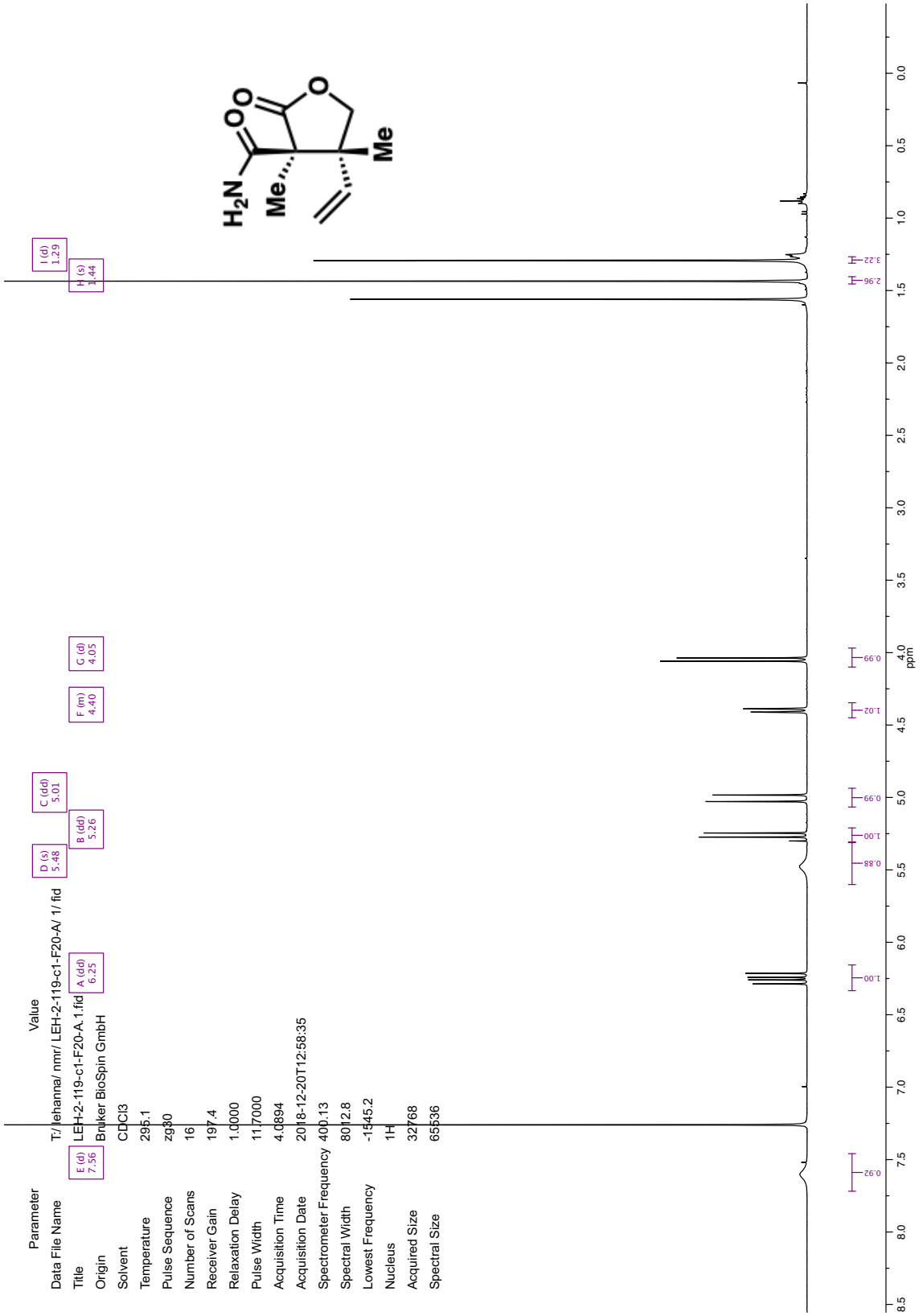
Parameter
Value
Data File Name T:/ lehanna/ nmr/ LEH-2-119-c1-F20-A/ 1/ fid
Title LEH-2-119-c1-F20-A.1.fid
Origin Bruker BioSpin GmbH
Solvent CDCl3
Temperature 295.1
Pulse Sequence zg30
Number of Scans 16
Receiver Gain 197.4
Relaxation Delay 1.0000
Pulse Width 11.7000
Acquisition Time 4.0894
Acquisition Date 2018-12-20T12:58:35
Spectrometer Frequency 400.13
Spectral Width 8012.8
Lowest Frequency -1545.2
Nucleus 1H
Acquired Size 32768
Spectral Size 65536
E (d) 7.56
A (dd) 6.25
D (s) 5.48
C (dd) 5.01
B (dd) 5.26
F (m) 4.40
G (d) 4.05
H (s) 1.44
I (d) 1.29
Me
Me
H_2N
O
O
O
0.92
1.00
0.88
1.00
0.99
1.02
0.99
2.96
3.22
ppm

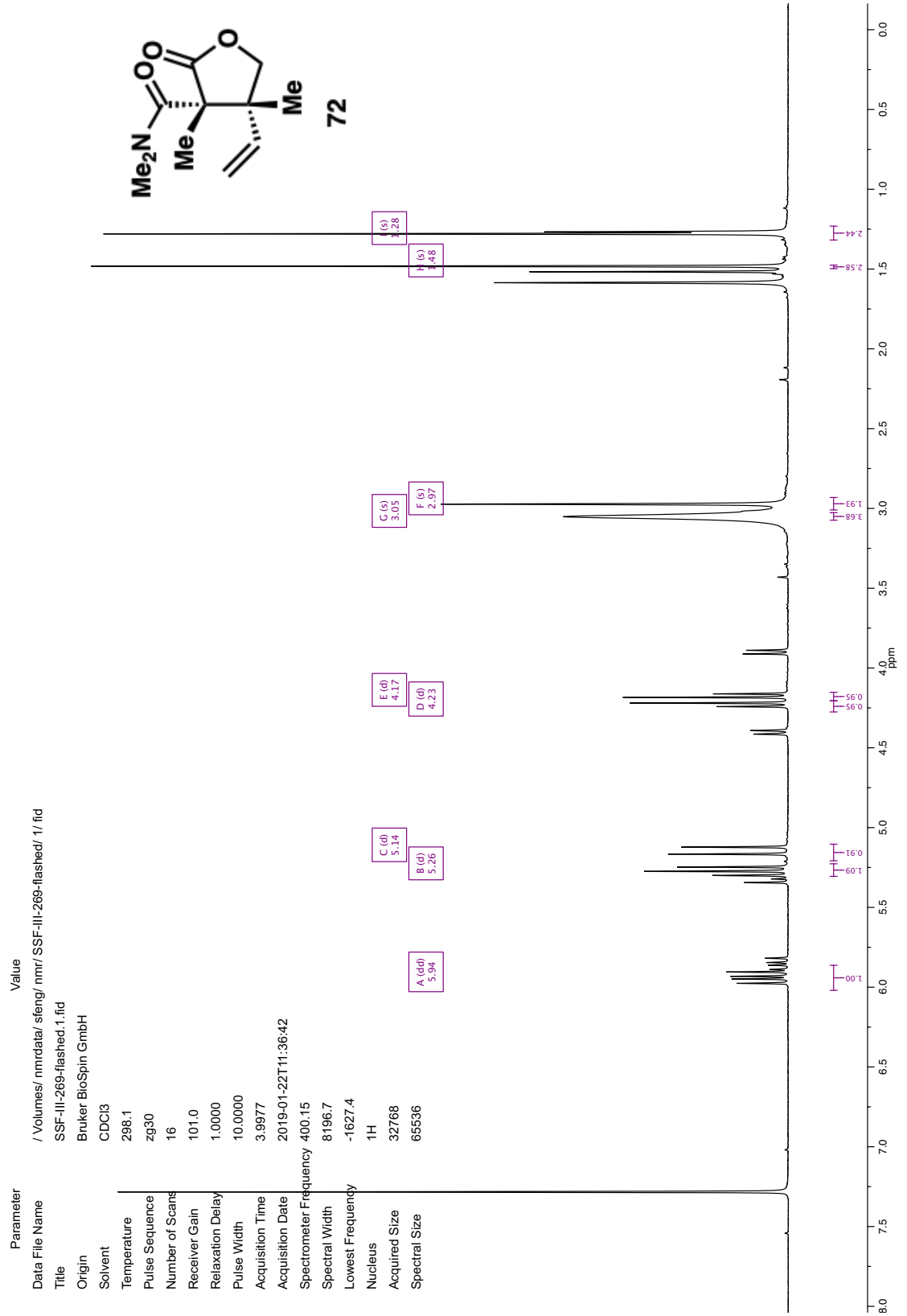
Parameter
Value
Data File Name / Volumes/ nmrdata/ sfeng/ nmr/ SSF-III-269-flashed/ 1/ fid
Title SSF-III-269-flashed.1.fid
Origin Bruker BioSpin GmbH
Solvent CDCl3
Temperature 298.1
Pulse Sequence zg30
Number of Scans 16
Receiver Gain 101.0
Relaxation Delay 1.0000
Pulse Width 10.0000
Acquisition Time 3.9977
Acquisition Date 2019-01-22T11:36:42
Spectrometer Frequency 400.15
Spectral Width 8196.7
Lowest Frequency -1627.4
Nucleus 1H
Acquired Size 32768
Spectral Size 65536
A (dd) 5.94
B (d) 5.26
C (d) 5.14
D (d) 4.23
E (d) 4.17
F (s) 2.97
G (s) 3.05
H (s) 1.48
I (s) 1.28
1.00
1.09
0.91
0.95
0.95
1.93
3.68
2.58
2.44
Me2N
Me
Me
O
O
O
72
ppm

Appendix 4

X-Ray Crystallography Reports Relevant to Chapter 3: Progress Towards the Total Synthesis of (–)-Merrilactone A

X-Ray Structure Determination

Low-temperature diffraction data (φ- and ω-scans) was collected on a Bruker AXS D8 VENTURE KAPPA diffractometer coupled to a PHOTON 100 CMOS detector with Cu-K_α radiation (λ = 1.54178 Å) from a $I_\mu S$ HB micro-focus sealed X-ray tube. All diffractometer manipulations, including data collection, integration, and scaling were carried out using the Bruker APEXII software.[1] Absorption corrections were applied using SADABS.[2] The structure was solved by intrinsic phasing using SHELXT[3] and refined against F^2 on all data by full-matrix least squares with SHELXL-2014[3] using established refinement techniques.[4] All non-hydrogen atoms were refined anisotropically. Unless otherwise noted, all hydrogen atoms were included into the model at geometrically calculated positions and refined using a riding model. The isotropic displacement parameters of all hydrogen atoms were fixed to 1.2 times the *U* value of the atoms they are linked to (1.5 times for methyl groups). Compound **72** crystallizes in the monoclinic space group $P2_1$ with one molecule in the asymmetric unit. The Flack parameter was determined to be 0.11(6); absolute configuration was determined by anomalous dispersion. Graphical representation of the structures with 50% probability thermal ellipsoids was generated using Mercury visualization software.

Table 1: Crystal data and structure refinement for 72.

Identification code	V18640	
Empirical formula	C11 H17 N O3	
Formula weight	211.25	
Temperature	99.98 K	
Wavelength	1.54178 Å	
Crystal system	Monoclinic	
Space group	P 2_1	
Unit cell dimensions	a = 6.7743(13) Å	α= 90°.
	b = 11.832(2) Å	β= 109.879(4)°.
	c = 7.2005(13) Å	γ = 90°.
Volume	542.76(18) $Å^3$	
Z	2	
Density (calculated)	1.293 Mg/m^3	
Absorption coefficient	0.768 mm^{-1}	
F(000)	228.0	
Crystal size	0.41 x 0.3 x 0.21 mm^3	
Theta range for data collection	15.074 to 159.652°.	
Index ranges	-8<=h<=8, -15<=k<=14, -7<=l<=9	
Reflections collected	8035	
Independent reflections	2266 [R(int) = 0.0499, R(sigma)=0.0444]	
Completeness to theta = 67.679°	94.4 %	
Absorption correction	Semi-empirical from equivalents	
Max. and min. transmission	0.7543 and 0.5508	
Refinement method	Full-matrix least-squares on F^2	
Data / restraints / parameters	2266 / 1 / 148	
Goodness-of-fit on F^2	1.045	
Final R indices [I>2sigma(I)]	R1 = 0.0353, wR2 = 0.0794	
R indices (all data)	R1 = 0.0314, wR2 = 0.0795	
Absolute structure parameter	0.11(6)	
Largest diff. peak and hole	0.19 and -0.16 $e.Å^{-3}$	

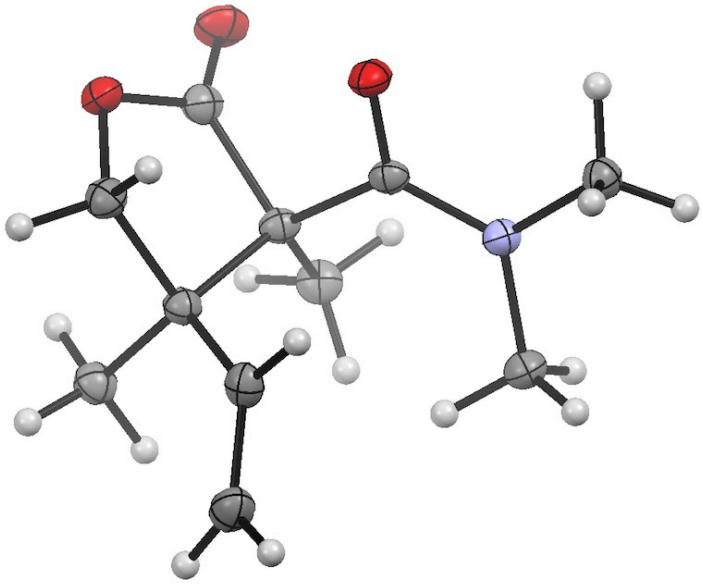

Compound **72** crystallizes in the monoclinic space group $P2_1$ with one molecule in the asymmetric unit. Absolute configuration was determined by anomalous dispersion (Flack = 0.11(6)).

References:

[1] APEX2, Version 2 User Manual, M86-E01078, Bruker Analytical X-ray Systems, Madison, WI, June 2006.
[2] Sheldrick, G.M. "SADABS (version 2008/1): Program for Absorption Correction for Data from Area Detector Frames", University of Göttingen, 2008.
[3] Sheldrick, G. *Acta Crystallogr., Sect. A: Found. Crystallogr*. **2008**, *64*, 112.
[4] Müller, P. *Crystallogr. Rev.* **2009**, *15*, 57.

ABOUT THE AUTHOR

Sean S. Feng was born on April 26th, 1993 to John and Jolyn Feng in Los Angeles, CA and grew up in the small town of Walnut in the San Gabriel Valley, just 45 minutes east of Pasadena. Sean graduated from Walnut High School in 2011 where she played varsity tennis and was dubbed class clown. It turns out, chemistry and math (not anymore) were really the only classes she excelled at, so here we are!

Sean then went on to attend University of California, Irvine just 45 minutes (south this time) of home where she began her undergraduate career as a chemistry major. Beginning as a premed student as many do, it wasn't until she took her first organic chemistry class with Professor Chris Vanderwal that she realized her true passion was total synthesis. Shortly after her first quarter of sophomore organic chemistry, she began performing research in the Vanderwal Group where she worked with graduate student and postdoc mentors, Sam Tartakoff and Allen Hong, on the total synthesis of clionastatins A and B until the completion of her bachelor's degree (not the molecule).

After receiving her B.S. in Chemistry from UC Irvine in 2015, Sean enrolled in the California Institute of Technology in Pasadena to pursue a Ph. D. in synthetic organic chemistry with Professor Sarah Reisman. Following graduation from Caltech in 2020, Sean will begin a career at Gilead Sciences, Inc. in the Bay Area as a process chemist.

On her spare time, you can catch Sean traveling to remote locations to go sport climbing, snuggling with her dogs, Woodson and Julep, and cooking brunch on the weekends.